

MICROFUNGI ASSOCIATED WITH TROPICAL AND SUBTROPICAL PALMS (*ARECACEAE*) IN CHINA AND THAILAND

YINRU XIONG

DOCTOR OF PHILOSOPHY
IN
BIOLOGICAL SCIENCE

SCHOOL OF SCIENCE
MAE FAH LUANG UNIVERSITY
2025

©COPYRIGHT BY MAE FAH LUANG UNIVERSITY

MICROFUNGI ASSOCIATED WITH TROPICAL AND SUBTROPICAL PALMS (*ARECACEAE*) IN CHINA AND THAILAND

YINRU XIONG

THIS DISSERTATION IS A PARTIAL FULFILLMENT OF THE REQUIREMENTS FOR THE DEGREE OF DOCTOR OF PHILOSOPHY IN BIOLOGICAL SCIENCE

SCHOOL OF SCIENCE
MAE FAH LUANG UNIVERSITY
2025
©COPYRIGHT BY MAE FAH LUANG UNIVERSITY

DISSERTATION APPROVAL

MAE FAH LUANG UNIVERSITY

FOR

DOCTOR OF PHILOSOPHY IN BIOLOGICAL SCIENCE

Dissertation Title: Microfungi Associated with Tropical and Subtropical Palms (*Arecaceae*) in China and Thailand

Author: Yinru Xiong

Examination Committee:

Professor Sajeewa Sandeshya Nilukana Maharachchikumbura, Ph. D.	Chairperson
Adjunct Professor Kevin David Hyde, Ph. D.	Member
Ishara Sandeepani Manawasinghe, Ph. D.	Member
Thilini Chethana Kandawatte Wedaralalage, Ph. D.	Member
Joanne Elizabeth Taylor, Ph. D.	Member

Advisors:

.....Advisor

(Adjunct Professor Kevin David Hyde, Ph. D.)

.....Co-Advisor

(Ishara Sandeepani Manawasinghe, Ph. D.)

Dean:

.....

(Professor Surat Laphookhieo, Ph. D.)

ACKNOWLEDGEMENTS

A thousand thoughts in silence grow, yet none find ink in the lines below. Looking back on this doctoral journey, while the summit reached after weathering countless challenges stands lofty, the scenery along the way is what remains most deeply etched in my memory.

I extend my most heartfelt gratitude to my supervisor, Prof. Kevin D. Hyde. It was he who granted me the invaluable opportunity to pursue my Ph.D. at the Excellent Center of Fungal Research, Mae Fah Luang University, Thailand. I am profoundly thankful for his meticulous guidance and insightful instruction throughout this process, enabling me to grow rapidly and master the relevant professional knowledge and skills. His rigorous work ethic, unwavering attention to detail, and relentless pursuit of high standards have constantly inspired me to strive for excellence in my work.

I also offer my sincere gratitude to my co-supervisor, Dr. Ishara S. Manawasinghe. Becoming her student has been my great fortune. During my doctoral studies, she taught me specialized knowledge and guided our progress. She meticulously reviewed every piece of my work and provided invaluable suggestions, fostering in me the ability for independent thinking and a spirit of scientific rigor in scholarship. In life, she provided me with meticulous care, always seeking solutions for me at the first sign of any problem. Consistently, she has watched over my growth like a caring sister.

I am deeply grateful to Dr. Ausana Mapook. She assisted in my studies and stayed in Thailand and offered extremely valuable suggestions on my thesis.

I also express my sincere thanks to Prof. Lu Yongzhong. It was he who introduced me to Prof. Hyde, opening a new door for my research career. This opportunity not only altered the course of my life but also gave me the chance to explore the mysteries of mycology. I will forever be grateful to them.

My heartfelt thanks also go to Prof. Sajeewa Maharachchikumbura, and Dr. Joanne Taylor for helping me improve my writing manuscripts and sharing their knowledge and experience in fungal taxonomy and palm fungi and also serving as my committee members. I would like to thank Dr. Thilini Chethana Kandawatte

Wedaralalage for serving as my committee member and providing me with valuable professional insights and guidance.

I wish to thank Dr. Dhanusha Wanasinghe, Dr. Ma Jian, Dr. Chada, Dr. Sun Yaru, Dr. Shen Hongwei, and Dr. Xu Rongju for their help and comments on my thesis and research topic. I thank Shaun Pennycook for checking the nomenclature for all my published work. I also sincerely thank all my fellow students for their care and support during my Ph.D. studies. Persisting through this process would have been far more challenging without you. You have given me precious memories that I will forever cherish throughout my academic career. Special thanks to Xia Guiyan, Liao Chunfang, Zhao Haijun, Shu Yongxin, Liu Xiangfu, Yang Erfu, Gao Ying, Xu Ruifang, Du Tianye, Lu Wenhua, Zhang Xian, Peng Xingcan, Su Hongli, Wu Na, Tang Xia, Tharindu, Omid, and Ishika. Special thanks to Yang Yunhui and Chen Chao for assisting me with specimen preservation and handling urgent experiments, ensuring the smooth progress of my research. Simultaneously, I thank all the teachers at the Excellent Center of Fungal Research, Mae Fah Luang University, and Zhongkai University of Agriculture and Engineering. Special thanks to P'Pooh and P'Bank for assisting me with school documents. I will forever be grateful for your help and support.

I am grateful to Mae Fah Luang University for providing the tuition fee scholarship and dissertation writing grant. I also thank the High-level Talent Project of Zhongkai University of Agriculture and Engineering (Grant No.: J2201080102).

Finally, I express my deepest gratitude to my beloved father. He has always provided me with steadfast support like a mountain, giving me the courage to forge ahead. He is my most unwavering pillar during times of distress and discouragement. I also extend special thanks to my girlfriend, Lu Li, for her years of care and support. Her diligence and dedication have also subtly influenced me, helping me to set sail anew during moments of laziness and slackness. She always offers me the most heartfelt support, restoring my confidence when disheartened. The future is no longer distant for us; we look forward to our even more brilliant tomorrow.

Yinru Xiong

Dissertation Title	Microfungi Associated with Tropical and Subtropical Palms (*Arecaceae*) in China and Thailand
Author	Yinru Xiong
Degree	Doctor of Philosophy (Biological Science)
Advisor	Adjunct Professor Kevin David Hyde, Ph. D.
Co-Advisor	Ishara Sandeepani Manawasinghe, Ph. D.

ABSTRACT

Tropical regions harbor one-third of global fungal biodiversity, yet many areas, particularly in Asia, remain underexplored. Palms (Arecaceae), thriving in these climates as culturally and ecologically significant monocots, support rich tropical biodiversity and host diverse fungal communities. Over the past three decades, extensive studies have revealed numerous novel palm-associated fungi at the species, genus, and higher taxonomic levels. However, these valuable records remain scattered and often lack DNA sequences or preserved specimens. This study consolidates global data from 1990 to 2025 to comprehensively analyze the diversity, distribution, and host associations of palm-associated fungi. In addition, fresh samples were collected from southern China and southern Thailand between 2021 and 2024. A total of 105 well-preserved collections were obtained from Guangdong, Guangxi, Jiangxi, and Yunnan provinces in China, and Narathiwat Province in Thailand. Based on morphological characteristics and multi-locus phylogenetic analysis, these collections were identified as belonging to 27 orders (including four *incertae sedis* within Dothideomycetes), 51 families, and 70 genera (including one *incertae sedis* genus each in Pleosporales and Sordariales, and six in Xylariales) within Ascomycota. Among these, six new families were identified: Cannoniaceae, Ganzhomycetaceae, Ganzhofusosporaceae, Leucocellomycetaceae, Pseudoconlariaceae, and Sporodochyalomycetaceae. The genera *Calamomyces*, *Ganzhomyces*, *Ganzhofusospora*, *Leucocellomyces*, *Pseudoconioscypha*, *Proliferirostrum*, *Sporodochyalomyces*, and *Tropicomicromyces* are described here as new. In total, 61 new species and 44 new records are introduced. For all introductions, detailed descriptions, illustrations, and phylogenetic analyses are provided. Additionally, two new combinations,

Tropicomicromyces magnoliae and *Tropicomyces palmae* are proposed based on morphological and multi-locus phylogenetic evidence. A comprehensive global checklist of palm-associated fungi, comprising 6,099 detailed records from 1990 to 2025, is included in this study. Using East Asia as a focal point, we integrated these data to assess fungal diversity and host preferences. Based on weighted global records, the estimated total number of palm-associated fungal species ranges between 44,509 and 72,136. Host preferences were categorized into three groups: typical, atypical, and suspected. To unify data access, we developed palmfungi.org, an interactive platform integrating host, geographic, and taxonomic information to bridge traditional and modern research. This study fills critical knowledge gaps, standardizes scattered data, establishes a foundation for studying host specificity, and highlights the urgent need for further exploration in tropical regions. Furthermore, results from this study consolidate global knowledge on palm-fungal relationships, enable exploration of host specificity, ecological trends, and sustainable applications, and foster collaboration among taxonomists, ecologists, and pathologists to advance understanding of the roles of palm fungi in biodiversity and ecosystem health.

Keywords: 105 Saprobic Collections, 61 New Species, Six New Families, Eight New Genera, Palm Fungal Checklist, Fungal Diversity, Phylogeny, Taxonomy, Platform

TABLE OF CONTENTS

CHAPTER	Page
1 INTRODUCTION	**1**
1.1 Background and Rationale	1
1.2 Research Questions	7
1.3 Research Objectives	7
1.4 Expected Outcomes	7
1.5 Research Contents	8
2 BIODIVERSITY OF MICROFUNGI ASSOCIATED WITH TROPICAL AND SUBTROPICAL PALM (ARECACEAE) IN CHINA AND THAILAND	**9**
2.1 Introduction	9
2.2 Materials and Methods	11
2.3 Results	14
2.4 Discussion	343
3 PALM FUNGI DATA PLATFORM	**350**
3.1 Introduction	350
3.2 Why Do We Need Palmfungi.Org?	352
3.3 What Is Palmfungi.Org?	353
3.4 Association with Plant Classification	355
3.5 Construction	355
3.6 Use Palmfungi.Org to Briefly Discuss the Current Status of Research on the Population Distribution of Palm Fungi	368
3.7 Discussion	370
4 CHECKLIST OF PALM FUNGI	**372**
4.1 Weighted Data Processing Methods	372
4.2 Results with Discussion	376

TABLE OF CONTENTS

CHAPTER	Page
5 CONCLUSIONS	**380**
5.1 Overall Conclusion	380
5.2 Research Advantages	384
5.3 Future Work	386
5.4 Publications	387
REFERENCES	**391**
APPENDICES	**464**
APPENDIX A MEDIA AND CHEMICAL REAGENTS	464
APPENDIX B ABSTRACT OF PUBLICATIONS	465
CURRICULUM VITAE	**471**

LIST OF TABLES

Table	Page
2.1 Details of genes/loci with PCR primers used in this study	13
3.1 List of expert curators with their contact information	356
4.1 Macro-classification of climate zones based on the U.S. Department of Energy (2014) merging perspective and the Köppen-Geiger climate classification (Beck et al. 2018)	373
4.2 The optimal $\beta_{Climate}$ value, β_{YEAR} value and $Intercept$ value of each climate in this study	376
4.3 Model prediction results	379

LIST OF FIGURES

Figure	Page
2.1 Phylogenetic tree of Asterinales	15
2.2 *Proliferirostrum licualicola* (MFLU 25-0156, holotype)	18
2.3 Phylogenetic tree of *Dothiorella*	20
2.4 *Dothiorella sarmentorum* (MHZU 24-0512, new host record)	23
2.5 Phylogenetic tree of *Neodeightonia*	25
2.6 *Neodeightonia guineensis* (MHZU 24-0149, holotype)	27
2.7 *Neodeightonia rattanicola* (MHZU 24-0504, new host record)	29
2.8 Phylogenetic tree of *Pseudofusicoccum*	31
2.9 *Pseudofusicoccum trachycarpi* (MHZU 24-0514, holotype)	33
2.10 Phylogenetic tree of *Gloniopsis*	35
2.11 *Gloniopsis coryphae* (MHZU 23-0132, holotype)	37
2.12 Phylogenetic tree of Eriomycetaceae	39
2.13 *Heleiosa brunnea* (MHZU 23-0183, holotype)	41
2.14 *Heleiosa phoenicis* (MHZU 23-0126, holotype)	43
2.15 *Phellinocrescentia caryotae* (MHZU 23-0164, holotype)	46
2.16 Phylogenetic tree of *Fissuroma*	48
2.17 *Fissuroma caryotae* (MHZU 23-0193, holotype)	50
2.18 Phylogenetic tree of *Anteaglonium*	51
2.19 *Anteaglonium caryotae* (MHZU 23-0160, holotype)	54
2.20 Phylogenetic tree of *Corylicola*	56
2.21 *Corylicola coffeae* (MHZU 24-0511, new host record)	58
2.22 Phylogenetic tree of Dictyosporiaceae	60
2.23 *Dictyocheirospora xishuiensis* (MHZU 23-0151, new host record)	62
2.24 Phylogenetic tree of *Paraconiothyrium*	63
2.25 *Paraconiothyrium guangdongensis* (MHZU 22-0176, holotype)	65
2.26 Phylogenetic tree of Pleosporales	68
2.27 *Ganzhofusospora phoenicis* (MHZU 24-0458, holotype)	73

LIST OF FIGURES

Figure	Page
2.28 *Ganzhomyces phoenicis* (MHZU 24-0456, holotype)	77
2.29 Phylogenetic tree of *Atrocalyx*	79
2.30 *Atrocalyx trachycarpi* (MHZU 24-0463, holotype)	81
2.31 Phylogenetic tree of Lophiotremataceae	83
2.32 *Lophiotrema guineensis* (MHZU 24-0451, holotype)	85
2.33 Phylogenetic tree of *Byssosphaeria*	86
2.34 *Byssosphaeria guangdongense* (MHZU 22-0177, holotype)	89
2.35 *Byssosphaeria lataniicola* (MHZU 23-0144, holotype)	91
2.36 *Byssosphaeria musae* (MHZU 23-0180, new host record)	93
2.37 Phylogenetic tree of *Camposporium*	95
2.38 *Camposporium livistonae* (MHZU 23-0129, holotype)	97
2.39 Phylogenetic tree of *Neomassaria*	98
2.40 *Neomassaria livistonae* (MHZU 23-0136, new host record)	101
2.41 *Neomassaria formosana* (MHZU 23-0150, new host record)	103
2.42 Phylogenetic tree of *Neooccultibambusa*	105
2.43 *Neooccultibambusa calami* (MFLU 25-0157, holotype)	107
2.44 *Seriascoma didymosporum* (MHZU 23-0141, new host record)	110
2.45 Phylogenetic tree of *Pleopunctum*	112
2.46 *Pleopunctum phoenicis* (MHZU 24-0483, holotype)	114
2.47 Phylogenetic tree of *Pseudomassarina*	115
2.48 *Pseudomassarina roystoneae* (MHZU 24-0453, holotype)	118
2.49 Phylogenetic tree of Sulcatisporaceae	120
2.50 *Parasulcatispora bismarckiae* (MHZU 23-0190, holotype)	122
2.51 *Tropicomicromyces livistonae* (MHZU 24-0448, holotype)	125
2.52 Phylogenetic tree of Teichosporaceae	126
2.53 Magnibotryascoma mali (MHZU 22-0178, new host record)	128
2.54 Pseudoteichospora borassi (MHZU 23-0177, holotype)	131

LIST OF FIGURES

Figure	Page
2.55 Phylogenetic tree of Tetraplosphaeriaceae	132
2.56 Tetraploa borassi (MHZU 23-0179, holotype)	135
2.57 Phylogenetic tree of some Pleosporales families	136
2.58 *Inflatispora licualae* (MFLU 25-0155, holotype)	139
2.59 Phylogenetic tree of Tubeufiaceae	140
2.60 *Helicoma oleifera* (MHZU 23-0157, holotype)	145
2.61 *Helicoma guttulatum* (MHZU 23-0166, new host record)	148
2.62 *Helicoma rufum* (MHZU 23-0168, new host record)	151
2.63 *Neohelicosporium guineensis* (MHZU 23-0153, holotype)	154
2.64 *Neohelicosporium xishuangbannaensis* (MHZU 23-0156, holotype)	157
2.65 Phylogenetic tree of *Cladophialophora*	159
2.66 *Cladophialophora licualae* (MFLU 25-0146, holotype)	161
2.67 Phylogenetic tree of Herpotrichiellaceae	163
2.68 *Veronaea pinangae* (MFLU 25-0151, holotype)	165
2.69 Phylogenetic tree of Herpotrichiellaceae	167
2.70 *Sclerococcum caryotae* (MHZU 23-0159, holotype)	169
2.71 Phylogenetic tree of Lachnaceae	171
2.72 *Proliferodiscus chiangraiensis* (MHZU 24-0513, new host and geography record)	173
2.73 Phylogenetic tree of *Orbilia*	175
2.74 *Orbilia phoenicis* (MHZU 24-0457, holotype)	177
2.75 Phylogenetic tree of *Codinaeella*	179
2.76 *Codinaeella plagiogyriae* (MHZU 24-0461, new host record)	181
2.77 Phylogenetic tree of *Chaetosphaeria*-like taxa in Chaetosphaeriaceae	183
2.78 *Fusichloridium licualae* (MFLU 25-0145, holotype)	186
2.79 Phylogenetic tree of *Rattania*	188
2.80 *Rattania pinangae* (MFLU 25-0150, holotype)	190

LIST OF FIGURES

Figure	Page
2.81 Phylogenetic tree of some of Chaetosphaeriales	192
2.82 *Kramasamuha arengae* (MHZU 23-0188, holotype)	194
2.83 Phylogenetic tree of Conioscyphaceae	196
2.84 *Conioscypha verrucosa* (MHZU 24-0486, new host record)	198
2.85 *Pseudoconioscypha licualae* (MFLU 25-0152, holotype)	201
2.86 Phylogenetic tree of *Conlarium*	203
2.87 *Conlarium thailandense* (MFLU 25-0149, new host record)	205
2.88 Phylogenetic tree of *Cytospora*	207
2.89 *Cytospora phoenicis* (MHZU 24-0508, holotype)	210
2.90 *Cytospora pingbianensis* (MHZU 24-0449, new host record)	212
2.91 Phylogenetic tree of *Distoseptispora*	214
2.92 *Distoseptispora elongata* (MFLU 25-0154, holotype)	217
2.93 *Distoseptispora nanchangensis* (MHZU 24-0500, new host record)	219
2.94 *Distoseptispora saprophytica* (MHZU 24-0470, new host record)	221
2.95 *Distoseptispora yichunensis* (MHZU 24-0484, new host record)	223
2.96 Phylogenetic tree of Plectosphaerellaceae	224
2.97 *Acremoniisimulans cocois* (MHZU 24-0477, new host and new geography record)	227
2.98 *Acrostalagmus luteoalbus* (MHZU 24-0460, new host and new geography record)	231
2.99 Phylogenetic tree of Hypocreales	233
2.100 *Verticimonosporium livistonae* (MHZU 24-0459, holotype)	235
2.101 Phylogenetic tree of *Alfaria*	237
2.102 *Alfaria cyperi-esculenti* (MHZU 24-0509, new host and new geography record)	239
2.103 Phylogenetic tree of *Memnoniella*	241
2.104 *Memnoniella ellipsoidea* (MHZU 23-0175, new host record)	243

LIST OF FIGURES

Figure	Page
2.105 Phylogenetic tree of *Neomyrmecridium*	245
2.106 *Neomyrmecridium trachycarpi* (MHZU 24-0466, holotype)	247
2.107 Phylogenetic tree of *Phaeoisaria*	249
2.108 *Phaeoisaria clematidis* (MHZU 24-0485, new host record)	251
2.109 Phylogenetic tree of *Pseudodactylaria*	253
2.110 *Pseudodactylaria caryotae* (MHZU 23-0192, holotype)	255
2.111 Phylogenetic tree of Rhamphoriaceae	257
2.112 *Xylolentia licualae* (MFLU 25-0153, holotype)	259
2.113 Phylogenetic tree of Sordariomycetidae and related families	261
2.114 *Rhexodenticula acaciae* (MHZU 24-0469, new host record)	263
2.115 Phylogenetic tree of *Sporidesmium*	265
2.116 *Sporidesmium phoenicis* (MHZU 24-0481, holotype)	267
2.117 Phylogenetic tree of Vermiculariopsiellaceae	269
2.118 *Vermiculariopsis pediculata* (MHZU 24-0497, new host record)	272
2.119 Phylogenetic tree of Beltraniaceae	274
2.120 *Beltraniella brevis* (MHZU 24-0488, new host record)	276
2.121 Phylogenetic tree of Coniocessiaceae	278
2.122 *Circinotrichum phoenicis* (MHZU 23-0195, holotype)	280
2.123 *Pirozynskiomyces trachycarpi* (MHZU 24-0468, holotype)	283
2.124 *Pseudoconiocessia arengicola* (MHZU 25-1055, holotype)	285
2.125 Phylogenetic tree of Fasciatisporaceae	287
2.126 *Fasciatispora elaeidis* (MHZU 24-0452, holotype)	290
2.127 *Fasciatispora sichuanensis* (MHZU 23-0142, new host record)	292
2.128 Phylogenetic tree of Xylariales	294
2.129 *Longicollium trachycarpi* (MHZU 24-0443, holotype)	299
2.130 Phylogenetic tree of Vamsapriyaceae	301
2.131 *Vamsapriya rhapidicola* (MHZU 23-0171, holotype)	303

LIST OF FIGURES

Figure	Page
2.132 *Vamsapriya trachycarpi* (MHZU 23-0186, holotype)	305
2.133 Phylogenetic tree of some genera of Xylariales	306
2.134 Virgaria nigra (MHZU 24-0489, new host and new geography record)	308
2.135 Phylogenetic tree of some families of Xylariales	310
2.136 *Anthostomella chinensis* (MHZU 23-0130, holotype)	312
2.137 *Anthostomella umbraculiferae* (MHZU 25-1053, holotype)	314
2.138 *Calamomyces brunneisporus* (MFLU 25-0148, holotype)	317
2.139 Phylogenetic tree of some families of Xylariales	319
2.140 *Melanographium citri* (MHZU 23-0189, new geography record)	321
2.141 *Melanographium coryphae* (MHZU 23-0133, holotype)	323
2.142 *Melanographium elaeidis* (MHZU 23-0155, holotype)	325
2.143 Phylogenetic tree of some orders in Sordariomycetes	326
2.144 *Leucocellomyces licualae* (MFLU 25-0144, holotype)	331
2.145 Phylogenetic tree of *Sporidesmiella*	333
2.146 *Sporidesmiella trachycarpi* (MHZU 24-0494, holotype)	335
2.147 *Pseudoconlarium trachycarpi* (MHZU 24-0464, holotype)	338
2.148 *Sporodochyalomyces trachycarpi* (MHZU 24-0465, holotype)	342
2.149 Germination rate based on different fruiting body morphologies	347
2.150 Germination rate based on collection locations	348
2.151 Unidentified fruiting bodies and spores	349
3.1 Palmfungi.org operation process	354
3.2 A single species entry of the palm web	358
3.3 Right toolbar and search result	359
3.4 Bottom border	360
3.5 Homepage	361
3.6 Host/Substrate	362
3.7 Archive	363

LIST OF FIGURES

Figure	Page
3.8 Curators: Website curator information	364
3.9 History: Website history information	365
3.10 References: Website reference information	366
3.11 Notes: a important news. b updated log	367
3.12 Contact: Website contact information	367
3.13 A diagram of the numbers of palm fungi vs. the number of palm species or Arecaceae	369
4.1 Palm fungi population trend chart from 1990 to 2025	377
4.2 Data on palm fungus records and palm species by climate within countries (reported fungus records)	378
4.3 Based on triple integration weights data, the data of palm fungi in each climate zone are presented each year	378
5.1 Host-fungus Sankey diagram based on the number of species	382

ABBREVIATIONS AND SYMBOLS

com.	combination
diam.	diameter
e.g.	for example
et al.	and others
h	hours
gen.	genus/genera
ibid.	ibidem
min	minute
ml	maximum likelihood support
mm	millimetre
nov.	novum (Latin for new thing)
pp	posterior probabilities
sp.	species
spp.	species (plural)
viz.	that is
vs.	versus
$\bar{x}$	average
°C	degree centigrade
µm	micrometer
µl	microliter
%	percent

CHAPTER 1

INTRODUCTION

1.1 Background and Rationale

1.1.1 Overview of Arecaceae Worldwide

Palm trees (Arecaceae) are important and more prominent in the tropics due to their extensive uses as food sources, construction materials, handicrafts, landscaping, and alternative medicine (Mendes et al., 2019). In addition, the beauty and uniqueness of palms in tropical landscapes are aesthetically important (Dransfield et al., 2008). Arecaceae is a monotypic family in Arecales and contains many important commercial species, such as coconuts, oil palm, date palm, and many ornamental species (Basu et al., 2014). Naturally, palms grow in almost all tropical and subtropical regions, whereas in temperate regions, introduced palm species can also survive because of their special freeze resistance (Reichgelt et al., 2018).

It has been suggested that palms may have originated in South America and Africa (West Gondwana) in the late Jurassic or early Cretaceous times (Chen et al., 2015). In fossil records, palms are one of the earliest recognizable angiosperm families (Dransfield et al., 2008), and as a modern monocot family, they have a rich fossil record (Poinar, 2002). Arecaceae is the fifth most species-rich monocot family with a long evolutionary history (Chen et al., 2022). In addition, Arecaceae has almost all possible androgynous and/or unisexual flower combinations (Douira et al., 2014). Berchtold et al. (1820) is the first study on palms that reported Arecaceae with two genera and 10 species. Currently, the palm family includes about 2,600 species, divided into climbing plants, shrubs, and trees belonging to 181 genera (Baker & Dransfield, 2016; Nadot et al., 2016). Members of Arecaceae can be readily identified by their “woody” type growth, with primary thickening of their vascular tissues, plicate leaves with unique development, and inflorescences subtended by adaxial two-keeled bracts (Dransfield et al., 2008).

Palms are a dominant feature of tropical forest communities (Marín-Spiotta et al., 2007; Ter Steege et al., 2013). Especially in southeastern Asia to Australia and Northern America to Southern America (Reichgelt et al., 2018). Their abundance can directly influence the functional composition of forest communities by the differences in the construction of forest structure, resulting in differences in functional traits (Boukili & Chazdon, 2017). The unique columnar architecture of arborescent palms inhibits liana growth and limits the amount of light reaching the forest floor (Salm et al., 2005). Meanwhile, the foraging activities around the base of palms can alter plant community composition (Queenborough et al., 2012). Because of these characteristic features and functions, the abundance of palm species influences tropical forest succession from acquisitive traits to resource conservation traits (Boukili & Chazdon, 2017). In addition, palms provide ideal subjects for demographic studies on woody plants because they are easily recognized and counted (Tomlinson, 1979). Palm tree stems are initially geotropic, and colonizing growth of the stems can occur one meter or more below the surface (Dransfield et al., 2008). The roots of palm trees are mostly very thick. When the palm tree finally dies, gaps will appear in the soil and be filled with soil and debris, causing a lot of turning of the soil (Furley, 1975). Moreover, palms are a keystone resource for frugivorous animals in the tropics because they provide a large amount and wide variety of fruits to animal consumers (Avalos et al., 2022; Pyszko et al., 2022; Muñoz-Gallego et al., 2023). Palms play as frugivory through regulating and structuring the nitrogen cycle, an important role in the zoogeochemistry of tropical forests (Villar et al., 2021). More importantly, palm provides important economic and cultural services for humans (FAOSTAT, 2019; EL-Mously et al., 2023).

1.1.2 Fungi Associated with Palms

Fungi associated with Arecaceae are referred as “palm fungi” by the mycological community (Pereira & Phillips, 2023; Xiong et al., 2024; Zhang et al., 2024), a guild which was first formally documented by Kunze and Schmidt (1817). Since then, over two centuries of sustained investigations have predominantly focused on saprophytic taxa colonizing palm substrates. With foundational contributions by 19th-century mycologists, including Saccardo PA, Paoletti G, and Penzig AJO, who initiated pioneering taxonomic documentation of saprophytic palm fungi, laying the groundwork for systematic studies (Saccardo & Paoletti, 1888; Penzig & Saccardo,

1897). Throughout the 20th century, Hennings P, Rehm H, Sydow H, Sydow P, Ellis MB, Pirozynski KA, Deighton FC, and their collaborators expanded these foundations through elaborative morphological analyses, addressing critical gaps in species diversity and biogeographic distributions (Hennings, 1902; Rehm, 1914; Sydow & Sydow, 1917; Ellis, 1957, 1967; Pirozynski, 1972; Deighton, 1985). The late 20th and early 21st centuries marked a paradigm shift as Hyde KD, Fröhlich J, McKenzie EHC, Ho WH, Pinruan U, Jones EBG, Taylor JE, Pinnoi A, Liu JK, and colleagues established this field as a focal point in mycology and pioneered molecular-based fungal taxonomy (Hyde, 1992; Hyde et al., 2000; Hyde & Fröhlich, 2003; McKenzie et al., 2004; Ho et al., 2005; Pinruan et al., 2004, 2010; Pinnoi et al., 2010; Liu et al., 2010). Their integration of phylogenetic methodologies with ecological studies catalyzed advancements in host-specificity and evolutionary classifications. Building upon these advances, Konta S, Pereira DS, Zhang SN, Xiong YR, and Karimi O have further expanded the taxonomic classification of palm fungi through integrative approaches combining multi-locus phylogenetics and ecological trait analysis, highlighting the critical role of this field in understanding fungal contributions to decomposition processes in tropical ecosystems (Konta et al., 2016; Pereira & Phillips, 2020; Zhang et al., 2020; Xiong et al., 2022; Karimi et al., 2024).

Phytopathogens affecting Arecaceae species remain perennially significant due to their economic impacts (Mendes et al., 2019; Hassan et al., 2021). *Graphiola phoenicis*, the causative agent of false smut on *Phoenix canariensis* (Canary Island Date Palm), has been epidemiologically monitored across two centuries (Mendes et al., 2019; Hassan et al., 2021). Furthermore, reports of diseases caused by taxonomically diverse genera, including *Fusarium* (Elliott, 2011; Hernández-Hernández et al., 2010), *Marasmiellus* (Jackson & McKenzie, 1988), *Palmeiromyces* (Pereira & Phillips, 2020), *Phyllachora* (Hyde & Cannon, 1999), *Pseudopestalotiopsis* (Tao et al., 2021), *Serenomyces* (Elliott & Des Jardin, 2014) and *Thielaviopsis* (Klotz & Fawcett, 1932) continue to expand, underscoring the ecological and agricultural significance of these pathogens.

In contrast to saprobic and pathogenic fungi, research on palm endophytic fungi emerged later, with the first documented study not appearing until 1990 (Rodrigues & Samuels, 1990). Rodrigues (1994) subsequently elucidated colonization dynamics of endophytes in *Euterpe oleracea*, demonstrating positive correlations with leaf age,

developmental stage, geographic location, and seasonal variation. Fröhlich et al. (2000) further revealed compartmentalized endophytic assemblages across distinct leaf tissues and aged organs of *Licuala ramsayi*. Taylor et al. (1999) provided foundational insights into climatic drivers shaping endophytic community structures. Advancing methodological rigor, Rungjindamai et al. (2008) and Pinruan et al. (2010) characterized basidiomycetous endophyte diversity in *Elaeis guineensis* foliar, rachis, and petiole tissues through integrated morphological and molecular analyses. Mahmouda et al. (2017) delineated root-associated endophytic diversity in coastal dune-inhabiting *Phoenix dactylifera*, highlighting strains with potential as biocontrol agents against root pathogens. Recent investigations by Azuddin et al. (2021) systematically profiled spine-associated endophytes of *Calamus castaneus*, evaluating their antagonistic activity toward phytopathogens, while Dhillon et al. (2024) identified antagonistic endophytic consortia from *Butyagrus nabonnandii* foliage with efficacy against lethal palm pathogens. Although palm endophyte research began later than other mycological studies, the recent molecular-era, multidisciplinary advances have brought it on par with broader fungal research. These advances now allow researchers to dissect host-microbe interactions at a mechanistic level more precisely than ever before.

1.1.3 Fungal Data Platforms

The storage and continuous updating of data are critical concerns that every field consistently prioritizes the proper data preservation and data preservation and continuous update is essential yet challenging in mycology due to the continuous update is essential yet challenging in mycology due to the exponential rate of taxonomic updates. To achieve this, update of fungal species resources cannot be achieved without the joint efforts of collaboration among various databases around the world are required. Index Fungorum (2023, http://www.indexfungorum.org), Species Fungorum (2023, http://www.speciesfungorum.org) and Mycobank (2004) continue to store and update fungal taxonomic updates where as T the National Center for Biotechnology Information (NCBI) continues to store and update molecular data. In addition to these major data depositories, Tthere are many similar online databases which are often focus on collecting information on the entire fungal kingdom.

In recent years, data platforms focused on a specific group of fungi have become a trend. For instance, “Marine fungi” (Jones et al., 2019, http://marinefungi.org); and

“Freshwater fungi” (Calabon et al., 2020, http://freshwaterfungi.org) are focus on specific fungal habitats, whereas “Sordariomycetes” (Bundhun et al., 2020, https://sordariomycetes.org) are focusing on specific fungal groups and web pages like gmsmicrofungi" (Chaiwan et al., 2021; http://gmsmicrofungi.org) focus on specific regional aspects. To a certain extent, these platforms saves researchers in mycology and related fields time when gathering information on specific fungal groups. However, there is still no outstanding platform for host-related fungal information, which significantly hinders progress in studies on fungal host specificity and biological control.

Pereira and Phillips (2023) periodize palm mycological research into three distinct phases, with both syntheses identifying the molecular era as the inflexion point for exponential growth in study intensity. The documented diversity of palm fungi has expanded substantially alongside intensified investigationsIn Pereira and Phillips (2023), the authors propose a global estimate exceeding 2,500 fungal taxonomic entities symbiotically associated with palms. This contrasts with the more conservative estimate by Zhang et al. (2024), who report approximately 1,050 formally described species. Earlier Hyde et al. (1997) suggested that Ascomycota fungi constituted approximately 41% of palm-associated taxa, respectively. However, Pereira and Phillips (2023) predict a revised taxonomic distribution: approximately 55% Ascomycota, 35% other fungi, and 10% Basidiomycota. Based on the current advancement in phylogeny and molecular data, it is obvious that these findings must be validated.

These scattered records and the rate of describing new taxa are not moving in parallel, thus creating a knowledge gap in understanding the true diversity of palm fungi. Collectively, previous findings underscore substantial unrealized diversity within palm-fungi systems, encompassing persistently documented saprotrophic and pathogenic guilds, alongside rapidly expanding endophytic lineages, while simultaneously indicating the need for unified taxonomic frameworks to address lingering ambiguities and accelerate discovery (Wanasinghe et al., 2018). Therefore, it is necessary to provide a platform related to palm fungi which could provide researchers with concise but relatively complete information on palm fungal species, and as a directory of palm fungal diversity and host specificity.

1.1.4 Re-evaluating the Total Diversity of Palm-associated Fungi

Pereira and Phillips (2023) emphasize the hyperdiversity of palm fungi and their complex community architectures enable macroecological syntheses to dissect fungal community structure and functional dynamics within ecosystems. This paradigm builds on foundational work by Fröhlich and Hyde (1999), who designated palms as critical substrates for fungal diversity exploration due to their exceptionally heterogeneous mycobiota. Recognizing palms as model systems for fungal biodiversity studies not only enhances inventory precision but also delivers a novel framework to dissect evolutionary drivers of plant-fungal specificity (Pereira & Phillips, 2023). Hyde (2001) catalogued multiple fungal taxa endemic to *Archontophoenix alexandrae* and allied palm genera, while Fröhlich and Hyde (1999) demonstrated 88% species-level dissimilarity between fungal communities of sympatric *Licuala congeners*. This trend of high beta diversity is corroborated by Yanna et al. (2001), who documented merely 6–17% fungal overlap within conspecific palm populations. Pereira and Phillips (2023) hypothesized that such pronounced host specificity may reflect coevolutionary adaptations between palms and their mycobionts. However, Hawksworth (2012) underscored limitations in these analyses while advocating continuous and unified reference datasets to refine diversity estimates. Building on this, Hawksworth and Lücking (2017) underscore temporally resolved longitudinal data, essential for both predicting fungal diversity patterns and guiding targeted discovery efforts.

Hyde et al. (1997) and McKenzie et al. (2004) established taxonomically annotated inventories of palm fungi, and Pereira and Phillips (2023) contributed a systematic synthesis of their ecological distributions. These fragmented occurrence records and inconsistent reporting standards as major impediments to robust assessments of palm fungal biodiversity and investigations into host specificity. Also, the lack of time-resolved longitudinal datasets remains a critical gap, hindering our ability to comprehensively track the diversification of palm fungi and their host interactions. Finally, there is a necessity for advanced standardized frameworks through a dedicated web platform for fungal data integration.

1.2 Research Questions

1.2.1 What is the diversity of saprobic fungi associated with tropical and subtropical palms in China and Thailand?

1.2.2 How to access palm fungal data using standardized frameworks?

1.2.3 How to define host association in palm fungi?

1.3 Research Objectives

1.3.1 To identify and describe novel/known fungal taxa associated with tropical and subtropical palms in China and Thailand based on morphology and multigene phylogeny.

1.3.2 To build a continued and diverse information platform for palm fungi that connects with other international data platforms.

1.3.3 To provide an updated checklist of fungi associated with palms worldwide from 1990 to 2025, with predictions of the number of palm fungi.

1.3.4 To provide a new perspective for interpreting the host specificity of palm fungi based on the data from this study.

1.4 Expected Outcomes

1.4.1 A diversity analysis of saprobes associated with tropical and subtropical palms known from cultures in China and Thailand.

1.4.2 Novel species, host/geological records of saprobes associated with tropical and subtropical palms in China and Thailand.

1.4.3 A checklist of fungi associated with palms worldwide from 1990 to 2025.

1.4.4 A global prediction of the number of palm fungi

1.4.5 A new perspective for interpreting the host specificity of palm fungi based on the data from this study.

1.5 Research Contents

This study mainly focuses on the diversity, taxonomy, and phylogeny of palm saprobic fungi in tropical and subtropical regions of China and saprobic fungi in tropical regions of Thailand. In addition, this study established a sustainable and updated palm fungus data platform and collected a list of palm fungi records from 1990 to 2025. Based on this list, this study proposed a new total palm fungal diversity. Finally, it proposed a definition for palm host-preferential fungal genera. The study is divided into five chapters.

Chapter 1 is a general introduction, introducing the research background and basic principles, reviewing the research history and status of palm fungi, and exploring the importance of palm and its related microfungi in these biodiverse areas. It outlines the significance of the study, clearly stating the research objectives, expected outcomes and the outline of the thesis.

Chapter 2 provides the diversity, taxonomy and phylogeny of palm saprobes. In this chapter, 105 specimens, which were collected from tropical and subtropical regions of China and tropical regions of Thailand, were characterised. Based on morphological comparisons and multi-gene phylogenetic analysis, I introduce seven new families, nine new genera, 61 new species, and 44 new records. The description and illustrations for each taxon are provided.

Chapter 3 provides a portal for sustainable and comprehensive palm fungal species information. It provides a new platform, www.plamfungi.org, for fungal researchers to explore the host specificity of palm fungi.

Chapter 4 provides a checklist for all palm-associated fungal records from 1995 to 2025. It details the taxonomic position of the fungi, the palm species, and their known distribution. Based on this record, a new total number of palm fungal diversity is proposed.

Chapter 5 provides an overall conclusion, the research advantages, and future work.

CHAPTER 2

BIODIVERSITY OF SAPROBIC MICROFUNGI ASSOCIATED WITH TROPICAL AND SUBTROPICAL PALM (ARECACEAE) IN CHINA AND THAILAND

2.1 Introduction

Palms (Arecaceae), comprising around 2,600 species of arborescent monocots, constitute an iconic botanical group. These species play a critical socio-ecological role across pantropical forest ecosystems (Cámara-Leret et al., 2017; Levis et al., 2017). As keystone components of neotropical rainforest ecosystems, palm species frequently dominate arborescent communities, constituting over 50% of the emergent tree stratum while modulating forest structure and microclimatic conditions through their distinctive crown architectures and phenological patterns (ter Steege et al., 2013; Reichgelt et al., 2018; Fehr et al., 2020). Furthermore, these angiosperms maintain complex trophic interdependencies by hosting diverse mycobiota that mediate critical biogeochemical processes (Schuessler et al., 2018; Muscarella et al., 2020; Rathna et al., 2025). The rhizospheric and phyllospheric fungal consortia associated with palms demonstrate specialized enzymatic capabilities for lignocellulose decomposition and phosphorus solubilization, integral to maintaining the nutrient dynamics and carbon sequestration capacities characteristic of these hyperdiverse ecosystems (Nisa et al., 2015; Outamamat et al., 2021; Toapanta-Alban et al., 2022).

Palm fungi are well known for their diversity and uniqueness in tropical and subtropical regions. Thus, studies in palm fungi have a long history, which could be divided into two phases. Phase one is between 1820 and 1990, which is the “Historical palm fungi era”. Poiteau (1824) reported the earliest record of palm fungi: *Graphiola phoenicis* from *Phoenix dactylifera*. Most of these species are published with Saccardo's Syll. Fung. The second period can be the “Classical palm fungi era”, which was led by KD Hyde and his colleagues from the end of the 20th century to the beginning of the 21st century (Taylor & Hyde, 2003). Hyde et al. (2000) provided 100

palm fungal genera with illustrations, their first monograph in the modern century. Fröhlich and Hyde (2000) introduced 20 palm fungal species distributed in Australia, Brunei, Ecuador, and China, with palm species geography distribution. Taylor and Hyde (2003) introduced and summarized 288 palm fungal species from Australia and China (Hunan, Hubei and Hong Kong).

The diversity of palm fungi is extremely high, covering almost all major fungal classifications (Fröhlich et al., 2000; Taylor & Hyde, 2003). More than 500 new fungal species were reported only in the second phase (Fröhlich et al., 2000; Hyde et al., 2000; Taylor & Hyde, 2003). After the second phase, more than 500 new species were reported (Index Fungorum, 2023). In recent years, research on palm fungi has emerged endlessly. Pinruan et al. (2010), Zhang et al. (2012), Xiong et al. (2022a) and Konta et al. (2023) reported saprophytic fungi on palm plants whereas Zheng et al. (2017), Pandian et al. (2021) and Xiong et al. (2022b) reported pathogenic fungi on palm plants. In addition, Guo et al. (1998) and Mahmoud et al. (2016, 2017) reported endophytic fungi on palm plants. However, most of these studies on palm fungi were assembled in several key areas viz. Australia, Brazil, China, India, Thailand and USA (Index Funguram, 2023). However, there are still gaps in the understanding systematic and sustained monograph, and ecologicalimpact of these fungi.

Fungi commonly associated with palms are often non- host specific (Pinnoi et al., 2006) yet *Oxydothis alexandrarum* is thus far exclusive to *Archontophoenix alexandrae*. Furthermore, peat swamps involved a large distinctively resource of palm fungi (Pinnoi et al., 2006; Pinruan et al., 2007). Peat swamp forests are unique ecosystems that are extremely important globally because of their rich species biodiversity. Meanwhile, peat swamps both have terrestrial and aquatic habitats for palm fungi (Pinruan et al., 2002, 2007). Interestingly, peat swamps keep highly distinctive fungal biodiversity in each habitat compared with other ecosystems (Pinnoi et al., 2006; Pinruan et al., 2007).

Palm fungi are still hidden in inapproximable fungal resources as a biodiversity treasury. To excavate palm fungi resources, we need further collections and studies in this unique group. Moreover, the research performed on palm fungi is scattered, lacking a complete and sustainable source of knowledge to precisely document palm fungi. In this study, I provide and compare the diversity analyses for 105 collections associated with

palm from tropical and subtropical regions of China and tropical regions of Thailand. In addition, I introduced 105 species with full (macro and micro characteristics) descriptions, illustrations, and a phylogenetic tree that shows the phylogenetic position of these taxa. All species illustrated below are in alphabetical order. They represent 88 genera in 60 families, 27 orders and five classes in Ascomycota.

2.2 Materials and Methods

2.2.1 Sampling Collection, Examination, and Collection

Decayed tissues of palm species were collected from 2021 to 2025 in Guangxi Province (Guilin City), Jiangxi Province (Ganzhou, Nanchang, Pingxiang City), Yunnan Province (Kunming, Qujing, Xishuangbanna City), China and Narathiwat Province, Thailand. After the collection information was recorded (Rathnayaka et al., 2024), the specimens were sent to the Mycology Laboratories at Zhongkai University of Agriculture and Engineering, Guangdong Province, China, and Mae Fah Luang University, Chiang Rai, Thailand for examination. Morphological observations and single spore collection were performed following the procedures outlined by Senanayake et al. (2020). The Cnoptec SZ650 series (Cnoptec, China) stereomicroscope was used to observe the macro morphological characteristics and photographs were taken using SteReo Discovery V20. Nikon Eclipse 80i and the industrial DigitaL Sight DS-Fi1 (Panasonic, Japan) microscope and imaging system were used to take pictures of micromorphological characters. The measured data were processed using Tarosoft (R) Image Frame Work v. 0.9.7, and photographic negatives were prepared using Adobe Photoshop 2023. Pure cultures are deposited in Zhongkai University of Agriculture and Engineering (ZHKUCC) or the Fungus Culture Collection Center of Mae Fah Luang University (MFLUCC), Chiang Rai, Thailand. Specimens are deposited in the Fungal Herbarium of Zhongkai University of Agriculture and Engineering (MHZU) or the Herbarium of Mae Fah Luang University (MFLU), Chiang Rai, Thailand. The methods for obtaining the fungal FoF number and fungal index (IF) number are described in Jayasiri et al. (2015) and Fungal Index (2025).

All taxonomic information will be deposited in the Palm Fungi Database (Xiong et al., 2024).

2.2.2 Molecular Studies

Pure cultures were grown on PDA plates for 1–2 weeks, and approximately 500 mg of fresh fungal mycelia were scraped. Total genomic DNA was extracted from mycelia using the MagPure Plant AS Kit (Magen Biotech, China) according to the manufacturer's instructions. The total volume of the polymerase chain reaction (PCR) was 25 µl, which contained 12.5 µl 2xMaster Mix, 1 µl of each primer (10 pM) (forward and reverse), 2 µl genomic DNA template, and 8.5 µl ddH_2O. The PCR thermal cycle program and primers are shown in Table 2.1. The PCR procedure is as follows: for ITS/LSU/SSU, the initial denaturation step is performed at 95°C for 2 minutes, then 35 amplification cycles at 95°C for 1 minute, 50°C for 1 minute and 72°C for 1 minute. Finally, extension for 10 minutes at 72°C. For *tef* 1-α/*tub* 2, an initial step of 2 minutes at 95°C followed by 35 cycles of 1 minute at 95°C, 1 minute at 52°C, 1 minute at 72°C and 7 minutes at 72°C. For *rpb* 2 PCR conditions, an initial denaturation step was per formed at 95°C for 5 minutes and then 30 cycles at 94°C for 1 minute, 53°C for 30 seconds, 72°C for 90 seconds and finally 72°C for 10 minutes. After PCR amplification, the product was observed on a 1% agarose gel under ultraviolet light. DNA sequencing was performed by Guangzhou Tianyi Technology Co., Ltd. The new sequences have been deposited in GenBank.

2.2.3 Phylogenetic Analyses

To clarify the taxonomic status collections in this study, preliminary identification was done using ITS sequences through BLASTn (https://blast.ncbi.nlm.nih.gov/Blast.cgi) searches in the search engine of the National Centre for Biotechnology Information (NCBI). Phylogenetic analyses were conducted using multi-gene markers recommended in recent publications. The relevant sequence data and newly generated DNA sequences were combined, and automatic alignment and editing were completed using OFPT (Zeng et al., 2023). Afterward, all datasets were concatenated into fasta files format; the alignments were checked visually and improved manually where necessary in the AliView program (Larsson, 2014). Phylogenetic analyses were referred to Dissanayake et al. (2020) and conducted with maximum likelihood (ML) and Bayesian posterior probability (BYPP) algorithms on the CIPRES Science Gateway

portal (https://www. phylo.org/). Maximum likelihood analysis was performed using RAxML-HPC v.8, with rapid bootstrap analysis, followed by 1,000 bootstrap replicates using the GTRGAMMA substitution model. The Bayesian analyses were performed using MrBayes 3.2.7a, and the best nucleotide substitution model for each data partition was evaluated with MrModeltest 2.2 (Nylander, 2004). The Markov Chain Monte Carlo (MCMC) sampling approach was used to calculate posterior probabilities (BYPP) (Rannala & Yang, 1996). Six simultaneous Markov chains were run for 2 million generations, and trees were sampled every 1,000th generation. The first 20% of trees, representing the burn-in phase of the analyses, were discarded, and the remaining trees were used for the BYPP value in the majority rule consensus tree. The phylogenetic trees were visualized using FigTree (v 1.4.2) (Rambaut, 2014) and edited using Microsoft Office PowerPoint (2020) and Adobe Illustrator CS6 (Adobe Systems Inc., USA). The bootstrap support values for ML equal to or greater than 70% and BYPP equal to or greater than 0.90 are given above the nodes.

Table 2.1 Details of genes/loci with PCR primers used in this study

Gene[1]	Primer	Sequence (5'-3')	Reference
ITS	ITS5	GGAAGTAAAAGTCGTAACAAGG	White et al.,
	ITS4	TCCTCCGCTTATTGATATGC	(1990)
LSU	LR0R	ACCCGCTGAACTTAAGC	Vilgalys and
	LR5	TCCTGAGGGAAACTTCG	Hester (1990)
SSU	NS1	GTAGTCATATGCTTGTCTC	White et al.,
	NS4	CTTCCGTCAATTCCTTTAAG	(1990)
tef 1-α	EF1-983F	GCYCCYGGHCAYCGTGAYTTYAT	Carbone and
	EF1-2218R	TACTTGAAGGAACCCTTACC	Kohn (1999)
tub 2	T1	AACATGCGTGAGATTGTAAGT	Glass and
	Bt2b	CCRGAYTGRCCRAARACRAAGTT	Donaldson
		GTC	(1995)
rpb 2	fRPB2-5F	GAYGAYMGWGATCAYTTYGG	O'Donnell et al.,
	fRPB2-7CR	CCCATRGCTTGYTTRCCCAT	(2007)

2.3 Results

2.3.1 Taxonomy

2.3.1.1 Dothideomycetes

Asterinales M.E. Barr ex D. Hawksw. & O.E. Erikss. (1986)

Stictographaceae D.Q. Dai & K.D. Hyde, Phytotaxa 369 (2): 70 (2018)

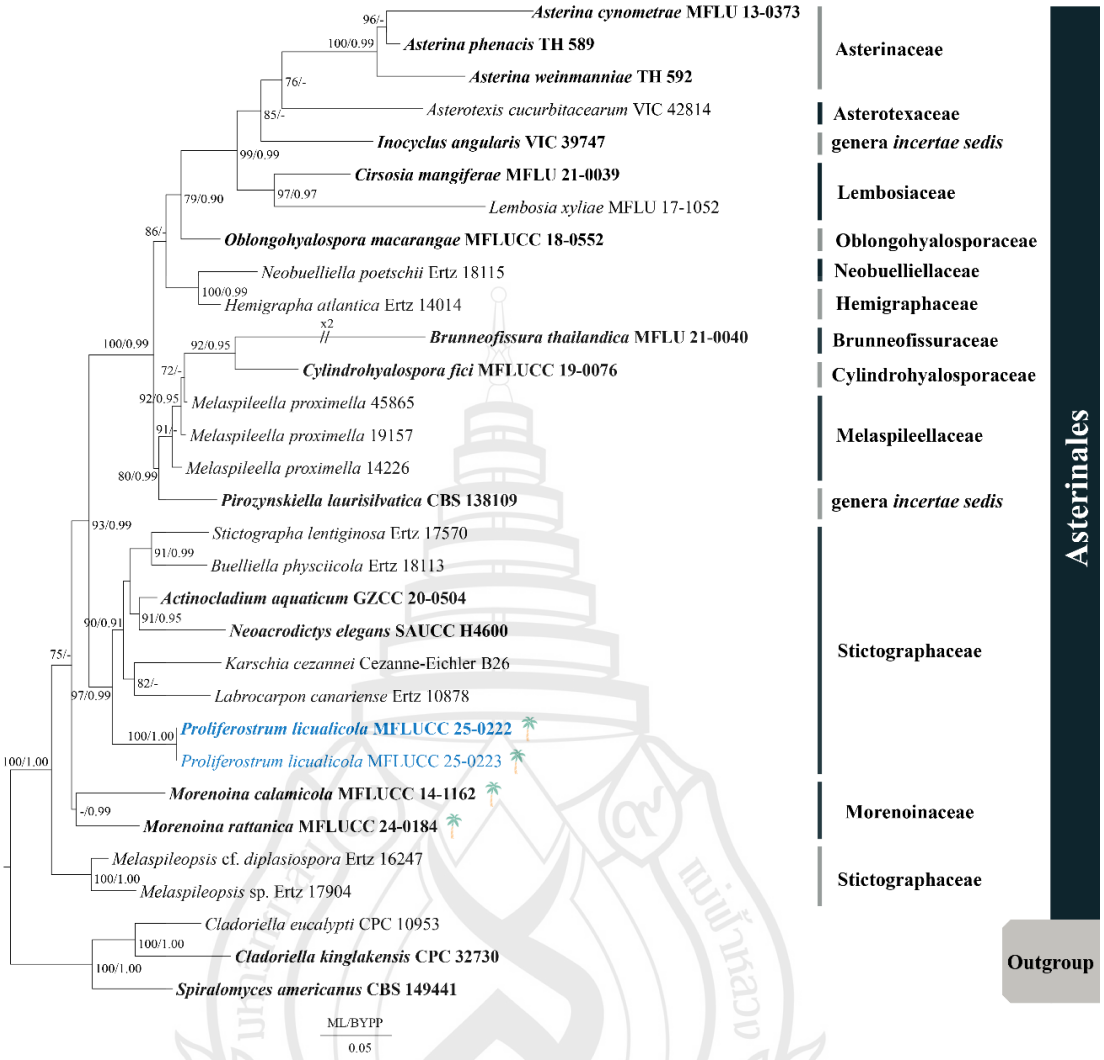
Proliferirostrum Y.R. Xiong, Manawas. & K.D. Hyde, ***gen. nov.***

Etymology: referring to the "proliferations" conidiogenous cell and "rostrate" conidia of type species.

Type species: *Proliferirostrum licualicola* Y.R. Xiong, Manawas. & K.D. Hyde

Saprobic on dead palm substrates. Asexual morph: Hyphomycetous. *Colonies* on natural substrate effuse, hairy, velvety. *Mycelium* immersed in the substratum, branched. *Conidiophores* macronematous, mononematous, solitary, cylindrical, straight or slightly flexuous, successive profilerations, signification constricted at remnants of proliferation. *Conidiogenous cell* integrated, terminal, holoblastic, monoblastic, cylindrical, successive profilerations. *Conidia* acrogenous, solitary, pyriform, short rostrate, tapering to the apex and round, truncate at basal, septate, guttulate, terminal cells pale, medium cells dark. Sexual morph: Not observed.

Notes: *Proliferirostrum* (*P.*) is introduced here as monotypic genus to accommodate type species *Proliferirostrum licualicola*. Based on our phylogenetic result (Figure 2.1), *Proliferirostrum* formed an independent clade within Stictographaceae with high supported value (97% ML and 0.99 BYPP bootstrap support). The phylogenetic result was similar to previous phylogenetic analyses on Asterinales by Hongsanan et al. (2020), Tennakoon et al. (2021) and Marasinghe et al. (2022). However, molecular data are lacking for most species of Stictographaceae. Morphologically, *Proliferirostrum* is distinct from Stictographaceae being hyphomycetous in which conidia are rostrate and club-shape, conidiogenous cell successive proliferations. However, *Neoacrodictys* is the only taxon reported as hyphomycetous in Stictographaceae which is characterised by schizolytic conidial secession and conidia that have one longitudinal and a few transverse oblique septa, turbinate to obpyriform (Xia et al., 2022). According to morphological differences and phylogenetic placement, we propose a new genus typified by *Proliferirostrum licualicola*.



Note Phylogram generated from maximum likelihood analysis of Asterinales based on combined ITS, LSU, and SSU sequence data. Bootstrap values for maximum likelihood (ML) equal to or greater than 70 and BYPP values equal to or greater than 0.90 are indicated above the branches. The new collections are indicated in blue and ex-type strains are indicated in bold.

Figure 2.1 Phylogenetic tree of Asterinales

Figure 2.2

Etymology: The epithet refers to the host genus name "*Licuala*", from which the species was collected.

Saprobic on dead petiole of *Licuala* sp. Asexual morph: Hyphomycetous. *Colonies* on natural substrate effuse, hairy, velvety, dark brown to black. *Mycelium* immersed in the substratum, branched and brown with smooth hyphae. *Conidiophores* 50–140 × 5–6 μm ($\overline{x}$ = 76.6 × 5.4 μm, n = 15), macronematous, mononematous, solitary, cylindrical, straight or slightly flexuous, successive profilerations, signification constricted at remnants of proliferation, olivaceous to dark brown. *Conidiogenous cell* 7–9 × 4–5 μm ($\overline{x}$ = 7.9 × 4.4 μm, n = 25), integrated, terminal, holoblastic, monoblastic, cylindrical, pale olivaceous, successive profilerations. *Conidia* 25–35 × 8.5–9.5 μm ($\overline{x}$ = 29.6 × 8.9 μm, n = 25), acrogenous, solitary, dry, pyriform, short rostrate, tapering to the apex and round, truncate at basal, 4-6-septate, guttulate, terminal cells hyaline to pale olivaceous, three medium cells dark olivaceous.

Culture characteristics: Colonies on PDA fast growing, after 2 weeks reaching 4 cm diam., at 25°C, circular, raised, brown mycelium velvety, filiform margin, pale brown; reverse black to dark brown.

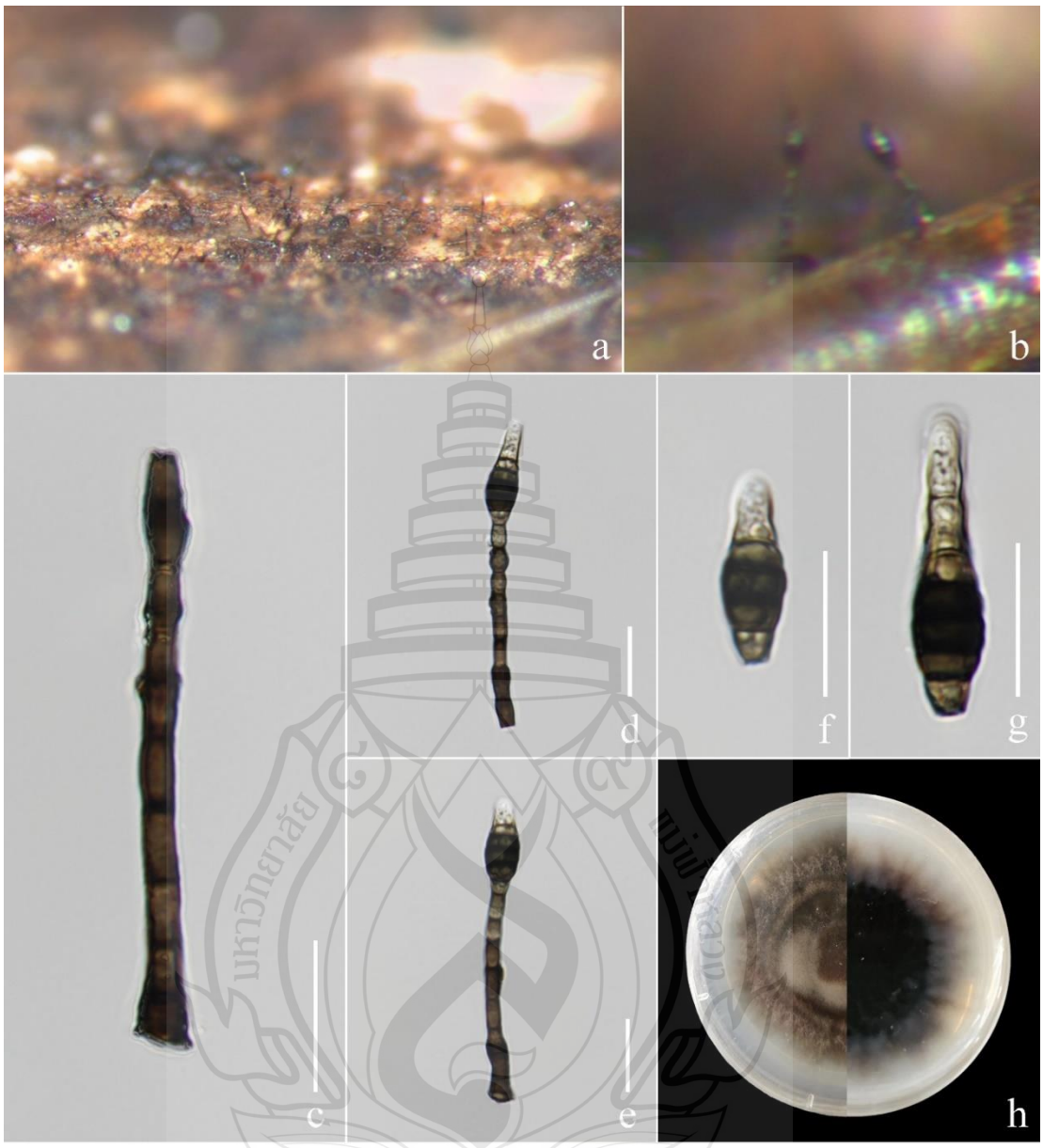
Known distribution: Thailand (this study).

Material examined: Thailand, Narathiwat Province, Toh Daeng Peat swamp, on dead petiole of *Licuala* sp., 4 Aug 2023, Y.R. Xiong and L. Lu, XG353 (MFLU 25-0156, holotype); ex-type MFLUCC 25-0222, other living culture MFLUCC 25-0223.

GenBank numbers: MFLUCC 25-0222: ITS – PV578230, LSU – PV578396, SSU – PV578534, *tef* 1-α – PV608880, *rpb*2 – PV595350; MFLUCC 25-0223: ITS – PV578231, LSU – PV578397, SSU – PV578535, *tef* 1-α – PV608881, *rpb*2 – PV595351.

Notes: Two collections from this study formed a separate lineage in the phylogenetic tree (Figure 2.1). Based on a MegaBLAST (Query cover ≥ 70%) search using the ITS sequence, the closest matches in NCBIs GenBank nucleotide database were *Neolinocarpon rachidis* (GenBank MK120273; Identities 452/540 (83.70%), 26 gaps), Dothideomycetes sp. (GenBank OR658706; Identities 421/501 (84.03%), 15 gaps) and Dothideomycetes sp. (GenBank AB986427; Identities 425/505 (84.16%), 23 gaps). The highest similarities using the LSU sequence were *Rhizodiscina* sp. (GenBank PQ608030; Identities 808/843 (95.85%), 2 gap), Dothideomycetes sp. (GenBank AB986427; Identities

800/835 (95.81%), 2 gaps) and *Rhizodiscina lignyota* (GenBank OP763385; Identities 791/826 (95.76%), 2 gaps). The highest similarities using the SSU sequence were *Actinocladium aquaticum* (GenBank NG_242859; Identities 986/1001 (98.50%), 1 gap), *Morenoina palmicola* (GenBank MK120299; Identities 1003/1020 (98.33%), 0 gaps) and *Rhizodiscina lignyota* (GenBank MF599193; Identities 1001/1020 (98.14%), 0 gaps). The highest similarities using the *rpb2* sequence were *Morenoina rattanica* (GenBank PP780229; Identities 860/1077 (79.85%), 0 gap). The highest similarities using the *tef* 1-α sequence were *Helicosporium multidentatum* (GenBank OR058863; Identities 818/897 (91.19%), 0 gap), *Neohelicosporium guangxiense* (GenBank MF535243; Identities 827/907 (91.18%), 1 gaps) and *Helicosporium flavum* (GenBank KY873285; Identities 822/903 (91.03%), 0 gaps). *Proliferirostrum licualicola* were distinct by conidiophores signification constricted at remnants of proliferation, conidiogenous cell successive profilerations, conidia short rostrate, tapering to the apex and round, truncate at basal, 4-6-septate and terminal cells hyaline to pale olivaceous, three medium cells dark olivaceous (Figure 2.2). Based on the phylogenetic placement and morphological variations, we introduce *P. licualicola* as a new species.



Note a, b Colonies on natural substrate. c–e Conidiophores, conidiogenous cells with conidia. f, g Conidia. h The front of culture on PDA at 25°C and the reverse of culture on PDA at 25°C. Scale bars: c–g = 20 µm.

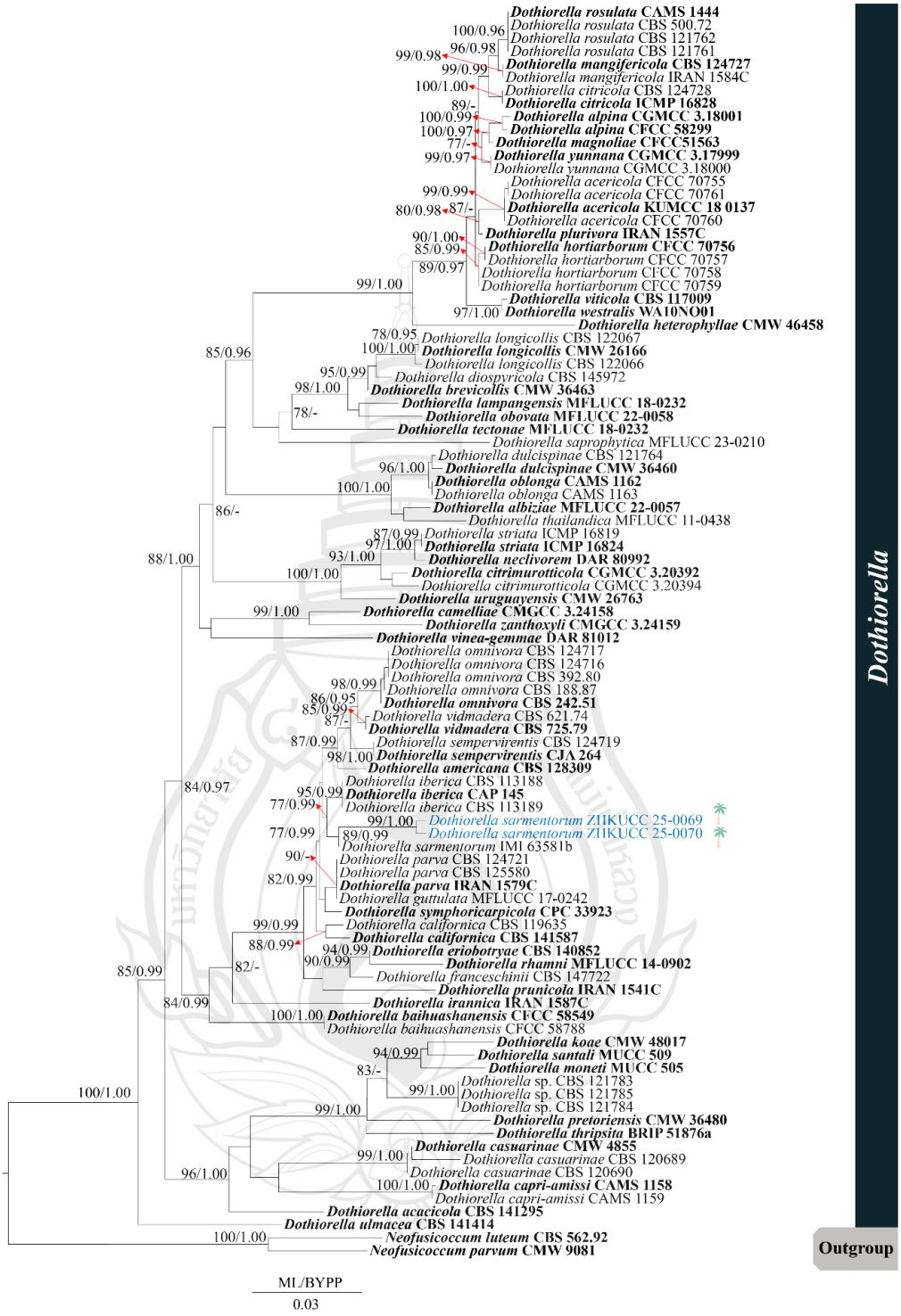
Figure 2.2 *Proliferirostrum licualicola* (MFLU 25-0156, holotype)

Botryosphaeriales C.L. Schoch, Crous & Shoemaker, Mycologia 98 (6): 1050 (2006)

Botryosphaeriaceae Theiss. & P. Syd., Annales Mycologici 16 (1-2): 16 (1918)

Dothiorella Sacc., Michelia 2(6): 5 (1880)

Notes: Saccardo (1880) initially introduced *Dothiorella* (*D.*) with *D. pyrenophora* as the type species. However, Crous and Palm (1999) reduced it to synonymy under *Diplodia*. Phillips et al. (2005) reinstated *Dothiorella* as a separate genus based on morpho-molecular data of ITS and *tef* 1-α and conidia are brown and 1-septate before they are discharged from the pycnidia. Based on phylogenetic results, Yang et al. (2017) proposed *Spencermartinsia,* which was introduced to accommodate *Dothiorella*-like species by Phillips et al. (2008) was not reliable in distinguishing from *Dothiorella* according to the morphological character of apiculate ascospores. Supported by further studies of morphology and phylogeny, *Spencermartinsia* had to be synonymized with *Dothiorella* (Hyde et al., 2019; Phookamsak et al., 2019). *Dothiorella* species are characterised by pigmented, 1-septate ascospores and conidia that become brown and 1-septate while they are attached to the conidiogenous cells (Phillips et al., 2005; Dissanayake et al., 2016). Phillips et al. (2005) used phylogenetic analysis combined ITS and *tef* 1-α to resurrect *Dothiorella*. Subsequently, phylogenetic studies mainly use ITS, *tef* 1-α and *tub*2 for analysis (Zhang et al., 2021; Li et al., 2023; Lin et al., 2023; Wu et al., 2024). In this study, we use ITS, *tub*2 and *tef* 1-α to update phylogenetic studies for *Dothiorella*. Currently, 334 epithets are listed under *Dothiorella* and only 39 species are available for molecular data in *Dothiorella* (Zhang et al., 2021; Li et al., 2023; Hyde et al., 2024; Index Fungorum, 2024). Although four species have been reported on palms (Xiong et al., 2024; Xiong et al., 2025), molecular data for three of these species remain unavailable.



Notes Phylogram generated from maximum likelihood analysis of *Dothiorella* based on combined ITS, *tub*2 and *tef* 1-α sequence data. Bootstrap values for maximum likelihood (ML) equal to or greater than 70 are indicated above the branches. The new collections are indicated in blue and ex-type strains are indicated in bold.

Figure 2.3 Phylogenetic tree of *Dothiorella*

Dothiorella sarmentorum (Fr.) A.J.L. Phillips, J. Luque & A. Alves, Mycologia 97: 52. (2005)

Figure 2.4

Sphaeria sarmentorum Fr., K. svenska Vetensk-Acad. Handl. 39: 107. (1818). Basionym.

≡ *Diplodia sarmentorum* (Fr.) Fr., Summ. veg. Scand. (Stockholm) 2: 417. (1849).

= *Diplodia pruni* Fuckel, Jahrb. Nassauischen Vereins Naturk., 23–24: 169. (1870) [1869].

= *Botryosphaeria sarmentorum* A.J.L. Phillips, J. Luque & A. Alves, Mycologia 97: 522. 2005.

Saprobic on dead segment of *Livistona chinensis*. Asexual morph: *Conidiomata* 240–260 × 270–310 μm, stromatic, erumpent, forming split-like opening on the host, solitary or scattered in small groups, immersed, uni-loculate, individual or aggregated, black, with globose to subglobose, ostiole. *Peridium* 25–40 μm, comprising several layers; outer layers thick-walled, dark brown cells of textura angularis; inner layers of thin-walled, lightly pigmented cells. *Conidiophores* reduced to conidiogenous cells. *Conidiogenous cells* 12–16 × 3.5–6 μm ($\bar{x}$ = 15 × 4.7 μm, n = 30), lining the pycnidial cavity, holoblastic, discrete, hyaline, subcylindrical, smooth, indeterminate, proliferating at the same level giving rise to periclinal thickenings. *Conidia* 18–23 × 9–13 μm ($\bar{x}$ = 20 × 11 μm, n = 30), ellipsoid to obovoid, with a broadly rounded apex and truncate base, initially hyaline and aseptate becoming pigmented brown and 1-septate often while still attached to conidiogenous cell, brown walled, smooth-walled, slightly constricted at the septum. Sexual morph: Not observed.

Culture characteristics: Colonies on PDA fast growing, after 2 weeks reaching 6 cm diam., at 25°C, raised with concave edge, circular, flat, filiform, grey, mycelium groups.

Known distribution: worldwide (Zhang et al., 2021; Jayawardena et al., 2023, this study).

Material examined: China, Jiangxi Province, Nanchang City, road next to Meiling National Forest Park, on dead petiole of *Livistona chinensis*, 10 Apr 2024, Y.R. Xiong, XG423 (MHZU 24-0512, new host record), living culture ZHKUCC 25-0069,

other living culture ZHKUCC 25-0070.

GenBank numbers: ZHKUCC 25-0069: ITS – PV578172, *tub* 2 – PV584059; ZHKUCC 25-0070: ITS – PV578173, *tef* 1-α – PV584060.

Notes: Two collections obtained in this study clustered with *D. sarmentorum* (= *D. sempervirentis*) by 97% ML and 0.99 BYPP bootstrap support (Figure 2.3). Morphological evidence of conidiogenous cells and brown and 1-septate conidia are well fit with *D. sarmentorum* (Phillips et al., 2016; Zhang et al., 2021, Figure 2.4). Therefore, based on morphology and phylogenetic analysis, we identified our collections as a new record of *D. sarmentorum*. *Dothiorella sarmentorum* was formally recognized as a holomorphic species by Phillips et al. (2005). Zhang et al. (2021) placed nine species (*D. californica*, *D. iberica*, *D. italica*, *D. guttulata*, *D. omnivora*, *D. parva*, *D. sempervirentis*, *D. symphoricarpicola*, and *D. vidmadera*) in synonymy with *D. sarmentorum* based on morphological evidence and phylogenetic analysis. This species has a wide range of host and geographic distribution worldwide (Zhang et al., 2021; Jayawardena et al., 2023, this study).

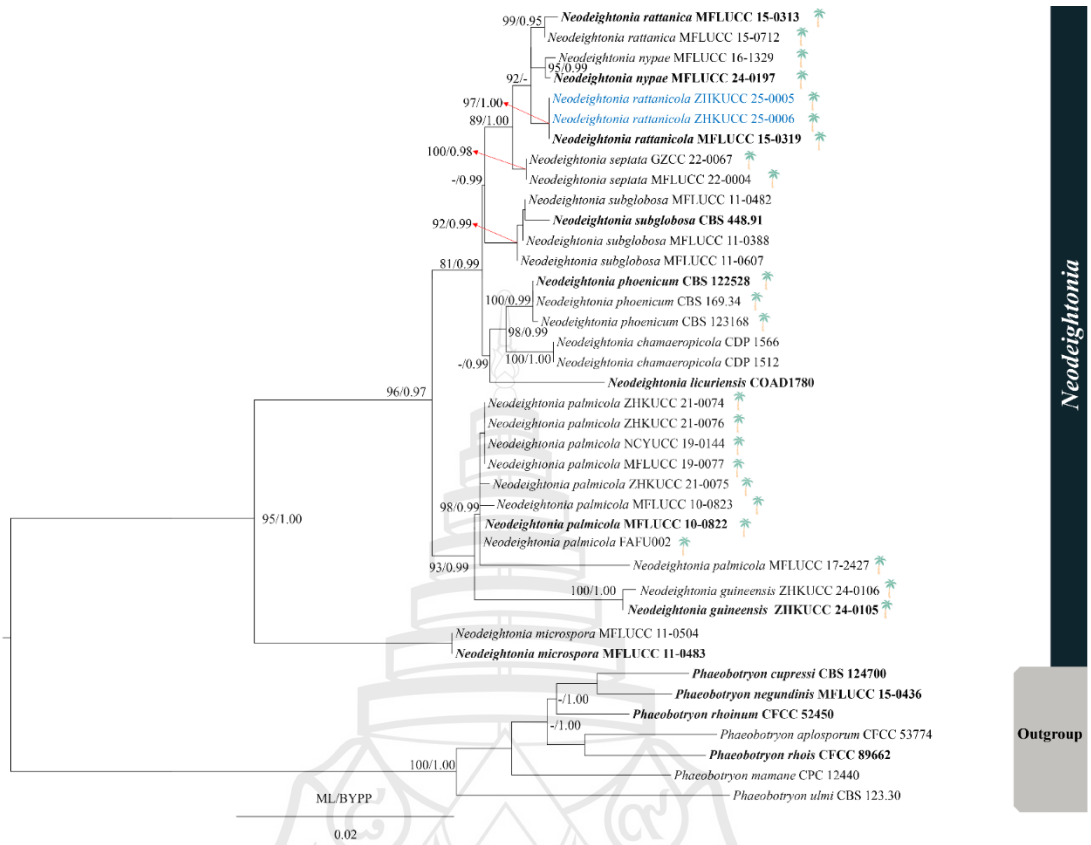


Note a, b Condiomata. c Section of conidioma. d Peridium. e, f Conidiogenous cells. g–j Conidia. k The front of culture on PDA at 25°C and the reverse of culture on PDA at 25°C. Scale bars: c = 20 µm; d–j = 10 µm.

Figure 2.4 *Dothiorella sarmentorum* (MHZU 24-0512, new host record)

Neodeightonia C. Booth, Mycol. Pap. 119: 17 (1970) [1969]

Notes: Punithalingam (1969) introduced *Neodeightonia* (*N.*) with *N. subglobosa* as the type species. Later on, *Neodeightonia* was synonymized with *Botryosphaeria* following the transfer of *N. subglobosa* to *Botryosphaeria* (Arx & Müller, 1975). However, Phillips et al. (2008) recognized *Neodeightonia* as a separate genus by distinguishing it from *Botryosphaeria* based on morpho-molecular data. The sexual morph characters of *Neodeightonia* by hyaline, aseptate ascospores with bipolar germ pores, surrounded by a membrane that swells in water acquiring a wing-like appearance, asexually they develop hyaline, aseptate conidia that may become pigmented, 1-septate and smooth to finely roughened or striate (Liu et al., 2012; Phillips et al., 2013, 2019). Phillips et al. (2008) first used phylogenetic analysis combined SSU, LSU, ITS, β-tubulin and *tef* 1-α to identify *Neodeightonia*. Subsequently, phylogenetic studies mainly use SSU, LSU, ITS and *tef* 1-α for analysis (Konta et al., 2016; Wu et al., 2022; Xiong et al., 2022). In this study, we use ITS, LSU, SSU and *tef* 1-α to update phylogenetic studies for *Neodeightonia*. Based on Pereira and Phillips (2023) and Zhang et al. (2024), 11 species were listed in *Neodeightonia*, and all species are associated with molecular data. Eight species have been reported from palm species (Xiong et al., 2025), including a new host from *Rhapis excelsa* from China in this study.



Note Phylogram generated from maximum likelihood analysis of *Neodeightonia* based on combined ITS, LSU, SSU and *tef* 1-α sequence data. Bootstrap values for maximum likelihood (ML) equal to or greater than 70 are indicated above the branches. The new collections are indicated in blue and ex-type strains are indicated in bold.

Figure 2.5 Phylogenetic tree of *Neodeightonia*

Neodeightonia guineensis Y.R. Xiong, Manawas. & K.D. Hyde, ***sp. nov.*** Figure 2.6

Etymology: Epithet refers to the host species from which the fungus was isolated.

Saprobic on petiole of *Elaeis guineensis* (Arecaceae). Sexual morph: *Ascomata* 150–180 × 210–290 µm ($\bar{x}$ = 160 × 240 µm; n = 10), semi-immersed, solitary, gregarious, unilocular, raising host surface and producing papillate black dots of dehiscence. *Peridium* 15–55 µm wide ($\bar{x}$ = 30 µm; n = 20), thick-walled, brown-black cells of *textura angularis*, smooth, asci developing amongst partially disintegrating sterile thin-walled

tissue in locule. *Hamathecium* 3–6.5 µm wide ($\bar{x}$ = 4.5 µm, n = 30), pseudoparaphyses, gelatinized, pluricellular, hyaline, constricted at the septa. *Asci* 80–165 × 20–35 µm ($\bar{x}$ = 110 × 30 µm; n = 20), bitunicate with a thick endotunica, fissitunicate, separated from one another by stromatic tissue, clavate, 8-spored, with a minute club pedicel. *Ascospores* 28–32 × 13–15 µm ($\bar{x}$ = 30 × 14 µm; n = 30), biseriate, hyaline to pale brown, ellipsoidal, muriform when mature, aseptate, rough, surrounded by a tightly fitting mucilaginous sheath. Asexual morph: not observed.

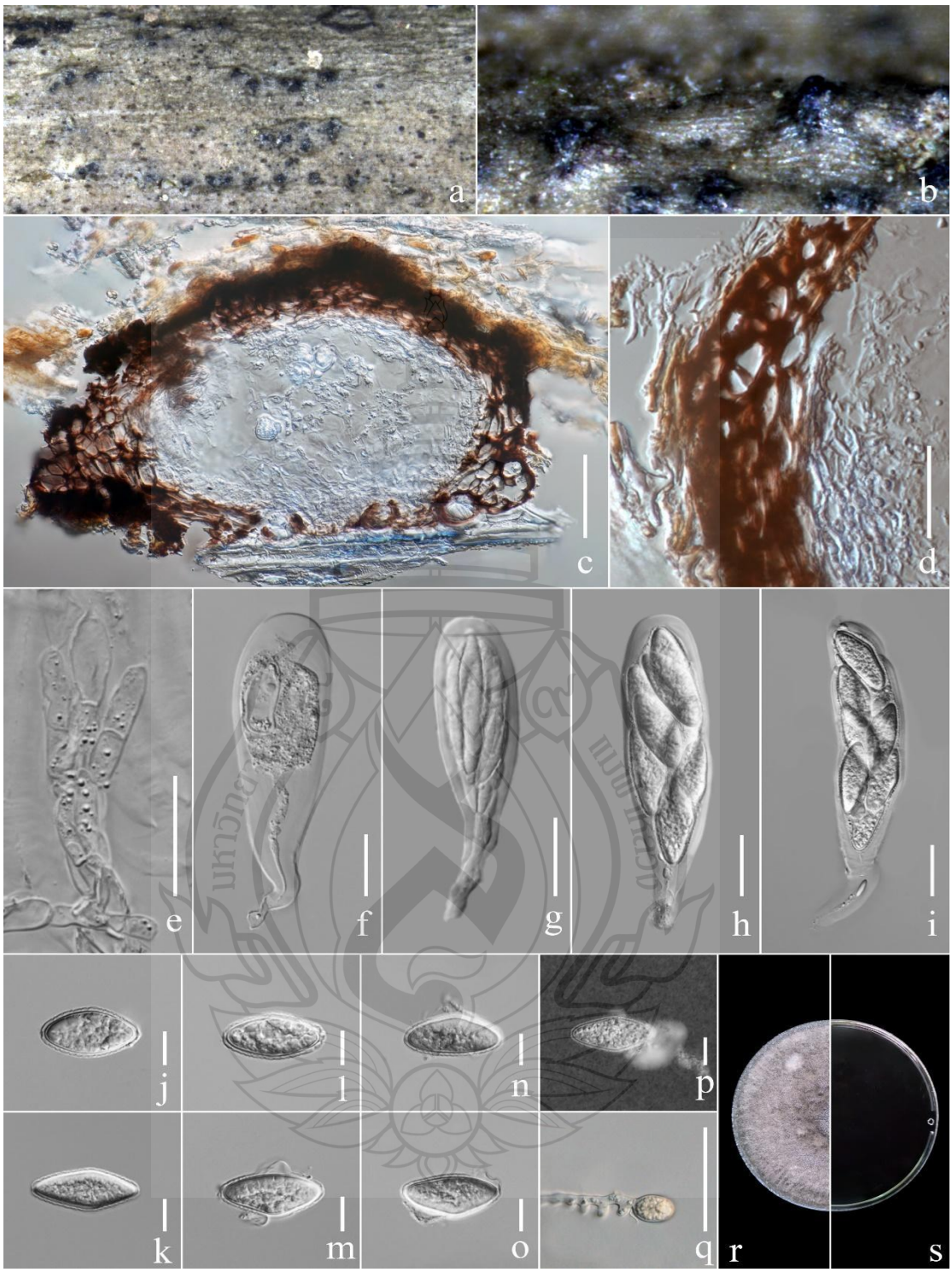
Culture characteristics: Colonies on PDA reaching 7 cm diam., at 28°C after five days. Upper view wrinkled, filamentous, entire margin, flat, cloudy, fluffy for aerial hyphae, becoming grey-black with age, dense aerial hyphae, reverse becoming black.

Known distribution: China (this study).

Material examined: China, Yunnan Province: Xishuangbanna City, in an unidentified forest beside National Highway 219 (21°93'N, 101°24E, 549.6 m), on rotting petiole of *Elaeis guineensis*, 5 February 2023, Y.R. Xiong and Li Lu, XG180 (MHZU 24-0149, holotype); ex-type, ZHKUCC 24-0105, other living culture ZHKUCC 24-0106.

GenBank numbers: ZHKUCC 24-0105: ITS – PQ594884, *tef* 1-α – PQ613915; ZHKUCC 24-0106: ITS – PQ594885, *tef* 1-α – PQ613916.

Notes: Two collections from this study formed a well-separated lineage with 93% ML, 99% MP and 0.99 BIPP support within *Neodeightonia* species, clustering with *N. palmicola*. The nucleotide differences excluding gaps of ITS between *N. guineensis* (ZHKUCC 24-0105) and *N. palmicola* (MFLUCC 10-0822) is 3.65% (19/521 base pairs). *Neodeightonia guineensis* is a sexual morph and differs from *N. palmicola*, which has slightly larger asci – (154.2 × 20.5 µm) and smaller ascospores (27 × 10 µm) (Liu et al., 2010). In addition, *N. palmicola* has ascospores with bipolar germ pores (Liu et al., 2010), whereas they are absent in *N. guineensis*. Moreover, *N. palmicola* has ascospores surrounded by a thick complex sheath (Liu et al., 2010), while *N. guineensis* is surrounded by a thin, tightly fitting mucilaginous sheath. Based on the phylogenetic placement and morphological variations, we introduce *N. guineensis* as a novel *Neodeightonia* species.



Note a–b. Conidiomata on decaying *Elaeis guineensis*. c. Section of ascoma. d. Peridium. e. Hamathecium. f–i. Asci. j–p. Ascospores (p stained in India ink). q. Germinating conidium. r, s. The front of culture on PDA at 25°C and the reverse of culture on PDA at 25°C. Scale bars: c = 40 µm, d–i = 20 µm, j–p = 10 µm, q = 50 µm.

Figure 2.6 *Neodeightonia guineensis* (MHZU 24-0149, holotype)

Neodeightonia rattanicola Konta & K.D. Hyde, Mycosphere 7(7): 950–961 (2016)

Figure 2.7

Saprobic on dead segment of *Rhapis excelsa*. Asexual morph: Coelomycetous. *Conidiomata* stromatic 200–240 × 220–250 μm ($\overline{x}$ = 220 × 240 μm, n = 10), pycnidial, semi-immersed, solitary, globose, unilocular, black dots, with a neck, papillate on the surface of the host where the conidiomata is located. *Peridium* 30–40 μm, composed of thick-walled, brown-black cells, *textura angularis*, thin inner wall with hyaline cells. *Conidiogenous cell* 15–25 × 5–10 μm ($\overline{x}$ = 19 × 7.5 μm, n = 25), holoblastic, cylindrical to subcylindrical, hyaline. *Conidia* 20–25 × 10–12 μm ($\overline{x}$ = 22 × 11 μm, n = 25), hyaline, unicellular, ellipsoid to obovoid, thick-walled, granulate, rounded at apex. Sexual morph: not observed.

Culture characteristics: Colonies on PDA, after 2 weeks reaching 4–5 cm diam., at 25°C, white at the edge, grey in the middle and outwardly strongly radiating. After 1 month of incubation, the colonies on PDA, grey-olivaceous and spongy, hyphae, septate, branched and smooth.

Known distribution: China (Xiong et al., 2025, this study), Thailand (Konta et al., 2016).

Material examined: China, Yunnan Province, Xishuangbanna City, in an unidentified forest beside National Highway 219, on a dead petiole of *Rhapis excelsa*, 5 Feb 2023, Y.R. Xiong and L. Lu, XG224 (MHZU 24-0504, new host record), living culture ZHKUCC 25-0005, other living culture ZHKUCC 25-0006.

GenBank numbers: ZHKUCC 25-0005: ITS – PV578204; ZHKUCC 25-0006: ITS – PV578205.

Notes: Two collections obtained in this study clustered with *Neodeightonia rattanicola* by 97% ML and 1.00 BYPP bootstrap support. The nucleotide differences excluding gaps between our collections and *N. rattanicola* (MFLUCC 15-0319) in ITS is 0.19% (1/513 base pairs). Morphological evidence of conidiogenous cells and hyaline conidia are well fit with *N. rattanicola* (Konta et al., 2016; Xiong et al., 2025) although brown mature conidia were not observed in our collections. Based on morphology and phylogenetic analysis, we identified our collections as a new record of *N. rattanicola*. *Neodeightonia rattanicola* was first introduced on decaying rachis of *Calamus* sp. from

Thailand by Konta et al. (2016), Xiong et al. (2024) reported a new record on dead petiole of *Wodyetia bifurcate* from China. In this study, we introduced a new record for *N. rattanicola* from *Rhapis excelsa*.



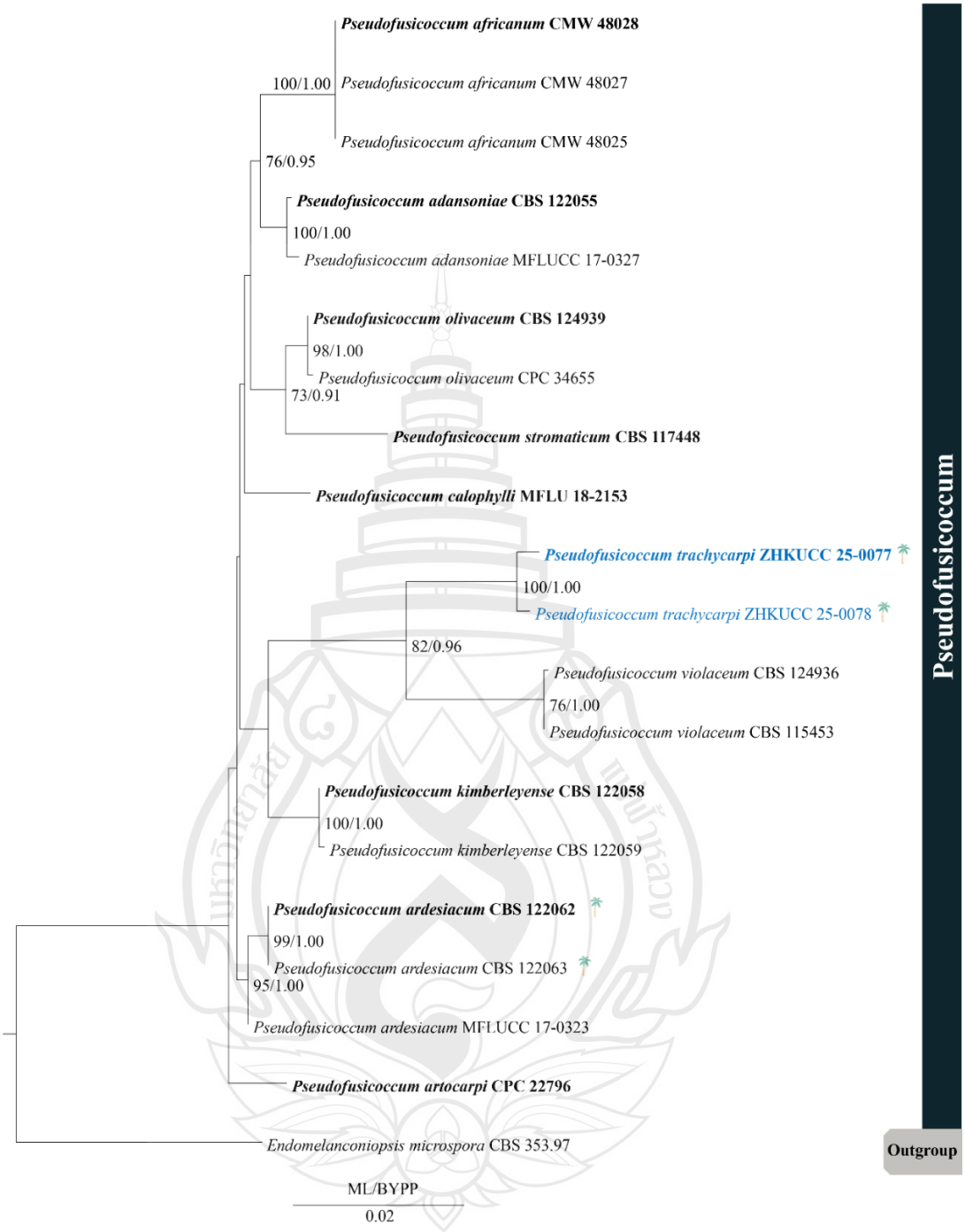
Note a, b Conidiomata. c Section of conidioma. d Peridium. e, f Conidiogenous cells. g–k Conidia. l Germinating conidium. m The front of culture on PDA at 25°C and the reverse of culture on PDA at 25°C. Scale bars: c = 40 µm; d–f = 20 µm; g–k = 10 µm; l = 50 µm.

Figure 2.7 *Neodeightonia rattanicola* (MHZU 24-0504, new host record)

Phyllostictaceae Fr. (as "Phyllostictei"), Summa vegetabilium Scandinaviae 2: 420 (1849)

Pseudofusicoccum Mohali, Slippers & M.J. Wingf., Stud. Mycol. 55: 249 (2006)

Notes: Crous et al. (2006) established *Pseudofusicoccum* (*Ps.*) with *Ps. stromaticum* as type species after combining *Fusicoccum stromaticum* as *Ps. stromaticum* based on morphological evidence and phylogenetic analysis with LSU. *Pseudofusicoccum* was placed in Botryosphaeriaceae and distinct from *Fusicoccum* by conidia with a mucilaginous sheath and phylogeny result (Crous et al., 2006). Although Yang et al. (2017) elevated *Pseudofusicoccum* to the familial rank as Pseudofusicoccaceae, the genus remains accepted within Phyllostictaceae, as phylogenetic analyses show its clustering between *Phyllosticta* and *Neofusicoccum* in Botryosphaeriaceae phylogenies (Minnis et al., 2012; Slippers et al., 2013; Liu et al., 2017; Phillips et al., 2019). The asexual morph is characterized by corticolous, coriaceous, uni- to multilocular, immersed to erumpent pycnidial conidiomata, and hyaline, aseptate, cylindrical to ellipsoid conidia covered by mucilaginous sheath (Crous et al., 2006; Senwanna et al., 2020). The sexual morph is characterized by scattered to clustered, uniloculate ascomata, bitunicate, cylindro-clavate asci with ocular chambers, and hyaline, uni to bi-seriate, aseptate, short clavate, smooth-walled ascospores with fine granules and surrounded by a mucilaginous sheath (Senwanna et al., 2020). Subsequently, phylogenetic studies use ITS and *tef* 1-α (Mehl et al., 2011; Trakunyingcharoen et al., 2015; Jami et al., 2018; Tibpromma et al., 2018; Jayasiri et al., 2019) first, then add LSU or *tub*2 to analysis (Senwanna et al., 2020; Li et al., 2023; Hyde et al., 2024). In this study, we use ITS, LSU, SSU, *tub*2 and *tef* 1-α to update phylogenetic studies for *Pseudofusicoccum*. Currently, nine epithets are listed under *Pseudofusicoccum* (Index Fungorum, 2024) with all species associated with molecular data. Among these two species have been reported from palm species including a new species described in this study (Xiong et al., 2025).



Note Phylogram generated from maximum likelihood analysis of *Pseudofusicoccum* based on combined ITS, LSU, SSU, *tub*2 and *tef* 1-α sequence data. Bootstrap values for maximum likelihood (ML) equal to or greater than 70 are indicated above the branches. The new collections are indicated in blue and ex-type strains are indicated in bold.

Figure 2.8 Phylogenetic tree of *Pseudofusicoccum*

Pseudofusicoccum trachycarpi Y.R. Xiong, Manawas. & K.D. Hyde, ***sp. nov.***

Figure 2.9

Etymology: The epithet refers to the host genus "*Trachycarpus*", from which the species was collected.

Saprobic on dead segment of *Trachycarpus fortunei*. Asexual morph: Coelomycetous. *Colonies* 230–290 × 120–150 μm ($\overline{x}$ = 265 × 133 μm, n = 10) on natural substrate superficial, raising host surface and producing a dark brown area of dehiscence of pseudo clypeus, superfcial to erumpent, solitary, gregarious, uni- to multi-loculate, immature functions as the locule for the mature conidiomata, black, short papillate, ostiolate. *Ostiole* central, papillate, periphysate. *Peridium* 20–50 μm wide, comprising several layers of heavily pigmented to hyaline, thick-walled, cells of *textura epidermoidea*, the exterior cells separate from the adjacent locules with cells become darker when locules mature. *Conidiophores* unbranched, reduced to conidiogenous cells. *Conidiogenous cells* 8–15 × 4–6 μm ($\overline{x}$ = 11 × 4.6 μm, n = 25) blastic-sympodial, phialidic, formed from the innermost layer of pycnidial wall, hyaline, smooth-walled. *Conidia* 4–6 × 1.5–2.5 μm ($\overline{x}$ = 4.8 × 2 μm, n = 25), hyaline, ellipsoid, occasionally slightly bent, apices rounded, smooth with fine granular content, unicellular, thin-walled. Sexual morph: Not observed.

Culture characteristics: Colonies on PDA, after 2 weeks reaching 4 cm diam., at 25°C, cream to grey cottony mycelium, regular margin, thin mycelium. Initially reverse white and with age it becomes grey.

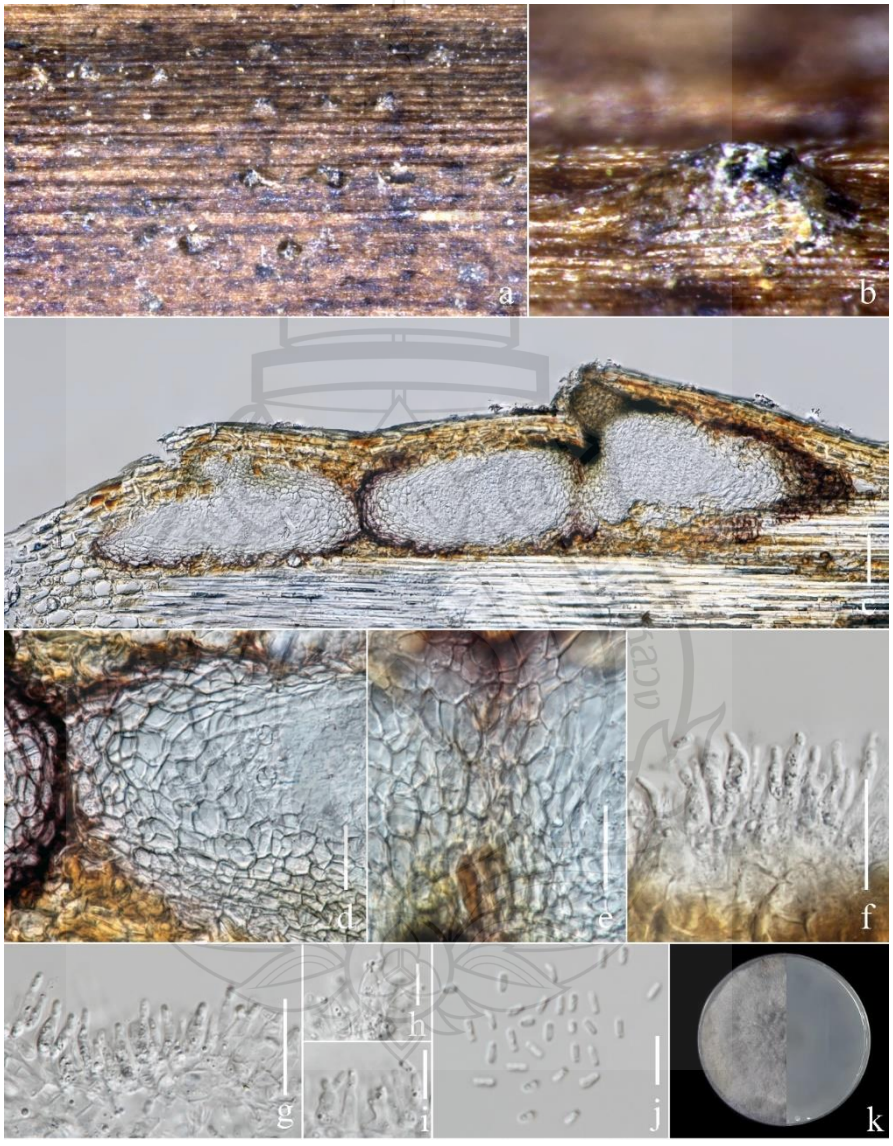
Known distribution: China (this study).

Material examined: China, Jiangxi Province, Nanchang City, road next to Meiling National Forest Park, on dead segment of *Trachycarpus fortunei*, 11 Apr 2024, Y.R. Xiong, XG430 (MHZU 24-0514, holotype); living culture ZHKUCC 25-0077, other living culture ZHKUCC 25-0078.

GenBank numbers: ZHKUCC 25-0077: ITS – PV578240, LSU – PV578408, SSU – PV578542, *tef* 1-α – PV608888, *tub* 2 – PV584067; ZHKUCC 25-0078: ITS – PV578241, LSU – PV578409, SSU – PV578543, *tef* 1-α – PV608889, *tub* 2 – PV584068.

Notes: Two collections from this study formed a separate lineage and clustered with *Pseudofusicoccum violaceum* in the phylogenetic tree with 82% ML and 1.00 BYPP bootstrap support. The nucleotide differences excluding gaps, between *Ps. trachycarpi* and *Ps*. *violaceum* were checked and given as follows, ITS: 0.72% (4/557

base pairs), *tef* 1-α: 4.61% (15/326 base pairs) and *tub*2: 0.66% (3/452 base pairs). *Pseudofusicoccum trachycarpi* differs from *Ps*. *violaceum* by blastic-sympodial conidiogenous cells and smaller conidia (*Ps*. *trachycarpi*: $\bar{x}$ = 4.8 × 2 µm vs *Ps*. *violaceum*: $\bar{x}$ = 6.6 × 3.7 µm). However, *Ps*. *violaceum* is holoblastic conidiogenous cells and bigger conidia ($\bar{x}$ = 33 × 9.5 µm) (Mehl et al., 2011). Based on the phylogenetic placement and morphological variations, we introduce *Ps*. *trachycarpi* as a new species.



Note a, b Conidiomata on the substrate. c Sections through conidiomata. d, e Peridium. f–i Conidiogenous cells and developing conidia. j Conidia. k The front of culture on PDA at 25°C and the reverse of culture on PDA at 25°C. Scale bars: c = 50 µm, d–g = 20 µm, h–j = 10 µm.

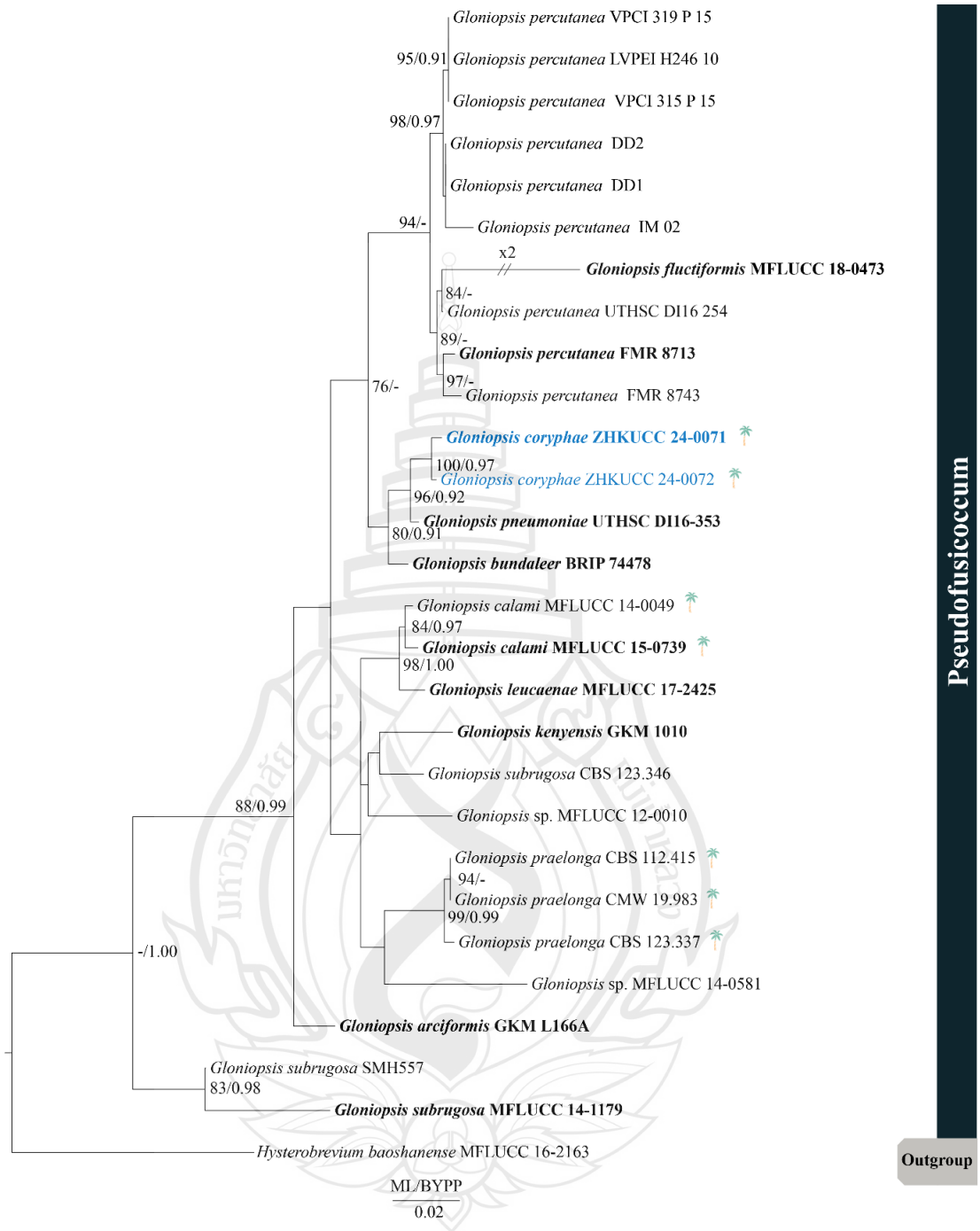
Figure 2.9 *Pseudofusicoccum trachycarpi* (MHZU 24-0514, holotype)

Hysteriales Lindau, Die Natürlichen Pflanzenfamilien nebst ihren Gattungen und wichtigeren Arten 1 (1): 265 (1897)

Hysteriaceae Chevall. [as 'Hysterineae'], Fl. gén. env. Paris (Paris) 1: 432 (1826)

Gloniopsis De Not., G. bot. ital. 2(7–8): 12, 23 (1847)

Notes: De Notaris (1847) established *Gloniopsis* (*Gl.*), without a designated type for the genus. Clements and Shear (1931) chose *Gl. decipiens* as the lectotype, following Höhnel (1918). Late on Zogg (1962) regarded *Gl. decipiens* as a doubtful taxon and suggested *Gl. praelonga* as the type species. However, *Gloniopsis decipiens* remains widely recognized as the type species (Boehm et al., 2009; Hyde et al., 2024; Index Fungorum, 2025 January). *Gloniopsis* is characterised by hysterothecioid, globose to subglobose ascomata, cellular, hyaline, septate pseudoparaphyses, and ellipsoid, hyaline to yellowish ascospores with transverse septa and longitudinal septa surrounded by a gelatinous sheath or not (Boehm et al., 2009; Jayasiri et al., 2018). Boehm et al. (2009) based on morphological evidence and phylogenetic analysis combined SSU, LSU, *tef* 1-α and *rpb*2 to place *Gloniopsis* in Hysteriaceae. Subsequently, phylogenetic studies mainly use SSU, LSU, *tef* 1-α and *rpb*2 or without SSU and *rpb*2 for analysis (Jayasiri et al., 2018, 2019; Valenzuela-Lopez et al., 2019). In this study, we use ITS, LSU and *tef* 1-α to update phylogenetic studies for *Gloniopsis*. Currently, 32 epithets are listed under *Gloniopsis* (Index Fungorum, 2025 January), and only 11 species are associated with molecular data. Totally three species have been reported from palm species including a new species described in this study (Xiong et al., 2025).



Note Phylogram generated from maximum likelihood analysis of *Gloniopsis* based on combined ITS, LSU and *tef* 1-α sequence data. Bootstrap values for maximum likelihood (ML) equal to or greater than 70 are indicated above the branches. The new collections are indicated in blue and ex-type strains are indicated in bold.

Figure 2.10 Phylogenetic tree of *Gloniopsis*

Gloniopsis coryphae Y.R. Xiong, Manawas. & K.D. Hyde, ***sp. nov.***

Figure 2.11

Etymology: The epithet refers to the host genus name "*Corypha*", from which the species was collected.

Saprobic on dead leaf sheath of *Corypha umbraculifera*. Asexual morph: Not observed. Sexual morph: *Ascomata* 150–230 × 160–220 µm ($\bar{x}$ = 192.5 × 184 µm, n = 10), hysterothecia erumpent, erumpent to superficial, oval or ellipsoid to elongate, labiate, carbonaceous, scattered, dark, with a sunken longitudinal slit-like opening. *Peridium* 20–60 µm composed of brown and thick textura globulosa cells. *Hamathecium* pseudoparaphyses, hyaline, septate, branched, borne in a gelatinous matrix. *Asci* 60–70 × 15–20 µm ($\bar{x}$ = 65 × 17 µm, n = 25), bitunicate, cylindrical to clavate, 8-spored, fissitunicate, apically rounded, short pedicellate, sinuous stipe. *Ascospore* 16–20 × 8–9 µm ($\bar{x}$ = 17.9 × 8.3 µm, n = 25), overlapping, bi-seriate, dictyosporous, asymmetric, 3–5 transverse and 1–2 vertical septa, fusiform, oblong or ellipsoidal, curved, constricted at the septa, smooth-walled, brown.

Culture characteristics: Colonies on PDA, after 2 weeks reaching 4 cm diam., at 25°C, circular, with fluffy, dense, spongy, cream mycelium on the surface with entire margin; in reverse dark-brown in the middle and brown at the margin.

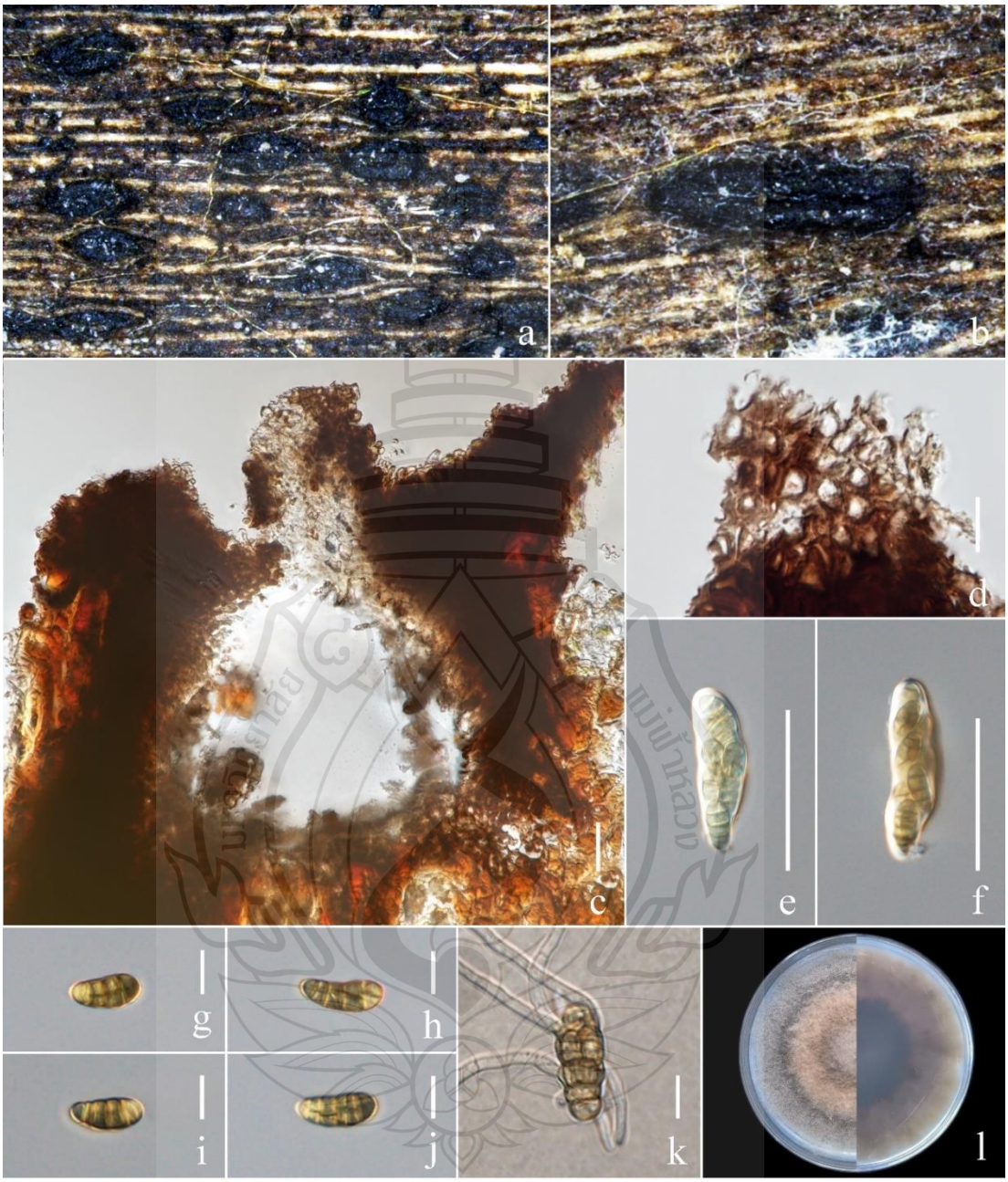
Known distribution: China (this study).

Material examined: China, Yunnan Province, Xishuangbanna City, in an unidentified forest beside National Highway 219, on dead leaf sheath of *Corypha umbraculifera*, 5 Feb 2023, Y.R. Xiong and L. Lu, XG148 (MHZU 23-0132, holotype), ex-type ZHKUCC 24-0071, other living culture ZHKUCC 24-0072.

GenBank numbers: ZHKUCC 24-0071: ITS – PV578188, LSU – PV578352; ZHKUCC 24-0072: ITS – PV578189, LSU – PV578353.

Notes: Two collections from this study formed a separate lineage and clustered with *Gloniopsis pneumoniae* in the phylogenetic tree with 96% ML bootstrap support and 1.00 BYPP. The nucleotide differences excluding gaps between *Gl. coryphae* (ZHKUCC 24-0071) and *Gl. pneumoniae* (UTHSC DI16.353) were checked and given as follows, ITS: 2.02% (13/643 base pairs). *Gloniopsis coryphae* differs from other species in *Gloniopsis* by 3–5 transverse and 1–2 vertical septa of ascospores with curved. However, *Gl. pneumoniae* only reported asexual morph with aseptate, hyaline and moderately thick-

walled conidia (Valenzuela-Lopez et al., 2019). Based on phylogenetic placement and sexual morphological variations, we introduce *Gl. coryphae* as a new species.



Note a, b Ascomata on substrate. c Vertical sections of ascomata. d Cells of peridium. e, f Asci. g–j Ascospore. k Germinating ascospore. l The front of culture on PDA at 25°C and the reverse of culture on PDA at 25°C. Scale bars: c = 20 µm, d, g–k = 10 µm, e, f = 50 µm.

Figure 2.11 *Gloniopsis coryphae* (MHZU 23-0132, holotype)

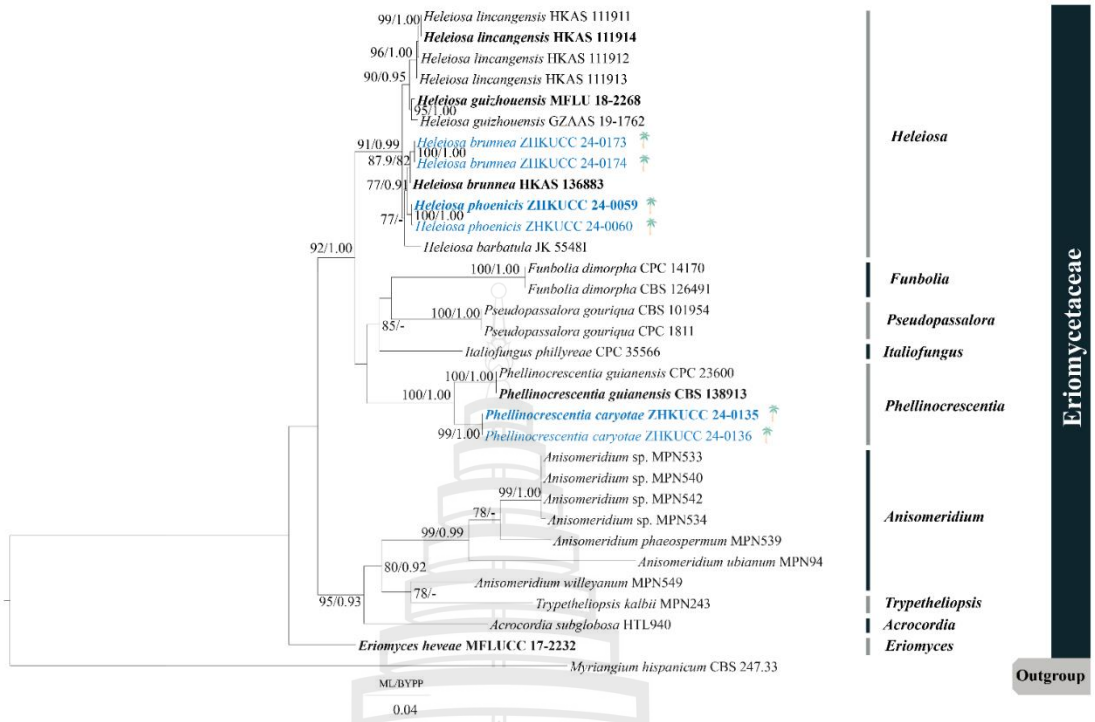
Monoblastiales Lücking, M.P. Nelsen & K.D. Hyde, Fungal Diversity 63: 313 (2013)

Eriomycetaceae Huanraluek & Hyde, Fungal Diversity 100: 146 (2020)

Heleiosa Kohlm., Volkm.-Kohlm. & O.E. Erikss., Can. J. Bot. 74(11): 1830 (1996)

= *Neoheleiosa* Mortimer, Frontiers in Microbiology: 6 (2021)

Notes: Kohlmeyer et al. (1996) introduced *Heleiosa* (*H.*) with *H. barbatula* as the type species. Based on both ascospore morphological and phylogenetic evidence which combined LSU, ITS and SSU sequence data, Sun et al. (2025) synonymize *Neoheleiosa* under *Heleiosa* due to the nomenclature priority. *Heleiosa* only reported sexual morph which is characterized by ascomata which are solitary, scattered, immersed to erumpent, globose to subglobose or obpyriform, dark brown to black, and coriaceous. Asci are bitunicate, fissitunicate, cylindric, pedicellate, with a rounded and thick-walled apex containing an ocular chamber; Ascospores overlapping uniseriate, narrowly ovoid to clavate, 1-septate, hyaline when young, becoming dark brown at maturity, conically rounded at both ends, guttulate, thick-walled, faintly longitudinally striated, having or lacking a mucilaginous sheath (Kohlmeyer et al., 1996; Mortimer et al., 2021). Zhang et al. (2023) based on morphology and phylogenetic analysis combined LSU, SSU, ITS and *tef* 1-α placed *Heleiosa* to Eriomycetaceae. In this study, we use ITS, LSU, SSU and *tef* 1-α to update phylogenetic studies for *Heleiosa* (Figure 2.12). Currently, four epithets are listed under *Heleiosa* (Index Fungorum, 2024 November), with all species associated with molecular data. To date, three species have been reported from palm species including one new species and one new host record introduced in this study (Xiong et al., 2025).



Note Phylogram generated from maximum likelihood analysis of Eriomycetaceae based on combined ITS, LSU, SSU and *tef* 1-α sequence data. Bootstrap values for maximum likelihood (ML) equal to or greater than 70 are indicated above the branches. The new collections are indicated in blue and ex-type strains are indicated in bold.

Figure 2.12 Phylogenetic tree of Eriomycetaceae

Heleiosa brunnea Y.R. Sun, Yong Wang bis & K.D. Hyde, Fungal Diversity 131: 127 (2025)

Figure 2.13

Saprobic on dead segment of *Livistona chinensis*. Asexual morph: Not observed. Sexual morph: *Ascomata* 320–370 × 170–200 µm ($\bar{x}$ = 340 × 188 µm, n = 5), immersed to erumpent, globose to subglobose or horizontally pyriform, coriaceous, ostiolate. *Ostiole* central or eccentric, with a minute papilla, periphysate, composed of thick-walled cells of *textura intricata*. *Peridium* 14–22 µm thick, hyaline to brown, contraction area becomes darker, *textura intricata*. *Hamathecium* comprise sparse, 1.5–3 µm wide, septate, branched pseudoparaphyses, intermixed with the asci, and embedded in matrix. *Asci* 90–125 × 9–13 µm ($\bar{x}$ = 107 × 11.4 µm, n = 25), 8-spored, bitunicate,

fissitunicate, cylindrical, pedicel furcate, rounded and thick-walled at the apex, ocular chamber. *Ascospores* 13–20 × 6–12 µm ($\overline{x}$ = 16 × 8.5 µm, n = 25), uniseriate, ellipsoidal to narrowly ovoid or clavate, 1-septate, constricted at the septum, initially hyaline, becoming brown at maturity, guttulate, thick walled, longitudinally striated, smooth-walled.

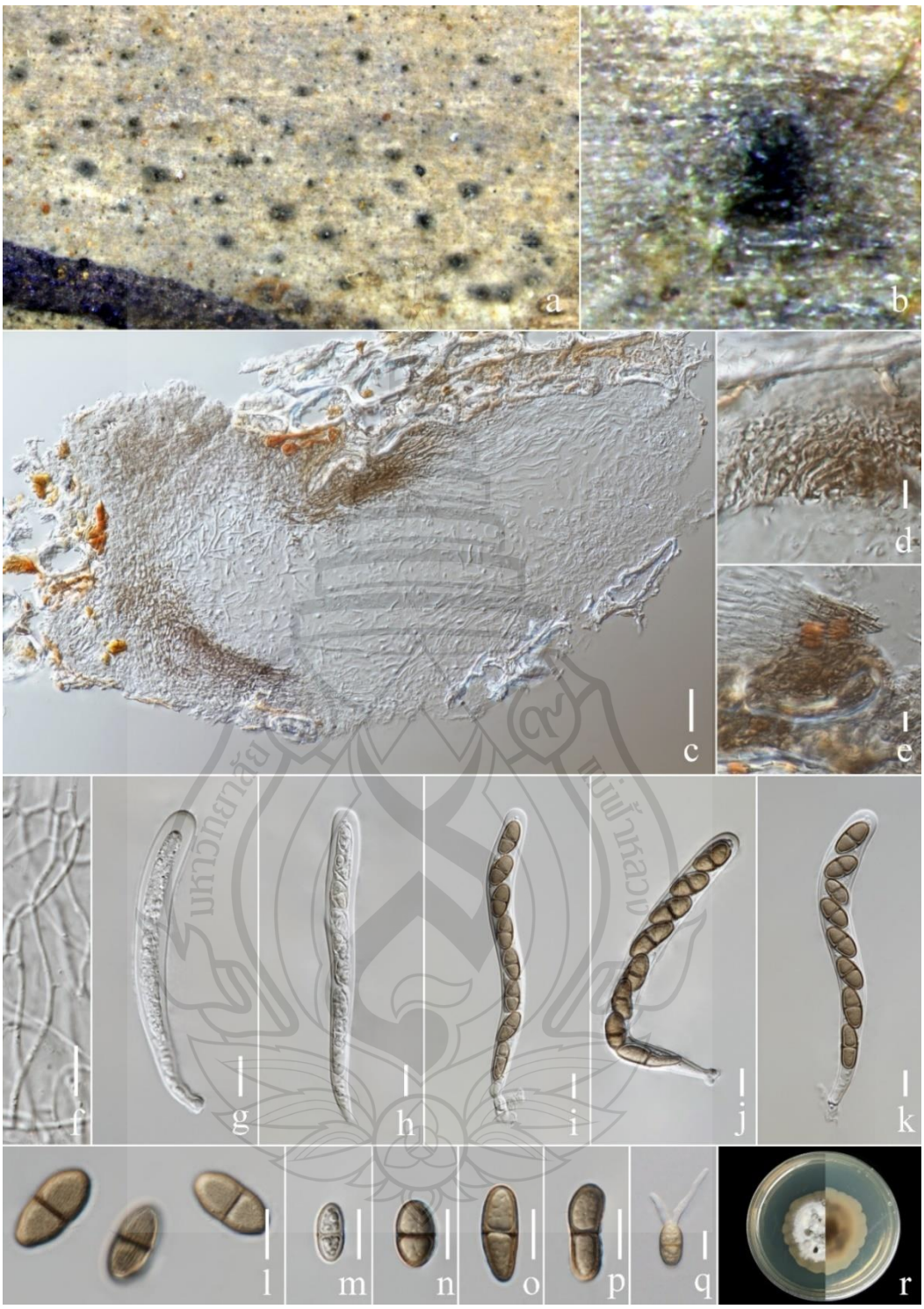
Culture characteristics: Colonies on PDA fast growing, after 2 weeks reaching 35 mm diam., at 25°C, circular, raised, cottony, producing mucus, glistening, white, reverse pastel yellow, with a yellowish-grey margin.

Known distribution: China (Sun et al., 2025, this study).

Material examined: China, Yunnan Province, Sanyuan District, on dead segment of *Livistona chinensis*, 29 Dec 2022, Y.R. Xiong and L. Lu, XG257 (MHZU 23-0183, holotype) – ex-type ZHKUCC 24-0173, other living culture ZHKUCC 24-0174.

GenBank numbers: ZHKUCC 24-0173: ITS – PV578206, LSU – PV578372, SSU – PV578516, *tef* 1-α – PV608864; ZHKUCC 24-0174: ITS – PV578207, LSU – PV578373, SSU – PV578517, *tef* 1-α – PV608865.

Notes: Two collections from this study assembled with *Heleiosa brunnea* in the phylogenetic tree with 100% ML and 1.00 BYPP bootstrap support (Figure 2.12). The nucleotide differences excluding gaps between our collection and *H. brunnea* (HKAS 136883) were as below: LSU: 0.02% (1/640 base pairs), ITS and SSU are the same. Our collections consisted of the morphological characteristics of *H. brunnea* from ascospores shape (Sun et al., 2025). *Heleiosa brunnea* was first introduced on twigs of *Osmanthus fragrans* from China by Sun et al. (2025). Although our collections ascospore have longitudinally striated which is not observed in *H. brunnea* (Sun et al., 2025), based on the phylogenetic analysis, we identified our collections as a new host record of *H. brunnea.*



Note a, b Ascomata on substrate. c Vertical sections of ascomata. d, e Cells of peridium. f Pseudoparaphyses. g–k Asci. l–p Ascospores s (l longitudinally striated). q Germinating conidium. r The front of culture on PDA at 25°C and the reverse of culture on PDA at 25°C. Scale bars: c–e = 20 µm, f–q = 10 µm.

Figure 2.13 *Heleiosa brunnea* (MHZU 23-0183, holotype)

Heleiosa phoenicis Y.R. Xiong, Manawas. & K.D. Hyde, ***sp. nov.***

Figure 2.14

Etymology: The epithet refers to the host genus "*Phoenix*", from which the species was collected.

Saprobic on a dead segment of *Phoenix canariensis*. Asexual morph: Coelomycetous. *Conidiomata* 150–200 × 100–150 μm ($\overline{x}$ = 170 × 125 μm, n = 10), pycnidial, semi-immersed, solitary, globose, unilocular, ostioles, papillate. *Peridium* 20–35 μm, composed of thick-walled, brown-black cells, *textura angularis*, inner wall with hyaline cells. *Conidiophores* reduce to conidiogenous cells. *Conidiogenous cell* 8–14 (–25) × 2.5–4 μm ($\overline{x}$ = 12.4 × 3.4 μm, n = 25), enteroblastic, phialidic to cylindrical, hyaline, smooth-walled, arising from stratum. *Conidia* 35–65 × 4–6.5 μm ($\overline{x}$ = 60 × 5.4 μm, n = 25), clavate to elongate-acicular, slightly curved, truncate to rounded or acute apex, constricted at septa, 7–11 (–12) septate, hyaline, 1–2 guttulate within the cell. Sexual morph: Not observed.

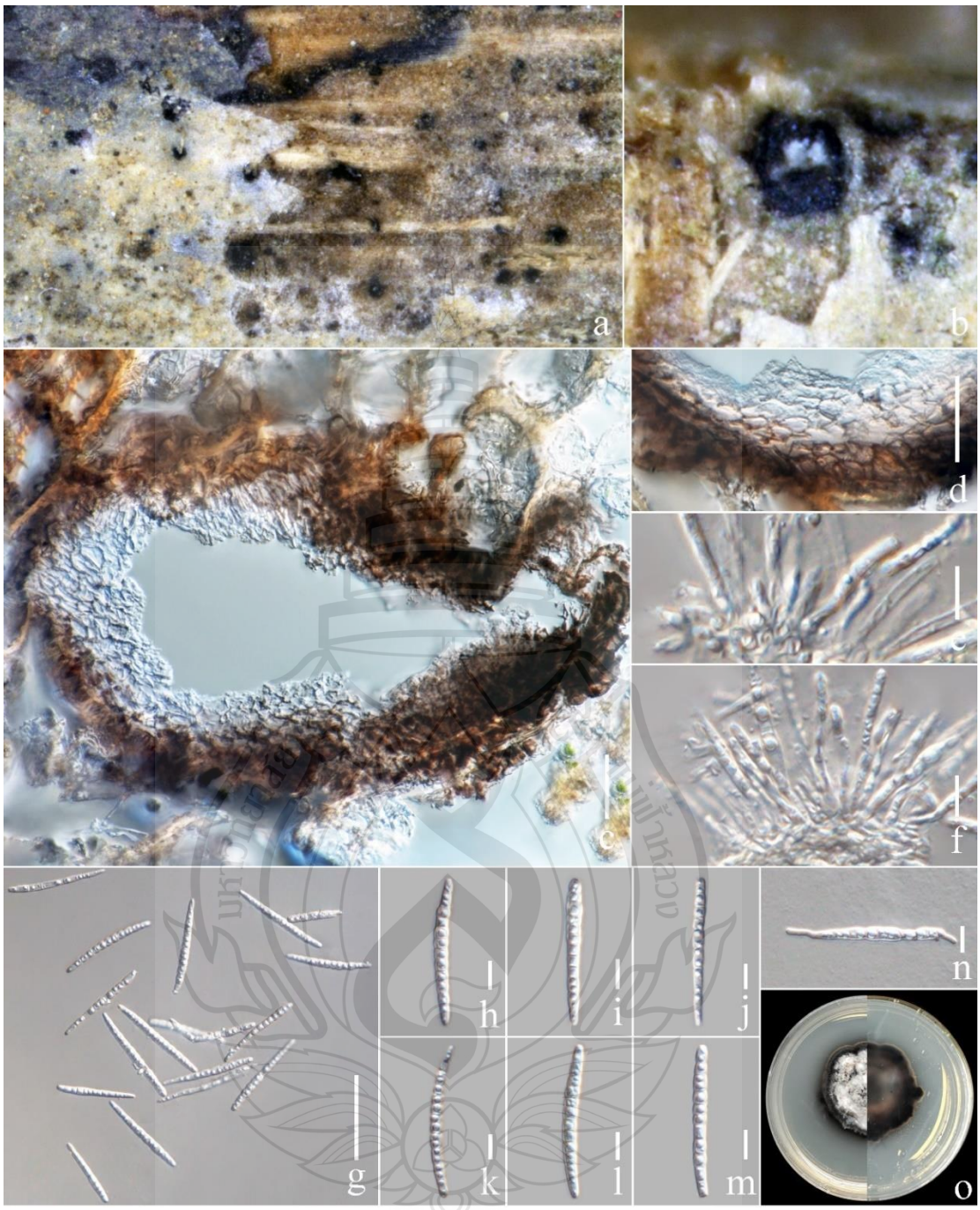
Culture characteristics: Colonies on PDA fast growing, after 2 weeks reaching 4 cm diam. at 25°C, irregular growth, with fluffy, dense, white mycelium on the surface, grey at the edge, black base, reverse dark.

Known distribution: China (this study).

Material examined: China, Yunnan Province, Sanyuan District, on dead sheath of *Phoenix canariensis*, 29 Dec 2022, Y.R. Xiong and L. Lu, XG116 (MHZU 23-0126, holotype) – ex-type ZHKUCC 24-0059, other living culture ZHKUCC 24-0060.

GenBank numbers: ZHKUCC 24-0059: ITS – PV578208, LSU – PV578374, SSU – PV578518, *tef* 1-α –PV608866; ZHKUCC 24-0060: ITS – PV578209, LSU – PV578375, SSU – PV578519, *tef* 1-α – PV608867.

Notes: Two collections from this study formed a sister lineage with *Heleiosa brunnea* in the phylogenetic tree with 100% ML and 1.00 BYPP bootstrap support (Figure 2.12). The nucleotide differences excluding gaps between *H. phoenicis* and *H. brunnea* were as below: ITS: 1.16% (6/518 base pairs), LSU: 1.12% (13/1158 base pairs), and *tef* 1-α: 2.08% (20/960 base pairs). Morphologically, *H. phoenicis* represents the first reported asexual morph in *Heleiosa*. Based on phylogenetic placement and morphological variations, we introduce *H. phoenicis* as a new species.



Note a, b Conidiomata on the substrate. c Sections through conidiomata. d Peridium. e, f Conidiogenous cells and developing conidia. g–m Conidia. n Germinating conidium. o The front of culture on PDA at 25°C and the reverse of culture on PDA at 25°C. Scale bars: c, d = 20 µm, e, f, h–n = 10 µm, g = 50 µm.

Figure 2.14 *Heleiosa phoenicis* (MHZU 23-0126, holotype)

Phellinocrescentia Crous & Decock, Persoonia 33: 235 (2014)

Notes: Crous et al. (2014) introduced *Phellinocrescentia* (*Ph.*) with *Ph. guianensis* as the type species based on morphological evidence and MegaBLAST results which combined ITS and LSU sequence data. *Phellinocrescentia* only reported asexual morphs characterized by conidiomata are pycnidial, globose, solitary or aggregated, uni- to multilocular; the wall is composed of textura angularis, with the outer surface covered by warty hyphae; conidia are aseptate, solitary, hyaline, smooth, guttulate, thin-walled, and ellipsoid to teardrop-shaped (Crous et al., 2014). In this study, we used ITS, LSU, and *tef* 1-α to update phylogenetic studies for *Phellinocrescentia* (Figure 2.12). Currently, one epithet is listed under *Phellinocrescentia* (Index Fungorum, 2024) with all species associated with molecular data. Here we described a new species of *Phellinocrescentia* which is the first time reported from palm species (Xiong et al., 2025).

Phellinocrescentia caryotae Y.R. Xiong, Manawas. & K.D. Hyde, ***sp. nov.***

Figure 2.15

Etymology: The epithet refers to the host genus "*Caryota*", from which the species was collected.

Saprobic on dead petiole of *Caryota mitis*. Asexual morph: Coelomycetous. *Conidiomata* 120–180 × 80–120 μm ($\overline{x}$ = 151 × 98 μm, n = 10), pycnidial, separate, gregarious to confuent, globose to subglobose, semi-immersed, unilocular, ostiolate, thick-walled. *Peridium* 10–40 μm, composed of thick-walled, brown-black cells, *textura epidermoidea*, hyaline cell at base with thin-walled. *Conidiophores* reduced to conidiogenous cells. *Conidiogenous cell* 5–8 × 1.5–2.5 μm ($\overline{x}$ = 6.4 × 1.9 μm, n = 25), hyaline, enteroblastic, phialidic, cylindrical, integrated, determinate, smooth-walled, periclinal wall thickened towards the apex. *Conidia* 2–3 × 1–1.5 μm ($\overline{x}$ = 2.8 × 1.3 μm, n = 25), hyaline, elliptical, unicellular, smooth-walled, guttulate. Sexual morph: Not observed.

Culture characteristics: Colonies on PDA fast growing, after 2 weeks reaching 35 mm diam., at 25°C, circular, raised, producing mucus, glistening, pale creamy, reverse pastel yellow, with a yellowish-grey margin.

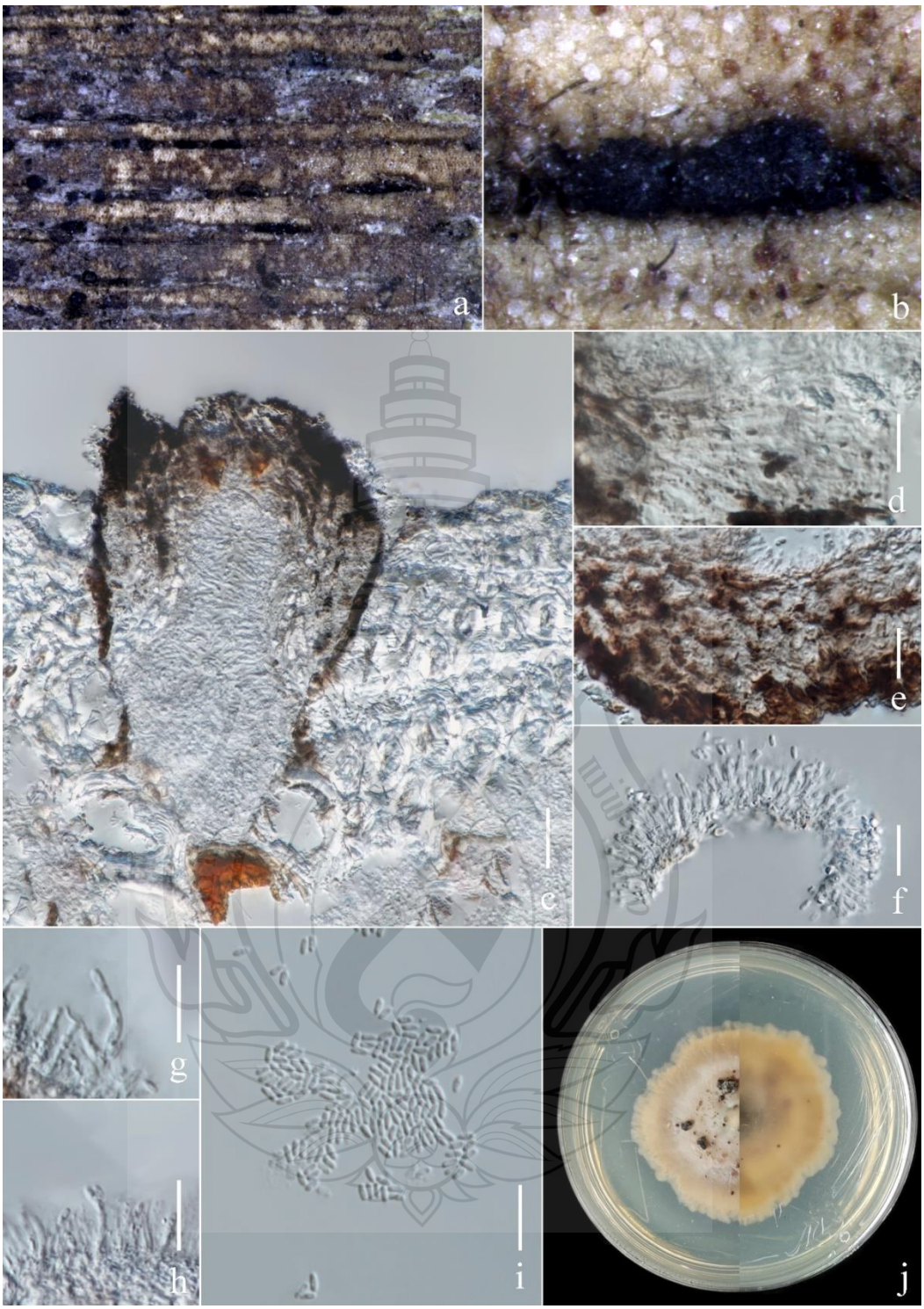
Known distribution: China (this study).

Material examined: China, Yunnan Province, Xishuangbanna City, an unidentified forest beside National Highway 219, on dead petiole of *Caryota mitis*, 5 Feb

2023, Y.R. Xiong and L. Lu, XG213 (MHZU 23-0164, holotype) – ex-type ZHKUCC 24-0135, other living culture ZHKUCC 24-0136.

GenBank numbers: ZHKUCC 24-0135: ITS – PV578224, LSU – PV578390; ZHKUCC 24-0136: ITS – PV578225, LSU – PV578391.

Notes: Two collections from this study formed a separate lineage and clustered with *Phellinocrescentia guianensis* in the phylogenetic tree with 100% ML and 1.00 BYPP bootstrap support (Figure 2.12). The nucleotide differences excluding gaps, between *Ph. caryotae* and *Ph. guianensis* were checked and given as follows, ITS: 7.05% (38/539 base pairs), and LSU: 4.06% (36/886 base pairs). Morphologically, *Phellinocrescentia guianensis* has brown and warty hyphae covered at the surface while *Ph. caryotae* is not observed in this character (Crous et al., 2014). *Phellinocrescentia caryotae* has a special structure with brown thick-walled *textura epidermoidea* cells at the upper part and hyaline cells at the base with thin-walled. Based on the phylogenetic placement and morphological variations, we introduce *Ph. caryotae* as a new species.



Note a, b Conidiomata on the substrate. c Sections through conidiomata. d, e Cells of peridium (d is basal cells, e is upper cells). f–h Conidiogenous cells and developing conidia. i Conidia. j The front of culture on PDA at 25°C and the reverse of culture on PDA at 25°C. Scale bars: c = 20 µm, d–i = 10 µm.

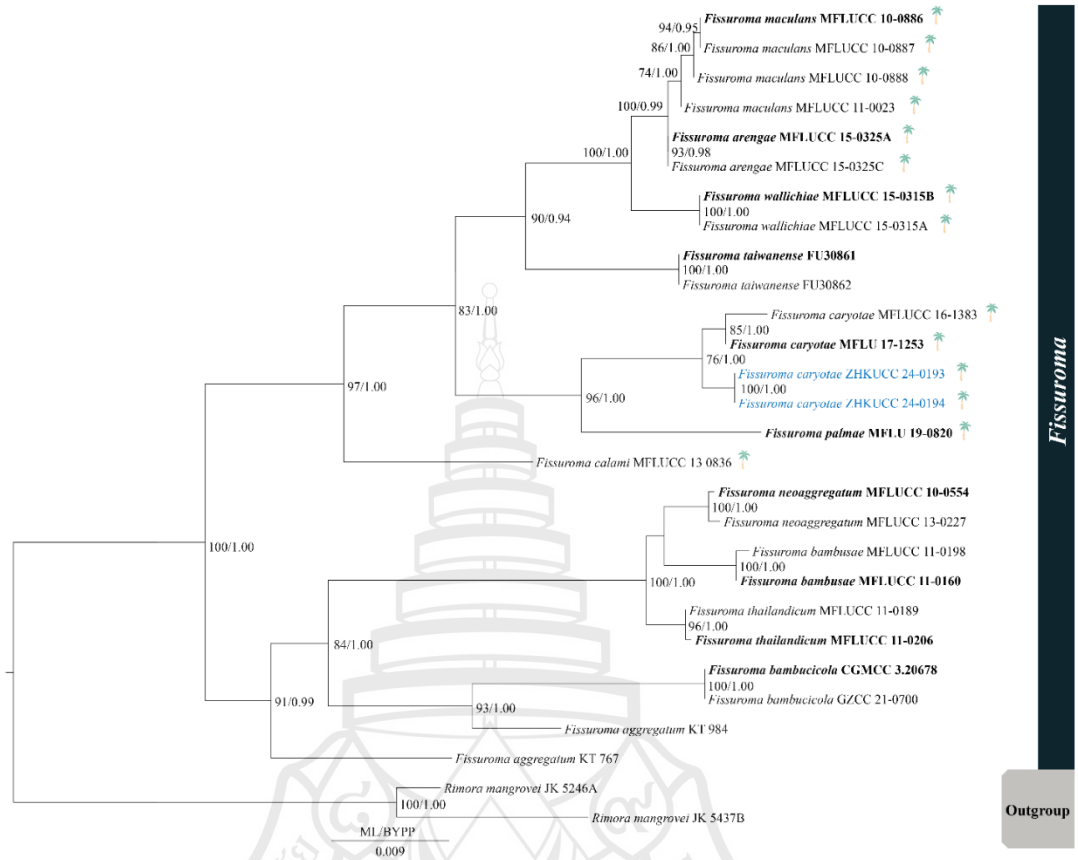
Figure 2.15 *Phellinocrescentia caryotae* (MHZU 23-0164, holotype)

Pleosporales Luttr. ex M.E. Barr (1987)

Aigialaceae Suetrong, Sakay., E.B.G. Jones, Kohlm., Volkm.-Kohlm. & C.L. Schoch, Studies in Mycology 64: 166 (2009)

Fissuroma J.K. Liu, Phook., E.B.G. Jones & K.D. Hyde, Fungal Diversity 51 (1): 145 (2011)

Notes: Liu et al. (2011) established *Fissuroma* (*F.*) with *F. maculans* as the type species. *Fissuroma* is a holomorphic genus, with the asexual morph known as pleurophomopsis-like coelomycetes. The sexual morph is characterized by hemispherical, black ascomata with a slit-like ostiole and flattened base, trabeculate pseudoparaphyses (Liew et al., 2000), obclavate to cylindrical asci, and ascospores which are fusiform, hyaline, 1-septate and surrounded by a distinctive sheath (Tanaka & Harada, 2005; Liu et al., 2011; Phookamsak et al., 2015; Tennakoon et al., 2018). Liu et al. (2011) used morphological evidence and phylogenetic analysis of combined SSU and LSU sequence data to introduce *Fissuroma* as a new genus. Subsequently, phylogenetic studies mainly use SSU, LSU, ITS and *tef* 1-α or without ITS for analysis (Phookamsak et al., 2015; Tennakoon et al., 2018; Wanasinghe et al., 2018; Zhang et al., 2020; Feng & Zhang, 2022). Following Feng and Zhang (2022), in this study, we employed ITS, LSU, SSU and *tef* 1-α to update the phylogenetic tree of *Fissuroma* (Figure 2.16). Currently, 15 epithets are listed under *Fissuroma* (Index Fungorum, 2024) with 12 molecular data available, among these 9 species have been reported from the palm (Xiong et al., 2025). Including a new host record for *F. caryotae* from *Arenga tremula* from China in this study.



Note Phylogram generated from maximum likelihood analysis of *Fissuroma* based on combined ITS, LSU, SSU and *tef* 1-α sequence data. Bootstrap values for maximum likelihood (ML) equal to or greater than 70 are indicated above the branches. The new collections are indicated in blue and ex-type strains are indicated in bold.

Figure 2.16 Phylogenetic tree of *Fissuroma*

Fissuroma caryotae Wanas., E.B.G. Jones & K.D. Hyde, Mycol. Progr. 17 (5): 579 (2018)

Index Fungorum number: IF 554088; *Facesoffungi number*: FoF 03608; Figure 2.17

Saprobic on dead rachis of *Arenga tremula*. Asexual morph: Not observed. Sexual morph: *Ascomata* 900–1100 × 250–370 µm ($\bar{x}$ = 971 × 301 µm, n = 10), solitary, scattered, semi-immersed, immersed beneath host epidermis, appearing numerous, raised, dome-shaped areas on the host surface, conical, hemisphaerical, coriaceous, flattened at the base, unilocular, black, ostiolate. *Ostioles* carbonaceous slit-like opening, central. *Peridium* 30–100 µm wide, unequal thickness, poorly developed at the base, thick at sides towards

the apex, base and corners comprising a mixture of host tissue and dark brown to hyaline fungal cells, black to dark brown, *textura angularis* to *textura prismatica*. *Hamathecium* 1–2 µm wide, pseudoparaphyses, composed of dense, hyaline, filiform, trabeculate, branched, anastomosing among the asci. *Asci* 120–170 × 14–18 µm ($\overline{x}$ = 141 × 17.4 µm, n = 30), 8-spored, bitunicate, fissitunicate, cylindric-clavate, or obclavate, short furcate pedicel, apically rounded with a truncate ocular chamber. *Ascospores* 45–50 × 10–13 µm ($\overline{x}$ = 47.8 × 11.2 µm, n = 40), overlapping 1–2-seriate at the base, 1-seriate at the apex, fusiform, hyaline, smooth-walled, tapering to pointed apices, 1–3-septate, constricted at the medium septum, smooth-walled, guttules, surrounded by a thin distinctive sheath.

Culture characteristics: Colonies on PDA, after 2 weeks reaching 2 cm diam., at 25°C, medium dense, circular, tufted colony center elevated, surface slightly rough with white edge entire, velvety to hairy, white greyish mycelium, becoming obverse grey to chestnut, reverse dark brown.

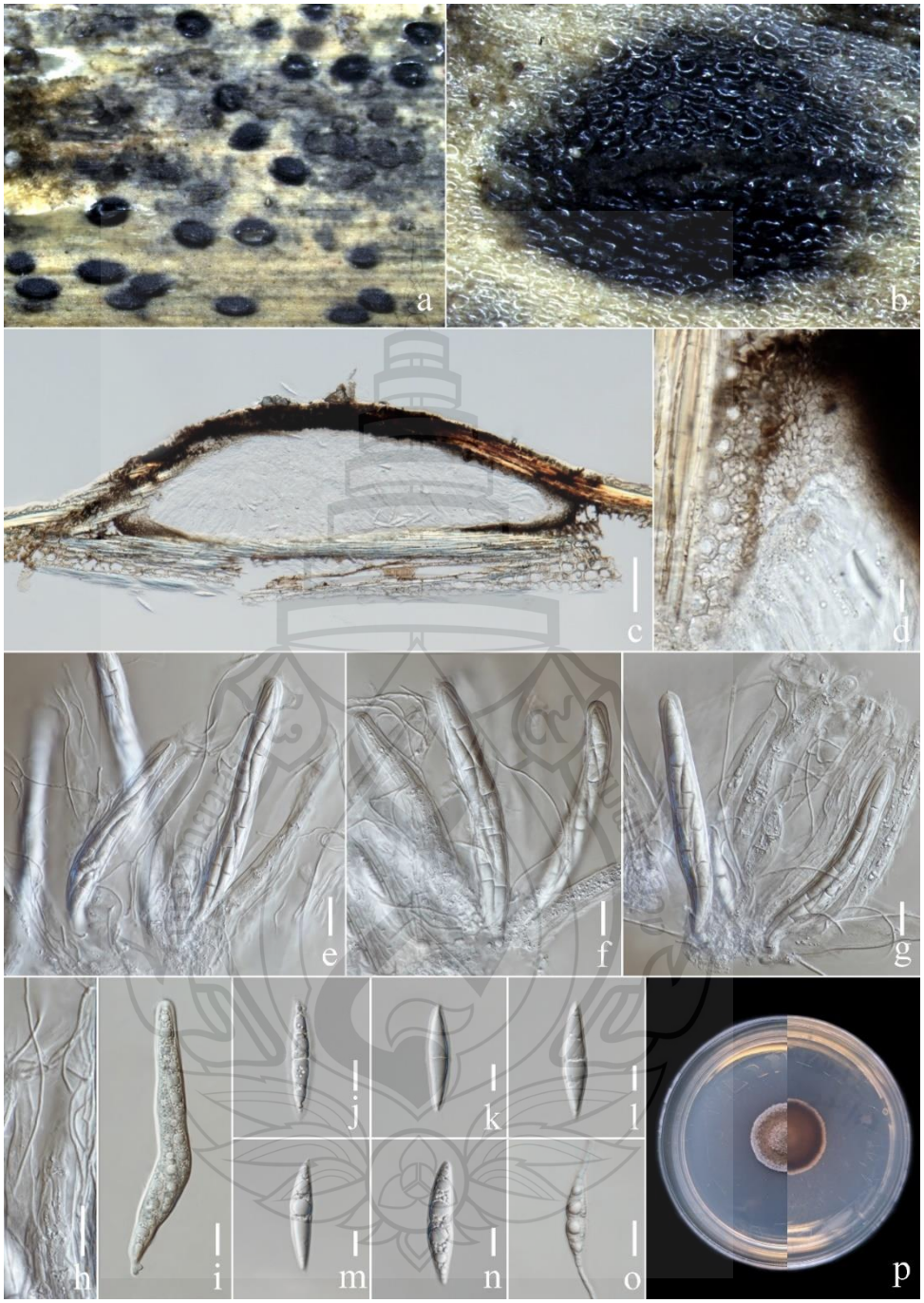
Known distribution: China (this study) and Thailand (Wanasinghe et al., 2018; Zhang et al., 2020).

Material examined: China, Yunnan Province, Xishuangbanna City, Xishuangbanna National Forest Park, on dead rachis of *Arenga tremula*, 4 Feb 2023, Y.R. Xiong and L. Lu, XG294 (MHZU 23-0193, holotype) – ex-type ZHKUCC 24-0193, other living culture ZHKUCC 24-0194.

GenBank numbers: ZHKUCC 24-0193: ITS – PV578180, LSU – PV578344, SSU – PV578500, *tef* 1-α – PV608850; ZHKUCC 24-0194: ITS – PV578181, LSU – PV578345, SSU – PV578501, *tef* 1-α – PV608851.

Notes: Two collections obtained in this study clustered with *Fissuroma caryotae* by 76% ML bootstrap support and 1.00 BYPP bootstrap support (Figure 2.16). The nucleotide differences excluding gaps between our collections and *F. caryotae* (MFLU 17-1253) in ITS is 1.83% (10/547 base pairs), LSU: 0.03% (3/829 base pairs), *tef* 1-α: 1.26% (11/871 base pairs). Although our collections have 1–3-septate ascospores, the size of ascospores are similar with *F. caryotae* ($\overline{x}$ = 47.8 × 11.2 µm vs $\overline{x}$ = 44.2 × 7.5 µm) (Wanasinghe et al., 2018). Therefore, based on morphology and phylogenetic analysis, we identified our collections as a new record of *F. caryotae* from *Arenga tremula*. *Fissuroma caryotae* was first introduced on a dead trunk of *Caryota urens* from Thailand by Wanasinghe et al. (2018). Zhang et al. (2020) reported a new record of dead petiole of *Calamus* sp. from

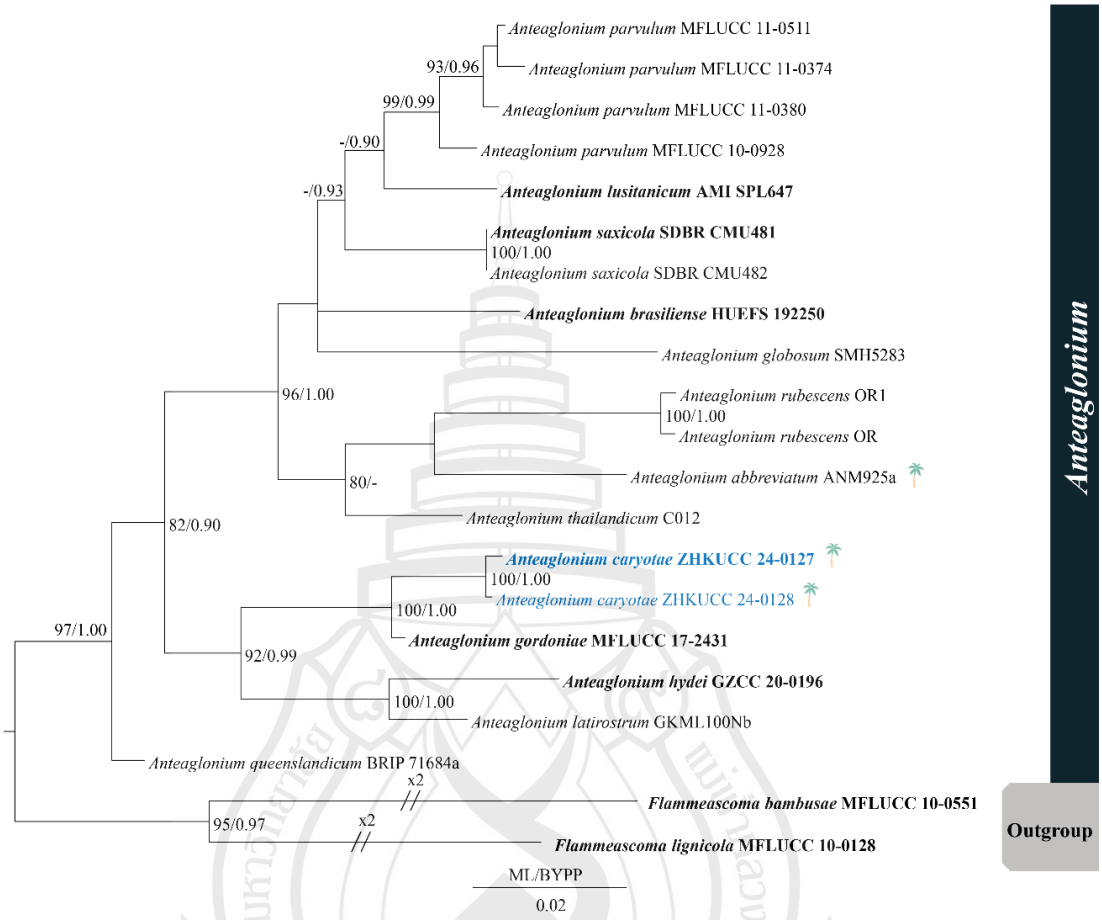
Thailand.



Note a, b Ascomata on substrate. c Vertical sections of ascomata. d Cells of peridium. e–i Asci with pseudoparaphyses (h Pseudoparaphyses, i Asci). j–k Ascospores. r The front of culture on PDA at 25°C and the reverse of culture on PDA at 25°C. Scale bars: c = 100 µm, d–i, o = 20 µm, j–n = 10 µm.

Figure 2.17 *Fissuroma caryotae* (MHZU 23-0193, holotype)

Anteagloniaceae K.D. Hyde, Jian K. Liu & A. Mapook, Fungal Diversity 63: 33 (2013)



Note Phylogram generated from maximum likelihood analysis of *Anteaglonium* based on combined ITS, LSU, SSU, *rpb2* and *tef* 1-α sequence data. Bootstrap values for maximum likelihood (ML) equal to or greater than 70 are indicated above the branches. The new collections are indicated in blue and ex-type strains are indicated in bold.

Figure 2.18 Phylogenetic tree of *Anteaglonium*

Anteaglonium Mugambi & Huhndorf, Syst. Biodiv. 7(4): 460 (2009)

Notes: Mugambi and Huhndorf (2009) established *Anteaglonium* (*An.*) to accommodate four species with *An. abbreviatum* (synonym of *Glonium abbreviatum*) as the type species. *Anteaglonium* is holomorphic genus which asexual morph characterized by coelomycetous conidiomata, pseudoparenchymatous conidioma wall, holoblastic conidiogenous cells and aseptate, globose, hyaline, guttulate conidia (Jaklitsch et al., 2018;

Hyde et al., 2020); Asexual morph characterized by hysterothecial ascomata, carbonaceous navicular with a longitudinal slit, bitunicate, fissitunicate, cylindrical clavate asci and septate, hyaline ascospores (Mugambi & Huhndorf, 2009). Mugambi and Huhndorf (2009) based on morphological evidence and phylogenetic analysis combined LSU and *tef* 1-α to introduce *Anteaglonium* as a new genus. Subsequently, phylogenetic studies mainly use ITS, LSU, SSU, *rpb*2 and *tef* 1-α or without ITS and *rpb*2 for analysis (Jayasiri et al., 2016, 2019; Jaklitsch et al., 2018; Zhang et al., 2023). In this study, we use ITS, LSU, SSU, *rpb*2 and *tef* 1-α to update phylogenetic studies for *Dictyocheirospora* (Figure 2.18). Currently, 11 epithets are listed under *Dictyocheirospora* (Index Fungorum, 2025 January) with all species associated with molecular data. Here we described a new species of *Anteaglonium* which is the first time reported from palm species (Xiong et al., 2025).

Anteaglonium caryotae Y.R. Xiong, Manawas. & K.D. Hyde, ***sp. nov.***

Figure 2.19

Etymology: The epithet refers to the host genus name "*Caryota*", from which the species was collected.

Saprobic on dead segment of *Caryota mitis*. Asexual morph: Not observed. Sexual morph: *Hysterothecia* 400–640 × 400–510 μm ($\bar{x}$ = 494 × 445 μm, n = 10), superficial, solitary, scattered, globose to subglobose, black, carbonaceous, straight, slightly striatelaterally, with a longitudinal slit, sulcus shallow. *Peridium* 40–150 μm wide, carbonaceous, brittle, thick, thickened towards apex, base thin, comprising pigmented cells of *textural prismatica*. *Hamathecium* 1–1.5 μm wide, comprising numerous, aseptate pseudoparaphyses, branched above the asci. *Asci* 60–80 × 8–10 μm ($\bar{x}$ = 68 × 9.2 μm, n = 25), 8-spored, bitunicate, cylindrical, short pedicellate, club shape, apically rounded, obliquely to irregularly uniseriate. *Ascospore* 20–27 × 5–7 μm ($\bar{x}$ = 23 × 5.9 μm, n = 25), biseriate, fusiform to obovoid, slight curve, smooth-walled, 1–3-septate, 1-septate at medium and constricted, upper cell frequently exhibits a septum, the lower cell rarely has a septum, hyaline to pare brown, guttulate.

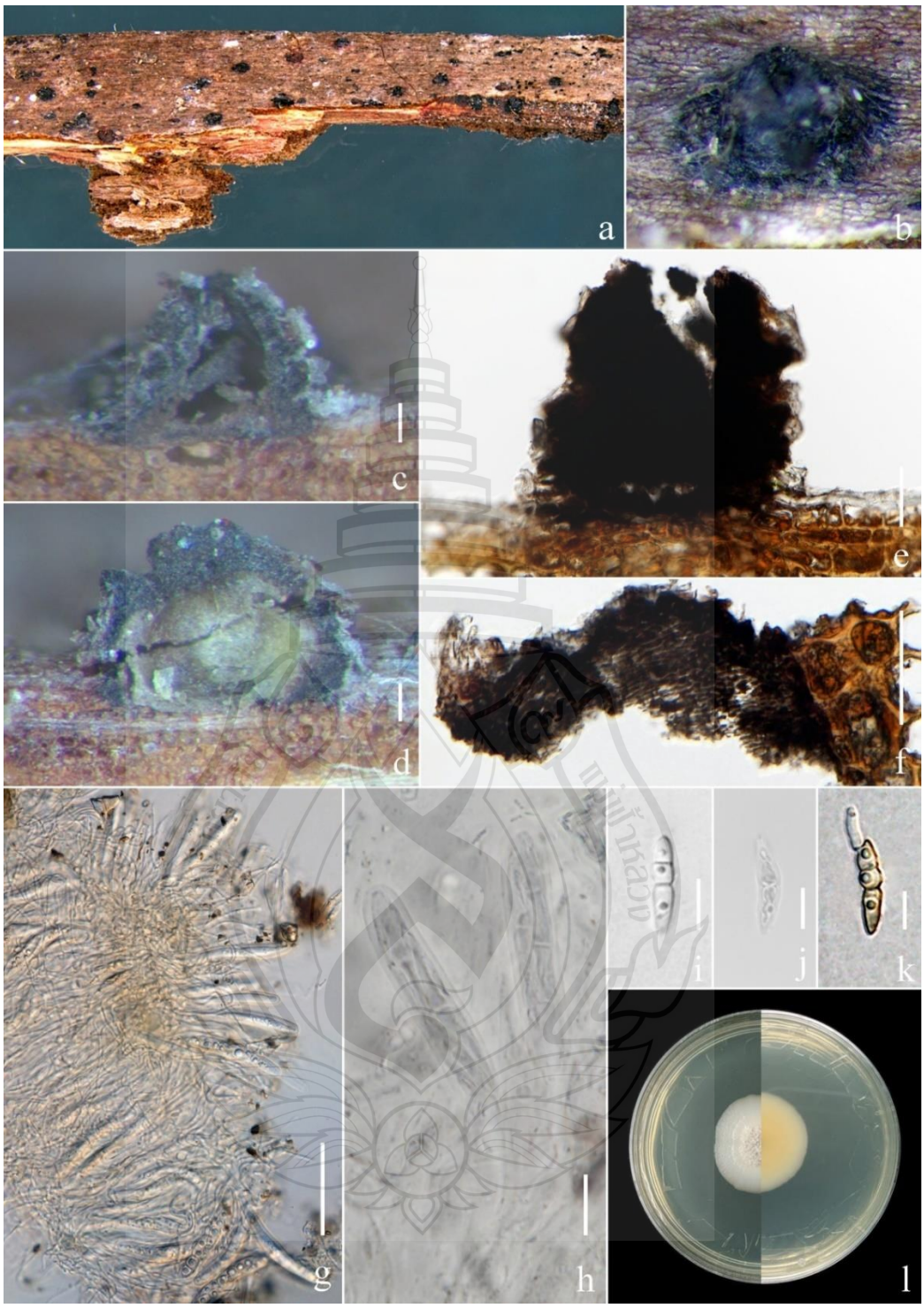
Culture characteristics: Colonies on PDA fast growing, after 2 weeks reaching 4 cm diam., at 25°C, circular, white and flattened with immersed mycelium with entire margin; in reverse cream in the middle and white at the margin.

Known distribution: China (this study).

Material examined: China, Yunnan Province, Xishuangbanna City, in an unidentified forest beside National Highway 219, on dead leaf sheath of *Caryota mitis*, 5 Feb 2023, Y.R. Xiong and L. Lu, XG205 (MHZU 23-0160, holotype) – ex-type ZHKUCC 24-0127, other living culture ZHKUCC 24-0128.

GenBank numbers: ZHKUCC 24-0127: ITS – PV578128, LSU – PV578298, SSU – PV578482, *tef* 1-α – PV608812, *rpb*2 – PV595300; ZHKUCC 24-0128: ITS – PV578129, LSU – PV578299, SSU – PV578483, *tef* 1-α – PV608813, *rpb*2 – PV595301.

Notes: Two collections from this study formed a separate lineage sister to *Anteaglonium gordoniae* in the phylogenetic tree with 100% ML bootstrap support and 1.00 BYPP (Figure 2.18). The nucleotide differences excluding gaps between our collection (ZHKUCC 24-0127) and *An. gordoniae* (MFLUCC 17-2431) were checked and given as follows, ITS: 3.94% (20/507 base pairs), LSU: 1.42% (12/844 base pairs), *rpb*2: 2.22% (24/1079 base pairs), and *tef* 1-α: 3.43% (30/874 base pairs). Morphologically, *An. caryotae* have short pedicellate, club-shaped asci and peridium comprising pigmented cells of *textural prismatica* which are different from *An. gordoniae* have short pedicellate asci and peridium comprising pigmented cells of *textura angularis*. Based on phylogenetic placement and morphological variations, we introduce *An. caryotae* as a new species.



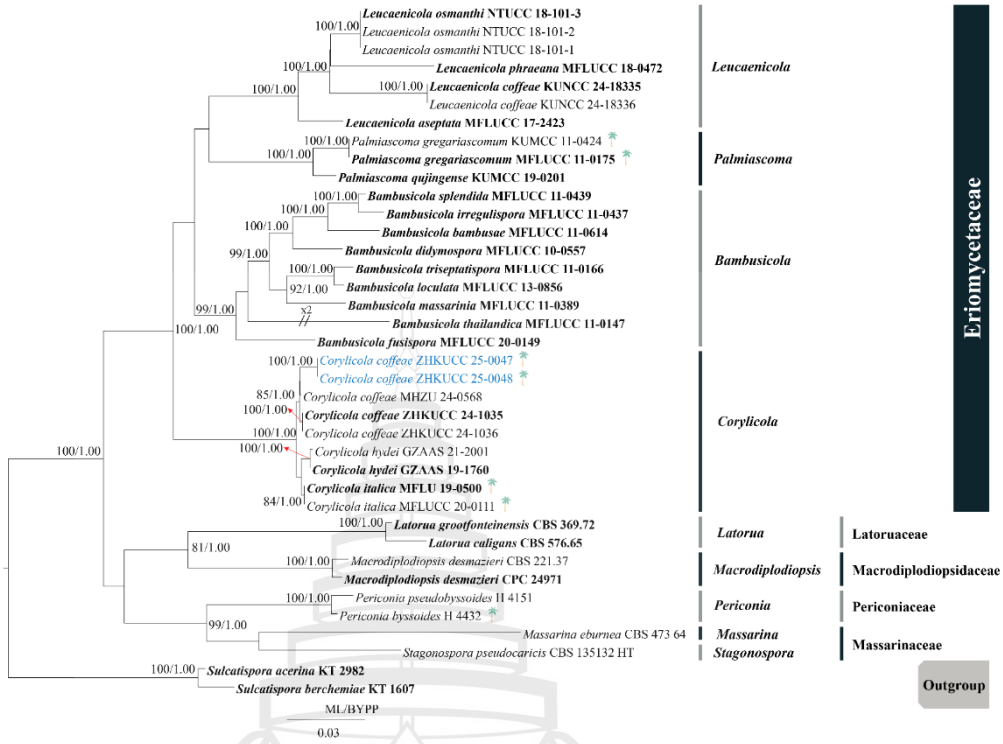
Note a, b Sporodochia on the substrate. c–e Vertical sections of ascomata. f Cells of peridium. g, h Asci. i–k Ascospores (k germinating ascospore). l The front of culture on PDA at 25°C and the reverse of culture on PDA at 25°C. Scale bars: c, d = 100 µm, e–g = 50 µm, h–k = 10 µm.

Figure 2.19 *Anteaglonium caryotae* (MHZU 23-0160, holotype)

Bambusicolaceae D.Q. Dai & K.D. Hyde, Fungal Diversity 63 (1): 49 (2013)

Corylicola Wijesinghe, Camporesi, Yong Wang bis & K.D. Hyde, Biodivers. Data J. 8: e55957, 7 (2020)

Notes: Corylicola (*C.*) was introduced by Wijesinghe et al. (2020) to accommodate the type species *C. italica*, which is isolated from dead branches of *Corylus avellana* (common hazel) in Italy. The genus is distinguished from other genera in Bambusicolaceae by the presence of yellowish-brown ascospore masses at the apex of the ascomatal neck (Wijesinghe et al., 2020). The sexual morph of *Corylicola* is characterized by globose to subglobose, ostiolate ascomata, cylindrical asci, and 1-septate ascospores (Wijesinghe et al., 2020; Zhang et al., 2023). The asexual morph is characterized by holoblastic, phialidic conidiogenous cells and one-celled, and aseptate conidia (Wijesinghe et al., 2020). In this study, we use ITS, LSU, SSU, *rpb*2 and *tef* 1-α to update phylogenetic studies for *Corylicola* (Figure 2.20). *Corylicola* comprises only three species, *C. italica*, *C. hydei* and *C. coffeae* (Index Fungorum, 2025), all species were reported as saprobic from various plants and verified with DNA sequences (Wijesinghe et al., 2020; Zhang et al., 2023; Lu et al., 2025). No species have been reported from palm species. Herein, we introduce a new host record in *Corylicola* and record the first report of *Corylicola* species from *Trachycarpus fortunei* from China.



Note Phylogram generated from maximum likelihood analysis of *Corylicola* based on combined ITS, LSU, SSU, *rpb*2 and *tef*1-α sequence data. Bootstrap values for maximum likelihood (ML) equal to or greater than 70 are indicated above the branches. The new collections are indicated in blue and ex-type strains are indicated in bold.

Figure 2.20 Phylogenetic tree of *Corylicola*

Corylicola coffeae L. Lu, K.D. Hyde & Tibpromma, Fungal diversity (2025, in press)

Figure 2.21

Saprobic on dead segment of *Trachycarpus fortunei*. Asexual morph: Coelomycetous. *Conidiomata* 150–200 × 180–260 µm ($\bar{x}$ = 179.8 × 217.5 µm, n = 20), pycnidial, immersed, solitary or aggregated, globose to subglobose, unilocular, dark brown to black, ostiolate. *Ostiole* central and circular. *Conidiomata wall* 15–20 µm ($\bar{x}$ = 16.5 µm, n = 20), composed of several layers of hyaline to brown cells of *textura angularis*. *Conidiophores* reduced to conidiogenus cells. *Conidiogenus cells* 4.5–6.5 × 2.5–4 µm ($\bar{x}$ = 5.1 × 3.3 µm, n = 20), holoblastic, phialidic, ampulliform, hyaline, smooth-walled. *Conidia* 3–4.5 × 2–2.5 ($\bar{x}$ = 3.8 × 2.3 µm, n = 20), solitary, subglobose or ovoid to

ellipsoid, rounded or obtuse ends, hyaline to light brown, aseptate, guttulated, one-celled, smooth-walled. Sexual morph: Not observed.

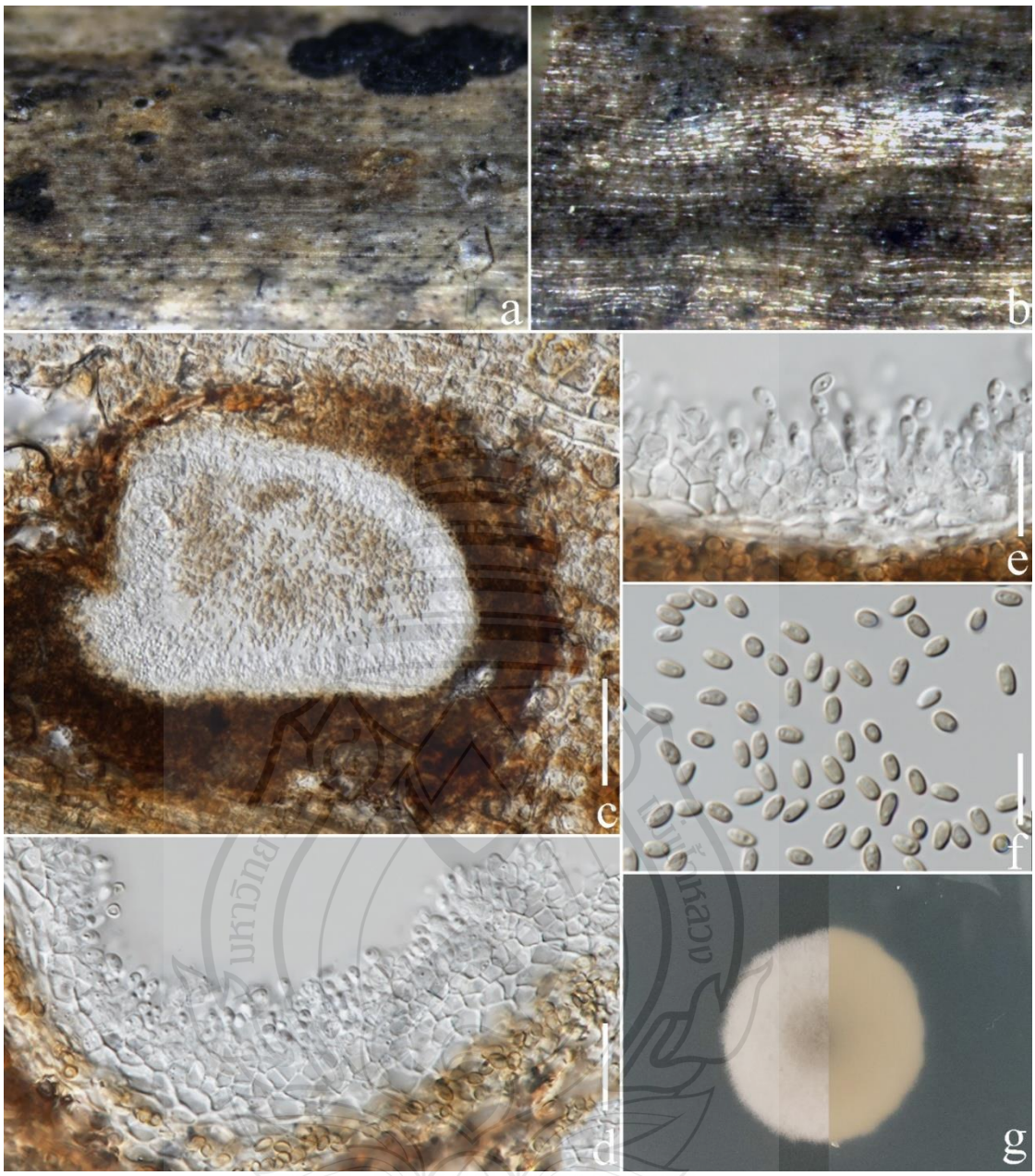
Culture characteristics: Colonies on PDA slowly growing, after 2 weeks reaching 1–2 cm diam., at 25°C, circular, flat, with filiform margin, dense, furry, whitish in upper and yellowish in the reverse of the colony.

Known distribution: China (Lu et al., 2025, this study).

Material examined: China, Jiangxi Province, Nanchang City, Meiling National Forest Park, on a dead segment of *Trachycarpus fortunei*, 11 April 2024, Y.R. Xiong, XG389 (MHZU 24-0511, new host record), living culture ZHKUCC 25-0047, other living culture ZHKUCC 25-0048.

GenBank numbers: ZHKUCC 25-0047: ITS – PV578156, LSU – PV578326, SSU – PV578494, *tef*1-α – PV608830, *rpb*2 – PV595312; ZHKUCC 25-0048: ITS – PV578157, LSU – PV578327, SSU – PV578495, *tef*1-α – PV608831, *rpb*2 – PV595313.

Notes: Two collections obtained in this study clustered with *C. coffeae* (MHZU 24-0568, ZHUKCC 21-1035 (ex-type), ZHUKCC 21-1036) by 85% ML bootstrap support and 1.00 BYPP (Figure 2.20). The nucleotide differences excluding gaps between our isolate (ZHKUCC 25-0047) and *C. coffeae* (ZHUKCC 21-1035) were checked and shown - ITS: 1.3% (7/501 base pairs), *rpb*2: 1.6% (18/1078 base pairs), *tef* 1-α: 0.3% (3/992 base pairs), while LSU and SSU are identical. *Corylicola coffeae* was introduced by Lu et al. (2025) with only sexual morph. Our species exhibits only an asexual morph, making morphological comparison with the sexual morph of *C. coffeae* unavailable (Lu et al., 2025). However, our species exhibits characteristics consistent with the asexual morph of *Corylicola*, particularly in the presence of holoblastic, phialidic and ampulliform conidiogenous cells, as well as hyaline and aseptate conidia (Wijesinghe et al., 2020, Figure 2.21). Therefore, based on morphology and phylogenetic analysis, we identified our collections as new host record of *C. coffeae*. It represents the asexual morph of *C. coffeae.*



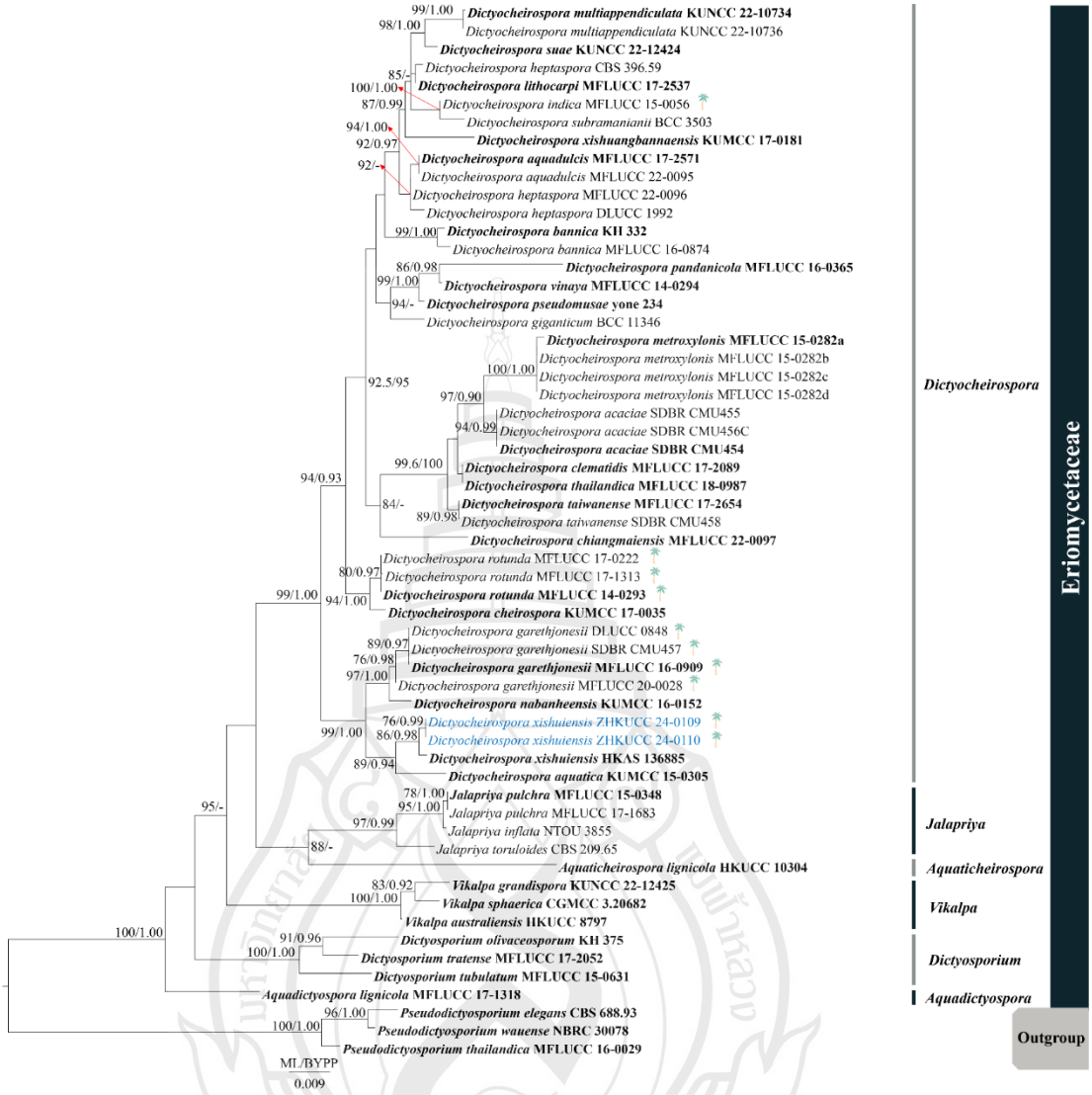
Note a, b Conidioma on natural substrate. c Vertical section of a conidiomata. d Peridium. e Conidiogenous cells with conidia lining the inner wall of a conidiomata. f Conidia. g The front of culture on PDA at 25°C and the reverse of culture on PDA at 25°C. Scale bars: c = 50 µm; d–f = 10 µm.

Figure 2.21 *Corylicola coffeae* (MHZU 24-0511, new host record)

Dictyosporiaceae Boonmee & K.D. Hyde, Fungal Diversity 80: 462 (2016)

Dictyocheirospora M.J. D'souza, Boonmee & K.D. Hyde, Fungal Diversity 80: 465 (2016).

Notes: Boonmee et al. (2016) established *Dictyocheirospora* (*Di.*) with *Di. rotunda* as the type species based on morphological evidence and phylogenetic analysis which combined SSU, LSU, and *tef* 1-α sequence data. *Dictyocheirospora* is hyphomycetous genus characterized by sporodochial conidiomata, dark-pigmented, micronematous or semi-macronematous conidiophores and acrogenous, cheiroid, and coloured conidia (Boonmee et al., 2016; Tennakoon et al., 2023). Subsequently, phylogenetic studies mainly use SSU, LSU, ITS and *tef* 1-α or without SSU for species delineation in this genus (Boonmee et al., 2016; Yang et al., 2018; Shen et al., 2022; Tennakoon et al., 2023; Shu et al., 2024). In this study, we use ITS, LSU, and *tef* 1-α to update phylogenetic studies for *Dictyocheirospora* (Figure 2.22). Currently, 31 epithets are listed under *Dictyocheirospora* (Index Fungorum, 2024), and only 24 species are associated with molecular data. Totally six species have been reported from palm species including the new host record described in this study (Xiong et al., 2025).



Note Phylogram generated from maximum likelihood analysis of Dictyosporiaceae based on combined ITS, LSU, and *tef* 1-α sequence data. Bootstrap values for maximum likelihood (ML) equal to or greater than 70 are indicated above the branches. The new collections are indicated in blue and ex-type strains are indicated in bold.

Figure 2.22 Phylogenetic tree of Dictyosporiaceae

Dictyocheirospora xishuiensis Y.R. Sun, Yong Wang bis & K.D. Hyde, Fungal Diversity 131: 141 (2025)

Figure 2.23

Saprobic on dead segment of *Elaeis guineensis*. Asexual morph: Hyphomycetous. *Colonies* on natural substrate superficial, scattered. *Mycelium* immersed,

composed of hyaline, smooth, septate, branched hyphae. *Conidiomata* sporodochial, dark brown to black. *Conidiophores* micronematous, undifferentiated from vegetative hyphae, short. *Conidiogenous cells* holoblastic, integrated, terminal, pale brown, smooth-walled. *Conidia* 27–43 × 14–19 μm ($\overline{x}$ = 37 × 17 μm, n = 25), solitary, acrogenous, cheiroid, brown, arranged in 3–5 compact rows, with rows digitate, cylindrical, inwardly curved at apex, arising from a basal cell, with each row composed of 3–7 cells, euseptate, slightly constricted at septa, smooth-walled; with 1–3 rounded to cylindrical appendages (normal 2 cylindrical appendages), arising from two sides of conidial rows, grow toward both ends, hyaline. Sexual morph: Not observed.

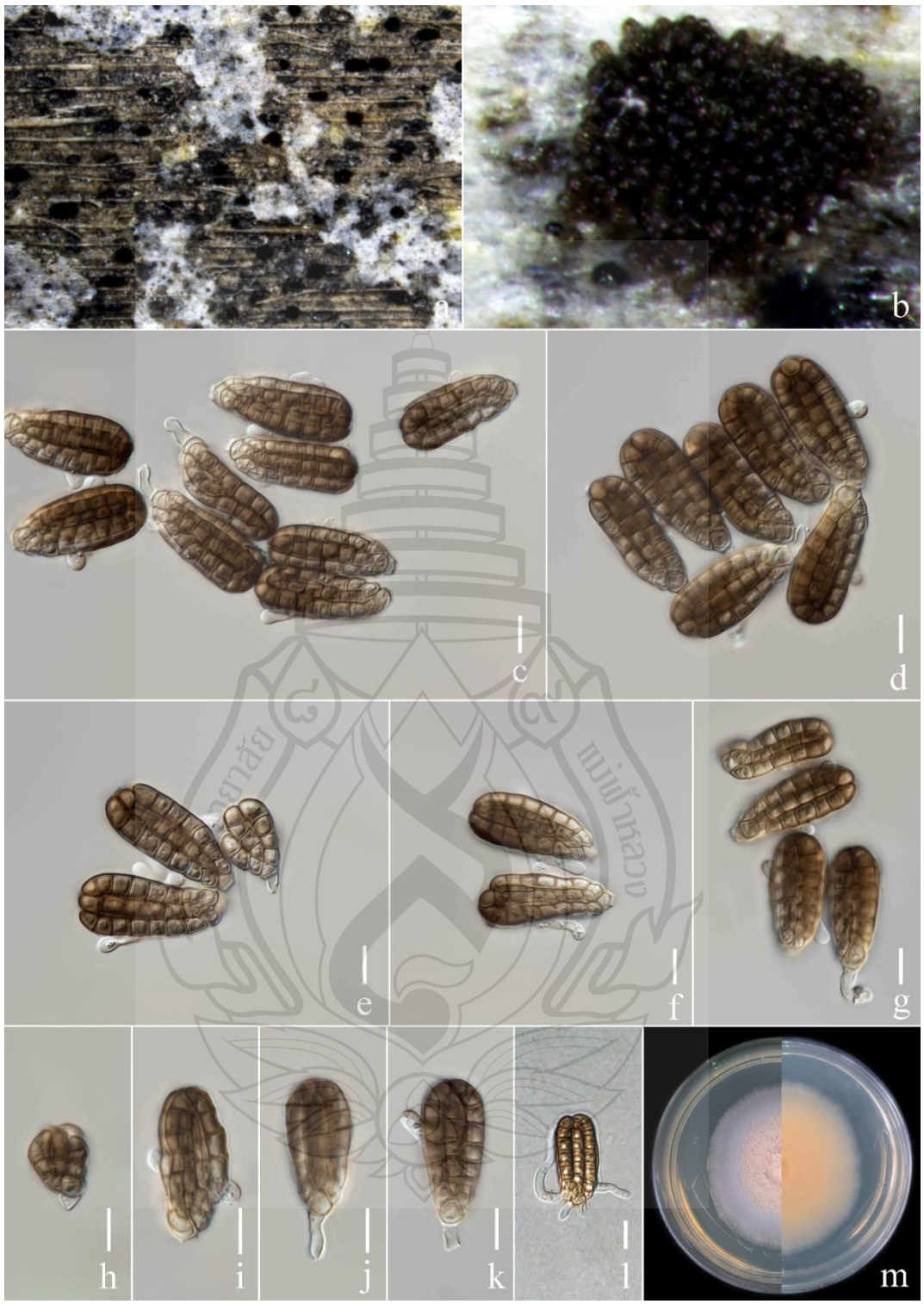
Culture characteristics: Colonies on PDA fast growing, after 2 weeks reaching 4 cm diam., at 25°C, circular, with fluffy, dense, white mycelium on the surface with entire margin; in reverse yellow in the middle and white at the margin.

Known distribution: China (this study).

Material examined: China, Yunnan Province, Xishuangbanna City, in an unidentified forest beside National Highway 219, on a dead segment of *Elaeis guineensis*, 5 Feb 2023, Y.R. Xiong and L. Lu, XG183 (MHZU 23-0151, new host record), living culture ZHKUCC 24-0109, other living culture ZHKUCC 24-0110.

GenBank numbers: ZHKUCC 24-0109: ITS – PV578162, LSU – PV578328, *tef* 1-α – PV608834; ZHKUCC 24-0110: ITS – PV578163, LSU – PV578329, *tef* 1-α – PV608835.

Notes: Two collections from this study formed a sister lineage and clustered with *Dictyocheirospora xishuiensis* in the phylogenetic tree with 86% ML and 0.99 BYPP bootstrap support. The nucleotide differences excluding gaps, between our collection (ZHKUCC 24-0109) and *Di. xishuiensis* (HKAS 136885) were checked and given as follows: ITS: 0.06% (3/499 base pairs), LSU are same. Our collections are similar with *Di. xishuiensis* in conidial morphology (Sun et al., 2025). Based on phylogenetic placement and morphological variations, we introduce our collections as a new host record of *Di. xishuiensis*. *Dictyocheirospora xishuiensis* was first introduced by Sun et al. (2025) from dead twigs of *Camphora* sp. from China.



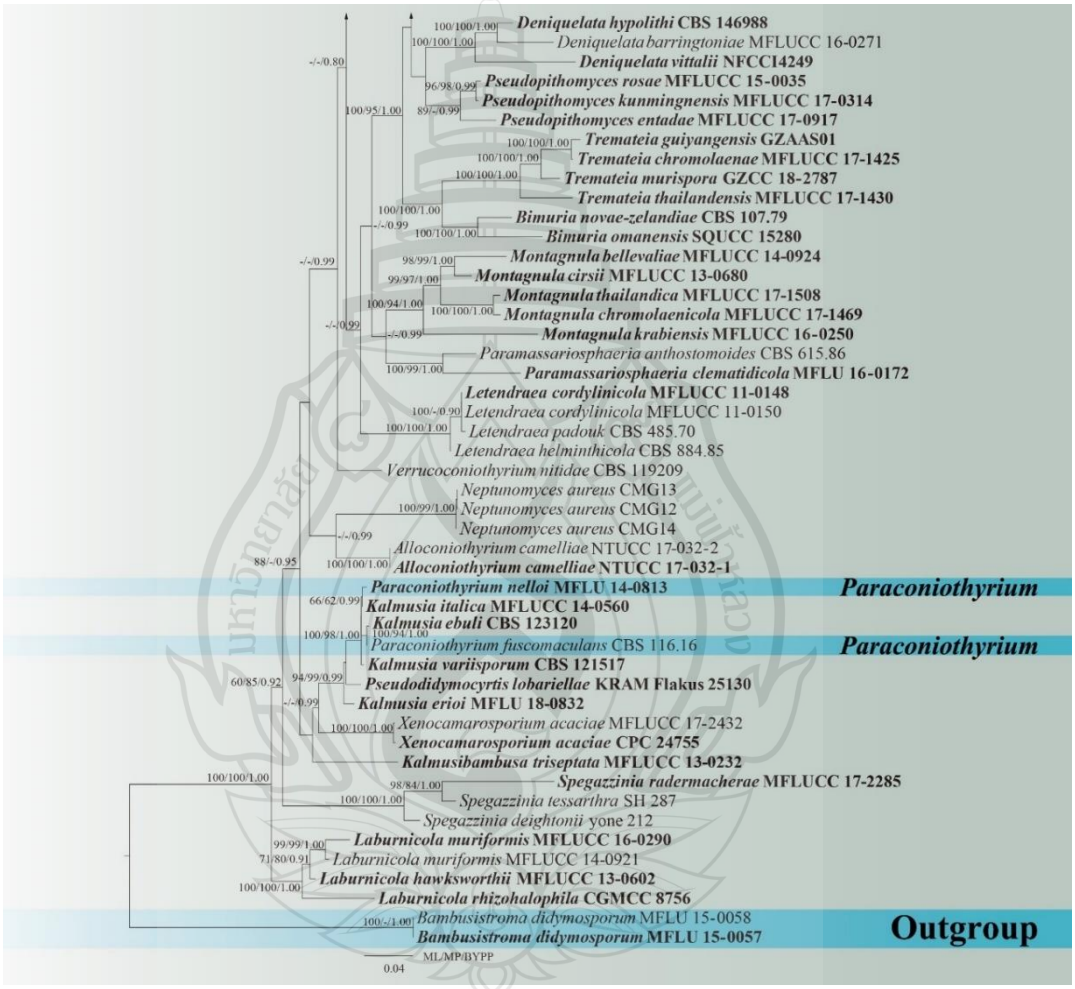
Note a, b Sporodochia on the substrate. c–k Conidia. l Germinating conidium. m The front of culture on PDA at 25°C and the reverse of culture on PDA at 25°C. Scale bars: c–k = 10 µm.

Figure 2.23 *Dictyocheirospora xishuiensis* (MHZU 23-0151, new host record)

Didymosphaeriaceae Munk, Dansk botanisk Arkiv 15 (2): 128 (1953)

Paraconiothyrium Verkley & M. da Silva (2004).

Notes: Paraconiothyrium is an asexual genus introduced by Verkley et al. (2004) to accommodate four species, *P. estuarinum*, *P. brasiliense*, *P. cyclothyrioides* and *P. fungicola*. *Paraconiothyrium* was confirmed to be polyphyletic in Didymosphaeriaceae by Ariyawansa et al. (2020). For taxonomic treatment of this genus, we follow Ariya wansa et al. (2014), Hongsanan et al. (2020) and Wijayawardene et al. (2022).



Note The maximum-likelihood phylogram of *Paraconiothyrium* based on a combined ITS, LSU, SSU, *rpb*2 and *tef* 1-α sequence dataset with Bambusistroma didymosporum (MFLU 15-0057 and MFLU 15-0058) as the outgroup taxa. The maximum-likelihood bootstrap values (ML ≥ 70%), Maximum parsimony values (MP ≥ 70%) and Bayesian Inference Posterior Probability values (BIPP ≥ 0.85) are shown above the nodes. Strains derived from the current study are in red, while type strains are in bold black.

Figure 2.24 Phylogenetic tree of *Paraconiothyrium*

Paraconiothyrium guangdongensis Y.R. Xiong, Manawas., & K. D. Hyde, sp. nov.

Figure 2.25

Saprobic on rotting leaf of *Licuala peltata* var. *sumawongii* (*Arecaceae*). *Sexual morph*: Not observed. *Asexual morph*: Coelomycetous. Conidiomata 60–180 µm length, 30–85 µm diam ($\overline{x}$ = 139 × 61 µm, n = 10), pycnidial, solitary, scattered, immersed, unilocular, ellipsoid, raising host surface and producing a dark area of dehiscence. Pycnidial wall 20–30 µm wide, multi-layered, several layers of black to lightly pigmented thick-walled cells of textura angularis, becoming flattened and highly pigmented. Conidiophores 5.5–7 µm long, fasciculate, subcylindrical to ampulliform, discrete, hyaline. Conidiogenous cell 1.5–2.5 × 1–1.5 µm ($\overline{x}$ = 2.2 × 1.2 µm, n = 20), discrete, cylindrical to subcylindrical, irregular, phialidic, hyaline. Conidia 3.5–4.5 × 1.5–2 µm ($\overline{x}$ = 4.1 × 1.8 µm, n = 50), ellipsoidal to cylindrical, initially hyaline, pale brown at maturity, thin-walled, smooth, aseptate.

Culture characteristics: Colonies on PDA attaining 5 cm diam after a week at 25°C, dentate, curled, raised, outermost papillate surface, white; middle smooth surface, buff; rhizoid brown in the centre.

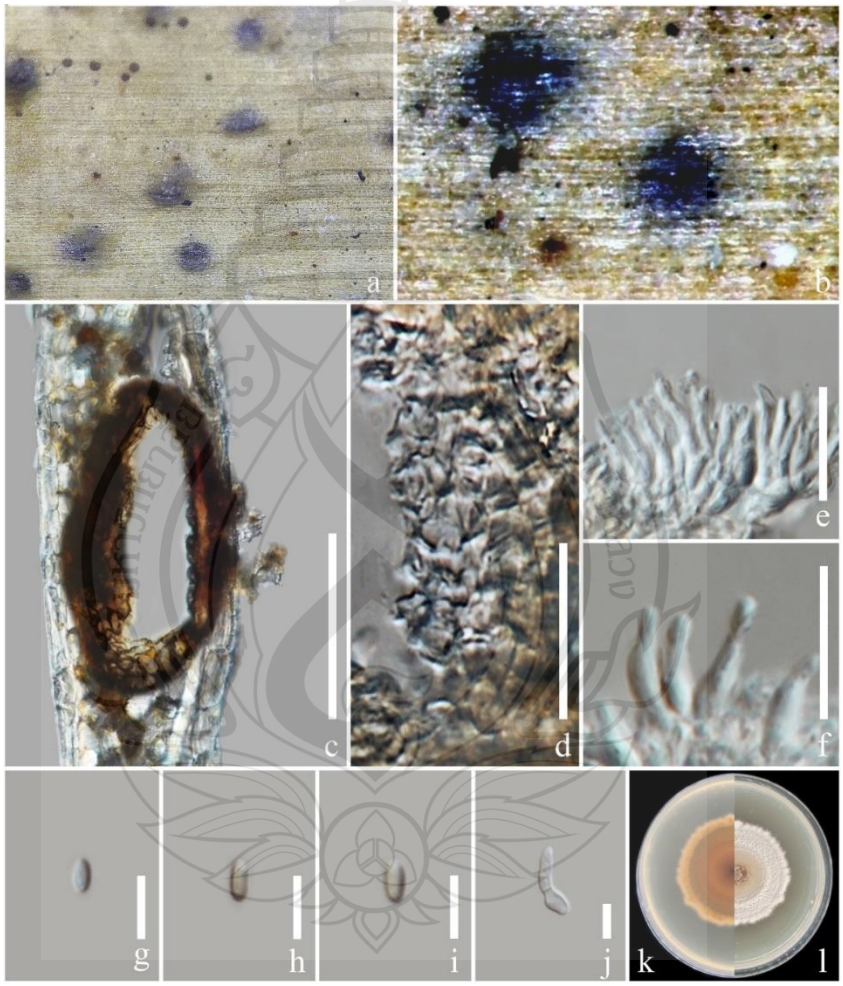
Known distribution: China (this study).

Material examined: China, Guangdong Province, Guangzhou City, South China Botanical Garden (23°11'23" N, 113°21'13" E), rotting leaf of the *Licuala peltata* var. *sumawongii* (Arecaceae), 17 December 2020, Y.R. Xiong (holotype, MHZU 22-0176; ex-type culture, ZHKUCC 22-0332); other living cultures, ZHKUCC 22-0333, ZHKUCC 22-0334.

GenBank numbers: ZHKUCC 22-0332: ITS – OQ449317, LSU – OQ449285, *tef* 1-α – OQ458719; ZHKUCC 22-0333: ITS – OQ449318, LSU – OQ449286, *tef* 1-α – OQ458720; ZHKUCC 22-0334: ITS – OQ449319, LSU – OQ449287, *tef* 1-α – OQ458721.

Notes: The identification of *Paraconiothyrium* species is confusing, and ITS alone is not sufficient to provide a good resolution (Gonçalves et al., 2020; Phukhamsakda et al., 2022). It is necessary to combine morphological and multi-gene locus phylogenetic analysis. The nucleotide differences between *Paraconiothyrium guangdongensis* and its phylogenetically related species are *P. cyclothyrioides* (CBS 972.95) LSU: 1.03% (9/876 bases), ITS: 6.01% (30/499 bases); *P. estuarinum* (CBS 109850) LSU: 1.12% (10/894

bases), ITS: 6.01% (30/499 bases); *P. iridis* (CBS 146036) LSU: 0.95% (8/846 bases), ITS: 7.26% (39/537 bases); *P. maculicutis* (CBS 101461) LSU: 0.93% (8/864 bases); *P. salinum* (CMG 50) ITS: 8.75% (46/526 bases) and *P. thysanolaenae* (MFLUCC 10–0550) LSU: 0.88% (7/795 bases), ITS: 5.38% (29/539 bases) excluding gaps. Morphologically, *P. guangdongensis* has distinct fasciculate, subcylindrical to ampulliform conidiophores, and other *Paraconiothyrium* species all reduced to conidiogenous cells. Therefore, our collections are introduced as a new species *P. guangdongensis* based on both phylogeny and morphological evidence.



Note a–b, Conidiomata on the rotting leaf of *Licuala peltata* var. *sumawongii*; c, Section of conidiomata; d, Peridium; e–f, Conidiogenous cells giving rise to conidia; g–j, Conidia; k–l, Culture on PDA from above and reverse. Scale bars c = 100 µm. d–f = 10 µm. g–j = 5 µm. j = 10 µm.

Figure 2.25 *Paraconiothyrium guangdongensis* (MHZU 22-0176, holotype)

Ganzhofusosporaceae Y.R. Xiong, Manawas. & K.D. Hyde, ***fam. nov.***

Index Fungorum number: IF XXXX; *Facesoffungi number*: FoF XXXX

Etymology: refers to the name of the type genus.

Type genus: *Ganzhofusospora* Y.R. Xiong, Manawas. & K.D. Hyde

Saprobic on dead palm substrates. Asexual morph: Not observed. Sexual morph: *Ascomata* perithecium, semi-immersed, solitary, aggregated, globose to subglobose, setose. *Setae* brown, septate. *Peridium* dark brown to brown cells, normally arranged in *textura angularis* and *textura prismatica*. *Hamathecium* paraphyses, numerous, branched, anastomosing, multi-septate, hyaline, embedded in a gelatinous matrix. *Asci* 8-spored, bitunicate, cylindric to clavate, with a short-stalked, apically rounded, with ocular chamber. *Ascospores* overlapping, fusiform to cylindrical, septate, guttulate, with mucilaginous sheath.

Notes: Ganzhofusosporaceae is introduced to accommodate the new genus *Ganzhofusospora* (*G.*) which formed a sister clade with Hermatomycetaceae and Pseudoberkleasmiaceae within Pleosporales (Figure 2.26). Ganzhofusosporaceae shares the typical Pleosporales characters in having perithecioid ascomata with bitunicate, and fissitunicate asci. However, Ganzhofusosporaceae is different from Hermatomycetaceae by pseudostromatic, perithecium ascomata and multi-septate ascospores (de Silva et al., 2022). Pseudoberkleasmiaceae has only a reported asexual morph, thus we cannot compare (Tibpromma et al., 2018). We provide an updated phylogenetic tree for Pleosporales including Ganzhofusosporaceae and Ganzhomycetaceae.

Ganzhofusospora Y.R. Xiong, Manawas. & K.D. Hyde, ***gen. nov.***

Index Fungorum number: IF XXXX; *Facesoffungi number*: FoF XXXX

Etymology: referring to the location "Ganzhou" from where samples were collected and "fusiform" shape of ascospores of the type species.

Type species: *Ganzhofusospora phoenicis* Y.R. Xiong, Manawas. & K.D. Hyde

Saprobic on dead palm substrates. Asexual morph: Not observed. Sexual morph: *Ascogenous stromata* immersed, pseudostromatic. *Ascomata* perithecium, semi-immersed, solitary, aggregated, globose to subglobose, dark, setose. *Setae* brown, septate. *Peridium* dark brown to brown, normally arranged in *textura angularis* and *textura prismatica*, heterogeneous compactness. *Hamathecium* paraphyses, numerous, branched, anastomosing, septate, embedded in a gelatinous matrix. *Asci* 8-spored, bitunicate, cylindric-clavate, with a short-stalked, apically rounded, with broadly ocular chamber

when immature. *Ascospores* overlapping biseriate, fusiform to cylindrical, 1–5-septate, constricted at the medium septum, widest at the central cells, hyaline, guttulate, surrounded by mucilaginous sheath.

Notes: Based on our phylogenetic result (Figure 2.26), *Ganzhofusospora* formed a distinct clade in Pleosporales and clustered with *Hermatomyces*. Morphologically, *Ganzhofusospora* differs from *Hermatomyces* by ascospores are 1–5-septate, constricted at the septum, widest at the central cells with mucilaginous sheath present (de Silva et al., 2022). *Pseudoberkleasmium* only reported asexual morph which we cannot compare (Tibpromma et al., 2018). According to Morphological differences evidence and phylogenetic results, we proposed a monotypic genus *Ganzhofusospora* to accommodate the type species *G. phoenicis*. More fresh collections of *Ganzhofusospora* are needed to stabilize the placement of this genus and the family Ganzhofusosporaceae. One species has been reported from palm species including a new species described in this study (Xiong et al., 2025).

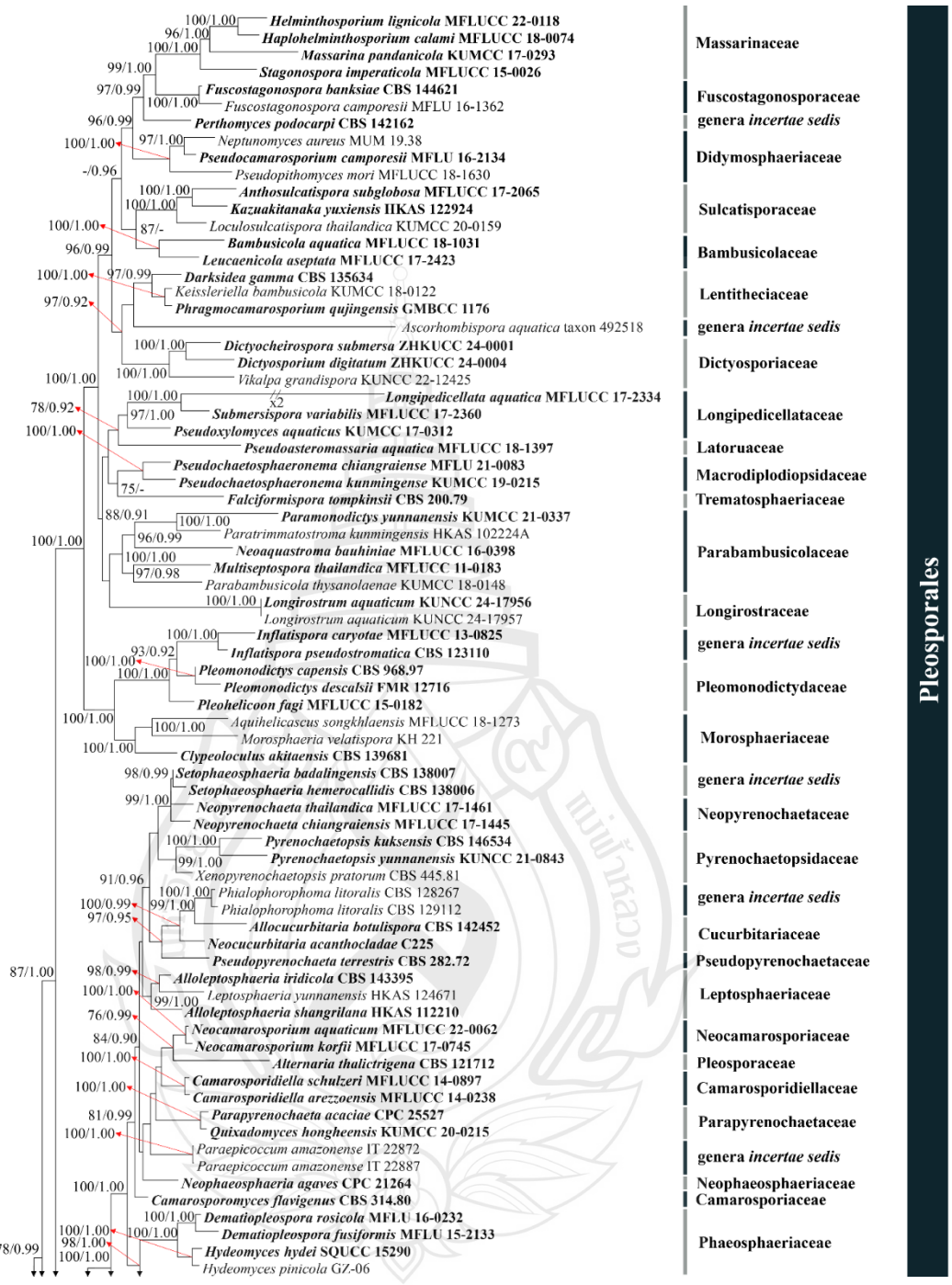


Figure 2.26 Phylogenetic tree of Pleosporales

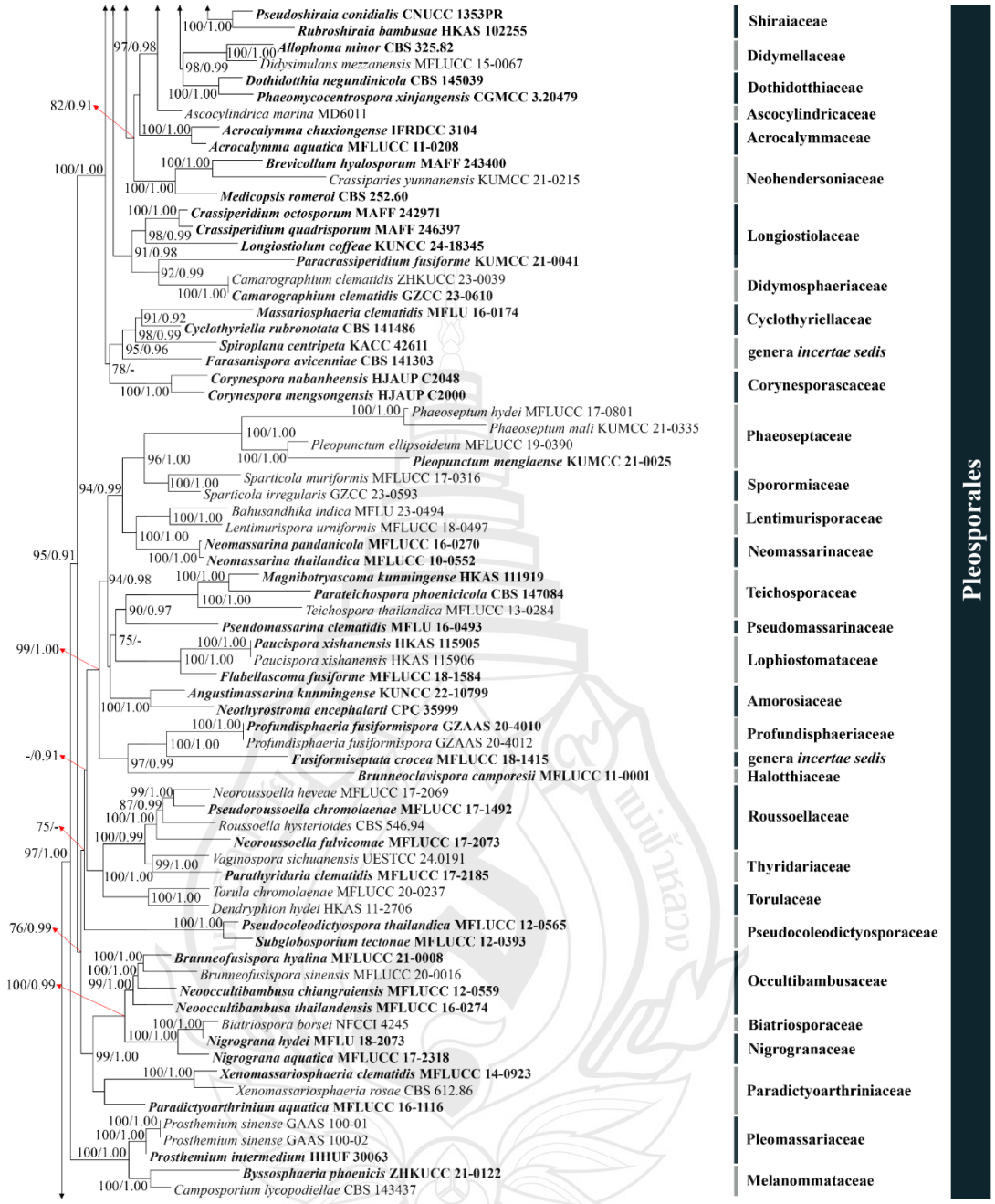
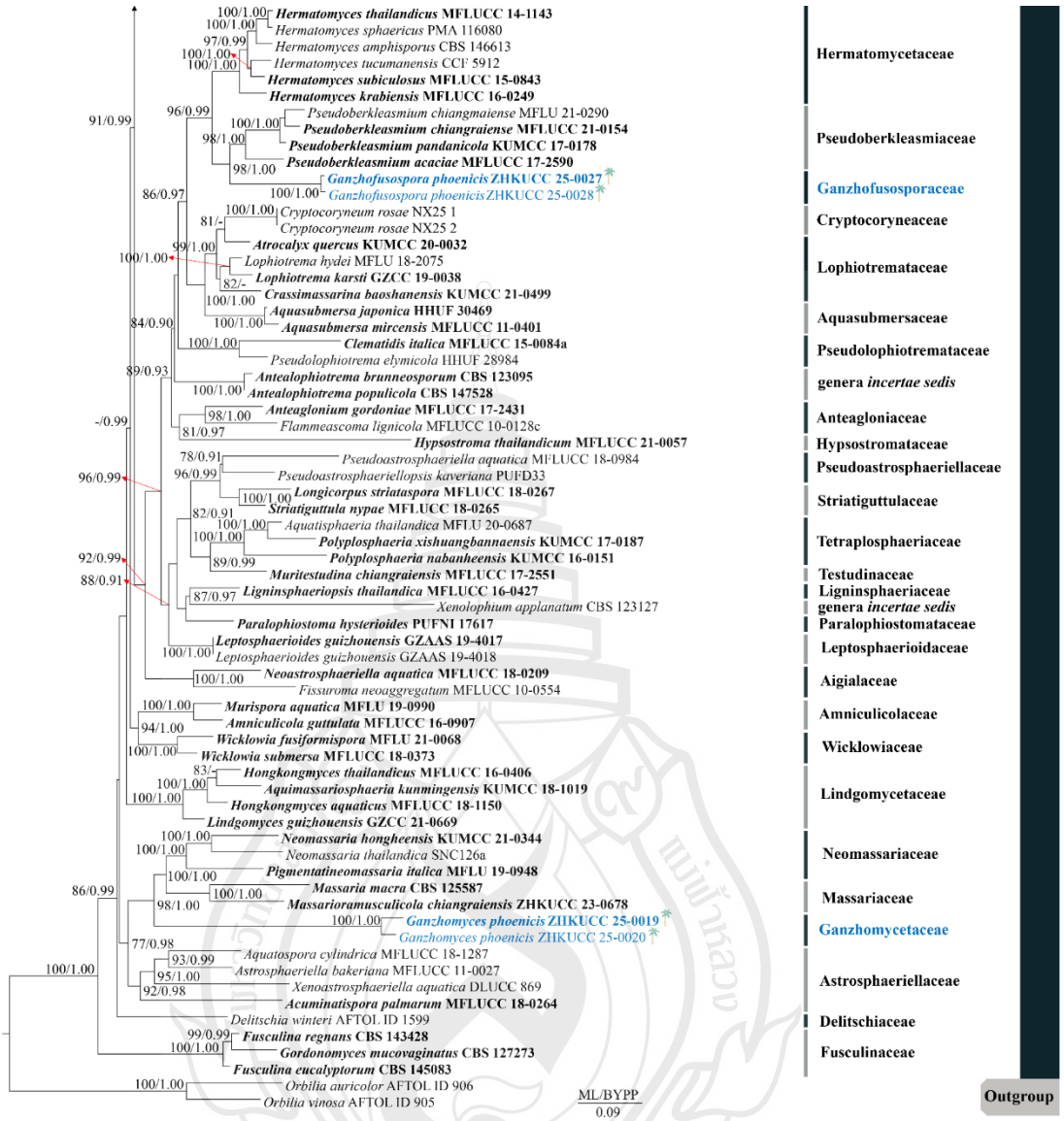


Figure 2.26 (continued)



Note Phylogram generated from maximum likelihood analysis of Pleosporales based on combined ITS, LSU, SSU, *tef* 1-α and *rpb2* sequence data. Bootstrap values for maximum likelihood (ML) equal to or greater than 70 are indicated above the branches. The new collections are indicated in blue and ex-type strains are indicated in bold.

Figure 2.26 (continued)

Ganzhofusospora phoenicis Y.R. Xiong, Manawas. & K.D. Hyde, ***sp. nov.***

Figure 2.27

Etymology: The epithet refers to the host genus name "*Phoenix*", from which the species was collected.

Saprobic on dead leaf sheath of *Phoenix sylvestris*. Asexual morph: Not observed. Sexual morph: *Ascogenous stromata* immersed, pseudostromatic. *Ascomata* 200–300 × 200–280 μm ($\overline{x}$ = 255 × 230 μm, n = 10), perithecium, semi-immersed, solitary, aggregated, globose to subglobose, dark, uniloculate, erumpent black dot, coriaceous, setose. *Setae* brown, septate, straight or slightly curved. *Peridium* 30–55 μm, dark brown to brown cells of *textura angularis* and *textura prismatica*, heterogeneous compact, part of slit-like loosely arranged. *Hamathecium* 1.5–2.5 μm wide paraphyses, numerous, branched, anastomosing, septate, hyaline, embedded in a gelatinous matrix. *Asci* 115–190 × 20–25 μm ($\overline{x}$ = 135 × 21 μm, n = 25) 8-spored, bitunicate, cylindric-clavate, with a short-stalk, apically rounded, with broadly ocular chamber when immature. *Ascospores* 40–47 × 6–10 μm ($\overline{x}$ = 43 × 8.5 μm, n = 40) overlapping biseriate, fusiform to cylindrical, 1–3-septate when immature, 5-septate when mature, constricted at the medium septum, widest at the central cells, hyaline, guttulate, surrounded by 1.5–3 μm mucilaginous sheath.

Culture characteristics: Colonies on PDA fast growing, after 2 weeks reaching 2 cm diam., at 25°C, circular, margin entire, dense, surface filamentous, cream at the margin, olivaceous in the center; reverse cream at the margin, dark olivaceous in the center.

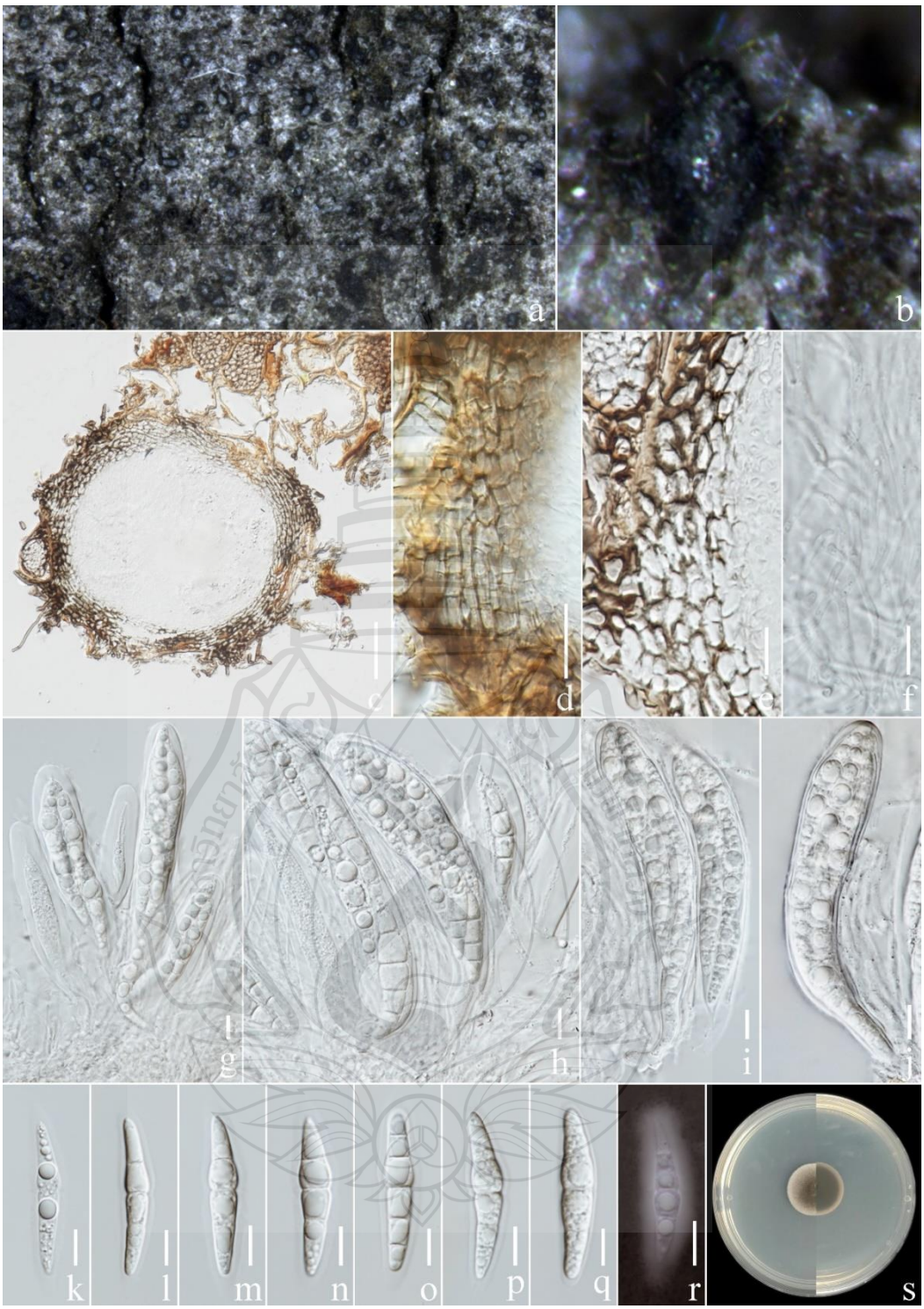
Known distribution: China (this study).

Material examined: China, Jiangxi Province, Ganzhou City, Xingda Restaurant, on dead leaf sheath of *Phoenix sylvestris*, 9 Apr 2024, Y.R. Xiong, XG371 (MHZU 24-0458, holotype), ex-type ZHKUCC 25-0027, other living culture ZHKUCC 25-0028.

GenBank numbers: ZHKUCC 25-0027: ITS – PV578184, LSU – PV578348, SSU – PV578502, *tef* 1-α – PV608852, *rpb*2 – PV595328; ZHKUCC 25-0028: ITS – PV578185, LSU – PV578349, SSU – PV578503, *tef* 1-α – PV608853, *rpb*2 – PV595329.

Notes: Two collections from this study formed a separate lineage in the phylogenetic tree with 98% ML and 1.00 BYPP bootstrap support (Figure 2.26). Based on a MegaBLAST (Query cover ≥ 70%) search using the ITS sequence, the closest matches in NCBIs GenBank nucleotide database were *Hermatomyces sphaericus* (GenBank PP779923; Identities 419/455 (92.09%), 7 gaps), *Hermatomyces* sp. (GenBank LS398264;

Identities 448/487 (91.99%), 10 gaps) and *Hermatomyces constrictus* (GenBank NR_191060; Identities 448/487 (91.99%), 10 gaps). The highest similarities using the LSU sequence were *Hermatomyces jinghaensis* (GenBank MW989519; Identities 863/896 (96.32%), 1 gap), *Hermatomyces trangensis* (GenBank KY790601; Identities 858/891 (96.30%), 0 gaps) and *Pseudoberkleasmium chiangmaiense* (GenBank MZ420759; Identities 844/877 (96.24%), 1 gaps). The highest similarities using the *rpb*2 sequence were *Hermatomyces sphaericus* (GenBank LS398358; Identities 439/517 (84.91%), 0 gap), *Hermatomyces turbinatus* (GenBank MZ042638; Identities 697/834 (83.57%), 4 gaps) and *Hermatomyces amphisporus* (GenBank LR812668; Identities 689/825 (83.52%), 4 gaps). The highest similarities using the *tef* 1-α sequence were *Anteaglonium gordoniae* (GenBank MK360042; Identities 824/873 (94.39%), 2 gap), *Atrocalyx lignicola* (GenBank LC194387; Identities 864/921 (93.81%), 0 gaps) and *Lophiotrema eburnoides* (GenBank LC194403; Identities 843/900 (93.67%), 2 gaps). *Ganzhofusospora phoenicis* was distinct by peridium is heterogeneous compactness which part of slit-like and loosely arranged, and ascospores are 1–3-septate when immature with 5-septate when mature. Based on phylogenetic placement and morphological variations, we introduce *G. phoenicis* as a new species.



Note a, b Ascomata on substrate. c Vertical sections of ascomata. d, e Peridium. f Hamathecium. g–i Asci. k–r Ascospore (r ascospore in Indian ink). s The front of culture on PDA at 25℃ and the reverse of culture on PDA at 25℃. Scale bars: c = 50 µm, d = 20 µm, e–r = 10 µm.

Figure 2.27 *Ganzhofusospora phoenicis* (MHZU 24-0458, holotype)

Ganzhomycetaceae Y.R. Xiong, Manawas. & K.D. Hyde, ***fam. nov.***

Etymology: refers to the name of the type genus.

Type genus: *Ganzhomyces* Y.R. Xiong, Manawas. & K.D. Hyde

Saprobic on dead palm substrates. Asexual morph: Coelomycetous. *Conidiomata* pycnidial, semi-immersed, solitary, oval to irregulate elliptical, unilocular, papillate. *Peridium* 20–35 μm, thick-walled, brown-black cells, *textura angularis*. *Conidiophores* reduced to conidiogenous cells. *Conidiogenous cells* enteroblastic, phialidic, cylindrical, smooth-walled. *Conidia* hyaline, spermatia, oblong or ellipsoidal, smooth-walled, guttulate. Sexual morph: Not observed.

Notes: Ganzhomycetaceae is introduced to accommodate the new genus *Ganzhomyces* (*Ga*.) which formed an independent branch with Massariaceae and Neomassariaceae within Pleosporales (Figure 2.26). Massariaceae have cylindrical to ampulliform conidiophore which differs with Ganzhomycetaceae's conidiophore reduced to conidiogenous cells (Hongsanan et al., 2020). However, Neomassariaceae has only reported asexual morph, thus we cannot compare (Yang et al., 2024).

Ganzhomyces Y.R. Xiong, Manawas. & K.D. Hyde, ***gen. nov.***

Etymology: referring to the location name "Ganzhou" were collected and "fungus".

Type species: *Ganzhomyces phoenicis* Y.R. Xiong, Manawas. & K.D. Hyde

Saprobic on dead palm substrates. Asexual morph: Coelomycetous. *Conidiomata* pycnidial, semi-immersed, solitary, oval to irregulate elliptical, unilocular. *Peridium* composed of thick-walled, brown-black cells, *textura angularis*. *Conidiophores* reduced to conidiogenous cells. *Conidiogenous cells* enteroblastic, phialidic, cylindrical, hyaline, smooth-walled, arising from stratum. *Conidia* hyaline, spermatia, oblong or ellipsoidal, unicellular, smooth-walled, with 1–2 small guttules. Sexual morph: Not observed.

Notes: Based on our phylogenetic result (Figure 2.26), *Ganzhomyces* formed a distinct clade in Pleosporales. Morphologically, *Ganzhofusospora* is characterised by enteroblastic and phialidic cylindrical conidiogenous cells. According to morphological differences and phylogenetical results, we propose a monotypic genus *Ganzhomyces* to accommodate the type species *Ga. phoenix*. More fresh collections of *Ganzhomyces* are needed to stabilize the placement of this genus and the family Ganzhomycetaceae.

Ganzhomyces phoenicis Y.R. Xiong, Manawas. & K.D. Hyde, ***sp. nov.***

Figure 2.28

Etymology: The epithet refers to the host genus "*Phoenix*", from which the species was collected.

Saprobic on dead leaf sheath of *Phoenix sylvestris*. Asexual morph: Coelomycetous. *Conidiomata* 150–200 × 100–150 μm ($\overline{x}$ = 170 × 125 μm, n = 10), pycnidial, semi-immersed, solitary, oval to irregulate elliptical, unilocular, distribute in fibrous bundle ridges with forming papillate. *Peridium* 20–30 μm, composed of thick-walled, brown-black cells, *textura angularis*. *Conidiophores* reduced to conidiogenous cells. *Conidiogenous cells* 4–8 × 2–3 μm ($\overline{x}$ = 5.4 × 2.2 μm, n = 25), enteroblastic, phialidic, cylindrical, hyaline, smooth-walled, arising from stratum. *Conidia* 2.5–4 × 1.5–2 μm ($\overline{x}$ = 3.4 × 1.7 μm, n = 25), hyaline, spermatia, oblong or ellipsoidal, unicellular, smooth-walled, with 1–2 small guttules. Sexual morph: Not observed.

Culture characteristics: Colonies on PDA fast-growing, after 2 weeks reaching 2 cm diam., at 25°C, circular, margin entire, dense, mycelium velvety towards the margin, cream; reverse cream at the margin, grey in the center.

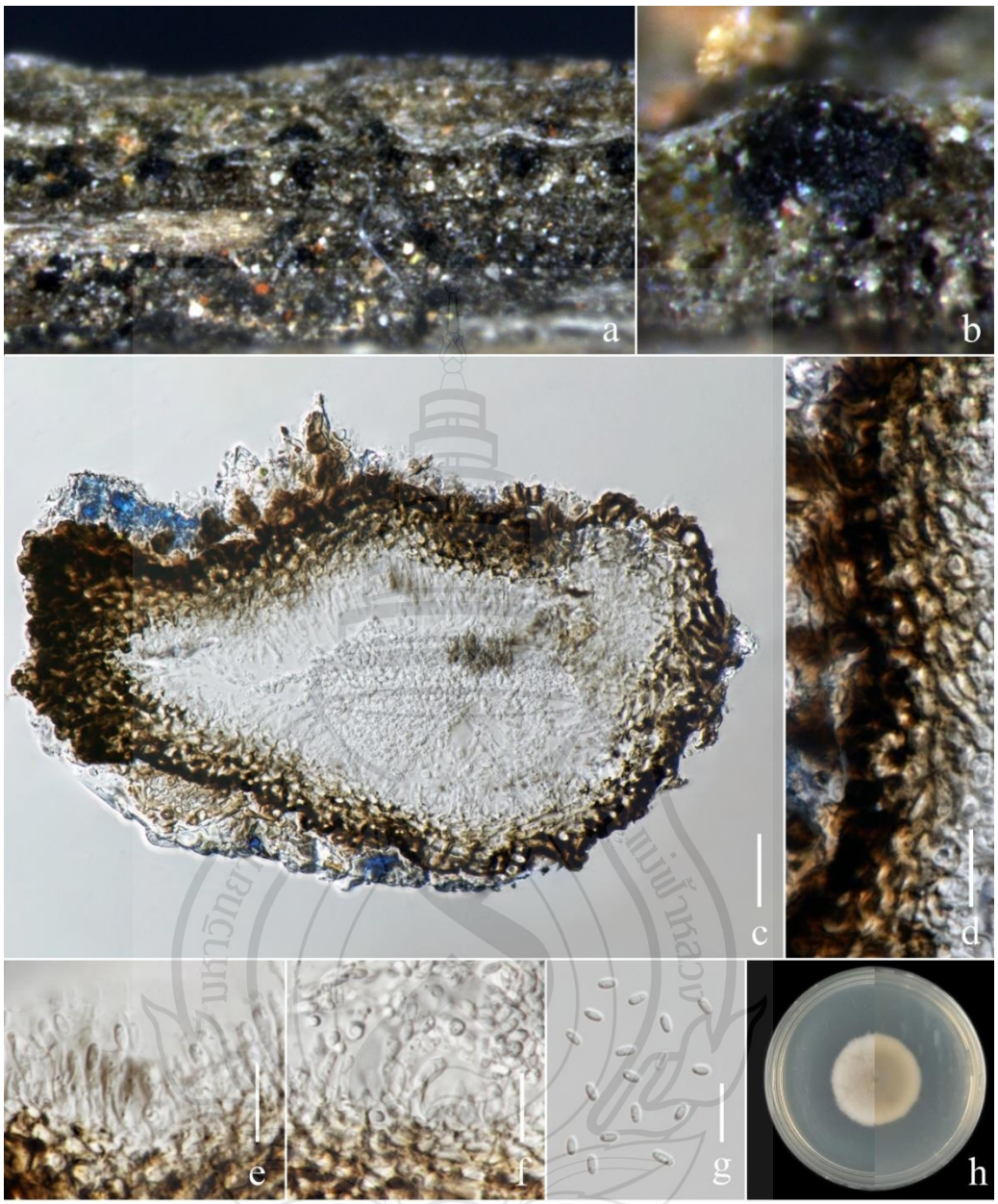
Known distribution: China (this study).

Material examined: China, Jiangxi Province, Ganzhou City, Xingda Restaurant, on dead leaf sheath of *Phoenix sylvestris*, 9 Apr 2024, Y.R. Xiong, XG362 (MHZU 24-0456, holotype), ex-type ZHKUCC 25-0019, other living culture ZHKUCC 25-0020.

GenBank numbers: ZHKUCC 25-0019: ITS – PV578186, LSU – PV578350, SSU – PV578504, *tef* 1-α – PV608854; ZHKUCC 25-0020: ITS – PV578187, LSU – PV578351, SSU – PV578505, *tef* 1-α – PV608855.

Notes: Two collections from this study formed a separate lineage in the Pleosporales phylogenetic tree with 98% ML and 1.00 BYPP bootstrap support (Figure 2.26). Based on a MegaBLAST (Query cover ≥ 70%) search using the ITS sequence, the closest matches in NCBIs GenBank nucleotide database were *Lorrainsmithia elkeae* (GenBank PQ066529; Identities 404/465 (86.88%), 16 gap), *Trichomerium syzygii* (GenBank MN901487; Identities 405/466 (86.91%), 17 gaps) and *Pseudocercospora sphaerellae-eugeniae* (GenBank KC731558; Identities 402/466 (86.27%), 21 gaps). The highest similarities using the LSU sequence were *Trichomerium syzygii* (GenBank MN901474; Identities 785/813 (96.56%), 0 gaps), Ascomycota sp. (GenBank MH323446;

Identities 887/919 (96.52%), 3 gaps) and *Lorrainsmithia elkeae* (GenBank PQ060439; Identities 832/865 (96.18%), 1 gaps). The highest similarities using the SSU sequence were *Ophiosphaerella herpotricha* (GenBank KC841054; Identities 1022/1051 (97.24%), 4 gaps), *Neomassaria* sp. (GenBank ON804892; Identities 1017/1046 (97.23%), 4 gaps) and *Triseptatospora calami* (GenBank NG_242833; Identities 1016/1047 (97.04%), 4 gapss). The highest similarities using the *tef* 1-α sequence were *Tamaricicola muriformis* (GenBank KU600013; Identities 880/935 (94.12%), 0 gap), *Bambusicola meishanensis* (GenBank PQ278548; Identities 896/956 (93.72%), 1 gaps) and *Pyrenochaeta* sp. (GenBank LT797110; Identities 920/984 (93.50%), 1 gaps). *Ganzhomyces phoenicis* were distinct by oval to irregulate elliptical and unilocular conidiomata, and conidia are unicellular and oblong or ellipsoidal. Based on phylogenetic placement and morphological variations, we introduce *Ga. phoenicis* as a new species.



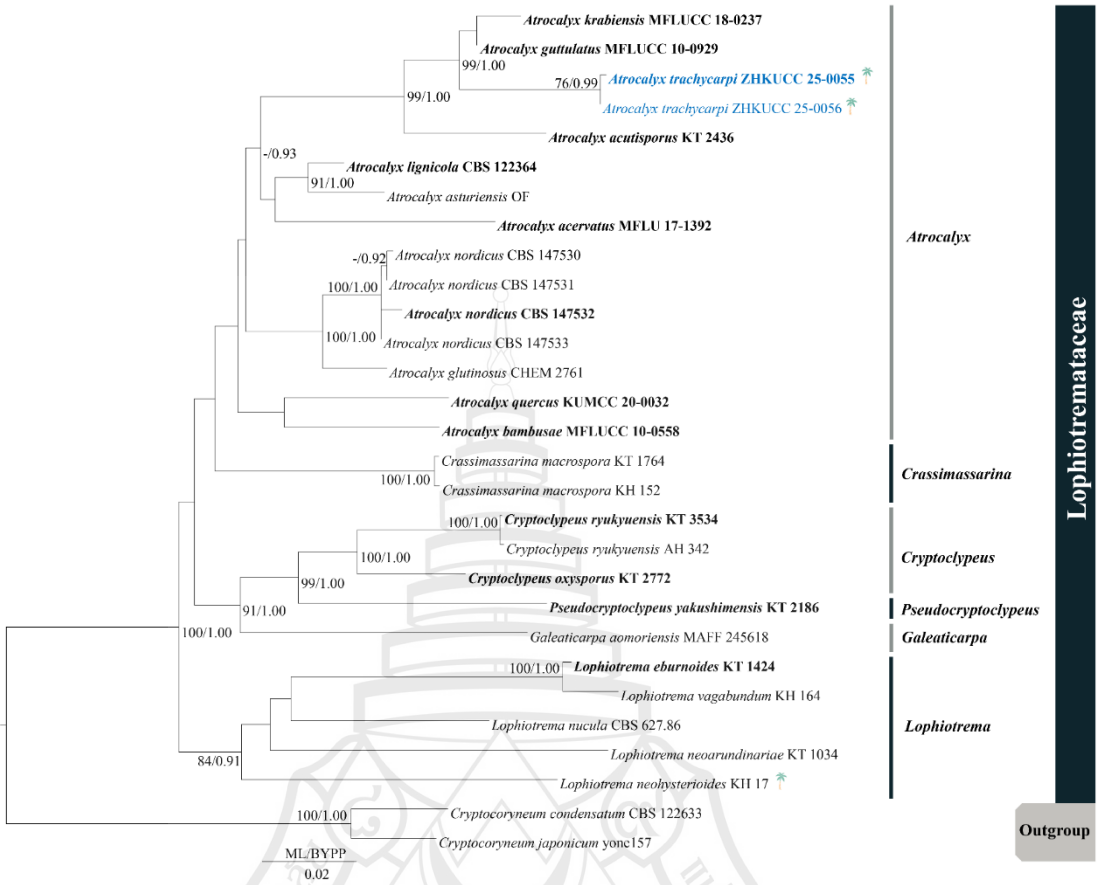
Note a, b Conidiomata on the substrate. c Sections through conidiomata. d Peridium. e, f Conidiogenous cells and developing conidia. g Conidia. h The front of culture on PDA at 25°C and the reverse of culture on PDA at 25°C. Scale bars: c = 20 µm, d–g = 10 µm.

Figure 2.28 *Ganzhomyces phoenicis* (MHZU 24-0456, holotype)

Lophiotremataceae K. Hiray. & Kaz. Tanaka, Mycoscience 52: 405 (2011)

Atrocalyx A. Hashim. & Kaz. Tanaka, Persoonia 39: 59 (2017)

Notes: Hashimoto et al. (2017) established *Atrocalyx* (*A*.) with *A. acutisporus* as the type species based on morphological evidence and phylogenetic analysis combined SSU, ITS, LSU, *tef* 1-α and *rpb*2 sequence data. *Atrocalyx* is a holomorphic genus, with the asexual morph characterized by pycnidial conidiomata which are globose to subglobose, superficial, black, ostiolate, holoblastic, ampliform to cylindrical, hyaline conidiogenous cells, and ellipsoidal, hyaline, smooth, aseptate conidia. The sexual morph is characterized by solitary to grouped, semi-immersed to immersed ascomata with a crest-like, elongated ostiolar neck, a peridium with two zones, septate, branched, and anastomosed pseudoparaphyses, and bitunicate, fissitunicate, cylindrical, 8-spored asci, with broadly fusiform, hyaline, 1- to multi-septate, and smooth ascospores (Hashimoto et al., 2017; Jayasiri et al., 2019; Hyde et al., 2020a; Andreasen et al., 2021). Subsequently, phylogenetic studies mainly use SSU, ITS, LSU, *tef* 1-α and *rpb*2 or without SSU for analysis (de Silva et al., 2018; Jaklitsch et al., 2018; Jayasiri et al., 2019; Hyde et al., 2020a, 2020b; Andreasen et al., 2021; Mack et al., 2024). In this study, we use ITS, LSU, *rpb*2 and *tef* 1-α to update phylogenetic studies for *Atrocalyx* (Figure 2.29). Ten epithets are listed under *Atrocalyx* (Index Fungorum, 2024), and all species have molecular data. Here we described a new species of *Atrocalyx* which is the first time the genus has been reported from palms (Xiong et al., 2025).



Note Phylogram generated from maximum likelihood analysis of *Atrocalyx* based on combined ITS, LSU, *rpb*2 and *tef* 1-α sequence data. Bootstrap values for maximum likelihood (ML) equal to or greater than 70 are indicated above the branches. The new collections are indicated in blue and ex-type strains are indicated in bold.

Figure 2.29 hylogenetic tree of *Atrocalyx*

Atrocalyx trachycarpi Y.R. Xiong, Manawas. & K.D. Hyde, ***sp. nov.***

Figure 2.30

Etymology: The epithet refers to the host species "*Trachycarpus*", from which the species was collected.

Saprobic on dead leaflet of *Trachycarpus fortune*. Asexual morph: Not observed. Sexual morph: *Ascomata* 300–370 × 170–200 µm ($\bar{x}$ = 343 × 183 µm, n = 10), multilocular, solitary, scattered, immersed, erumpent through host surface, sub-globose, ostiolate. *Ostiolar neck* 30–45 × 45–50 µm ($\bar{x}$ = 39 × 47 µm, n = 10), dark, carbonaceous, fragile, with irregular opening, plugged by periphyses. *Peridium* 20–60 µm, composed of

dark cells of *textura angularis*, inner layer of light pigmented to hyaline cells of *textura angularis*. *Hamathecium* 1.5–2.5 µm wide, dense, branched, septate, cylindrical pseudoparaphyses. *Asci* 65–100 × 9–13 µm ($\overline{x}$ = 78 × 11 µm, n = 25), 8-spored, bitunicate, fissitunicate, cylindrical, with a short furcate pedicel, apically rounded with an ocular chamber. *Ascospores* 18–22 × 4.5–8 µm ($\overline{x}$ = 20 × 6 µm, n = 25), biseriate, ellipsoidal to broadly fusiform, constricted at sub-medially of each cell, 1-septate, constricted at the septum, with distinct large guttules in each cell, surrounded by a thick mucilaginous sheath.

Culture characteristics: Colonies on PDA fast growing, after 2 weeks reaching 3.5 cm diam., at 25°C, colonies dense, circular, flattened, raised surface rough with crenate edge, velvety, colour of colonies in the upper part: dark grey at the margin light grey at the centre; reverse black at the margin dark grey at the centre.

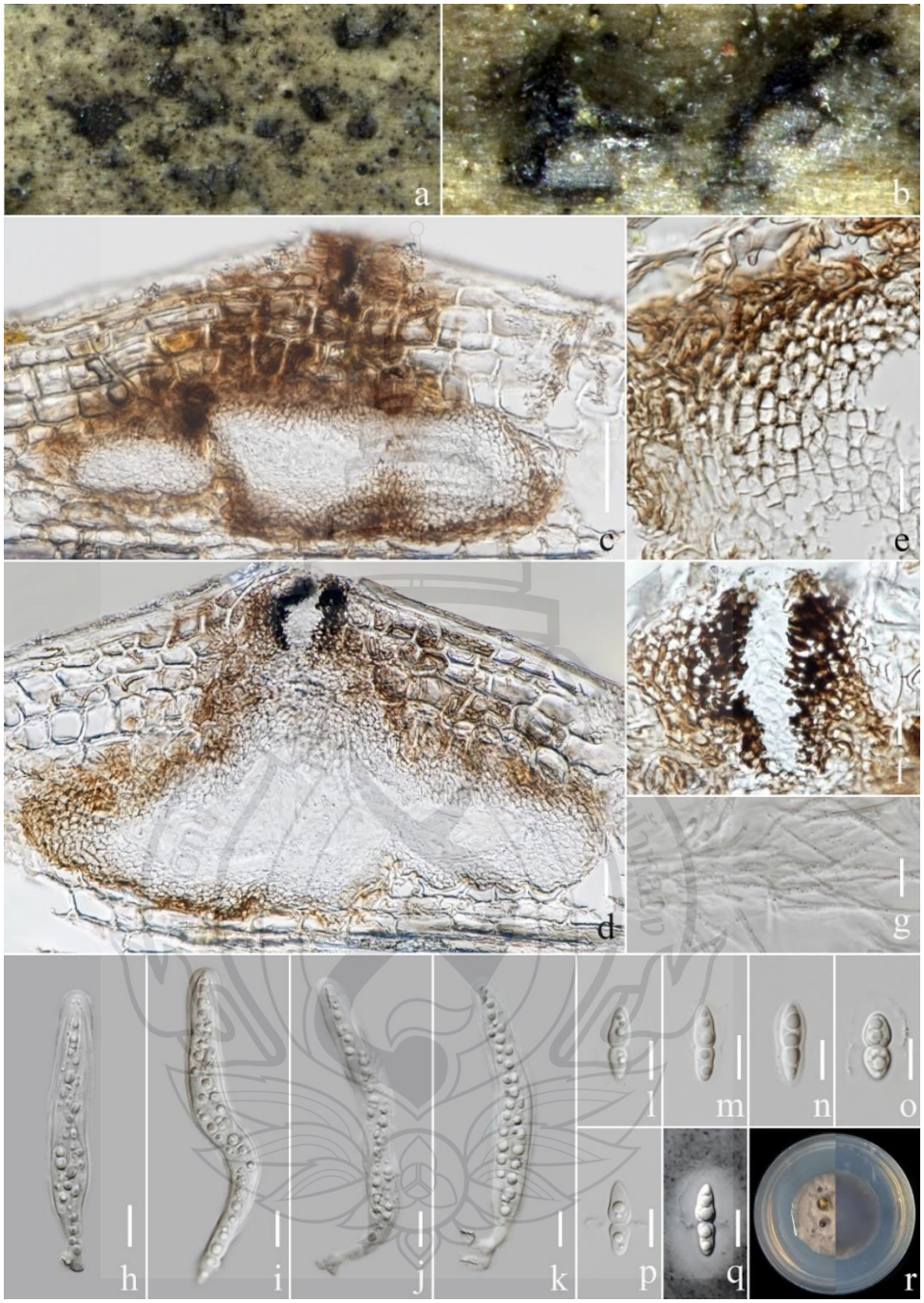
Known distribution: China (this study).

Material examined: China, Jiangxi Province, Nanchang City, The road next to Meiling National Forest Park, on a dead leaflet of *Trachycarpus fortunei*, 11 Apr 2024, Y.R. Xiong, XG399 (MHZU 24-0463, holotype), ex-type ZHKUCC 25-0055, other living culture ZHKUCC 25-0056.

GenBank numbers: ZHKUCC 25-0055: ITS – PV578134, LSU – PV578304, *tef* 1-α – PV608818, *rpb*2 – PV595306; ZHKUCC 25-0056: ITS – PV578135 LSU – PV578305, *tef* 1-α – PV608819, *rpb*2 – PV595307.

Notes: Two collections from this study clustered in *Atrocalyx* clade and formed a sister lineage to *A. guttulatus* and *A. krabiensis* in the phylogenetic tree with 99% ML and 1.00 BYPP bootstrap support (Figure 2.29). The nucleotide differences excluding gaps between *A. trachycarpi* and its phylogenetically related species were checked: *A. guttulatus* (MFLUCC 10-0929) - LSU: 0.23% (2/858 base pairs), and *tef* 1-α: 5.14% (47/914 base pairs); *A. krabiensis* (MFLUCC 18-0237) - ITS: 5.86% (27/461 base pairs), LSU: 0.35% (3/870 base pairs), and *tef* 1-α: 2.22% (20/900 base pairs). *Atrocalyx trachycarpi* differs from *A. guttulatus* and *A. krabiensis* by multilocular ascomata. Moreover, *A. guttulatus*, characterized by uniseriate ascospores with terminal appendages, is clearly distinguished from *A. trachycarpi*, which has biseriate ascospores surrounded by a thick mucilaginous sheath (Tibpromma et al., 2017). In addition, *A. krabiensis*, which has 1–6-septate ascospores, can be differentiated from *A. trachycarpi*, which has 1-septate ascospores (Jayasiri et al., 2019). Based on phylogenetic placement and morphological variations, we

introduce *A. trachycarpi* as a new species.

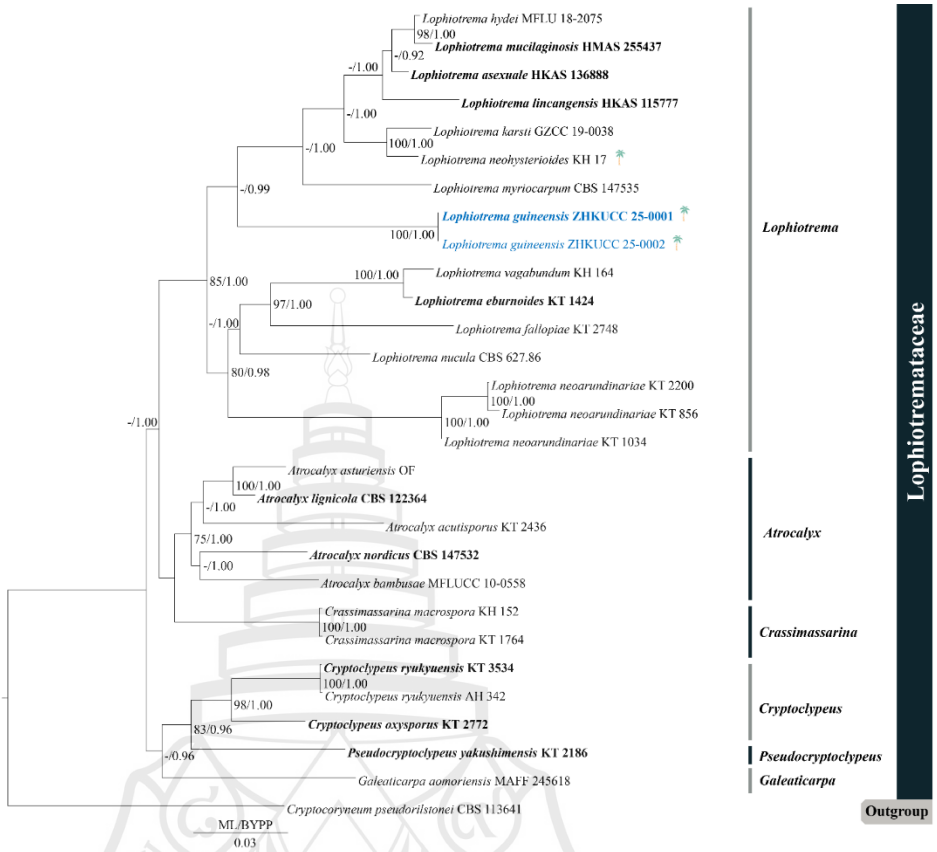


Note a, b Ascomata on substrate. c, d Vertical sections of ascomata. e Cells of peridium. f Ostiolar neck. g Pseudoparaphyses. h–k Asci. l–q Ascospores (q ascospore in Indian ink). r The front of culture on PDA at 25°C and the reverse of culture on PDA at 25°C. Scale bars: c = 50 µm, d = 20 µm, e–q = 10 µm.

Figure 2.30 *Atrocalyx trachycarpi* (MHZU 24-0463, holotype)

Lophiotrema Sacc., Michelia 1 (no. 3): 338 (1878)

Notes: Saccardo 1878 established *Lophiotrema* (*L.*), and Chesters and Bell (1970) synonymized this genus with *Lophiostoma*, arguing that neither ascospore color nor the number of transverse septa provided a sufficient basis for generic distinction. However, Holm and Holm (1988) restore *Lophiotrema* based on cylindrical or oblong asci and nearly equal thickness of peridium. *Lophiotrema* is characterized by ascomata with a slit-like ostiole and nearly equal in thickness to peridium, cylindrical or oblong asci (Hirayama & Tanaka, 2011; Hashimoto et al., 2017). Moreover, although the asexual morph of *Lophiotrema* was reported in *Pleurophomopsis* and characterized by pycnidial, this connection has never been successfully demonstrated (Leuchtmann, 1985; Zhang et al., 2009; Li et al., 2020). Zhang et al. (2009) updated phylogenetic analysis using combined LSU, SSU, *tef* 1-α, *rpb*1 and *rpb*2 for *Lophiotrema.* Subsequently, phylogenetic studies mainly use LSU, ITS, SSU, *tef* 1-α, *rpb*2 or only LSU and SSU for analysis (Tibpromma et al., 2017; Phookamsak et al., 2019; Li et al., 2023). In this study, we use ITS, LSU, *rpb*2 and *tef* 1-α to update phylogenetic studies for *Lophiotrema* (Figure 2.31). Currently, 48 epithets are listed under *Lophiotrema* (Index Fungorum, 2024 December), but only 12 species have molecular data. Three species have been reported from palms including a new species described in this study (Xiong et al., 2025).



Note Phylogram generated from maximum likelihood analysis of Lophiotremataceae based on combined ITS, LSU, *rpb*2 and *tef* 1-α sequence data. Bootstrap values for maximum likelihood (ML) equal to or greater than 70 are indicated above the branches. The new collections are indicated in blue and ex-type strains are indicated in bold.

Figure 2.31 Phylogenetic tree of Lophiotremataceae

Lophiotrema guineensis Y.R. Xiong, Manawas. & K.D. Hyde, ***sp. nov.***

Figure 2.32

Etymology: The epithet refers to the host species "*Elaeis guineensis*", from which the species was collected.

Saprobic on dead petiole of *Elaeis guineensis*. Asexual morph: Coelomycetous. *Conidiomata* 170–200 × 100–130 µm ($\overline{x}$ = 182 × 112 µm, n = 10), pycnidial, immersed, solitary, coalescing, hemispherical or pyriform, unilocular, cracks epidermis of substrate. *Peridium* 15–25 µm, composed of thick-walled, brown cells, inner wall with hyaline cells, *textura angularis*. *Conidiophores* reduced to conidiogenous cells. *Conidiogenous cell* 2–5

× 1–2 µm ($\overline{x}$ = 3.4 × 1.5 µm, n = 25), enteroblastic, phialidic to cylindrical, hyaline, smooth-walled, arising from stratum. *Conidia* 5–7 × 2–3 µm ($\overline{x}$ = 6 × 2.3 µm, n = 25), spermatia, oblong to ellipsoid, slightly curved, truncate to rounded, aseptate, hyaline, 1–2 small guttule within the cell. Sexual morph: Not observed.

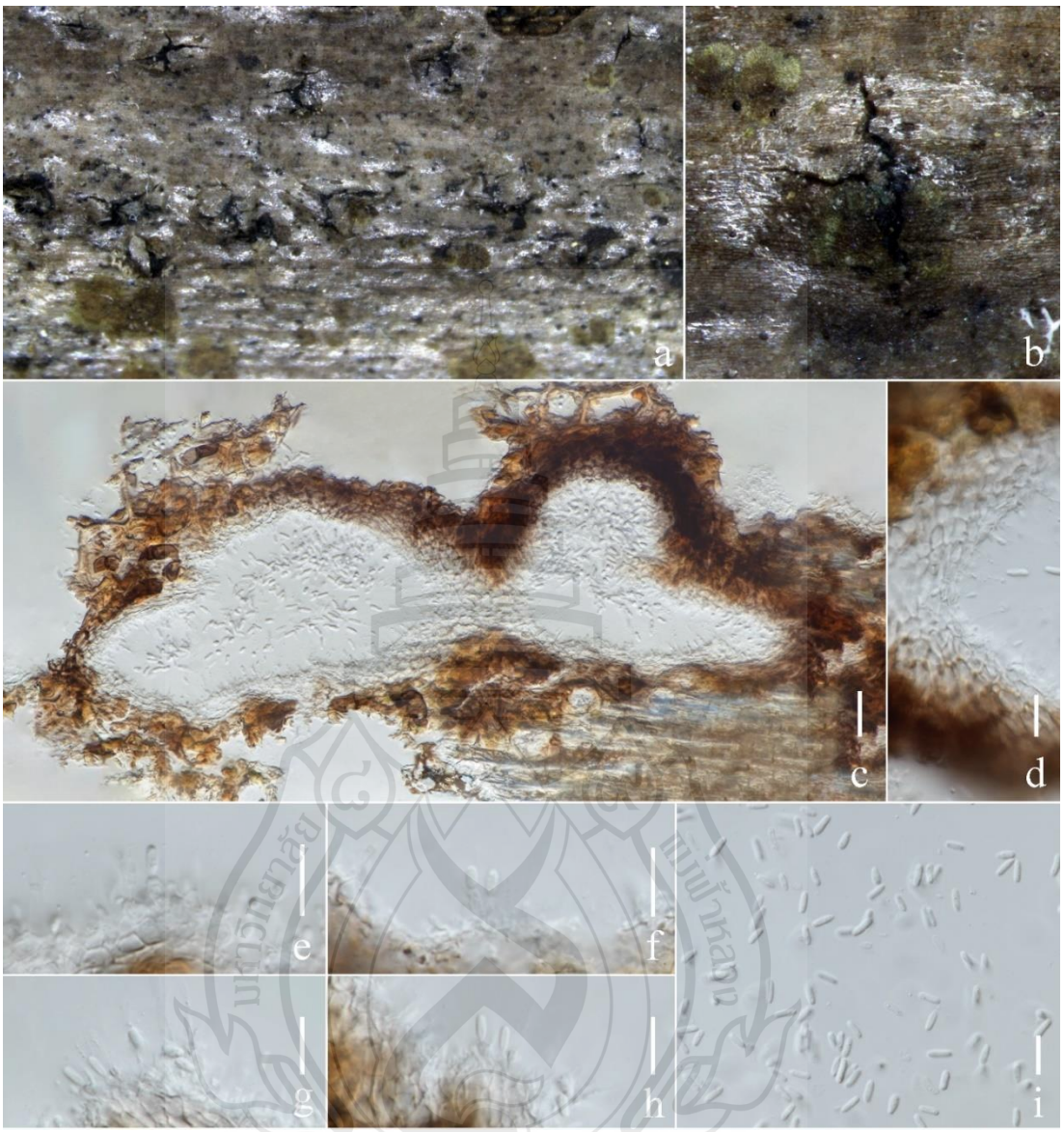
Culture characteristics: Colonies on PDA fast growing, after 2 weeks reaching 4 cm diam., at 25°C, circular, with fluffy, dense, white mycelium on the surface with entire margin; in reverse yellow in the middle and white at the margin.

Known distribution: China (this study).

Material examined: China, Yunnan Province, Xishuangbanna City, in an unidentified forest beside National Highway 219, on dead petiole of *Elaeis guineensis*, 5 Feb 2023, Y.R. Xiong and L. Lu, XG175 (MHZU 24-0451, holotype), ex-type ZHKUCC 25-0001, other living culture ZHKUCC 25-0002.

GenBank numbers: ZHKUCC 25-0001: LSU – PV578362, *tef* 1-α – PV608856; ZHKUCC 25-0002: LSU – PV578363, *tef* 1-α – PV608857.

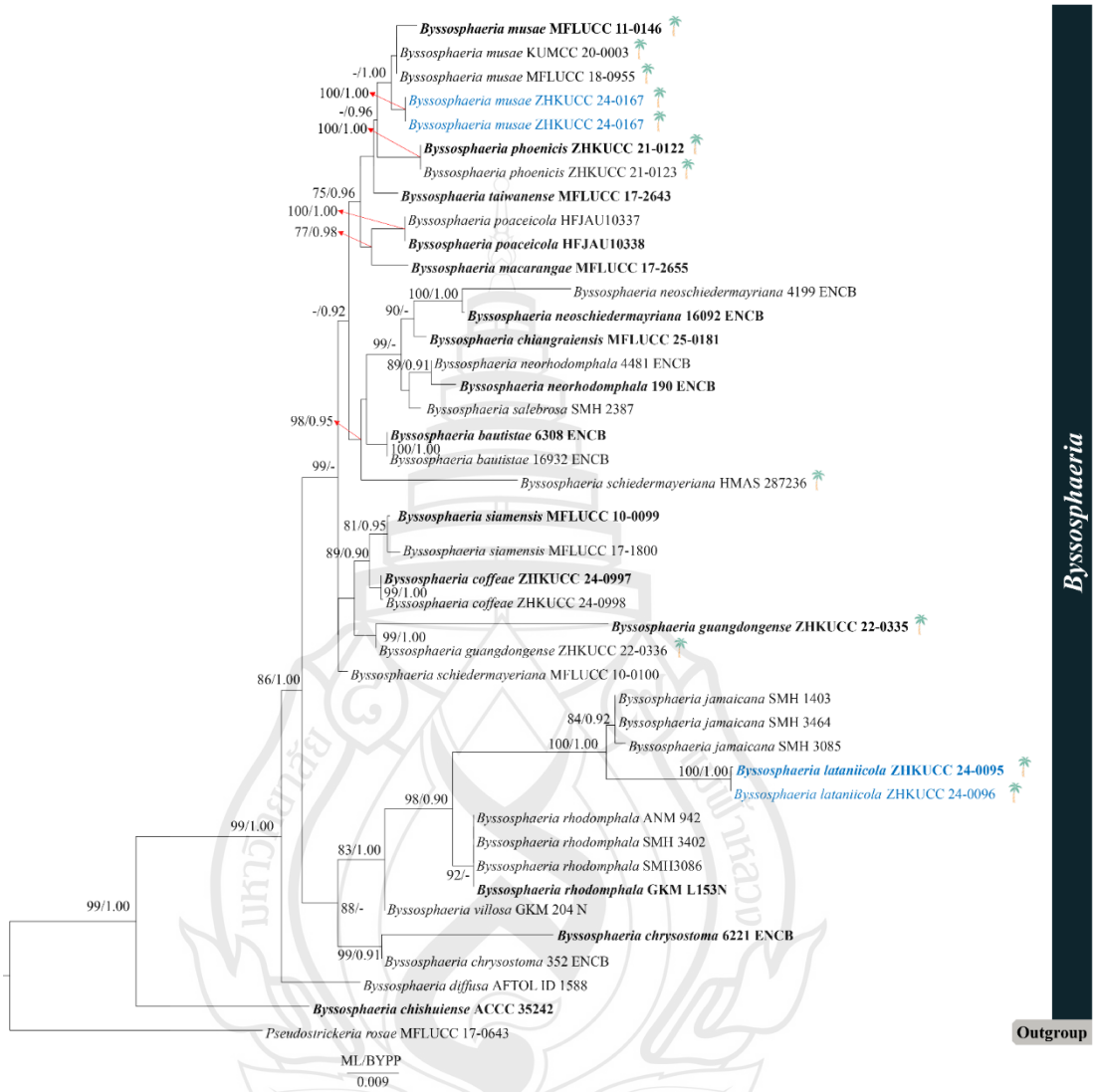
Notes: Two collections from this study formed an independent lineage within *Lophiotrema* in the phylogenetic tree with 70% ML bootstrap support and 1.00 BYPP (Figure 2.31). Based on a MegaBLAST (Query cover ≥ 70%) search using the LSU sequence, the closest matches in NCBIs GenBank nucleotide database were *L. neoarundinaria* (GenBank OR253247; Identities 842/855 (98.48%), 0 gap), *L. hydei* (GenBank OR253264; Identities 840/853 (98.48%), 0 gaps) and *L. mucilaginosis* (GenBank OQ771954; Identities 837/850 (98.47%), 0 gaps). The highest similarities using the *tef* 1-α sequence were *Atrocalyx lignicola* (GenBank GU349072; Identities 743/813 (91.39%), 1 gap), *Cryptoclypeus ryukyuensis* (GenBank LC194392; Identities 830/912 (91.01%), 2 gaps) and *L. hydei* (GenBank MK108984; Identities 838/924 (90.69%), 2 gaps). Morphologically, *Lophiotrema guineensis* fits well with *Lophiotrema* by asexual morph (Tanaka & Harada, 2003). However, *L. guineensis* is distinct in *Lophiotrema* by its asexual morph which is oblong to ellipsoid and aseptate conidia. Based on phylogenetic placement and morphological variations, we introduce *L. guineensis* as a new species.



Note a, b Conidiomata on the substrate. c Sections through conidiomata. d Peridium. e–h Conidiogenous cells and developing conidia. i Conidia. Scale bars: c = 20 µm, d–i = 10 µm.

Figure 2.32 *Lophiotrema guineensis* (MHZU 24-0451, holotype)

Melanommataceae G. Winter, Rabenh. Krypt. -Fl., Edn 2 (Leipzig) 1.2: 220 (1885)



Note Phylogram generated from maximum likelihood analysis of *Byssosphaeria* based on combined ITS, LSU, SSU and *tef* 1-α sequence data. Bootstrap values for maximum likelihood (ML) equal to or greater than 70 are indicated above the branches. The new collections are indicated in blue and ex-type strains are indicated in bold.

Figure 2.33 Phylogenetic tree of *Byssosphaeria*

Byssosphaeria Cooke, Grevillea 7(no. 43): 84 (1879)

Notes: Cooke (1879) introduced *Byssosphaeria* (*B*.) with *B. keithii* as the type species. *Byssosphaeria* was once considered to be assigned to *Herpotrichia* (Bose, 1961; Sivanesan, 1971; von Arx & Müller, 1975). *Byssosphaeria* was reinstated as a genus by Barr (1984) and formally described later (Barr, 1990). Most of the *Byssosphaeria* species are reported in sexual morphs which is characterized by the superficial ascomata, usually gregarious, with bright yellow, orange or red fat ostiole, and a subiculum of dense hypha around the ascomata, with fusiform, hyaline to pale brown ascospores, surrounded by a mucilaginous sheath that is drawn out at both ends (Barr, 1990; Tian et al., 2015). Mugambi and Huhndorf (2009) conducted the first phylogenetic analysis of *Byssosphaeria* using combined LSU and *tef* 1-α sequences, which supported *Byssosphaeria* as a distinct genus within Melanommataceae. Subsequent phylogenetic studies primarily used LSU, SSU, *tef* 1-α, and, with or without, *rpb*2 or ITS for analysis (Zhang et al., 2012; Liu et al., 2015; Tian et al., 2015; Tibpromma et al., 2018; Hongsanan et al., 2020; Yang et al., 2022; Kularathnage et al., 2022; Tennakoon et al., 2024; Zhang et al., 2024). In this study, we use ITS, LSU, SSU and *tef* 1-α to update phylogenetic studies for *Byssosphaeria* (Figure 2.33). Currently, 29 epithets are listed under *Byssosphaeria* (Index Fungorum 2024), but only 15 species have molecular data. Five species have been reported from palms including a new species described in this study (Xiong et al., 2025).

Byssosphaeria guangdongense Y.R. Xiong, Manawas. & K.D. Hyde, ***sp. nov.***

Figure 2.34

Etymology: Species Epithet refers to the locale from where the fungus was isolated.

Saprobic on rotting branch of *Phoenix roebelenii* O'Brien., (*Arecaceae*). *Sexual morph*: Ascomata 480–640 length, 310–500 µm diam ($\bar{x}$ = 540 × 378 µm, n = 10), globose to subglobose, superficial, with dehiscent base, middle collapsed of the top, unilocular, black, scattered to gregarious, conspicuous at the surface, black, hairy, ostiole, with pore-like opening, surrounded discoid by orange to light brown. Setae 4.5–7 µm wide, filiform, brown to black, septate. Ostiole collapsed, comprised of orange to light brown angular cells. Peridium 40–70 µm wide, thick-walled, of equal thickness, multi-layered, outer layers dark-brown to black, textura angularis; inner layer 25–40 µm wide, hyaline, and some areas are light yellow, textura prismatica. Hamathecium 1.5–3 µm wide, hypha-like, unbranched,

bushy, septate, filamentous. Asci 110–160 × 10–25 µm ($\overline{x}$ = 138 × 15 µm, n = 50), 8-spored, bitunicate, fissitunicate, long pedicellate with club-like, rounded, with a small ocular chamber at the apex of asci. Ascospores 30–40 × 5–10 µm, ($\overline{x}$ = 33 × 6 µm, n = 50), bi-seriate, oblong to fusiform, 1-septate, lightly constricted at the septate, verrucose, slightly curved, initially hyaline, maturity brown, surrounded by a thick gelatinous sheath. *Asexual morph*: Not observed.

Culture Characteristics: Colonies on PDA attaining 8 cm diam after a week at 25°C, irregular, undulate, dull, white aerial mycelium mixed with yellow; reverse pale brown with yellow.

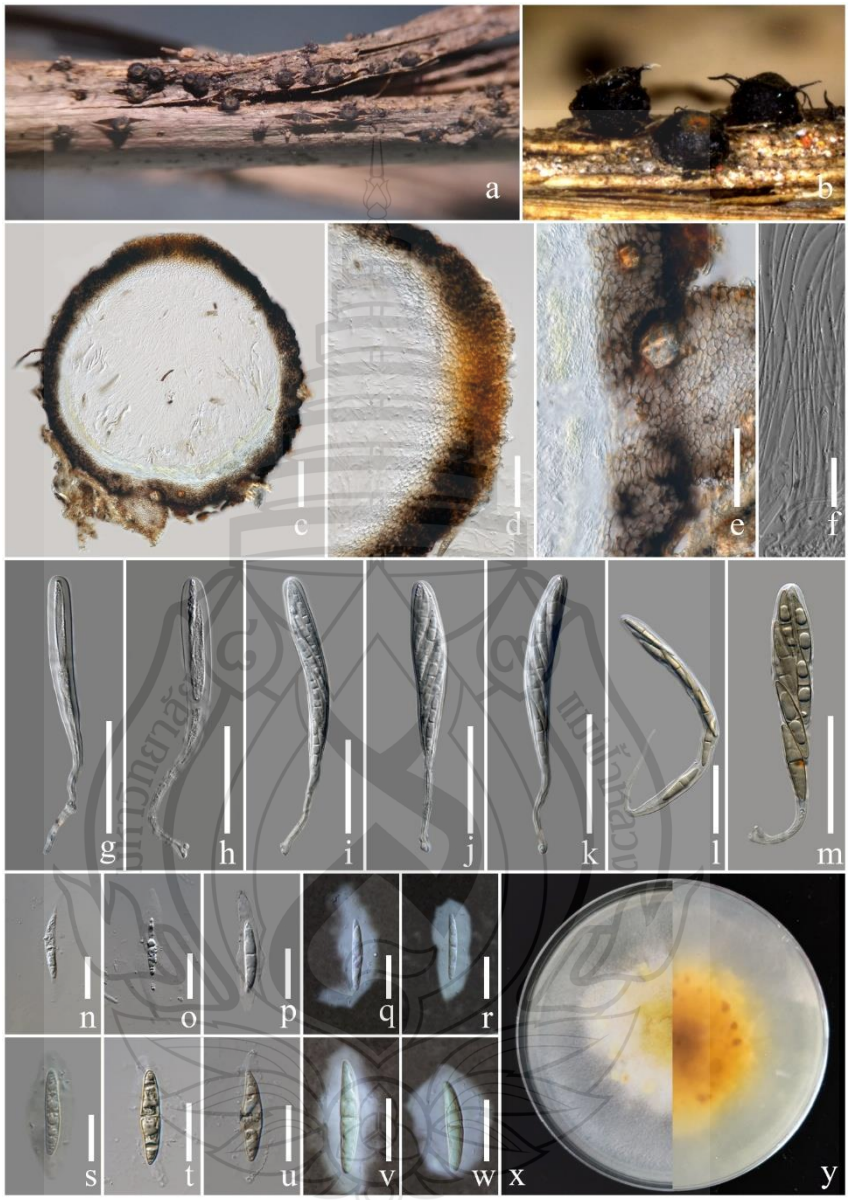
Known distribution: China (this study).

Material examined: China, Guangdong Province, Guangzhou City, Zhongkai University of Agriculture and Engineering (23°6'14" N, 113°16'34" E), rotting branch of the *Phoenix roebelenii* (*Arecaceae*), 12 August 2021, Y.R. Xiong (MHZU 22-0177, holotype; ex-type culture, ZHKUCC 22-0335); ibid. 12 August 2021, Y.R. Xiong (living culture, ZHKUCC 22-0336).

GenBank numbers: ZHKUCC 22-0335: ITS – OQ449320, LSU – OQ449288, SSU – OQ449337; ZHKUCC 22-0336: ITS – OQ449321, LSU – OQ449289, SSU – OQ449338.

Notes: In the phylogenetic tree, two collections from this study developed a clade with 99% ML and 87% MP bootstrap support and 0.99 BYPP value. Our species; *Byssosphaeria guangdongense* is closely related to *B. schiedermayeriana*. (MFLUCC 10-0100). *Byssosphaeria schiedermayeriana* was reported as 1−(3−5−) septate by Barr (1984), or 1−3-septate by Hyde et al. (1999). *Byssosphaeria guangdongense* is different from *B. schiedermayeriana* by 1-septate. In addition, *B. schiedermayeriana* with thin sheath extending at the apices (Hyde et al., 1999), and protruding at ends as appendages (Tanaka & Hosoya, 2006) although the sheath was not mentioned by Barr (1984). However, *B. guangdongense* has a thick sheath surrounding the spores, and no appendages. The nucleotide difference between *Byssosphaeria guangdongense* and its phylogenetically related species are *B. schiedermayeriana*. (MFLUCC 10-0100) LSU: 1.17% (9/765 bases) excluding gaps, SSU are similar in this clade. Furthermore, *B. phoenicis* was reported same host and location as the above collections. It is different from *B. guangdongense* by swells around the septum and protruding at both ends of a thin sheath, as well as branches with

significantly different taxonomic positions on the phylogenetic tree. Combining both phylogeny and morphological evidence, collections obtained in this study were identified as a new *Byssosphaeria* species.



Note a–b, Ascomata on the branch of *Phoenix roebelenii*; c–d, Section of ascomata; e, Peridium; f, Hamathecium; g–m, Asci; n–w, Ascospores; x–y, Culture on PDA from above and reverse. Scale bars c = 100 µm (c). d–e = 50 µm. f = 20 µm. g–m = 50 µm. n–w = 20 µm.

Figure 2.34 *Byssosphaeria guangdongense* (MHZU 22-0177, holotype)

Byssosphaeria lataniicola Y.R. Xiong, Manawas. & K.D. Hyde, ***sp. nov.***

Figure 2.35

Etymology: The epithet refers to the host genus "*Latania*", from which the species was collected.

Saprobic on dead segment of *Latania verschaffeltii*. Asexual morph: Not observed. Sexual morph: *Ascomata* 480–500 × 470–500 μm ($\bar{x}$ = 493 × 484 μm, n = 10), perithecial, clusters on surface or semi-immersed, superficial, subglobose, dark brown, coriaceous, ostiolated canal, setae 5.7 μm. *Peridium* 60–95 μm wide, comprising two cell types, outer layer comprising thick brown *textura prismatica* cell layers, and inner composed of thin hyaline *textura angularis* cells to *textura globosa*. *Hamathecium* 2–3 μm wide, composed of dense, trabeculate, branched, anastomosing, pseudoparaphyses, embedded in a hyaline gelatinous matrix. *Asci* 120–150 × 13–16 μm ($\bar{x}$ = 140 × 14.7 μm, n = 30), 8-spored, bitunicate, fissitunicate, cylindric-clavate, knob-like to furcated-like pedicel, apically rounded, with ocular chamber. *Ascospore* 30–35 × 7–9 μm ($\bar{x}$ = 32 × 7.9 μm, n = 30), overlapping 1–2-seriate, fusiform with acute ends, hyaline to brown, 1–3-septate, straight to slightly curved, slightly constricted at septum, smooth-walled, guttulate, surrounded by a gelatinous sheath when hyaline, delicate, sometimes appearing as a wing-like expansion near the central septum

Culture characteristics: Colonies on PDA reaching 28 mm diameter after 1 week at room 25°C, circular, convex, effuse, velvety to fluffy, light orange to white from the above; yellowish-brown at the centre, yellowish brown to orange at the margin from the reverse.

Known distribution: China (this study).

Material examined: China, Yunnan Province, Xishuangbanna City, in an unidentified forest beside National Highway 219, on dead segment of *Latania verschaffeltii*, 5 Feb 2023, Y.R. Xiong and L. Lu, XG165 (MHZU 23-0144, holotype), ex-type ZHKUCC 24-0095, other living culture ZHKUCC 24-0096.

GenBank numbers: ZHKUCC 24-0095: ITS – PV578138, LSU – PV578308, SSU – PV578486, *tef* 1-α – PV608820; ZHKUCC 24-0096: ITS – PV578139, LSU – PV578309, SSU – PV578487, *tef* 1-α – PV608821.

Notes: Two collections from this study formed a separate lineage and clustered with *Byssosphaeria jamaicana* in the phylogenetic tree with 100% ML bootstrap support

and 1.00 BYPP (Figure 2.33). The nucleotide differences excluding gaps between *B. lataniicola* and *B. jamaicana* were checked: LSU: 2.04% (18/882 base pairs), and *tef* 1-α: 1.92% (14/730 base pairs). *Byssosphaeria lataniicola* is characterized by 1–3-septate ascospores, which differ from the strongly constricted ascospores of *B. jamaicana* which possess a single median septum (Niranjan & Sarma, 2019). In addition, *B. lataniicola* have a gelatinous hyaline sheath of ascospores which is not observed in *B. jamaicana* (Niranjan & Sarma, 2019). Based on phylogenetic placement and morphological variations, we introduce *B. lataniicola* as a new species.



Note a, b Ascomata on substrate. c Vertical sections of ascomata. d Cells of peridium. e Setae. f Pseudoparaphyses. g–k Asci. l–o Ascospores. p Germinating conidium. q the front of culture on PDA at 25℃ and the reverse of culture on PDA at 25℃. Scale bars: c = 100 µm, d–p = 10 µm.

Figure 2.35 *Byssosphaeria lataniicola* (MHZU 23-0144, holotype)

Byssosphaeria musae Phookamsak & K.D. Hyde, Fungal Diversity 72: 119 (2015)

Figure 2.36

Saprobic on dead segment of *Borassus flabellifer*. Asexual morph: Not observed. Sexual morph: *Ascomata* 400–450 × 370–400 μm ($\bar{x}$ = 420 × 395 μm, n = 10), gregarious, scattered, superficial on subiculum, visible as dark spots on host, orange to yellow around pore, uni-loculate, globose to subglobose, setose, apex rounded, ostiole central, with pore-like opening, setae 5.5 μm. *Peridium* 60–100 μm wide, thick-walled, of equal thickness, composed of several layers of dark brown to black cells, arranged in *textura angularis* to *textura prismatica*. *Hamathecium* 1–2 μm wide, composed of dense, trabeculate, distinctly septate, anastomosing, pseudoparaphyses, embedded in a hyaline gelatinous matrix. *Asci* 75–135 × 10–15 μm ($\bar{x}$ = 108 × 13.7 μm, n = 25), 8-spored, bitunicate, fissitunicate, clavate, long pedicellate with knob-like pedicel, apically rounded, with well-developed ocular chamber. *Ascospores* 30–35 ×5–8 μm ($\bar{x}$ = 32 × 7 μm, n=30), overlapping 1–2-seriate, fusiform, with acute ends, hyaline to pale brown when young, becoming light brown at maturity, 1(–3)-septate, not constricted at the septa, slightly curved, smooth-walled, bearing delicate hyaline appendages over ends with wing-like appendages near the central septum.

Culture characteristics: Colonies on PDA growing, 40 mm diam., after 1 week at 25°C, circular, white to cream or pale yellowish, intermixed with yellowish to orangish hyphae; reverse cream to white yellowish at the margin, yellowish-brown at the centre, medium dense to dense, irregular, flattened to slightly raised, fluffy to feathery, effuse.

Known distribution: China (Hyde et al., 2020; Zhang et al., 2024, this study), Thailand (Liu et al., 2015).

Material examined: China, Yunnan Province, Xishuangbanna City, Xishuangbanna Dai Nationality Park, on dead segment of *Borassus flabellifer*, 5 Feb 2023, Y.R. Xiong and L. Lu, XG250 (MHZU 23-0180, new host record), living cultures ZHKUCC 24-0167, ZHKUCC 24-0168.

GenBank numbers: ZHKUCC 24-0167: ITS – PV578140, LSU – PV578310, SSU – PV578488, *tef* 1-α – PV608822; ZHKUCC 24-0168: ITS – PV578141, LSU – PV578311, SSU – PV578489, *tef* 1-α – PV608823.

Notes: Two collections obtained in this study clustered with *Byssosphaeria musae* by 97% ML bootstrap support and 1.00 BYPP (Figure 2.33). The nucleotide differences excluding gaps between our collections and *B. musae* (MFLUCC 11-0146) in ITS is 0.59% (4/675 base pairs), LSU: 0.62% (5/812 base pairs), SSU: 0.11% (1/933 base pairs), *tef* 1-α: 0.32% (3/938 base pairs). Morphological evidence of conidiogenous cells and hyaline conidia well fit with *B. musae* (Liu et al., 2015; Hyde et al., 2020; Zhang et al., 2024) thus we identify our collection as *B. musae*. *Byssosphaeria musae* was first introduced on the leaf sheath of *Musa* sp. from Thailand by Liu et al. (2015). Subsequently, Hyde et al. (2020) reported a new record on the decaying frond of a palm from China. Zhang et al. (2024) reported a new record on decaying rachides and petioles of *Cocos nucifera* from China. To our knowledge, this is the first record of *B. musae* from *Borassus flabellifer*.

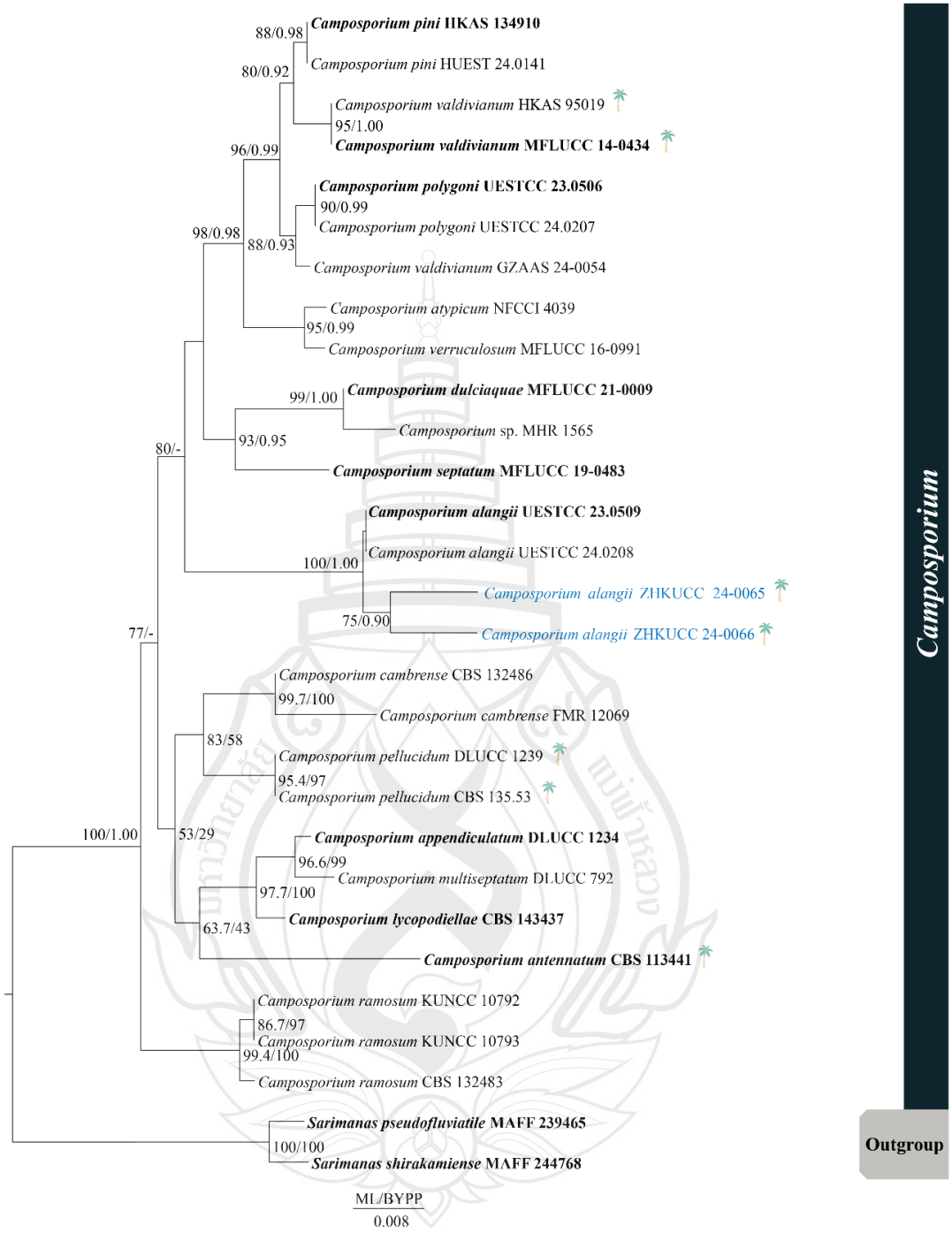


Note a, b Ascomata on substrate. c Vertical sections of ascomata. d Cells of peridium. e Setae. f–h Asci. i–m Ascospores (k ascospore in Indian ink). n Germinating conidium. o The front of culture on PDA at 25°C and the reverse of culture on PDA at 25°C. Scale bars: c = 50 µm, d–n = 10 µm.

Figure 2.36 *Byssosphaeria musae* (MHZU 23-0180, new host record)

Camposporium Harkn., Bull. Calif. Acad. Sci. 1(no. 1): 37 (1884)

Notes: Harkness (1884) proposed *Camposporium* (*Ca*.) with *Ca. antennatum* as the type species. *Camposporium* is hyphomycetous genus characterized by dematiaceous, simple conidiophores, terminal, integrated, denticulate conidiogenous cells, and the conidia are typically cylindrical and elongate, multi-septate, rounded at one or both ends, often the cells at each end are paler in pigmentation than the central cells, the apex is either simple or has one or more cylindrical appendages, the base typically has a persistent portion of the denticle attached (Hughes, 1951; Ellis, 1971; Ichinoe, 1971; Whitton et al., 2002; Koukol & Delgado, 2021). Crous et al. (2018) established the phylogenetic tree for *Camposporium* using LSU. Subsequently, phylogenetic studies mainly use SSU, LSU, ITS and *tef* 1-α or add *rpb2* to analysis (Hyde et al., 2020; Calabon et al., 2021; Tian et al., 2024). Based on phylogenetic analysis combined SSU, LSU, ITS and *tef* 1-α, *Fusiconidium* was proposed need combined under *Camposporium* (Hyde et al., 2020). Koukol and Delgado (2021) formally synonymized *Fusiconidium* as *Camposporium* according to previous phylogenetic analysis and morphological evidence. In this study, we use ITS, LSU, SSU and *tef* 1-α to update phylogenetic studies for *Camposporium* (Figure 2.37). Although 29 epithets are listed under *Camposporium* (Index Fungorum, 2024), only 13 species are associated with molecular data. Totally five species have been reported from palm species including a new species described in this study (Xiong et al., 2025).



Note Phylogram generated from maximum likelihood analysis of *Campospurium* based on combined ITS, LSU, SSU and *tef* 1-α sequence data. Bootstrap values for maximum likelihood (ML) equal to or greater than 70 are indicated above the branches. The new collections are indicated in blue and ex-type strains are indicated in bold.

Figure 2.37 Phylogenetic tree of *Campospurium*

Camposporium alangii H.Z. Du & Jian K. Liu, Mycology. 1–60 (2025)

Figure 2.38

Etymology: The epithet refers to the host genus "*Livistona*", from which the species was collected.

Saprobic on dead segment of *Livistona chinensis*. Asexual morph: Hyphomycetous. *Colonies* on natural substrate, effuse, dark brown, velvety. *Mycelium* immersed, composed of hyaline, smooth, septate, branched hyphae. *Conidiophores* 17–30 × 7–10 μm ($\overline{x}$ = 23 × 8.5 μm, n = 25) macronematous, mononematous, often procumbent on substrate, short, light brown to brown, unbranched, irregularly cylindrical, flexuous, septate, thick-walled. *Conidiogenous cells* monoblastic, terminal, integrated, subcylindrical, pale brown to hyaline. *Conidia* 50–80 (–100) × 9–13 μm ($\overline{x}$ = 69 × 11 μm, n = 25), solitary, acrogenous, dry, cylindrical, elongate or irregular crooked, light brown, paler at apex and base cell, surface rugose, 9–12(–16)-septate, apex rounded, basal cell truncate. Sexual morph: Not observed.

Culture characteristics: Colonies on PDA fast growing, after 2 weeks reaching 4 cm diam., at 25°C, mycelia superficial, circular, with entire edge, flat, rugose in the centre; in reverse yellowish.

Known distribution: China (this study).

Material examined: China, Province, Yunnan, Sanyuan District, on dead segment of *Livistona chinensis*, 29 Dec 2022, Y.R. Xiong and L. Lu, XG131 (MHZU 23-0129, new host record); ex-type culture ZHKUCC 24-0065, other living culture ZHKUCC 24-0066.

GenBank numbers: ZHKUCC 24-0065: ITS – PV578144, LSU – PV578314, SSU – PV578490; ZHKUCC 24-0066: ITS – PV578145, LSU – PV578315, SSU – PV578491.

Notes: Two collections from this study formed a separate lineage and clustered with *Camposporium dulciaquae* and *Ca. septatum* in the phylogenetic tree with 100% ML bootstrap support and 1.00 BYPP (Figure 2.37). The nucleotide differences excluding gaps, between *Ca. livistonae* and its phylogenetically related species were checked and given as follows; *Ca. dulciaquae* (MFLUCC 21-0009), ITS: 6.52% (35/537 base pairs), LSU: 0.94% (8/849 base pairs), and SSU: 1.77% (17/960 base pairs); *Ca. septatum* - ITS: 4.59% (23/501 base pairs), LSU: 1.05% (9/856 base pairs), and SSU: 1.88% (18/960 base pairs).

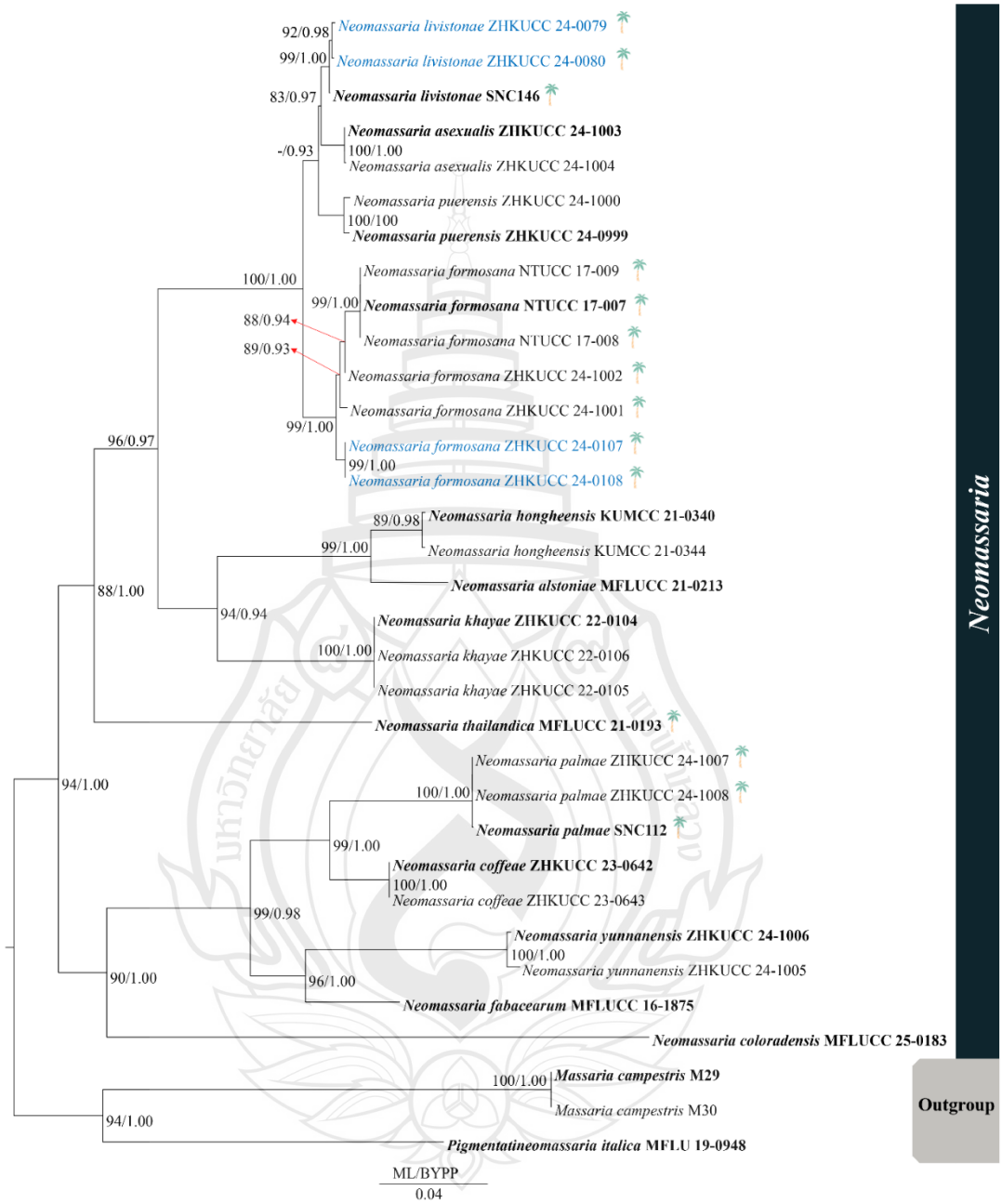
Camposporium livistonae differs from its closely related species by having no appendages at the apical cell. In addition, *Ca. dulciaquae* have 8–11-septate conidia and *Ca. septatum* have (8–)9(–11)-septate (Hyde et al., 2020; Calabon et al., 2021). However, *Ca. livistonae* has 9–12-septate conidia. Based on the phylogenetic placement and morphological variations, we introduce *Ca. livistonae* as a new species.



Note a, b Sporodochia on the substrate. c, g–i Conidia. d, e Conidiophores with conidia. f Conidia surface. j Germinating conidium. k The front of culture on PDA at 25°C and the reverse of culture on PDA at 25°C. Scale bars: c = 50 µm, d–j = 10 µm.

Figure 2.38 ***Camposporium livistonae*** (MHZU 23-0129, holotype)

Neomassariaceae Ariyaw., Jaklitsch & Voglmayr, Cryptog. Mycol. 39 (3): 367 (2018)



Note Phylogram generated from maximum likelihood analysis of *Neomassaria* based on combined ITS, LSU, SSU, *rpb*2 and *tef*1-α sequence data. Bootstrap values for maximum likelihood (ML) equal to or greater than 70 are indicated above the branches. The new collections are indicated in blue and ex-type strains are indicated in bold.

Figure 2.39 Phylogenetic tree of *Neomassaria*

Neomassaria Mapook, Camporesi & K.D. Hyde, Fungal Diversity 80: 74 (2016)

Notes: *Neomassaria* (*Neom.*) was first proposed by Hyde et al. (2016), in Massariaceae, and typified by *Neom. fabacearum*. Then the second species *Neom. formosana* was introduced by Ariyawansa et al. (2018) and proposed a new family Neomassariaceae, to accommodate this genus based on phylogenetic analyses of concatenated LSU, *RPB*2, SSU and *tef*1-α sequence, as *Neom. fabacearum* and *Neom. formosana* formed a monophyletic lineage with an uncertain phylogenetic placement within the Pleosporales (Ariyawansa et al., 2018). This genus has been reported with sexual and asexual morphs (Coelomycetous and Hyphomycetous), the sexual morph of *Neomassaria* is characterized by having immersed, subglobose to globose ascomata, central ostiole, peridium comprising cells of *textura angularis*, pseudoparaphyses, 8-spored, bitunicate oblong to cylindrical asci, with pedicellate, containing ellipsoid to fusiform, 1-septate, hyaline ascospores, and with or without a gelatinous sheath (Hyde et al., 2016; Zhang et al., 2024). The Coelomycetous asexual morph is characterized by immersed conidiomata, with ostiole central, conidiomatal wall composed of brown cells of *textura angularis*, conidiophores reduced to conidiogenous cells, polyphialidic sporodochial conidiogenous cells, terminal, integrated, subcylindrical to cylindrical, with minute periclinal thickenings, with oblong conidia, hyaline and aseptate, forming conidial chains that remain attached (Lu et al., 2025, in press). Hyphomycetous is characterized by macronematous and mononematous conidiophores, solitary, erect, unbranched, brown, septate, smooth-walled; monoblastic and holoblastic conidiogenous cells, terminal, brown, with pale brown to brown conidia, acrogenous, solitary, obclavate, septate, hyaline towards the apex (Zhang et al., 2024). In this study, we use ITS, LSU, SSU, *rpb*2 and *tef*1-α to update phylogenetic studies for *Neomassaria* (Figure 2.39). There are 12 species accepted in *Neomassaria* (Index Fungorum, 2025 January; Lu et al., 2025, in press), and all species are confirmed by molecular data (Liu et al., 2024; Zhang et al., 2024). Totally four species have been reported from palm species (Xiong et al., 2025) including two new host records of *Neomassaria* introduced from different palm species from China in this study.

Neomassaria livistonae S.N. Zhang, K.D. Hyde & Jian K. Liu, Fungal Diversity 127: 149 (2024)

Figure 2.40

Saprobic on a dead segment of *Phoenix loureiroi*. Sexual morph: *Ascomata* 100–210 × 180–240 μm ($\bar{x}$ = 148 × 207 μm, n = 15), immersed to semi-immersed, visible

as black dots or lenticular shape black area on host surface, solitary or scattered, with a central ostiole, coriaceous, subglobose, unilocular. *Ostiole* central, crest-like. *Peridium* 20–40 µm wide ($\bar{x}$ = 29 µm, n = 20), composed of cells of *textura angularis*, outer layer brown and thicker, inner layer hyaline. *Hamathecium* 1.5–2.5 µm wide ($\bar{x}$ = 2.1 µm, n = 20), pseudoparaphyses, embedded in a gelatinous matrix. *Asci* 80–100 × 7–9 µm ($\bar{x}$ = 86 × 8.1 µm, n = 20), bitunicate, fssitunicate, cylindrical, 8-spored, hyaline, apically rounded, with a short pedicel, apically rounded with an inconspicuous ocular chamber. *Ascospores* 25–30 × 3–4 µm ($\bar{x}$ = 27 × 3.6 µm, n = 20), overlapping 1–2-seriate, fusiform and tapering to both ends, hyaline, 1-septate, constricted at septum, guttulate, smooth-walled, sheath absent. Asexual morph: Not observed.

Culture characteristics: Colonies on PDA fast growing, after 2 weeks reaching 4–5 cm diam., at 25°C, filamentous, slight raised, with undulate edge, dense, furry, cottony white aerial hyphae covered the colony, above white, below green in the middle, wrinkled, with a distinct pale-yellow halo outside.

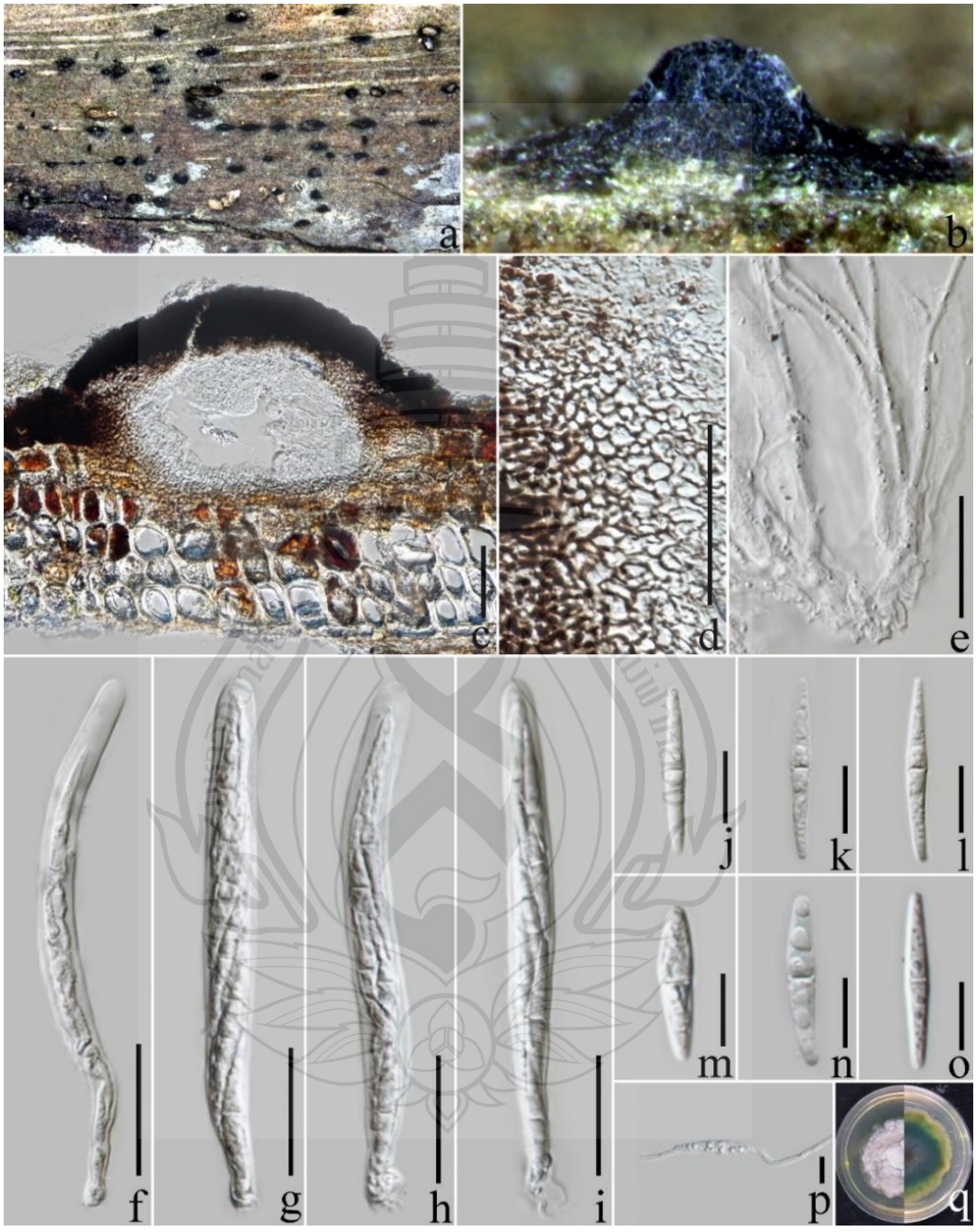
Known distribution: China (Zhang et al., 2024, this study).

Material examined: China, Yunnan Province, Xishuangbanna, Xishuangbanna Tropical Botanical Garden, Chinese Academy of Sciences, on dead segment of *Phoenix loureiroi*, 5 February 2023, Y.R. Xiong, XG154 (MHZU 23-0136, new host record), living culture ZHKUCC 24-0079, other living culture ZHKUCC 24-0080.

GenBank numbers: ZHKUCC 24-0079: ITS – PV578212, LSU – PV578378, SSU – PV578522, *tef*1-α – PV608870, *rpb*2 – PV595338; ZHKUCC 24-0080: ITS – PV578213, LSU – PV578379, SSU – PV578523, *tef*1-α – PV608871, *rpb*2 – PV595339.

Notes: Two collections obtained in this study clustered with *Neom. livistonae* (SNC 146, holotype) by 99% ML bootstrap support and 1.00 BYPP (Figure 2.39). Pairwise nucleotide differences (excluding gaps) between our isolate (ZHKUCC 24-0079) and *Neom. livistonae* (SNC 146) were analyzed, ITS, LSU, SSU, and *rpb*2 sequences were identical, whereas the *tef*1-α gene exhibited minor differences (0.4%, 4/946 bp). Morphologically, our species aligns with the generic concepts of *Neom. livistonae*; however, a minor difference was observed in asci and ascospores when compared to the holotype, our collection has cylindrical asci and ascospores lacking a sheath, whereas the holotype exhibits cylindric-clavate asci with a distinct ocular chamber and ascospores surrounded by a thin mucilaginous sheath (Zhang et al., 2024, Figure 2.40). Therefore, based on the

phylogenetic analysis, we identified our collections as new host record of *Neom. livistonae*. *Neomassaria livistonae* was reported by Zhang et al. (2024) from decaying petioles of *Livistona chinensis* (Zhang et al., 2024).



Note a, b Appearance of ascomata on the host surface. c Vertical section of an ascoma. d Peridium. e Pseudoparaphyses. f–i Asci. j–o Ascospores. p Germinating ascospore. q The front of culture on PDA at 25°C and the reverse of culture on PDA at 25°C. Scale bars: c = 50 µm; d–i = 20 µm; j–p = 10 µm.

Figure 2.40 *Neomassaria livistonae* (MHZU 23-0136, new host record)

Neomassaria formosana H.A. Ariyaw., Jaklitsch & Voglmayr, Cryptogamie, Mycologie 39 (3): 368 (2018)

Figure 2.41

Saprobic on dead segment of *Elaeis guineensis*. Sexual morph: *Ascomata* 120–210 × 170–260 µm ($\bar{x}$ = 155.4 × 219.6 µm, n = 15), immersed to erumpent, visible as black dots on host surface, solitary to scattered, with a central ostiole, coriaceous, subglobose, unilocular. *Ostiole* central. *Peridium* 15–25 µm wide ($\bar{x}$ = 19.8 µm, n = 20), hyaline to brown, comprising several layers of *textura angularis* cells, thinner-walled and lighter to the inner side, outside fusing with the host. *Hamathecium* 1–2 µm wide ($\bar{x}$ = 1.3 µm, n = 20), pseudoparaphyses, embedded in a gelatinous matrix. *Asci* 65–95 × 6–8.5 µm ($\bar{x}$ = 79o.6 × 7.2 µm, n = 20), bitunicate, fssitunicate, cylindrical, 8-spored, hyaline, apically rounded, with a short pedicel. *Ascospores* 17–25 × 2.5–5 µm ($\bar{x}$ = 21.2 × 3.7 µm, n = 20), overlapping 1–2-seriate, fusiform and tapering to both ends, hyaline, 1-septate, constricted at septum, guttulate, smooth-walled. Asexual morph: Not observed.

Culture characteristics: Colonies on PDA fast growing, after 2 weeks reaching 5–6 cm diam., at 25°C, circular, flat, filiform margin, with white aerial mycelium, floccose, above white to greyish green, reverse pale yellow to greenish.

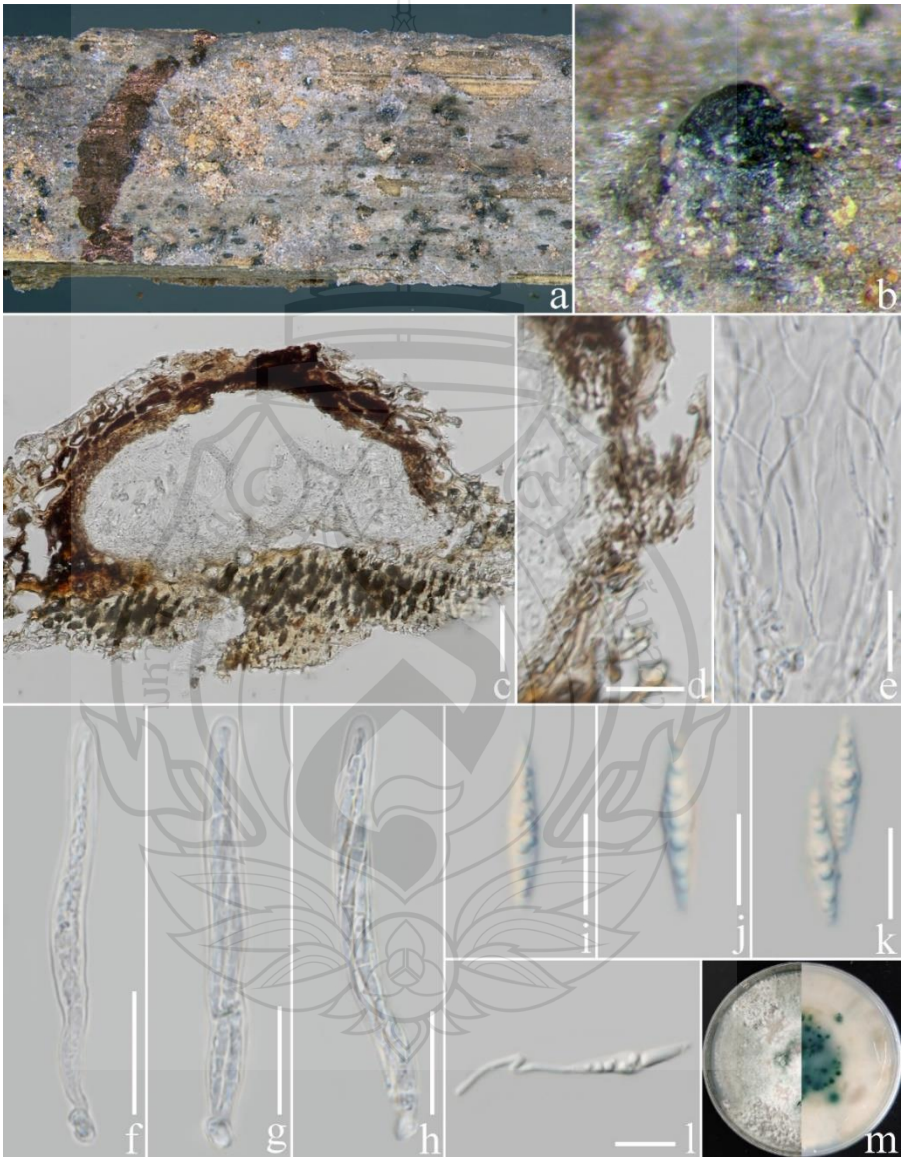
Known distribution: China (Ariyawansa et al., 2018; Zhang et al., 2024; Lu et al., 2025, this study).

Material examined: China, Yunnan Province, Xishuangbanna, Xishuangbanna Tropical Botanical Garden, Chinese Academy of Sciences, on dead segment of *Elaeis guineensis*, 5 February 2023, Y.R. Xiong, XG181 (MHZU 23-0150, new host record), living culture ZHKUCC 24-0107, other living culture ZHKUCC 24-0108.

GenBank numbers: ZHKUCC 24-0107: ITS – PV578210, LSU – PV578376, SSU – PV578520, *rpb*2 – PV595336, *tef*1-α – PV608868; ZHKUCC 24-0108: ITS – PV578211, LSU – PV578377, SSU – PV578521, *rpb*2 – PV595337, *tef*1-α – PV608869.

Notes: Two collections obtained in this study clustered with *Neom. formosana* by 99% ML bootstrap support and 1.00 BYPP (Figure 2.39). Pairwise nucleotide differences (excluding gaps) between our isolate (ZHKUCC 24-0107) and the ex-type species *Neom. formosana* (NTUCC 17-007) were analyzed, SSU and *rpb*2 sequences were similar, whereas the LSU and *tef*1-α gene exhibited minor differences (0.1%, 1/879 bp and 0.1%, 1/723 bp, respectively). Morphologically, our species aligns with the generic concepts of *Neom.*

formosana by cylindrical asci and fusiform ascospores, 1-septate (Ariyawansa et al., 2018; Zhang et al., 2024, Figure 2.41). Therefore, based on the phylogenetic analysis, we identified our collections as new host records of *Neom. formosana*. *Neomassaria formosana* was reported by Ariyawansa et al. (2018) as saprobic fungi on dead stems of *Rhododendron* sp. Another two host records were collected from *Trachycarpus fortunei* and *Coffea* sp. (Zhang et al., 2024; Lu et al., 2025).



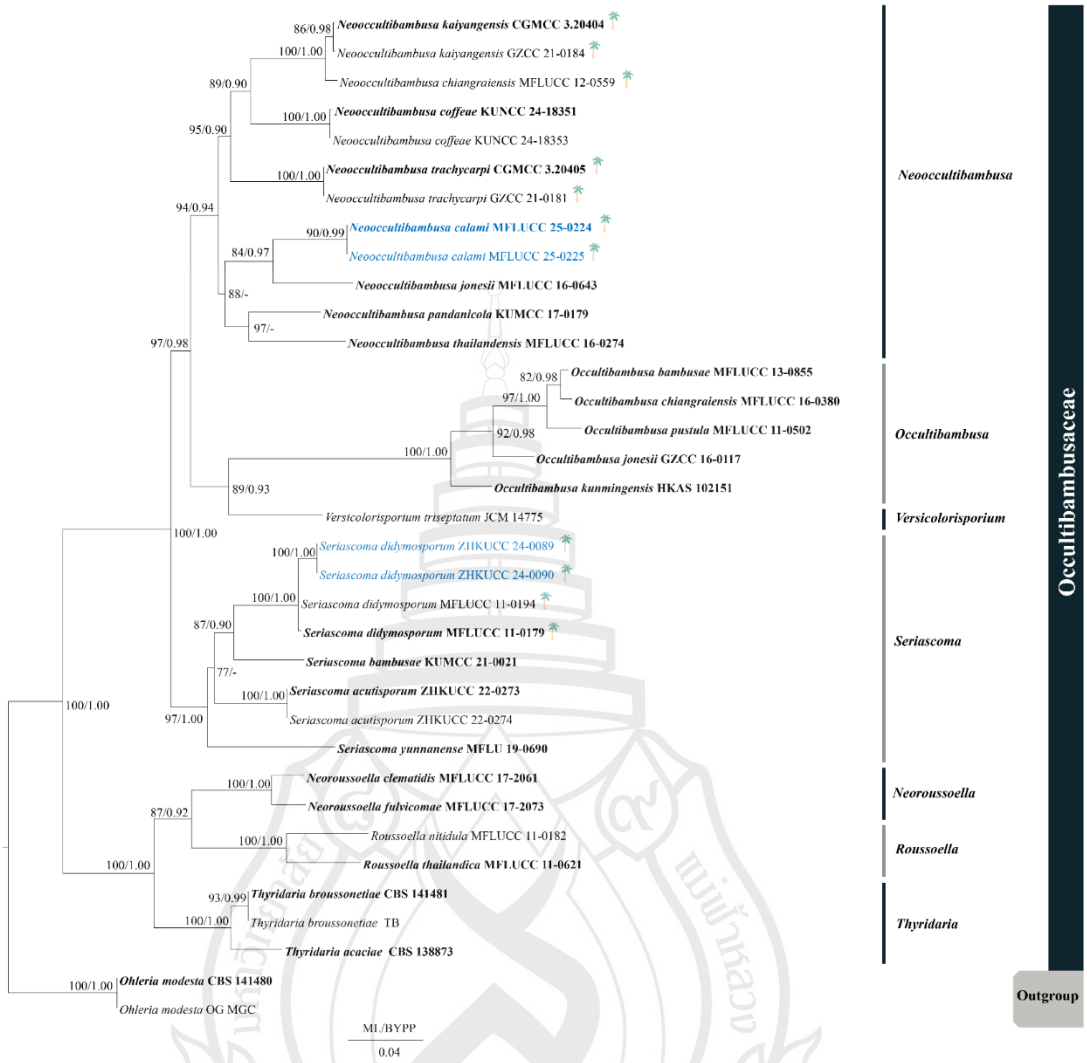
Note a, b Appearance of ascomata on the host surface. c Vertical section of an ascoma. d Peridium. e Pseudoparaphyses. f–h Asci. i–k Ascospores. l Germinating ascospore. m The front of culture on PDA at 25°C and the reverse of culture on PDA at 25°C. Scale bars: c = 50 µm; d–h = 20 µm; i–l = 10 µm.

Figure 2.41 *Neomassaria formosana* (MHZU 23-0150, new host record)

Occultibambusaceae D.Q. Dai & K.D. Hyde, Fungal Diversity 82: 25 (2016)

Neooccultibambusa Doilom & K.D. Hyde, Fungal Diversity 82: 126 (2016)

Notes: Doilom et al. (2017) established *Neooccultibambusa* (*Neoo*.) with *Neoo. chiangraiensis* as the type species based on morphological evidence and phylogenetic analysis combined SSU, LSU, and *rpb*2 sequence data. *Neooccultibambusa* species are mostlyreported as sexual morphs characterized by black and immersed to semi-immersed ascomata with a central ostiole, hyphae-like and pseudoparaphyses hamathecium, bitunicate and furcate to rounded pedicel asci with an ocular chamber, conidia 1–3 transverse septa and surrounded or without by a gelatinous sheath (Doilom et al., 2017). Several *Neooccultibambusa* species have been reported with asexual morph which forms chlamydospores in culture (Doilom et al., 2017). Phylogenetic analyses of *Neooccultibambusa* mainly use SSU, LSU, ITS and *rpb*2 or add *tef* 1-α sequence data (Tibpromma et al., 2018; Yu et al., 2021). In this study, we use ITS, LSU, SSU and *tef 1-α* to update phylogenetic studies for *Neooccultibambusa* (Figure 2.42). Currently, six epithets are listed under *Dictyocheirospora* (Index Fungorum, 2025 January) and all species are associated with molecular data. Totally three species have been reported from palm species including a new species described in this study (Xiong et al., 2025).



Note Phylogram generated from maximum likelihood analysis of *Neoocculitibambusa* based on combined ITS, LSU, SSU and *tef* 1-α sequence data. Bootstrap values for maximum likelihood (ML) equal to or greater than 70 and BYPP values equal to or greater than 0.90 are indicated above the branches. The new collections are indicated in blue and ex-type strains are indicated in bold.

Figure 2.42 Phylogenetic tree of *Neoocculitibambusa*

Neoocculitibambusa calami Y.R. Xiong, Manawas. & K.D. Hyde, ***sp. nov.***

Figure 2.43

Etymology: The epithet refers to the host genus name "*Calamus*", from which the species was collected.

Saprobic on dead rachis of *Calamus* sp. Asexual morph: Not observed. Sexual

morph: *Ascomata* 150–190 × 200–300 µm ($\bar{x}$ = 172 × 256 µm, n = 15), solitary or gregarious, scattered, immersed, uni-loculate to multi-loculate, black papillate dots on host surface, subglobose or irregular, ostiolate. *Loculate* 100–150 × 200–240 µm ($\bar{x}$ = 124 × 221 µm, n = 10), subglobose or irregular, ostiolate. *Ostiole* 65–90 × 55–70 µm ($\bar{x}$ = 80 × 61 µm, n = 15), circular, central, periphysate, composing brown *textura angularis* cells. *Peridium* 15–35 µm wide, composing brown to dark brown *textura angularis* cells, thicker outwardly. *Hamathecium* 2–3 µm wide, hyphae-like, pseudoparaphyses, septate, embedded in a gelatinous matrix. *Asci* 50–120 × 9–10 µm ($\bar{x}$ = 67 × 9.5 µm, n = 25), 8-spored, bitunicate, cylindric-clavate, with a short furcate to rounded pedicel, apically rounded, with an ocular chamber. *Ascospores* 16–18 × 3–5 µm ($\bar{x}$ = 16.7 × 3.8 µm, n = 25), overlapping biseriate, hyaline, fusiform to fusoid, tapering and round towards the ends, 1-septate, constricted at the center septum, becoming pale brown and present one pseudosepta when senescent (Figure 2.43), guttulate, smooth, surrounded by mucilaginous sheath.

Culture characteristics: Colonies on PDA fast growing, after 2 weeks reaching 4 cm diam., at 25°C, circular, convex, aerial in the centre, edge entire, white to black mycelium with entire margin; in reverse black.

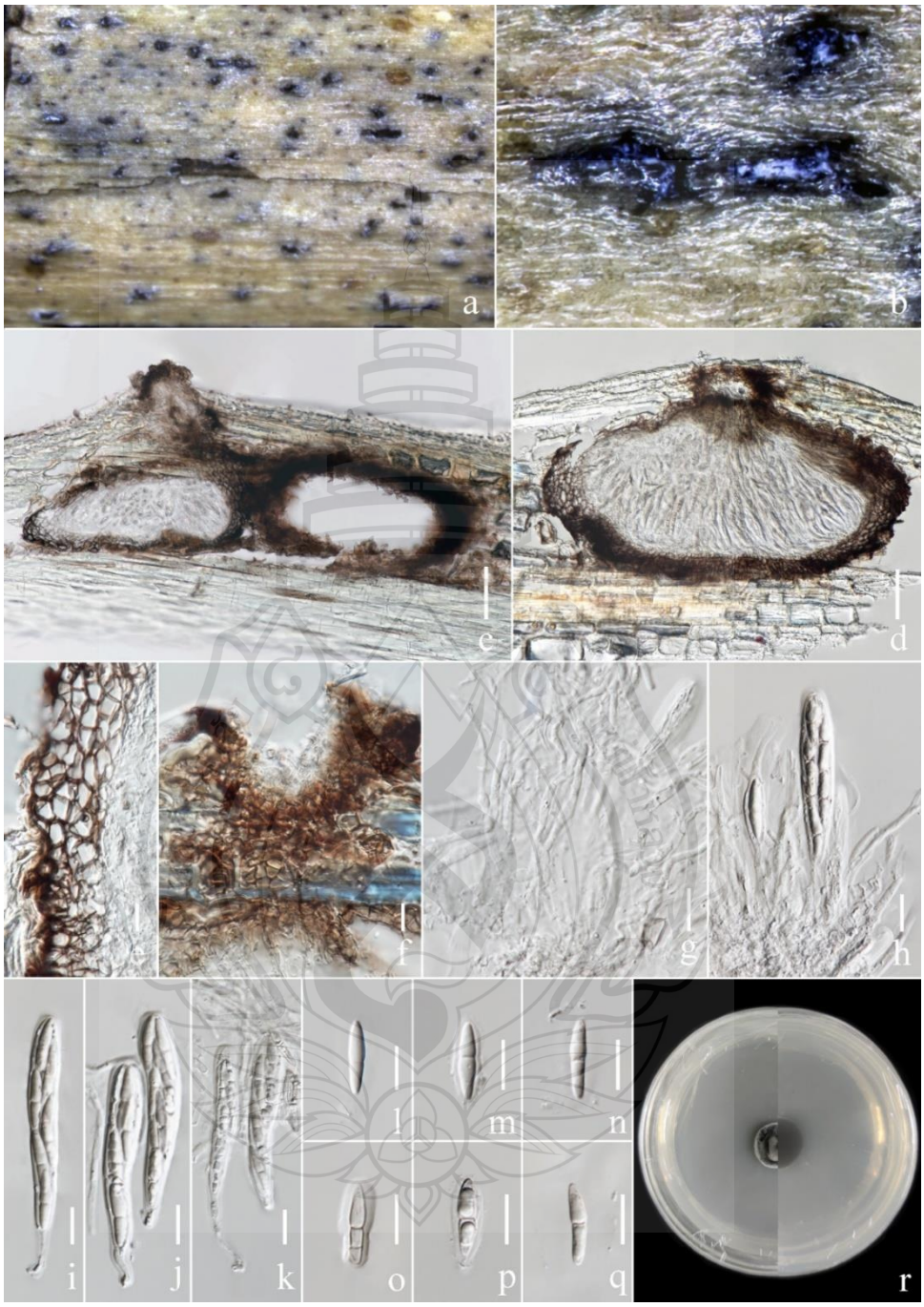
Known distribution: Thailand (this study).

Material examined: Thailand, Narathiwat Province, in an unidentified beach, on dead rachis of *Calamus* sp., 6 Aug 2023, Y.R. Xiong, XG357 (MFLU 25-0157, holotype); ex-type MFLUCC 25-0224, other living culture MFLUCC 25-0225.

GenBank numbers: MFLUCC 25-0224: ITS – PV578216, LSU – PV578382, SSU – PV578526, *tef* 1-α – PV608874; MFLUCC 25-0225: ITS – PV578217, LSU – PV578383, SSU – PV578527, *tef* 1-α – PV608875.

Notes: Two collections from this study formed a separate lineage and clustered with *Neooccultibambusa thailandensis* in the phylogenetic tree with 94% ML bootstrap support and 1.00 BYPP (Figure 2.42). The nucleotide differences exclude gaps between *Neoo. calami* (MFLUCC) and *Neoo. thailandensis* (MFLUCC 16-0274) were checked and given as follows, ITS: 11.78% (55/467 base pairs), LSU: 2.17% (20/923 base pairs), SSU: 0% (0/857 base pairs), *tef* 1-α: 4.99% (50/1002 base pairs). *Neooccultibambusa calami* has ascospores which are surrounded by mucilaginous sheath and hyaline differs from *Neoo. thailandensis* have ascospores without appendages or mucilaginous sheath and are

yellow-brown (Tibpromma et al., 2018, Figure 2.43). Based on phylogenetic placement and morphological variations, we introduce *Neoo. calami* as a new species.



Note a, b Ascomata on substrate. c, d Vertical sections of ascomata. e Cells of peridium. f Cells of ostiole. g Pseudoparaphyses. h–k Asci. l–q Ascospores. r The front of culture on PDA at 25°C and the reverse of culture on PDA at 25°C. Scale bars: c, d = 50 µm, e–q = 10 µm.

Figure 2.43 *Neooccultibambusa calami* (MFLU 25-0157, holotype)

Seriascoma Phookamsak, D.Q. Dai & K.D. Hyde, Fungal Diversity 82: 30 (2016)

Notes: *Seriascoma* (*Se*.) was proposed by Dai et al. (2017) and typified by *Se. didymosporum*. *Seriascoma* species are saprobic, mainly found on bamboo and decaying wood in terrestrial or freshwater habitats in China and Thailand (Dai et al., 2017; Rathnayaka et al., 2019; Dong et al., 2020; Calabon et al., 2024). The sexual morph of *Seriascoma* is characterized by solitary or gregarious, erumpent, subglobose to elongated, uni- to multi-loculate, coriaceous ascostromata, which are immersed under a clypeus; bitunicate and fissitunicate asci, 8-spored, clavate, with short to long furcate pedicels, and contain fusiform ascospores, asymmetric, 1-septate, hyaline (Dai et al., 2017; Hongsanan et al., 2020). The asexual morph is characterized by eustromatic and conical conidiomata, black, uni- to multi-loculate, with enteroblastic, conidiogenous cells, phialidic, cylindrical to ampulliform, producing oblong, hyaline and aseptate conidia (Dai et al., 2017; Calabon et al., 2024). In this study, we use ITS, LSU, SSU, *rpb*2 and *tef*1-α to update phylogenetic studies for *Seriascoma* (Figure 2.42). There are five species are accepted in *Seriascoma* (Index Fungorum, 2025 January), all species were confirmed by molecular data of combined ITS, LSU, SSU, *rpb*2 and *tef*1-α sequence (Dai et al., 2017; Senanayake et al., 2023). There are no previous records of *Seriascoma* species occurring on palm hosts. In this study, we report a new host record *Se. didymosporum* on *Arenga obtusifolia* in China, representing the first documented occurrence of *Seriascoma* on a palm species.

Seriascoma didymosporum Phookamsak, D.Q. Dai, Karun. & K.D. Hyde, Fungal Diversity 82: 32 (2016)

Figure 2.44

Saprobic on dead segment of *Arenga obtusifolia*. Sexual morph: *Ascomata* 90–130 × 170–260 µm ($\bar{x}$ = 104.9 × 218 µm, n = 15), gregarious, immersed beneath clypeus, erumpent in linear rows, coriaceous, subglobose, unilocular, ostiolate. *Peridium* 15–20 µm wide ($\bar{x}$ = 16.6 µm, n = 20), composed of cells of *textura angularis*, outer layer brown and thicker, inner layer hyaline. *Hamathecium* 2–3 µm wide ($\bar{x}$ = 2.5 µm, n = 20), pseudoparaphyses, numerous, cellular, hypha-like, hyaline, septate. *Asci* 55–65 × 9–11 µm ($\bar{x}$ = 61.7 × 9.9 µm, n = 20), bitunicate, fssitunicate, 8-spored, clavate, long pedicellate with club-like, hyaline, apically rounded, with an ocular chamber when mature. *Ascospores* 13–16 × 4–6.5 µm ($\bar{x}$ = 14.6 × 5.4 µm, n = 20), overlapping 1–2-seriate, clavate to fusiform,

hyaline, 1-septate, constricted at septum, upper cell shorter and wider than lower cell, guttulate, slight-curved, smooth-walled. Asexual morph: Not observed.

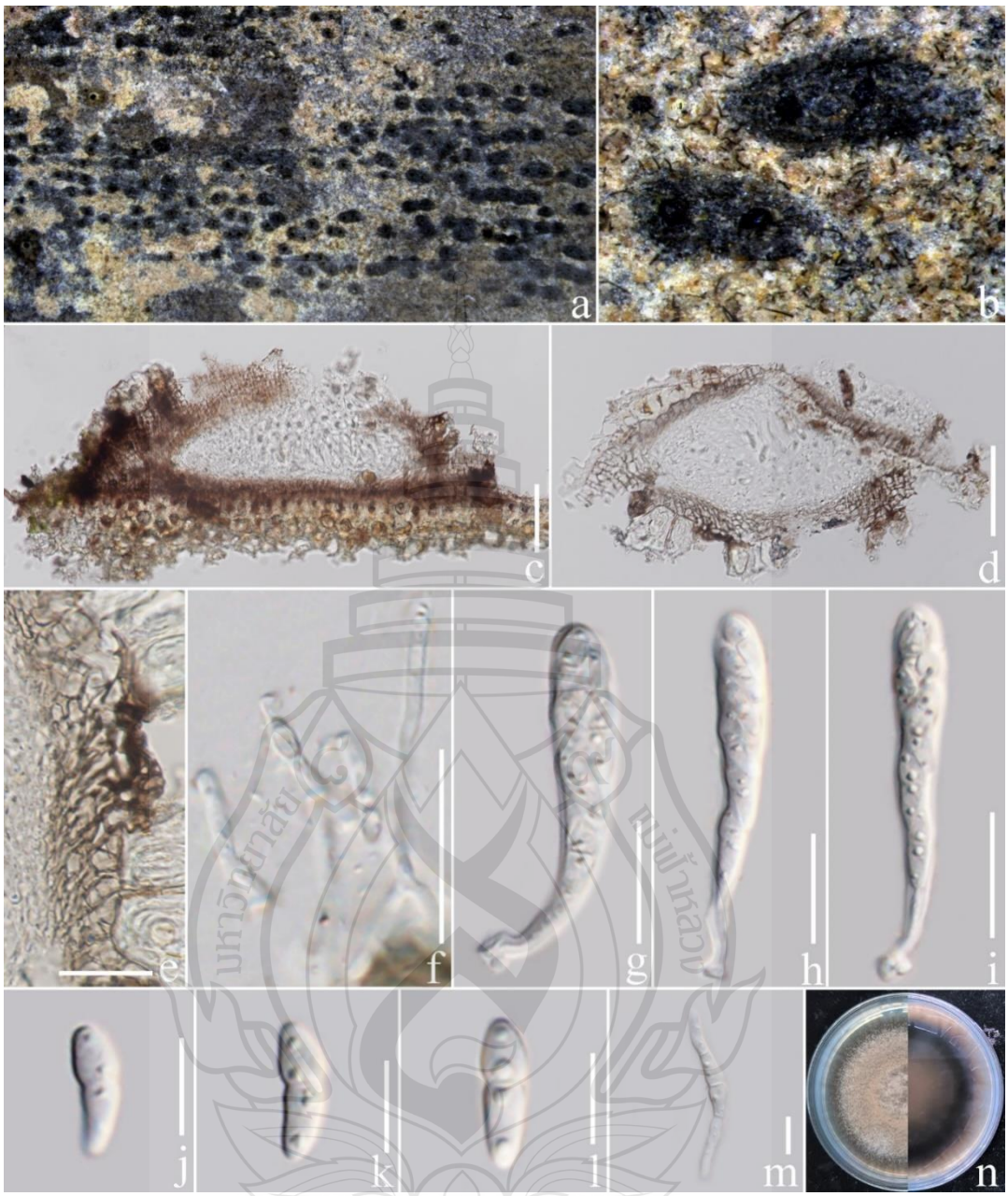
Culture characteristics: Colonies on PDA fast growing, after 2 weeks reaching 4–5 cm diam. at 25°C, circular, dense, flat, smooth with entire edge, velvety to floccose, slightly radiating, reddish brown to dark green from above, reddish brown to black from below.

Known distribution: Thailand (Dai et al., 2017), China (Dong et al., 2020, this study).

Material examined: China, Yunnan Province, Xishuangbanna, Xishuangbanna Tropical Botanical Garden, Chinese Academy of Sciences, on dead segment of *Arenga obtusifolia*, 5 February 2023, Y.R. Xiong, XG160 (MHZU 23-0141, new host record) – living culture ZHKUCC 24-0089, other living culture ZHKUCC 24-0090.

GenBank numbers: ZHKUCC 24-0089: ITS – PV578252, LSU – PV578420, SSU – PV578550, *rpb*2 – PV595360; ZHKUCC 24-0090: ITS – PV578253, LSU – PV578421, SSU – PV578551, *rpb*2 – PV595361.

Notes: Two collections obtained in this study clustered with *Se. didymosporum* (MFLUCC 11-0179 (ex-type) and MFLUCC 11-0194) by 100% ML bootstrap support and 1.00 BYPP (Figure 2.42). Pairwise nucleotide differences (excluding gaps) between our isolate (ZHKUCC 24-0089) and *Se. didymosporum* (MFLUCC 11-0179, ex-type) were analyzed, LSU, SSU, and *rpb*2 sequences were identical, whereas the ITS gene exhibited minor differences (1.6%, 9/546 bp). Morphologically, our species aligns with the generic concepts of the holotype *Se. didymosporum* by clavate asci and clavate to fusiform ascospores, hyaline, 1-septate (Dai et al., 2017, Figure 2.44). *Seriascoma didymosporum*, the type species of the genus *Seriascoma*, has previously been reported from terrestrial habitats associated with bamboo (Dai et al., 2017) and from submerged, unidentified wood in freshwater environments (Dong et al., 2020). Therefore, based on the phylogenetic analysis, we identified our collections as new host records of *Se. didymosporum.*



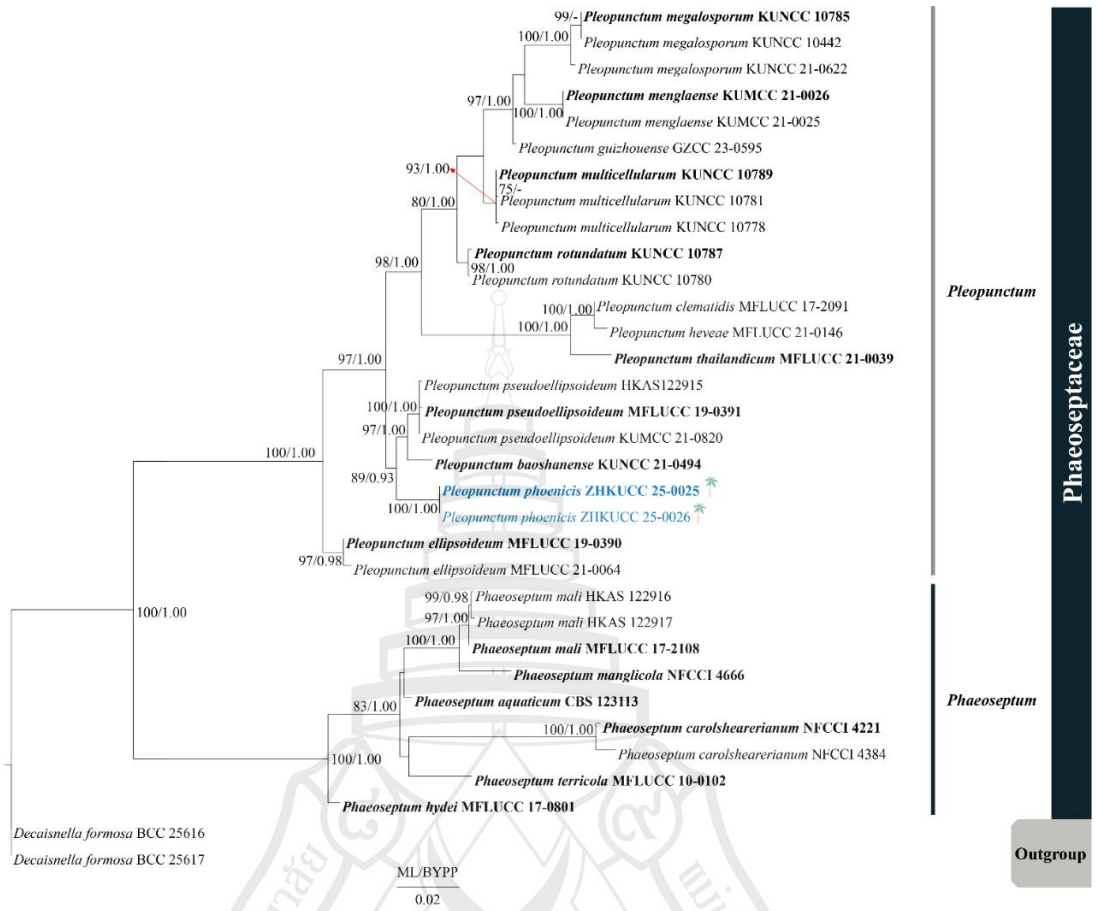
Note a, b Appearance of ascomata on the host surface. c, d Vertical section of an ascomata. e Peridium. f Pseudoparaphyses. g–i Asci. j–l Ascospores. m Germinating ascospore. n The front of culture on PDA at 25°C and the reverse of culture on PDA at 25°C. Scale bars: c, d = 50 µm; e–i = 20 µm; j–m = 10 µm.

Figure 2.44 *Seriascoma didymosporum* (MHZU 23-0141, new host record)

Phaeoseptaceae Boonmee, Thambugala & K.D. Hyde, Mycosphere 9: 323 (2018)

Pleopunctum N.G. Liu, K.D. Hyde & J.K. Liu, Mycosphere 10 (1): 767 (2019)

Notes: Liu et al. (2019) established *Pleopunctum* (*Pl.*) with *Pl. ellipticum* as the type species. *Pleopunctum* is a hyphomycetous genus characterized by gregarious, superficial, brown to black colonies, mononematous, septate conidiophores, monoblastic conidiogenous cells, multi-septate, muriform and oval to ellipsoidal conidia, often with a hyaline, elliptical to globose basal cell (Liu et al., 2019). Based on morphological evidence and phylogenetic analysis combined SSU, LSU, ITS and *tef* 1-α Liu et al. (2019) introduced *Pleopunctum* as a new genus. Subsequently, phylogenetic studies mainly use SSU, LSU, ITS, *tef* 1-α and *rpb*2 or without *rpb*2 for analysis (Phukhamsakda et al., 2020; Boonmee et al., 2021; Senwann et al., 2021; Wanasinghe et al., 2022; Xu et al., 2023; Ren et al., 2024; Yu et al., 2024). In this study, we use ITS, LSU, SSU, *tef* 1-α and *rpb*2 to update phylogenetic studies for *Pleopunctum* (Figure 2.45). Currently, 11 epithets are listed under *Pleopunctum* (Index Fungorum, 2024 November) with all species associated with molecular data. Here is the first-time report species from the palm in *Pleopunctum*, we provide a new species in *Pleopunctum* described from the palm in this study (Xiong et al., 2025).



Note Phylogram generated from maximum likelihood analysis of *Pleopunctum* based on combined ITS, LSU, SSU, *tef* 1-α and *rpb*2 sequence data. Bootstrap values for maximum likelihood (ML) equal to or greater than 70 are indicated above the branches. The new collections are indicated in blue and ex-type strains are indicated in bold.

Figure 2.45 Phylogenetic tree of *Pleopunctum*

Pleopunctum phoenicis Y.R. Xiong, Manawas. & K.D. Hyde, ***sp. nov.***

Figure 2.46

Etymology: The epithet refers to the host genus name "*phoenix*", from which the species was collected.

Saprobic on dead leaf sheath of *Phoenix sylvestris*. Asexual morph: Hyphomycetous. *Colonies* on natural substrate superficial, punctiform, scattered to gregarious, dark brown to black, glistening. *Mycelium* immersed, composed of dark brown to hyaline, smooth, septate, branched hyphae. *Conidiophores* 2–3 µm diam.,

macronematous, mononematous, pale brown to hyaline. *Conidiogenous cells* monoblastic, integrated, terminal, pale brown, smooth-walled. *Conidia* 25–30 × 15–20 µm ($\overline{x}$ = 29 × 18 µm, n = 25), solitary, ellipsoidal, subcylindrical or muriform, rounded at the apex, multi-septate, slightly constricted at the septa, slightly curved, brown to dark brown, paler at the base, observed sheath surrounded, thick at medium part, often with a hyaline, elliptical to globose basal cell 10–20 × 10–15 µm ($\overline{x}$ = 15 × 14 µm, n = 25), multiple small hyaline basal cells are occasionally observed. Sexual morph: Not observed.

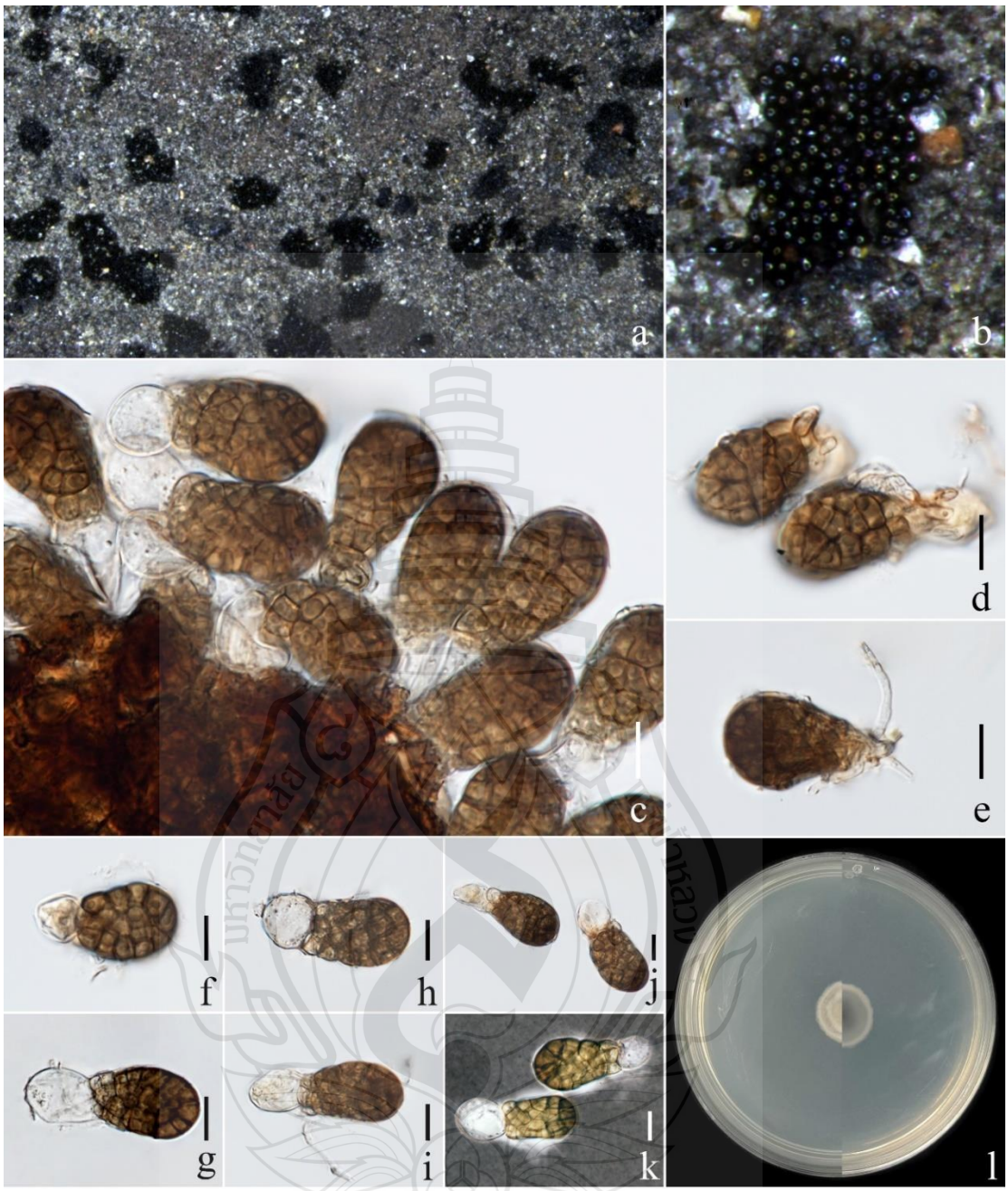
Culture characteristics: Colonies on PDA fast growing, after 2 weeks reaching 1.5 cm diam., at 25°C, irregular circular, striated, umbonate, white margin between grey in the central cycle and pale grey in the outer circle; in reverse black in the middle and white at the margin.

Known distribution: China (this study).

Material examined: China, Jiangxi Province, Ganzhou City, Xingda Restaurant, on dead leaf sheath of *Phoenix sylvestris*, 9 Apr 2024, Y.R. Xiong, XG368 (MHZU 24-0483, holotype), ex-type ZHKUCC 25-0025, other living culture ZHKUCC 25-0026.

GenBank numbers: ZHKUCC 25-0025: ITS – PV578228, LSU – PV578394, SSU – PV578532, *tef* 1-α – PV608878, *rpb*2 – PV595348; ZHKUCC 25-0026: ITS – PV578229, LSU – PV578395, SSU – PV578533, *tef* 1-α – PV608879, *rpb*2 – PV595349.

Notes: Two collections from this study clustered in *Pleopunctum* clade and formed a sister lineage to *Pl. baoshanense* and *Pl. pseudoellipsoideum* in the phylogenetic tree with 89% ML and 0.93 BYPP (Figure 2.46). The nucleotide differences excluding gaps between *Pl. phoenicis* (MHZU 24-0483) and its phylogenetically related species were checked and given as follows, *Pl. baoshanense* (KUNCC 21-0494) - *tef* 1-α: 2.90% (27/930 base pairs), *rpb*2: 5.19% (53/1020 base pairs); *Pl. pseudoellipsoideum* (MFLUCC 19-0391) - ITS: 1.16% (6/519 base pairs), LSU: 1.39% (12/866 base pairs), *tef* 1-α: 3.12% (30/961 base pairs), *rpb*2: 4.36% (44/1010 base pairs). Morphologically, *Pl. phoenicis* has conidia with sheath surrounded which is not reported in *Pl. baoshanense* and *Pl. pseudoellipsoideum* (Liu et al., 2019; Ren et al., 2024). Moreover, *Pl. phoenicis* occasionally has multiple small hyaline basal cells in conidia while *Pl. baoshanense* only has one elliptical to globose basal cell (Ren et al., 2024). Based on phylogenetic placement and morphological variations, we introduce *Pl. phoenicis* as a new species.



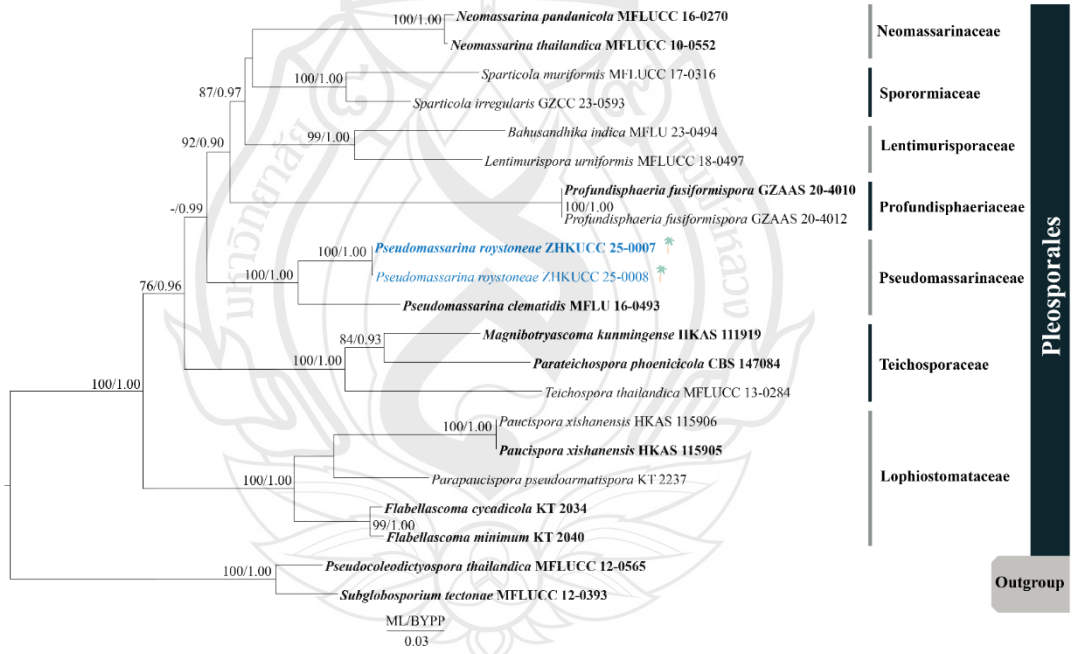
Note a, b Sporodochia on the substrate. c–e Conidiophore and conidiogenous cells with conidia. f–k Conidia (k conidia in Indian ink). m The front of culture on PDA at 25°C and the reverse of culture on PDA at 25°C. Scale bars: c–k = 10 µm.

Figure 2.46 *Pleopunctum phoenicis* (MHZU 24-0483, holotype)

Pseudomassarinaceae Phukhams. & K.D. Hyde, Fungal Diversity 102: 99 (2020)

Pseudomassarina Phukhams. & K.D. Hyde, Fungal Diversity 102: 101 (2020)

Notes: Phukhamsakda et al. (2020) established *Pseudomassarina* (*Pseu.*) with *Pseu. clematidis* as the type species. *Pseudomassarina* was reported as a teleomorphic genus characterized by obpyriform to subglobose, coriaceous, and carbonaceous ascomata, papillate ostioles, with septum, deeply constricted at the septum, cell above septum longer and wider than below cell ascospores, mucilaginous sheath surround ascospores (Phukhamsakda et al., 2020). *Pseudomassarina* was established as a novel genus in Pseudomassarinaceae based on morphological evidence and phylogenetic analysis combined ITS, SSU, LSU, *tef* 1-α and *rpb*2 (Phukhamsakda et al., 2020) and in the present study, we followed and updated the phylogenetic analysis for *Pseudomassarina* (Figure 2.47). Currently, one epithet is listed under *Pseudomassarina* (Index Fungorum, 2024 December) and one species is associated with molecular data. Here we described a new species of *Pseudomassarina* which is the first time reported from palm species (Xiong et al., 2025).



Note Phylogram generated from maximum likelihood analysis of *Pseudomassarina* based on combined ITS, SSU, LSU, *tef* 1-α and *rpb*2 sequence data. Bootstrap values for maximum likelihood (ML) equal to or greater than 70 are indicated above the branches. The new collections are indicated in blue and ex-type strains are indicated in bold.

Figure 2.47 Phylogenetic tree of *Pseudomassarina*

Pseudomassarina roystoneae Y.R. Xiong, Manawas. & K.D. Hyde, ***sp. nov.***

Figure 2.48

Etymology: The epithet refers to the host genus name "*Roystonea*", from which the species was collected.

Saprobic on dead rachis of *Roystonea regia*. Asexual morph: Not observed. Sexual morph: *Ascomata* 350–500 × 250–350 μm ($\overline{x}$ = 380 × 290 μm, n = 10), solitary, scattered or gregarious, semi-immersed, part immersed beneath host dehiscent epidermis, appearing numerous, raised, papillate shaped areas on the host surface, subglobose, coriaceous, unilocular, black, ostiolate. *Ostioles* carbonaceous perforated-like opening, central. *Setae* 2–3.5 μm wide, erect or slightly curved, pale brown. *Peridium* 40–80 μm wide, multilayered, outer layered comprising thick-walled brown to dark brown cells of *textura angularis*, inner layers comprising pale brown to hyaline cells of *textura prismatica*. *Hamathecium* 1.5–2.5 μm wide, pseudoparaphyses, composed of dense, hyaline, filiform, trabeculate, branched, anastomosing among the asci. *Asci* 110–120 × 14–18 μm ($\overline{x}$ = 114 × 15.4 μm, n = 30), 8-spored, bitunicate, fissitunicate, cylindric-clavate, short furcate pedicel, apically rounded with ocular chamber clearly visible. *Ascospores* 30–40 × 5–9 μm ($\overline{x}$ = 35 × 6 μm, n = 40), overlapping, fusiform, hyaline, smooth-walled, tapering towards the ends, rounded or acute at both ends, guttulate, 1–3-septate, constricted at the medium septum, cell above septum wider than below cell, smooth-walled, surrounded by a thin mucilaginous sheath.

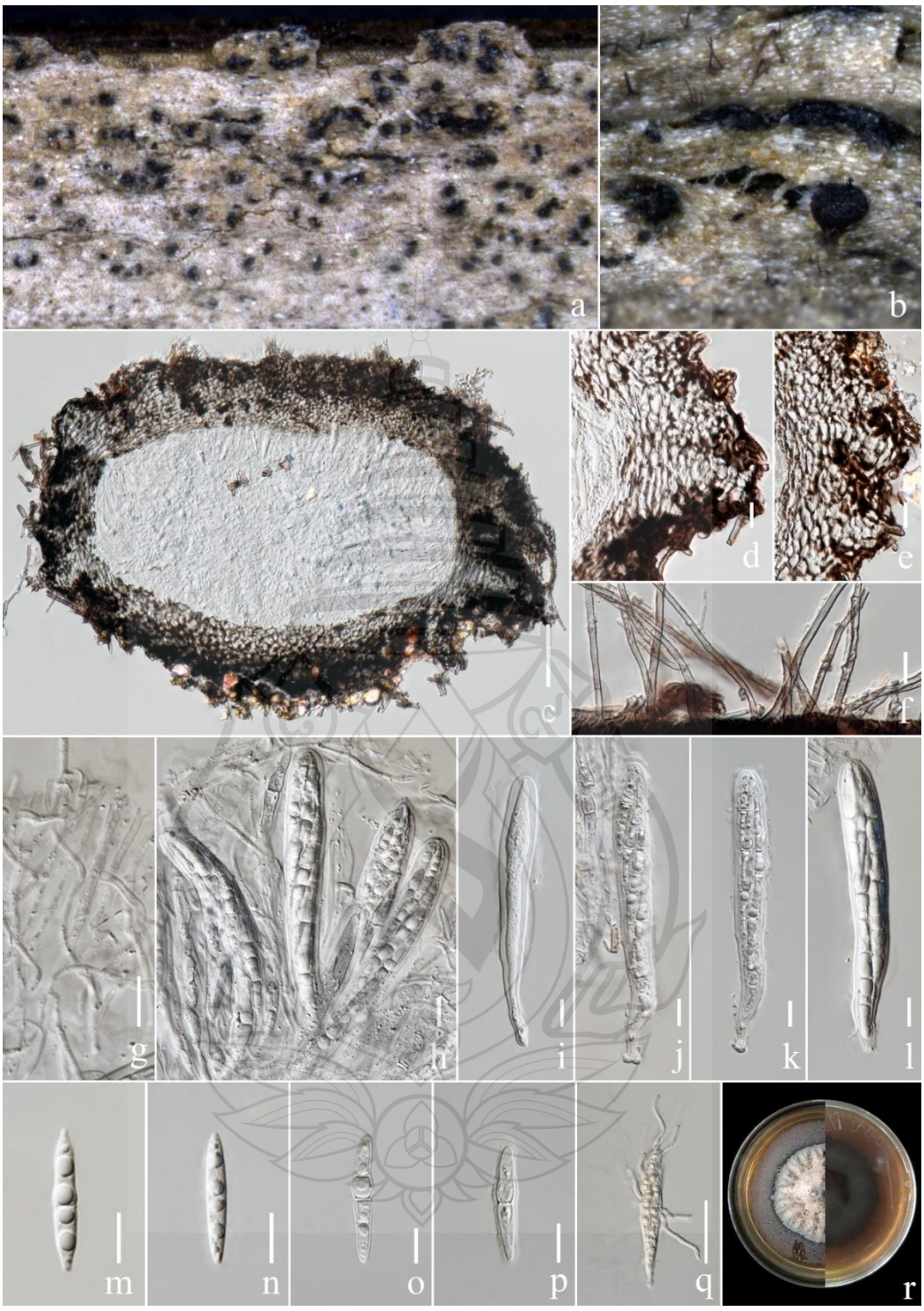
Culture characteristics: Colonies on PDA fast growing, after 2 weeks reaching 4 cm diam., at 25°C, circular, with fluffy, dense, striated, white mycelium on the surface with entire margin; in reverse black in the middle and brown at the margin.

Known distribution: China (this study).

Material examined: China, Yunnan Province, Xishuangbanna City, Xishuangbanna Dai Nationality Park, on dead rachis of *Roystonea regia*, 6 Feb 2023, Y.R. Xiong and L. Lu, XG228 (MHZU 24-0453, holotype), ex-type ZHKUCC 25-0007, other living culture ZHKUCC 25-0008.

GenBank numbers: ZHKUCC 25-0007: ITS – PV578242, LSU – PV578410, SSU – PV578544, *tef* 1-α – PV608890, *rpb*2 – PV595356; ZHKUCC 25-0008: ITS – PV578243, LSU – PV578411, SSU – PV578545, *tef* 1-α – PV608891, *rpb*2 – PV595357.

Notes: Two collections from this study clustered in *Pseudomassaria* clade and formed a sister lineage to *Pseu. clematidis* in the phylogenetic tree with 100% ML bootstrap support and 1.00 BYPP (Figure 2.47). The nucleotide differences exclude gaps between our collection (ZHKUCC 25-0007) and *Pseu. clematidis* (MFLU 16-0493) were checked and given as follows; ITS: 13.59% (64/471 base pairs), LSU: 2.86% (23/804 base pairs), SSU: 0.45% (4/884 base pairs), *tef* 1-α: 6.69% (60/896 base pairs), and *rpb2*: 13.19% (128/970 base pairs). Morphologically, *Pseu. roystoneae* have setae which are not reported from *Pseu. clematidis* (Phukhamsakda et al., 2020). In addition, *Pseu. roystoneae* have 1–3-septate ascospores while *Pseu. clematidis* only reported 1-septate ascospores (Phukhamsakda et al., 2020). Based on phylogenetic placement and morphological variations, we introduce *Pseu. roystoneae* as a new species.



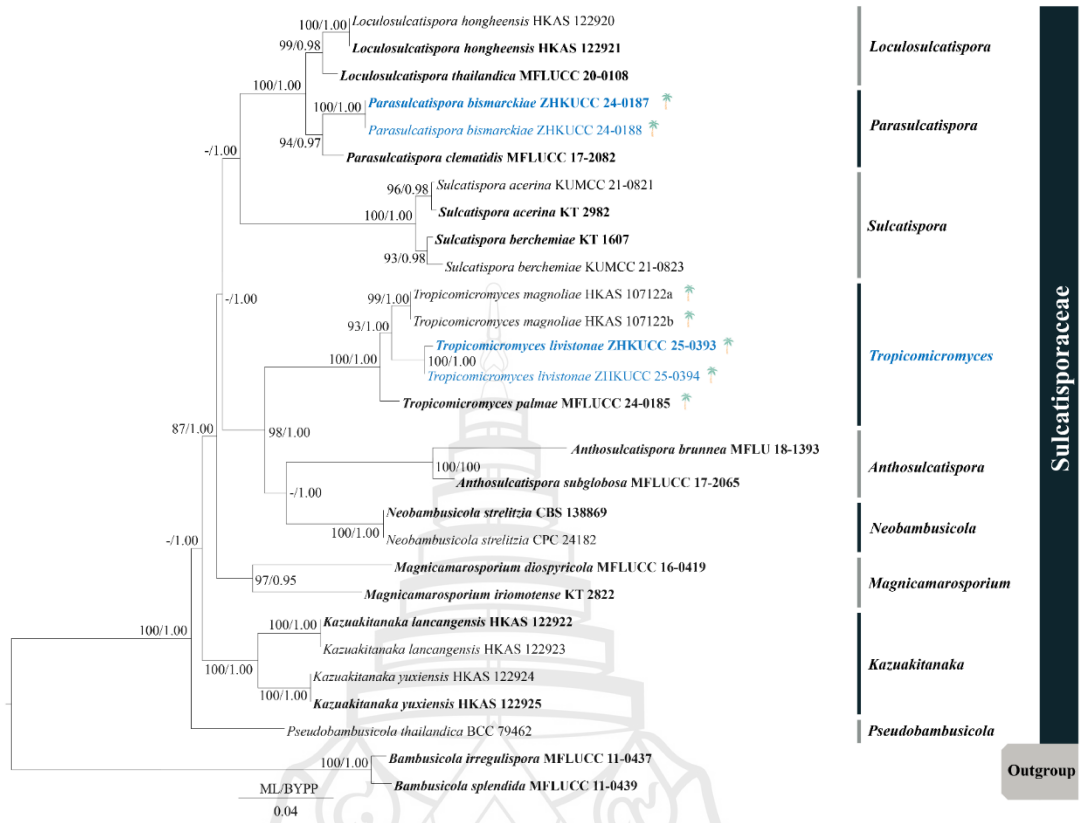
Note a, b Ascomata on substrate. c Vertical sections of ascomata. d, e Cells of peridium. f Setae. g Pseudoparaphyses. h–l Asci. m–p Ascospores. q Germinating asci. r The front of culture on PDA at 25°C and the reverse of culture on PDA at 25°C. Scale bars: c, q = 50 µm, d–p = 10 µm.

Figure 2.48 *Pseudomassarina roystoneae* (MHZU 24-0453, holotype)

Sulcatisporaceae Kaz. Tanaka & K. Hiray., Stud. Mycol. 82: 119 (2015)

Parasulcatispora Phukhams. & K.D. Hyde, Fungal Diversity 102: 1–203 (2020).

Notes: Phukhamsakda et al. (2020) established *Parasulcatispora* (*Pa*.) with *Pa. clematidis* as the type species. The sexual morph of *Parasulcatispora* is characterized by coriaceous semi-immersed ascomata, central ostioles filled with hyaline periphyses, trabeculate pseudoparaphyses, bitunicate and fissitunicate asci and 1-euseptate ascospore (Phukhamsakda et al., 2020). Following Phukhamsakda et al. (2020) herein, we used phylogenetic analysis of combined SSU, LSU, *tef* 1-α and *rpb*2 to update the phylogenetic tree for *Parasulcatispora* (Figure 2.49). Currently, one epithet is listed under *Parasulcatispora* (Index Fungorum, 2024 December) this species is associated with molecular data. Here we described a new species of *Parasulcatispora* which is the first time reported from palm species (Xiong et al., 2025).



Note Phylogram generated from maximum likelihood analysis of Sulcatisporaceae based on combined ITS, LSU, *rpb2*, SSU and *tef* 1-α sequence data. Bootstrap values for maximum likelihood (ML) equal to or greater than 70 are indicated above the branches. The new collections are indicated in blue and ex-type strains are indicated in bold.

Figure 2.49 Phylogenetic tree of Sulcatisporaceae

Parasulcatispora bismarckiae Y.R. Xiong, Manawas. & K.D. Hyde, ***sp. nov.***

Figure 2.50

Etymology: The epithet refers to the host genus name "*Bismarckia*", from which the species was collected.

Saprobic on dead segment of *Bismarckia nobilis*. Asexual morph: Coelomycetous. *Conidiomata* 250–320 × 80–100 µm ($\bar{x}$ = 286 × 90 µm, n = 10), pycnidial, immersed to semi-immersed, solitary, multilocular, raising host epidermal and form clypeus or slit-like. *Peridium* 8–15 µm, composed of thin-walled, brown cells, *textura angularis*, inner wall with hyaline *textura globulosa* cells. *Conidiophores* reduced to

conidiogenous cells. *Conidiogenous cell* 3–4 × 1–2 µm ($\bar{x}$ = 3.6 × 1.6 µm, n = 25), holoblastic, annellate, phialidic to cylindrical, slight curve, hyaline, smooth-walled, arising from stratum. *Conidia* 7–11 × 3–4 µm ($\bar{x}$ = 8.3 × 3.5 µm, n = 25), oblong to ellipsoid, slightly curved, truncate to rounded apex, aseptate, hyaline, 1–2 guttulate within the cell. Sexual morph: Not observed.

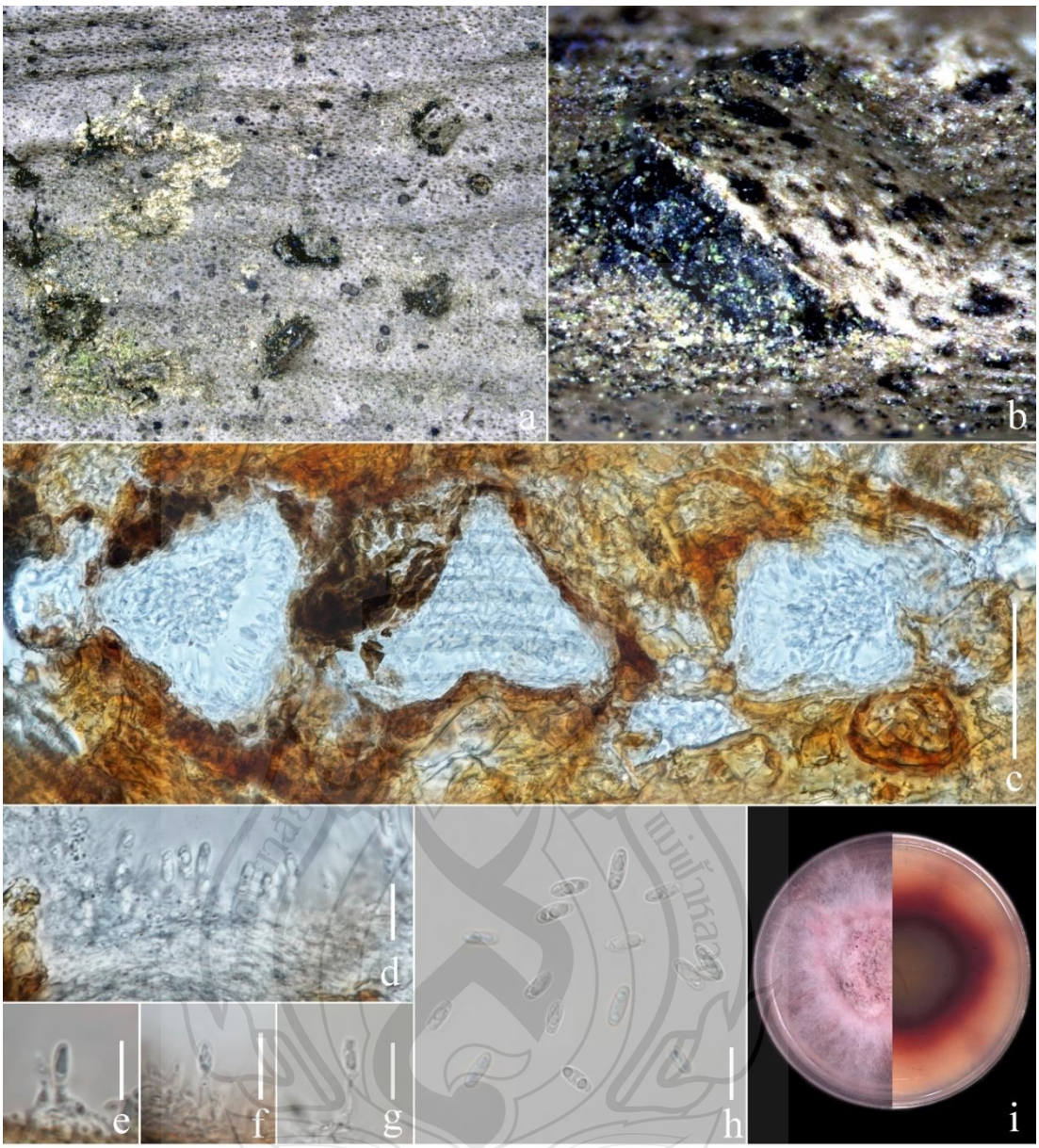
Culture characteristics: Colonies on PDA fast growing, after 2 weeks reaching 4 cm diam., at 25°C, filamentous and irregular, with fluffy, dense, pale pink mycelium on the surface; in reverse yellow-brown in the middle and red-brown at the margin.

Known distribution: China (this study).

Material examined: China, Yunnan Province, Xishuangbanna City, on dead leaf sheath of *Bismarckia nobilis*, 4 Feb 2023, Y.R. Xiong and L. Lu, XG283 (MHZU 23-0190, holotype) – ex-type ZHKUCC 24-0187, other living culture ZHKUCC 24-0188.

GenBank numbers: ZHKUCC 24-0187: ITS – PV578220, LSU – PV578386, SSU – PV578528, *tef* 1-α – PV608876, *rpb*2 – PV595342; ZHKUCC 24-0188: ITS – PV578221, LSU – PV578387, SSU – PV578529, *tef* 1-α – PV608877, *rpb*2 – PV595343.

Notes: Two collections from this study clustered in *Parasulcatispora* clade and formed a sister lineage to *Pa. clematidis* in the phylogenetic tree with 94% ML bootstrap support and 1.00 BYPP (Figure 2.49). The nucleotide differences excluding gaps between *Pa. bismarckiae* (ZHKUCC 24-0187) and *Pa. clematidis* (MFLUCC 16-0909) were checked and given as follows, ITS: 8.10% (41/506 base pairs), LSU: 1.65% (14/847 base pairs), and *tef* 1-α: 2.58% (23/892 base pairs). *Parasulcatispora bismarckiae* is characterised by oblong to ellipsoid conidia and annellate conidiogenous cells in *Parasulcatispora*. In addition, *Parasulcatispora clematidis* is a sexual morph of *Parasulcatispora* (Phukhamsakda et al., 2020). Based on phylogenetic placement and asexual morphological variations, we introduce *Pa. bismarckiae* as a new species.



Note a, b Conidiomata on the substrate. c Sections through conidiomata. d–g Conidiogenous cells and developing conidia. h Conidia. i The front of culture on PDA at 25°C and the reverse of culture on PDA at 25°C. Scale bars: c = 50 µm, d–h = 10 µm.

Figure 2.50 *Parasulcatispora bismarckiae* (MHZU 23-0190, holotype)

Tropicomicromyces Y.R. Xiong, Manawas. & K.D. Hyde, ***gen. nov.***

Etymology: referring to the tropical habitats and microfungal of the type species.

Saprobic on dead petiole of *Livistona* sp. Asexual morph: not observed. Sexual morph: *Ascomata* semi-immersed, solitary or aggregated in small groups, scattered, globose to subglobose, dark brown, visible as the dark brown area with an erumpent black dot or papilla, coriaceous, ostiolate. *Peridium* blackish to dark brown cells of *textura angularis*. *Hamathecium* anastomosing, septate, branched, hyaline, pseudoparaphyses. *Asci* 8-spored, bitunicate, cylindric-clavate, with a short pedicel, apically rounded, with minutely an ocular chamber. *Ascospores* overlapping biseriate, lunate to ellipsoid, 1-septate, constricted at the septum, slightly constricted at the central of cells, hyaline, brown when mature, surrounded by a mucilaginous sheath.

Type species: *Tropicomicromyces livistonae* Y.R. Xiong, Manawas. & K.D. Hyde

Notes: Based on our phylogenetic result (Figure 2.49), *Tropicomicromyces* (*Tr.*) formed a distinct clade in Sulcatisporaceae and clustered with *Anthosulcatispora* and *Neobambusicola*. Morphologically, *Tropicomicromyces* consist of the basial character of Sulcatisporaceae (Tanaka et al., 2015). However, it differs from *Anthosulcatispora* and *Neobambusicola* by 8-spored asci with minutely an ocular chamber, with ascospores lunate to ellipsoid, 2-celled, and mucilaginous sheath present (Phookamsak et al., 2019; de Silva et al., 2022). According to Morphological differences evidence and phylogenetic results, we proposed a new genus *Tropicomicromyces* typified by of *Tr. livistonae*. Moreover, based on *N. magnoliae* and *N. palmae* cluster with *Tr. livistonae* in phylogenetic analysis (Figure 2.49), we proposed two new combinations for them (see notes on *Tr. magnoliae* and *Tr. palmae*). The genus has two species hosts on the palm (Xiong et al., 2025).

Tropicomicromyces livistonae Y.R. Xiong, Manawas. & K.D. Hyde, ***sp. nov.***

Figure 2.51

Etymology: The epithet refers to the host genus "*Livistona*", from which the species was collected.

Saprobic on dead petiole of *Livistona* sp. Asexual morph: Not observed. Sexual morph: *Ascomata* 300–400 × 390–500 μm ($\overline{x}$ = 365 × 440 μm, n = 10) semi-immersed, solitary or aggregated in small groups, scattered, globose to subglobose, dark brown, visible

as dark brown area with an erumpent black dot or papilla, coriaceous, ostiolate. *Peridium* 35–50 µm, blackish to dark brown cells of *textura angularis*. *Hamathecium* 1.5–2 µm wide anastomosing, septate, branched, hyaline, pseudoparaphyses. *Asci* 60–85 × 8.5–12.5 µm ($\overline{x}$ = 74.5 × 10 µm, n = 25) 8-spored, bitunicate, cylindric-clavate, with a short pedicel, apically rounded, with minutely an ocular chamber. *Ascospores* 17–27 × 3.5–6.5 µm ($\overline{x}$ = 21.6 × 4.8 µm, n = 40) overlapping biseriate, lunate to fusiform, 1-septate, constricted at the septum, slightly constricted at the central of cells, hyaline, brown when mature, surrounded by a mucilaginous sheath.

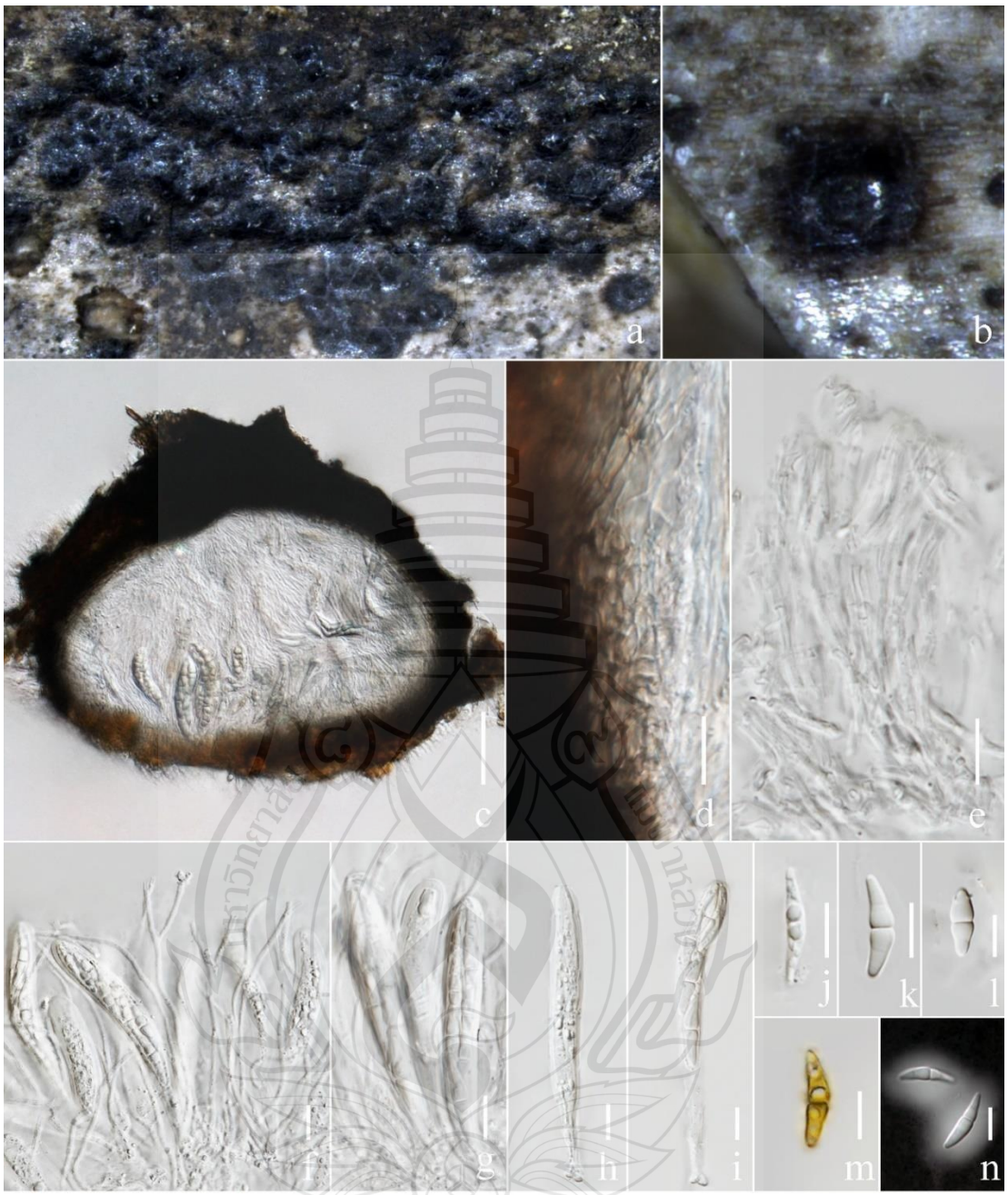
Culture characteristics: Colonies on PDA, after 2 weeks reaching 4 cm diam., at 25°C, circular or irregular, flat to slightly raised, mycelium velvety towards the margin, greyish green, reverse dull dark brown.

Known distribution: China (this study).

Material examined: China, Yunnan Province, Xishuangbanna City, in an unidentified forest beside National Highway 219, on dead petiole of *Livistona* sp., 8 Jul 2022, Y.R. Xiong and L. Lu, XG066 (MHZU 24-0448, holotype), ex-type ZHKUCC 25-0393, other living culture ZHKUCC 25-0394.

GenBank numbers: ZHKUCC 25-0393: ITS – PV578260, LSU – PV578428, SSU – PV578556, *tef* 1-α – PV608898, *rpb*2 – PV595364; ZHKUCC 25-0394: ITS – PV578261, LSU – PV578429, SSU – PV578557, *tef* 1-α – PV608899, *rpb*2 – PV595365.

Notes: Two collections from this study formed a separate lineage and clustered with *Tropicomicromyces magnoliae* and *Tr. palmae* in the phylogenetic tree with 93% ML and 1.00 BYPP bootstrap support (Figure 2.49). The nucleotide differences excluding gaps between *Tr. livistonae* and its phylogenetically related species were as follows, *Tr. magnoliae* (HKAS 107122a) - ITS: 3.55% (23/647 base pairs), *tef* 1-α: 3.19% (29/909 base pairs); *Tr. palmae* - ITS: 5.60% (27/482 base pairs), *tef* 1-α: 3.08% (29/942 base pairs), *rpb*2: 5.77% (52/901 base pairs). *Tropicomicromyces magnoliae* was reported as an asexual morph and *Tr. palmae* was reported as a sexual morph (de Silva et al., 2022; Zhang et al., 2024). *Tropicomicromyces livistonae* differs from *Tr. palmae* by ascospore are lunate to ellipsoid and brown when mature. However, *Tr. palmae* has hyaline ascospore with fusiform (Zhang et al., 2024). Based on phylogenetic placement and morphological variations, we introduce *Tr. livistonae* as a new species.



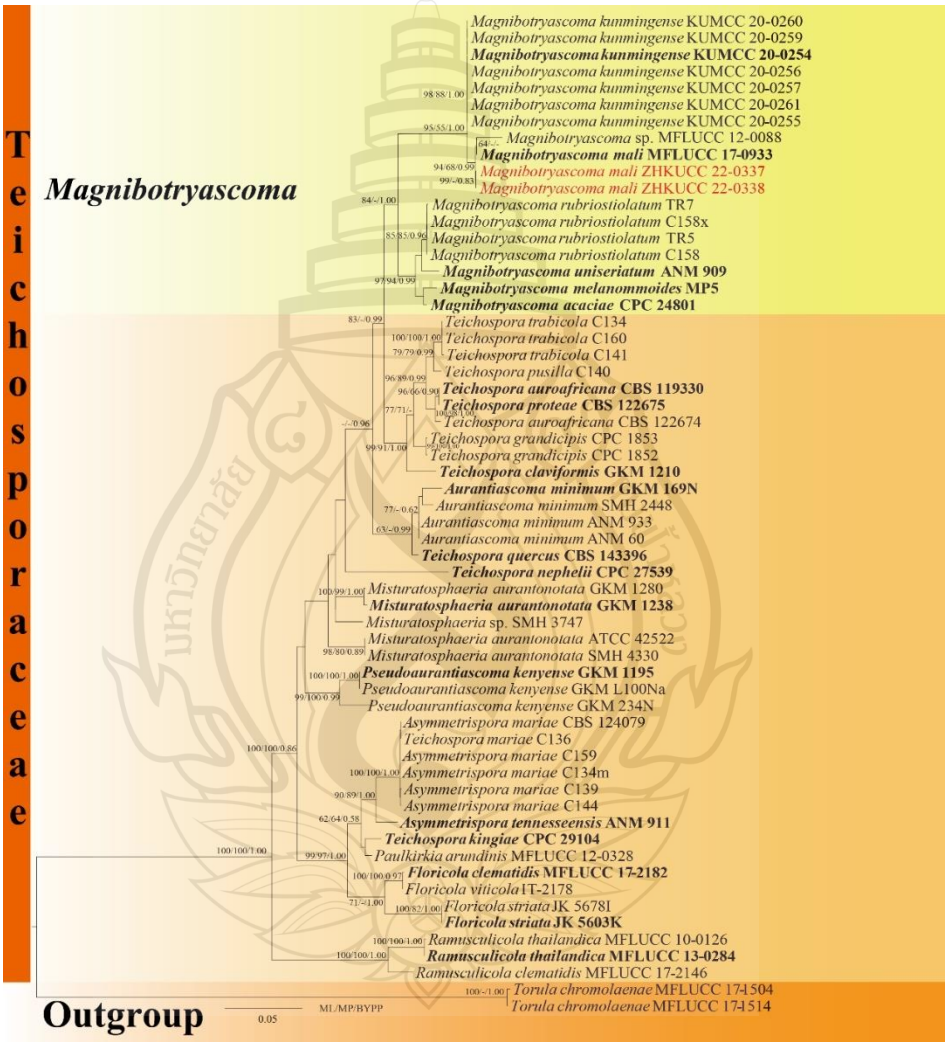
Note a, b Ascomata on substrate. c Vertical sections of ascomata. d Peridium. e Hamathecium. f–i Asci. j–n Ascospore (n ascospore in Indian ink). Scale bars: c = 50 µm, d–n = 10 µm.

Figure 2.51 *Tropicomicromyces livistonae* (MHZU 24-0448, holotype)

Teichosporaceae M.E. Barr, Mycotaxon 82: 374 (2002)

Magnibotryascoma Thambugala & K.D. Hyde (2024)

Notes: *Magnibotryascoma* was proposed to accommodate *M. uniseriatum* which was transferred from *Misturatosphaeria uniseriatum* based on its unique morphology (Mugambi & Huhndorf, 2009; Thambugala et al., 2015). For taxonomic treatment of this genus, we follow Hongsanan et al. (2020), Tennakoon et al. (2021) and Wijayawardene et al. (2022).



Note Phylogram generated from maximum likelihood analysis of Teichosporaceae based on combined ITS, LSU, SSU, *rpb*2 and *tef* 1-α sequence data. Bootstrap values for maximum likelihood (ML) equal to or greater than 70 are indicated above the branches. The new collections are indicated in red and ex-type strains are indicated in bold.

Figure 2.52 Phylogenetic tree of Teichosporaceae

Magnibotryascoma mali Phukhams., Wanas. & K.D. Hyde, Fungal Diversity 87: 105 (2017)

Figure 2.53

Saprobic on rotting branch of *Trachycarpus fortunei* (*Arecaceae*). *Sexual morph*: Not observed. *Asexual morph*: Coelomycetous. Pycnidia 90–220 µm diam, 150–250 µm length ($\overline{x}$ = 156 × 223 µm, n = 10), pycnidial, solitary, scattered, unilocular, semi-immersed, coriaceous, papillate, dark brown to brown. Pycnidial wall 15–25 µm wide, thick, multi-layered, composed of light brown to brown cells of textura angularis. Conidiophores 3–5 × 1.5–2 µm ($\overline{x}$ = 4 × 1.9 µm, n = 20) fasciculate, subcylindrical, hyaline. Conidiogenous cell 1.5–5 × 2–2.5 µm ($\overline{x}$ = 3 × 2.1 µm, n = 20), enteroblastic, discrete, cylindrical to irregular, hyaline. Conidia 3–4 × 2.5–3.5 µm ($\overline{x}$ = 3.6 × 2.9 µm, n = 50), globose to oval, guttulate, hyaline when immature, brown at maturity, aseptate, smooth-walled.

Culture characteristics: Colonies on PDA attaining 2 cm diam after a week at 25°C, erose, convex, rough, rugose, buff; reverse cream.

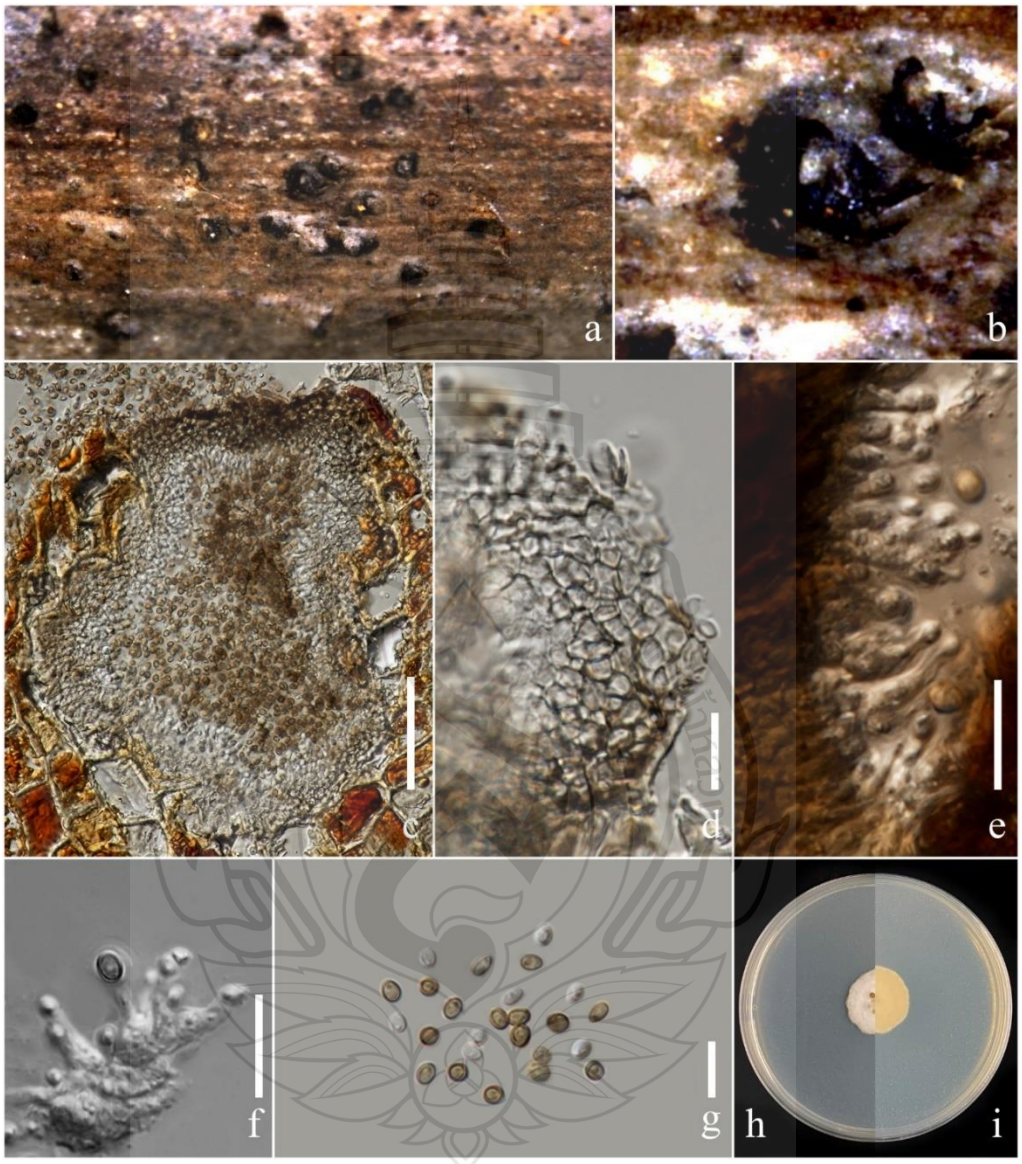
Known distribution: China (Hyde et al., 2017; Mortimer et al., 2021, this study).

Material examined: China, Yunnan Province, Kunming City, Kunming Institute of Botany, Chinese Academy of Sciences (25°08'17" N, 102°44'34" E), a rotting branch of the *Trachycarpus fortunei* (*Arecaceae*), 20 October 2021, Y.R. Xiong (MHZU 22-0178, new host record; living culture, ZHKUCC 22-0337); ibid. 20 October 2021, Y.R. Xiong (living cultures, ZHKUCC 22-0338).

GenBank numbers: ZHKUCC 22-0337: ITS – OQ449322, LSU – OQ449290, SSU – OQ449339, *rpb2* – OQ458724, *tef* 1-α – OQ458717; ZHKUCC 22-0338: ITS – OQ449323, LSU – OQ449291, SSU – OQ449340, *rpb2* – OQ458725, *tef* 1-α – OQ458718.

Notes: *Magnibotryascoma mali* was introduced by Hyde et al. (2017), but the ITS sequence of the type strain has obvious deletions and differs from other species of this genus. Thus, the ITS sequence of this species was excluded from the phylogenetic analysis in this study. *Magnibotryascoma kunmingense* was introduced by Mortimer et al. (2021). However, the nucleotide of *M. mali* and *M. kunmingense* strains are not significantly different as follow *M. kunmingense* (KUMCC 20-0254) LSU: 0.98% (8/817 bases), *rpb2*: 0.92% (7/757 bases), SSU: 0.11% (1/981 bases), *tef* 1-α: 0.65% (6/926 bases) excluding gaps. Tennakoon et al. (2021) also compared the morphological data of these two species,

which mentioned that their morphology is almost identical. Therefore, *M. kunmingense* could be a possible synonym for *M. mali*. However, both species were introduced with their asexual morph. Therefore, we proposed in the future, these two species could be synonymized based on the sexual morph and more sampling.



Note a–b, Conidiomata on the rotting branch of *Trachycarpus fortune*; c Section of conidiomata; d Peridium; e–f, Conidiogenous cells giving rise to conidia; g Conidia; h–i, Culture on PDA from above and reverse. Scale bars c = 50 μm, d–g = 10 μm.

Figure 2.53 *Magnibotryascoma mali* (MHZU 22-0178, new host record)

Pseudoteichospora X.G. Tian, K.D. Hyde & Tibpromma, Mycosphere 15(1): 1–274 (2024).

Notes: Tian et al. (2024) established *Pesudoteichospora* (*Pesudotei.*) with *Pesudotei. thailandensis* as the type species. *Pseudoteichospora* is coelomycetous genus characterized by immersed or semi-immersed pycnidial conidiomata, papillate ostiole, phialidic and cylindrical conidiogenous cells and ellipsoidal to oval aseptate conidia (Tian et al., 2024). Based on morphological evidence and phylogenetic analysis combined ITS, LSU, SSU, *rpb*2 and *tef* 1-α Tian et al. (2024) introduced *Pseudoteichospora* as a new genus. In this study, we use ITS, LSU, SSU, *rpb*2 and *tef* 1-α to update phylogenetic studies for *Pseudoteichospora* (Figure 2.52). Currently, one epithets are listed under *Pseudoteichospora* (Index Fungorum, 2024 December) and all species are associated with molecular data. Here we described a new species of *Pseudoteichospora* which is the first time reported from palm species (Xiong et al., 2025).

Pseudoteichospora borassi Y.R. Xiong, Manawas. & K.D. Hyde, ***sp. nov.***

Figure 2.54

Etymology: The epithet refers to the host genus name "*Borassus*", from which the species was collected.

Saprobic on dead segment of *Borassus flabellifer*. Asexual morph: Coelomycetous. *Conidiomata* 150–200 × 100–190 µm ($\overline{x}$ = 183 × 153 µm, n = 10), pycnidial, semi-immersed, unilocular, dark brown to black, solitary, globose to sub-globose, ostiolate. *Ostiole* central, cylindrical papillate on substrate surficial. *Peridium* 16–20 µm wide, with outer layers of brown, cells of *textura angularis*, with a hyaline inner lining. *Conidiophores* reduced to conidiogenous cells. *Conidiogenous cells* 10–20 × 2–4 µm ($\overline{x}$ = 15 × 2.8 µm, n = 25), hyaline, phialidic, indeterminate, cylindrical and smooth-walled, most 1-cell, scattered 2-cells. *Conidia* 5–7 × 2–4 µm ($\overline{x}$ = 6 × 3.4 µm, n = 25), hyaline, 1-cell, oval to clavate with obtuse ends, guttulate. Sexual morph: Not observed.

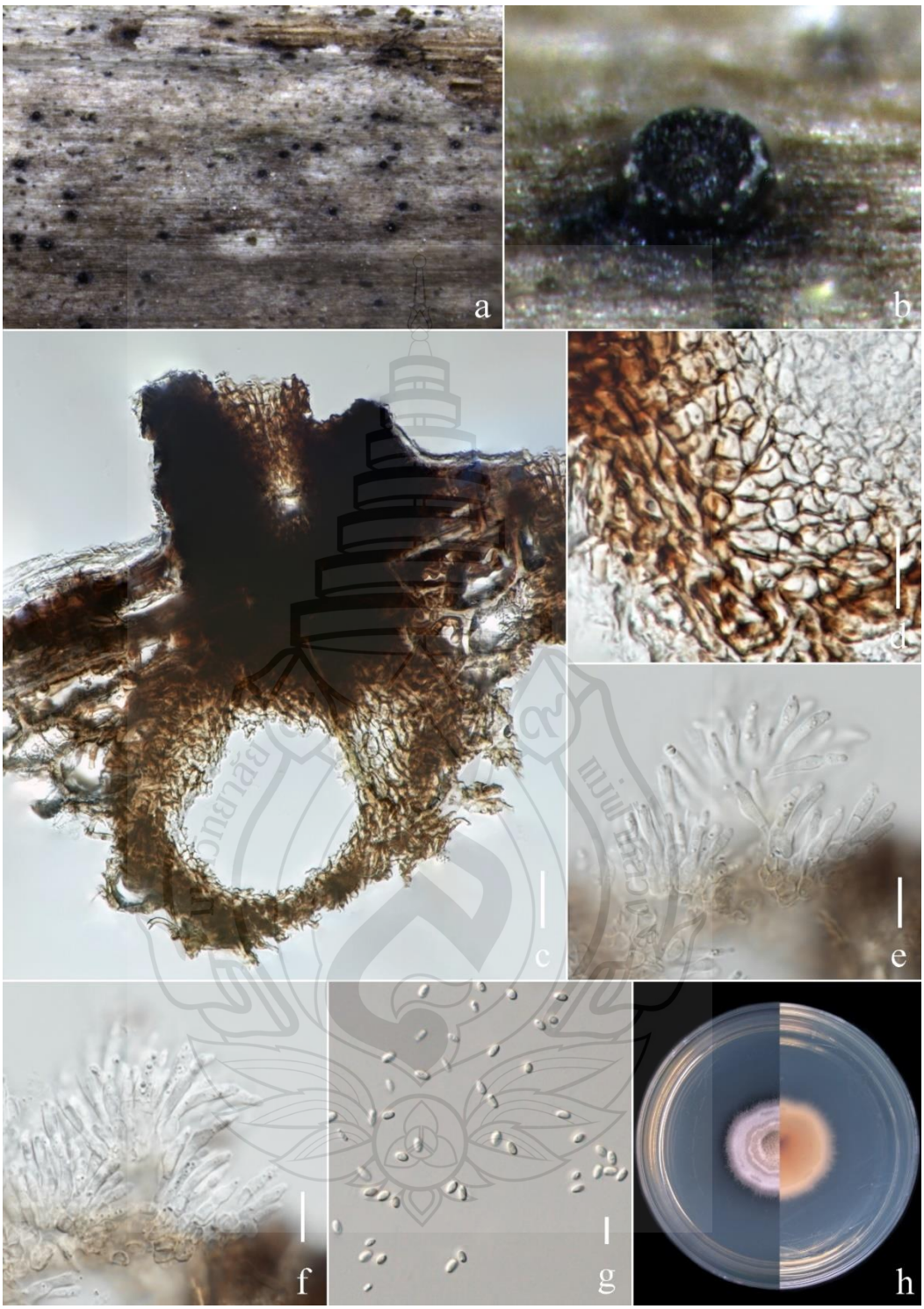
Culture characteristics: Colonies on PDA fast growing, after 2 weeks reaching 4 cm diam., at 25°C, circular, filamentous, umbonate, with fluffy, dense, white mycelium, grey in centre; in reverse cream in the middle and white at the margin.

Known distribution: China (this study).

Material examined: China, Yunnan Province, Xishuangbanna City, Xishuangbanna Dai Nationality Park, on dead segment of *Borassus flabellifer*, 6 Feb 2023, Y.R. Xiong and L. Lu, XG246 (MHZU 23-0177, holotype) – ex-type ZHKUCC 24-0161, other living culture ZHKUCC 24-0162.

GenBank numbers: ZHKUCC 24-0161: ITS – PV578244, LSU – PV578412, *rpb*2 – PV595358, *tef* 1-α – PV608892; ZHKUCC 24-0162: ITS – PV578245, LSU – PV578413, *rpb*2 – PV595359, *tef* 1-α – PV608893.

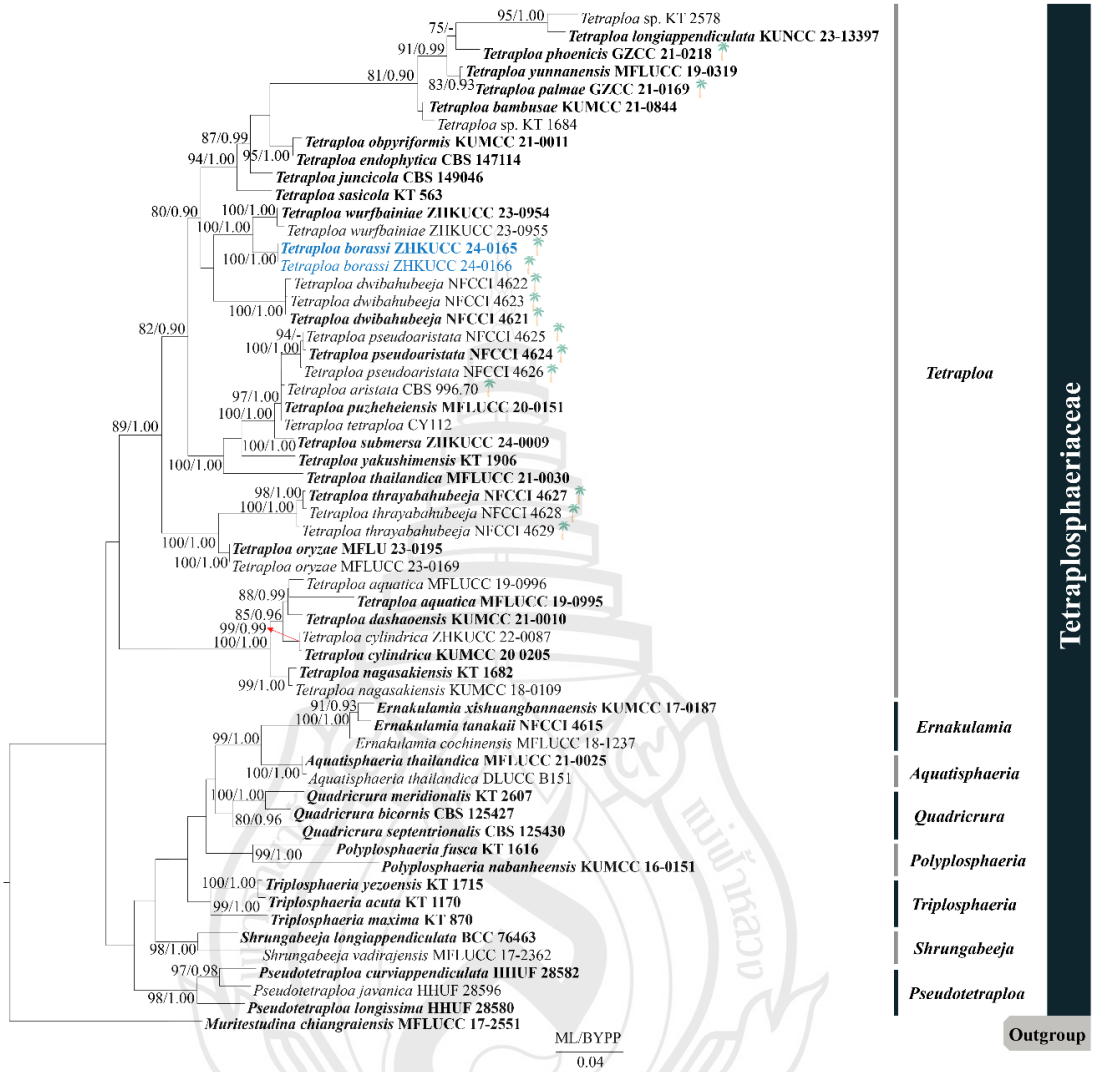
Notes: Two collections from this study clustered in *Pseudoteichospora* clade and formed a sister lineage to *Pseudotei. thailandensis* in the phylogenetic tree with 100% ML and 1.00 BYPP (Figure 2.52). The nucleotide differences exclude gaps between *Pseudotei. borassi* and *Pseudotei. thailandensis* (MFLUCC 23-0121) were checked and given as follows, ITS: 1.95% (10/512 base pairs), *rpb*2: 4.41% (46/1044 base pairs), *tef* 1-α: 3.06% (28/914 base pairs). *Pseudoteichospora borassi* has a cylindrical ostiole superficial on the substrate which differs from *Pseudotei. thailandensis* which has only a central, papillate ostiole (Tian et al., 2024). Based on phylogenetic placement and morphological variations, we introduce *Pseudotei. borassi* as a new species.



Note a, b Appearance of conidiomata on host. c Section through of conidiomata. d Section of peridium. c, f Conidiogenous cells and conidia. l Conidia. m The front of culture on PDA at 25°C and the reverse of culture on PDA at 25°C. Scale bars: c = 20 μm, d–g = 10 μm.

Figure 2.54 *Pseudoteichospora borassi* (MHZU 23-0177, holotype)

Tetraplosphaeriaceae Kaz. Tanaka & K. Hiray, Stud. Mycol. 64: 177 (2009)



Note Phylogram generated from maximum likelihood analysis of Tetraplosphaeriaceae based on combined ITS, LSU, SSU, *tub*2 and *tef* 1-α sequence data. Bootstrap values for maximum likelihood (ML) equal to or greater than 70 are indicated above the branches. The new collections are indicated in blue and ex-type strains are indicated in bold.

Figure 2.55 Phylogenetic tree of Tetraplosphaeriaceae

Tetraploa Berk. & Broome, Ann. Mag. nat. Hist., Ser. 2 5: 459 (1850)

Notes: Berkeley and Broome (1850) established *Tetraploa* (*Te*.) with *Te. aristata* as the type species. Although Tanaka et al. (2009) redefined *Tetraploa* as *Tetraploasphaeria* based on its massarina-like sexual morph and *Tetraploa sensu stricto* asexual morphs, Hyde et al. (2013) reinstated *Tetraploa* over *Tetraplosphaeria* which is currently accepted (Hyde et al., 2024). *Tetraploa* is a holomorphic genus with the asexual morph characterized by brown, euseptate, short cylindrical with 3–4 columnar conidial body, and coarsely verrucose base having setose appendages at the apex. The sexual morph characterized by globose to subglobose ascomata, cylindrical to clavate asci, narrowly fusiform, and uniseptate ascospores with an appendage-like sheath (Tanaka et al., 2009; Hyde et al., 2013, 2020; Dong et al., 2020; Jayawardena et al., 2022). Based on morphological evidence and phylogenetic analysis combined SSU and LSU, Tanaka et al. (2009) proposed *Tetraplosphaeria* to include *Tetraploa* species. However, Hyde et al. (2013) based on morphological evidence and phylogenetic analysis combined LSU, SSU, *tef* 1-α and *rpb*2 reinstated *Tetraploa*. Subsequently, phylogenetic studies mainly use LSU, SSU, ITS, *tef* 1-α and *tub*2 or *rpb*2 replaced instead of *tub*2 in species delineation (Dong et al., 2020; Hyde et al., 2020; Jayawardena et al., 2022; Liao et al., 2024; Zhang et al., 2024; Zhao et al., 2024). In this study, we use ITS, LSU, SSU, *tub*2 and *tef* 1-α to update phylogenetic studies for *Tetraploa* (Figure 2.55). Currently, 38 epithets are listed under *Tetraploa* (Index Fungorum 2024 December), with 24 species associated with molecular data. Totally seven species have been reported from palm species including a new species described in this study (Xiong et al., 2025).

Tetraploa borassi Y.R. Xiong, Manawas. & K.D. Hyde, ***sp. nov.***

Figure 2.56

Etymology: The epithet refers to the host genus name "*Borassus*", from which the species was collected.

Saprobic on dead petiole of *Borassus flabellifer*. Asexual morph: Hyphomycetous. *Colonies* on natural substrate superficial, effuse. *Mycelium* superficial, composed of hyaline, smooth, septate, branched hyphae. *Conidiophores* absent. *Conidiogenous cells* indistinct. *Conidia* 25–35 × 10–20 µm ($\bar{x}$ = 29 × 16.5 µm, n = 25), obovate to short cylindrical, with truncate to obtuse basal end, brown to dark brown, verruculose, inconspicuous euseptate, composed of 3–4 columns when mature, 2–3-septate

in each column, with 2–4 appendages. Appendage 55–200 µm long ($\bar{x}$ = 121.5 µm, n = 20), 5–7.5 µm wide at the base, 3–4 µm wide at the apex, pare brown, euseptate, smooth, straight, rigid.

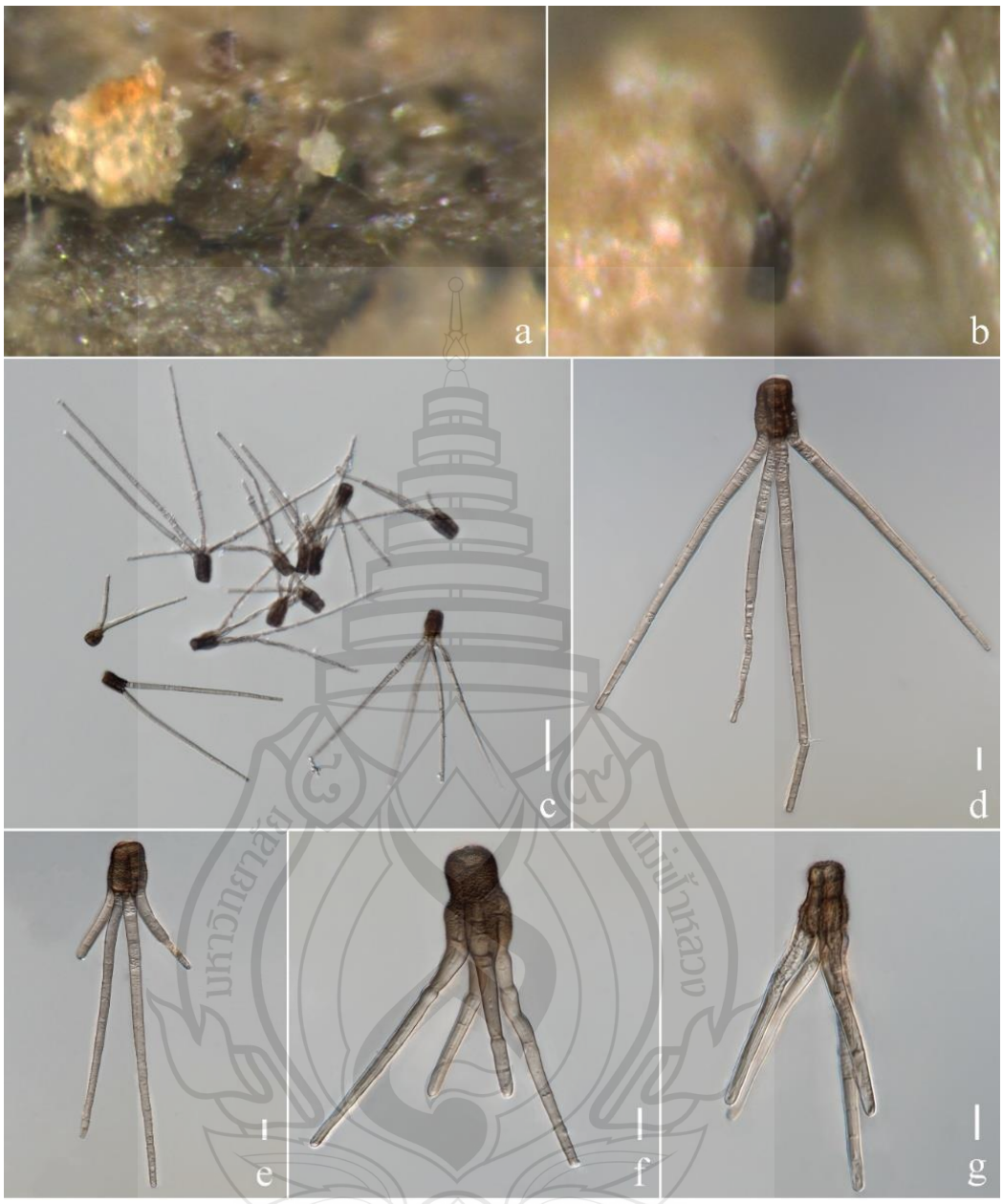
Culture characteristics: Colonies on PDA fast growing, after 2 weeks reaching 4 cm diam., at 25°C, circular, dense, grey, flossy, velvety; reverse centre dark brown to orange-brown, turning white towards the margin.

Known distribution: China (this study).

Material examined: China, Yunnan Province, Xishuangbanna City, Xishuangbanna Dai Nationality Park, on dead petiole of *Borassus flabellifer*, 6 Feb 2023, Y.R. Xiong and L. Lu, XG248 (MHZU 23-0179, holotype) – ex-type ZHKUCC 24-0165, other living culture ZHKUCC 24-0166.

GenBank numbers: ZHKUCC 24-0165: ITS – PV578258, LSU – PV578426, SSU – PV578554, *tef* 1-α – PV608896, *tub*2 – PV607968; ZHKUCC 24-0166: ITS – PV578259, LSU – PV578427, SSU – PV578555, *tef* 1-α – PV608897, *tub*2 – PV607969.

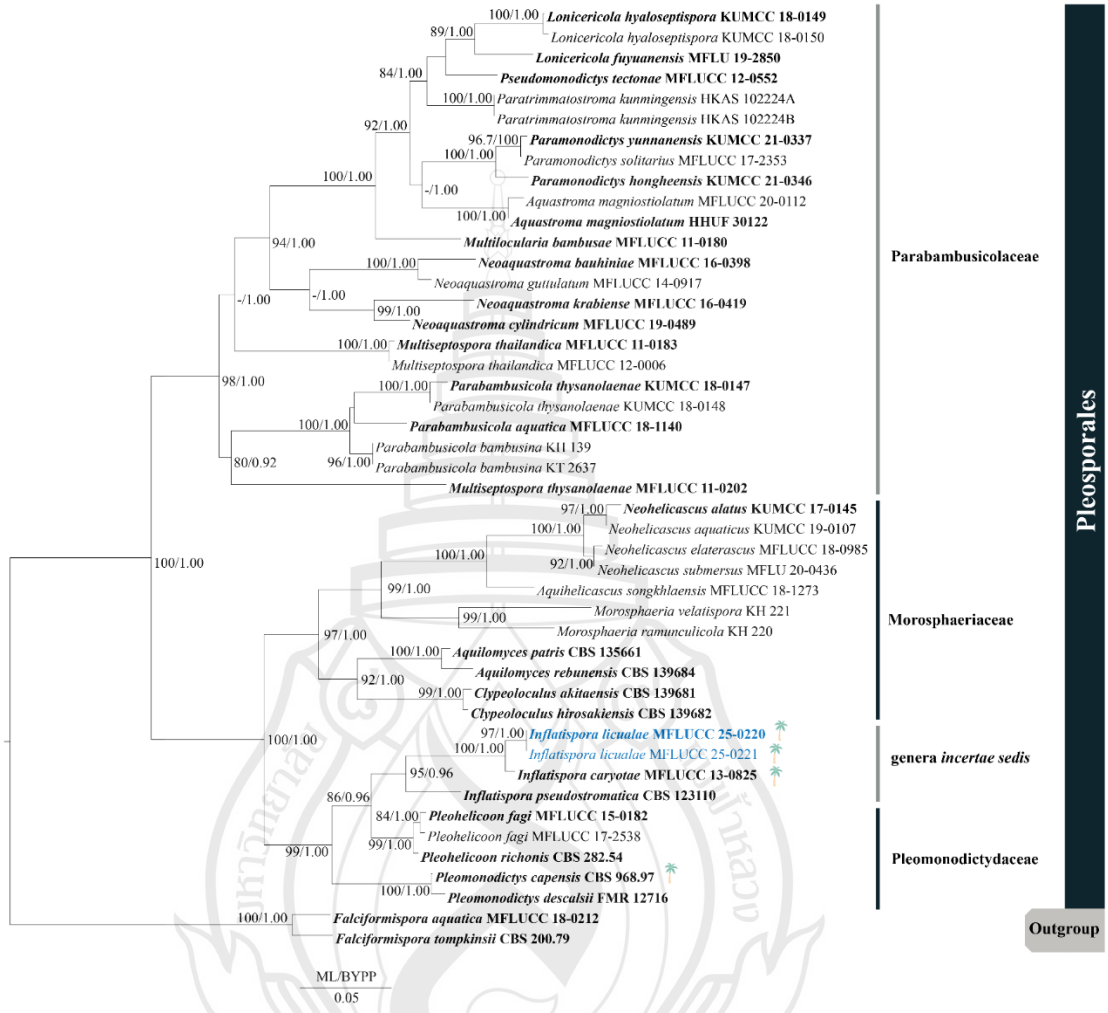
Notes: Two collections from this study clustered in *Tetraploa* clade and formed a sister lineage to *Te. wurfbainiae* in the phylogenetic tree with 100% ML bootstrap support and 1.00 BYPP (Figure 2.55). The nucleotide differences excluding gaps between *Te. borassi* (ZHKUCC 24-0165) and *Te. wurfbainiae* (ZHKUCC 23-0954) were checked and given as follows, ITS: 2.67% (13/487 base pairs), LSU: 1.38% (12/868 base pairs), *tub*2: 4.56% (27/592 base pairs), and *tef* 1-α: 4.06% (11/271 base pairs). Morphologically, *Te. borassi* have verruculose conidia which is not observed in *Te. wurfbainiae* (Liao et al., 2024). Moreover, *Te. borassi* have 2–3-septate in each column of conidia with 2–4 appendages, which is different from *Te. wurfbainiae* 3–4-septate or sometimes 5-septate in each column of conidia with one (in young conidia) or three appendages (Liao et al., 2024). Based on phylogenetic placement and morphological variations, we introduce *Te. borassi* as a new species.



Note a, b Sporodochia on the substrate. c–g Conidia. Scale bars: c = 50 µm, d–g = 10 µm.

Figure 2.56 *Tetraploa borassi* (MHZU 23-0179, holotype)

Pleosporales genera *incertae sedis*



Note Phylogram generated from maximum likelihood analysis of some Pleosporales families based on combined ITS, LSU, SSU and *rpb2* sequence data. Bootstrap values for maximum likelihood (ML) equal to or greater than 70 are indicated above the branches. The new collections are indicated in blue and ex-type strains are indicated in bold.

Figure 2.57 Phylogenetic tree of some Pleosporales families

Inflatispora Y. Zhang ter, J. Fourn. & K.D. Hyde, Sydowia 62: 290 (2011)

Notes: Zhang et al. (2011) established *Inflatispora* (*I.*) *I. pseudostromatica* as the type species. The sexual morph of *Inflatispora* was characterized by globose to subglobose, semi-immersed ascomata, which are covered under a pseudostroma, scattered

or in small groups, and black, asci consisting of 8-spores, clavate, bitunicate and ascospores are hyaline with an enlarged supra-median cell (Zhang et al., 2011; Tibpromma et al., 2017). In addition, the asexual morph of *Inflatispora* is characterized by colonies on natural substrates with composed of immersed, septate, smooth-walled hyphae, macronematous, mononematous, cylindrical, unbranched, dark to mid-brown conidiophores tapering towards the apex, conidiogenous cells are monophialidic, terminal, hyaline, and conidia are acrogenous, slimy, aggregated, oblong to ellipsoidal, hyaline, aseptate, and guttulate. Based on morphological evidence and phylogenetic analysis combined ITS, SSU and LSU sequence data Zhang et al. (2011) introduce *Inflatispora* as genera *incertae sedis* in Pleosporales. Subsequently, Tibpromma et al. (2017) use morphology and phylogenetic analysis combined SSU, LSU, *tef* 1-α and *rpb*2 to introduce a new sexual species *I. caryotae*. In our phylogenetic analyses based on ITS, SSU, LSU, and *rpb*2, *Inflatispora* clustered within Pleomonodictydaceae with 68% ML bootstrap support and 1.00 BYPP (Figure 2.57). Although Hyde et al. (2024) placed *Inflatispora* as genera incertae sedis in Pleosporales, more collections with molecular data are needed to confirm the taxonomic placement of the genus. Currently, two epithets are listed under *Inflatispora* (Index Fungorum, 2025 January), with all species associated with molecular data. Totally two species have been reported from palm species including a new species described in this study (Xiong et al., 2025).

Inflatispora licualae Y.R. Xiong, Manawas. & K.D. Hyde, ***sp. nov.***

Figure 2.58

Etymology: The epithet refers to the host genus "*Licuala*", from which the species was collected.

Saprobic on a dead segment of *Licuala* sp. Asexual morph: Hyphomycetous. *Colonies* on natural substrates effuse, hairy, scattered, hyaline to pare brown, with glistening conidial masses at apex. *Mycelium* immersed, composed of hyaline, smooth, septate, ale brown to hyaline hyphae. *Conidiophores* 50–60 × 3.5–4 µm ($\bar{x}$ = 53 × 3.8 µm, n = 25), macronematous, mononematous, erect, solitary, straight or slightly flexuous, cylindrical, smooth-walled, septate, unbranched, dark brown or mid brown, becoming narrow down towards the apex. *Conidiogenous cells* 4.5–8.5 × 1.5–2 µm ($\bar{x}$ = 6.6 × 1.9 µm, n = 25), monophialidic, integrated, terminal, hyaline, smooth-walled. *Conidia* 4–5 × 1.5–2 µm ($\bar{x}$ = 4.7 × 1.8 µm, n = 40), acrogenous, aggregated in slimy masses, oblong to

ellipsoidal, hyaline, aseptate, smooth-walled, guttulate at both ends. Sexual morph: Not observed.

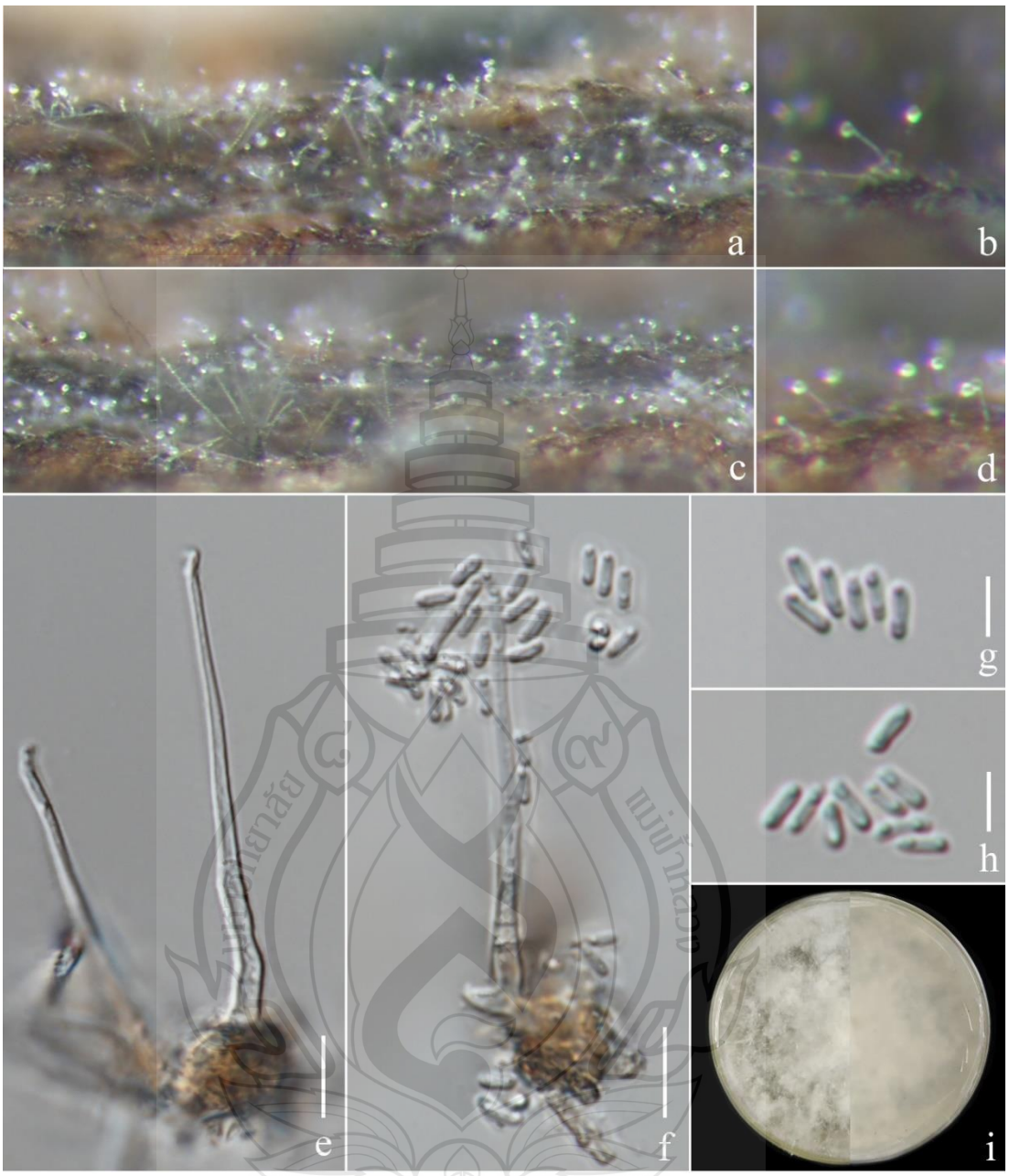
Culture characteristics: Colonies on PDA fast growing, after 2 weeks reaching 4 cm diam., at 25°C, circular, with fluffy, dense, white mycelium on the surface, curled; in reverse yellow in the middle and white at the margin.

Known distribution: Thaliand (this study).

Material examined: Thailand, Narathiwat, Toh Daeng Peat swamp, on dead segment of *Licuala* sp., 5 Aug 2024, Y.R. Xiong, XG350 (MFLU 25-0155, holotype), ex-type MFLUCC 25-0220, other living culture MFLUCC 25-0221.

GenBank numbers: MFLUCC 25-0220: ITS – PV578190, LSU – PV578354, SSU – PV578506, *rpb*2 – PV595330; MFLUCC 25-0221: ITS – PV578191, LSU – PV578355, SSU – PV578507, *rpb*2 – PV595331.

Notes: One collection from this study formed a separate lineage and clustered with *Inflatispora caryotae* with 100% ML bootstrap support and 1.00 BYPP (Figure 2.57). The nucleotide differences excluding gaps between our collection and *I. caryotae* (MFLUCC 13-0825) were checked: ITS: 1.91% (9/472 base pairs), LSU: 1.27% (11/869 base pairs). *Inflatispora licualae* is first reported as an asexual morph in *Inflatispora*. Based on the phylogenetic placement and morphological variations, we introduce *I. licualae* as a new species.



Note a–d Sporodochia on the substrate. e, f Conidiophore, conidiogenous cells with conidia. g, h Conidia. i The front of culture on PDA at 25°C and the reverse of culture on PDA at 25°C. Scale bars: e, f = 10 µm, g, h = 5 µm.

Figure 2.58 *Inflatispora licualae* (MFLU 25-0155, holotype)

Tubeufiales Boonmee & K.D. Hyde

Tubeufiaceae M.E. Barr, Mycologia 71(5): 948 (1979)

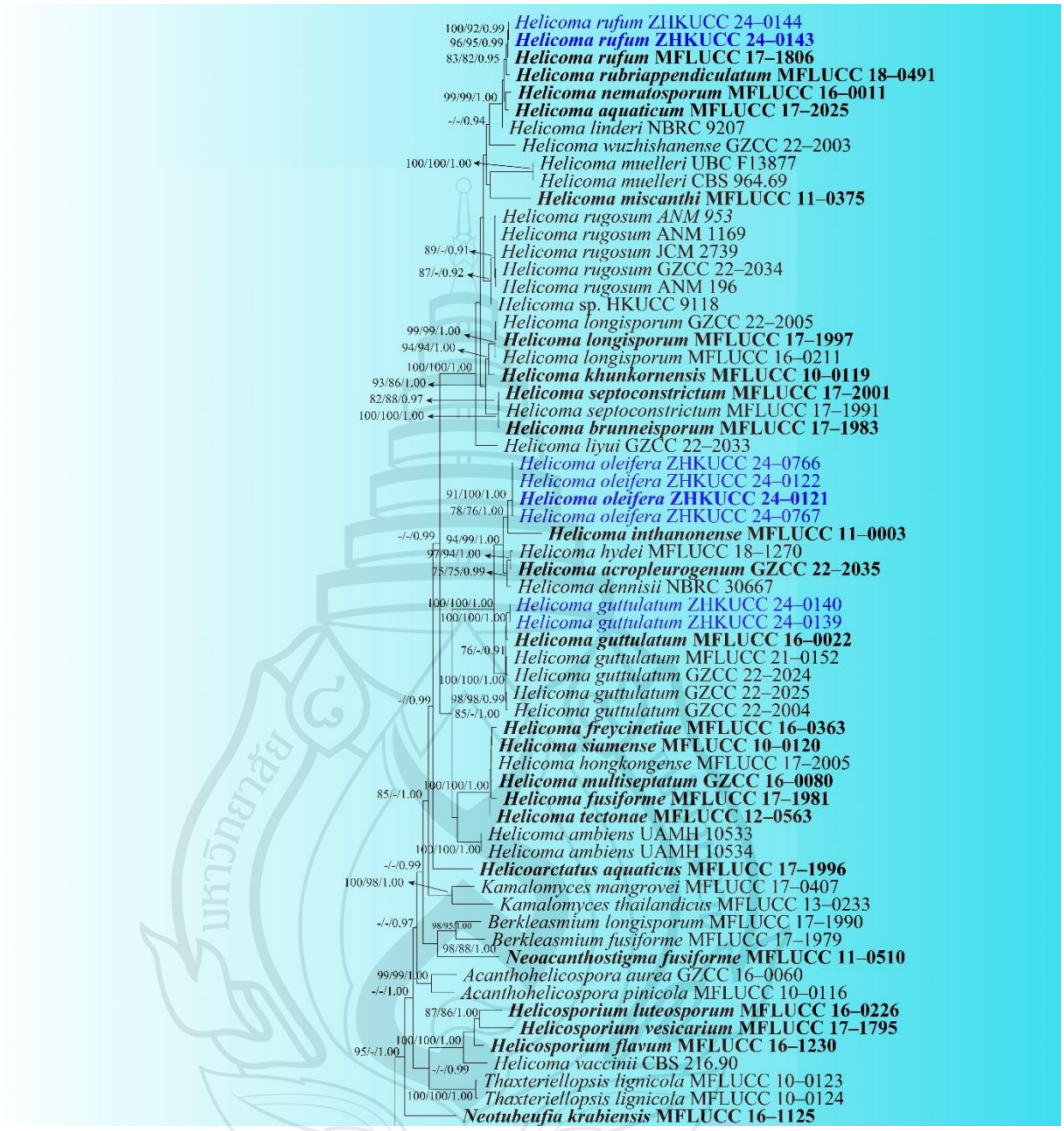
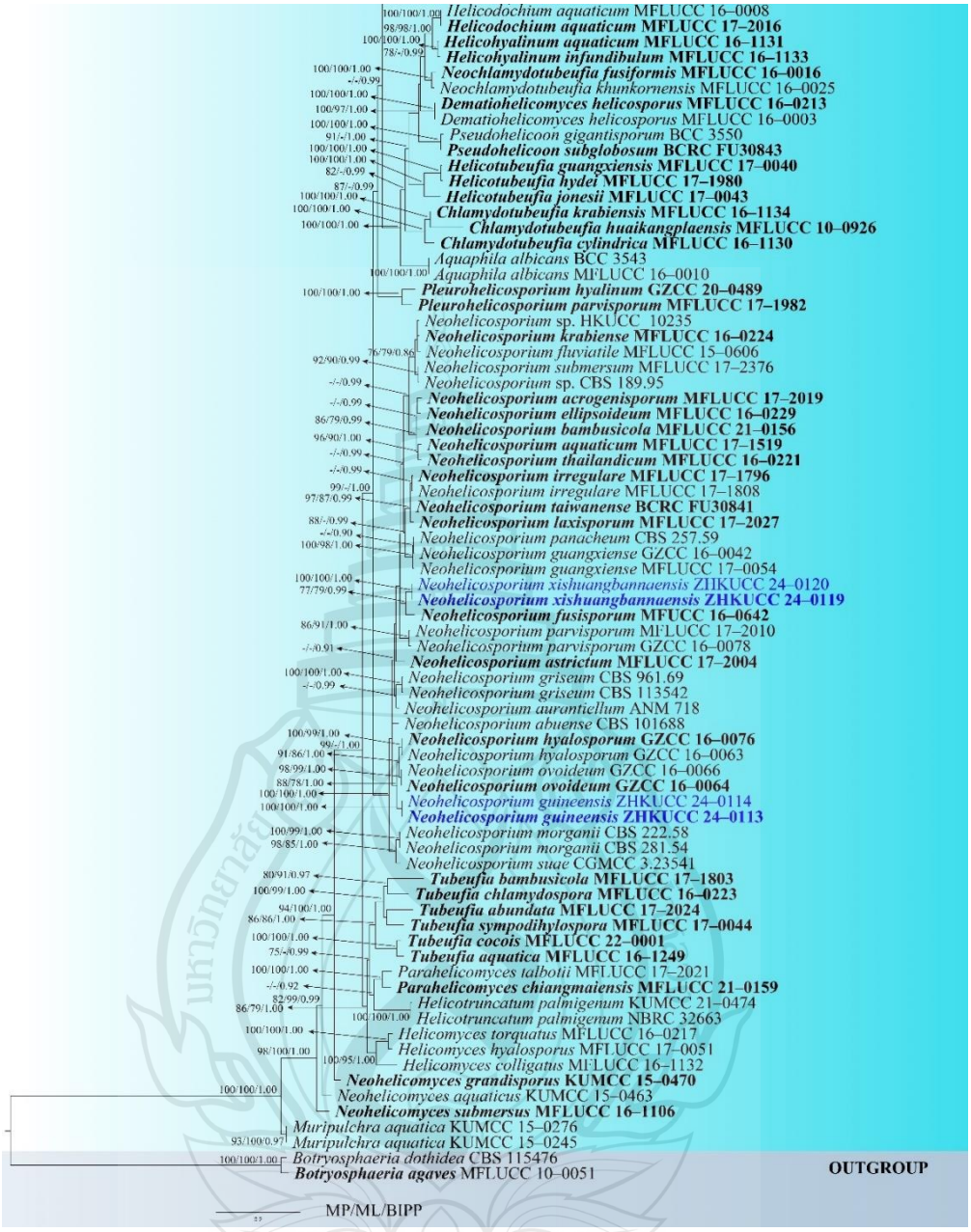


Figure 2.59 Phylogenetic tree of Tubeufiaceae



Note Maximum Likelihood majority rule consensus tree for Tubeufiaceae using ITS, LSU, *rpb*2 and *tef* 1-*α* sequence dataset with *Botryosphaeria agaves* (MFLUCC 10-0051) and *B. dothidea* (CBS 115476) as the outgroup taxa. Bootstrap support for Maximum Likelihood (ML) and Maximum Parsimony (MP) equal to or greater than 75% and Bayesian Inference posterior probability (BIPP) equal to or greater than 0.90 are indicated above branches as MP/ML/BIPP. The scale bar indicates 0.2 nucleotide changes per site. Collections from this study are marked in blue and ex-type strains are marked in bold.

Figure 2.59 (continued)

Helicoma Corda, Icon. fung. (Prague) 1: 15 (1837)

Notes: *Helicoma* was proposed by Corda (1837), with *H. muelleri* as the type species. It is one of the earliest genera of helicosporous hyphomycetes (Linder, 1929; Moore, 1955; Goos, 1986; Boonmee et al., 2014; Lu et al., 2018b). *Helicoma* species are frequently reported as saprobes inhabiting terrestrial and aquatic environments (Zhao et al., 2007; Boonmee et al., 2011, 2014; Hyde et al., 2016; Lu et al., 2018b, 2023; Liu et al., 2019; Tian et al., 2022). Based on phylogenetic analysis of combined ITS, LSU, *tef* 1-*α* and *rpb*2, Lu et al. (2018b) accepted species that are different from typical-Helicoma morphs described by Goos (1986) as *Helicoma*. These species are characterised by conidiogenous cells that are intercalary, cylindrical, with denticles, arising laterally from the lower portion of conidiophores as tooth-like protrusions. Conidia are pleurogenous, helicoid, hygroscopic, tapering towards the apex and rounded at the tip, coiled 1½–5 times, becoming loosely coiled in water. Subsequently, *H. hydei* (Liu et al., 2019), *H. wuzhishanense* (Lu et al., 2022), *H. acropleurogenum* and *H. liyui* (Lu et al., 2023) were reported in this genus.

Helicoma oleifera Y.R. Xiong, Manawas. & K.D. Hyde, ***sp. nov.***

Figure 2.60

Etymology: Species epithet refers to the host species name "*oleifera*" from which the fungus was isolated.

Saprobic on the rotting petiole of *Elaeis oleifera*. **Sexual morph:** Not observed. **Asexual morph:** Hyphomycetous, helicosporous. *Colonies* on the substratum superficial, effuse, gregarious, brown. ***Mycelium*** composed of partly immersed, partly superficial, hyaline, septate, branched hyphae. ***Conidiophores*** 145–360 µm long, 6.5–7.5 µm wide ($\bar{x}$ = 210 × 6.5 µm, n = 20), macronematous, mononematous, cylindrical, unbranched or branched at base, straight to slightly bent, septate, deep brown at root part, brown at apex, pale brown at middle part mixing with some brown areas, smooth-walled with irregular inclusion. ***Conidiogenous cells*** 13–22 µm long, 5–7.5 µm wide ($\bar{x}$ = 17 × 6.4 µm, n = 20), monoblastic, integrated, sympodial, terminal, cylindrical or fertile at the apex of conidiophores, brown, smooth-walled with irregular inclusion; with denticles, 1.3–2.3 µm long, 1.4–2.5 µm wide ($\bar{x}$ = 1.6 × 1.8 µm, n = 20), arising from the apex portion of conidiophores as tooth-like and papillate protrusions, exposed or imbedded in the apex of conidiophore, mono- to polyblastic, brown, smooth-wall. ***Conidia*** 18–22.5 µm diam.

($\overline{x}$ = 20.4 µm, n = 40) and conidial filament 6.8–9 µm wide ($\overline{x}$ = 8.2 µm, n = 40), 45–55 µm long ($\overline{x}$ = 50.6 µm, n = 40), solitary, acrogenous, helicoid, rounded at tip, tapering towards flat end, conic truncate at base, tightly coiled 1½ times, 8-septate, not becoming loose in water, guttulate, hyaline to pale brown, smooth-walled, the third cell shrinking and producing the root canal.

Culture characteristics: ***Conidia*** germinating on water agar and germ tubes produced from conidia within 12 h. ***Colonies*** growing on PDA attaining 2.5 cm diam. after six weeks at 25ºC, irregular, undulate, rough, superficial and partially immersed, brown aerial mycelium mixed with pale brown, deep brown at up and down junction area; reverse brown with pale brown.

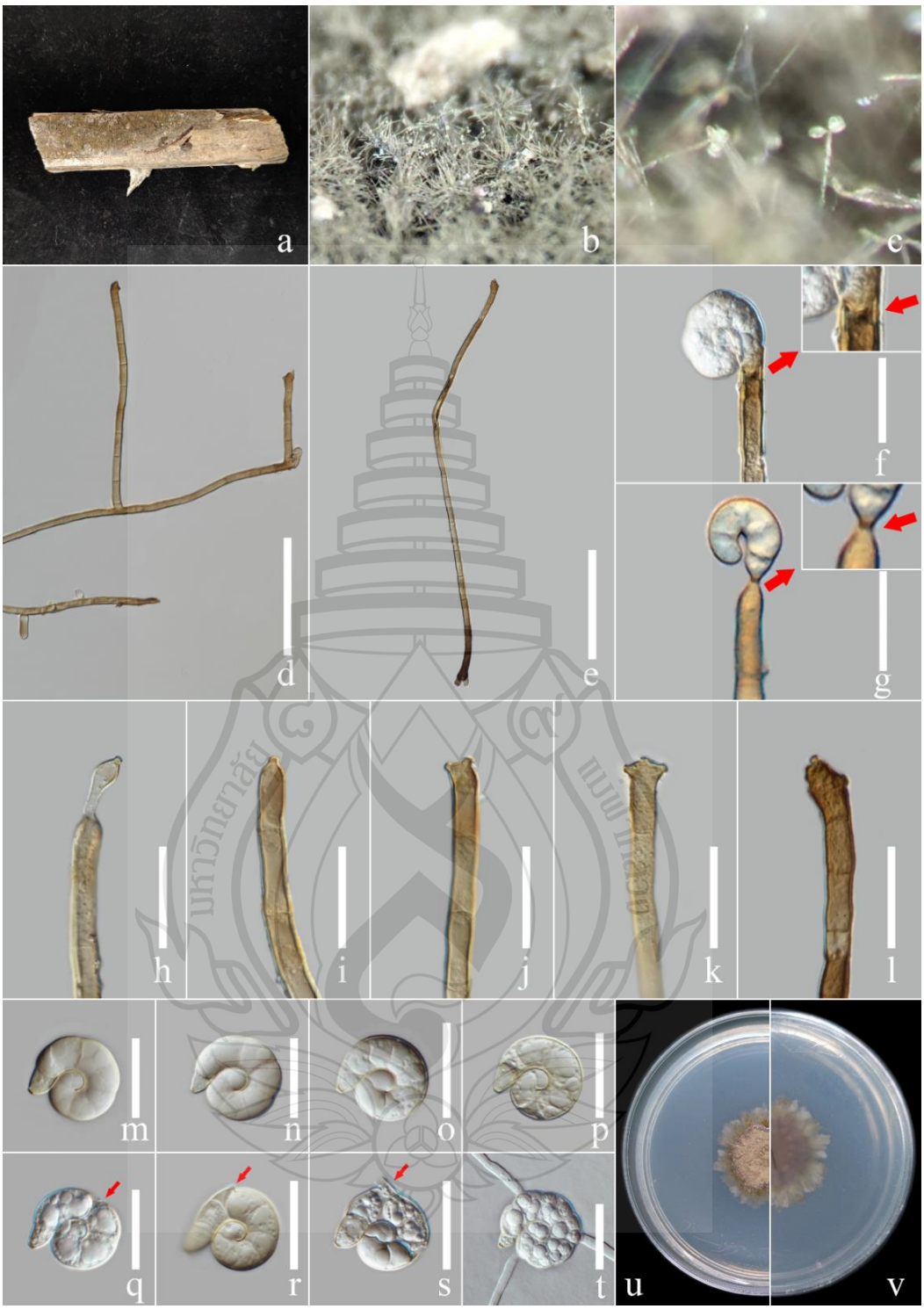
Known distribution: China (this study).

Material examined: China, Yunnan Province, Xishuangbanna City, An unidentified forest beside National Highway 219 (21°93′N, 101°24E, 549.6 m elev.), rotting petiole of the *Elaeis oleifera*, 5 February 2023, Y.R. Xiong and Li Lu, XG198 (MHZU 23-0157, holotype); ex-type culture, ZHKUCC 24-0121, other living cultures ZHKUCC 24-0122, ZHKUCC 24-0766, ZHKUCC 24-0767.

GenBank numbers: ZHKUCC 24-0121: ITS – PP860086, LSU – PP860098, *tef* 1-α – PP858056, *rpb*2 – PP858068; ZHKUCC 24-0122: ITS – PP860087, LSU – PP860099, *tef* 1-α – PP858057, *rpb*2 – PP858069; ZHKUCC 24-0766: ITS – PP860088, LSU – PP860100, *tef* 1-α – PP858058, *rpb*2 – PP858070; ZHKUCC 24-0767: ITS – PP860089, LSU – PP860101, *tef* 1-α – PP858059, *rpb*2 – PP858071.

Notes: Four collections obtained in this study from the rotting petiole of the *Elaeis oleifera* clustered in an independent clade in the phylogenetic tree with 78% ML, 76% MP bootstrap support and 1.00 BIPP bootstrap support. The nucleotide differences between *Helicoma oleifera* and its phylogenetically related species were checked, excluding gaps: *H. acropleurogenum* (GZCC 22-2035) - ITS: 3.53% (18/510 base pairs), LSU: 0.71% (6/844 base pairs), *tef* 1-*α*: 2.85% (26/912 base pairs), *rpb*2: 3.92% (41/1045 base pairs); *H. dennisii* (NBRC 30667) - ITS: 4.36% (25/573 base pairs), LSU: 0.35% (2/564 base pairs), *tef* 1-*α* and *rpb*2 sequence unavailable; *H. hydei* (MFLUCC 18-1270) - ITS: 3.50% (26/744 base pairs), LSU: 0.71% (6/847 base pairs), *tef* 1-*α*: 2.74% (25/912 base pairs), *rpb*2 sequence is unavailable; *H. inthanonense* (MFLUCC 11-0003) - ITS: 4.56% (26/570 base pairs), LSU: 1.63% (14/860 base pairs), *tef* 1-*α* and *rpb*2 sequence is

unavailable. *Helicoma oleifera* is different from related species not only in the size of conidia and conidiophores, but also in conidia, which shrink and produce the tubular structure at the third cell (Figs. 2.60), while other species do not produce any deformation. In addition, *H. acropleurogenum* (Lu et al., 2023) has intercalary and mostly monoblastic, rarely polyblastic conidiogenous cells; however, *H. oleifera* has terminal and monoblastic or polyblastic conidiogenous cells. *Helicoma dennisii* (Tsui et al., 2006) has intercalary and polyblastic conidiogenous cells and fertile denticle structure at several cells on the upper end of the conidiophore. However, *H. oleifera* only has fertile denticle structures at the apex cell of the conidiophore. Furthermore, *H. oleifera* differs from *H. hydei* (Liu et al., 2019) by having an embedded denticle structure, while *H. hydei* (Liu et al., 2019) has an exposed denticle structure. Furthermore, *H. inthanonense* (Boonmee et al., 2011) has acropleurogenous and brown conidia with 7-septate and produces an asexual morph from MEA culture, while *H. oleifera* has acrogenous and hyaline to pale brown conidia with 8-septate. Therefore, we introduce *H. oleifera* as a new species.



Note a specimen observed; b, c colony on decaying *Elaeis oleifera*; d, e conidiophores; f, g conidiogenous cell with attached conidia; h–l conidiogenous cells; m–p conidia; q–s conidia produce the tubular structure at the third cell; t germinated conidium; u, v culture on PDA from above and reverse. Scale bars: 100 μm (d, e); 20 μm (f–t).

Figure 2.60 *Helicoma oleifera* (MHZU 23-0157, holotype)

Helicoma guttulatum Y.Z. Lu, Boonmee & K.D. Hyde, Fungal Diversity 80: 1–270 (2016)

Figure 2.61

Saprobic on the rotting petiole of *Caryota mitis*. **Sexual morph:** Not observed. **Asexual morph:** Hyphomycetous, helicosporous. ***Colonies*** on the substratum superficial, effuse, gregarious, brown. ***Mycelium*** composed of partly immersed, partly superficial, brown, septate hyphae. ***Conidiophores*** 75–225 μm long, 5.5–6 μm wide ($\overline{x}$ = 152 × 5.7 μm, n = 20), macronematous, crowded, erect, straight to slightly bent, brown, deep brown towards the base, septate, branched, smooth-walled with irregular inclusion. ***Conidiogenous cells*** 10–29 μm long, 5–8.8 μm wide ($\overline{x}$ = 18 × 6.3 μm, n = 20), mono- to polyblastic, integrated, cylindrical, terminal, pale brown to brown, smooth-walled with irregular inclusion; with denticles, 1.6–3.5 μm long, 1.6–2.5 μm wide ($\overline{x}$ = 2.4 × 2.1 μm, n = 20), arising from the apex portion of conidiophores as tooth-like protrusions, mono- to polyblastic, brown, smooth-wall. ***Conidia*** 21–30 μm diam. ($\overline{x}$ = 25.1 μm, n = 40) and conidial filament 7.2–10 μm wide ($\overline{x}$ = 8.4 μm, n = 40), 48–69 μm long ($\overline{x}$ = 57.4 μm, n = 40), solitary, acropleurogenous, tightly coiled 1½ times, guttulate, not becoming loose in water, hyaline to pale brown, tapering towards flat end, 8–9-septate, rounded at the apex, conic truncate at the base, smooth-walled.

Culture characteristics: ***Conidia*** germinating on water agar and germ tubes produced from conidia within 12 h. ***Colonies*** growing on PDA attaining 2.5 cm diam. after six weeks at 25ºC, irregular, undulate, rough, superficial and partially immersed, brown aerial mycelium mixed with pale brown, deep brown at up and down junction area; reverse brown with pale brown.

Known distribution: China (this study).

Material examined: China, Yunnan Province, Xishuangbanna City, An unknown forest beside National Highway 219 (21°93'N, 101°24E, 549.6 m elev.), rotting petiole of the *Caryota mitis*, 5 February 2023, Y.R. Xiong and Li Lu, XG215 (MHZU 23-0166, new host record; living culture, ZHKUCC 24-0139, ZHKUCC 24-0140).

GenBank numbers: ZHKUCC 24-0139: ITS – PP860094, LSU – PP860106, *tef* 1-α – PP858054, *rpb*2 – PP858066; ZHKUCC 24-0140: ITS – PP860095, LSU – PP860107, *tef* 1-α – PP858055, *rpb*2 – PP858067.

Notes: Two collections on rotting petiole of the *Caryota mitis* obtained in this study clustered with the *H. guttulatum* clade, based on the phylogenetic tree with 100% ML, 100% MP bootstrap support and 0.91 BIPP bootstrap support. The nucleotide differences excluding gaps between *H. guttulatum* (ZHKUCC 24-0139) and *H. guttulatum* (MFLUCC 16-0022) in ITS is 3.60% (17/472 base pairs), while there is no difference in LSU and one base pair difference in *tef* 1-*α* and *rpb*2. Our two collections are similar to *H. guttulatum* (Hyde et al., 2016) in shape, colour and size of conidia. Although the conidiophores are longer than in previous collections, this might be due to the branching of the conidiophore of the collections in this study, whereas the previous collections are unbranched. In addition, the location of the denticles is the same. Therefore, based on morphology and phylogenetic analysis, we identified our collections as *H. guttulatum* and this is a new record of *H. guttulatum* on *Caryota mitis*. *Helicoma guttulatum* was first introduced on decaying wood from Thailand by Hyde et al. (2016), based on morphology and phylogeny. Tian et al. (2022) reported a new collection of *H. guttulatum* on decaying wood of an unidentified host from Thailand.



Note a specimen observed; b, c colony on decaying *Caryota mitis*; d conidiophores; e–j conidiogenous cells, thereinto; j with attached conidia; k–o conidia; p germinated conidium; q, r culture on PDA from above and reverse. Scale bars: 50 µm (d); 20 µm (e–j); 10 µm (k–o); 20 µm (p).

Figure 2.61 *Helicoma guttulatum* (MHZU 23-0166, new host record)

Helicoma rufum Y.Z. Lu, J.C. Kang & K.D. Hyde, Fungal Diversity 92: 131–344 (2018)

Figure 2.62

Saprobic on the rotting inflorescence of *Caryota mitis*. **Sexual morph:** Not observed. **Asexual morph:** Hyphomycetous, helicosporous. ***Colonies*** on the substratum superficial, effuse, gregarious, pale brown. ***Mycelium*** composed of partly immersed, partly superficial, hyaline to brown, septate, branched hyphae. ***Conidiophores*** 150–270 µm long, 4–7.5 µm wide ($\overline{x}$ = 225 × 5.9 µm, n = 20), macronematous, mononematous, cylindrical, erect, straight to slightly bent, pale brown to deep brown from top towards the base, apex hyaline, septate, mostly unbranched, smooth-walled. ***Conidiogenous cells*** 7–15 µm long, 4–7 µm wide ($\overline{x}$ = 12 × 5.9 µm, n = 20), mono- to polyblastic, cylindrical, integrated, intercalary, brown, smooth-walled; with denticles, 3–6 µm long, 1.5–3 µm wide ($\overline{x}$ = 4.6 × 2.5 µm, n = 20), arising from the lower portion of conidiophores as tooth-like protrusions, mono- to polyblastic, pale brown to brown, smooth-walled. ***Conidia*** 21–47 µm diam. ($\overline{x}$ = 36.2 µm, n = 40) and conidial filament 2–5 µm wide ($\overline{x}$ = 3.8 µm, n = 40), 145–345 µm long ($\overline{x}$ = 257.7 µm, n = 40), solitary, pleurogenous, tightly coiled 3–4½ times, guttulate, become loose in water, hyaline to pale brown, 25–35-septate, smooth-walled.

Culture characteristics: ***Conidia*** germinating on water agar and germ tubes produced from conidia within 12 h. ***Colonies*** growing on PDA attaining 3 cm diam. after six weeks at 25ºC, irregular, undulate, rough, superficial and partially immersed, brown aerial mycelium mixed with pale brown; reverse brown with pale brown.

Known distribution: China (this study).

Material examined: China, Yunnan Province, Xishuangbanna City, an unidentified forest beside National Highway 219 (21°93'N, 101°24E, 549.6 m), rotting inflorescence of the *Caryota mitis*, 5 February 2023, Y.R. Xiong and Li Lu, XG217 (MHZU 23-0168, new host record; living culture, ZHKUCC 24-0143, ZHKUCC 24-0144).

GenBank numbers: ZHKUCC 24-0143: ITS – PP860096, LSU – PP860108, *tef* 1-α – PP858060, *rpb*2 – PP858072; ZHKUCC 24-0144: ITS – PP860097, LSU – PP860109, *tef* 1-α – PP858061, *rpb*2 – PP858073.

Notes: Two collections on rotting inflorescence of *Caryota mitis* obtained in

this study clustered with the *H. rufum* clade in the phylogenetic tree with 96% ML, 95% MP bootstrap values and 0.99 BIPP bootstrap support. The nucleotide differences between *H. rufum* (ZHKUCC 24-0143) and *H. rufum* (MFLUCC 17-1806) are LSU: 0.09% (1/1171 base pairs), *tef* 1-*α*: 0.22% (2/912 base pairs), *rpb*2 sequence unavailable and no difference in ITS, excluding gaps. Our collection is similar to *H. rufum* (Lu et al., 2018b) in the shape, colour and size of conidia. Although the conidiophores and conidia are longer than in previous collections, this might be because the collections came from a different area, resulting in branching at the top of the conidiophores. Therefore, based on phylogenetic and morphological analysis, we identified our collections as a new host record of *H. rufum* on *Caryota mitis*. *Helicoma rufum* was introduced from decaying wood in Thailand by Lu et al. (2018b), based on the distinguished phylogenetic clade, wider conidiophores and larger tooth-like conidiogenous protrusions and larger conidia.



Note a specimen observed; b, c colony on decaying *Caryota mitis*; d, e conidiophores; f–i conidiogenous cells; j–l conidia; m germinated conidium. Scale bars: 50 µm (d, e, m); 10 µm (f–i); 20 µm (j–l).

Figure 2.62 *Helicoma rufum* (MHZU 23-0168, new host record)

Neohelicosporium Y.Z. Lu, J.C. Kang & K.D. Hyde, Mycol Prog 17:631–646 (2018)

Notes: *Neohelicosporium* was introduced by Lu et al. (2018a) to accommodate taxa with special helicosporous spores based on morphology and phylogenetic analysis of combined ITS, LSU, *tef* 1-*α*, and *rpb*2. Their unique characteristics include branched or unbranched conidiophores arising from creeping hyphae, mono- to polyblastic, integrated, sympodial conidiogenous cells with denticles and acrogenous and/or acropleurogenous conidia, which are used to distinct *Neohelicosporium* from *Helicosporium* (Lu et al., 2018b). After synonymising several species from *Helicoma, Helicomyces, Helicosporium,* and *Tubeufia*, 25 species are accepted in *Neohelicosporium* (Lu et al., 2018b; Index Fungorum, 2024).

Neohelicosporium guineensis Y.R. Xiong, Manawas. & K.D. Hyde, ***sp. nov.***

Figure 2.63

Etymology: Species epithet refers to the host species name "*guineensis*" from which the fungus was isolated.

Saprobic on the rotting petiole of *Elaeis guineensis*. **Sexual morph:** Not observed. **Asexual morph:** Hyphomycetous, helicosporous. ***Colonies*** on the substratum superficial, effuse, gregarious, brown. ***Mycelium*** composed of partly immersed, partly superficial, pale brown, glistening, septate, branched hyphae. ***Conidiophores*** 50–160 µm long, 4–6 µm wide ($\overline{x}$ = 120 × 5.2 µm, n = 20), macronematous, mononematous, cylindrical, unbranched or branched at apex, straight, septate, pale brown, brown at root part, smooth-walled. ***Conidiogenous cells*** 11.5–20 µm long, 3.5–5.5 µm wide ($\overline{x}$ = 15.5 × 4.8 µm, n = 20), mono- to polyblastic, integrated, sympodial, terminal or intercalary, cylindrical, yellowish to pale brown, smooth-walled; with denticles, 1.4–2.7 µm long, 1.2–2 µm wide ($\overline{x}$ = 1.9 × 1.6 µm, n = 20), arising from the juncture portion of two conidiogenous cells as tooth-like protrusions, mono- to polyblastic, hyaline, smooth-walled. ***Conidia*** 16–20 µm diam. ($\overline{x}$ = 18 µm, n = 40) and conidial filament 1.8–3 µm wide ($\overline{x}$ = 2.4 µm, n = 40), 90–130 µm long ($\overline{x}$ = 112.9 µm, n = 40), solitary, mostly pleurogenous, rarely acrogenous, helicoid, rounded at tip, obvious hump and constricted at septa, coiled 2½–3½ times, 11–12-septate, becoming loose in water, guttulate, hyaline, smooth-walled.

Culture characteristics: ***Conidia*** germinating on water agar and germ tubes produced from conidia within 12 h. ***Colonies*** growing on PDA attaining 3.5 cm diam. after

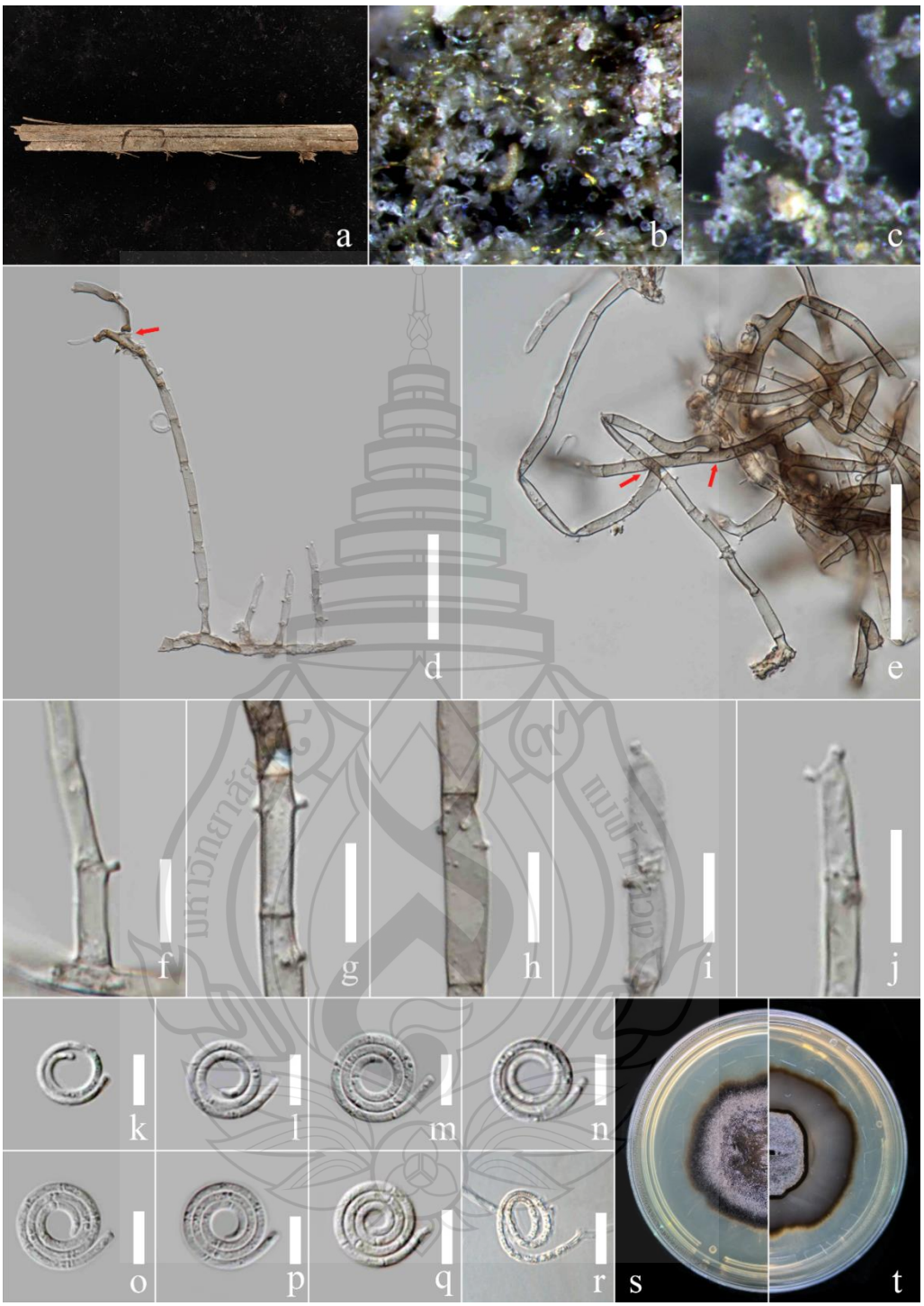
six weeks at 25ºC, irregular, undulate, umbonate, rough, superficial and partially immersed, white aerial mycelium, deep brown at immersed area; reverse white to deep brown.

Known distribution: China (this study).

Material examined: China, Yunnan Province, Xishuangbanna City, an unidentified forest beside National Highway 219 (21°93'N, 101°24E, 549.6 m elev.), rotting petiole of the *Elaeis guineensis*, 5 February 2023, Y.R. Xiong and Li Lu, XG186 (MHZU 23-0153, holotype); ex-type, ZHKUCC 24-0113, other living culture ZHKUCC 24-0114.

GenBank numbers: ZHKUCC 24-0113: ITS – PP860090, LSU – PP860102, *tef* 1-α – PP858062, *rpb*2 – PP858074; ZHKUCC 24-0114: ITS – PP860091, LSU – PP860103, *tef* 1-α – PP858063, *rpb*2 – PP858075.

Notes: Two collections from this study formed a separate lineage and clustered with *Neohelicosporium hyalosporum* and *N. ovoideum* in the phylogenetic tree with 88% ML, 78% MP bootstrap support and 1.00 BIPP bootstrap support. The nucleotide differences excluding gaps between *N. guineensis* and its phylogenetically related species were checked: *N. hyalosporum* (GZCC 16-0076) - ITS: 1.56% (8/513 base pairs), LSU: 0.83% (7/840 base pairs), *tef* 1-*α*: 1.32% (12/912 base pairs), *rpb*2: 3.63% (38/1045 base pairs); *N. ovoideum* (GZCC 16-0064) - ITS: 1.50% (8/534 base pairs), LSU: 0.48% (4/826 base pairs), *tef* 1-*α*: 1.21% (11/912 base pairs), *rpb*2: 3.16% (33/1045 base pairs). *Neohelicosporium guineensis* differs from its closely-related species in the size of conidia and conidiophores. *Neohelicosporium hyalosporum* and *N. ovoideum* are multi-septate and are not constricted at the septa, while *N. guineensis* are 11–12-septate and constricted at the septa (Lu et al., 2018a, 2018b). *Neohelicosporium hyalosporum* (Lu et al., 2018a) has multi-denticles in one conidiogenous cell, while *N. guineensis,* has no more than three denticles (Figures. 2.63f–e) in one conidiogenous cell. Furthermore, *N. ovoideum* (Lu et al., 2018b) has 1–2 short-connecting cells between conidiophores, while *N. guineensis* has one long connecting cell (Figures. 2.63d and 2.63e) which connects conidiophores at the apex. Based on the phylogenetic placement and morphological variations, we introduce *N. guineensis* as a new species.



Note a specimen observed; b, c colony on decaying *Elaeis guineensis*; d, e apical branches forming long connected conidiophores; f–j conidiogenous cells; k–q conidia; r germinated conidium; s, t culture on PDA from above and reverse. Scale bars: 50 µm (d, e); 10 µm (f–q); 20 µm (r).

Figure 2.63 *Neohelicosporium guineensis* (MHZU 23-0153, holotype)

Neohelicosporium xishuangbannaensis Y.R. Xiong, Manawas. & K.D. Hyde, ***sp. nov.***

Figure 2.64

Etymology: Species epithet refers to the location name "Xishuangbanna" from where the holotype was collected.

Saprobic on the rotting petiole of *Elaeis guineensis*. **Sexual morph:** Not observed. **Asexual morph:** Hyphomycetous, helicosporous. ***Colonies*** on the substratum superficial, effuse, gregarious, brown. ***Mycelium*** composed of partly immersed, partly superficial, brown, septate, unbranched hyphae. ***Conidiophores*** 40–125 µm long, 3–6 µm wide (x = 68.4 × 4.4 µm, n = 20), macronematous, mononematous, flexuous, long, cylindrical, branched, septate, smooth-walled. ***Conidiogenous cells*** 7–14 µm long, 2.5–5.5 µm wide ($\overline{x}$ = 11.2 × 3.9 µm, n = 20), mono- to polyblastic, integrated, sympodial, terminal or intercalary, cylindrical, pale brown, smooth-walled; with denticles, 1.8–3.3 µm long, 1.1–2.3 µm wide ($\overline{x}$ = 2.4 × 1.4 µm, n = 20), arising from the juncture portion of two conidiogenous cells as tooth-like and papillate protrusions, mono- to polyblastic, pale brown or hyaline, smooth-walled. ***Conidia*** 16.5–20.5 µm diam. ($\overline{x}$ = 18.5 µm, n = 40) and conidial filament 1.8–3.2 µm wide ($\overline{x}$ = 2.4 µm, n = 40), 90–125 µm long ($\overline{x}$ = 107 µm, n = 40), solitary, acropleurogenous, helicoid, rounded at tip, coiled 2–3¼ times, 9–13-septate, becoming loose in water, guttulate, slightly constricted at septa, hyaline to pale brown, smooth-walled.

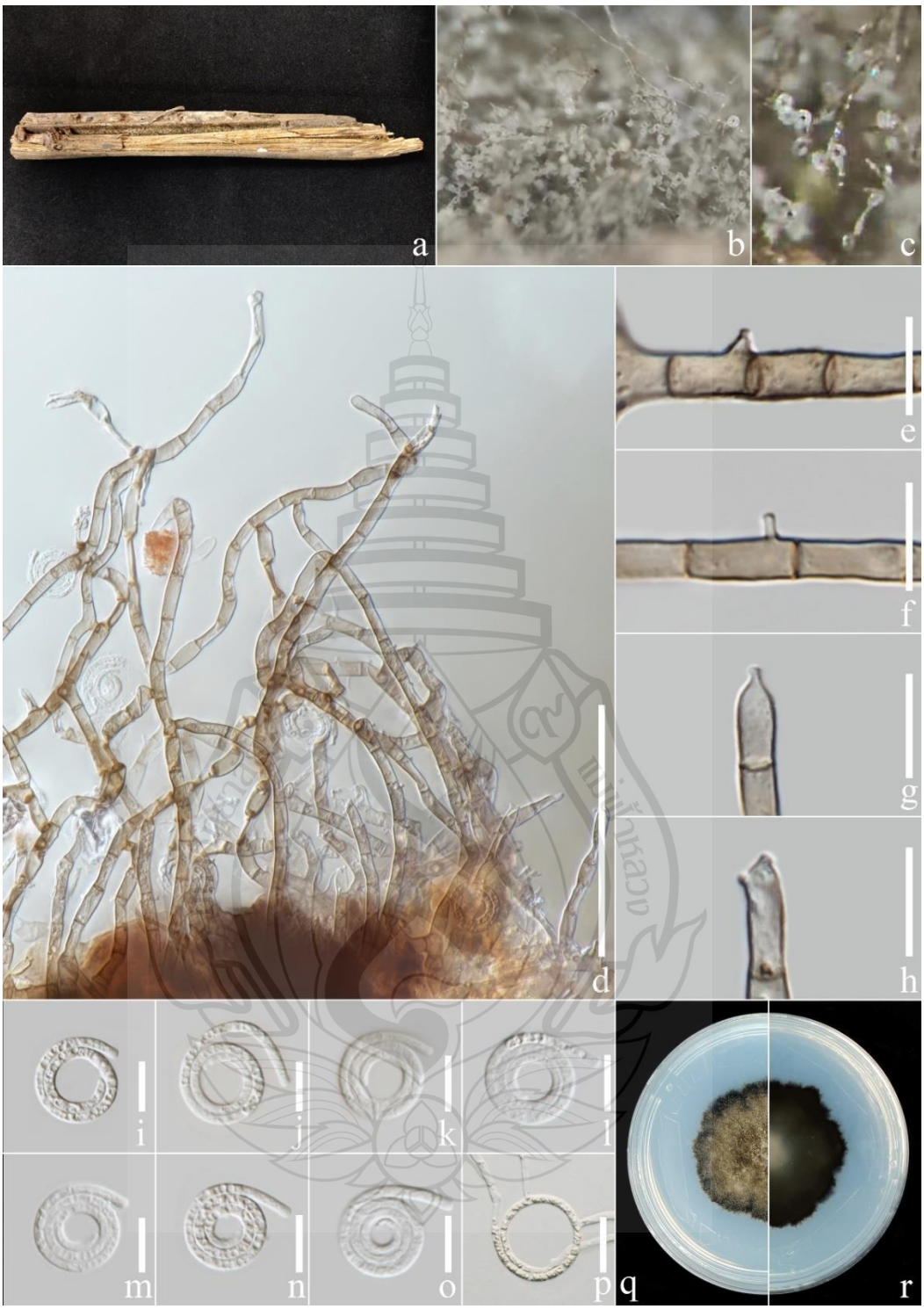
Culture characteristics: ***Conidia*** germinating on water agar and germ tubes produced from conidia within 12 h. ***Colonies*** growing on PDA attaining 2.5 cm diam. after six weeks at 25ºC, irregular, undulate, umbonate, rough, superficial and partially immersed, brown aerial mycelium mixed with pale brown, deep brown at up and down junction area; reverse brown with deep brown.

Known distribution: China (this study).

Material examined: China, Yunnan Province, Xishuangbanna City, an unidentified forest beside National Highway 219 (21°93'N, 101°24E, 549.6 m elev.), rotting petiole of the *Elaeis guineensis*, 5 February 2023, Y.R. Xiong and Li Lu, XG197 (MHZU 23-0156, holotype); ex-type, ZHKUCC 24-0119, other living culture ZHKUCC 24-0120.

GenBank numbers: ZHKUCC 24-0119: ITS – PP860092, LSU – PP860104, *tef* 1-α – PP858064, *rpb*2 – PP858076; ZHKUCC 24-0120: ITS – PP860093, LSU – PP860105, *tef* 1-α – PP858065, *rpb*2 – PP858077.

Notes: Two collections obtained in this study developed an independent clade in the phylogenetic tree with 77% ML, 79% MP bootstrap support and 0.99 BIPP bootstrap support. The nucleotide differences excluding gaps between *Neohelicosporium xishuangbannaensis* and *N. fusisporum* (MFUCC 16-0642) are ITS: 2.81% (15/533 base pairs), LSU: 1.06% (9/852 base pairs), *tef* 1-*α*: 2.41% (22/912 base pairs) and *rpb*2 sequence is unavailable. *Neohelicosporium fusisporum* was reported as a sexual and asexual morph by Jayasiri et al. (2017). *Neohelicosporium xishuangbannaensis* is different from the asexual morph of *N. fusisporum* (Jayasiri et al., 2017) in the size of conidia and conidiogenous cells. In addition, the asexual morph of *N. fusisporum* (Jayasiri et al., 2017) has an intercalary conidiogenous cell, while *N. xishuangbannaensis* has an intercalary (Figures. 2.64e and 2.64f) or terminal (Figures. 2.64g and 2.64h) conidiogenous cell. Furthermore, the asexual morph of *N. fusisporum* (Jayasiri et al., 2017) has denticles with tooth-like or long neck cells, while *N. xishuangbannaensis* has a denticle with tooth-like and papillate protrusions. Based on these differences, herein we introduce *N. xishuangbannaensis* as a new species.



Note a specimen observed; b, c colony on decaying *Elaeis guineensis*; d conidiophores; e, f intercalary conidiogenous cells; g, h terminal conidiogenous cells; i–o conidia; p germinated conidium; q, r culture on PDA from above and reverse. Scale bars: 50 µm (d); 10 µm (e–o); 20 µm (p).

Figure 2.64 *Neohelicosporium xishuangbannaensis* (MHZU 23-0156, holotype)

2.3.1.2 Eurotiomycetes

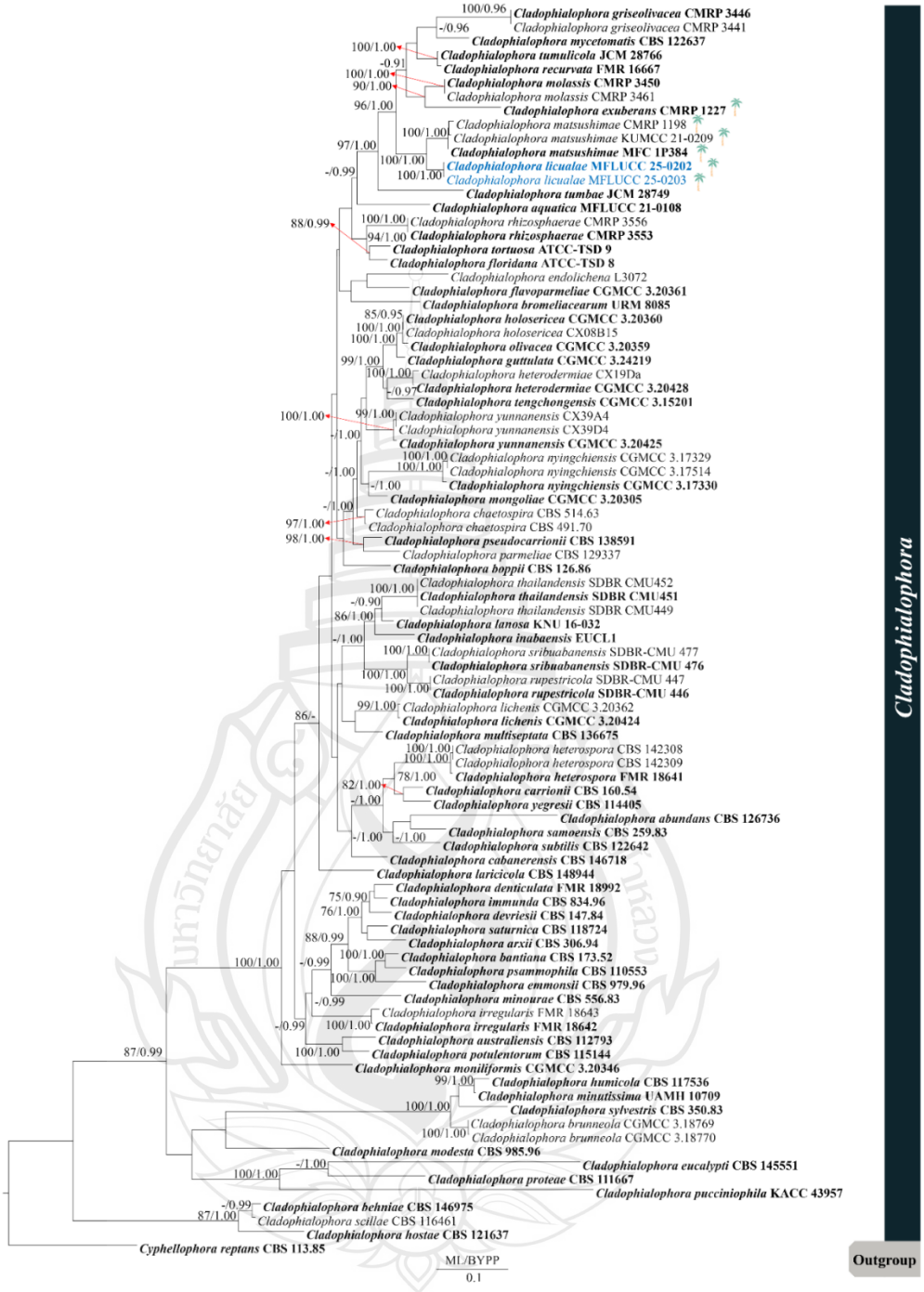
Asterinales M.E. Barr ex D. Hawksw. & O.E. Erikss. (1986)

Chaetothyriales M.E. Barr, Mycotaxon 29: 502 (1987)

Herpotrichiellaceae Munk, Dansk botanisk Arkiv 15 (2): 131 (1953)

Cladophialophora Borelli, Proceedings of the 5th International Conference on Mycoses: 355 (1980)

Notes: Borelli (1980) established *Cladophialophora* (*Cl.*) with *Cl. carrionii* (Trejos) de Hoog, Kwon-Chung and McGinnis (= *Cl. ajelloi* Borelli) as the type species to accommodate species that exhibit spore formation resembling *Cladosporium* and conidiogenous cells similar to *Phialophora* (Borelli, 1980; Badali et al., 2008; Bensch et al., 2012). This genus is known to exhibit diverse ecological roles, functioning as opportunistic pathogens or pathogens in plants, animals, and humans, as well as existing as saprobes and endophytes (de Hoog et al., 2007; Crous et al., 2007; Badali et al., 2008; Feng et al., 2014). *Cladophialophora* is characterized by 1-celled, globose to elongate, dry conidia arising through blastic, acropetal conidiogenesis, most are arranged in branched chains, as melanized conidia with inconspicuous scars (Borelli, 1980; Ho et al., 1999; de Hoog et al., 2000; Badali et al., 2008). Haase et al. (1999) and Untereiner (2000) based on morphological evidence and phylogenetic analysis combined SSU to define *Cladophialophora* belongs to the Chaetothyriales. Subsequently, phylogenetic studies mainly use LSU, ITS or add SSU, *tub*2 and *tef* 1-α to analysis (Crous et al., 2007; de Hoog et al., 2007; Diederich et al., 2013; Boonmee et al., 2021; Torres-Garcia et al., 2023; Chang et al., 2023). In this study, we use ITS, LSU, SSU, *tub*2 and *tef* 1-α to update phylogenetic studies for *Cladophialophora* (Figure 2.65). Currently, 70 epithets are listed under *Cladophialophora* (Index Fungorum, 2025 January) with 65 species associated with molecular data. Among these three species have been reported from palm species including a new species described in this study (Xiong et al., 2025).



Note Phylogram generated from maximum likelihood analysis of *Cladophialophora* based on combined ITS, LSU, SSU, *tub*2 and *tef* 1-α sequence data. Bootstrap values for maximum likelihood (ML) equal to or greater than 70 are indicated above the branches. The new collections are indicated in blue and ex-type strains are indicated in bold.

Figure 2.65 Phylogenetic tree of *Cladophialophora*

Cladophialophora licualae Y.R. Xiong, Manawas. & K.D. Hyde, ***sp. nov.***

Figure 2.66

Etymology: The epithet refers to the host genus name "*Licuala*", from which the species was collected.

Saprobic on dead petiole of *Licuala* sp. Asexual morph: Hyphomycetes. *Colonies* on natural substrate effuse, scattered, brown to dark brown, hairy. *Mycelium* is superficial and immersed, composed of branched, septate, smooth-walled, pale brown to brown hyphae. *Conidiophores* 40–120 × 4–7 µm ($\bar{x}$ = 71.5 × 5.3 µm, n = 20), macronematous, mononematous, dark brown to brown, septate, single or caespitose, straight or flexuous, unbranched, smooth, and cylindrical. *Conidiogenous cells* 10–15 × 4–5 µm ($\bar{x}$ = 13.2 × 4.7 µm, n = 20), brown to pale brown, monoblastic, integrated, determinate, terminal, cylindrical, cylindrical. *Conidia* (15–)20–40 × 4–5.5 µm ($\bar{x}$ = 28 × 4.8 µm, n = 30), solitary, easy to dry, cylindrical, elongate, pale brown, concolorous, slightly thickened walls and septa, 3–7-septate, cells vary in size, apex rounded, basal cell truncate and elongate-conical. Sexual morph Not observed.

Culture characteristics: Colonies on PDA fast growing, after 2 weeks reaching 4 cm diam., at 25°C, circular, umbonate, with fluffy, dense, white mycelium on the surface with entire margin; in reverse black in the middle and white at the margin.

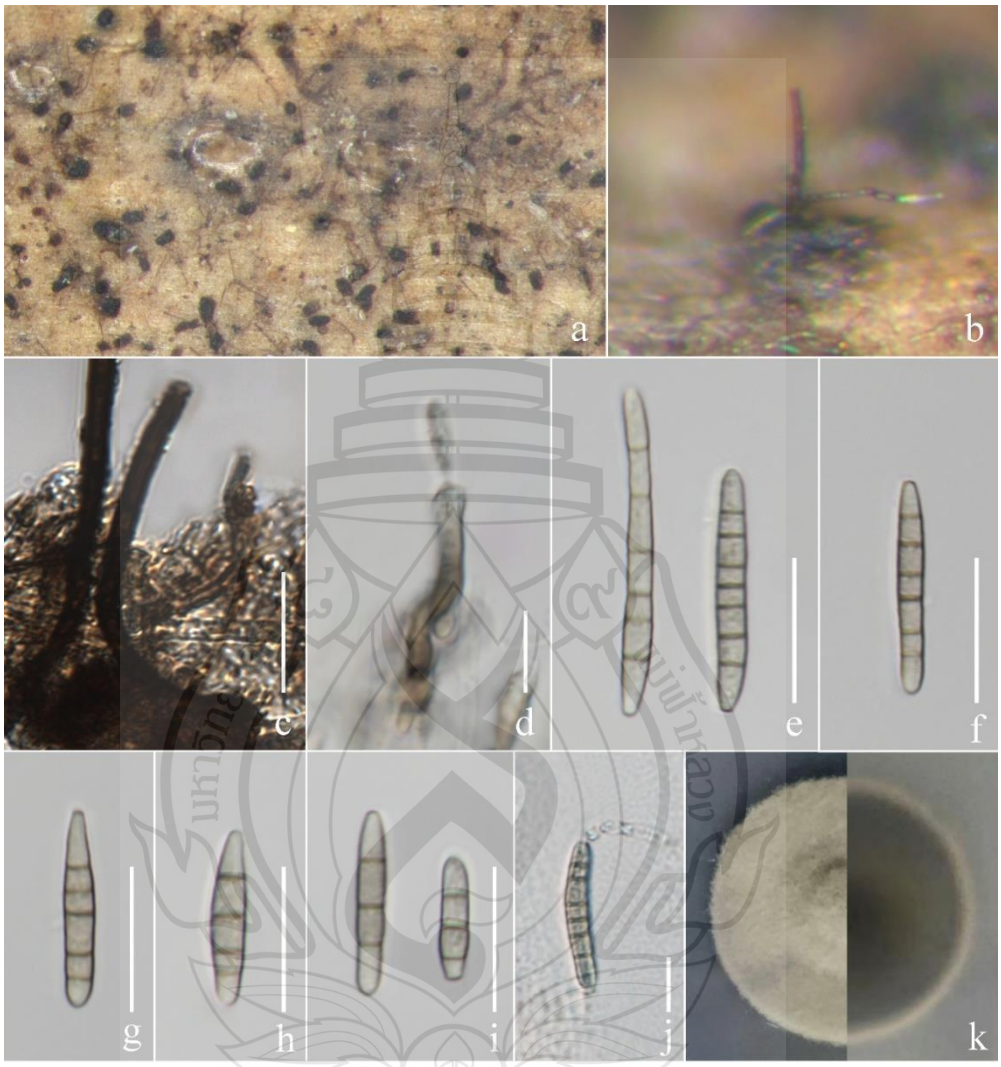
Known distribution: Thailand (this study).

Material examined: Thailand, Narathiwat Province, Toh Daeng Peat swamp, on dead petiole of *Licuala* sp., 4 Aug 2023, Y.R. Xiong, XG327 (MFLU 25-0146, holotype), ex-type MFLUCC 25-0202, other living culture MFLUCC 25-0203.

GenBank numbers: MFLUCC 25-0202: ITS – PV578148, LSU – PV578318, *tub*2 – PV584055, *tef* 1-α – PV608826; MFLUCC 25-0203: ITS – PV578149, LSU – PV578319, *tub*2 – PV584056, *tef* 1-α – PV608827.

Notes: Two collections from this study clustered in *Cladophialophora* clade and formed a sister lineage to *Cl. matsushimae* in the phylogenetic tree with 100% ML bootstrap support and 1.00 BYPP (Figure 2.65). The nucleotide differences excluding gaps between *Cl. licualae* (MFLUCC XG327) and *Cl. matsushimae* (MFC 1P384) were checked and given as follows, ITS: 5.41% (30/555 base pairs), LSU: 0.91% (6/658 base pairs). Morphologically, *Cl. licualae* have 3–7-septate cylindrical to elongate conidia which is not a classical *Cladophialophora*-like morph (Feng et al., 2014). In addition, this conidia

character is different from *Cl. matsushimae* whose conidia are branched chains, 0–1(–2)-septate and smaller "microconidia" oval to broadly fusiform 0–1-septate are produced (Koukol, 2010; Kularathnage et al., 2025). Based on the phylogenetic placement and morphological variations, we introduce *Cl. licualae* as a new species.

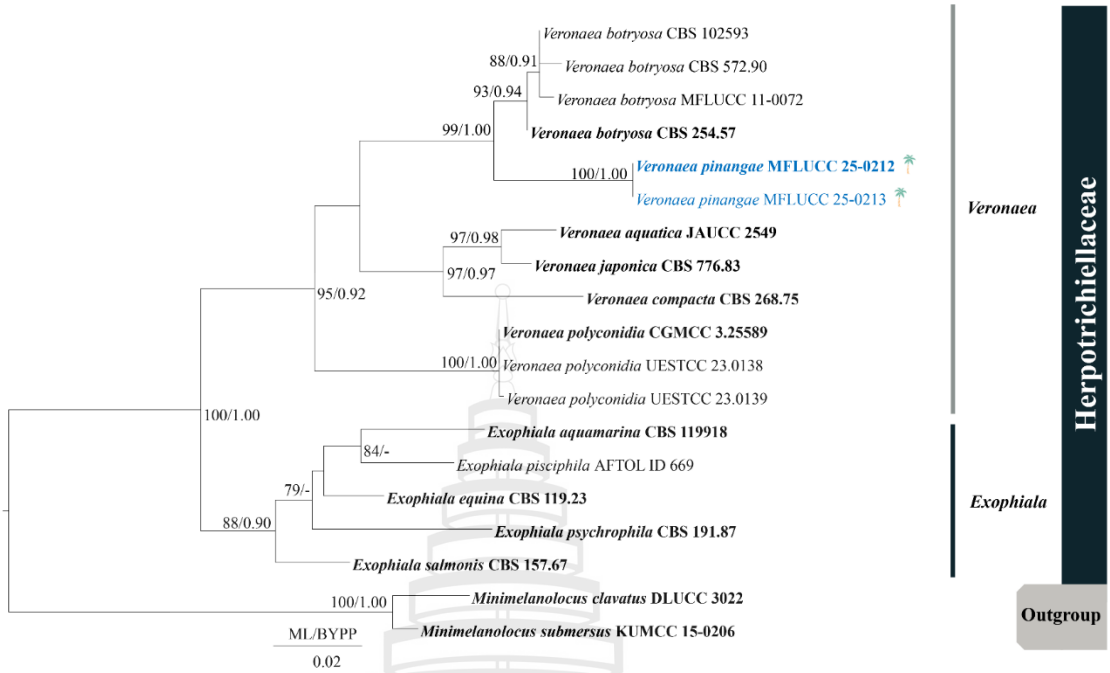


Note a, b Appearance of sporodochia on host substrate. c, d Conidiophores, conidiogenous cells, and conidia. e–i Conidia. j Germinating conidium. k The front of culture on PDA at 25°C and the reverse of culture on PDA at 25°C. Scale bars: d, j = 10 µm, c, e–i = 20 µm.

Figure 2.66 *Cladophialophora licualae* (MFLU 25-0146, holotype)

Veronaea Cif. & Montemart., Atti Ist. bot. Univ. Lab. crittog. Pavia, Ser. 4 15: 68 (1957)

Notes: Ciferi and Montemartini (1957) established *Veronaea* (*V.*) with *V. botryose* as the type species. *Veronaea* is reported as an asexual genus characterized by erect, mostly unbranched, pale to medium brown conidiophores with polyblastic, sympodial, terminal or intercalary, and cylindrical conidiogenous cells and smooth-walled, septate, cylindrical to pyriform pale brown to brown conidia (Papendorf, 1976; Arzanlou et al., 2007; Rambelli, 2011; Zhang, 2019). Based on morphological evidence and phylogenetic analysis combined ITS and LSU Arzanlou et al. (2007) redefine *Veronaea* and subsequently most of the phylogenetic studies use ITS, LSU and SSU or add *tub*2 for species delineation (Dong et al., 2018; Chandrasiri et al., 2021; Yang et al., 2023; Su et al., 2023). In this study, we use ITS, LSU, SSU and *tub*2 to update phylogenetic studies for *Veronaea* (Figure 2.67). Currently, 21 epithets are listed under *Veronaea* (Index Fungorum, 2025 January), and only five species have molecular data. We describe a new species of *Veronaea* which is the first report from a palm (Xiong et al., 2025).



Note Phylogram generated from maximum likelihood analysis of Herpotrichiellaceae based on combined ITS, LSU, SSU and *tub*2 sequence data. Bootstrap values for maximum likelihood (ML) equal to or greater than 70 are indicated above the branches. The new collections are indicated in blue and ex-type strains are indicated in bold.

Figure 2.67 Phylogenetic tree of Herpotrichiellaceae

Veronaea pinangae Y.R. Xiong, Manawas. & K.D. Hyde, ***sp. nov.***

Figure 2.68

Etymology: The epithet refers to the host genus name "*Pinanga*", from which the species was collected.

Saprobic on dead rachis of *Pinanga riparia*. Asexual morph: Hyphomycetous. *Colonies* on the natural substrate, effuse, widely spreading, superficial, scattered, hairy, brown to dark brown. *Conidiophores* 160–180 × 5–6 µm ($\bar{x}$ = 167 × 5.6 µm, n = 10), macronematous, mononematous, solitary, unbranched, straight with irregularly twisted, smooth to slightly roughened, cylindrical, brown to dark brown. *Conidiogenous cells* 20–23 × 5–6 µm ($\bar{x}$ = 22 × 5.5 µm, n = 25), monoblastic, integrated, sympodial, terminal, cylindrical or fertile at the apex of conidiophores, brown to hyaline, irregular inclusion. *Conidia* 18–20 × 5–7 µm ($\bar{x}$ = 18.8 × 6.2 µm, n = 25), solitary, acropleurogenous, elliposoid

to fusiform, 3–5-septate, smooth, tapering to a pointed apex and truncate at base, pale brown. Sexual morph: Not observed.

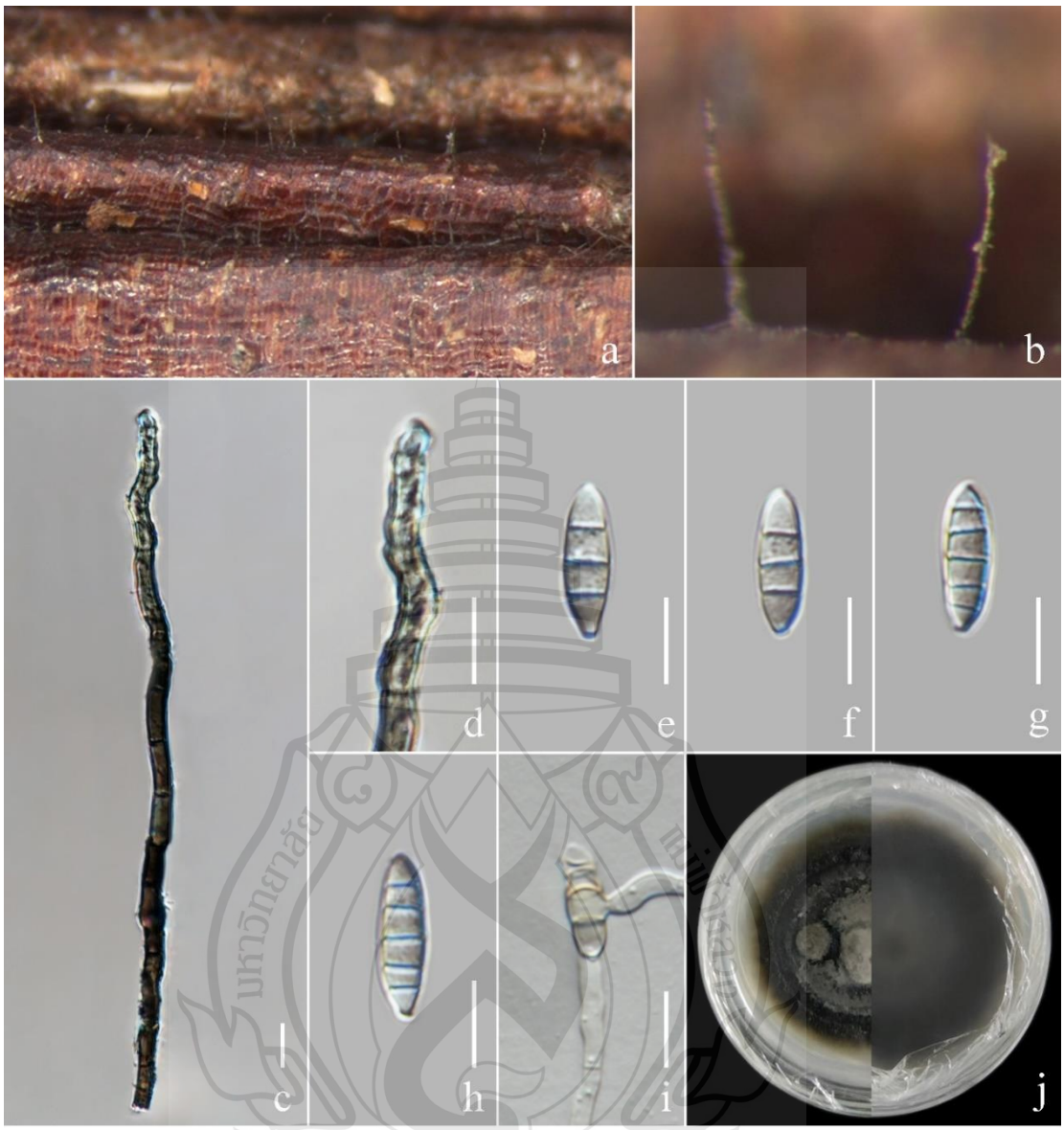
Culture characteristics: Colonies on PDA fast growing, after 2 weeks reaching 4 cm diam., at 25°C, circular, raised, fluffy, dense, convex or dome-shaped, with dark-brown papillate, surface, brown in the centre, lighter on the outside, dark-brown at the margins, consistently dark-brown in reverse.

Known distribution: Thailand (this study).

Material examined: Thailand, Narathiwat Province, in an unidentified beach, on dead rachis of *Pinanga riparia*, 6 Aug 2023, Y.R. Xiong, XG341 (MFLU 25-0151, holotype), ex-type MFLUCC 25-0212, other living culture MFLUCC 25-0213.

GenBank numbers: MFLUCC 25-0212: ITS – PV578268, LSU – PV578436, *tub*2 – PV607970; MFLUCC 25-0213: ITS – PV578269, LSU – PV578437, *tub*2 – PV607971.

Notes: Two collections from this study formed a separate lineage and clustered with *Veronaea botryosa* in the phylogenetic tree with 100% ML bootstrap support and 1.00 BYPP (Figure 2.67). The nucleotide differences excluding gaps between *V. pinangae* (XG341) and *Veronaea botryosa* (CBS 102593) were checked and given as follows, ITS: 5.52% (34/616 base pairs), LSU: 1.12% (10/895 base pairs), and *tub*2: 11.83% (44/372 base pairs). Morphologically, *V. pinangae* have 3–5-septate and tapering to a pointed apex and truncate at the base of conidia which differs from *Veronaea botryose* have rounded at apex and (0–)1–2(–3) septate conidia (Bonifaz et al., 2013; Dong et al., 2018). Based on phylogenetic placement and morphological variations, we introduce *V. pinangae* as a new species.



Note a, b Sporodochia on the substrate. b Conidiophores. b Conidiogenous cells. e–h Conidia. i Germinating conidium. j The front of culture on PDA at 25°C and the reverse of culture on PDA at 25°C. Scale bars: c–i = 10 µm.

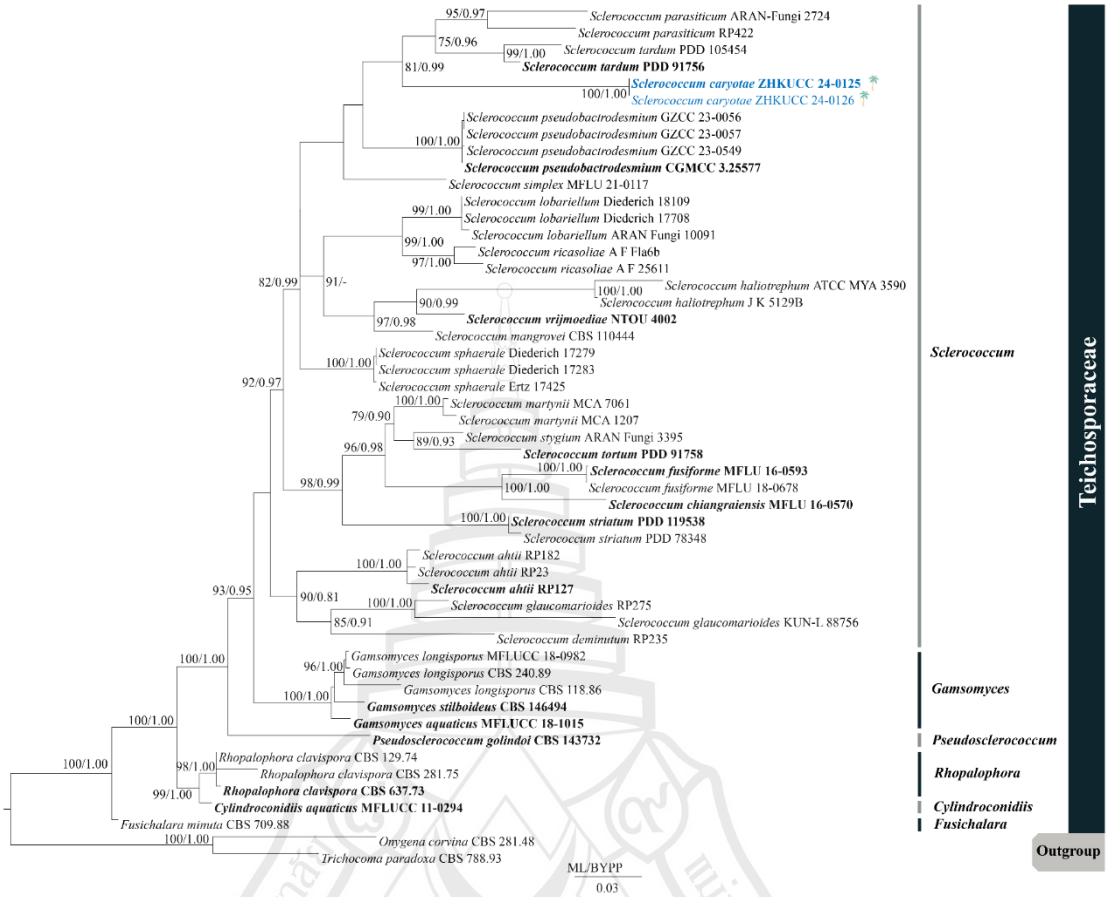
Figure 2.68 *Veronaea pinangae* (MFLU 25-0151, holotype)

Sclerococcales Réblová, Unter. & W. Gams, Mycological Progress 16 (1): 34 (2016)

Dactylosporaceae Bellem. & Hafellner, Cryptog. Mycol. 3: 79 (1982) (=Sclerococcaceae Réblová, Unter. & W. Gams)

Sclerococcum Fr., Novitiae forae svecicae 5 (2): 79 (1819)

Notes: Fries (1819, 1825) established *Sclerococcum* (*S.*) with *Sclerococcum sphaerale* (synonym: *Spiloma sphaerale*) as the type species. *Sclerococcum* is a holomorpic genus which is asexually characterized by conidiomata characterized by blackish and sporodochial-stromatic, with conidiogenesis being thallic, probably meristem thallic (meristem arthric) (Kiffer & Morelet, 2000; Seifert et al., 2011), and conidia are dark brown, ranging from uni- to multi-cellular (Diederich et al., 2013; Miadlikowska et al., 2014). The sexual morph of this genus is characterized by superficial to stalked blackish apothecia, with an excipulum composed of *textura angularis* to *globulosa* cells, hymenium features a thick gelatinous matrix, and the paraphyses are sparingly branched, with apices that are slightly swollen and pigmented. Asci are cylindrical to clavate, amyloid with an I– tholus, and are covered by an I+ blue external gelatinous cap. Ascospores are subglobose to ellipsoid, 8-spores, and bearing one to several transverse septa (Bellemère & Hafellner, 1982; Döbbeler & Buck, 2017; Hafellner, 1979). Diederich et al. (2013, 2018) re-circumscribed *Sclerococcum* based on morphological evidence and phylogenetic analysis combined ITS, LSU and LSU, mtSSU. Subsequently, phylogenetic studies mainly use SSU, mtSSU, LSU and ITS or exclude SSU and mtSSU (Ekanayaka et al., 2019; Thiyagaraja et al., 2022; Ma et al., 2024). In this study, we use ITS, LSU, and SSU to update phylogenetic studies for *Sclerococcum* (Figure 2.69). Currently, 105 epithets are listed under *Sclerococcum* (Index Fungorum, 2024 January) with 19 species associated with molecular data. Totally four species have been reported from palm species including a new species described in this study (Xiong et al., 2025).



Note Phylogram generated from maximum likelihood analysis of Dactylosporaceae based on combined ITS, LSU, and SSU sequence data. Bootstrap values for maximum likelihood (ML) equal to or greater than 70 are indicated above the branches. The new collections are indicated in blue and ex-type strains are indicated in bold.

Figure 2.69 Phylogenetic tree of Herpotrichiellaceae

Sclerococcum caryotae Y.R. Xiong, Manawas. & K.D. Hyde, ***sp. nov.***

Figure 2.70

Etymology: The epithet refers to the host genus name "*Caryota*", from which the species was collected.

Saprobic on dead rachis of *Caryota mitis*. Asexual morph: Not observed. Sexual morph: *Ascomata* 360–670 × 130–250 µm ($\bar{x}$ = 476 × 190 µm, n = 10), apothecia, superficial, scattered, composed of a disc usually sitting on a distinct stipe, not clearly differentiate from the disc; disc shiny, black when dry, dark brown and somewhat

translucent when wet, epruinose, round, plane to somewhat concave. *Stipe* 70–140 µm wide, usually somewhat tapering towards the base, pale to medium brown, much paler than the disc or occasionally concolourous dark brown cells of *textura angularis* to *globulosa*. *Hymenium* hyaline, enclosed in a thick gelati-nous matrix. *Pseudoepithecium* composed of hyaline to brown amorphous matter surrounding the paraphysis tips. *Paraphyses* 1.5–2 µm wide numerous, cylindrical, hyaline. *Asci* 40–50 × 8–9.5 µm ($\overline{x}$ = 45 × 8.7 µm, n = 25), 8-spored, unitunicate, short sessile, cylindric-clavate, rounded at the apex. *Ascospores* 13–15.5 × 3.5–5 µm ($\overline{x}$ = 13.9 × 4.3 µm, n = 25), biseriate, hyaline or light brown, brown when old, homopolar to heteropolar (with a longer upper cell), ellipsoid to slightly obovate, occasionally oblong, straight or occasionally slightly curved, 1-septate, not or occasionally slightly constricted at the septum, guttulate, smooth.

Culture characteristics: Colonies on PDA fast growing, after 2 weeks reaching 4 cm diam., at 25°C, lobate, with fluffy, dense, yellow in the centre, white mycelium on the surface with entire margin; in reverse yellow in the middle and white at the margin.

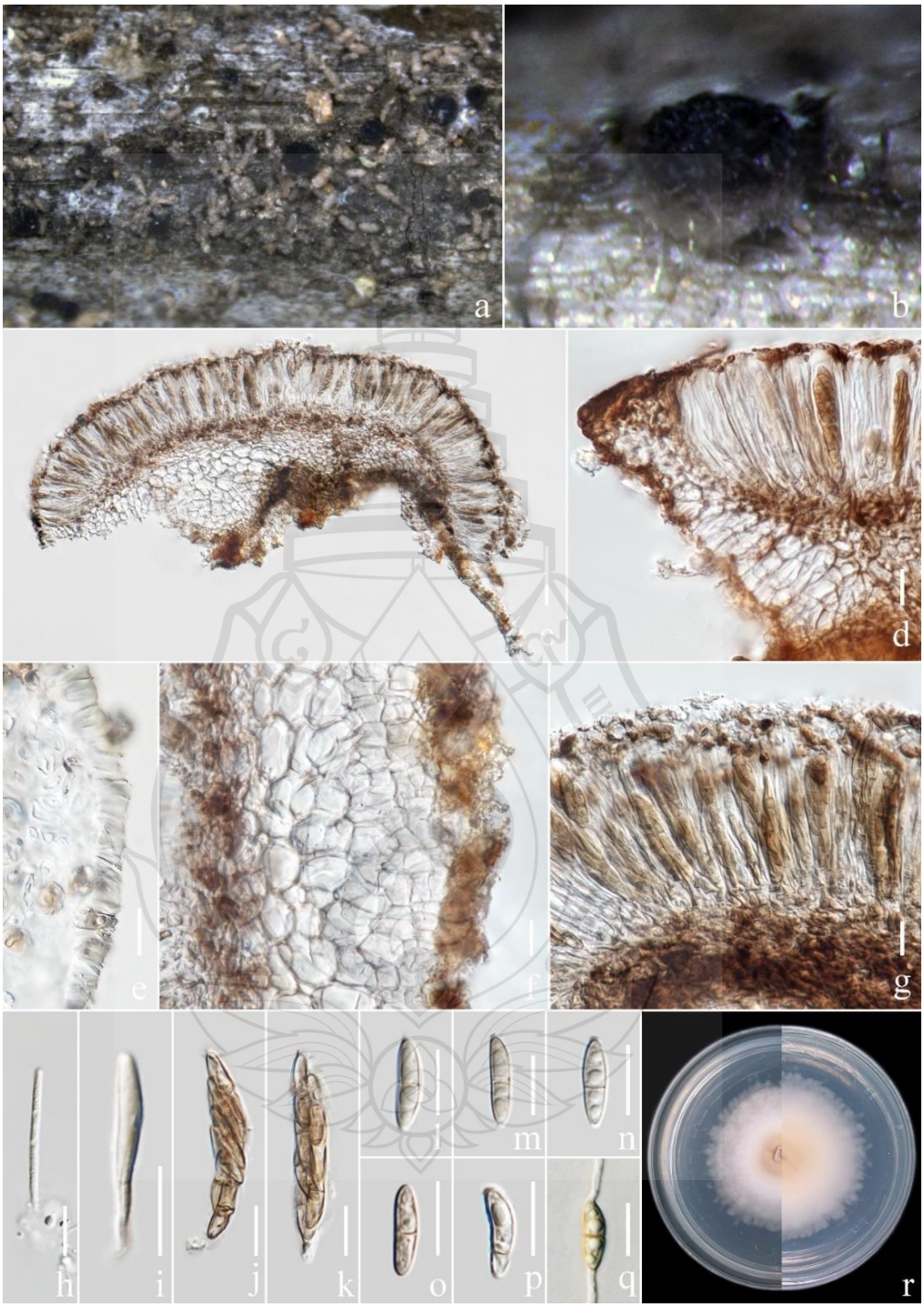
Known distribution: China (this study).

Material examined: China, Yunnan Province, Xishuangbanna City, in an unidentified forest beside National Highway 219, on dead rachis of *Caryota mitis*, 5 Feb 2023, Y.R. Xiong and L. Lu, XG204 (MHZU 23-0159, holotype) – ex-type ZHKUCC 24-0125, other living culture ZHKUCC 24-0126.

GenBank numbers: ZHKUCC 24-0125: ITS – PV578250, LSU – PV578418, SSU – PV578548; ZHKUCC 24-0126: ITS – PV578251, LSU – PV578419, SSU – PV578549.

Notes: Two collections from this study formed a separate lineage within *Sclerococcum* in the phylogenetic tree with 81% ML bootstrap support and 0.99 BYPP (Figure 2.69). Based on a MegaBLAST (Query cover ≥ 70%) search using the LSU sequence, the closest matches in NCBIs GenBank nucleotide database were *S. pseudobactrodesmium* (GenBank OR514702; Identities 807/842 (95.84%), 5 gap), *S. parasiticum* (GenBank MH698500; Identities 799/835 (95.69%), 3 gaps) and *S. simplex* (GenBank MZ655912; Identities 807/846 (95.39%), 5 gaps). The highest similarities using the SSU sequence were *S. parasiticum* (GenBank MK759888; Identities 588/596 (98.66%), 0 gaps), and *S. pseudobactrodesmium* (GenBank OR604485; Identities 588/597 (98.49%), 1 gap). Morphologically, *S. caryotae* is distinct in *Sclerococcum* by 1-septate homopolar to

heteropolar (with a longer upper cell) ascospores. Based on phylogenetic placement and morphological variations, we introduce *S. caryotae* as a new species.



Note a, b Appearance of apothecia. d–f Apothecial section. d–f hymenium, pseudoepithecium, paraphyses with asci (h paraphyses). i–k Asci. l–p Ascospore. q Germinating ascospore. r The front of culture on PDA at 25°C and the reverse of culture on PDA at 25°C. Scale bars: c = 50 µm, d–q = 10 µm.

Figure 2.70 *Sclerococcum caryotae* (MHZU 23-0159, holotype)

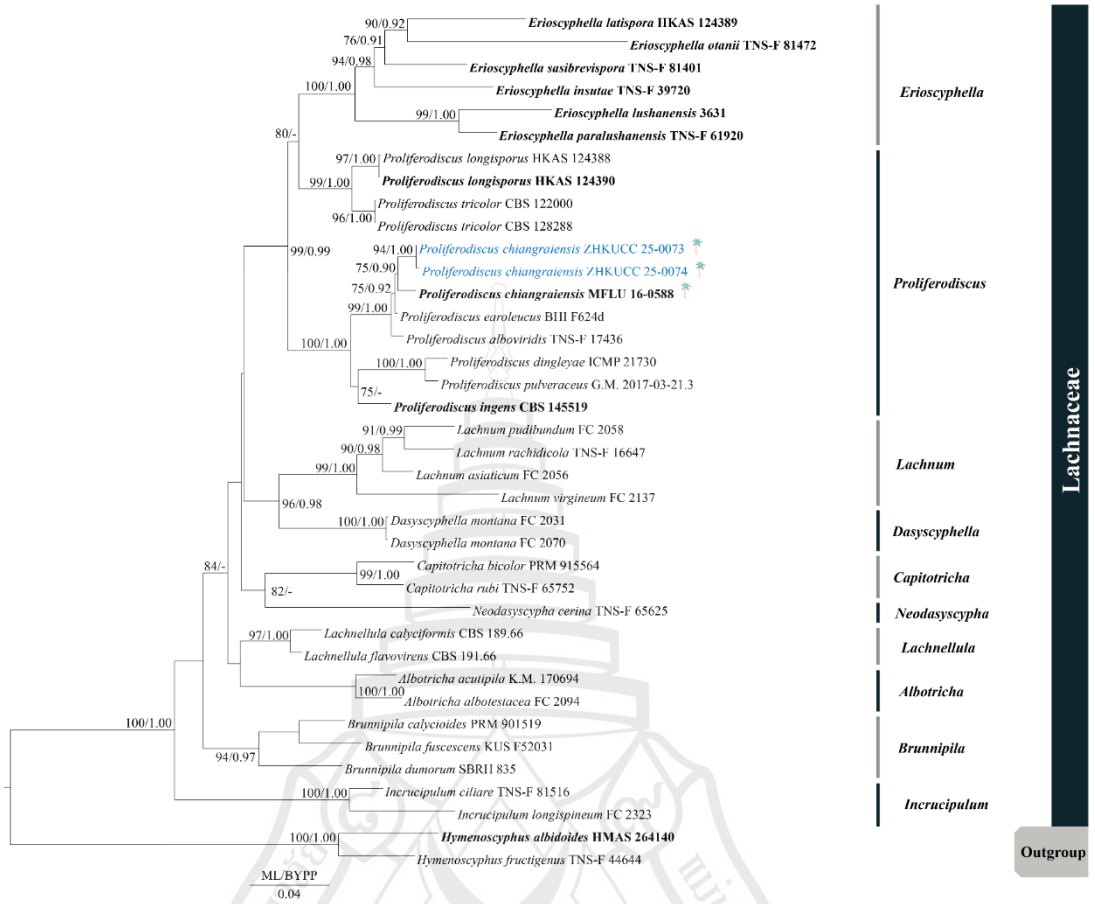
2.3.1.3 Leotiomycetes

Helotiales Nannf., Nova Acta Regiae Soc. Sci. Upsal. Ser. 4, 8 (2): 68 (1932)

Lachnaceae Raitv., Scripta Mycologica Tartu 20: 7 (2004)

Proliferodiscus J.H. Haines & Dumont, Mycologia 75: 536 (1983)

Notes: *Proliferodiscus* (*Pro*.) is a discomycetes genus, and was established by Haines and Dumont (1983) to accommodate species with proliferous hymenial discs, including *Pro. inspersus* (type) and *Pro. earoleuca* (Haines & Dumont, 1983). The genus is characterized by colourful, proliferous apothecia with a short stipe, hyaline, thin-walled, curled hairs that are densely granulated or covered by hyaline, amorphous material, an ectal excipulum composed of *textura prismatica* cells, filiform paraphyses, asci are 8-spored, and ascospores are hyaline (Haines & Dumont, 1983; Ekanayaka et al., 2019; Luo et al., 2025). The only known asexual morph in the genus is *Pro. ingens*, which consists subglobose conidiomata, hyaline, septate, smooth-walled conidiophores, and cylindrical to ellipsoidal, hyaline, aseptate conidia (Bien & Damm, 2020). *Proliferodiscus* species are primarily distributed in America, Asia, Australia, and Europe (Bien & Damm, 2020; Li et al., 2022). In this study, we use ITS and LSU to update phylogenetic tree of *Proliferodiscus* (Figure 2.71). There are 14 species accepted in *Proliferodiscus* (Index Fungorum, 2025 January) and 11 species were verified with DNA sequences (Li et al., 2022; Luo et al., 2025). Two species have been reported from palm species (Xiong et al., 2025) including a new host and geography record of *Pro. chiangraiensis* was introduced from *Livistona chinensis* from China in this study. In addition, our species is the first asexual morph of *Pro. chiangraiensis*.



Note Phylogram generated from maximum likelihood analysis of Lachnaceae based on combined ITS and LSU sequence data. Bootstrap values for maximum likelihood (ML) equal to or greater than 70 and BYPP values equal to or greater than 0.90 are indicated above the branches. The new collections are indicated in blue and ex-type strains are indicated in bold.

Figure 2.71 Phylogenetic tree of Lachnaceae

Proliferodiscus chiangraiensis Ekanayaka & K.D. Hyde, Mycosphere 10 (1): 403 (2019)

Figure 2.72

Saprobic on dead segment of *Livistona chinensis*. Asexual morph: Coelomycetous. *Stromatic conidiomata* 120–180 × 180–250 µm ($\overline{x}$ = 148.6 × 216.5 µm, n = 20), solitary or aggregated, subglobose or irregular, unilocular, semi-immersed, dark brown to black, almost glabrous, opening with an irregular rupture. *Peridium* 30–50 µm ($\overline{x}$ = 36.2 µm, n = 20), composed of thick-walled, hyaline to brown cells of *textura intricata*.

Paraphyses 1–1.8 µm ($\overline{x}$ = 1.3 µm, n = 20), filiform, unbranched, hyaline and aseptate. *Conidiophores* reduced to conidiogenus cells. *Conidiogenus cells* 7–10 × 1–2.5 µm ($\overline{x}$ = 9.2 × 1.7 µm, n = 20), enteroblastic, hyaline, smooth-walled, navicular to subulate, or cylindrical, tapering towards apices, collarettes hardly visible, periclinal thickening sometimes visible. *Conidia* 2.5–3.5 × 1.2–1.8 ($\overline{x}$ = 3.0 × 1.5 µm, n = 20), hyaline, smooth-walled, aseptate, cylindrical to ellipsoidal, straight, with both ends rounded, guttulate. Sexual morph: Not observed.

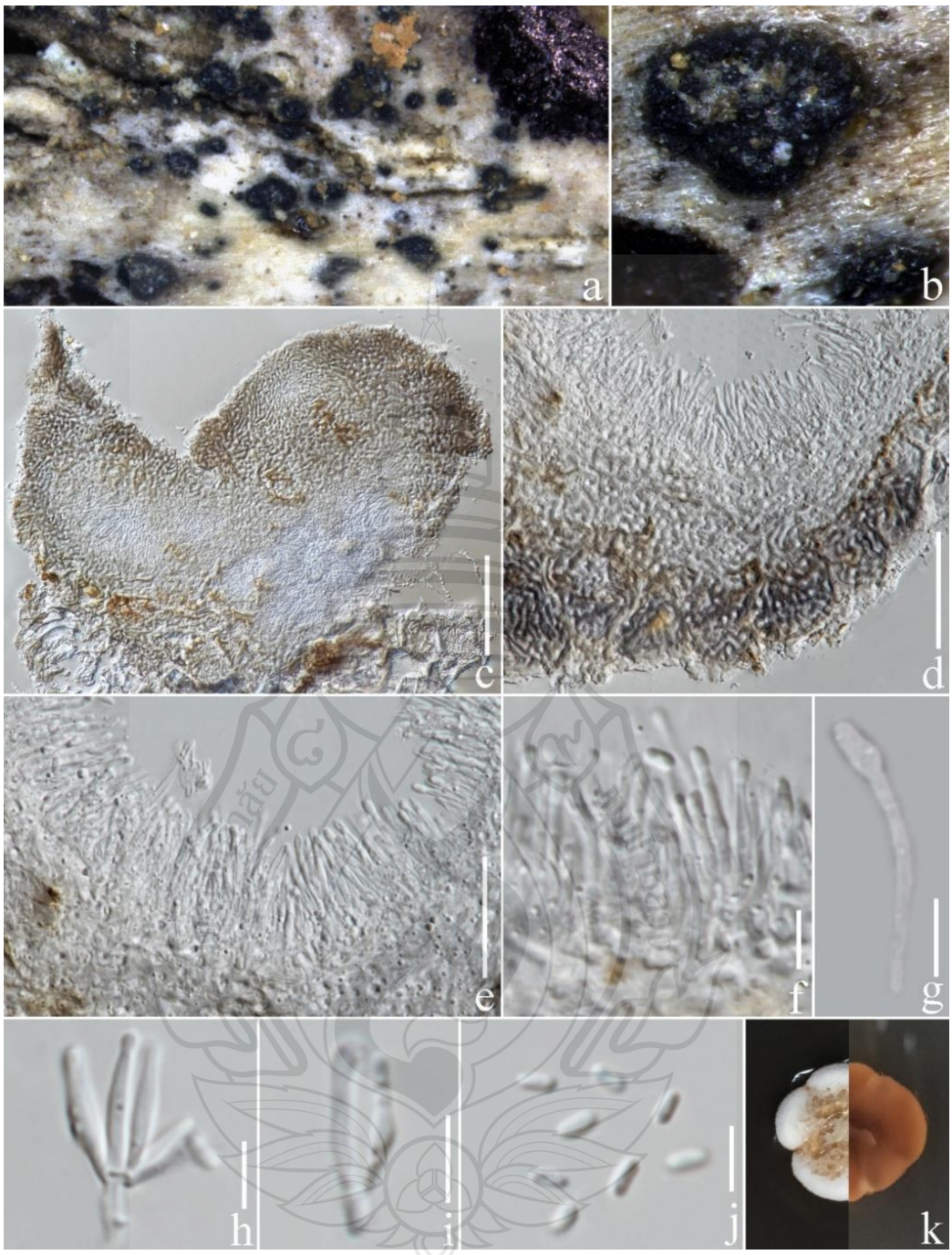
Culture characteristics: Colonies on PDA slowly growing, after 2 weeks reaching 1–2 cm diam., at 25 °C, slight raised, with lobate margin, cottony or floccose, light brown pigment or exudate accumulates at the colony center, above white, yellowish in reverse.

Known distribution: Thailand (Ekanayaka et al., 2019), China (this study).

Material examined: China, Jiangxi Province, Nanchang City, Meiling National Forest Park, on a dead segment of *Livistona chinensis*, 10 April 2024, Y.R. Xiong, XG425 (MHZU 24-0513, new host and geography record), living culture ZHKUCC 25-0073, other living culture ZHKUCC 25-0074.

GenBank numbers: ZHKUCC 25-0073: ITS – PV578232, LSU – PV578398, *rpb*2 – PV595352; ZHKUCC 25-0074: ITS – PV578233, LSU – PV578399, *rpb*2 – PV595353.

Notes: Two collections obtained in this study clustered with *Pro. chiangraiensis* (MFLU 16-0588, holotype) by 75% ML bootstrap support and 0.90 BYPP (Figure 2.71). The nucleotide differences excluding gaps between our isolate (ZHKUCC 25-0073) and *Pro. chiangraiensis* (MFLU 16-0588) were checked and shown - ITS: 1.1% (6/523 base pairs), LSU: 0.5% (4/867 base pairs), and SSU: 1.6% (14/844 base pairs). *Proliferodiscus chiangraiensis* was introduced by Ekanayaka et al. (2019) with only sexual morph. Our species exhibits only an asexual morph, making the morphological comparison with the sexual morph of *Pro. chiangraiensis* unavailable. Our species exhibits characteristics consistent with the asexual morph of *Proliferodiscus*, particularly in the presence of enteroblastic and cylindrical conidiogenous cells, as well as cylindrical to ellipsoidal, hyaline, and aseptate conidia (Bien & Damm, 2020, Figure 64). Therefore, based on morphology and phylogenetic analysis, we identified our collections as new a host and geography record of *Pro. chiangraiensis*. It represents the asexual morph of *Pro. chiangraiensis.*



Note a, b Conidioma on natural substrate. c Vertical section of a conidiomata. d Peridium and paraphyses. e, f Conidiogenous cells lining the inner wall of a conidiomata. g Germinated conidium. h, i Detached conidiogenous cells. j Conidia. k The front of culture on PDA at 25℃ and the reverse of culture on PDA at 25℃. Scale bars: c, d = 30 µm; e = 20 µm; f–j = 5 µm.

Figure 2.72 *Proliferodiscus chiangraiensis* (MHZU 24-0513, new host and geography record)

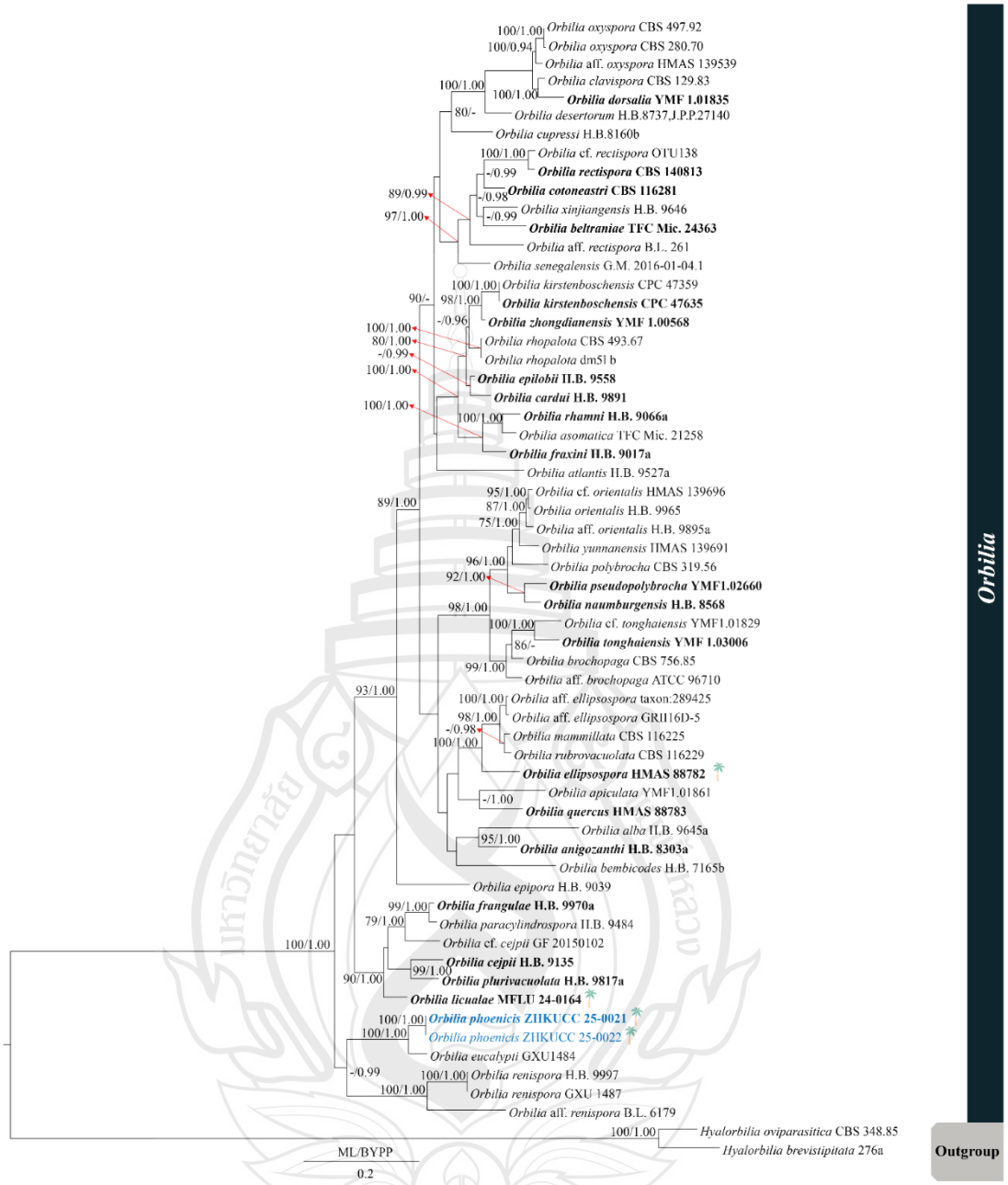
2.3.1.4 Orbiliomycetes

Orbiliales Baral, O.E. Erikss., G. Marson & E. Weber

Orbiliaceae Nannf., Nova Acta Regiae Societatis Scientiarum Upsaliensis 8 (2): 250 (1932)

Orbilia Fr., Corpus Florarum provincialium suecicae I. Floram Scanicam: 343 (1836)

Notes: Fries (1836) first introduced *Orbilia* (*O.*) with *O. xanthostigma* as the type species. Baral et al. (2020) list three subgenera within *Orbilia* based on morphology and phylogenetic results including *Hemiorbilia*, *Habrostictis*, and *Orbilia*. *Orbilia* is holomorphic subgenus characterized by teleomorph Apothecia hydrated mainly whitish, ochraceous, yellowish, rose, orange, lilaceous, margin glabrous or crenulate, denticulate to dentate, or hairy, and sessile or (short-)stipitate. Ascus apex is slightly or medium or strongly truncate, not or slightly to distinctly indented, thin-walled, rarely with dome, and sometimes with apical chamber. Ascospores are variously shaped, apical, globose to tear-shaped, subulate, rod-shaped, plug-shaped, dumbbell-shaped or ampulliform, and filum absent or very short. Paraphyses are apically uninflated to strongly capitate-clavate, and also spathulate to lanceolate (Baral et al., 2020). The asexual morph is characterized by unbranched conidia that vary in shape between ellipsoid, sub-cylindrical, clavate, obovoid, obpyramidal, fusiform, or top-shaped with mostly septate, either 1-septate (didymosporous) or with more septa (phragmosporous), and rarely non-septate (amerosporous). Conidia are branched (staurosporous) always multiseptated with one stipe and two, three, or four arms, and are mainly Y- or T-shaped, more rarely ┼-, H-, K-, U-, V- or tuning fork-shaped, thereby forming either 2- (flat) or 3-dimensional (spatial) structures, straight or curved (Baral et al., 2020). Moreover, trapping organs are unknown in this subgenus (Baral et al., 2020). Morphological evidence and phylogenetic analyses based on SSU, ITS, and LSU were used to define *Orbilia* in a narrow sense (Baral et al., 2020). In our study, we used ITS and LSU to update phylogenetic studies for subgenus *Orbilia* in *Orbilia* (Figure 2.73). Currently, 27 species are listed under *Orbilia* in a narrow sense (Baral et al., 2020). Totally nine species have been reported from palm species including a new species described in this study (Xiong et al., 2025).



Note Phylogram generated from maximum likelihood analysis of *Orbilia* based on combined ITS, and LSU sequence data. Bootstrap values for maximum likelihood (ML) equal to or greater than 70 are indicated above the branches. The new collections are indicated in blue and ex-type strains are indicated in bold.

Figure 2.73 Phylogenetic tree of *Orbilia*

Orbilia phoenicis Y.R. Xiong, Manawas. & K.D. Hyde, ***sp. nov.***

Figure 2.74

Etymology: The epithet refers to the host genus name "*Phoenix*", from which the species was collected.

Saprobic on dead leaf sheath of *Phoenix sylvestris*. Asexual morph: Hyphomycetous. *Colonies* on natural substratum superfcial, effuse, erect, cylindrical or tufted, yellowish to pale ochre. *Mycelium* immersed. *Conidiophores* 3.5–4.5 μm wide, synnematous, semi-macronematous, scattered, erect, rarely gregarious, unbranched, hyaline, septate, smooth. *Conidiogenous cells* 7–12 × 2–4 μm ($\overline{x}$ = 9.6 × 2.8 μm, n = 25), monoblastic, sympodial, obclavate, hyaline. *Hyphopodium* 10–15 × 4–5 μm ($\overline{x}$ = 13.5 × 4.8 μm, n = 25), 2–3-septate when mature, brown, oblong, round at apex. *Conidia* 14–20 × 7.5–8.5 μm ($\overline{x}$ = 17 × 8 μm, n = 25), (total size), U-shaped, stalk-like nodulous protuberance, the two arms ± equal in length, parallel, arms 12–15 × 4–5 μm ($\overline{x}$ = 13.8 × 4.8 μm, n = 25), cylindrical but slightly tapering above, 1–3-septate (each arm with an oblique basal septum). Sexual morph: Not observed.

Culture characteristics: Colonies on PDA fast-growing, after 2 weeks reaching 4 cm diam., at 25°C, circular, flat, filamentous, dense, white mycelium on the surface with entire margin; in reverse cream.

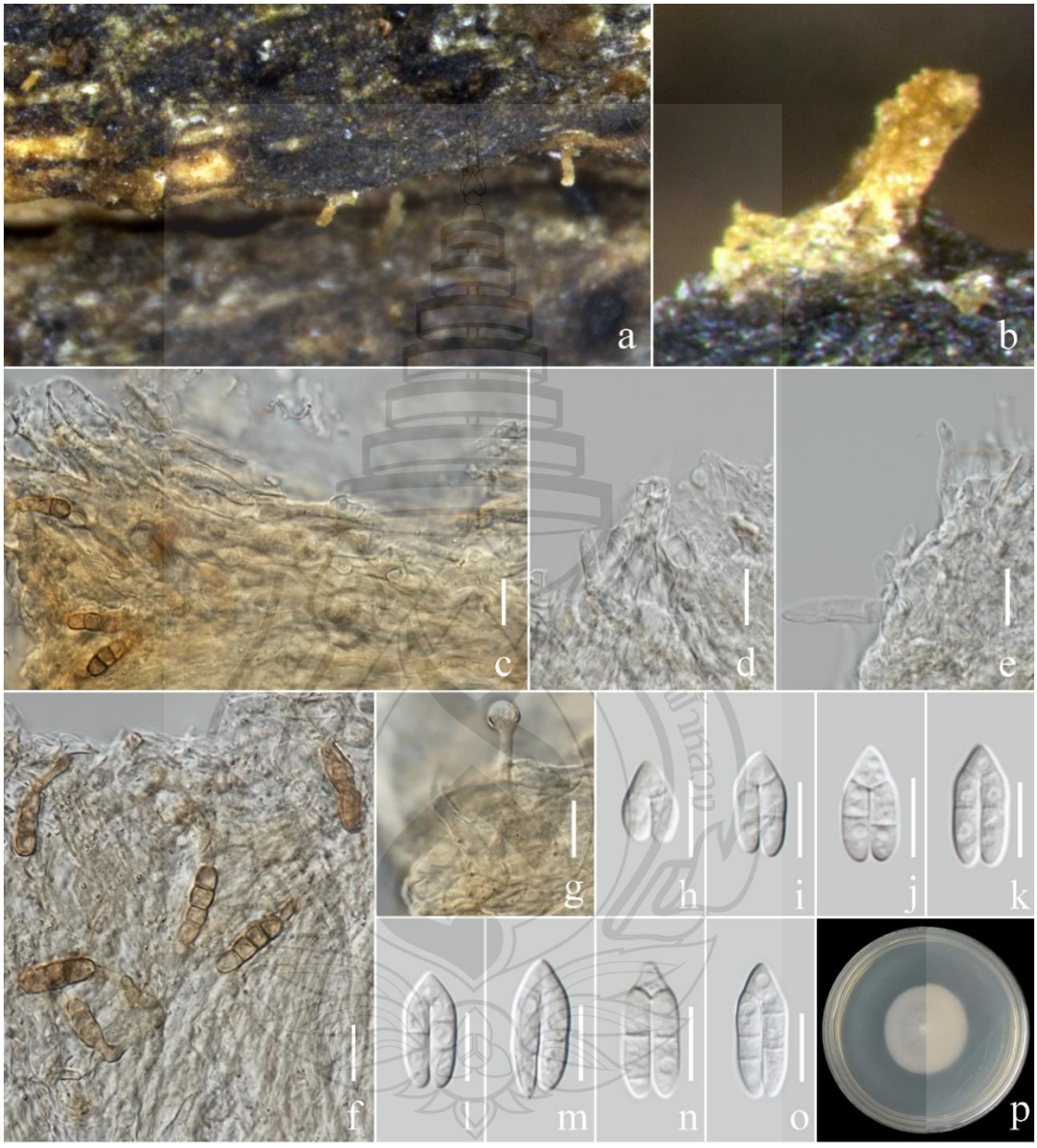
Known distribution: China (this study).

Material examined: China, Jiangxi Province, Ganzhou City, Xingda Restaurant, on dead leaf sheath of *Phoenix sylvestris*, 9 Apr 2024, Y.R. Xiong, XG364 (MHZU 24-0457, holotype), ex-type ZHKUCC 25-0021, other living culture ZHKUCC 25-0022.

GenBank numbers: ZHKUCC 25-0021: ITS – PV578218, LSU – PV578384; ZHKUCC 25-0022: ITS – PV578219, LSU – PV578385.

Notes: Two collections from this study formed a separate lineage and clustered with *Orbilia eucalypti* in the phylogenetic tree with 100% ML bootstrap support and 1.00 BYPP (Figure 2.73). The nucleotide differences excluding gaps between *O. phoenicis* (MHZU 24-0457) and *O. eucalypti* (GXU1484) its phylogenetically related species were checked and given as follows, ITS: 5.05% (24/475 base pairs), LSU: 2.24% (12/535 base pairs). Morphologically, *O. phoenicis* is distinct by 2–3-septate and brown hyphopodium with *O. eucalypti* (GXU1484) (Shao et al., 2018). Moreover, *O. phoenicis* has 1–3-septate (each arm with an oblique basal septum) which is different from *O. eucalypti* (GXU1484) has

1–2 septate (each arm with an oblique basal septum) (Shao et al., 2018). Based on phylogenetic placement and morphological variations, we introduce *O. phoenicis* as a new species.



Note a, b Colonies on substrate. c Synnematous conidiophores. d, e Conidiogenous cells. f, g Synnematous conidiophores. h–o Conidia. p The front of culture on PDA at 25°C and the reverse of culture on PDA at 25°C. Scale bars: c–o = 10 μm.

Figure 2.74 *Orbilia phoenicis* (MHZU 24-0457, holotype)

2.3.1.5 Sordariomycetes

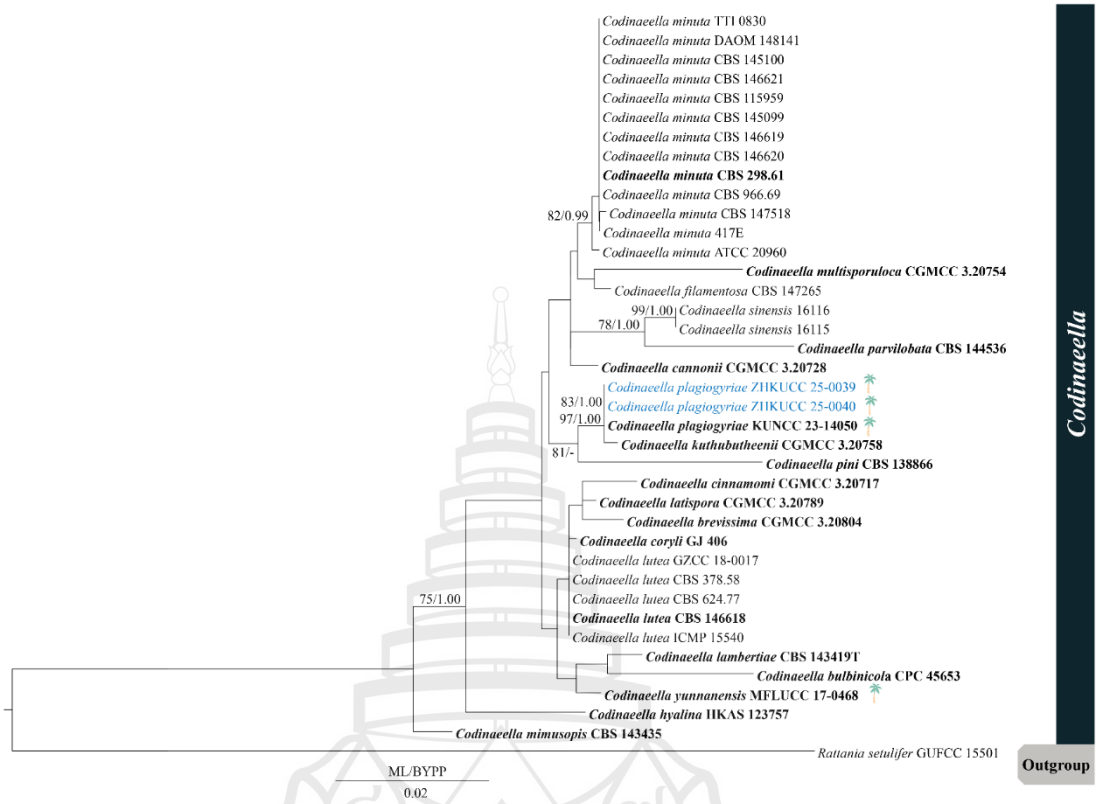
Orbiliales Baral, O.E. Erikss., G. Marson & E. Weber

Chaetosphaeriales Huhndorf, A.N. Mill. & F.A. Fernández, Mycological Research 108 (12): 378 (2004)

Chaetosphaeriaceae Réblová, M.E. Barr & Samuels, Sydowia 51: 56 (1999)

Codinaeella Réblová & Hern.-Restr., Journal of Fungi 7 (12, no. 1097): 45 (2021)

Notes: Based on molecular data and morphological evidence, *Codinaeella* (*Cod.*) was established by Réblová et al. (2021) to accommodate eight "*Codinaea*" -like fungi, typified by *Cod. minuta*. *Codinaeella* species are mainly saprobic and only reported with sexual morph, found on various plants and soil worldwide (Réblová et al., 2021; Wu et al., 2022; Zhang et al., 2022). *Codinaeella* is characterized by two morphotypes: Morphotype CA1, found in species like *Cod. minuta*, *Cod. lutea*, and *Cod. parvilobata*, features unbranched conidiophores that grow singly or in small groups, often accompanied by fertile setae terminating in mono- or poly-phialides. Morphotype CA2, represented only by *Cod. filamentosa*, has branched conidiophores with sterile setiform extensions and shorter, unbranched conidiophores (Réblová et al., 2021). *Codinaeella* can be distinguished from *Codinaea* by the arrangement of setae and conidiophores on natural substrates and its unique pigment production (Wu et al., 2022). *Codinaeella* often forms bright yellow, ochre, and orange to dark burgundy pigments dispersed in agar, whereas in *Codinaea* the pigments are rarely formed (Réblová et al., 2021). In our study, we used ITS and LSU to update phylogenetic studies for *Codinaeella* (Figure 2.75). There are 19 species accepted in *Codinaeella* (Index Fungorum, 2025 January; Zhang et al., 2025 in press) and all were verified with DNA sequences (Réblová et al., 2021; Wu et al., 2022; Zhang et al., 2022). Two species have been reported from palm species (Xiong et al., 2025) including a new host record of *Cod. plagiogyriae* was introduced from *Livistona chinensis* from China.



Note Phylogram generated from maximum likelihood analysis of *Codinaeella* based on combined ITS and LSU sequence data. Bootstrap values for maximum likelihood (ML) equal to or greater than 70 are indicated above the branches. The new collections are indicated in blue and ex-type strains are indicated in bold.

Figure 2.75 Phylogenetic tree of *Codinaeella*

Codinaeella plagiogyriae J.Y. Zhang & Y.Z. Lu, Fungal diversity: (2025)

Index Fungorum number: IF 903193; *Facesoffungi number*: FoF 17045; Figure 2.76

Saprobic on dead segment of *Livistona chinensis*. Asexual morph: Hyphomycetous. *Colonies* on natural substrate superficial, effuse, white to yellowish, dense, shining, globose aggregated in a large mass. *Mycelium* mostly immersed, composed of hyaline hyphae, branched, septate, smooth-walled. *Conidiophores* 80–120 × 4.5–5.5 µm ($\overline{x}$ = 97.2 × 4.9 µm, n = 20), macronematous, mononematous, single or in small groups, erect, straight or slightly flexuous, smooth-walled, dark brown at the base, becoming paler to subhyaline towards the apex, 3–8-septate, smooth, guttulate. *Conidiogenous cells* 15–25 × 3–5 ($\overline{x}$ = 19.4 × 3.7 µm, n = 20), mono- or polyphialidic, with discrete, lateral phialides,

integrated, terminal, with lateral openings formed by successive sympodial elongation, cylindrical to cylindrical-lageniform, with funnel-shaped collarettes, light brown at the base and becoming subhyaline to hyaline towards the apex, smooth-walled. *Conidia* 15–20 × 3–4.5 µm ($\bar{x}$ = 18.1 × 3.7 µm, n = 20), falcate, asymmetrical, tapering toward both ends, amerospores, aseptate, aggregated in large and slimy mass, smooth-walled, hyaline, with straight or gently curved setula at both end, 7–8µm-long. Sexual morph: Not observed.

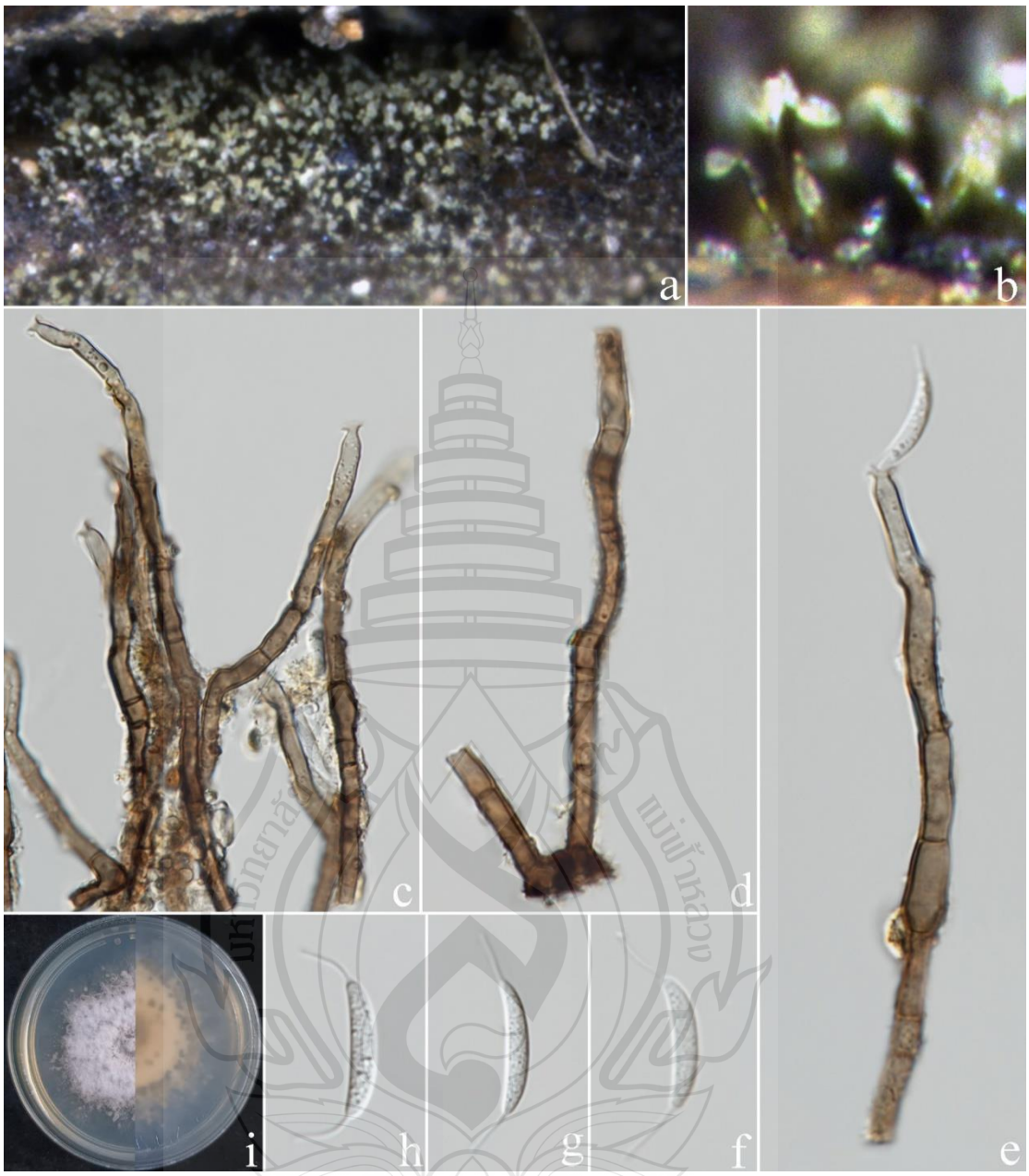
Culture characteristics: Colonies on PDA fast growing, after 2 weeks reaching 4–5 cm diam., at 25°C, filamentous, flat, with filiform edge, sparse, cotton-like, white aerial mycelium on surface, above white, yellowish in reverse.

Known distribution: China (Zhang et al., 2025, this study).

Material examined: China, Jiangxi Province, Nanchang City, Meiling National Forest Park, on dead segment of *Livistona chinensis*, 10 April 2024, Y.R. Xiong, XG380 (MHZU 24-0461, new host record), living culture ZHKUCC 25-0039, other living culture ZHKUCC 25-0040.

GenBank numbers: ZHKUCC 25-0039: ITS – PV578150, LSU – PV578320; ZHKUCC 25-0040: ITS – PV578151, LSU – PV578321.

Notes: Two collections obtained in this study clustered with *Cod. plagiogyriae* (KUNCC 23-14050, ex-type) by 97% ML bootstrap support and 1.00 BYPP (Figure 2.75). Based on a MegaBLAST (Query cover ≥ 70%) search using the ITS and LSU sequence, the closest matches in the NCBIs GenBank nucleotide database were *Cod. plagiogyriae* (GenBank PQ671254; Identities 498/498(100%), 0 gap) for ITS; *Cod. plagiogyriae* (GenBank PQ671174; Identities 882/884(99%), 2 gaps) for LSU. *Codinaeella plagiogyriae* was introduced by Zhang et al. (2025), which was collected from dead fronds and frond stalks of *Plagiogyria euphlebia* in China. Morphological evidence of conidiophores and conidia are well fit with the holotype descriptions of *Cod. plagiogyriae* (Zhang et al., 2025, Figure 2.76). Therefore, based on morphology and phylogenetic analysis, we identified our collections as a new host record of *Cod. plagiogyriae*.

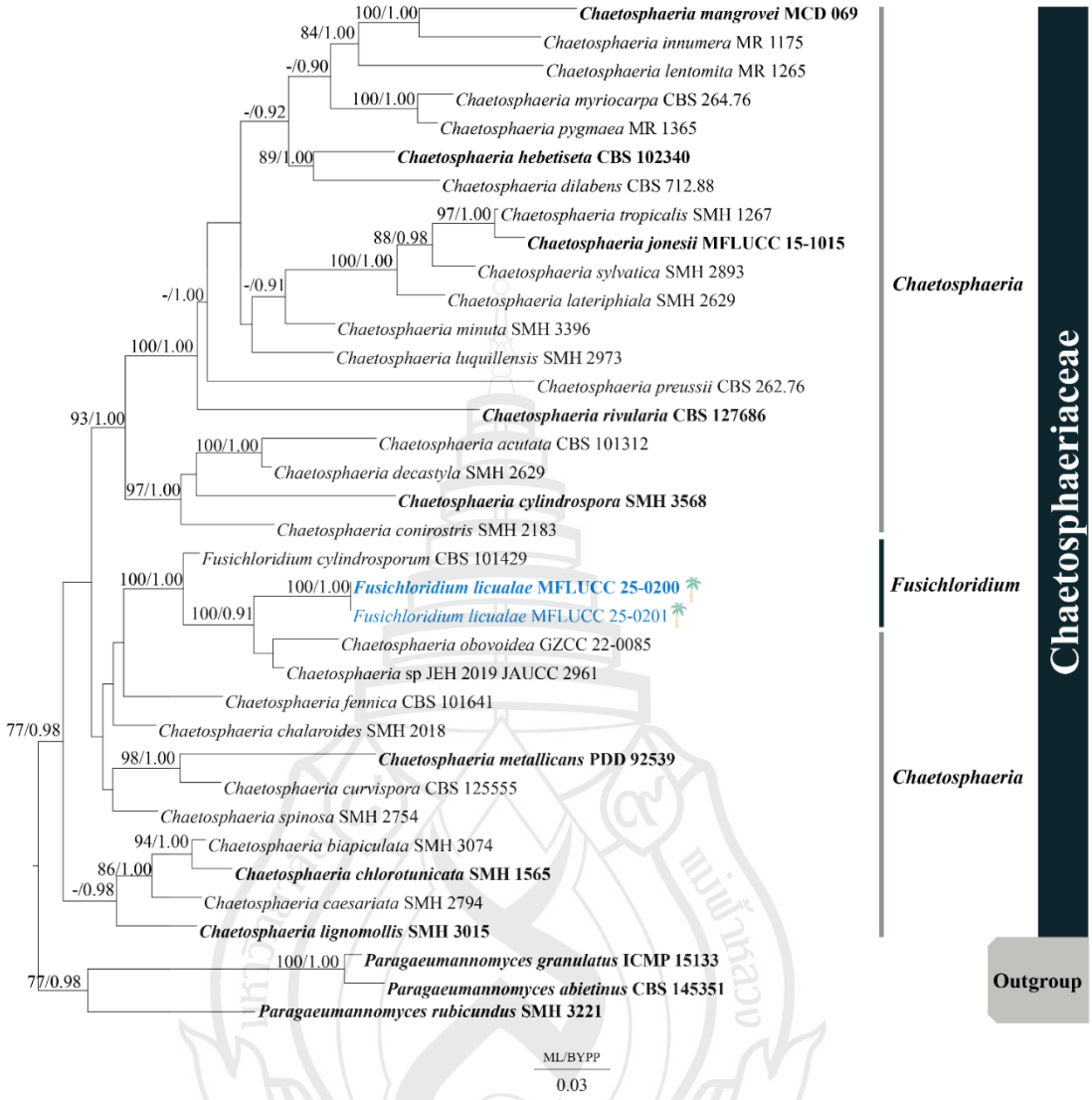


Note a, b Colonies on natural substrate. c–e Conidiophores and conidiogenous cells with conidia. f–h Conidia. i The front of culture on PDA at 25°C and the reverse of culture on PDA at 25°C. Scale bars: c–e = 30 µm; f–h = 10 µm.

Figure 2.76 *Codinaeella plagiogyriae* (MHZU 24-0461, new host record)

Fusichloridium W.P. Wu & Y.Z Diao, Fungal Diversity 116: 282 (2022)

Notes: Wu and Diao (2022) established *Fusichloridium* (*Fu*.) to accommodate the type species, *Fusichloridium cylindrosporum* (Réblová et al., 2022). *Fusichloridium* is a holomorphic genus with the asexual morph characterized by cylindrical and sympodially or sometimes percurrently proliferating conidiophores, monophialidic or polyphialidic with almost hyaline collarettes, and conidia are cylindrical with tapering and centrally some time slightly constricted (Wu & Diao, 2022). The sexual morph is characterized by perthecia and subglobose ascomata, ostiole is conical and covered with conidiophores, paraphyses are threadlike but soon evanescente, cylinderical to somewhat fusiform with a thin apical plate, and ascospore are fusiform and mostly 3-septate with guttulate (Wu & Diao, 2022). Wu and Diao (2022) based on morphological evidence and phylogenetic analysis combined ITS and LSU to introduce *Fusichloridium* as a new genus. Subsequently, phylogenetic studies mainly use SSU, LSU, ITS and *tef* 1-α or without SSU sequences data in analysis (Réblová et al., 2022). Following Réblová et al. (2022), in this study, we used ITS and LSU to update phylogenetic studies for *Fusichloridium* (Figure 2.77). Currently, one species is listed under *Fusichloridium* (Index Fungorum, 2025 January) and this species is associated with molecular data. Here is the first report of *Fusichloridium* on palm species (Xiong et al., 2025).



Note Phylogram generated from maximum likelihood analysis of *Chaetosphaeria*-like taxa in Chaetosphaeriaceae based on combined ITS and LSU sequence data. Bootstrap values for maximum likelihood (ML) equal to or greater than 70 are indicated above the branches. The new collections are indicated in blue and ex-type strains are indicated in bold.

Figure 2.77 Phylogenetic tree of *Chaetosphaeria*-like taxa in Chaetosphaeriaceae

Fusichloridium licualae Y.R. Xiong, Manawas. & K.D. Hyde, ***sp. nov.***

Figure 2.78

Etymology: The epithet refers to the host genus name "*Licuala*", from which the species was collected.

Saprobic on dead leaf sheath of *Licuala* sp. Asexual morph: Hyphomycetous. *Colonies* on natural substrate, superficial, effuse, hairy, with white and gold shining masses on the apex of conidiophores. *Mycelium* partly immersed, composed of septate, hyaline hyphae. *Conidiophores* 100–200 × 5–6.5 μm ($\bar{x}$ = 144 × 5.5 μm, n = 25), macronematous, mononematous, erect, straight or slightly flexuous, solitary, scattered, smooth, septate, brown, percurrent proliferations assuming a geniculate appearance. *Conidiogenous cells* 20–60 × 5–7 μm ($\bar{x}$ = 45 × 5.7 μm, n = 25), mono- to poly-phialidic, terminal, integrated, cylindrical, brown, with subhyaline funnel-shaped collarettes, narrow at below the collarette. *Conidia* 17–23 × 5–8 μm ($\bar{x}$ = 20 × 6.9 μm, n = 25), accumulating in slimy beige to pale brown heads, elongate mouse-shaped with tapering, centrally some time slightly constricted, one unconspicuous transverse septum at medium, hyaline when young, yellow-brown when mature, truncate base, appendage at apex; basal cushion subulate to narrowly lageniform 2–5 × 1.5–2 μm ($\bar{x}$ = 3 × 1.9 μm, n = 25), with filiform-like appendage up to 170 μm. Sexual morph: Not observed.

Culture characteristics: Colonies on PDA, after 2 weeks reaching 2 cm diam., at 25°C, circular, umbonate, with fluffy, dense, grey mycelium on the surface with undulate margin; in reverse yellow in the middle and cream at the margin.

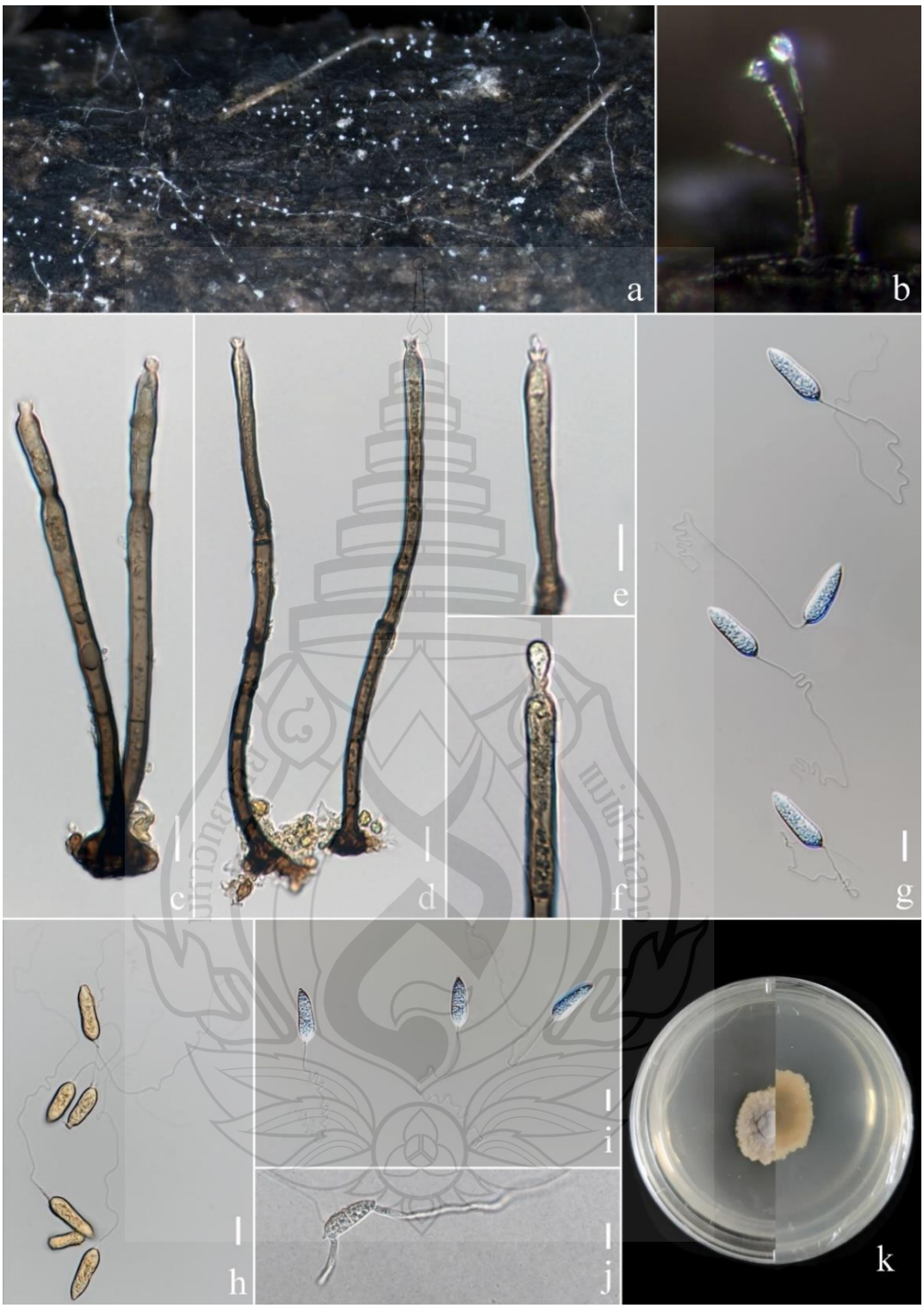
Known distribution: Thailand (this study).

Material examined: Thailand, Narathiwat Province, Toh Daeng Peat swamp, on dead leaf sheath of *Licuala* sp., 4 Aug 2023, Y.R. Xiong, XG326 (MFLU 25-0145, holotype), ex-type MFLUCC 25-0200, other living culture MFLUCC 25-0201.

GenBank numbers: MFLUCC 25-0200: ITS – PV578182, LSU – PV578346; MFLUCC 25-0201: ITS – PV578183, LSU – PV578347.

Notes: Two collections from this study formed a separate lineage, but both closed with *Chaetosphaeria obovoidea* and *Fusichloridium cylindrosporum* in the phylogenetic tree with 100% ML bootstrap support and 0.91 BYPP (Figure 2.77). The nucleotide differences excluding gaps between *Fu. licualae* (MFLUCC 25-0200) and its phylogenetically related species were checked and given as follows, *Chaetosphaeria*

obovoidea (GZCC 22-0085) - ITS: 5.15% (25/485 base pairs), LSU: 3.05% (28/918 base pairs); *Fusichloridium cylindrosporum* (CBS 101429) - ITS: 6.65% (34/511 base pairs), LSU: 3.66% (34/930 base pairs). Our collections have terminal conidiogenous cells and conidia elongate mouse-shaped with tapering which is distinct from *Chaetosphaeria obovoidea* and have aseptate and obovoid conidia intercalary conidiogenous loci (Zhang et al., 2022, Figure 2.78). In addition, our collections as long filiform-like appendages with basal cushions which is absent in *Fusichloridium cylindrosporum* (Réblová & Gams, 1999; Réblová et al., 2022, Figure 2.78). Our collections is similar to *Fusichloridium* by conidia centrally times slightly constricted (Wu & Diao, 2022, Figure 2.78) and phylogenetic placement, we introduce our collections as a new species in *Fusichloridium*, named *Fu. licualae*. Moreover, we proposed *Chaetosphaeria obovoidea* can be consider to synomized in *Fusichloridium* based on phylogenitc analysis result. However, this view still needs more evidence to support.



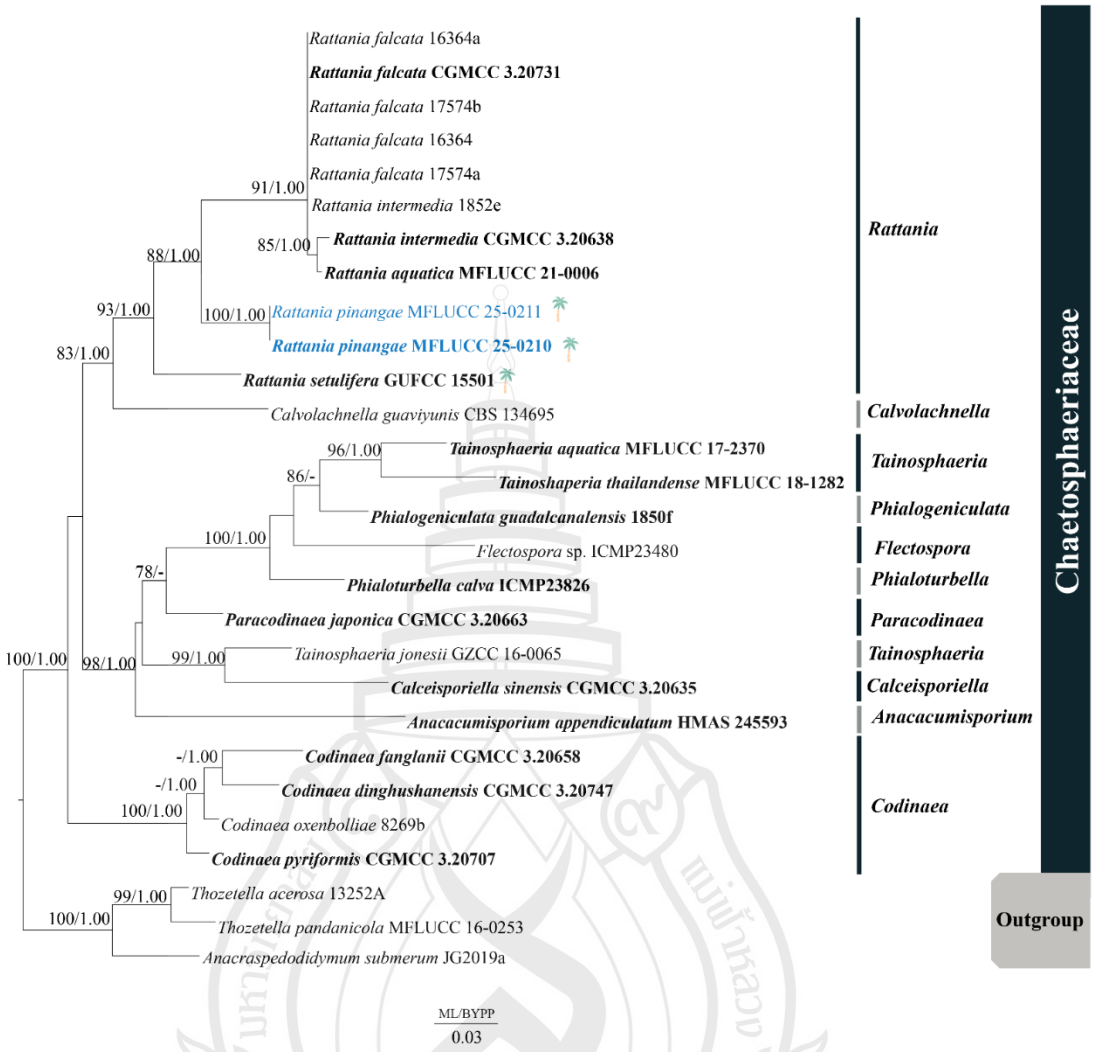
Note a, b Colonies on substrate surface. c, d Conidiophores. e, f Conidiogenous cells with growing conidia. g–i Conidia. j Germinating conidium. k The front of culture on PDA at 25°C and the reverse of culture on PDA at 25°C. Scale bars: c–k = 10 µm.

Figure 2.78 *Fusichloridium licualae* (MFLU 25-0145, holotype)

Chaetosphaeriaceae Réblová, M.E. Barr & Samuels, Sydowia 51: 56 (1999)

Rattania Prabhug. & Bhat, Mycotaxon 108: 218 (2009)

Notes: Prabhugaonkar and Bhat (2009) established *Rattania* (*R.*) with *R. setulifera* as the type species. *Rattania* is a hyphomycetous genus characterized by sporodochia with setose conidiomata, monoblastic conidiogenous cells and aseptate to multi-septate, and setulate conidia (Prabhugaonkar & Bhat, 2009). Shenoy et al. (2010) first placed *Rattania* in Chaetosphaeriales based on morphological evidence and phylogenetic analysis using LSU. Subsequently, phylogenetic studies mainly use ITS and LSU for analysis (Calabon et al., 2021). In this study, we use ITS and LSU to update phylogenetic studies for *Rattania* (Figure 2.79). Currently, four species are listed under *Rattania* (Index Fungorum, 2025 January), and all species are associated with molecular data. Totally two species have been reported from palm species including a new species described in this study (Xiong et al., 2025).



Note Phylogram generated from maximum likelihood analysis of *Rattania* based on combined ITS and LSU sequence data. Bootstrap values for maximum likelihood (ML) equal to or greater than 70 are indicated above the branches. The new collections are indicated in blue and ex-type strains are indicated in bold.

Figure 2.79 Phylogenetic tree of *Rattania*

Rattania pinangae Y.R. Xiong, Manawas. & K.D. Hyde, ***sp. nov.***

Figure 2.80

Etymology: The epithet refers to the host genus name "*Pinanga*", from which the species was collected.

Saprobic on dead leaf sheath of *Pinanga riparia*. Asexual morph: Hyphomycetous. *Colonies* on natural substrate superficial, scattered. *Mycelium* mostly

immersed, composed of branched, septate, smooth, thin-walled, brown hyphae. *Conidiomata* sporodochial, scattered, punctiform, pulvinate, dark brown to black, setose, dark brown, basal stroma composed of dark brown, irregular cells. *Setae* 200–450 × 7–13 μm ($\overline{x}$ = 361 × 9.8 μm, n = 25), sterile, arising from the lower part of the stroma, subulate, acutely pointed, mid to dark brown, becoming paler towards the apex, smooth, simple, straight or slightly curved, sometimes constrict at septate. *Conidiophores* formed a close palisade over the surface of the stroma, cylindrical, brown to pale brown. *Conidiogenous cells* 10–15 × 3–4 μm ($\overline{x}$ = 12.4 × 3.6 μm, n = 25), integrated, terminal, monophialidic, poroconidia, ampulliform or cylindrical, hyaline to pale brown. *Conidia* 10–13 × 3–4 μm ($\overline{x}$ = 11.5 × 3.4 μm, n = 25), holoblastic, solitary, hyaline, aseptate, naviculate to fusiform, curved, guttulate, with a single filiform setula at both ends, 3–5 μm long. Sexual morph: Not observed.

Culture characteristics: Colonies on PDA fast growing, after 2 weeks reaching 4 cm diam., at 25°C, circular, brown, with fluffy, dense, white mycelium on the surface with entire margin; in reverse dark brown.

Known distribution: Thailand (this study).

Material examined: Thailand, Narathiwat Province, in an unidentified beach, on dead leaf sheath of *Pinanga riparia*, 6 Aug 2023, Y.R. Xiong, XG340 (MFLU 25-0150, holotype), ex-type MFLUCC 25-0210, other living culture MFLUCC 25-0211.

GenBank numbers: MFLUCC 25-0210: ITS – PV578246, LSU – PV578414; MFLUCC 25-0211: ITS – PV578246, LSU – PV578414.

Notes: Two collections from this study formed an independent lineage within *Rattania* in the phylogenetic tree with 88% ML bootstrap support and 1.00 BYPP (Figure 2.79). Based on a MegaBLAST (Query cover ≥ 70%) search using the LSU sequence, the closest matches in NCBIs GenBank nucleotide database were *Rattania falcata* (GenBank OL655195; Identities 838/848 (98.82%), 1 gap), *Rattania setulifera* (GenBank HM171322; Identities 829/839 (98.81%), 2 gaps) and *Rattania aquatica* (GenBank OL655050; Identities 837/850 (98.47%), 0 gaps). The highest similarities using the ITS sequence were Chaetosphaeriales sp. (GenBank JX243872; Identities 452/479 (94.36%), 9 gap), Chaetosphaeriales sp. (GenBank JX243880; Identities 480/513 (93.57%), 9 gaps) and Chaetosphaeriales sp. (GenBank JX243871; Identities 479/512 (93.55%), 9 gaps). Moreover, *Rattania pinangae* is distinct in *Rattania* by poroconidia and ampulliform

conidiogenous cells. Based on phylogenetic placement and morphological variations, we introduce *R. pinangae* as a new species.



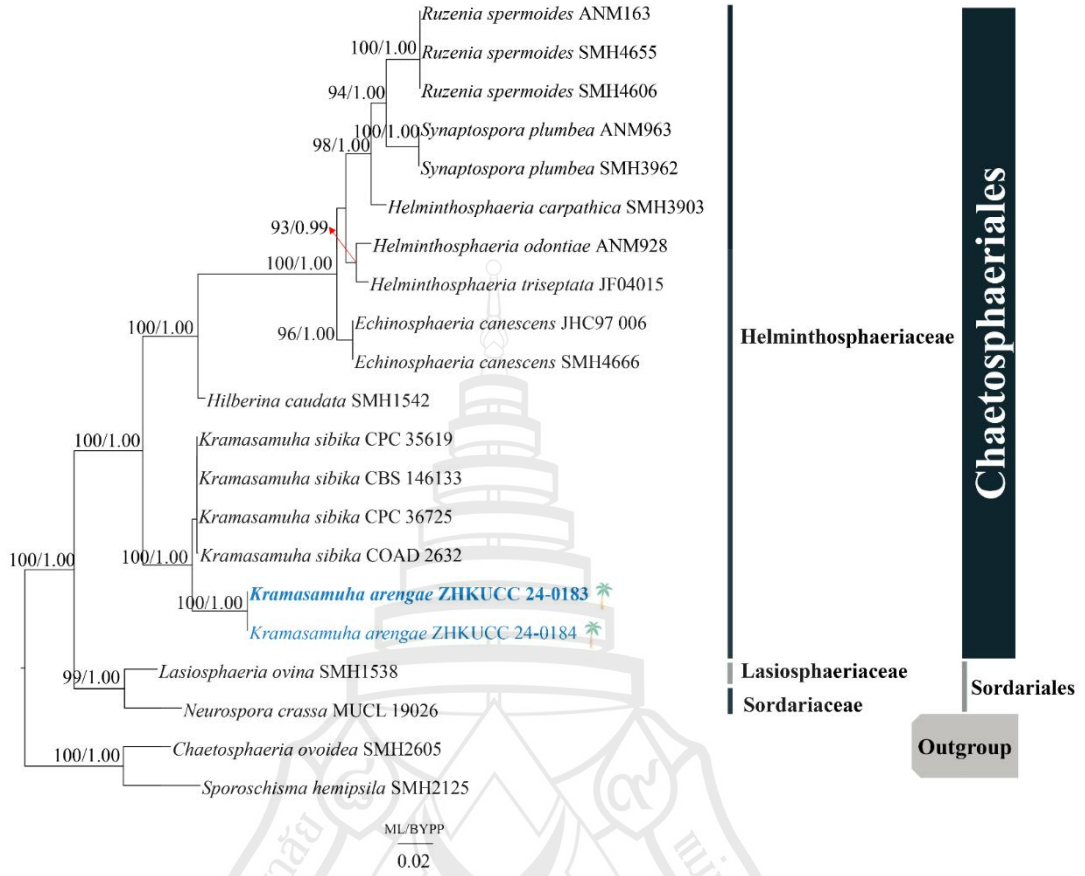
Note a, b Colonies on the substrate. c Sporodochial conidiomata with setae. d, e Setae. f, g Conidiophores and conidiogenous cells. h, i Conidia. j Germinating conidium. k The front of culture on PDA at 25°C and the reverse of culture on PDA at 25°C. Scale bars: c, d = 100 µm, e–j = 10 µm.

Figure 2.80 *Rattania pinangae* (MFLU 25-0150, holotype)

Helminthosphaeriaceae Samuels, Cand. & Magni, Mycologia 89: 144 (1997)

Kramasamuha Subram. & Vittal, Canadian Journal of Botany 51 (6): 1128 (1973)

Notes: Subramanian and Vittal (1973) established a monotypic genus *Kramasamuha* (*K*.) with *K. sibiki* as the type species. *Kramasamuha* only reported asexual morph characterized by erect or flexuous, simple or branched and septate of conidiophores, monoblastic, solitary or in clusters and terminal and intercalary of conidiogenous cells, septate, and obovoid to pyriform with short narrow separating cell at base as remnant from conidiogenous cell of conidia (Subramanian & Vittal, 1973; Hernández-Restrepo et al., 2020). Hernández-Restrepo et al. (2020) first provide ITS and LSU molecular data for *K. sibiki* which the only species in *Kramasamuha* to place the genus to Helminthosphaeriaceae. This study followed Hernández-Restrepo et al. (2020) and updated the phylogenetic analysis (Figure 2.81). Currently, two epithets are listed under *Kramasamuha* (Index Fungorum, 2025 January), and only one species is associated with molecular data. Here we described a new species of *Kramasamuha* which is the first time reported from palm species (Xiong et al., 2025).



Note Phylogram generated from maximum likelihood analysis of selected Chaetosphaeriales based on combined ITS and LSU sequence data. Bootstrap values for maximum likelihood (ML) equal to or greater than 70 are indicated above the branches. The new collections are indicated in blue and ex-type strains are indicated in bold.

Figure 2.81 Phylogenetic tree of some of Chaetosphaeriales

Kramasamuha arengae Y.R. Xiong, Manawas. & K.D. Hyde, ***sp. nov.***

Figure 2.82

Etymology: The epithet refers to the host genus name "*Arenga*", from which the species was collected.

Saprobic on dead petiole of *Arenga tremula*. Asexual morph: Hyphomycetous. *Colonies* on natural substrate superficial, effuse, scattered, dark brown. *Conidiophores* 190–220 × 4–6 µm ($\bar{x}$ = 210 × 5 µm, n = 10), erect, slightly flexuous, solitary to fasciculate, brown, smooth, multi-septate, simple, becoming paler towards the apex, terminating in an

acute. *Conidiogenous cells* 6–10 × 3.5–5.5 µm ($\overline{x}$ = 7.5 × 4.5 µm, n = 25), monoblastic, pale brown to hyaline, ampulliform, straight to curved, truncate apex, thin-walled, solitary, integrated or discrete, terminal or intercalary. *Conidia* 30–40 × 10–13 µm ($\overline{x}$ = 34 × 11.5 µm, n = 25), solitary, smooth, obovoid to pyriform, apex obtuse; when mature, 2-septate, medium cell thick-walled, dark brown, basal and apical cell pale, with short narrow separating cell at base as remnant from conidiogenous cell, some occur a papillate or a hyaline acicular appendage on apical cell. Sexual morph: Not observed.

Culture characteristics: Colonies on PDA fast growing, after 2 weeks reaching 4 cm diam., at 25°C, circular, with fluffy, dense, white mycelium on the surface with entire margin; in reverse yellow in the middle and white at the margin.

Known distribution: China (this study).

Material examined: China, Yunnan Province, Xishuangbanna City, on dead petiole of *Arenga tremula*, 4 Feb 2023, Y.R. Xiong and L. Lu, XG276 (MHZU 23-0188, holotype) – ex-type ZHKUCC 24-0183, other living culture ZHKUCC 24-0184.

GenBank numbers: ZHKUCC 24-0183: ITS – PV578192, LSU – PV578356; ZHKUCC 24-0184: ITS – PV578193, LSU – PV578357.

Notes: Two collections from this study formed a separate lineage and clustered with *Kramasamuha sibiki* in the phylogenetic tree with 98% ML bootstrap support and 1.00 BYPP (Figure 2.81). The nucleotide differences excluding gaps between *K. arengae* (ZHKUCC 24-0183) and *K. sibiki* (COAD 2632) were checked and given as follows, ITS: 4.00% (21/525 base pairs), and LSU: 0.88% (7/793 base pairs). Morphologically, *K. arengae* have a papillate or a hyaline acicular appendage on the apical cell of the conidia which is different from *K. sibiki* only has a short narrow separating cell at the base of the conidia (Hernández-Restrepo et al., 2020). Based on phylogenetic placement and morphological variations, we introduce *K. arengae* as a new species.



Note a–c Sporodochia on the substrate. d–i Conidiophore and conidiogenous cells with conidia. j–p Conidia. q Germinating conidium. r The front of culture on PDA at 25°C and the reverse of culture on PDA at 25°C. Scale bars: d–q = 10 µm.

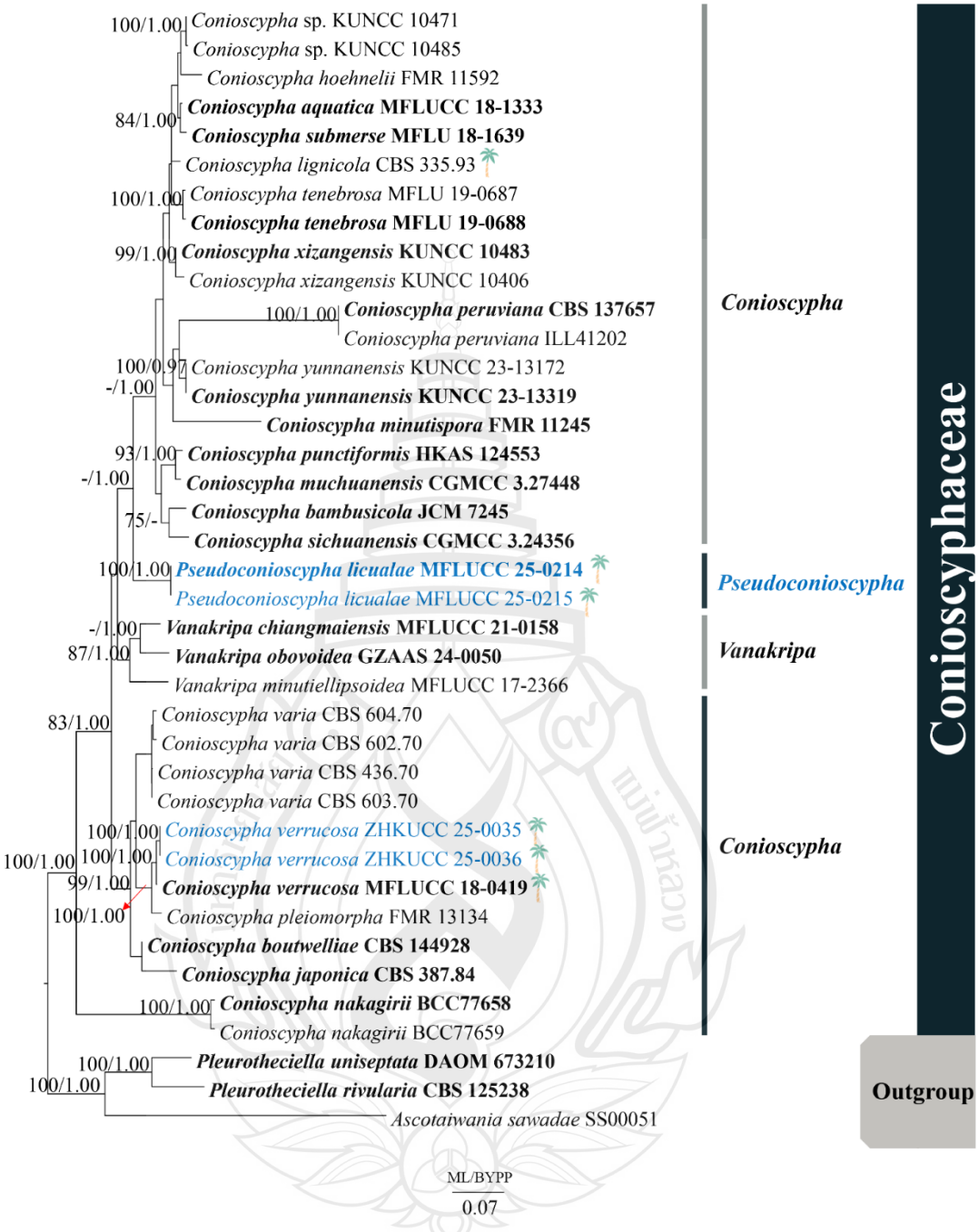
Figure 2.82 *Kramasamuha arengae* (MHZU 23-0188, holotype)

Conioscyphales Réblová & Seifert, Persoonia 37: 63 (2016)

Conioscyphaceae Réblová & Seifert, Persoonia 37: 63 (2015)

Conioscypha Höhn., Annls mycol. 2(1): 58 (1904)

Notes: Von Höhnel (1904) first introduced *Conioscypha* (*Co*.) with *Co. lignicola* as the type species. *Conioscypha* is a holomorph genus in which asexual morph characterised by unique conidiogenesis which occurs at inconspicuous loci along hyphae, a basipetal succession of blastically produced, aseptate, brown conidia leave behind hyaline, cup-like detachment remnant collarettes and subglobose or elliptical, and pigmented conidia (Shearer & Motta, 1973; Goh & Hyde, 1998). The sexual morph characters by immersed to superficial ascomata, papil late or elongated neck, cylindrical to clavate, unitunicate asci with a pronounced J-, apical ring, and narrowly fusiform to fusiform-navicular, and hyaline ascospores (Zelski et al., 2015; Hyde et al., 2020a). Réblová et al. (2016) introduced the family Conioscyphaceae based on morphological evidence and phylogenetic analysis combined ITS, SSU, LSU, *rpb*2, MCM7 and *tef* 1-α to accommodate *Conioscypha*. Subsequently, phylogenetic studies on this genus mainly use SSU, LSU, ITS and *rpb*2 sequence data (Liu et al., 2024; Xu et al., 2024). In this study, we use ITS, LSU, SSU, *rpb*2 and *tef* 1-α to update phylogenetic studies for *Conioscypha* (Figure 2.83). Currently, 23 epithets are listed under *Conioscypha* (Index Fungorum, 2025 January), and only 19 species are associated with molecular data. To date, two species have been reported from palm including a new host record described in this study (Xiong et al., 2025).



Note Phylogram generated from maximum likelihood analysis of Conioscyphaceae based on combined ITS, LSU, SSU, *rpb*2 and *tef* 1-α sequence data. Bootstrap values for maximum likelihood (ML) equal to or greater than 70 are indicated above the branches. The new collections are indicated in blue and ex-type strains are indicated in bold.

Figure 2.83 Phylogenetic tree of Conioscyphaceae

Conioscypha verrucosa J. Yang & K.D. Hyde, Fungal diversity 100: 5–277 (2020)

Figure 76

Saprobic on dead inflorescence rachis of *Livistona chinensis*. Asexual morph: Hyphomycetous. *Colonies* on natural substrate sporodochia, scattered, dark brown or black. *Mycelium* partly immersed, partly superficial, composed of septate, hyaline hyphae. *Conidiophores* reduced to conidiogenous cells. *Conidiogenous cells* 6–15 × 3–8 μm ($\overline{x}$ = 9.3 × 4.9 μm, n = 10), monoblastic, integrated, terminal, globose or subcylindrical, hyaline, smooth-walled. *Conidia* 16–20 × 12–16 μm ($\overline{x}$ = 18.6 × 14.2 μm, n = 25), acrogenous, globose, subglobose, ellipsoidal or obovoid, aseptate, thick-wall, verrucose, guttulate, brown, with a central basal pore. Sexual morph: Not observed.

Culture characteristics: Colonies on PDA fast growing, after 2 weeks reaching 8–9 cm diam., at 25°C, irregular, wrinkled, dense, white mycelium on the surface; in reverse cream.

Known distribution: China (Hyde et al., 2020b, this study).

Material examined: China, Jiangxi Province, Nanchang City, The road next to Meiling National Forest Park, on dead inflorescence rachis of *Livistona chinensis*, 10 Apr 2024, Y.R. Xiong, XG378 (MHZU 24-0486, new host record), living culture ZHKUCC 25-0035, other living culture ZHKUCC 25-0036.

GenBank numbers: ZHKUCC 25-0035: ITS – PV578152, LSU – PV578322, SSU – PV578492, *tef* 1-α – PV608828, *rpb*2 – PV595310; ZHKUCC 25-0036: ITS – PV578153, LSU – PV578323, SSU – PV578493, *tef* 1-α – PV608829, *rpb*2 – PV595311.

Notes: Two collections obtained in this study clustered with *Conioscypha verrucosa* by 100% ML bootstrap support and 1.00 BYPP (Figure 2.83). The nucleotide differences excluding gaps between our collections and *Co. verrucosa* (MFLUCC 18-0419) in ITS is 0.59% (3/511 base pairs) and *rpb*2 is 1.26% (14/1113 base pairs). Morphological evidence verrucose and aseptate conidia are well fit with *Co. verrucosa* (Hyde et al., 2020b). *Conioscypha verrucosa* was first introduced on decaying wood submerged in a freshwater stream from China by Hyde et al. (2020). To our knowledge, this is the first report of *Conioscypha verrucosa* associated with *Livistona chinensis*.



Note a, b Colonies on substrate surface. c–h Conidia. i Germinating conidium. j, k The front of culture on PDA at 25°C and the reverse of culture on PDA at 25°C. Scale bars: c–i = 10 μm.

Figure 2.84 *Conioscypha verrucosa* (MHZU 24-0486, new host record)

Pesudoconioscypha Y.R. Xiong, Manawas. & K.D. Hyde, ***gen. nov.***

Etymology: referring to distinct with *Conioscypha* on morph of the type species.

Type species: *Pseudoconioscypha licualae* Y.R. Xiong, Manawas. & K.D. Hyde

Saprobic on dead petiole of *Livistona* sp. Asexual morph: *Colonies* on the natural substrate, effuse, widely spreading, superficial, scattered, hairy, brown to dark brown. *Mycelium* superficial, hyaline hyphae. *Conidiophores* macronematous, mononematous, unbranched, solitary, erect or slightly flexuous, dark brown, brown towards the apex. *Conidiogenous cells* polyblastic, verticils, producing conidia from apex conidiogenous loci, forming distinct detachment scar, intercalary, indeterminate, cylindrical. *Conidia* solitary, straight to slightly curved, oblong to oval, smooth, 3-distoseptate with thick-wall, or aseptate with a concave shape with a hollow central cavity. Sexual morph: Not observed.

Notes: Based on our phylogenetic result (Figure 2.83), *Pseudoconioscypha* (*Pseudoc*.) formed a distinct clade in Conioscyphaceae which is sister to *Conioscypha* with 60% ML bootstrap support and 1.00 BYPP. Morphologically, *Pseudoconioscypha* forms a distinct detachment scar which is consistent with the characteristic of Conioscyphaceae by forming cup-like detachment remnant collarettes after unique conidiogenesis (Goh & Hyde, 1998; Réblová et al., 2016). However, it differs from *Conioscypha* by macronematous and mononematous conidiophores, and 3-distoseptate with thick-wall conidia (Goh & Hyde, 1998). Here we described a new species of *Pseudoconioscypha* which is the first time reported from palm species (Xiong et al., 2025).

Pseudoconioscypha licualae Y.R. Xiong, Manawas. & K.D. Hyde, ***sp. nov.***

Figure 2.85

Etymology: The epithet refers to the host genus name "*Licuala*", from which the species was collected.

Saprobic on dead rachis of *Licuala* sp. Asexual morph: *Colonies* on the natural substrate, effuse, widely spreading, superficial, scattered, hairy, brown to dark brown. *Mycelium* superficial, hyaline hyphae. *Conidiophores* 370–610 × 8–10 μm ($\overline{x}$ = 509 × 9 μm, n = 10), macronematous, mononematous, unbranched, solitary, erect or slightly flexuous, dark brown, brown towards the apex. *Conidiogenous cells* 25–35 × 6–8 μm ($\overline{x}$ = 27.5 × 7.3 μm, n = 25), polyblastic, verticils, producing conidia from apex conidiogenous loci,

forming distinct detachment scar, intercalary, indeterminate, cylindrical. *Conidia* 20–23 × 10–13 µm ($\overline{x}$ = 21.8 × 10.8 µm, n = 25), solitary, straight to slightly curved, oblong to oval, smooth, 3-distoseptate with thick-wall, or aseptate with a concave shape with a hollow central cavity. Sexual morph: Not observed.

Culture characteristics: Colonies on PDA fast growing, after 2 weeks reaching 2 cm diam., at 25°C, circular, with dense, white mycelium on the surface with entire margin; in reverse white.

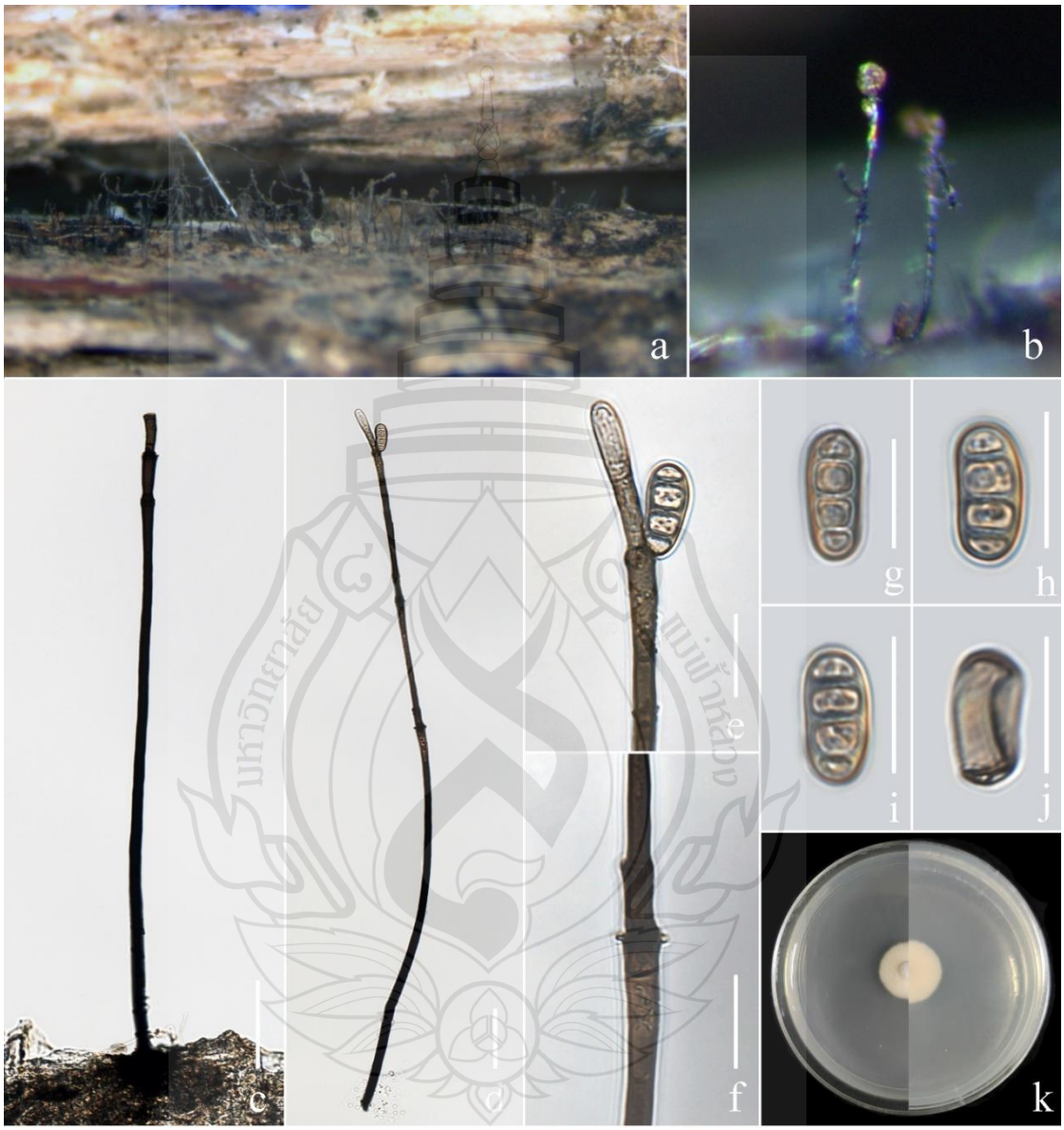
Known distribution: Thailand (this study).

Material examined: Thailand, Narathiwat Province, Toh Daeng Peat swamp, on dead rachis of *Licuala* sp., 4 Aug 2023, Y.R. Xiong, XG342 (MFLU 25-0152, holotype), ex-type MFLUCC 25-0214, other living culture MFLUCC 25-0215.

GenBank numbers: MFLUCC 25-0214: ITS – PV578236, LSU – PV578402, SSU – PV578536, *tef* 1-α – PV608884; MFLUCC 25-0215: ITS – PV578237, LSU – PV578403, SSU – PV578537, *tef* 1-α – PV608885.

Notes: Two collections from this study formed a distinct lineage within Conioscyphaceae in the phylogenetic tree with 60% ML bootstrap support and 1.00 BYPP (Figure 2.83). Based on a MegaBLAST (Query cover ≥ 70%) search using the ITS sequence, the closest matches in NCBIs GenBank nucleotide database were *Co. pleiomorpha* (GenBank LR025178; Identities 497/579 (85.84%), 32 gap (6 %)), *Vanakripa. chiangmaiense* (GenBank OL753684; Identities 497/584 (85.10%), 39 gaps (0 %)) and *Co. tenebrosa* (GenBank NR171089; Identities 462/560 (82.50%), 58 gaps (10 %)). The highest similarities using the LSU sequence were *Vanakripa minutiellipsoidea* (GenBank MN512342; Identities 824/853 (96.60%), 5 gaps (0 %)), *Co. lignicola* (GenBank AY484513; Identities 852/885 (96.27%), 4 gaps (0 %)) and *Co. tenebrosa* (GenBank MK804509; Identities 827/860 (96.16%), 1 gaps (0 %)). The highest similarities using the SSU sequence were *Co. submersa* (GenBank PQ218294; Identities 918/921 (99.67%), 0 gap (0 %)), *Co. lignicola* (GenBank JQ437439; Identities 978/982 (99.59%), 0 gaps (0 %)) and *Vanakripa chiangmaiense* (GenBank OP377997; Identities 992/998 (99.40%), 0 gaps (0 %)). The highest similarities using the *tef* 1-α sequence were *Co. muchuanensis* (GenBank PQ278582; Identities 852/915 (93.11%), 0 gap (0 %)), *Co. sichuanensis* (GenBank OR873430; Identities 875/941 (92.99%), 0 gaps (0 %)) and *Dematipyriforma aquilariae* (GenBank OP473035; Identities 843/911 (92.54%), 0 gaps

(0 %)). *Pseudoconioscypha licualae* is distinct from *Conioscypha* and *Vanakripa* by long macronematous and mononematous conidiophores and 3-distoseptate conidia. Based on phylogenetic placement and morphological variations, we introduce *Pseudoc. licualae* as a new species and type of *Pseudoconioscypha*.



Note a, b Colonies on substrate surface. c–f Conidiophore and conidiogenous cells with conidia. g–j Conidia. k The front of culture on PDA at 25°C and the reverse of culture on PDA at 25°C. Scale bars: c, d = 50 µm, e–j = 20 µm.

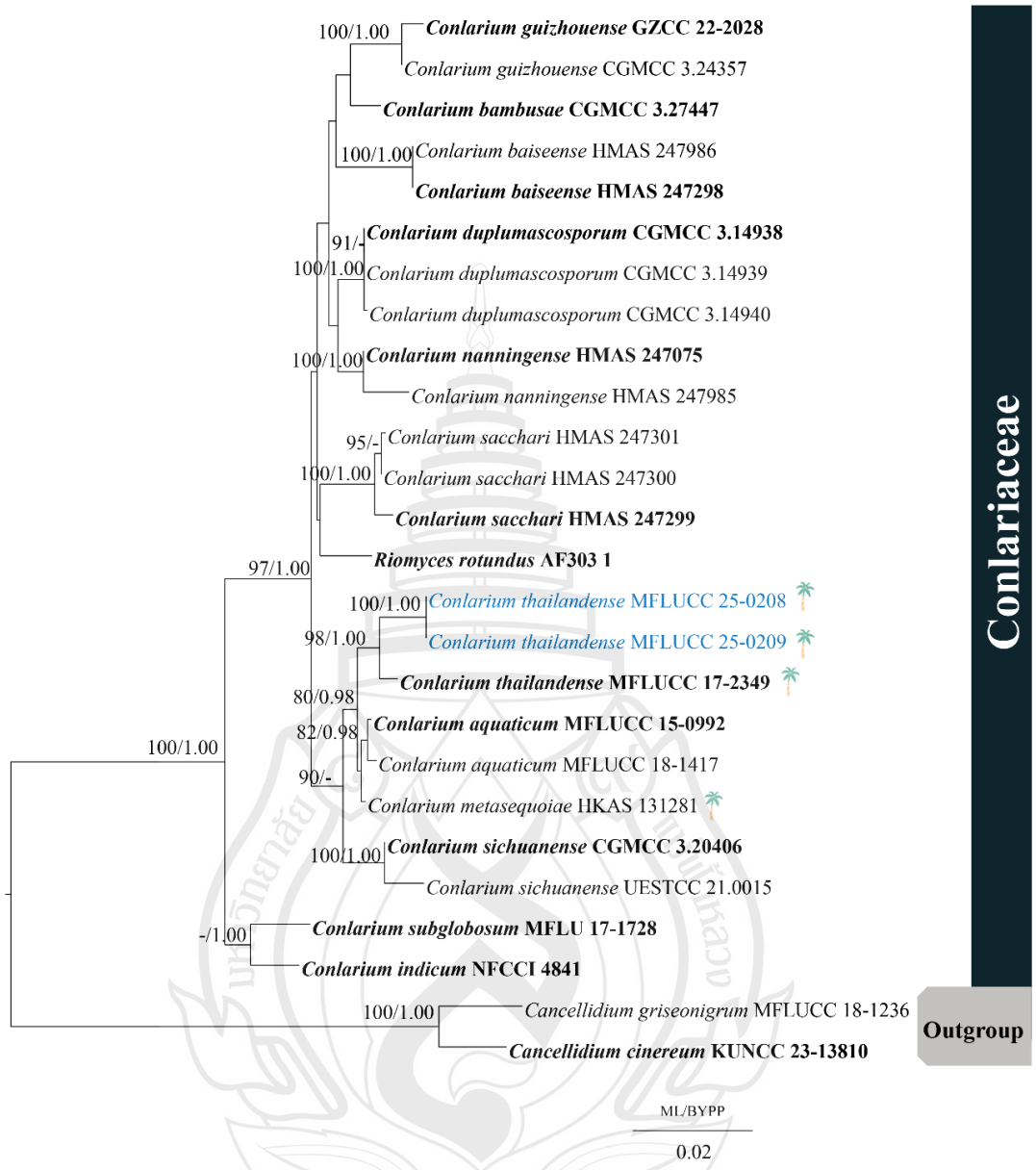
Figure 2.85 *Pseudoconioscypha licualae* (MFLU 25-0152, holotype)

Conlariales K.D. Hyde & Hongsanan, Fungal Diversity 107(14): 94 (2021)

Conlariaceae Huang Zhang, K.D. Hyde & Maharachch., Fungal Diversity 85: 90 (2017)

Conlarium F. Liu & L. Cai, Mycologia 104: 1180 (2012)

Notes: Liu et al. (2012) first introduced *Conlarium* (*Con*.) with *Con. duplumascospora* as the type species based on morphological evidence and phylogenetic analysis combined LSU. *Conlarium* species are mainly known by the asexual morph, which is characterized by muriform, irregularly globose or subglobose conidia (Hyde et al., 2021, 2024). Subsequently, phylogenetic studies mainly use ITS, LSU and SSU for analysis (Hyde et al., 2024; Tian et al., 2024). In this study, we use ITS, LSU and SSU to update phylogenetic studies for *Conlarium* (Figure 2.86). Currently, 29 epithets are listed under *Conlarium* (Index Fungorum, 2025 January), and only 13 species are associated with molecular data. Totally two species have been reported from palm species including a new host record described in this study (Xiong et al., 2025).



Note Phylogram generated from maximum likelihood analysis of *Conlarium* based on combined ITS, LSU, and SSU sequence data. Bootstrap values for maximum likelihood (ML) equal to or greater than 70 and BYPP values equal to or greater than 0.90 are indicated above the branches. The new collections are indicated in blue and ex-type strains are indicated in bold.

Figure 2.86 Phylogenetic tree of *Conlarium*

Conlarium thailandense X.D. Yu, H. Zhang & K.D. Hyde, Fungal Divers 95: 1–273 (2019)

Figure 2.87

Saprobic on dead petiole of *Licuala* sp. Asexual morph: Hyphomycetous. *Colonies* sporodochia, broadly punctiform, gregarious, dark brown, raised. *Mycelium* partly immersed on natural substratum, partly surficial, comprising branched, pale brown to hyaline, smooth hyphae. *Conidiophores* reduced to conidiogenous cells. *Conidiogenous cell* 10–15 × 5–9 μm ($\overline{x}$ = 12.6 × 6.8 μm, n = 15), monoblastic, holoblastic, integrated, determinate, cylindrical to obpyriform, pale brown to hyaline, smooth. *Conidia* 35–50 × 20–28 μm ($\overline{x}$ = 43 × 24 μm, n = 25), acrogenous, solitary, dry, mostly irregular, subglobose to ellipsoidal, brown to dark brown, clathrate, muriform, 5–6-transversely septate, 2–4-longitudinally septate, slightly constricted at the septa, smooth and thin-walled, with a small, sub-rounded, depressions on the surface of each cell. Conidial secession schizolytic. Sexual morph: Not observed.

Culture characteristics: Colonies on PDA fast growing, after 2 weeks reaching 2–3 cm diam. at 25°C, circular, raised, surface velvety, aerial, sparser, grey; reverse dark brown to black.

Known distribution: Thailand (Phookamsak et al., 2019, this study).

Material examined: Thailand, Narathiwat Province, Toh Daeng Peat swamp, on dead petiole of *Licuala* sp., 5 Feb 2023, Y.R. Xiong, XG336 (MFLU 25-0149, new host record), living culture MFLUCC 25-0208, other living culture MFLUCC 25-0209.

GenBank numbers: MFLUCC 25-0208: ITS – PV578154, LSU – PV578324; MFLUCC 25-0209: ITS – PV578155, LSU – PV578325.

Notes: Two collections obtained in this study clustered with *Conlarium thailandense* by 98% ML bootstrap support and 1.00 BYPP (Figure 2.86). The nucleotide differences excluding gaps between our collections and *Con. thailandense* (MFLUCC 17-2349) are 1.27% in ITS (6/471 base pairs), and 0.70% in LSU (6/858 base pairs). Morphological evidence of conidiogenous cells and the shape of conidia are well fit with *Con. thailandense* (Phookamsak et al., 2019). *Conlarium thailandense* was first introduced on dead wood from Thailand by Phookamsak et al. (2019). Therefore, based on morphology and phylogenetic analysis, we identified our collections as new records of *Con. thailandense*.



Note a, b Appearance of sporodochia on host substrate. c–f Conidia attached to conidiophore and conidia. g Germinated conidium. h The front of culture on PDA at 25°C and the reverse of culture on PDA at 25°C. Scale bars: c–f = 10 μm; g = 25 μm.

Figure 2.87 *Conlarium thailandense* (MFLU 25-0149, new host record)

Diaporthales Nannf., Nova Acta R. Soc. Scient. Upsal. 8: 53 (1932)

Cytosporaceae Fr. [as 'Cytisporei'], Syst. orb. veg. (Lundae) 1: 118 (1825)

Cytospora Ehrenb., Sylv. mycol. berol. (Berlin): 2 (1818)

Notes: Ehrenberg (1818) first described *Cytospora* (*Cy.*) Donk (1964) and designated *Cy. chrysosperma* (syn.: *Naemaspora chrysosperma*) as the lectotype species.

Following the “one fungus, one name” concept (Wingfield et al., 2012), *Cytospora* was established as the correct name by Fan et al. (2015a, 2015b) and Rossman et al. (2015), taking precedence over *Leucostoma*, *Leucocytospora*, *Valsa*, *Valsella*, and *Valseutypella*. *Cytospora* is holomorphic genus which asexual morph characterized by stromatic or pycnidial and ostiolate conidiomata, conceptacle or lacking, ectostromatic disc or lacking, single and undivided to multiple chambered with invaginations of locules, hyaline and branched or not of conidiophores, enteroblastic and phialidic, subcylindrical to cylindrical of conidiogenous cells, hyaline and allantoid, aseptate eguttulate of conidia (Lin et al., 2024); and sexual morph characterized by prosenchymatous or pseudoparenchymatous stromatic tissues, sometimes delimited by a black marginal line (conceptacle), perithecial ascomata inclined to upright, in valsoid or diatrypelloid configurations, numerous per disc with periphysate of ostioles, composing by *textura epidermoidea* to *textura angularis* cells of wall, paraphyses collapsed and broad but usually deliquescent at maturity, free floating and refractive with apical ring chitinoid of asci, ascospores hyaline, allantoid, aseptate, thin-walled, smooth, biseriate to irregularly multiseriate, 4, 8 or polysporous per ascus (Lin et al., 2024). Adams et al. (2005) first combined ITS molecular phylogeny and morphology evidence to analyse *Cytospora*. Subsequently Lin et al. (2024) based on morphological evidence and phylogenetic analysis combined ITS, *act*, *rpb*2, *tef* 1-α, and *tub*2 to re-evaluate *Cytospora* and related genera. In this study, we use ITS, *act*, *rpb*2, *tef* 1-α, and *tub*2 to update phylogenetic studies for *Cytospora* (Figure 2.88). Currently, 743 species are listed under *Cytospora* (Index Fungorum, 2025 January), and only 184 species are associated with molecular data. Totally eight species have been reported from palm species including a new species and a new host record described in this study (Xiong et al., 2025).

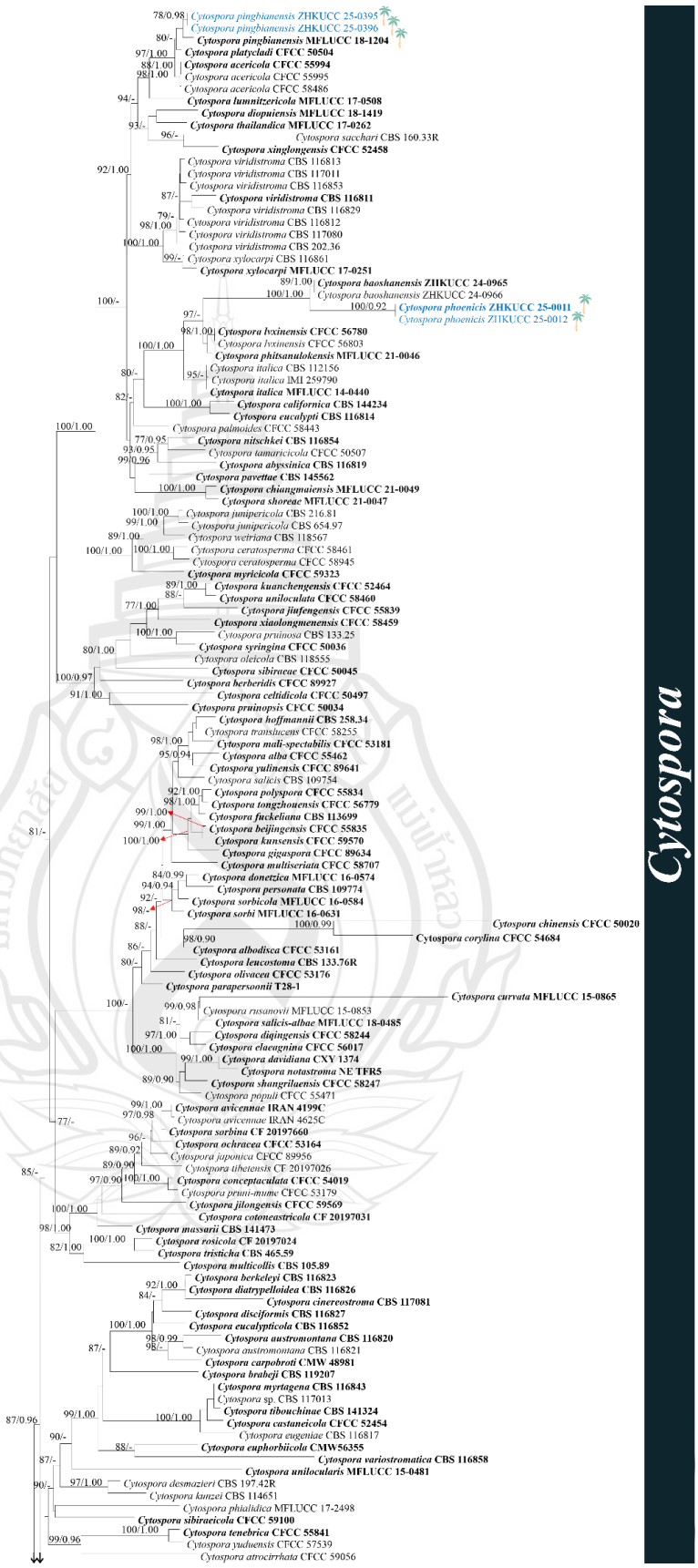
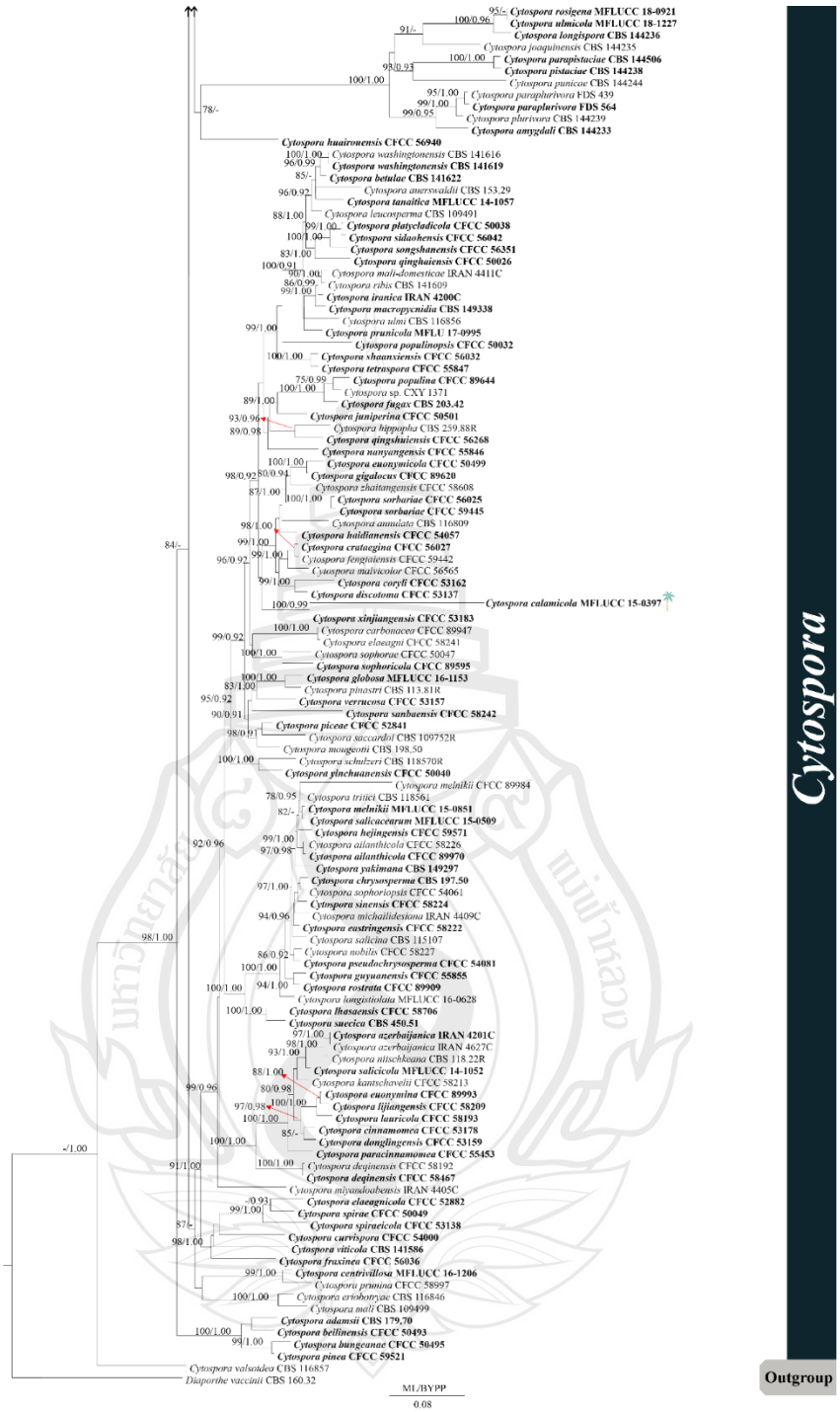


Figure 2.88 Phylogenetic tree of *Cytospora*



Note Phylogram generated from maximum likelihood analysis of *Cytospora* based on combined ITS, *act*, *rpb*2, *tef* 1-α and *tub*2 sequence data. Bootstrap values for maximum likelihood (ML) equal to or greater than 70 are indicated above the branches. The new collections are indicated in blue and ex-type strains are indicated in bold.

Figure 2.88 (continued)

Cytospora phoenicis Y.R. Xiong, Manawas. & K.D. Hyde, ***sp. nov.***

Figure 2.89

Etymology: The epithet refers to the host genus name "*Phoenix*", from which the species was collected.

Saprobic on dead petiole of *Phoenix canariensis*. Asexual morph: Coelomycetous. *Conidiomata* 750–900 × 260–300 μm ($\overline{x}$ = 823 × 281 μm, n = 10), stromatic, lamyelloid, scattered, or sometimes in small groups, immersed to partially erumpent, black, flat to discoid, multiple locules with separate walls and multiple ostioles. *Conceptacle* absent. *Locules* 60–120 ×60–100 μm ($\overline{x}$ = 94 × 88 μm, n = 25), numerous, subdivided frequently, independent walls composed of *textura epidermoidea* cells, irregular shape. *Conidiophores* 2.5–5 ×1–1.5 μm ($\overline{x}$ = 3.4 ×1.4 μm, n = 25), borne along the locules, hyaline, branched at the base, embedded in a gelatinous layer, or reduce to the conidiogenous cells. *Conidiogenous cell* 5–8 × 1.5–2 μm ($\overline{x}$ = 6.7 × 1.7 μm, n = 25), enteroblastic, phialidic, hyaline, smooth. *Conidia* 3.5–5.5 × 1–2 μm ($\overline{x}$ = 4.1 × 1.5 μm, n = 25), hyaline, elongate-allantoid, aseptate, thin-walled. Sexual morph: Not observed.

Culture characteristics: Colonies on PDA, after 2 weeks reaching 4–5 cm diam., at 25°C, circular, with fluffy, dense, white mycelium on the surface with entire margin; in reverse yellow in the middle and white at the margin.

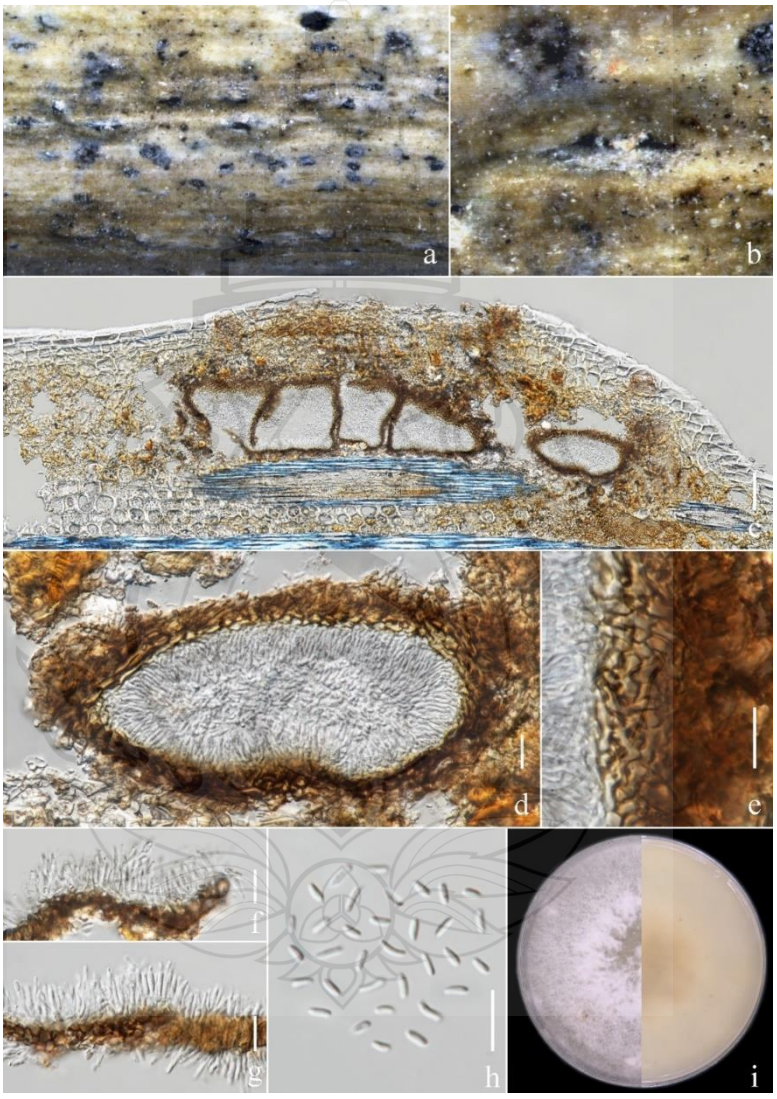
Known distribution: China (this study).

Material examined: China, Yunnan Province, Xishuangbanna City, in an unidentified forest beside National Highway 219, on dead petiole of *Phoenix canariensis*, 4 Feb 2023, Y.R. Xiong and L. Lu, XG300 (MHZU 24-0508, holotype), ex-type ZHKUCC 25-0011, other living culture ZHKUCC 25-0012.

GenBank numbers: ZHKUCC 25-0011: ITS – PV578158, *rpb2* – PV595314, *tub2* – PV607962, *tef* 1-α – PV608832; ZHKUCC 25-0012: ITS – PV578159, *rpb2* – PV595315, *tub2* – PV607963, *tef* 1-α – PV608833.

Notes: Two collections from this study formed a separate lineage and clustered with *Cytospora baoshanensis* in the phylogenetic tree with 100% ML bootstrap support and 1.00 BYPP (Figure 2.88). The nucleotide differences excluding gaps between *Cy. phoenicis* (ZHKUCC 25-0011) and *Cy. baoshanensis* (MHZU 24-0530) were checked and given as follows, ITS: 4.85% (26/536 base pairs), *rpb2*: 11.45% (118/1030 base pairs), *tub2*: 11.89% (63/530 base pairs), *tef* 1-α: 5.76% (60/1042 base pairs). *Cytospora phoenicis*

have independent walls composed of *textura epidermoidea* cells which are different with *Cy. baoshanensis* have peridium comprising brown cells of *textura angularis* (Lu et al., 2025, Figure 2.89). In addition, *Cy. phoenicis* conidiophores are branched at the base or reduced to conidiogenous cells and can be distinguished from *Cy. baoshanensis* where conidiophores are irregularly branched at the base and above (Lu et al., 2025, Figure 2.89). Based on phylogenetic placement and morphological variations, we introduce *Cy. phoenicis* as a new species.



Note a, b Colonies on substrate surface. c Sections through conidiomata. d Locules. e Peridium. f, g Conidiogenous cells and developing conidia. h Cconidia. i The front of culture on PDA at 25°C and the reverse of culture on PDA at 25°C. Scale bars: c = 50 µm, d–h = 10 µm.

Figure 2.89 *Cytospora phoenicis* (MHZU 24-0508, holotype)

Cytospora pingbianensis Q.J. Shang, K.D. Hyde & J.K. Liu, Mycosphere 11(1): 189–224 (2020)

Figure 2.90

Saprobic on dead petiole of *Phoenix canariensis*. Asexual morph: Coelomycetous. *Conidiomata* 620–950 × 350–510 μm ($\bar{x}$ = 793 × 431 μm, n = 10), stromatic, torsellioid, scattered, or sometimes in small groups, erumpent through the surface of bark, black, flat to discoid, multiple locules with separate walls and a single shared ostiole. *Conceptacle* absent. Ostioles converge to a shared single ostiole. *Locules* 120–310 × 60–100 μm ($\bar{x}$ = 200 × 98 μm, n = 25), numerous, subdivided frequently, independent walls composed by *textura angularis* cells, subglobose or obpyriform shape. *Conidiophores* 4–6 ×1–2 μm ($\bar{x}$ = 4.9 ×1.6 μm, n = 25), borne along the locules, hyaline, branched at the base, in the middle or occasionally unbranched, embedded in a gelatinous layer. *Conidiogenous cell* 7–9.5 × 1.5–2 μm ($\bar{x}$ = 7.6 × 1.7 μm, n = 25), enteroblastic, phialidic, hyaline, smooth. *Conidia* 3–4.5 × 1–1.5 μm ($\bar{x}$ = 3.8 × 1.3 μm, n = 25), hyaline, longate-allantoid, aseptate, thin-walled. Asexual morph: Not observed.

Culture characteristics: Colonies on PDA slowly growing, after 2 weeks reaching 2–3 cm diam. at 25°C, circular, flat, with entire edge, above brown in the middle and cream in the outer, yellowish in reverse.

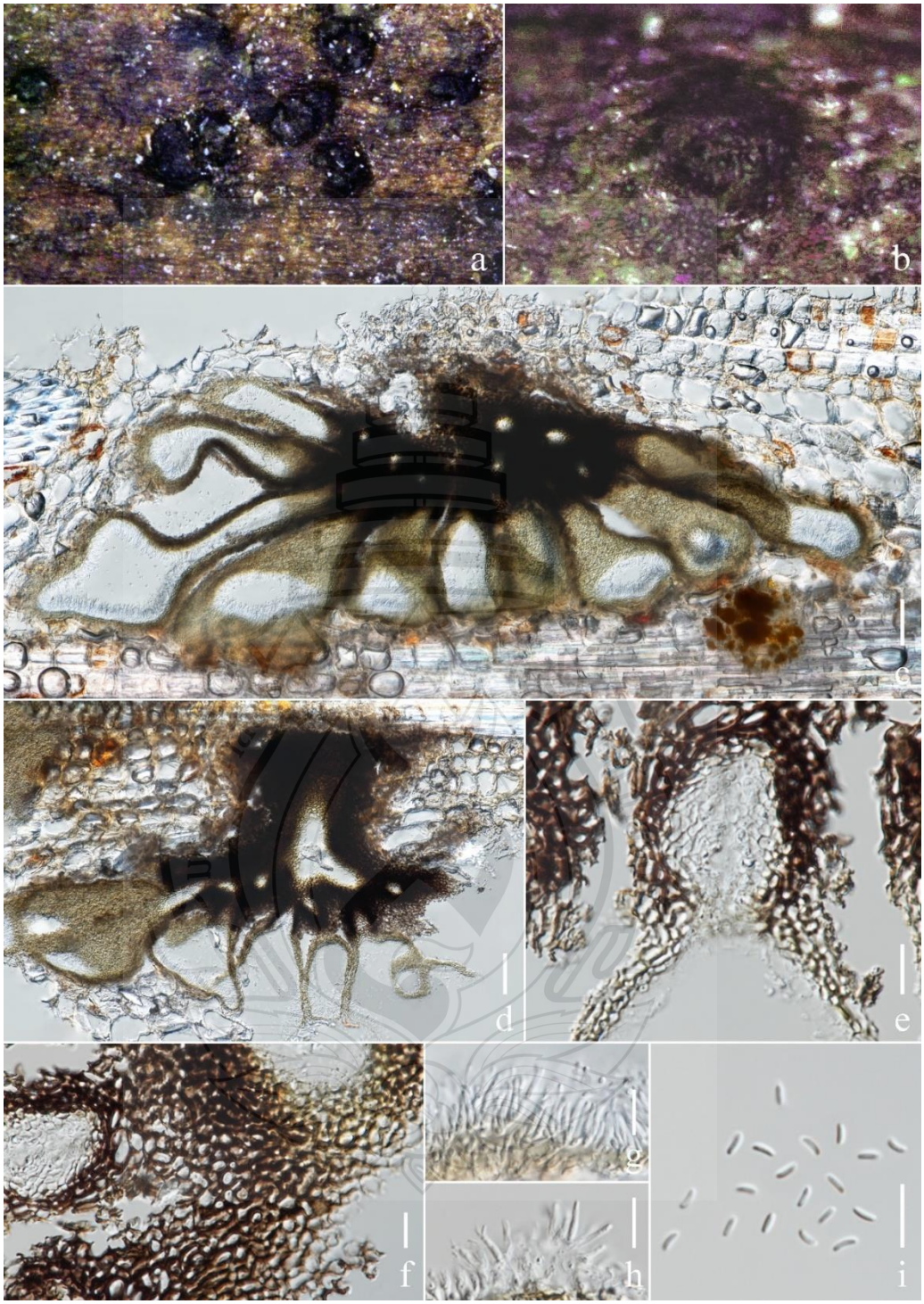
Known distribution: China (Shang et al., 2020; this study).

Material examined: China, Yunnan Province, Qujing City, Qujing Normal University, on dead petiole of *Phoenix canariensis*, 18 Aug 2022, Y.R. Xiong and L. Lu XG107 (MHZU 24-0449, new host record), living culture ZHKUCC 25-0395, other living culture ZHKUCC 25-0396.

GenBank numbers: ZHKUCC 25-0395: ITS – PV578160, *tub*2 – PV584057, *act* – PV584051; ZHKUCC 25-0396: ITS – PV578161, *tub*2 – PV584058, *act* – PV584052.

Notes: Two collections obtained in this study clustered with *Cy. pingbianensis* by 78% ML bootstrap support and 0.98 BYPP (Figure 2.88). The nucleotide differences excluding gaps between our collections and *Cy. pingbianensis* (MFLUCC 18-1204) in *act* is 1.79% (4/223 base pairs). Morphological evidence of conidiogenous cells and brown conidia are well fit with *Cytospora* (Lin et al., 2024, Figure 2.90). *Cytospora pingbianensis* was first introduced as a sexual morph on a dead branch of undetermined wood from China by Shang et al. (2020). Therefore, we identified our collections as the first asexual morph

record of *Cy. pingbianensis*.



Note a, b Colonies on natural substrate. c, d Conidiophores and conidia. e, f Conidiogenous cells with conidia. g Conidia. h The front of culture on PDA at 25°C and the reverse of culture on PDA at 25°C. Scale bars: c, d = 20 μm; e–g = 10 μm.

Figure 2.90 *Cytospora pingbianensis* (MHZU 24-0449, new host record)

Distoseptisporales Z.L. Luo, K.D. Hyde & Hong Y. Su, Fungal Diversity 99: 482 (2019)

Distoseptisporaceae K.D. Hyde & McKenzie, Fungal Diversity 80: 402 (2016)

Distoseptispora K.D. Hyde, McKenzie & Maharachch., Fungal Diversity 80: 402 (2016)

Notes: *Distoseptispora* (*Di*.) was established by Su et al. (2016) to accommodate *Di. aquatica* and *Di. fluminicola*, with *Di. fluminicola* as the type species based on morphological evidence and phylogenetic analysis based on LSU. Most *Distoseptispora* species are hyphomycetous, and characterized by macronematous conidiophores, percurrent or cylindrical conidiogenous cells, dematiaceous and euseptate or distoseptate conidia (Su et al., 2016); and sexual morph which characterized by solitary or gregarious, immersed to semi-immersed, subglobose to ellipsoidal, dark brown ascomata with a short neck, and hyaline, septate ascospores with a mucilaginous sheath (Yang et al., 2021). Subsequently, phylogenetic studies mainly use SSU, LSU, ITS, *rpb*2 and *tef* 1-α or without SSU in this genus (Hu et al., 2023; Yu et al., 2024). In this study, we use ITS, LSU, *tef* 1-α and *rpb*2 to update phylogenetic studies for *Distoseptispora* (Figure 2.91). Currently, 87 epithets are listed under *Distoseptispora* (Index Fungorum, 2025 January) and all species are associated with molecular data. Totally nine species have been reported from palm species including one new species and three new host records described in this study (Xiong et al., 2025).

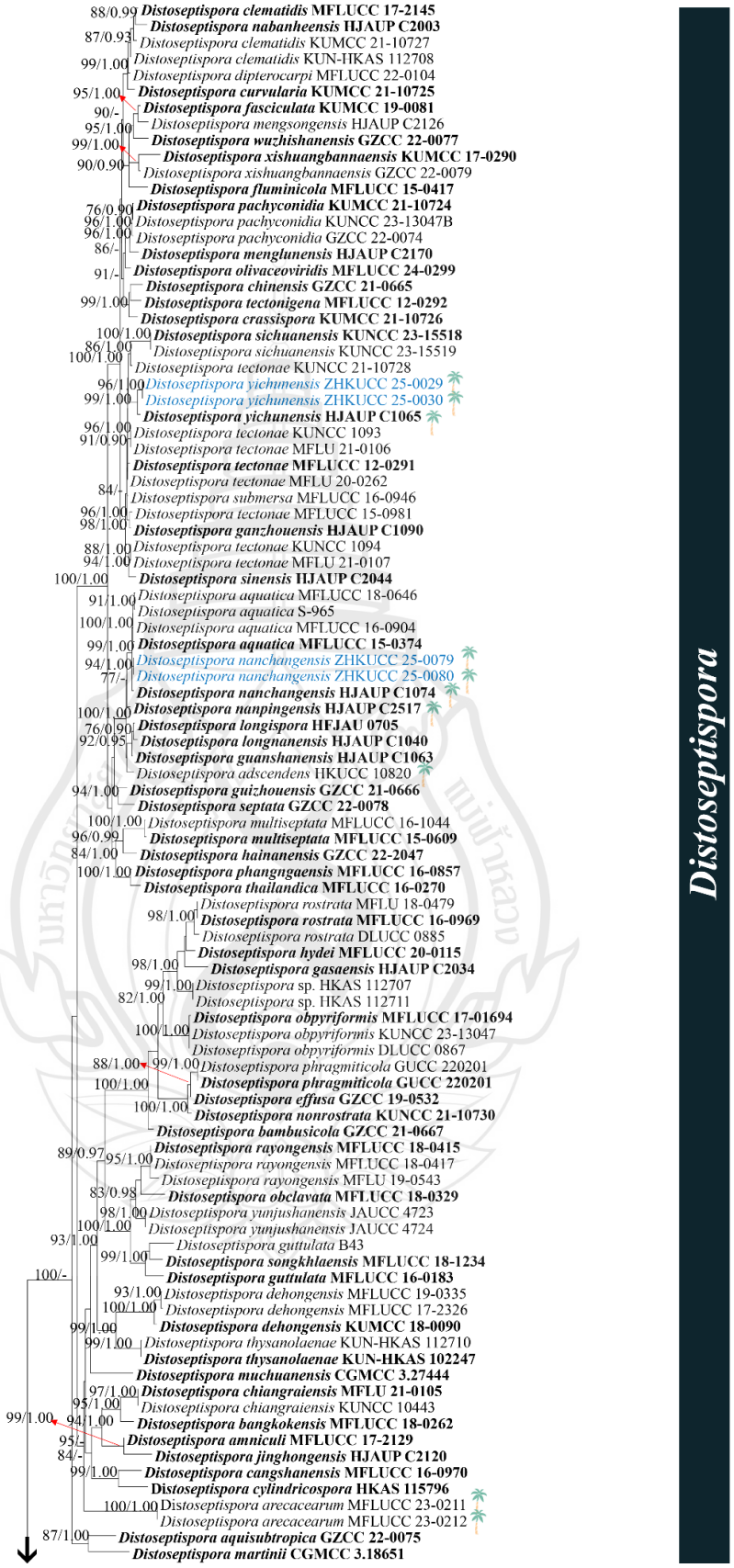
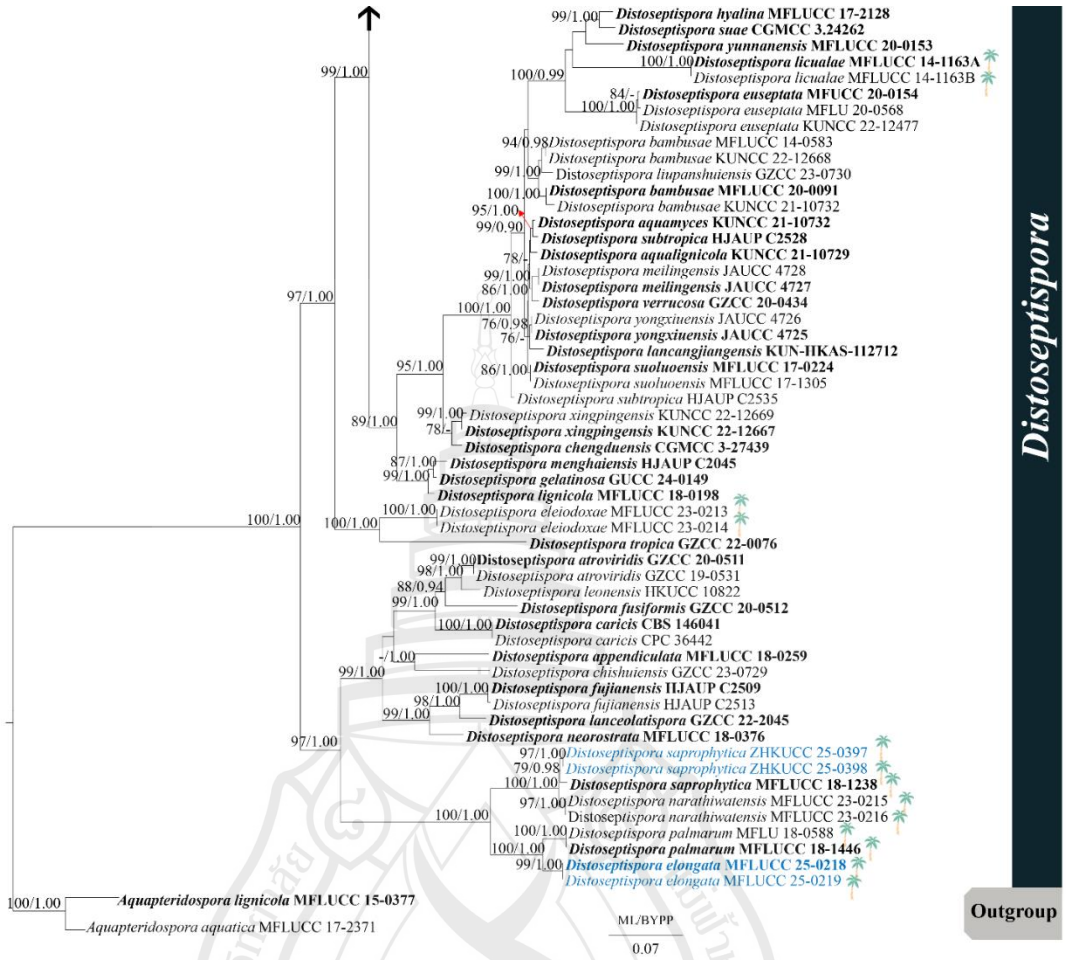


Figure 2.91 Phylogenetic tree of *Distoseptispora*



Note Phylogram generated from maximum likelihood analysis of *Distoseptispora* based on combined ITS, LSU, *tef* 1-α and *rpb2* sequence data. Bootstrap values for maximum likelihood (ML) equal to or greater than 70 are indicated above the branches. The new collections are indicated in blue and ex-type strains are indicated in bold.

Figure 2.91 (continued)

Distoseptispora elongata Y.R. Xiong, Manawas. & K.D. Hyde, ***sp. nov.***

Figure 2.92

Etymology: The epithet refers to the character of "long conidiophore" from which the species was observed.

Saprobic on dead petiole of *Licuala* sp. Asexual morph: Hyphomycetous. *Colonies* on natural substrate superficial, effuse, hairy, gregarious, dark brown to black. *Mycelium* partly immersed, partly superficial on host substrate, composed of septate,

branched, pale brown to hyaline hyphae. *Conidiophores* macronematous, mononematous, septate, erect, cylindrical, unbranched. *Conidiogenous cells* holoblastic, monoblastic, integrated, determinate, terminal, cylindrical, brown, smooth. *Conidia* 120–260 × 10–12 µm ($\bar{x}$ = 202 × 10.6 µm, n = 25), acrogenous, solitary, dry, thin-walled, smooth, obclavate, mostly erect or slight curved, thick-walled,15–27-distoseptate, brown to olivaceous, rounded at apex, with a truncate base, paler towards the apex. Sexual morph: Not observed.

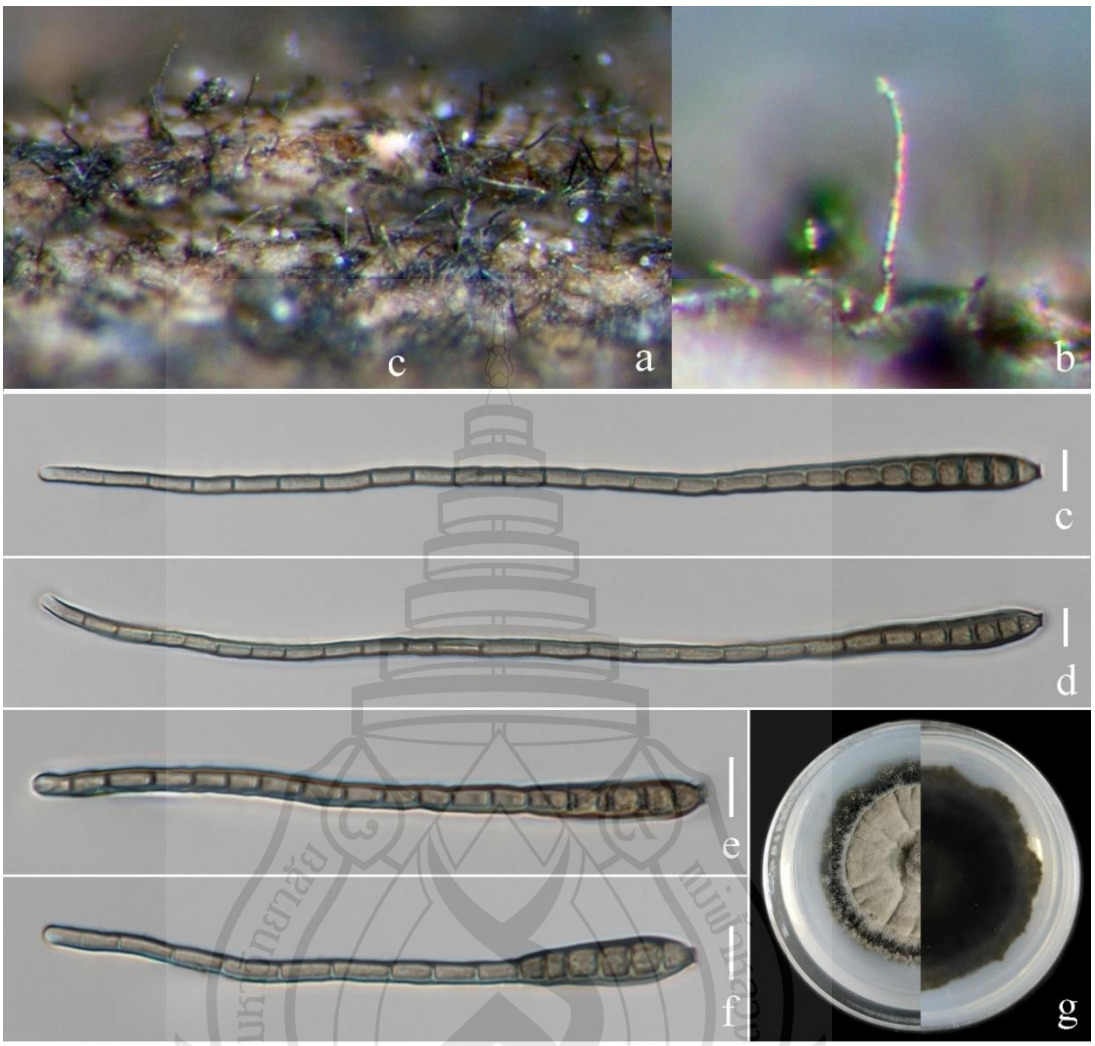
Culture characteristics: Colonies on PDA fast growing, after 2 weeks reaching 4 cm diam. at 25°C, circular, radially striated with lobate medium with fluffy, dense, white mycelium on the surface, with black crenated margin; in reverse black in the middle and grey at the margin.

Known distribution: Thailand (this study).

Material examined: Thailand, Narathiwat Province, Toh Daeng Peat swamp, on dead petiole of *Licuala* sp., 4 Aug 2023, Y.R. Xiong, XG345 (MFLU 25-0154, holotype), ex-type MFLUCC 25-0218, other living culture MFLUCC 25-0219.

GenBank numbers: MFLUCC 25-0218: ITS – PV578164, LSU – PV578330, *rpb*2 – PV595316, *tef* 1-α – PV608836; MFLUCC 25-0219: ITS – PV578165, LSU – PV578331, *rpb*2 – PV595317, *tef* 1-α – PV608837

Notes: Two collections from this study formed a separate lineage and clustered with *Distoseptispora palmarum* in the phylogenetic tree with 100% ML bootstrap support and 1.00 BYPP. The nucleotide differences excluding gaps between *Di. elongata* (MFLUCC 25-0218) and *Di. palmarum* (MFLUCC 18-1446) were checked and given as follows, ITS: 6.39% (35/547 base pairs), LSU: 0.25% (2/805 base pairs), *tef* 1-α: 3.66% (33/901 base pairs) and *rpb*2: 4.63% (49/1059 base pairs). Morphologically, *Di. elongata* has holoblastic conidiogenous cells which is different from *Di. palmarum* which has polyblastic conidiogenous cells (Hyde et al., 2019). Moreover, *Di. elongata* has longer conidia (120–260 µm) than *Di. palmarum* (35–180 µm) (Hyde et al., 2019). Based on phylogenetic placement and morphological variations, we introduce *Di. elongata* as a new species.



Note a, b Colonies on the substrate surface. c–f Conidiophores with conidiogenous cells. g–j Conidia. k The front of culture on PDA at 25°C and the reverse of culture on PDA at 25°C. Scale bars: c–f = 25 µm, g–j = 10 µm.

Figure 2.92 *Distoseptispora elongata* (MFLU 25-0154, holotype)

Distoseptispora nanchangensis Y.F. Hu & Jian Ma, Microbiology Spectrum 11: e02468–02423 (2023)

Index Fungorum number: IF 849134; *Facesoffungi number*: FoF 17068; Figure 2.93

Saprobic on dead petiole of *Livistona chinensis*. Asexual morph: Hyphomycetous. *Colonies* on natural substrate effuse, scattered, dark brown to black, and hairy. *Mycelium* immersed. *Conidiophores* 25–48 × 9–10 µm ($\overline{x}$ = 36.6 × 9.3 µm, n = 15), macronematous, mononematous, brown to dark brown, 2–3-septate, single or caespitose,

straight or slight flexuous, unbranched, smooth, and cylindrical, tapering distally, robust at the base. *Conidiogenous cell* 9–10.5 × 6–8 μm ($\overline{x}$ = 9.6 × 6.9 μm, n = 15), dark brown, monoblastic, integrated, determinate, terminal, cylindrical. *Conidia* 60–120 × 17–23 μm ($\overline{x}$ = 93.9 × 19.6 μm, n = 25), acrogenous, solitary, obclavate, straight or curved, 6–13-distoseptate, brown to dark brown, smooth, thick-walled, schizolytic, sometimes with percurrent regeneration forming a secondary conidium from the conidial apex, truncate at the base, rounded at the apex. Sexual morph: Not observed.

Culture characteristics: Colonies on PDA fast growing, after 2 weeks reaching 8–9 cm diam. at 25°C, circular, raised, surface velvety, aerial, sparser, dark brown; reverse dark brown to black.

Known distribution: China (Hu et al., 2023; Xiong et al., 2025, this study).

Material examined: China, Jiangxi Province, Nanchang City, The road next to Meiling National Forest Park, on dead petiole of *Livistona chinensis*, 11 Apr 2024, Y.R. Xiong, XG431 (MHZU 24-0500, new host record), living culture ZHKUCC 25-0079, other living culture ZHKUCC 25-0080.

GenBank numbers: ZHKUCC 25-0079: ITS – PV578166, LSU – PV578332, *rpb*2 – PV595318, *tef* 1-α –PV608838; ZHKUCC 25-0080: ITS – PV578167, LSU – PV578333, *rpb*2 – PV595319, *tef* 1-α –PV608839.

Notes: Two collections obtained in this study clustered with *Distoseptispora nanchangensis* by 99% ML bootstrap support and 1.00 BYPP (Figure 2.91). The nucleotide differences excluding gaps between our collections and *Di. nanchangensis* (HJAUP C1074) in ITS: 0.91% (5/551 base pairs), *tef* 1-α: 0.11% (1/931 base pairs) and *rpb*2: 0.44% (4/911 base pairs). Morphological evidence of conidiogenous cells and the shape of conidia are well fit with *Di. nanchangensis* (Hu et al., 2023; Xiong et al., 2025) although the numbers of distoseptate of mature conidia only 6–13 in our collections which is fewer than 21–43 (Hu et al., 2023) and 17–41 (Xiong et al., 2025). Therefore, based on morphology and phylogenetic analysis, we identified our collections as new host records of *Di. nanchangensis*. *Distoseptispora nanchangensis* was first introduced on dead branches of an unidentified broadleaf tree from China by Hu et al. (2023), Xiong et al. (2025) reported a new record on dead petiole of *Trachycarpus fortune* from China.



Note a, b Colonies on the substrate surface. c–f Conidiophores with conidiogenous cells bearing conidia. g–i Conidia. j The front of culture on PDA at 25°C and the reverse of culture on PDA at 25°C. Scale bars: c–i = 10 µm.

Figure 2.93 *Distoseptispora nanchangensis* (MHZU 24-0500, new host record)

Distoseptispora saprophytica W. Dong, H. Zhang & K.D. Hyde, Mycosphere 12 (1): 38 (2021)

Figure 2.94

Saprobic on dead primary rachis of *Corypha umbraculifera*. Asexual morph: Hyphomycetous. *Colonies* on natural substrate superficial, effuse, hairy, gregarious, brown. *Mycelium* partly immersed, partly superficial on host substrate, composed of septate, branched, pale brown, thin-walled hyphae. *Conidiophores* 25–48 × 9–10 μm ($\overline{x}$ = 36.6 × 9.3 μm, n = 15), macronematous, mononematous, erect, cylindrical, straight or slightly flexuous, or occasionally sharply curving near the base, septate, unbranched, brown, thin-walled, smooth. *Conidiogenous cell* 9–10.5 × 6–8 μm ($\overline{x}$ = 9.6 × 6.9 μm, n = 15), polyblastic, integrated, terminal and intercalary, determinate, subcylindrical, brown, smooth. *Conidia* 60–120 × 17–23 μm ($\overline{x}$ = 93.9 × 19.6 μm, n = 25), acrogenous, solitary, dry, thick-walled, smooth, subcylindrical to obclavate, straight or curved, 3–6-distoseptate, slightly constricted at septa, olivaceous to brown, rounded at apex, with an inconspicuous truncate base and faintly pigmented scar. Sexual morph: Not observed.

Culture characteristics: Colonies on PDA, after 2 weeks reaching 8–9 cm diam., at 25°C, white-brown from above, black from below, surface rough, dry, with dense mycelium, raised, entire at edge; reverse dark brown to black.

Known distribution: China (this study), Thailand (Dong et al., 2021).

Material examined: China, Yunnan Province, Xishuangbanna City, in an unidentified forest beside National Highway 219, on dead primary rachis of *Corypha umbraculifera*, 5 Feb 2023, Y.R. Xiong and L. Lu, XG146 (MHZU 24-0470, new host record), living culture ZHKUCC 25-0397, other living culture ZHKUCC 25-0398.

GenBank numbers: ZHKUCC 25-0397: ITS – PV578168, LSU – PV578334, *rpb2* – PV595320, *tef* 1-α – PV608840; ZHKUCC 25-0398: ITS – PV578169, LSU – PV578335, *rpb2* – PV595321, *tef* 1-α – PV608841.

Notes: Two collections obtained in this study clustered with *Distoseptispora saprophytica* by 79% ML bootstrap support and 0.98 BYPP (Figure 2.91). The nucleotide differences excluding gaps between our collections and *Di. saprophytica* (MFLUCC 18-1238) in ITS: 1.39% (8/572 base pairs), LSU: 0.46% (3/656 base pairs), *tef* 1-α: 1.26% (12/950 base pairs) and *rpb2*: 1.03% (9/876 base pairs). Morphological evidence of conidiogenous cells and hyaline conidia are well fit with *Di. saprophytica* (Dong et al.,

2021). Therefore, based on morphology and phylogenetic analysis, we identified our collections as new host record of *Di. saprophytica* from *Corypha umbraculifera*. *Distoseptispora saprophytica* was first introduced on submerged wood in a stream from Thailand by Dong et al. (2021).



Note a, b Colonies on the substrate surface. c–e Conidiophores with conidiogenous cells bearing conidia. f–i Conidia. j Germinating conidium. k The front of culture on PDA at 25°C and the reverse of culture on PDA at 25°C. Scale bars: c–e = 20 µm, f–j = 10 µm.

Figure 2.94 *Distoseptispora saprophytica* (MHZU 24-0470, new host record)

Distoseptispora yichunensis Y.F. Hu & Jian Ma, Microbiol. Spectrum 11 (6): e0246823, 13 (2023)

Figure 2.95

Saprobic on dead leaf sheath of *Livistona chinensis*. Asexual morph: Hyphomycetous. *Colonies* on natural substrate effuse, brown, and hairy. *Mycelium* superficial, hyaline hyphae. *Conidiophores* 25–48 × 9–10 μm ($\overline{x}$ = 36.6 × 9.3 μm, n = 15), macronematous, mononematous, solitary, straight or flexuous, septate, unbranched, smooth, cylindrical, and brown to dark brown. *Conidiogenous cell* 9–10.5 × 6–8 μm ($\overline{x}$ = 9.6 × 6.9 μm, n = 15), monoblastic, integrated, terminal, cylindrical, determinate, pale brown to brown, smooth. *Conidia* 60–120 × 17–23 μm ($\overline{x}$ = 93.9 × 19.6 μm, n = 25), acrogenous, solitary, obclavate, straight or curved, pale brown to brown (18–)34–45(–52)-distoseptate, smooth, truncate at the base, rounded at the apex. Sexual morph: Not observed.

Culture characteristics: Colonies on PDA fast growing, after 2 weeks reaching 8–9 cm diam., at 25°C, circular, surface velvety, with brown, denser mycelium at the center, becoming black at the entire margin; reverse dark brown to black.

Known distribution: China (Hu et al., 2023, this study).

Material examined: China, Jiangxi Province, Nanchang City, The road next to Meiling National Forest Park, on dead leaf sheath of *Livistona chinensis*, 5 Feb 2023, Y.R. Xiong, XG374 (MHZU 24-0484, new host record), living culture ZHKUCC 25-0029, other living culture ZHKUCC 25-0030.

GenBank numbers: ZHKUCC 25-0029: ITS – PV578170, LSU – PV578336, *rpb2* – PV595322, *tef* 1-α – PV608842; ZHKUCC 25-0030: ITS – PV578171, LSU – PV578337, *rpb2* – PV595323, *tef* 1-α – PV608843.

Notes: Two collections obtained in this study clustered with *Distoseptispora yichunensis* by 99% ML bootstrap support and 1.00 BYPP (Figure 2.91). The nucleotide differences excluding gaps between our collections and *Di. yichunensis* (HJAUP C1065) in ITS: 0.71% (4/564 base pairs), LSU: 0.35% (2/569 base pairs), *tef* 1-α: 0.11% (1/927 base pairs) and *rpb2*: 1.03% (2/900 base pairs). Morphological evidence of conidiogenous cells and hyaline conidia are well fit with *Di. yichunensis* (Hu et al., 2023). *Distoseptispora yichunensis* was first introduced on dead branches of an unidentified broadleaf tree from China by Hu et al. (2023). Based on morphology and phylogenetic analysis, we identified our collections as new host records of *Di. yichunensis*.

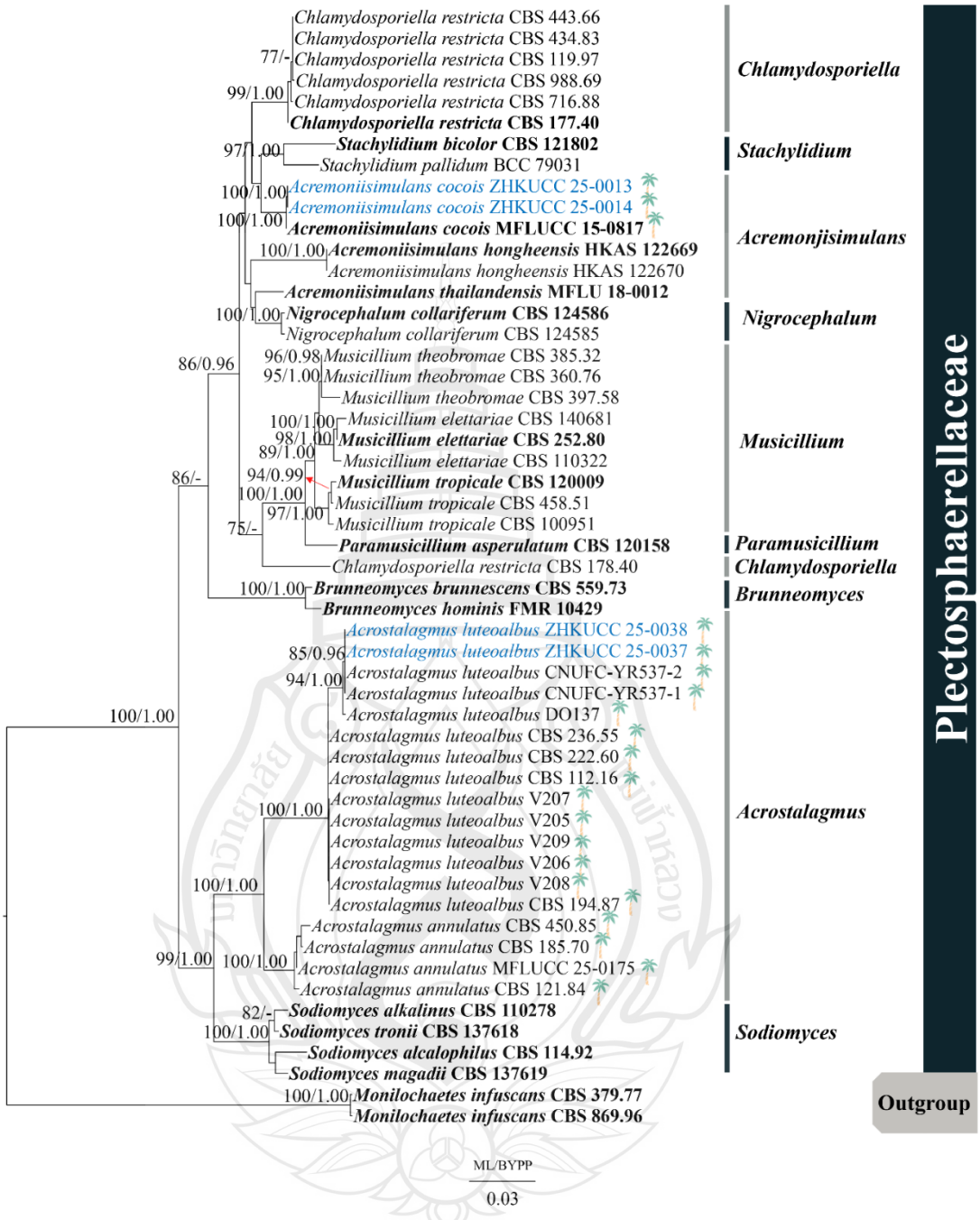


Note a, b Colonies on the substrate surface. c–e Conidiophores with conidiogenous cells. f–h Conidia. i The front of culture on PDA at 25°C and the reverse of culture on PDA at 25°C. Scale bars: c, f, g = 50 µm, d, e = 10 µm, h = 20 µm.

Figure 2.95 *Distoseptispora yichunensis* (MHZU 24-0484, new host record)

Glomerellales Chadef. ex Réblová, W. Gams & Seifert, Studies in Mycology 68: 170 (2011)

Plectosphaerellaceae W. Gams, Summerbell & Zare, Nova Hedwigia 85 (3-4): 476 (2007)



Note Phylogram generated from maximum likelihood analysis of Plectosphaerellaceae based on combined ITS, LSU and SSU sequence data. Bootstrap values for maximum likelihood (ML) equal to or greater than 70 are indicated above the branches. The new collections are indicated in blue and ex-type strains are indicated in bold.

Figure 2.96 Phylogenetic tree of Plectosphaerellaceae

Acremoniisimulans Tibpromma & K.D. Hyde, Fungal Diversity 93: 88 (2018)

Notes: Based on distinct morphology and phylogeny analyses of combined LSU, SSU, *tef*1-α and ITS sequence data, *Acremoniisimulans* (*Ac*.) was proposed to accommodate the hyphomycetous species *Ac. thailandensis* and is characterized by pale brown conidiophores and conidia (Tibpromma et al., 2018). Later, *Ac. cocois* and *Ac. hongheensis* were introduced to represent the sexual morph of this genus by Konta et al. (2023) and Yang et al. (2023), respectively. The sexual morph is characterized by oblong to clavate asci, 4–8-spored, unitunicate, with oblong to broadly oblong ascospores, biseriate, hyaline, 1-celled, guttules (Konta et al., 2023; Yang et al., 2023). In this study, we use ITS, LSU and SSU to update phylogenetic studies for *Acremoniisimulans* (Figure 2.96). There are only three species epithets available for *Acremoniisimulans* in Index Fungorum (2025, January), and all species with molecular data. Only one species has been reported from palm species (Xiong et al., 2025). In this study, a new geography record of *Ac. cocois* was introduced from *Cocos nucifera* from China.

Acremoniisimulans cocois Konta & K.D. Hyde, Mycosphere 14 (1): 135 (2023)

Figure 2.97

Saprobic on dead segment of *Cocos nucifera*. Asexual morph: Hyphomycetous. *Colonies* on natural substrate, effuse and velvety, brown and powdery. *Mycelium* hyaline, immersed, composed of septate, branched or unbranched. *Conidiophores* 20–50 × 3–4 µm ($\overline{x}$ = 32 × 3.4 µm, n = 20), macronematous, mononematous, scattered, hyaline to pale brown, smooth, thin-walled, septate, branched or unbranched, tapering toward the top, straight or slightly flexous. *Conidiogenous cells* 10–12 × 2.5–3 µm ($\overline{x}$ = 11.2 × 2.7 µm, n = 20), monophialidic, hyaline, cylindrical. *Conidia* 3–4 × 2.5–3 µm ($\overline{x}$ = 3.5 × 2.8 µm, n = 30), catenated, pale brown to brown, subglobose to oval, aseptate, rounded at each end, smooth-walled, guttulate. *Conidial secession* schizolytic. Sexual morph: Not observed.

Culture characteristics: Colonies on PDA reaching 2–3 cm diam., at 25°C after two weeks, circular, with lobate margin, dense, with an irregularly undulating surface, the central region covered by white, woolly mycelium, gelatinous-folded, while the peripheral mycelium more compact and dark brown to olive. A pale ring along the colony margin, cream. Reverse pale brown to brown, wrinkled.

Known distribution: China (this study), Thailand (Konta et al., 2023).

Material examined: China, Yunnan Province, Xishuangbanna, on a dead segment of *Cocos nucifera*, 4 February 2024, Y.R. Xiong & Li Lu, XG306 (MHZU 24-0477, new host and new geography record), living culture ZHKUCC 25-0013, other living culture ZHKUCC 25-0014.

GenBank numbers: ZHKUCC 25-0013: ITS – PV578122, LSU – PV578292; ZHKUCC 25-0014: ITS – PV578123, LSU – PV578293.

Notes: Two collections obtained in this study clustered with *Ac. cocois* (MFLUCC 15-0817, ex-type) by 100% ML bootstrap support and 1.00 BYPP (Figure 2.96). The nucleotide differences excluding gaps between our isolate (ZHKUCC 25-0013) and *Ac. cocois* (MFLUCC 15-0817, ex-type) were checked and shown - ITS: 0.1% (1/505 base pairs), LSU: 0% (0/789 base pairs). Morphologically, our collection is well fit with the asexual species of *Acremoniisimulans* (*Ac. thailandensis*) by having pale brown to brown, oval, aseptate conidia (Tibpromma et al., 2018; Figure 2.97). *Acremoniisimulans cocois* was introduced by Konta et al. (2023) with a sexual morph, was collected from the dead petiole of *Cocos nucifera* in Thailand. Therefore, based on morphological and phylogenetic analyses, we identified our collections as a new record of *Ac. cocois*, representing its asexual morph.



Note a, b Colonies on natural substrate. c Conidia. d, e Conidiophores, conidiogenous cells and conidia. f The front of culture on PDA at 25℃ and the reverse of culture on PDA at 25℃. j Conidiophores grown on PDA. k Conidia produced on PDA after two weeks. Scale bars: c–e = 10 μm.

Figure 2.97 *Acremoniisimulans cocois* (MHZU 24-0477, new host and new geography record)

Acrostalagmus Corda, Icones fungorum hucusque cognitorum 2: 15 (1838)

Notes: *Acrostalagmus* (*Acro*.) was established by Corda (1838) with the type species *Acro. cinnabarinus*. Later, some studies identified *Acro. cinnabarinus* as identical to *Verticillium luteoalbum*, leading to the proposal of the new combination *Acro. luteoalbus* as the type species of *Acrostalagmus* (Zare et al., 2004). This genus is characterized by mononematous or synnematous conidiophores, enteroblastic, monophialidic conidiogenous cells, and hyaline or bright orange to reddish, oval, ellipsoidal to oblong-ellipsoidal conidia, held together by slime (Zare et al., 2004; Nguyen et al., 2019). *Acrostalagmus* species are known for their alkalitolerant (Bondarenko et al., 2016; Bondarenko et al., 2018) or alkalophilic nature (Shi et al., 2023), enabling them to thrive in diverse ecological environments such as forests, sand ridges, marine ecosystems, and polar regions (Youssef et al., 2021; Shi et al., 2023). They are also found in specific substrates like saffron soil, needle mushroom, vermicompost, and cacao branches (Artigues & Davet, 1984; Rojas et al., 2011; Shi et al., 2023). The genus is notable for its ability to produce a variety of enzymes and bioactive secondary metabolites (Soprunov & Galiulina, 1951; Artigues & Davet, 1984; Shi et al., 2023), which contribute to its ecological adaptability and potential value in drug development (Shi et al., 2023). These bioactive compounds exhibit a range of activities, making *Acrostalagmus* a promising candidate for biotechnological and pharmaceutical applications. In this study, we use ITS, LSU and SSU to update phylogenetic studies for *Acrostalagmus* (Figure 2.96). There are 55 epithets deposited in Index Fungorum (2025, January), many species were synomumised and only 13 species are accepted in *Acrostalagmus* (Hyde et al., 2024), and only two species are associated with molecular data (Crous et al., 2023). In this study, a new host and new geography record of *A. luteoalbus* was introduced from *Livistona chinensis* in China. To date, two species have been reported from palm hosts including a new host record described in our study.

Acrostalagmus luteoalbus (Link) Zare, W. Gams and Schroers, Mycol. Res. 108 (5): 581 (2004)

Figure 2.98

Saprobic on dead segment of *Livistona chinensis*. Asexual morph: Hyphomycetous. *Colonies* on natural substrate, effuse and velvety. *Mycelium* 1–1.5 µm wide ($\overline{x}$ = 1.3 µm, n = 20), hyaline, thin and smooth-walled. *Conidiophores* 3.5–6 µm wide ($\overline{x}$ = 4.9 µm, n = 20), mononematous, main stipe erect, more or less straight, pale reddish

brown or yellowish at the base, almost hyaline at the apex, branched, septate, verruculose, thick-walled. *Conidiogenous cells* 15–18 × 3–5 µm ($\overline{x}$ = 17 × 3.8 µm, n = 20), phialides, subhyaline, narrowly flask-shaped, only very slightly swollen at the base, tapering in the middle or upper part into a narrow neck which opens with an inconspicuous collarette, denticulate. *Conidia* 4.5–5.5 × 2.5–3.5 µm ($\overline{x}$ = 4.8 × 2.9 µm, n = 30), forming rounded pale reddish brown slimy heads, oval, aseptate, smooth-walled, guttulate. Sexual morph: Not observed.

Culture characteristics: Colonies on PDA fast growing, after seven days reaching 4–5 cm diam., at 25°C, filamentous, flat, with filiform edge, flocculent, with loose, cotton-like clusters of mycelia, above dull orange, orange in reverse. Sporulated in cultures (PDA) after two weeks at 25°C. *Conidiophores* arise directly from aerial hyphae, septate and branched, pale-orange, 3.5–5 µm wide ($\overline{x}$ = 4 µm, n = 20), mononematous. *Conidiogenous cells* phialidic and hyaline. *Conidia* 4.5–5.5 × 2.5–3.5 µm ($\overline{x}$ = 4.9 × 2.9 µm, n = 30), oval, pale brown, smooth, aseptate, guttulate.

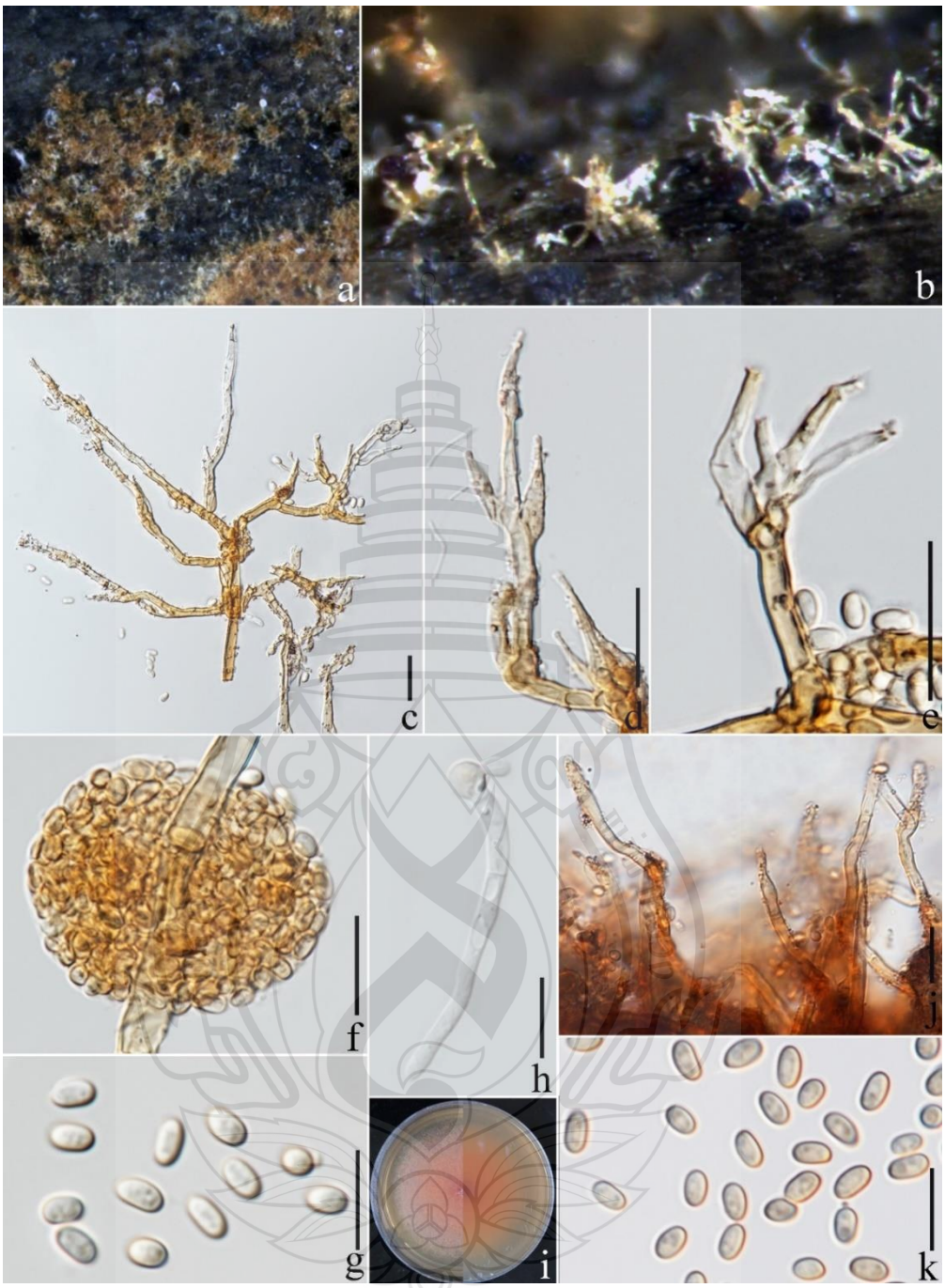
Known distribution: China (this study), England (Zare et al., 2004), Finland (Andersson et al., 2021), Iran (Mohammadi & Amini, 2015), Korea (Nguyen et al., 2019), Russia (Grum-Grzhimaylo et al., 2016), South Africa (Crous et al., 2023).

Material examined: China, Jiangxi Province, Nanchang City, Meiling National Forest Park, on dead segment of *Livistona chinensis*, 10 April 2024, Y.R. Xiong, XG379 (MHZU 24-0460, new host and new geography record), living culture ZHKUCC 25-0037, other living culture ZHKUCC 25-0038.

GenBank numbers: ZHKUCC 25-0037: ITS – PV578124, LSU – PV578294, SSU – PV578480; ZHKUCC 25-0038: ITS – PV578125, LSU – PV578295, SSU – PV578481.

Notes: Two collections obtained in this study clustered with *Acro. luteoalbus* by 97% ML bootstrap support and 0.99 BYPP (Figure 2.96). Based on a MegaBLAST (Query cover ≥ 70%) search using the ITS LSU and SSU sequence, the closest matches in the NCBI GenBank nucleotide database were *Acro. luteoalbus* (GenBank MH482849; Identities 537/537(100%), 0 gap), *Acro. luteoalbus* (GenBank PQ637402; Identities 538/539(99%), 1 gap) and *Acro. luteoalbus* (GenBank: OW983372; Identities 538/539(99%), 1 gaps) for ITS; *Acro. luteoalbus* (GenBank KJ443141; Identities 848/848(100%), 0 gap), *Acro. luteoalbus* (GenBank KJ443142; Identities 848/848(100%), 0 gap) and

Acro. luteoalbus (GenBank: KP671745; Identities 848/848(100%), 0 gap) for LSU; *Acro. luteoalbus* (GenBank KJ443096; Identities 1078/1091(99%), 3 gaps), *Acro. luteoalbus* (GenBank KJ443097; Identities 1078/1091(99%), 3 gaps) and *Acro. luteoalbus* (GenBank: KT587308; Identities 1075/1092(98%), 7 gaps) for SSU. Morphological evidence of conidiogenous cells and hyaline conidia are well fit with *Acro. luteoalbus* (Zare et al., 2004; Crous et al., 2023, Figure 2.98). Therefore, based on morphology and phylogenetic analysis, we identified our collections as new record of *Acro. luteoalbus*. *Acrostalagmus luteoalbus* is the type species of *Acrostalagmus* and has been widely recorded from indoor dust, soil and various plant substrates, across freshwater to terrestrial habitats (Zare et al., 2004; Mohammadi & Amini, 2015; Grum-Grzhimaylo et al., 2016; Nguyen et al., 2019; Andersson et al., 2021; Crous et al., 2023).



Note a, b Colonies on natural substrate. c–e Conidiophores and conidiogenous cells. f Conidial heads. g Conidia. h Germinated conidium. i The front of culture on PDA at 25°C and the reverse of culture on PDA at 25°C. j Conidiophores grown on PDA. k Conidia produced on PDA after two weeks. Scale bars: c–e, j = 20 µm; f–h, k = 10 µm.

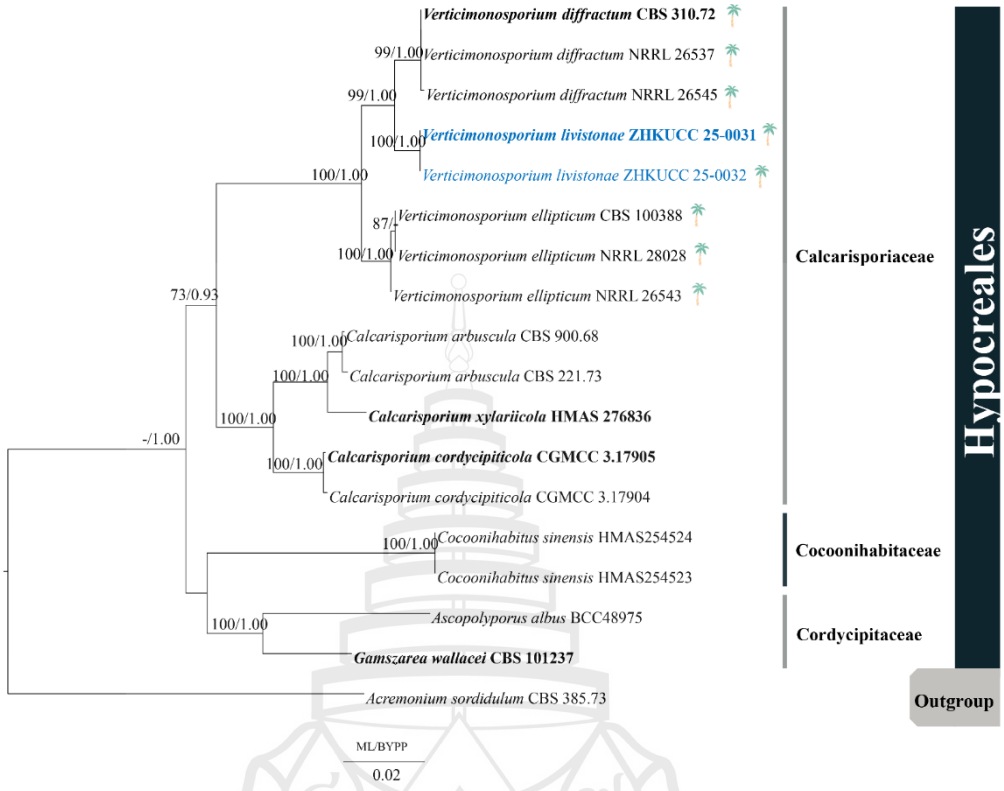
Figure 2.98 *Acrostalagmus luteoalbus* (MHZU 24-0460, new host and new geography record)

Hypocreales Lindau, Nat. Pflanzenfam., Teil. I (Leipzig) 1(1): 343 (1897)

Calcarisporiaceae Jing Z. Sun, Xing Z. Liu & K.D. Hyde, Mycol. Progr. 16(4): 435 (2017)

Verticimonosporium Matsush., Microfungi of the Solomon Islands and Papua-New Guinea: 68 (1971)

Notes: Matsushima (1971) established *Verticimonosporium* (*Ver*.) with *Ver. diffractum* as the type species. *Verticimonosporium* is a hyphomycetous genus characterized by conidiophore erect, simple or branched in the lower part, conidiogenous cells are swollen near the base, with a narrow tip and whorls on the aerial hyphae, conidia are globose to ellipsoidal and hyaline, and smooth-walled (Matsushima, 1971; Gams et al., 1999). Gams et al. (1999) first used molecular data for *Verticimonosporium* and based on morphological evidence and phylogenetic analysis combined SSU, and LSU to place *Verticimonosporium* in Hypocreales. In this study, we use ITS, LSU and SSU to update phylogenetic studies for *Verticimonosporium* (Figure 2.99). Currently, three epithets are listed under *Verticimonosporium* (Index Fungorum, 2025 January), and only two species are associated with molecular data. Totally three species have been reported from palm species including a new species described in this study (Xiong et al., 2025).



Note Phylogram generated from maximum likelihood analysis of some families of Hypocreales based on combined ITS, LSU and SSU sequence data. Bootstrap values for maximum likelihood (ML) equal to or greater than 70 and BYPP values equal to or greater than 0.90 are indicated above the branches. The new collections are indicated in blue and ex-type strains are indicated in bold.

Figure 2.99 Phylogenetic tree of Hypocreales

Verticimonosporium livistonae Y.R. Xiong, Manawas. & K.D. Hyde, ***sp. nov.*** Figure 2.100

Etymology: The epithet refers to the host genus name "*Livistona*", from which the species was collected.

Saprobic on dead petiole of *Livistona chinensis*. Asexual morph: Hyphomycetous. *Colonies* on natural substrate superficial. *Mycelium* superficial, composed of hyaline, smooth, septate, branched aerial hyphae, lanose to almost cobwebby. *Conidiophores* micronematous, undifferentiated from vegetative hyphae, short. *Conidiogenous cells* 8–15 × 3–5 µm (widest part) ($\bar{x}$ = 10 × 4 µm, n = 25), discrete or in clusters, ampulliform to flask shaped, swollen near the base, with a narrow tip, clustered in

regular terminal and intercalary whorls on the aerial hyphae, whorls of 1–4. *Conidia* 6–8 × 5.5–8 µm ($\overline{x}$ = 7 × 6.3 µm, n = 25), solitary, subglobose ovoid, with slightly raised truncated remnant at base, hyaline, aseptate, smooth-walled. Sexual morph: Not observed.

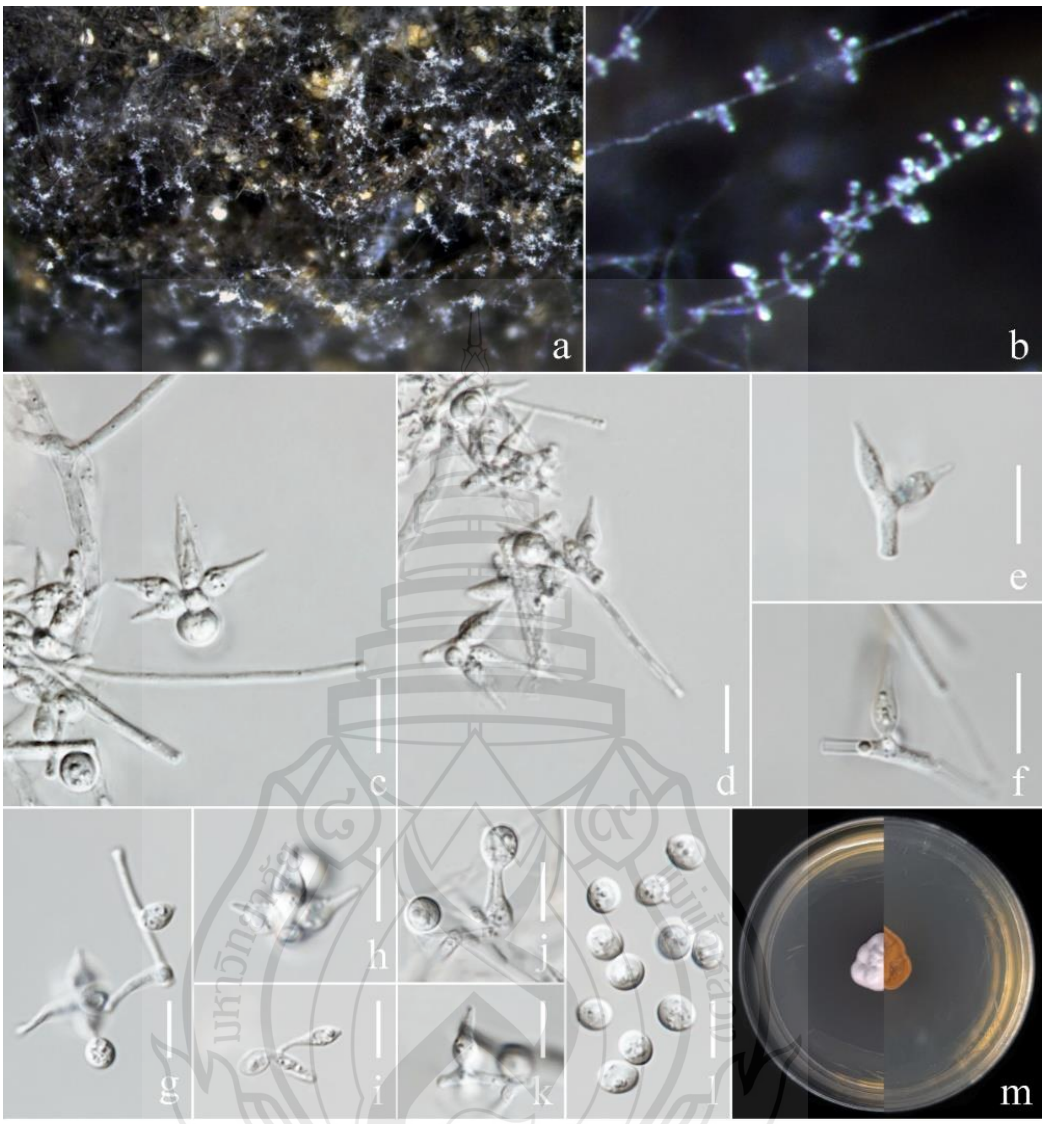
Culture characteristics: Colonies on PDA fast growing, after 2 weeks reaching 2 cm diam., at 25°C, irregular, convex with papillate surface, dense, white mycelium on the surface, radially striated with undulate edge; in reverse yellow.

Known distribution: China (this study).

Material examined: China, Jiangxi Province, Nanchang City, the road next to Meiling National Forest Park, on dead petiole of *Livistona chinensis*, 10 Apr 2024, Y.R. Xiong, XG375 (MHZU 24-0459, holotype), ex-type ZHKUCC 25-0031, other living culture ZHKUCC 25-0032.

GenBank numbers: ZHKUCC 25-0031: ITS – PV578270, LSU – PV578438, SSU – PV578558; ZHKUCC 25-0032: ITS – PV578271, LSU – PV578439, SSU – PV578559.

Notes: Two collections from this study formed a separate lineage and clustered with *Verticimonosporium diffractum* in the phylogenetic tree with 99% ML bootstrap support and 1.00 BYPP (Figure 2.99). The nucleotide differences excluding gaps between *Ver. livistonae* (ZHKUCC 25-0031) and *Ver. diffractum* (CBS 310.72) were checked and given as follows, ITS: 4.12% (24/583 base pairs), LSU: 1.01% (9/897 base pairs), and SSU: 0.41% (4/978 base pairs). *Verticimonosporium livistonae* produces subglobose to ovoid conidia measuring 6–8 × 5.5–8 µm, which are larger and morphologically distinct from the globose to subglobose conidia of *Ver. diffractum* that measures 4.5–6.5 or 5.5–7.5 × 4.5–6 µm (Gams et al., 1999, Figure 2.100). Moreover, *Verticimonosporium livistonae* has conidiogenous cells with whorls of 1–4 which is less than *Ver. diffractum* has conidiogenous cells with whorls of 1–8 (Gams et al., 1999, Figure 2.100). Based on phylogenetic placement and morphological variations, we introduce *Ver. livistonae* as a new species.



Note a, b Colonies on substrate surface. c–k Conidiogenous cells with conidia. l Conidia. m The front of culture on PDA at 25°C and the reverse of culture on PDA at 25°C. Scale bars: c–l = 10 µm.

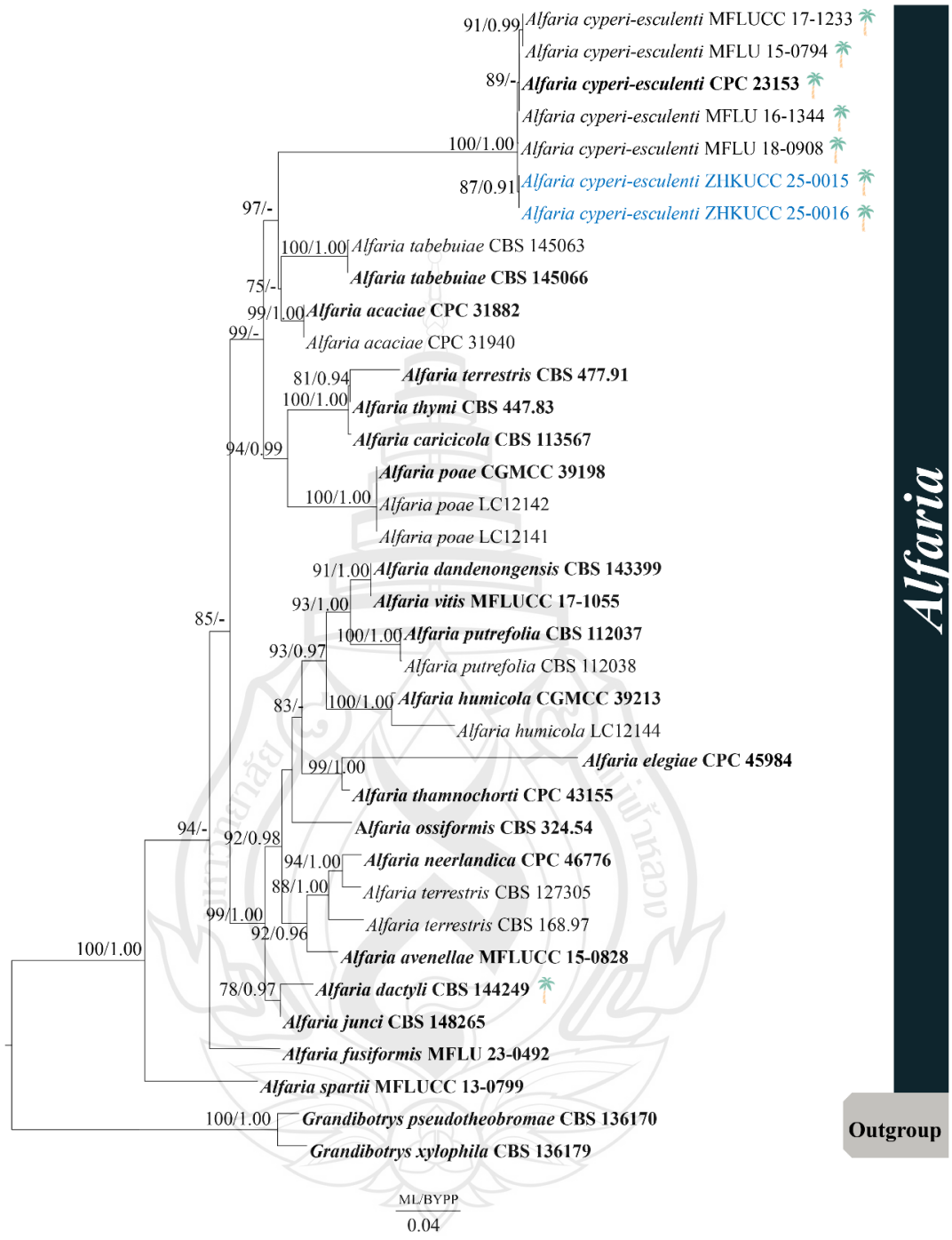
Figure 2.100 *Verticimonosporium livistonae* (MHZU 24-0459, holotype)

Stachybotryaceae L. Lombard & Crous, Persoonia 32: 283 (2014)

Alfaria Crous, N.J. Montaño-Mata & García-Jim., Persoonia 32: 239 (2014)

Notes: *Alfaria* (*Al.*) was introduced by Crous et al. (2014) to accommodate a pathogen, *Al. cyperi-esculenti* (type), which is associated with leaf tip dieback and tuber rot of *Cyperus esculentus* (Cyperaceae) in Spain (Crous et al., 2014). The genus is characterized by black, globose, immersed ascomata, fasciculate, subcylindrical asci with

obtuse apices, with 2–8 ascospores, hyaline, fusoid-ellipsoid, 0–3-septate (Crous et al., 2014; Liang et al., 2019). The asexual morph exhibits microthyrium-like features, including solitary or sporodochial, verticillately or penicillately branched, hyaline conidiophores, phialidic conidiogenous cells, and cylindrical to ellipsoidal conidia, hyaline to lightly pigmented, aseptate (Jayawardena et al., 2018; Manawasinghe et al., 2022). In this study, we use ITS, LSU, *rpb*2 and *tef* 1-α to update phylogenetic studies for *Alfaria* (Figure 2.101). There are 20 species epithets accepted in *Alfaria* (Index Fungorum, 2025 January), and all species are confirmed with molecular data (Manawasinghe et al., 2022; Liu et al., 2024). To date, two species have been reported from palm host including a new host and new geography record of *Al. cyperi-esculenti* was introduced from *Caryota mitis* from China in this study (Xiong et al., 2025).



Note Phylogram generated from maximum likelihood analysis of *Alfaria* based on combined ITS, LSU, *rpb*2 and *tef* 1-α sequence data. Bootstrap values for maximum likelihood (ML) equal to or greater than 70 and BYPP values equal to or greater than 0.90 are indicated above the branches. The new collections are indicated in blue and ex-type strains are indicated in bold.

Figure 2.101 Phylogenetic tree of *Alfaria*

Alfaria cyperi-esculenti Crous, Montaño-Mata & García-Jim., Persoonia 32: 239 (2014)

Index Fungorum number: IF 808924; *Facesoffungi number*: FoF 03602; Figure 2.102

Saprobic on dead segment of *Caryota mitis*. Asexual morph: Coelomycetous. *Conidiomata* 200–300 μm diam., sporodochial, stromatic, superficial, cupulate to discoid, solitary to gregarious, oval to elongate, composed of cells of *textura globulosa* or *textura angularis*. *Setae* arising from the basal to the fringe of stroma, 100–130 × 4–8 μm ($\overline{x}$= 113 × 6.6 μm, n = 25), brown, thick-walled, straight, smooth, septate, unbranched, narrowing to sharp apices. *Conidiophores* up to 47 μm long, arising from the basal stroma, unbranched or branched, hyaline to greenish-brown, smooth-walled. *Conidiogenous cells* 17–22 × 1–3 μm ($\overline{x}$= 18.7 × 1.8 μm, n = 25), monoblastic, annellidic, cylindrical to elongate doliiform, hyaline, covered by an olivaceous green mucoid layer, smooth, with conspicuous collarettes and periclinal thickenings. *Conidia* 6.5–9 × 3.7–5 μm ($\overline{x}$= 8.2 × 4.3 μm, n = 40), aseptate, smooth-walled, ellipsoidal, greenish-brown to dark brown, guttlate, with germ slit when mature. Sexual morph: Not observed.

Culture characteristics: Colonies on PDA slowly growing, after 2 weeks reaching 3–4 cm diam., at 25°C, lobate, slight raised, with filamentous edge, white aerial mycelium and luteous to pale luteous mycelium, fluffy, cotton, above white, yellowish in reverse.

Known distribution: China (this study); Spain (Crous et al., 2014); Italy (Jayawardena et al., 2018; Manawasinghe et al., 2022).

Material examined: China, Guangxi Province, Guilin City, Guilin Garden botanical garden, on dead segment of *Caryota mitis*, 3 June 2023, Y.R. Xiong, XG308 (MHZU 24-0509, new host and new geography record), living culture ZHKUCC 25-0015, other living culture ZHKUCC 25-0016.

GenBank numbers: ZHKUCC 25-0015: ITS – PV578126, LSU – PV578296, *rpb2* – PV595298, *tef* 1-α – PV608810; ZHKUCC 25-0016: ITS – PV578127, LSU – PV578297, *rpb2* – PV595299, *tef* 1-α – PV608811.

Notes: Two collections obtained in this study clustered with *Al. cyperi-esculenti* by 100% ML bootstrap support and 1.00 BYPP (Figure 2.101). The nucleotide differences excluding gaps between our isolate (ZHKUCC 25-0015) and *Al. cyperi-esculenti* (CPC

23153, ex-type) were checked and shown - ITS: 0% (0/549 base pairs), LSU: 0% (0/783 base pairs). Morphological evidence of sporodochial conidiomata and ellipsoidal conidia are well fit with *Al. cyperi-esculenti* (Jayawardena et al., 2018; Manawasinghe et al., 2022, Figure 2.102). Therefore, based on morphology and phylogenetic analysis, we identified our collections as the new host and new geography of *Al. cyperi-esculenti*.

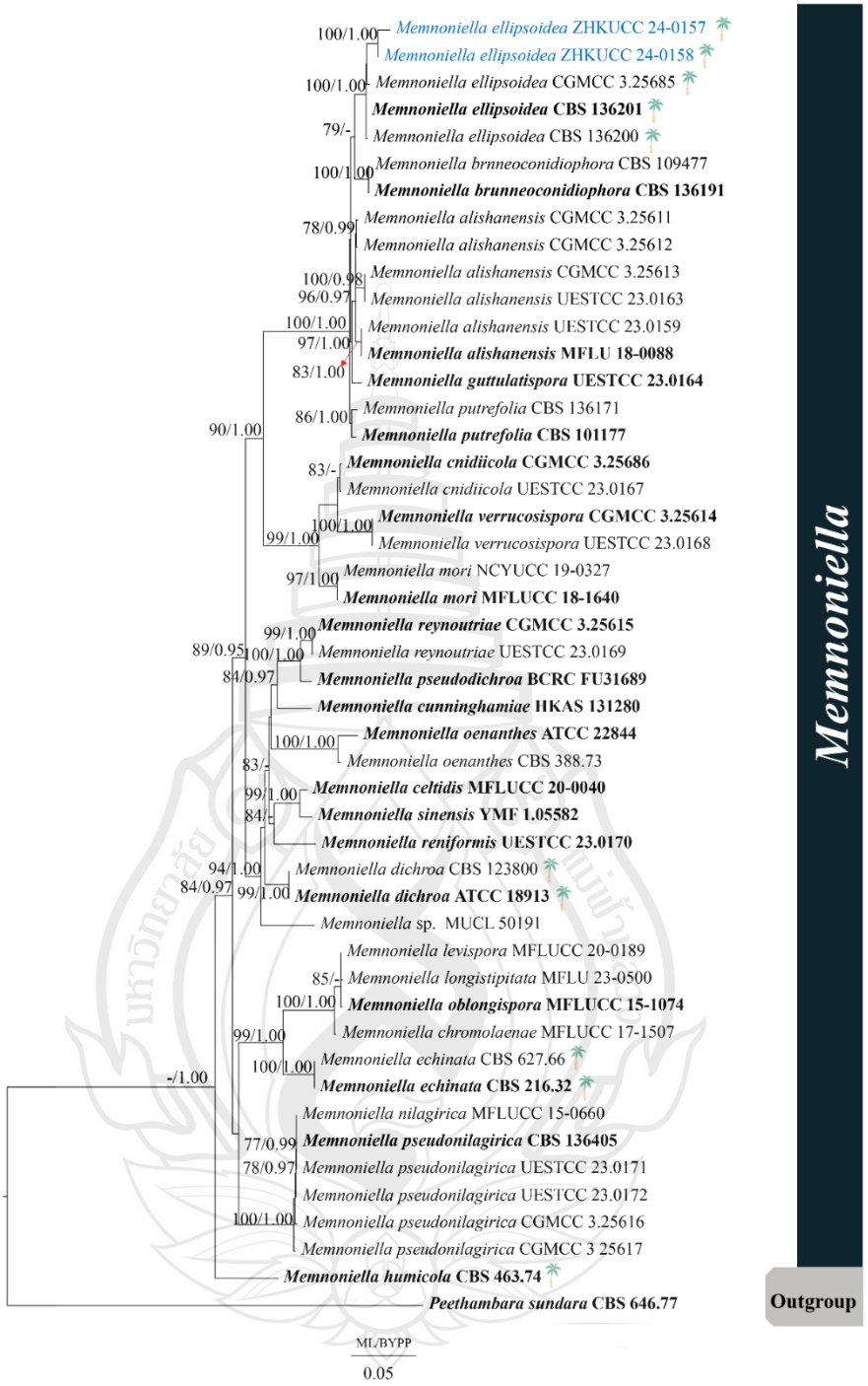


Note a, b Appearance of conidiomata on the host surface. c Vertical section through conidioma. d Germinated conidium. e, f Conidiophores, conidiogenous cells and conidia. g Conidia. h Setae. i The front of culture on PDA at 25°C and the reverse of culture on PDA at 25°C. Scale bars: c = 50 µm; h = 30 µm; d–g = 10 µm.

Figure 2.102 *Alfaria cyperi-esculenti* (MHZU 24-0509, new host and new geography record)

Memnoniella Höhn., Zentralblatt für Bakteriologie, Parasitenkunde, Infektionskrankheiten und Hygiene, 2. Abt. 60(1/6): 16 (1923)

Notes: *Memnoniella* (*Me.*) was established by von Höhnel (1923) with *Me. eChinata* as the type species. *Memnoniella* species exhibit saprobic lifestyles and are characterized by macronematous, mononematous, and unbranched conidiophores, phialidic conidiogenous cells with conspicuous collarettes, producing unicellular, aseptate, smooth to verrucose conidia that are arranged in dry chains or slimy masses (Hyde et al., 2020; Tennakoon et al., 2021; Du et al., 2025). Historically, *Memnoniella* was suggested to be synonymous with *Stachybotrys* due to morphological similarities (Smith, 1962; Wang et al., 2015). However, Lombard et al., (2016) reinstated *Memnoniella* as a distinct genus within the Stachybotryaceae family, supported by both morphological and phylogenetic evidence. Subsequent studies have further validated this classification (Tennakoon et al., 2021; Du et al., 2025). In this study, we use ITS, LSU, *rpb*2 and *tub*2 to update phylogenetic studies for *Memnoniella* (Figure 2.103). There are 31 species accepted in *Memnoniella* (Index Fungorum, 2025 January) and 24 species were verified with DNA sequences (Tennakoon et al., 2021; Du et al., 2025). To date, four species have been reported from palm species including a new host record of *Me. ellipsoidea* was introduced from *Dypsis lutescens* from China (Xiong et al., 2025).



Note Phylogram generated from maximum likelihood analysis of *Memnoniella* based on combined ITS, LSU, *rpb2* and *tub2* sequence data. Bootstrap values for maximum likelihood (ML) equal to or greater than 70 and BYPP values equal to or greater than 0.90 are indicated above the branches. The new collections are indicated in blue and ex-type strains are indicated in bold.

Figure 2.103 Phylogenetic tree of *Memnoniella*

Memnoniella ellipsoidea L. Lombard & Crous, Persoonia 36: 197 (2016)

Figure 2.104

Saprobic on dead segment of *Dypsis lutescens*. Asexual morph: Hyphomycetous. *Colonies* on natural substrate superficial, effuse, black, glistening, single or clustered, globose aggregated in a large mass. *Mycelium* is mostly immersed, partly superficial, hyaline. *Conidiophores* 120–200 × 7–10 µm ($\overline{x}$ = 167.5 × 8.7 µm, n = 20), macronematous, mononematous, single or in small groups, erect, straight or slightly flexuous, smooth, thick-walled, unbranched, olivaceous brown at the base, becoming subhyaline towards the apex, 2–4-septate, bearing 4–6 conidiogenous cells at its apex. *Conidiogenous cells* 10–15 × 4–8 ($\overline{x}$ = 13.9 × 5.7 µm, n = 20), monophialidic, clavate to subcylindrical, discrete, determinate, terminal, smooth, subhyaline to olivaceous brown, smooth-walled. *Conidia* 10–13 × 6–8 µm ($\overline{x}$ = 12.1 × 6.9 µm, n = 30), aggregated in black and glistening heads, subglobose to ellipsoidal, acrogenous, aseptate, with 2 globose guttules, verrucose, thick-walled, rounded at both ends, olivaceous brown to dark brown. Sexual morph: Not observed.

Culture characteristics: Colonies on PDA fast growing, after 2 weeks reaching 4–5 cm diam., at 25°C, filamentous, flat, with filiform edge, fluffy, white aerial mycelium on surface, above white, yellowish in reverse.

Known distribution: Brazil and Nepal (Lombard et al., 2016), China (Du et al., 2025; this study).

Material examined: China, Yunnan Province, Xishuangbanna, Dai Nationality Park, on dead segment of *Dypsis lutescens*, 6 February 2024, Y.R. Xiong, XG241 (MHZU 23-0175, new host record), living culture ZHKUCC 24-0157, other living culture ZHKUCC 24-0158.

GenBank numbers: ZHKUCC 24-0157: ITS – PV578202, LSU – PV578370, *rpb*2 – PV595334, *tub*2 – PV584065; ZHKUCC 24-0158: ITS – PV578203, LSU – PV578371, *rpb*2 – PV595335, *tub*2 – PV584066.

Notes: Two collections obtained in this study clustered with *Me. ellipsoidea* (CBS 136200, CBS 136201 (ex-type) and CGMCC 3.25685) by 100% ML bootstrap support and 1.00 BYPP (Figure 2.103). The nucleotide differences excluding gaps between our isolate (ZHKUCC 24-0157) and *Me. ellipsoidea* (CBS 136201, ex-type) were checked and shown - ITS: 3.6% (19/527 base pairs), LSU: 0% (0/795 base pairs), *rpb*2: 0% (0/721

base pairs), and *TUB*2: 1.1% (4/350 base pairs). Morphological evidence of clavate to subcylindrical conidiogenous cells and ellipsoidal conidia are well fit with the holotype descriptions of *Me. ellipsoidea* (Lombard et al., 2016; Figure 2.104). *Memnoniella ellipsoidea* was introduced by Lombard et al. (2016), which was collected from *Bromelia* sp. in Brazil and a dead twig in Nepal as a saprobic fungus. Recently, Du et al. (2025) introduced a new record of *Me. ellipsoidea* from dead stems of the medicinal plant *Reynoutria japonica* in China. Therefore, based on morphology and phylogenetic analysis, we identified our collections as a new host record of *Me. ellipsoidea*.



Note a, b Sporulation on the host substrate. c–f Conidiophores and conidiogenous cells with conidia. g Conidia. h Germinated conidium. i The front of culture on PDA at 25°C and the reverse of culture on PDA at 25°C. Scale bars: c–e = 30 µm; f–h = 15 µm.

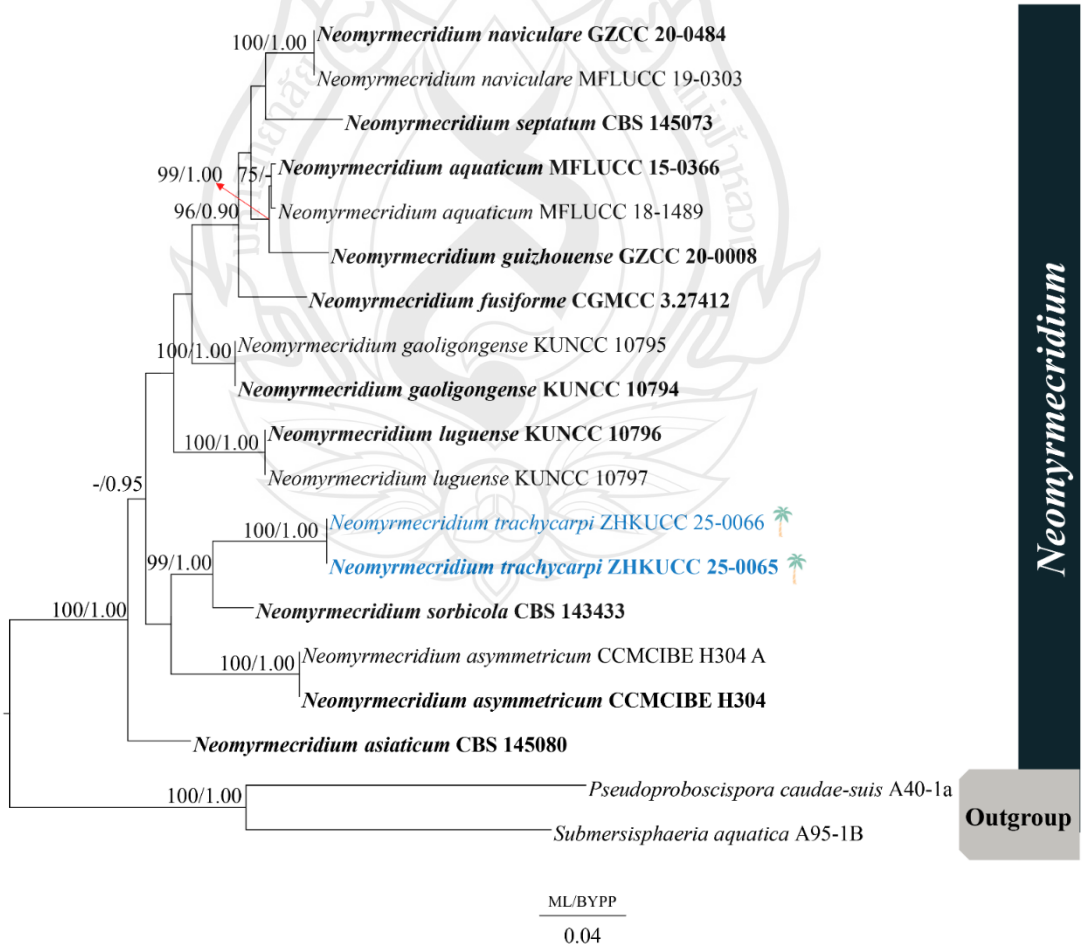
Figure 2.104 *Memnoniella ellipsoidea* (MHZU 23-0175, new host record)

Myrmecridiales Crous, Persoonia 34: 219 (2015)

Myrmecridiaceae Crous, Persoonia 34: 219 (2015)

Neomyrmecridium Crous, Persoonia 41: 287 (2018)

Notes: Crous et al. (2016) established *Neomyrmecridium* (*Neomy*.) with *Neomy. septatum* as the type species based on morphological evidence and phylogenetic analysis used LSU. *Neomyrmecridium* is a hyphomycetous genus characterized by conidiophores solitary and unbranched, conidiogenous cells polyblastic and denticulate, conidia fusoid-ellipsoid and septate with mucoid sheath (Crous et al., 2018a; Hyde et al., 2020). Hyde et al. (2020) and Zhang et al. (2024) used LSU, ITS, *rpb*2 and *tef* 1-α or without *rpb*2 and *tef* 1-α for phylogenetic analysis. In this study, we use LSU, SSU, ITS, *rpb*2 and *tef* 1-α to update phylogenetic studies for *Neomyrmecridium* (Figure 2.105). Currently, eight species are listed under *Neomyrmecridium* (Zhang et al., 2024, Index Fungorum, 2025 January) and all species are associated with molecular data. Here we described a new species of *Neomyrmecridium* which is the first time reported from palm species (Xiong et al., 2025).



Note Phylogram generated from maximum likelihood analysis of *Neomyrmecridium* based on combined ITS, LSU, SSU and *tef* 1-α sequence data. Bootstrap values for maximum likelihood (ML) equal to or greater than 70 are indicated above the branches. The new collections are indicated in blue and ex-type strains are indicated in bold.

Figure 2.105 Phylogenetic tree of *Neomyrmecridium*

Neomyrmecridium trachycarpi Y.R. Xiong, Manawas. & K.D. Hyde, ***sp. nov.***
Figure 2.106

Etymology: The epithet refers to the host genus name "*Trachycarpus*", from which the species was collected.

Saprobic on dead leaf sheath of *Trachycarpus fortunei*. Asexual morph: Hyphomycetous. *Colonies* on natural substrate effuse, pale brown, velvety, hair. *Mycelium* consists of branched hyphae, hyaline, smooth. *Conidiophores* 160–190 × 5–5.5 μm ($\overline{x}$ = 171 × 5.4 μm, n = 15), macronematous, mononematous, solitary, erect to flexuous, unbranched, subcylindrical, smooth, dark brown, paler towards apex. *Conidiogenous cells* 10–20 × 3–4 μm ($\overline{x}$ = 16.6 × 3.7 μm, n = 25), polyblastic, terminal and intercalary, integrated, subcylindrical, pale brown, hyaline towards apex, with a rachis of pimple-like denticles. *Conidia* 10–15 × 4–5.5 μm ($\overline{x}$ = 13 × 4.6 μm, n = 25), solitary, fusiform to obovoid, initially hyaline, but pale brown with age, apex obtuse, 0–4 septate, in lower to a truncate hilum, smooth-walled. Sexual morph: Not observed.

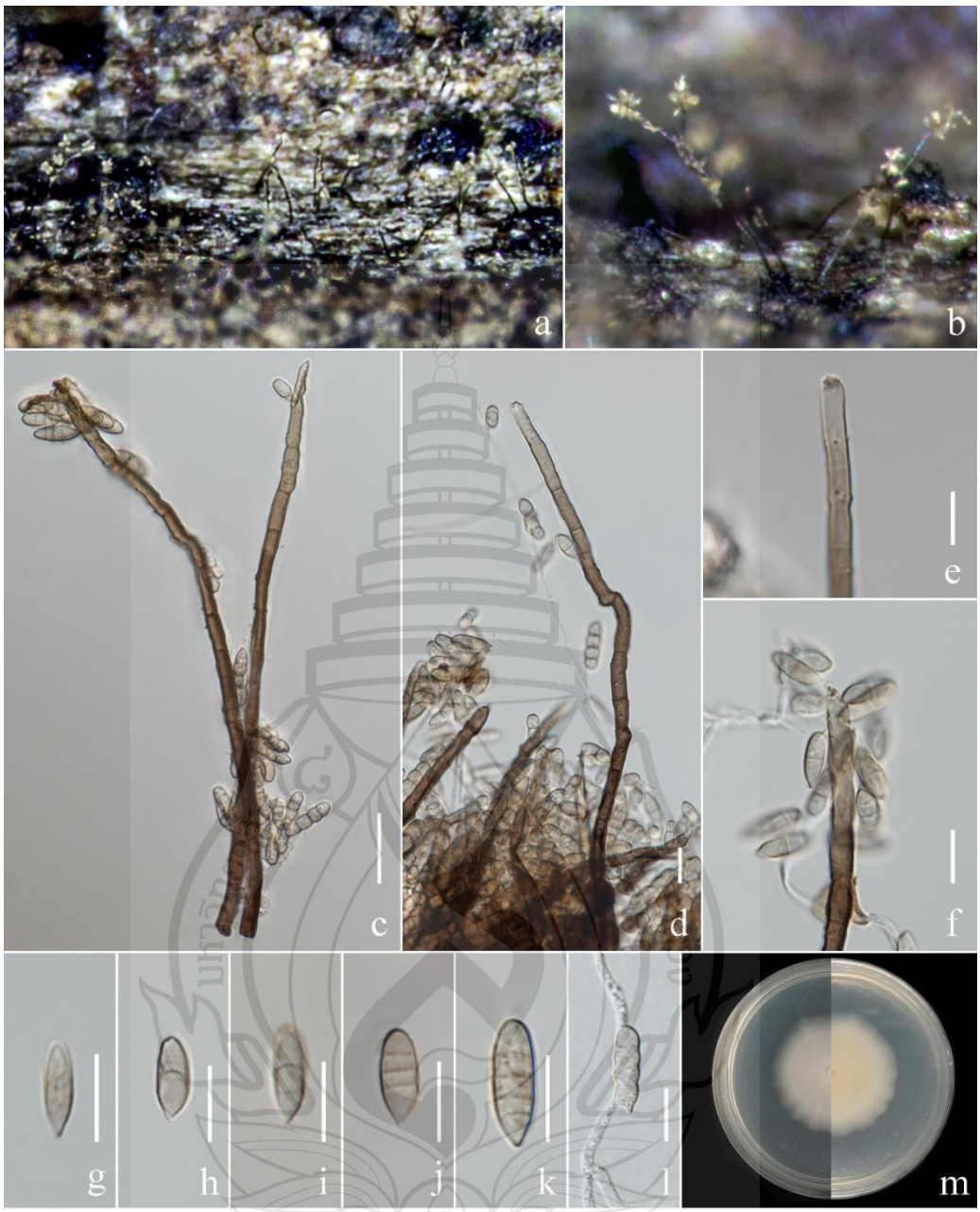
Culture characteristics: Colonies on PDA fast growing, after 2 weeks reaching 4 cm diam., at 25°C, circular, with fluffy, dense, white mycelium on the surface with entire margin; in reverse cream in the middle and white at the margin.

Known distribution: China (this study).

Material examined: China, Jiangxi Province, Pingxiang City, Wugong Mountain National Scenic Area, on dead leaf sheath of *Trachycarpus fortunei*, 12 Apr 2024, Y.R. Xiong, XG418 (MHZU 24-0466, holotype), ex-type ZHKUCC 25-0065, other living culture ZHKUCC 25-0066.

GenBank numbers: ZHKUCC 25-0065: ITS – PV578214, LSU – PV578380, SSU – PV578524, *tef* 1-α – PV608872, *rpb*2 – PV595340; ZHKUCC 25-0066: ITS – PV578215, LSU – PV578381, SSU – PV578525, *tef* 1-α – PV608873, *rpb*2 – PV595341.

Notes: Two collections from this study formed a separate lineage and clustered with *Neomyrmecridium sorbicola* in the phylogenetic tree with 99% ML bootstrap support and 1.00 BYPP (Figure 2.105). The nucleotide differences excluding gaps between *Neomy. trachycarpi* (ZHKUCC 25-0065) and *Neomy. sorbicola* (CBS 143433) were checked and given as follows, ITS: 7.65% (41/536 base pairs), LSU: 3.09% (26/841 base pairs). *Neomyrmecridium trachycarpi* have fusiform to obovoid conidia with 0–4 septate and without sheath which is different from *Neomy. sorbicola* have conidia with mucoid sheath surrounding conidium in the median region (Crous et al., 2018b). Based on phylogenetic placement and morphological variations, we introduce *Di. guineensis* as a new species.



Note a, b Colonies on the substrate surface. c–f Conidiophore, conidiogenous cells with conidia. g–k Conidia. l Germinating conidium. m The front of culture on PDA at 25°C and the reverse of culture on PDA at 25°C. Scale bars: c–l = 10 µm.

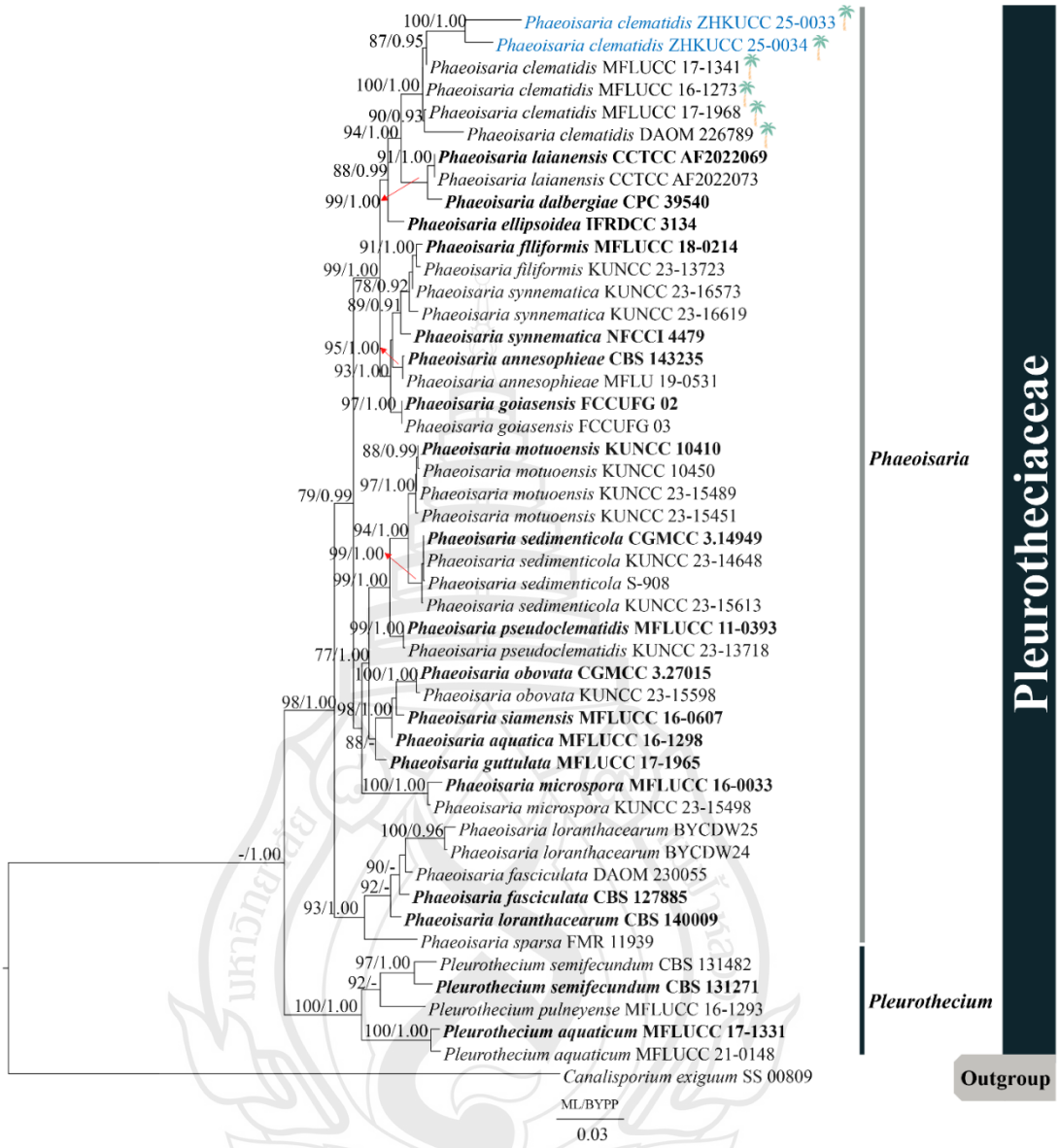
Figure 2.106 *Neomyrmecridium trachycarpi* (MHZU 24-0466, holotype)

Pleurotheciales Réblová & Seifert, Persoonia 37: 63 (2015)

Pleurotheciaceae Réblová & Seifert, Persoonia 37: 63 (2015)

Phaeoisaria Höhn., Sitzungsber. Kaiserl. Akad. Wiss., Wien. Math.-Naturwiss. Cl., Abt. 1 118 (4): 330 (1909)

Notes: *Phaeoisaria* (*Pha.*) was proposed by Höhnel (1909) to accommodate *P. bambusae* as the type species. Most of the *Phaeoisaria* species have been reported as saprobes (Luo et al., 2018) and few species are human pathogens (Guarro et al., 2000). Most of these species are reported from their asexual morph and it is characterized by long or short erect synnemata brush-like, with parallelly adpressed conidiophores, a flared fertile above half and apices, polyblastic, sympodially extending the denticulate, with short or long, recurved conidiogenous cells, aseptate or septate, and subglobose to fusiform, or ellipsoidal conidia (de Hoog & Papendorf, 1976; Luo et al., 2018; Jayawardena et al., 2022; Wang et al., 2024). Only *Pha. filiformis* has been reported asexual morph and is characterized by immersed, globose elongated ascomata with a long, cylindrical, black, ostiolar neck, filamentous, branched, septate paraphyses, unitunicate, cylindrical asci with a small refractive apical apparatus, and filiform, multi-septate, hyaline ascospores tapering at both ends (Luo et al., 2019). There are 38 species accepted in *Phaeoisaria* (Index Fungorum, 2025 January), and 20 species are associated with molecular data, and primarily derived from the combined analysis of LSU, ITS, SSU, and *rpb*2 sequences (Luo et al., 2018; Wang et al., 2024, Figure 2.107). In this study, we use ITS, LSU, SSU and *rpb*2 to update phylogenetic studies for *Phaeoisaria* (Figure 2.107). One species has been reported from palm species including a new host record of *Pha. clematidis* was introduced from *Livistona chinensis* from China in this study (Xiong et al., 2025).



Note Phylogram generated from maximum likelihood analysis of *Phaeoisaria* based on combined ITS, LSU, SSU and *rpb*2 sequence data. Bootstrap values for maximum likelihood (ML) equal to or greater than 70 are indicated above the branches. The new collections are indicated in blue and ex-type strains are indicated in bold.

Figure 2.107 Phylogenetic tree of *Phaeoisaria*

Phaeoisaria clematidis (Fuckel) S. Hughes, Can. J. Bot. 36: 794 (1958)

Figure 2.108

Saprobic on dead segment of *Livistona chinensis*. Asexual morph: Hyphomycetous. *Colonies* synnematal, indeterminate, scattered, erect, rigid, dark brown to black, composed of compactly and parallelly adpressed conidiophores. *Mycelium* 0.7–1 µm wide ($\overline{x}$ = 0.9 µm, n = 20), hyaline, branched, aseptate, smooth-walled. *Synnemata* erect, rigid, dark brown to black, velvety, smooth, composed of compactly and parallelly adpressed conidiophores, with flared conidiogenous cells in the above half. *Conidiophores* 120–330 × 2–3 µm ($\overline{x}$ = 195 × 2.5 µm, n = 30), macronematous, synnematous, dark brown at the base, paler towards the apex, smooth. *Conidiogenous cells* 8–16 µm× 2–3 µm ($\overline{x}$ = 11.3 × 2.4 µm, n = 30), polyblastic, terminal and intercalary, mostly discrete, sometimes integrated, recurved, smooth, sympodial extended, denticulate, subhyaline to pale brown, sympodial, each with one to several denticulate conidiogenous loci. *Conidia* 4–6 × 2–3 µm ($\overline{x}$ = 5.4 × 2.3 µm, n = 30), solitary, ellipsoidal to obovoidal, hyaline, aseptate, smooth and thin-walled, guttulate, rounded at the apex, obtuse and tapering towards base. Sexual morph: Not observed.

Culture characteristics: Colonies on PDA slowly growing, after 2 weeks reaching 2 cm diam., at 25°C, circular, raised, with entire edge, dense, brittle and rough at the surface, floccose, above white, olive green in reverse.

Known distribution: Argentina, Brazil, China, Germany, Indonesia, Japan, Philippines, Thailand, and Vietnam (Hoog & Papendorf, 1976; Guarro et al., 2000; Pinnoi et al., 2006; Mel'nik 2012; Luo et al., 2018; Wang et al., 2024; this study)

Material examined: China, Jiangxi Province, Nanchang City, Meiling National Forest Park, on a dead segment of *Livistona chinensis,* 10 April 2024, Y.R. Xiong, XG376 (MHZU 24-0485, new host record), living culture ZHKUCC 25-0033, other living culture ZHKUCC 25-0034.

GenBank numbers: ZHKUCC 25-0033: ITS – PV578222, LSU – PV578388, SSU – PV578530, *rpb*2 – PV595344; ZHKUCC 25-0034: ITS – PV578223, LSU – PV578389, SSU – PV578531, *rpb*2 – PV595345.

Notes: Two collections obtained in this study clustered with *Pha. clematidis* (MFLUCC 17-1341) by 97% ML bootstrap support and 0.95 BYPP (Figure 2.107). The nucleotide differences excluding gaps between our collections (ZHKUCC 25-0033) and

Pha. clematidis (MFLUCC 17-1341) in ITS is 0% (0/448 base pairs), LSU is 0% (0/817 base pairs), SSU is 0.11% (1/853 base pairs) and *rpb*2 is 0.19% (1/505 base pairs). Morphological evidence of conidiogenous cells and hyaline conidia are well fit with *Pha. clematidis* (Luo et al., 2018, Figure 2.108). Therefore, based on morphology and phylogenetic analysis, we identified our collections as *Pha. clematidis. Phaeoisaria clematidis* commonly occurs on various hosts and is distributed worldwide (de Hoog & Papendorf, 1976; Crous et al., 2015; Luo et al., 2018). Some records have been reported *Pha. Clematidis* can be human pathogens that cause a corneal ulcer (Guarro et al., 2000). To our knowledge this is the first record of *Phaeoisaria clematidis* on *Livistona chinensis.*



Note a, b Colonies on natural substrate. c, d Conidiophores. e Conidiogenous cells with conidia. f Conidia. g Germinated conidium. h The front of culture on PDA at 25°C and the reverse of culture on PDA at 25°C. Scale bars: c, d = 30 µm; e–g = 10 µm.

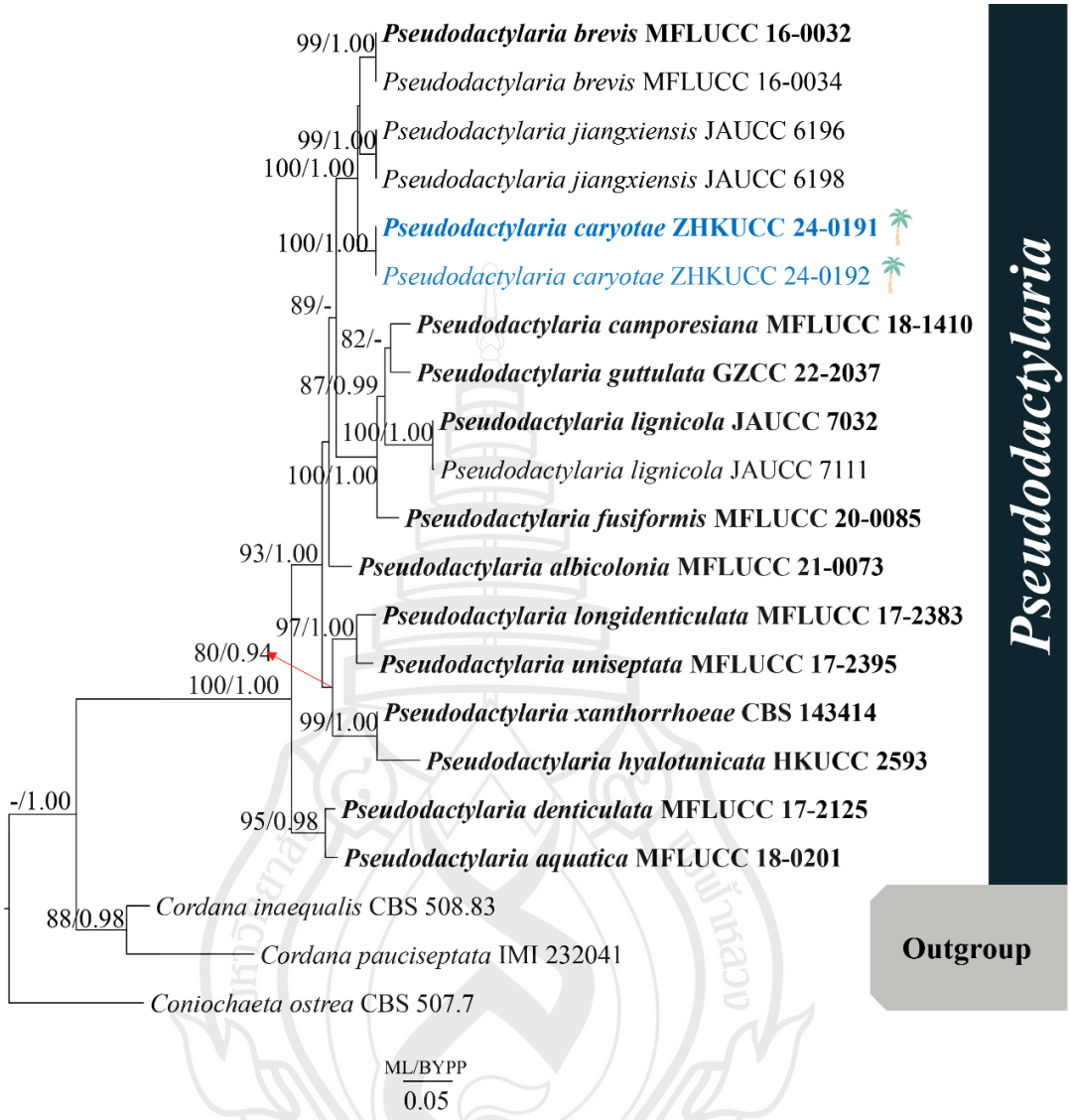
Figure 2.108 *Phaeoisaria clematidis* (MHZU 24-0485, new host record)

Pseudodactylariales Crous, Persoonia 39: 421 (2017)

Pseudodactylariaceae Crous, Persoonia 39: 421 (2017)

Pseudodactylaria Crous, Persoonia 39: 421 (2017)

Notes: Crous et al. (2017) established *Pseudodactylaria* (*Psudoda*.) with *Psudoda. xanthorrhoeae* as the type species. *Pseudodactylaria* is a hyphomycetous genus characterized by distinct, single, hyaline, unbranched or branched and septate conidiophores, terminal, integrated, polyblastic, denticulate conidiogenous cells and solitary, fusoid-ellipsoid, 1-septate or aseptate, and hyaline conidia (Hyde et al., 2020; Manawasinghe et al., 2024). Based on morphological evidence and phylogenetic analysis of LSU molecular data, Crous et al. (2017) introduced *Pseudodactylaria* as a new genus in Pseudodactylariaceae. Subsequently, phylogenetic studies mainly use LSU, and ITS for analysis (Boonmee et al., 2021; Manawasinghe et al., 2024). In this study, we use ITS, LSU, SSU, *rpb*2 and *tef* 1-α to update the phylogenetic tree for *Pseudodactylaria*. Currently, 13 species are listed under *Pseudodactylaria* (Index Fungorum, 2025 January, Xu et al., 2025), and all species are associated with molecular data. Here we described a new species of *Pseudodactylaria* which is the first time reported from palm species (Xiong et al., 2025).



Note Phylogram generated from maximum likelihood analysis of *Pseudodactylaria* based on combined ITS, LSU, SSU, *rpb2* and *tef* 1-α sequence data. Bootstrap values for maximum likelihood (ML) equal to or greater than 70 are indicated above the branches. The new collections are indicated in blue and ex-type strains are indicated in bold.

Figure 2.109 Phylogenetic tree of *Pseudodactylaria*

Pseudodactylaria caryotae Y.R. Xiong, Manawas., & K.D. Hyde, ***sp. nov.***

Figure 110

Etymology: The epithet refers to the host genus name "*Caryota*", from which the species was collected.

Saprobic on dead inflorescence rachis of *Caryota mitis*. Asexual morph: Hyphomycetous. *Colonies* on natural substrate superficial, effuse, scattered or aggregated, brown, with glistening conidial masses at the apex. *Mycelium* partly superficial. *Conidiophores* reduced to conidiogenous cells. *Conidiogenous cells* 9–14 × 1.5–2 μm ($\overline{x}$ = 12.5 × 1.6 μm, n = 10), polyblastic, integrated, sympodial, terminal, denticulate, straight or flexuous, hyaline, cylindrical, smooth. *Conidia* 15–19 × 4–5 μm ($\overline{x}$ = 16.8 × 4.4 μm, n = 25), solitary, acropleurogenous, simple, smooth, prominently big guttulate in cells or numerous small guttulate, 1-septate, narrowly fusiform, subtruncate at the base, sometime with denticles residue, subobtuse at apex, hyaline, sometimes with a hyaline, irregular appendage. Sexual morph: Not observed.

Culture characteristics: Colonies on PDA fast growing, after 2 weeks reaching 4 cm diam., at 25°C, circular, with fluffy, sparse, white mycelium on the surface with entire margin; in reverse yellow in the middle and white at the margin.

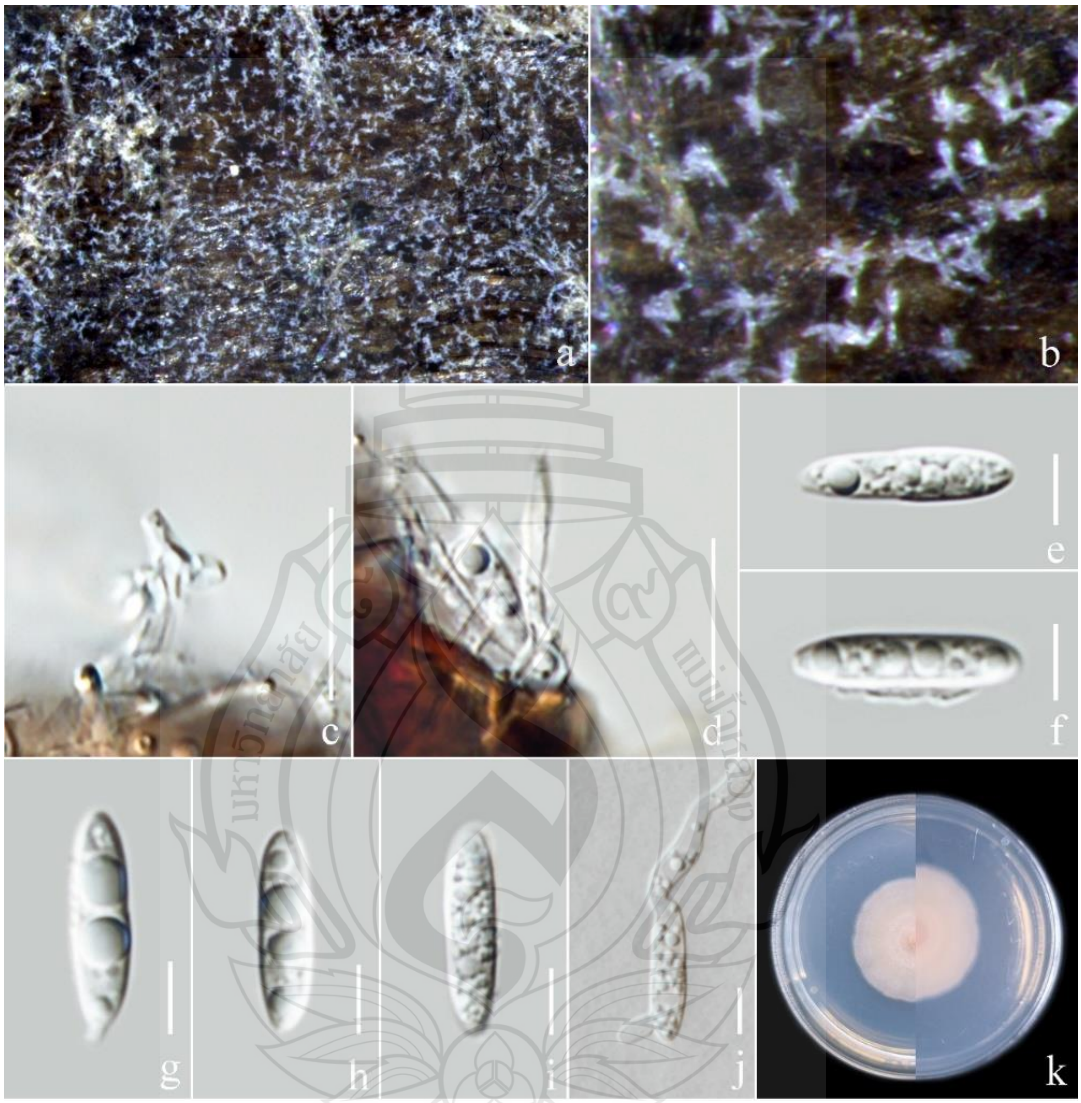
Known distribution: China (this study).

Material examined: China, Yunnan Province, Xishuangbanna City, Xishuangbanna National Forest Park, on dead inflorescence rachis of *Caryota mitis*, 4 Feb 2023, Y.R. Xiong and L. Lu, XG292 (MHZU 23-0192, holotype), ex-type ZHKUCC 24-0191, other living culture ZHKUCC 24-0192.

GenBank numbers: ZHKUCC 24-0191: ITS – PV578238, LSU – PV578406, SSU – PV578540, *tef* 1-α – PV608886, *rpb*2 – PV595354; ZHKUCC 24-0192: ITS – PV578239, LSU – PV578407, SSU – PV578541, *tef* 1-α – PV608887, *rpb*2 – PV595355.

Notes: Two collections from this study clustered in *Pseudodactylaria* clade and formed a sister lineage to *Pseudoda. brevis* in the phylogenetic tree with 98% ML bootstrap support and 1.00 BYPP. (Figure 2.109) The nucleotide differences excluding gaps between *Pseudoda. caryotae* (ZHKUCC 24-0191) and *Pseudoda. brevis* (MFLUCC 16-0032) was checked and given as follows, ITS: 4.55% (22/483 base pairs), and LSU: 0.24% (2/827 base pairs). *Pseudodactylaria caryotae* has conidiophores reduced to conidiogenous cells which are different from *Pseudoda. brevis* has conidiophores with macronematous,

mononematous and sometimes branched (Lin et al., 2018). In addition, *Pseudoda. caryotae* sometimes have conidia with a hyaline, irregular appendage which is absent in *Pseudoda. brevis* (Lin et al., 2018). Based on phylogenetic placement and morphological variations, we introduce *Pseudoda. caryotae* as a new species.



Note a, b Colonies on substrate surface. c, d conidiogenous cells. e–i Conidia. j Germinating conidium. k The front of culture on PDA at 25°C and the reverse of culture on PDA at 25°C. Scale bars: c, d = 10 µm, e–j = 5 µm.

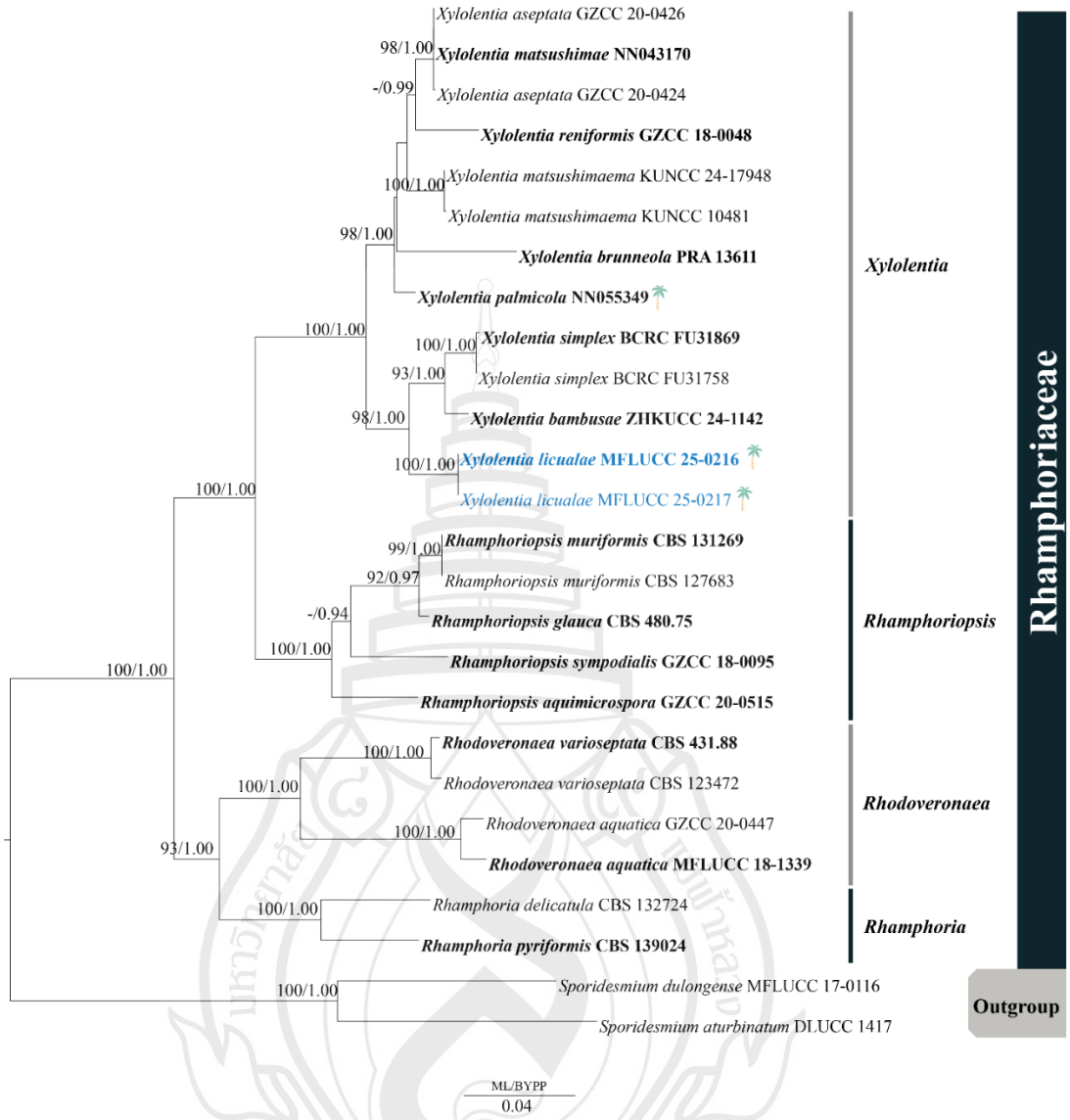
Figure 2.110 *Pseudodactylaria caryotae* (MHZU 23-0192, holotype)

Rhamphoriales K.D. Hyde & Hongsanan, Fungal Diversity 107: 94 (2021)

Rhamphoriaceae Réblová, Mycologia 11 (4): 754 (2018)

Xylolentia Réblová, Mycologia 11 (4): 759 (2018)

Notes: Réblová and Štěpánek (2018) established *Xylolentia* (*X.*) with *X. brunneola* as the type species. *Xylolentia* is a holomorphic genus with asexual morph characterized by macronematous, mononematous and unbranched or branched conidiophores, polyblastic conidiogenous cells with sympodially extending rachis, conidia ellipsoidal to obovoid, hyaline, becoming brown, and aseptate (Réblová & Štěpánek, 2018). Sexual morph is characterized by globose and glabrous ascomata with a cylindrical neck, unitunicate and cylindric-clavate asci with long pedicellate and an inamyloid apical ring, ascospores ellipsoidal to obovoid, brown, and septate (Réblová & Štěpánek, 2018). Based on morphological evidence and phylogenetic analysis combined SSU, LSU, and *rpb*2, Réblová and Štěpánek (2018) introduced *Xylolentia* as a new genus. Subsequently, phylogenetic studies mainly use ITS, LSU, SSU, *rpb*2 and *tef* 1-α or without ITS to analysis (Yang et al., 2023; Zhao et al., 2025). In this study, we use ITS, LSU, SSU, *rpb*2 and *tef* 1-α to update phylogenetic studies for *Xylolentia* (Figure 2.111). Currently, eight species are listed under *Xylolentia* (Index Fungorum, 2025 January) all species are associated with molecular data. Totally two species have been reported from palm species including a new species described in this study (Xiong et al., 2025).



Note Phylogram generated from maximum likelihood analysis of Rhamphoriaceae based on combined ITS, LSU, SSU, *rpb*2 and *tef* 1-α sequence data. Bootstrap values for maximum likelihood (ML) equal to or greater than 70 and BYPP values equal to or greater than 0.90 are indicated above the branches. The new collections are indicated in blue and ex-type strains are indicated in bold.

Figure 2.111 Phylogenetic tree of Rhamphoriaceae

Xylolentia licualae Y.R. Xiong, Manawas. & K.D. Hyde, ***sp. nov.***

Figure 2.112

Etymology: The epithet refers to the host genus name "*Licuala*", from which the species was collected.

Saprobic on dead petiole of *Licuala* sp. Asexual morph: Hyphomycetous. *Colonies* on wood effuse, hairy, scattered or aggregated, dark brown, with white conidial masses at the apex. *Mycelium* partly superficial, partly immersed, composed of septate, smooth-walled, brown hyphae. *Conidiophores* 80–130 × 3–4 μm ($\overline{x}$ = 110 × 3.7 μm, n = 25), macronematous, mononematous, erect, straight, or slightly flexuous, solitary or aggregated in small groups, cylindrical, smooth-walled, septate, unbranched, dark brown, becoming pale brown to subhyaline at the apex. *Conidiogenous cells* 15–20 × 3–4 μm ($\overline{x}$ = 17.7 × 3.5 μm, n = 25), polyblastic, integrated, elongating percurrently, terminal, determinate, cylindrical to cylindric-lageniform, phialidic at the apex, pale brown near the base, subhyaline to hyaline towards the apex, sympodially extending. *Conidia* 3.5–4.5 × 2–3 μm ($\overline{x}$ = 4.1 × 2.3 μm, n = 25), aggregated in slimy masses, acropleurogenous, simple, smooth, aseptate, reniform, exhibit a small concavity in the middle, hyaline. Sexual morph: Not observed.

Culture characteristics: Colonies on PDA, after 2 weeks reaching 3 cm diam. at 25°C, circular, dark, raised, with dark brown or white mycelium on the plicated and waxy-mucoid surface; reverse dark brown with entire margin.

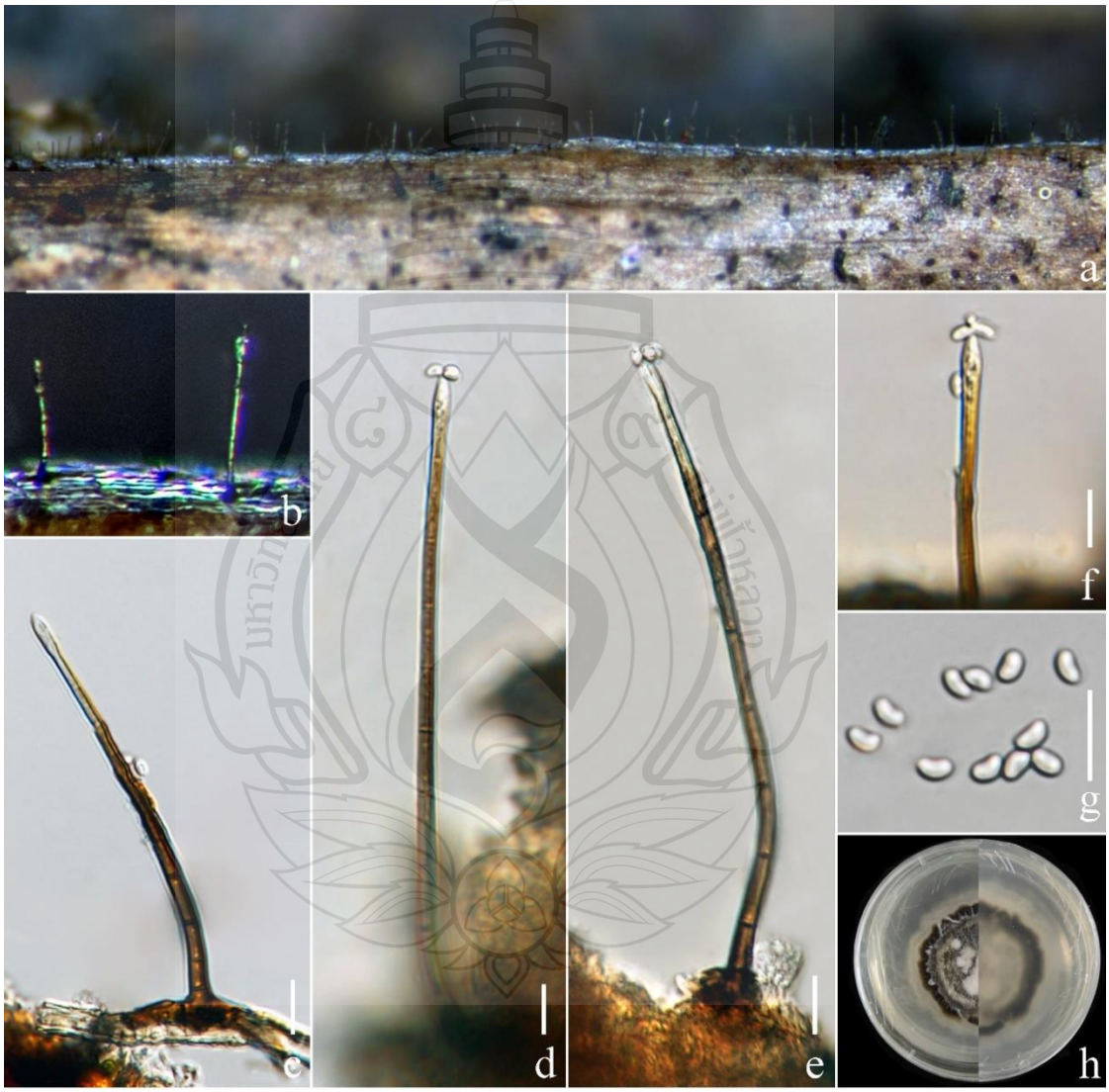
Known distribution: Thailand (this study).

Material examined: Thailand, Narathiwat Province, Toh Daeng Peat swamp, on dead petiole of *Licuala* sp., 4 Aug 2023, Y.R. Xiong, XG344 (MFLU 25-0153, holotype), ex-type MFLUCC 25-0216, other living culture MFLUCC 25-0217.

GenBank numbers: MFLUCC 25-0216: ITS – PV578274, LSU – PV578442, SSU – PV578560; MFLUCC 25-0217: ITS – PV578275, LSU – PV578443, SSU – PV578561.

Notes: Two collections from this study formed a separate lineage and clustered with *Xylolentia bambusae* and *X. simplex* in the phylogenetic tree with 98% ML bootstrap support and 1.00 BYPP (Figure 2.111). The nucleotide differences excluding gaps between *X. licualae* (MFLUCC 25-0216) and its phylogenetically related species were checked and given as follows *X. bambusae* (ZHKUCC 24-1142) - ITS: 5.00% (29/580 base pairs), LSU:

1.24% (11/888 base pairs); *X. simplex* (BCRC FU31869) - ITS: 5.56% (35/629 base pairs), LSU: 0.52% (3/575 base pairs). *Xylolentia licualae* has conidia with reniform and exhibits a small concavity in the middle (Figure 2.112). It not only differs from *X. bambusae* has hyaline, ellipsoidal, subglobose conidia, but it is also distinct from *X. simplex* has pale brown, ellipsoidal to reniform conidia (Kirschner & Hsieh, 2023; Zhao et al., 2025). Based on the phylogenetic placement and morphological variations, we introduce *X. licualae* as a new species.



Note a, b Colonies on substrate surface. c–f Conidiophore, conidiogenous cells with conidia. g Conidia. h The front of culture on PDA at 25°C and the reverse of culture on PDA at 25°C. Scale bars: c–g = 10 µm.

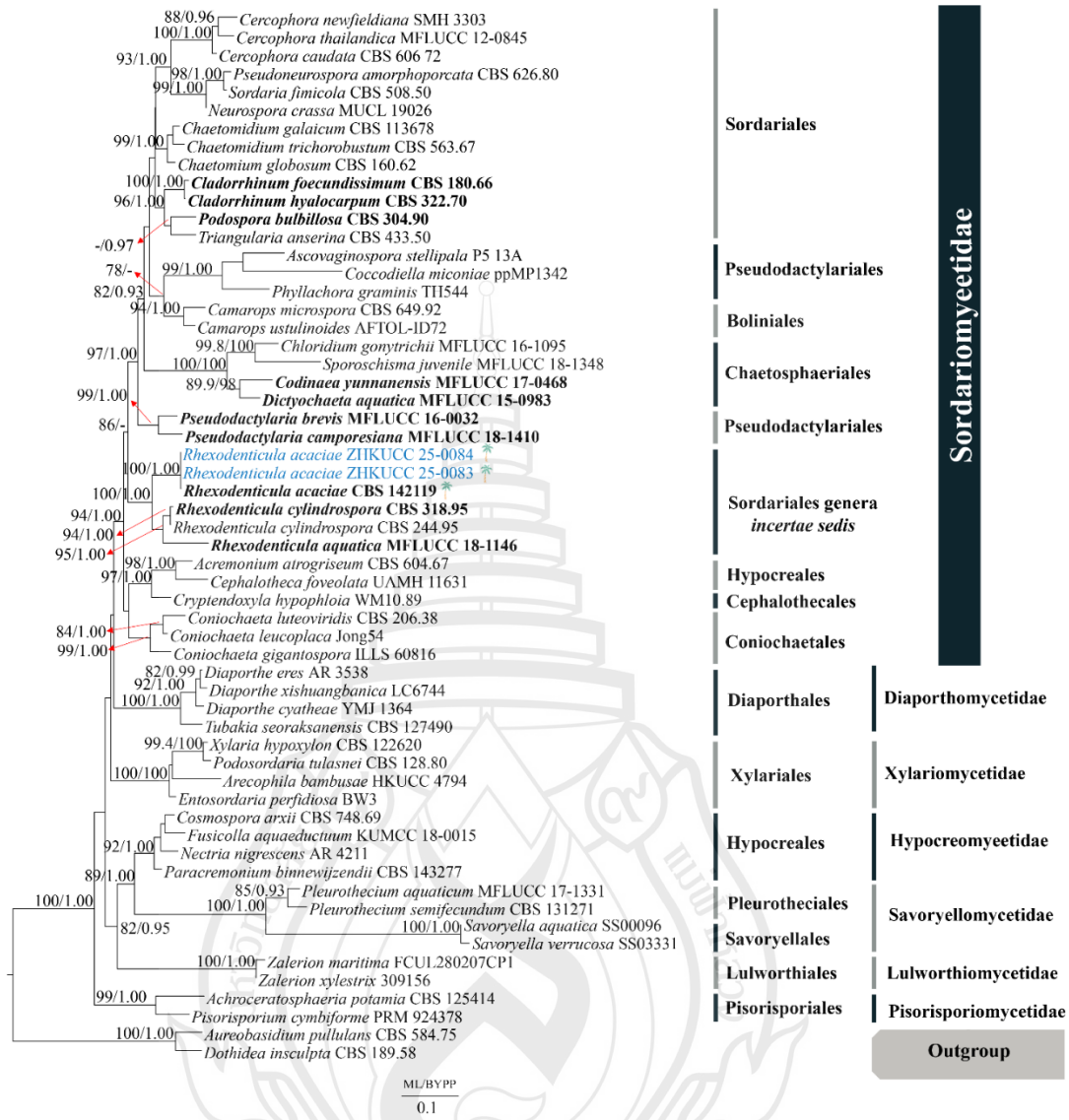
Figure 2.112 *Xylolentia licualae* (MFLU 25-0153, holotype)

Sordariales Chadef. ex D. Hawksw. & O.E. Erikss., Systema Ascomycetum 5: 182 (1986)

Sordariales genera *incertae sedis*

Rhexodenticula W.A. Baker & Morgan-Jones, Mycotaxon 79: 363 (2001)

Notes: Baker et al. (2001) established *Rhexodenticula* (*Rh*.) with *Rh. cylindrospora* as the type species. *Rhexodenticula* was reported as hyphomycetous genus which is characterized by macronematous, mononematous, solitary or caespitose, erect, cylindrical, simple, septate conidiophores polyblastic, integrated, denticulate conidiogenous cells, and cylindrical, fusiform, obclavate, fusoid-ellipsoid, pale to brown, and septate conidia (Baker et al., 2001; Crous et al., 2016). This study is the first report of the sexual morph for *Rhexodenticula* which is characterized by subglobose to ellipsoidal, subimmersed in the cortical tissue, erupting, papillate ascomata; peridium forming *textura angularis* cells; asci 8-spored, cylindrical, short pedunculate, bitunicate, fissitunicate, truncated ocular chamber and ascospores overlapping, biseriate, fusiform, septate, slightly constricted at septum, hyaline, with a gelatinous sheath. Klaubauf et al. (2014) first analysed *Rhexodenticula* by phylogenetic result which using LSU, combined morphological evidence placed *Rhexodenticula* to Sordariomycetes genera *incertae sedis*. Subsequently, phylogenetic studies mainly use ITS, LSU, SSU and *tef* 1-α for analysis (Dong et al., 2021). In this study, we use ITS, LSU, SSU and *tef* 1-α to update phylogenetic studies for *Rhexodenticula* (Figure 2.113). Currently, five epithets are listed under *Rhexodenticula* (Index Fungorum, 2025 January), and only three species are associated with molecular data. Here we described a new host record of *Rhexodenticula acaciae* from *Livistona chinensis*, which is the first time reported from palm species (Xiong et al., 2025)



Note Phylogram generated from maximum likelihood analysis of Sordariomycetidae and related families based on combined ITS, LSU, SSU and *tef* 1-α sequence data. Bootstrap values for maximum likelihood (ML) equal to or greater than 70 and BYPP values equal to or greater than 0.90 are indicated above the branches. The new collections are indicated in blue and ex-type strains are indicated in bold.

Figure 2.113 Phylogenetic tree of Sordariomycetidae and related families

Rhexodenticula acaciae Crous, Persoonia 37: 371 (2016)

Figure 2.114

Saprobic on dead segment of *Livistona chinensis*. Asexual morph: Not observed. Sexual morph: *Ascomata* 150–250 × 120–200 µm ($\overline{x}$ = 210 × 170 µm, n = 10), subglobose to ellipsoidal, subimmersed in the cortical tissue, erupting, papillate, dark brown, single or several joined together. *Peridium* 10–25 µm thick, composed of multi-layers of polygonal cells with large lumina, becoming flat towards the locule, forming *textura angularis* cells in longitudinal section, brow. *Hamathecium* 2.5–3 µm wide, composed of septate, pseudoparaphyses in a gelatinous matrix, sparingly branched. *Asci* 90–140 × 9–13 µm ($\overline{x}$ = 110 × 10.4 µm, n = 25), 8-spored, cylindrical, short pedunculate, bitunicate, fissitunicate, truncated ocular chamber. *Ascospores* 23–28 × 4–7 µm ($\overline{x}$ = 25 × 5.6 µm, n = 25), overlapping, biseriate, fusiform, 3-septate, slightly constricted at septum, hyaline, with a gelatinous sheath.

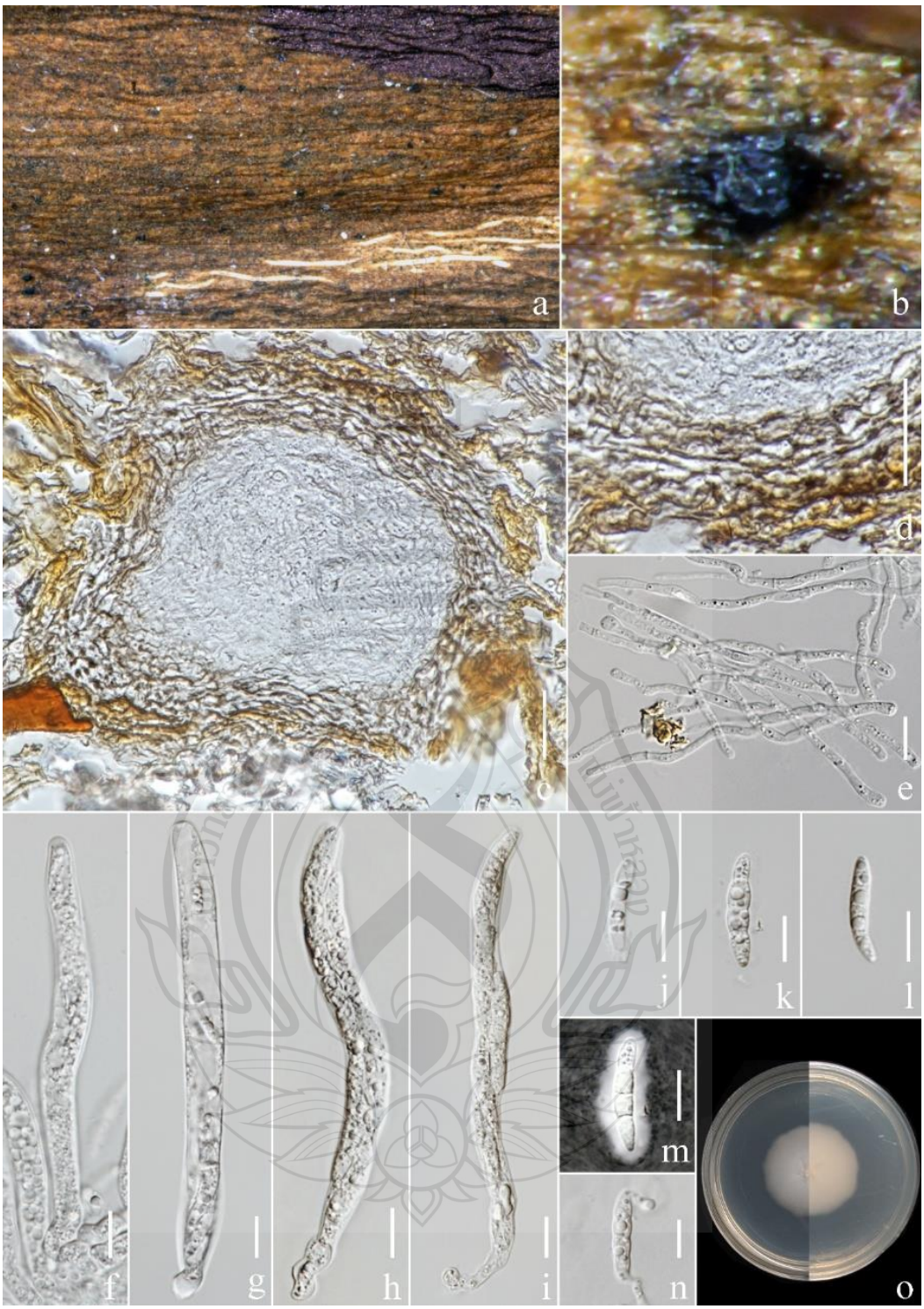
Culture characteristics: Colonies on PDA fast growing, after 2 weeks reaching 2–3 cm diam. at 25°C, circular, with fluffy, dense, white mycelium on the surface with entire margin; in reverse yellow in the middle and white at the margin.

Known distribution: Australia (Crous et al., 2016), China (this study)

Material examined: China, Jiangxi Province, Pingxiang City, Wugong Mountain National Scenic Area, on dead petiole of *Trachycarpus fortunei*, 13 Apr 2024, Y.R. Xiong, XG437 (MHZU 24-0469, new host record), living culture ZHKUCC 25-0083, other living culture ZHKUCC 25-0084.

GenBank numbers: ZHKUCC 25-0083: ITS – PV578248, LSU – PV578416, SSU – PV578546; ZHKUCC 25-0084: ITS – PV578249, LSU – PV578417, SSU – PV578547.

Notes: Two collections obtained in this study clustered with *Rhexodenticula acaciae* by 100% ML bootstrap support and 1.00 BYPP (Figure 2.113). The nucleotide differences excluding gaps between our collections and *Rh. acaciae* (CBS 142119) in ITS is 0.19% (1/521 base pairs). Our collection is the first sexual report for *Rh. acacia.* Therefore, based on phylogenetic analysis, we identified our collections as a new record of *Rh. acaciae*. *Rhexodenticula acaciae* was first introduced on leaves of *Acacia koa* from Australia by Crous et al. (2016).



Note a, b Ascomata on substrate. c Vertical sections of ascomata. d Peridium. e Hamathecium. f–i Asci. j–m Ascospore (m ascospore in Indian ink). n Germinating ascospore. o The front of culture on PDA at 25°C and the reverse of culture on PDA at 25°C. Scale bars: c, d = 20 µm; e–n = 10 µm.

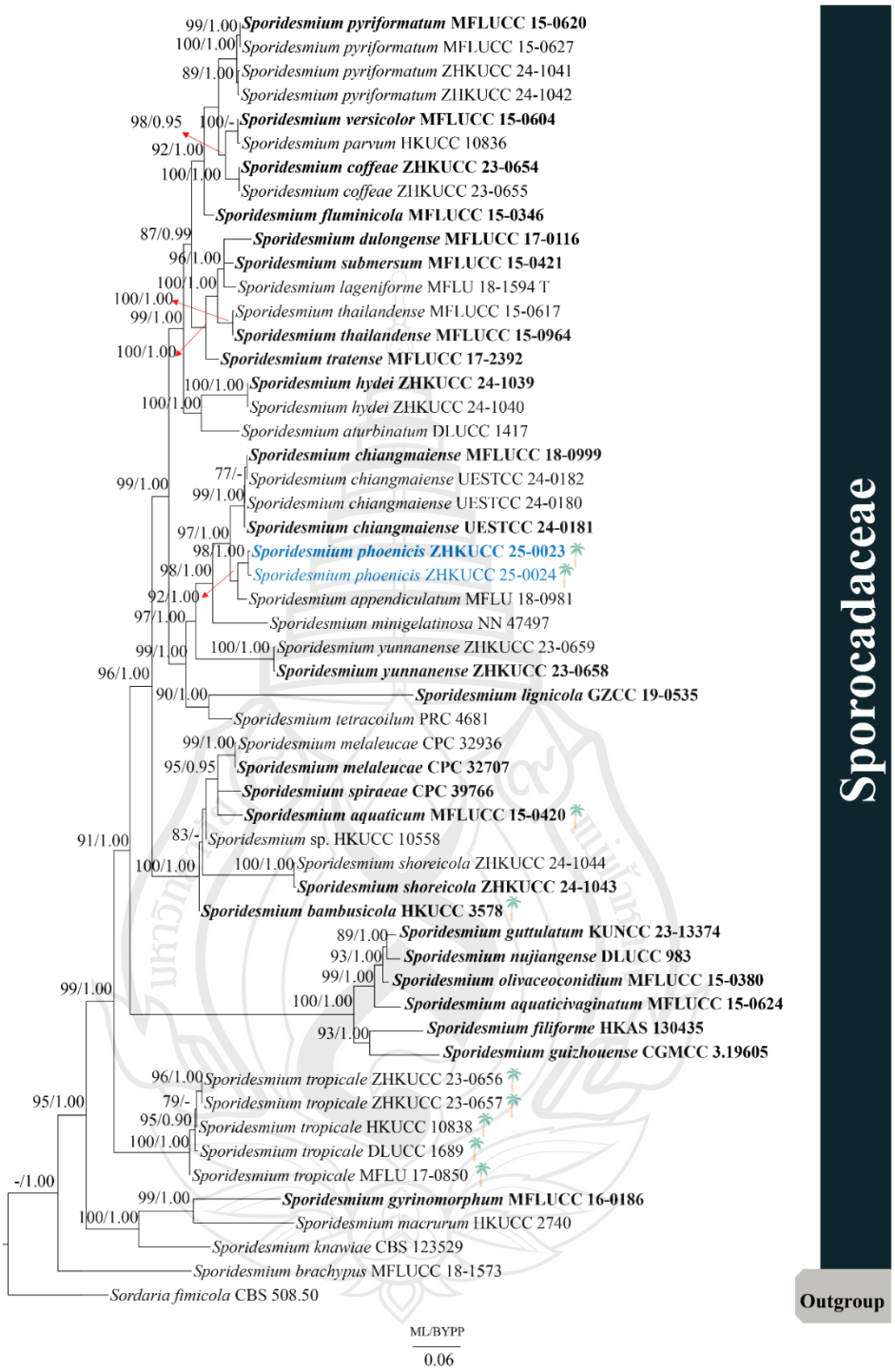
Figure 2.114 *Rhexodenticula acaciae* (MHZU 24-0469, new host record)

Sporidesmiales Crous, Persoonia 40: 377 (2018)

Sporidesmiaceae Fr., Summa vegetabilium Scandinaviae 2: 504 (1849)

Sporidesmium Link, Mag. Neuesten Entdeck. Gesammten Naturk. Ges. Naturf. Freunde Berlin 3 (1): 41 (1809)

Notes: *Sporidesmium* (*Sp.*) was established by Link (1809) with *S. atrum* as the type species. Most of *Sporidesmium* species reported as hyphomycetes, and the asexual morph is characterized by solitary or gregarious conidiophores, monoblastic conidiogenous cells, and pale brown to brown conidia with a hyaline apex and truncate base (Ellis, 1971; Su et al., 2016). Only *Sp. thailandense* and *Sp. lignicola* have been reported as sexual morphs, featuring cylindrical asci with a distinct, refractive, wedge-shaped and apical ring, and fusiform ascospores (Zhang et al., 2017; Luo et al., 2019). Shenoy et al. (2006) revealed the phenotypes of *Sporidesmium* and morphologically similar genera (*Ellisembia*, *Imimyces*, *Linkosia*, *Penzigomyces*, *Polydesmus*, *Repetophragma*, *Sporidesmiella* and *Stanjehughesia*) have multiple evolutionary origins, suggest *Sporidesmium* is polyphyletic. Later, many studies confirmed its polyphyletic in phylogenetics based on combined ITS, LSU, SSU, *rpb*2 and *tef*1-α sequence data, with species distributed across multiple families and orders in Dothideomycetes and Sordariomycetes (Su et al., 2016; Yang et al., 2018; Liu et al., 2019). In this study, we use ITS, LSU, SSU and *tef* 1-α to update phylogenetic studies for *Sporidesmium* (Figure 2.115). Over 500 epithets are listed under this genus (Index Fungorum, 2025), and only 32 species are associated with molecular data, as many species lack molecular data due to historical descriptions (Yang et al., 2018; Bao et al., 2021). Fifteen species have been reported from palm species including a new species described in this study (Xiong et al., 2025).



Note Phylogram generated from maximum likelihood analysis of *Sporidesmium* based on combined ITS, LSU, SSU and *tef* 1-α sequence data. Bootstrap values for maximum likelihood (ML) equal to or greater than 70 are indicated above the branches. The new collections are indicated in blue and ex-type strains are indicated in bold.

Figure 2.115 Phylogenetic tree of *Sporidesmium*

Sporidesmium phoenicis Y.R. Xiong, Manawas. & K.D. Hyde, ***sp. nov.***

Figure 2.116

Etymology: The epithet refers to the host species "*Phoenix*", from which the species was collected.

Saprobic on a dead segment of *Phoenix sylvestris*. Asexual morph: Hyphomycetous. *Colonies* effuse, hairy, scattered or in small groups, brown to black. *Mycelium* mostly immersed, composed of branched, septate, subhyaline, smooth hyphae. *Conidiophores* 35–65 × 6–7 µm ($\overline{x}$ = 44.6 × 6.2 µm, n = 20), macronematous, mononematous, solitary, cylindrical, straight or slightly flexuous, 1–3-septate, smooth-walled, reddish brown, truncate at apex. *Conidiogenous cells* 14–18 × 5.5–6.5 µm ($\overline{x}$ = 16.9 × 6.1 µm, n = 20), monoblastic, integrated, terminal, determinate, cylindrical, smooth-walled, brown. *Conidia* 45–65 × 12–15 µm ($\overline{x}$ = 58.5 × 13.1 µm, n = 20), acrogenous, solitary, brown, paler at the apex, obclavate, tapering gradually towards the apex, smooth-walled, straight, 10–11-distoseptate, guttulate, most with a mucilaginous sheath, subglobose, covering apical two cells, without appendages. Sexual morph: Not observed.

Culture characteristics: Colonies on PDA slowly growing, after 2 weeks reaching 2 cm diam., at 25°C, irregular, dense, flat, surface smooth, dry, with entire margin, white on the surface; reverse light yellow.

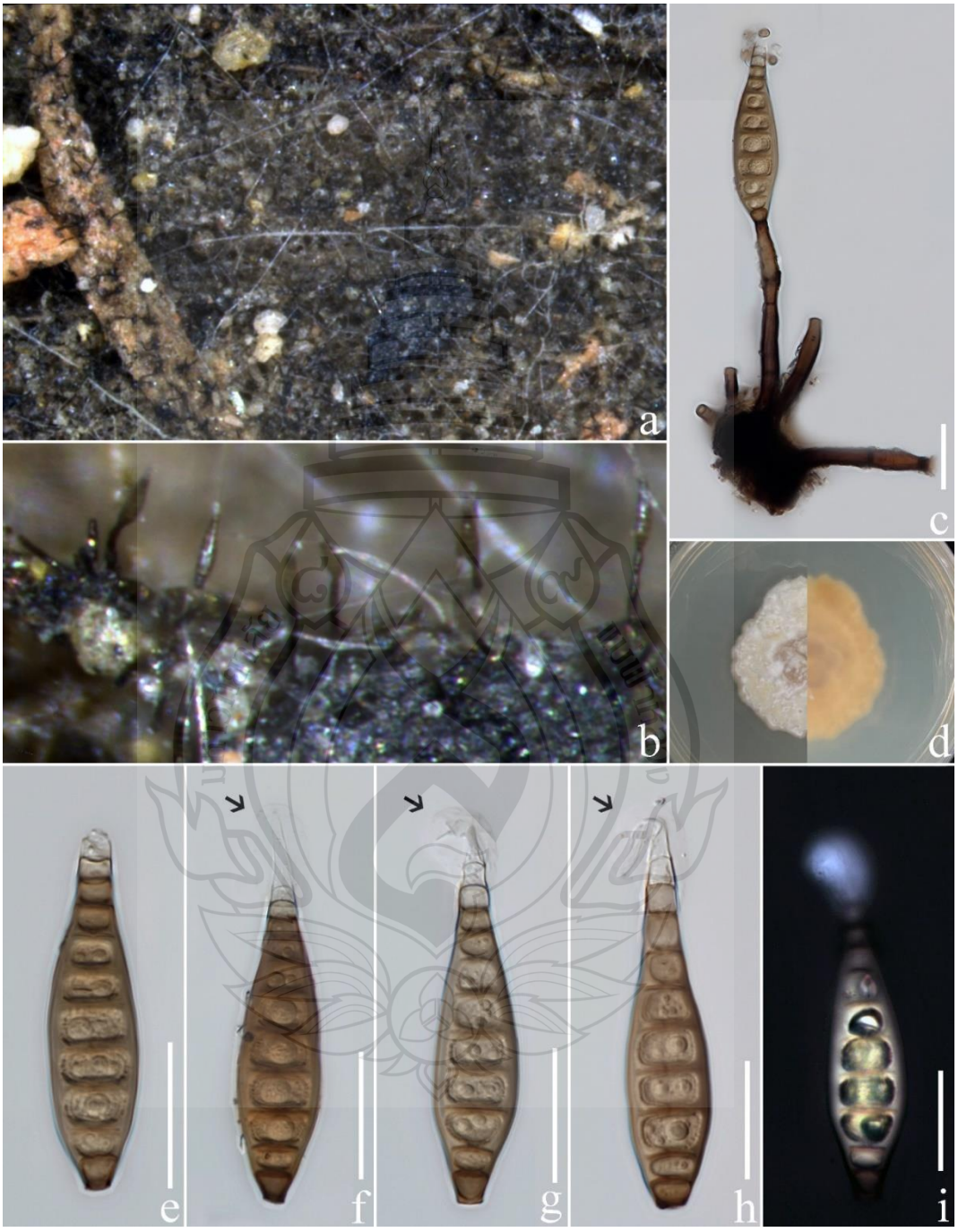
Known distribution: China (this study).

Material examined: China, Jiangxi Province, Ganzhou City, on dead segment of *Phoenix sylvestris*, 9 April 2024, Y.R. Xiong, XG366 (MHZU 24-0481, holotype), ex-type ZHKUCC 25-0023, other living culture ZHKUCC 25-0024.

GenBank numbers: ZHKUCC 25-0023: ITS – PV578256, LSU – PV578424, SSU – PV578552, *tef* 1-α – PV608894; ZHKUCC 25-0024: ITS – PV578257, LSU – PV578425, SSU – PV578553, *tef* 1-α – PV608895.

Notes: Two collections from this study formed a sister lineage to *Sporidesmium appendiculatum* in the phylogenetic tree with 94% ML bootstrap support and 1.00 BYPP (Figure 2.115). The nucleotide differences excluding gaps between our isolate (ZHKUCC 25-0023, ex-type) and *Sp. appendiculatum* (MFLU 18-0981, holotype) were checked and shown - ITS: 4.3% (22/507 base pairs), LSU: 0.7% (6/828 base pairs), and *Sp. appendiculatum* is lacking SSU and *tef* 1-α sequence data. Morphologically, our collection differs from *Sp. appendiculatum* by the subglobose sheath of conidia and without

appendages, while the conidia of *Sp. appendiculatum* has an oblong sheath and hypha-like appendages (Wang et al., 2016). Therefore, our collection introduced a new species, *Sp. phoenicis*, based on both phylogeny and morphology evidence.



Note a, b Colonies on the substrate. c Conidiophores with conidia. d The front of culture on PDA at 25°C and the reverse of culture on PDA at 25°C. e–h Conidia (arrows indicate the subglobose sheath). i Germinating conidium. Scale bars: c, e–i = 20 µm.

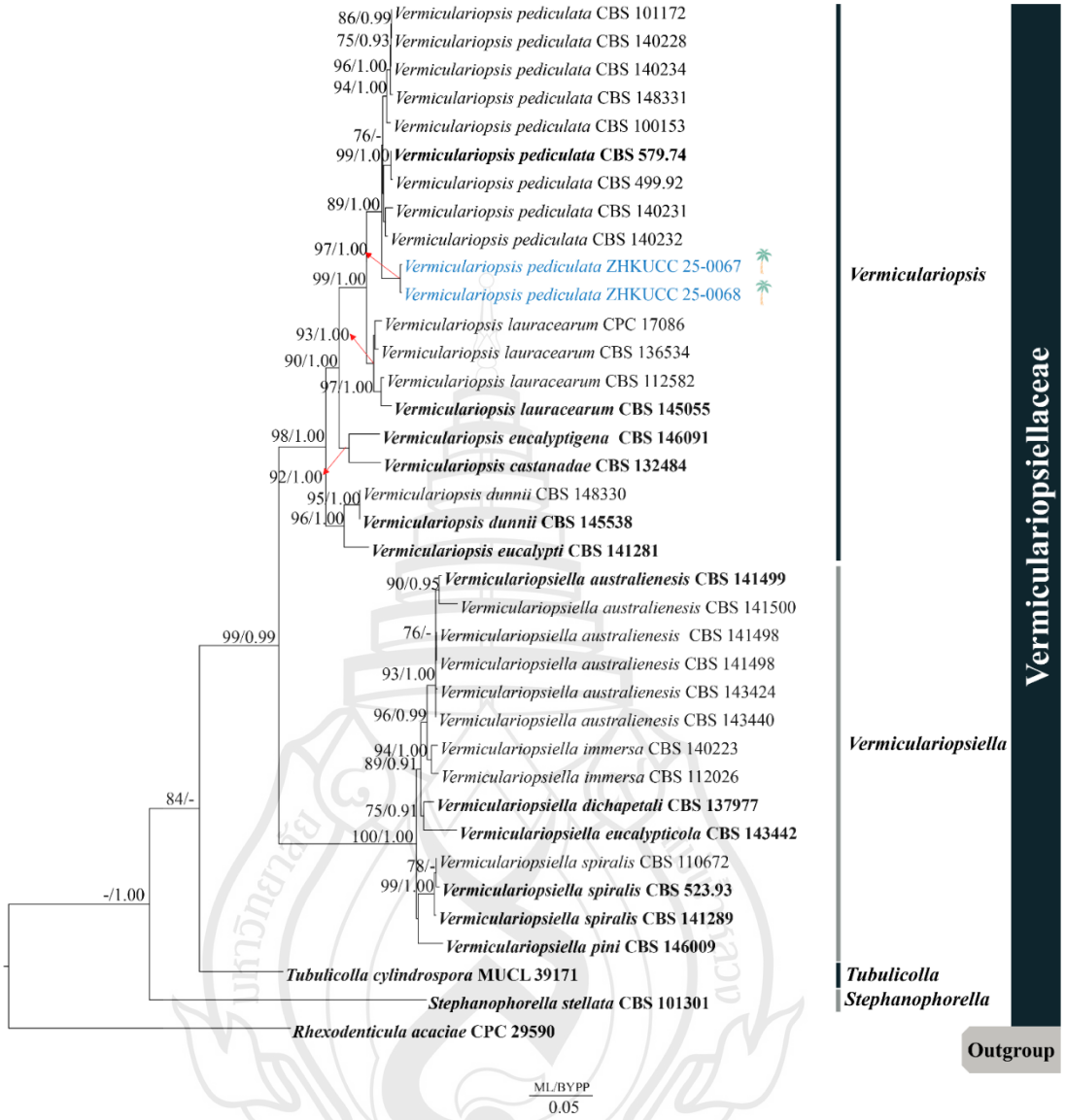
Figure 2.116 *Sporidesmium phoenicis* (MHZU 24-0481, holotype)

Vermiculariopsiellales Hern.-Rest., J. Mena, Gené & Crous, Studies in Mycology 86: 91 (2017)

Vermiculariopsiellaceae Hern.-Rest., J. Mena, Gené & Crous, Studies in Mycology 86: 91 (2017)

Vermiculariopsis Torrend, Brotéria Série Botânica 10: 41 (1912)

Notes: *Vermiculariopsis* (*Vs*.) was first introduced by Torrend (1912) and typified by *Vs. circinotricha*. The genus *Vermiculariopsis* has been resurrected to accommodate setose fungi characterized by branched setae (Hernãndez-Restrepo et al., 2022). Historically, *Vermiculariopsis* was considered a monotypic genus with morphological characters (branched setae) similar to those of some species in *Vermiculariopsiella* (Hernãndez-Restrepo et al., 2022). Crous et al. (2018) suggested that *Vermiculariopsis* might be the older name for *Vermiculariopsiella*, and no formal taxonomic changes were made at that time. Based on combined multi-locus analysis (ITS, LSU, *rpb*2) and morphological studies, Hernãndez-Restrepo et al. (2022) divided *Vermiculariopsiella* into two distinct clades. One clade, considered *Vermiculariopsiella*, includes the type species *V. immersa* along with *V. dichapetali* s.lat., *V. hongkongensis*, *V. eucalypticola*, *V. spiralis*, and *V. pini*. Another clade comprising *V. microsperma*, *V. pediculata*, *V. lauracearum*, *V. eucalyptigena*, *V. dunnii*, *V. eucalypti*, and additional collections previously classified as *Circinotrichum* sp. (CBS 148330) and *Gyrothrix* sp. (CBS 140234), has been reassigned to *Vermiculariopsis* (Hernãndez-Restrepo et al., 2022). In this study, we use ITS, LSU and *rpb*2 to update phylogenetic studies for *Vermiculariopsis* (Figure 2.117). There are eight species accepted in *Vermiculariopsis* (Index Fungorum, 2025 January), and only six species are associated with molecular data. To date, three species of *Vermiculariopsis* have been reported from palm species including a new host record described in this study (Xiong et al., 2025).



Note Phylogram generated from maximum likelihood analysis of Vermiculariopsiellaceae based on combined ITS, LSU and *rpb*2 sequence data. Bootstrap values for maximum likelihood (ML) equal to or greater than 70 are indicated above the branches. The new collections are indicated in blue and ex-type strains are indicated in bold.

Figure 2.117 Phylogenetic tree of Vermiculariopsiellaceae

Vermiculariopsis pediculata (J.L. Cunn.) Hern.-Restr & Crous, Persoonia 49: 130 (2022)

Figure 2.118

Saprobic on dead segment of *Trachycarpus fortunei*. Asexual morph: Hyphomycetous. *Colonies* on natural substrate superficial, effuse, velvety, brown, scattered. *Mycelium* superficial, composed of branched and anastomosing, smooth-walled, septate, subhyaline hyphae bearing conidiogenous cells and setae, becoming thickened and light brown at the point of origin of the setae. *Setae* 80–120 × 4–5 μm ($\overline{x}$ = 93 × 4.5 μm, n = 15), erect, dark brown to black, distinctly septate, surface rough and verruculose, upper part 2–4 times branched, half coiled, thin-walled, pale brown near the base, tapering at the tip and become subhyaline, branching imperfectly dichotomous, extremities spirally coiled, intertwined. *Conidiogenous cells* 5–10 × 3.5–5 μm ($\overline{x}$ = 7 × 3.8 μm, n = 20), phialidic, borne laterally on the superficial hyphae or swollen bases of setae, obclavate to ampullate, some subglobose, subhyaline, smooth-walled. *Conidia* adhering together to form a whitish pellicle at the base of setae, oblong to cylindrical when young, 6–11 × 2–3 μm ($\overline{x}$ = 9 × 2.9 μm, n = 25), fusiform when mature, 10–15 × 1.5–2.5 μm ($\overline{x}$ = 13 × 2 μm, n = 25), straight or slightly curved, hyaline, smooth-walled. Sexual morph: Not observed.

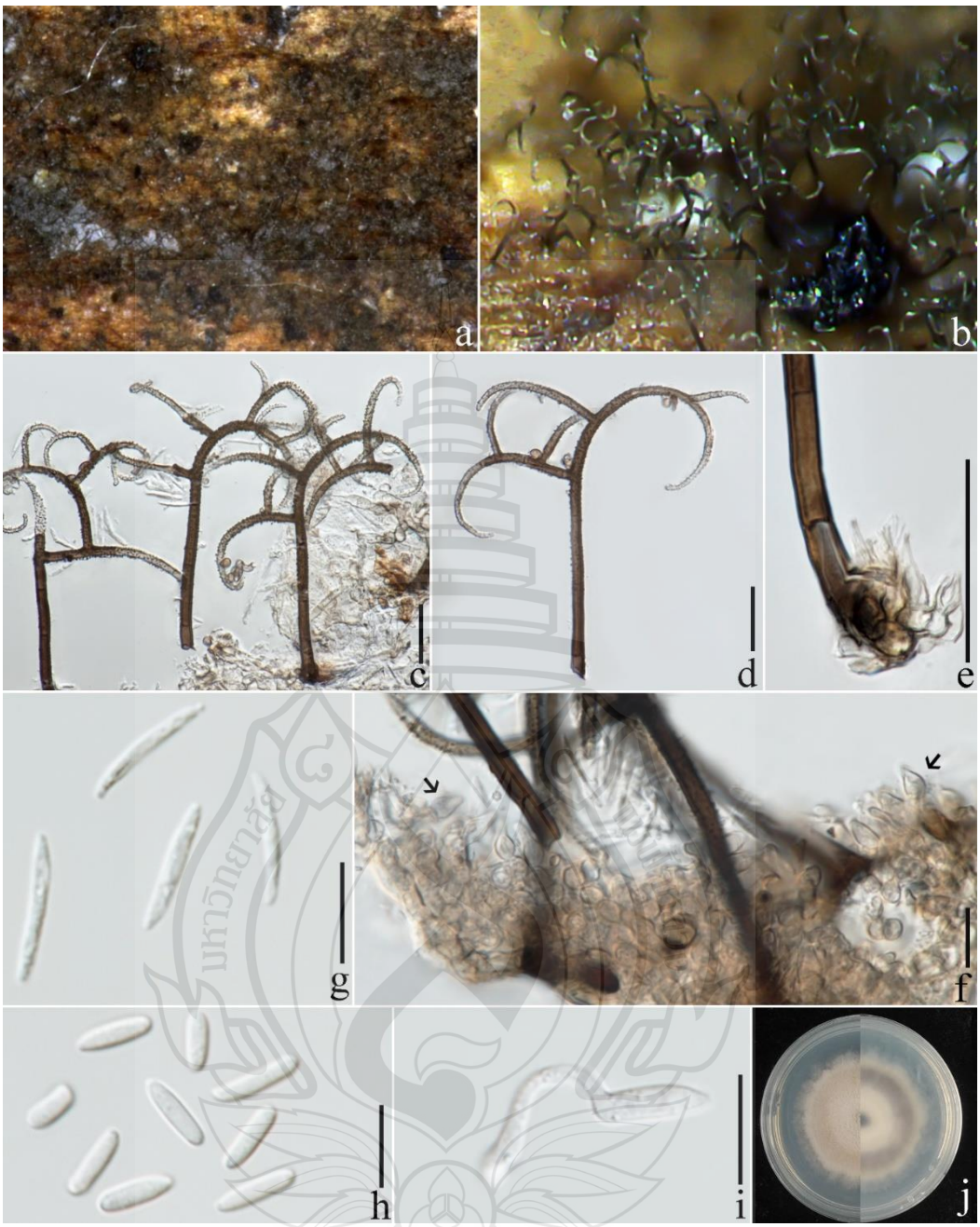
Culture characteristics: Colonies on PDA fast growing, after 2 weeks reaching 5 cm diam. at 25°C, circular, fluffy, flocculent, grey mycelium on the surface with lobate margin; in reverse white in the middle and light brown at the margin.

Known distribution: Australia (Hernãndez-Restrepo et al., 2022), Brazil (Hernãndez-Restrepo et al., 2022), Cuba (Hernãndez-Restrepo et al., 2022), France (Hernãndez-Restrepo et al., 2022), French Guiana (Hernãndez-Restrepo et al., 2022), Japan (Hernãndez-Restrepo et al., 2022), China (this study).

Material examined: China, Jiangxi Province, Pingxiang City, Wugong Mountain National Scenic Area, on dead segment of *Trachycarpus fortunei*, 12 Apr. 2024, Y.R. Xiong, XG419 (MHZU 24-0497, new host record), living culture ZHKUCC 25-0067, other living culture ZHKUCC 25-0068.

GenBank numbers: ZHKUCC 25-0067: ITS – PV578266, LSU – PV578434, *rpb2* – PV595370; ZHKUCC 25-0068: ITS – PV578267, LSU – PV578435, *rpb2* – PV595371.

Notes: Our collections formed a sister lineage under *Vs. pediculata* in the phylogenetic tree with 94% ML bootstrap support and 1.00 BYPP (Figure 2.117). The nucleotide differences excluding gaps between our collection and *Vs. pediculata* (CBS 579.74, ex-type) were checked and shown 0.8% (4/516 base pairs) in ITS, 0.5% (4/789 base pairs) in LSU, while 2.1% (15/693 base pairs) in *rpb*2. Our collections morph is well fit with *Vs. pediculata* (Hernãndez-Restrepo et al., 2022). Although our collections differ from *Vs. pediculata* by surface rough and verruculose of setae and shorter conidiogenous cells (5–10 × 3.5–5 µm vs. 10–24 × 3–5 µm) (Hernãndez-Restrepo et al., 2022). It might be caused by the environment and host. Based on phylogenetic placement and morphological variations, we introduce our collections as a new host record of *Vs. pediculata*.



Note a, b Colonies on substrate surface. c, d Setae. e, f Conidiogenous cells (arrows indicate the conidiogenous cells). g, h Conida. i Germinating conidium. j The front of culture on PDA at 25°C and the reverse of culture on PDA at 25°C. Scale bars: c, d = 20 µm, e–i = 10 µm.

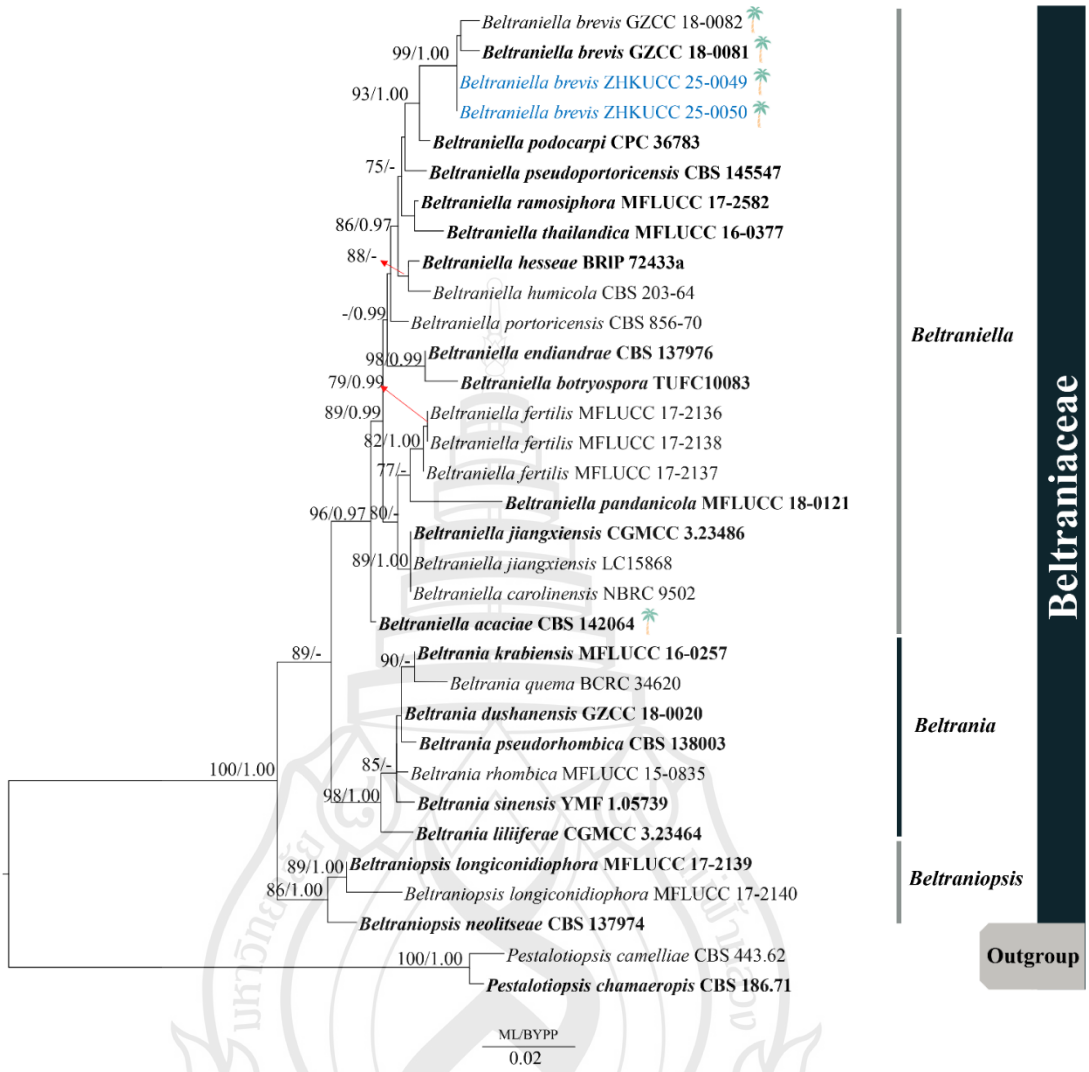
Figure 2.118 *Vermiculariopsis pediculata* (MHZU 24-0497, new host record)

Xylariales Nannf., Nova Acta Regiae Societatis Scientiarum Upsaliensis Ser. IV. 8 (2): 66 (1932)

Beltraniaceae Nann., Repertorio sistematico dei miceti dell' uomo e degli animali 4: 498 (1934)

Beltraniella Subram., Proc. Indian Acad. Sci., Sect. B 36 (6): 227 (1952)

Notes: *Beltraniella* (*Be.*) was introduced by Subramanian (1952) with *Be. odinae* as the type species. *Beltraniella* is anamorphic genus mainly consists of saprotrophic, litter-inhabiting ascomycetes, which are characterized by the presence of brown, unbranched setae and setiform conidiophores, polyblastic conidiogenous cells, sympodial, and denticulate, producing conidia in an acropleurogenous manner, turbinate or biconic conidia and feature a distinct hyaline transverse band at the equatorial zone (Subramanian, 1952; Hyde et al., 2020a). It is thought that their teleomorphs are in *Pseudomassaria* or *Leiosphaerella*, however, the detailed phylogenetic relationship of *Beltraniella* and these ascomycetous teleomorphs has not been examined (Kirk et al., 2008; Shirouzu et al., 2010). ITS and LSU are mainly used for phylogenetic analysis for this genus (Shirouzu et al., 2010; Hyde et al., 2020a, 2020b; Liu et al., 2024). Twenty-six species are accepted in Beltraniella (Crous et al., 2016b; Lin et al., 2017b; Tibpromma et al., 2018; Crous et al., 2019a). In this study, we use ITS, LSU and *rpb*2 to update phylogenetic studies for *Beltraniella* (Figure 2.119). There are 33 epithets accepted in *Beltraniella* (Index Fungorum, 2025 January), and only 15 species are associated with molecular data (Hyde, 2022a, 2020b; Liu et al., 2024). Two species have been reported from palm species including a new record described in this study (Xiong et al., 2025).



Note Phylogram generated from maximum likelihood analysis of Beltraniaceae based on combined ITS and LSU sequence data. Bootstrap values for maximum likelihood (ML) equal to or greater than 70 are indicated above the branches. The new collections are indicated in blue and ex-type strains are indicated in bold.

Figure 2.119 Phylogenetic tree of Beltraniaceae

Beltraniella brevis C.G. Lin, Jian K. Liu & K.D. Hyde, Asian Journal of Mycology 3 (1): 235 (2020)

Index Fungorum number: IF 556729; *Facesoffungi number*: FoF 06219; Figure 2.120

Saprobic on dead segment of *Trachycarpus fortunei*. Asexual morph: Hyphomycetous. *Colonies* on plant substrate effuse, straight, brown to black. *Mycelium*

mostly immersed in the substratum. *Setae* 100–282 × 4–7 μm ($\overline{x}$ = 192 × 5.5 μm, n = 10), numerous, erect, arising from radially lobed basal cells, straight or flexuous, unbranched, single or in small groups, thick-walled, verrucose, dark brown, paler at the apex, tapering to a pointed apex. *Conidiophores* macronematous, short, simple or branched, septate, sometimes reduced to conidiogenous cells, smooth-walled, subhyaline to pale brown, thin-walled, arising from basal cells of setae or from separate. *Conidiogenous cells* 5–12 × 4–7 μm ($\overline{x}$ = 9.2 × 5.6 μm, n = 20), polyblastic, integrated, determinate, terminal, ampulliform or subcylindrical, hyaline to subhyaline, smooth. *Separating cells* 10–17 × 3.7–5 μm ($\overline{x}$ = 14.5 × 4 μm, n = 25), fusiform, tapering to a pointed apex, thin-walled, smooth, hyaline to subhyaline, 1-denticulate at each end. *Conidia* 19–25 × 5.5–7 μm ($\overline{x}$ = 22 × 6.4 μm, n = 25), arise directly from conidiogenous cells or from separating cells, aggregated, acrogenous, simple, dry, straight, smooth, thin-walled, turbinate to pyriform, rostrate to pointed at proximal end, truncate at distal end, hyaline with a hyaline supraequatorial transverse band. Sexual morph: Not observed.

Culture characteristics: Colonies on PDA fast growing, after 2 weeks reaching 9 cm diam. at 25°C, dense, cream from above, spongy, velutinous, with filiform edge, grey from reverse., septate.

Known distribution: China (Hyde et al., 2020b; this study).

Material examined: China, Jiangxi Province, Nanchang City, Meiling National Forest Park, on dead segment of *Trachycarpus fortunei*, 11 April 2024, Y.R. Xiong, XG392 (MHZU 24-0488, new host record), living culture ZHKUCC 25-0049, other living culture ZHKUCC 25-0050.

GenBank numbers: ZHKUCC 25-0049: ITS – PV578136, LSU – PV578306; ZHKUCC 25-0050: ITS – PV578137, LSU – PV578307.

Notes: Two collections obtained in this study clustered with *Beltraniella brevis* by 99% ML bootstrap support and 1.00 BYPP (Figure 2.119). The nucleotide differences excluding gaps between our collection (ZHKUCC 25-0049) and *Be. brevis* (GZCC 18-0081, ex-type) in ITS is 0.17% (1/556 base pairs) and LSU is 0.6% (5/766 base pairs). Morphological evidence of brown and erect setae and hyaline conidia with separating cells are well fit with *Be. brevis* (Hyde et al., 2020b). Therefore, based on morphology and phylogenetic analysis, we identified our collections as new records of *Be. brevis*. *Beltraniella brevis* was first introduced on decaying leaves of unknown hosts from China

by Hyde et al. (2020b). To our knowledge, this is the first report of this species collected from *Trachycarpus fortune* from China.



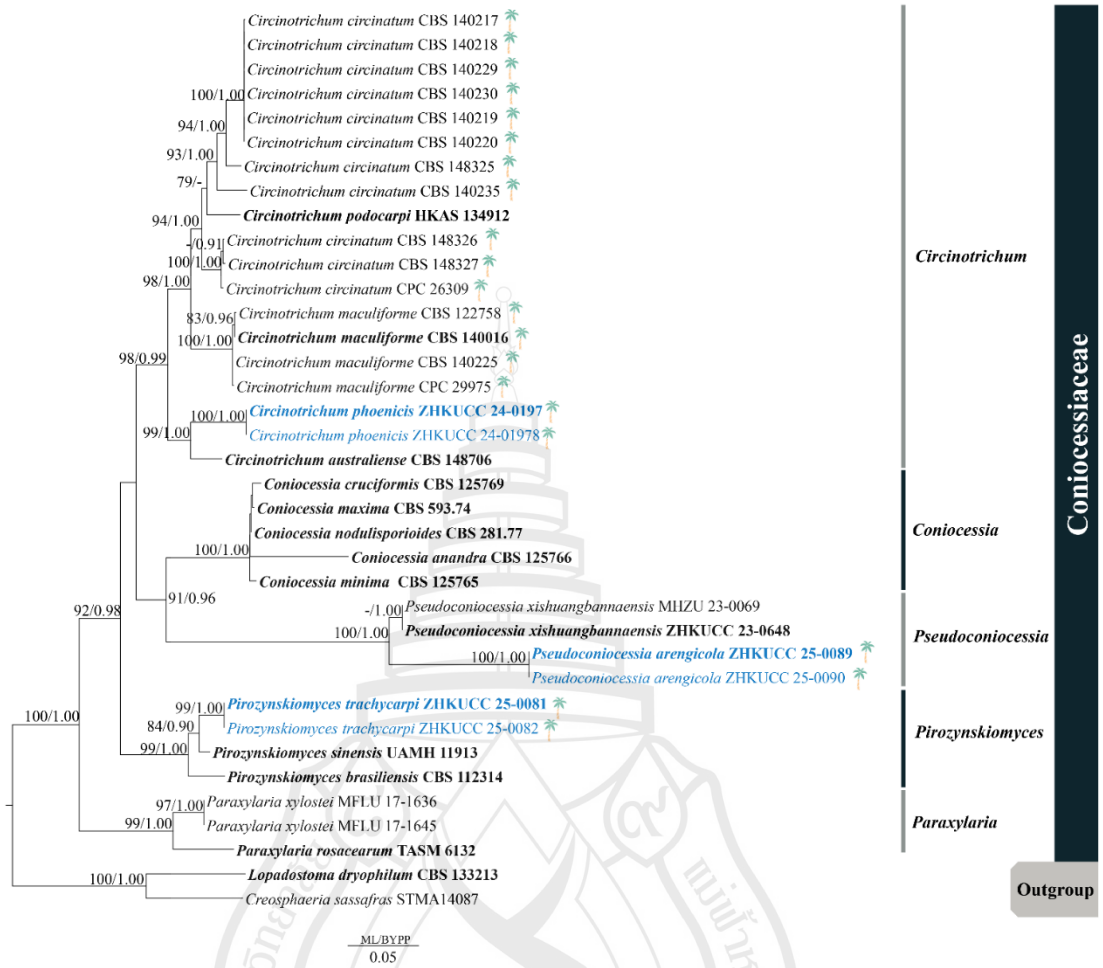
Note a, b Conidiophores on host surface. c, d Setae. e, f Conidiogenous cells. g–j Conidia. k, l Conidia with separating cells. m The front of culture on PDA at 25°C and the reverse of culture on PDA at 25°C. Scale bars: c, d = 30 µm; e–l = 10 µm.

Figure 2.120 *Beltraniella brevis* (MHZU 24-0488, new host record)

Coniocessiaceae Asgari & Zare, Mycological Progress 10 (2): 195 (2011)

Circinotrichum Nees, Syst. Pilze (Würzburg): 19 (1816)

Notes: Nees von Esenbeck (1817) established *Circinotrichum* (*Cir*.) with *Cir. maculiforme* as the type species. *Circinotrichum* is a hyphomycetous genus characterized by setae simple or branched and initially smooth becoming verrucose, conidiogenous cells born laterally on the superficial hyphae and polyblastic, and conidia cylindrical to fusoid and aggregated into a dry whitish layer at the base of the setae (Nees von Esenbeck, 1817; Hernández-Restrepo et al., 2022). Hernández-Restrepo et al. (2022) reassessed *Circinotrichum* based on morphological evidence and phylogenetic analysis combined ITS, LSU, and *rpb*2. Subsequently, phylogenetic studies mainly use ITS, LSU, and *rpb*2 in species identification (Tian et al., 2024). In this study, we use ITS, LSU, *rpb*2 and *tub*2 to update phylogenetic analysis of *Circinotrichum* (Figure 2.121). Currently, 20 species are listed under *Circinotrichum* (Index Fungorum, 2025 January), and only four species are associated with molecular data. To date, only two species have been reported palm species including a new species described in this study (Xiong et al., 2025).



Note Phylogram generated from maximum likelihood analysis of Coniocessiaceae based on combined ITS, LSU, *rpb*2 and *tub*2 sequence data. Bootstrap values for maximum likelihood (ML) equal to or greater than 70 are indicated above the branches. The new collections are indicated in blue and ex-type strains are indicated in bold.

Figure 2.121 Phylogenetic tree of Coniocessiaceae

Circinotrichum phoenicis Y.R. Xiong, Manawas. & K.D. Hyde, ***sp. nov.***

Figure 2.122

Etymology: The epithet refers to the host genus name "*Phoenix*", from which the species was collected.

Saprobic on dead petiole of *Phoenix canariensis*. Asexual morph: Hyphomycetous. *Colonies* on natural substrate superficial, effuse, velvety, dark brown to black. *Mycelium* superficial, branched, smooth-walled, aseptate, hyaline. *Setae* 2–4 µm

wide, multi-times sub-dichotomously to irregularly branched, brown, numerous, intertwined, erect, septate, thick-walled, initially root smooth-walled, becoming verrucose; branches terminatio paler in colour, verrucose, circinate. *Conidiogenous cells* 5–7 × 2–4 µm ($\overline{x}$ = 6.4 × 3 µm, n = 15), borne laterally on the superficial hyphae or swollen bases of setae, short ampulliform, subhyaline, smooth. *Conidia* 10–13 × 1.5–2.5 µm ($\overline{x}$ = 11.9 × 2 µm, n = 25), adhering together to form a greyish pellicle at the base of setae, hyaline, smooth, straight or slightly curved, cylindrical to fusiform. Sexual morph: Not observed.

Culture characteristics: Colonies on PDA, after 2 weeks reaching 4 cm diam., at 25°C, irregular, with fluffy, dense, white mycelium on the surface with undulate margin; in reverse yellow in the middle and white at the margin.

Known distribution: China (this study).

Material examined: China, Yunnan Province, Xishuangbanna City, on dead petiole of *Phoenix canariensis*, 4 Feb 2023, Y.R. Xiong and L. Lu, XG301 (MHZU 23-0195, holotype) – ex-type ZHKUCC 24-0197, other living culture ZHKUCC 24-0198.

GenBank numbers: ZHKUCC 24-0197: ITS – PV578146, LSU – PV578316, *rpb*2 – PV595308; ZHKUCC 24-0198: ITS – PV578147, LSU – PV578317, *rpb*2 – PV595309.

Notes: Two collections from this study clustered in *Circinotrichum* clade and formed a sister lineage to *Cir. australiense* in the phylogenetic tree with 100% ML bootstrap support and 1.00 BYPP. The nucleotide differences excluding gaps between *Cir. phoenicis* (ZHKUCC 24-0197) and *Cir. australiense* (CBS 148706) were checked and given as follows, ITS: 4.67% (24/514 base pairs), LSU: 1.12% (9/802 base pairs), and *rpb*2: 10.41% (69/663 base pairs). *Circinotrichum phoenicis* has setae with multi-times sub-dichotomously to irregularly branched and intertwined which is different from *Cir. australiense* have setae with L- or T-basal cells giving rise to a network of aggregated conidiogenous cells and irregularly branched (Hernández-Restrepo et al., 2022, Figure 2.122). Moreover, conidiogenous cells also a characteristic to distinct them which *Cir. phoenicis* are short ampulliform, *Cir. australiense* are subcylindrical to lageniform (Hernández-Restrepo et al., 2022, Figure 2.122). Based on the phylogenetic placement and morphological variations, we introduce *Cir. phoenicis* as a new species.



Note a, b Colonies on substrate surface. c–e Branched setae. f–h Conidiogenous cells. i Conidia. j The front of culture on PDA at 25°C and the reverse of culture on PDA at 25°C. Scale bars: c–i = 10 µm.

Figure 2.122 *Circinotrichum phoenicis* (MHZU 23-0195, holotype)

Pirozynskiomyces Hern.-Restr. & Crous, Persoonia 49: 111 (2022)

Notes: Hernández-Restrepo et al. (2022) established *Pirozynskiomyces* (*Pir*.) with *Pir. brasiliensis* as the type species and accommodate *Pir. sinensis* based on morphological evidence and phylogenetic analysis combined ITS, LSU, and *rpb2* sequence data. *Pirozynskiomyces* is hyphomycetous genus characterized by simple or branched and verrucose setae with straight or flexuous or coiled, conidiophores reduced to conidiogenous cells, polyblastic and ampulliform to lageniform conidiogenous cells, conidia curved or falcate and obtuse at the base and abruptly attenuate with a cellular appendage at the apex (adjust according to Hernández-Restrepo et al., 2022). In this study, we use ITS, LSU and *rpb*2 to update phylogenetic studies for *Pirozynskiomyces* (Figure 2.121). Currently, three epithets are listed under *Pirozynskiomyces* (Index Fungorum, 2025 January) with all species associated with molecular data. Here we described a new species of *Pirozynskiomyces* which is the first time reported from palm species (Xiong et al., 2025).

Pirozynskiomyces trachycarpi Y.R. Xiong, Manawas. & K.D. Hyde, ***sp. nov.***

Figure 2.123

Etymology: The epithet refers to the host genus name "*Trachycarpus*", from which the species was collected.

Saprobic on dead leaf sheath of *Trachycarpus fortunei*. Asexual morph: Hyphomycetous. *Colonies* on natural substrate superficial, hair, white to grey, aggregate. *Mycelium* immersed, composed of hyaline, smooth, septate, branched hyphae. *Setae* 110–140 × 4.5–5.5 μm ($\overline{x}$ = 127 × 4.9 μm, n = 15), erect, unbranched, solitary or in clusters of 2, evenly distributed throughout colony, lower part verruculose, upper part coiled in 1–2 coiledloops, thick-walled, dark brown. *Conidiophores* reduced to conidiogenous cells. *Conidiogenous cells* 5–15 × 4–5 μm ($\overline{x}$ = 9.5 × 4.5 μm, n = 25), ampulliform to lageniform, polyblastic, thin-walled, smooth, solitary or gregarious at the base of setae, pale brown to hyaline. *Conidia* 15–25 × 2–3 μm ($\overline{x}$ = 18.9 × 2.4 μm, n = 25), falcate, hyaline, smooth, attenuate with a short cellular appendage at the apex, base with small truncatescar or attenuate. Sexual morph: Not observed.

Culture characteristics: Colonies on PDA fast growing, after 2 weeks reaching 4 cm diam. at 25°C, irregular, umbonate, with dense, dirty white mycelium on the surface with crateriform and entire margin; in reverse yellow in the middle and white at the margin.

Known distribution: China (this study).

Material examined: China, Jiangxi Province, Nanchang City, The road next to Meiling National Forest Park, on dead leaf sheath of *Trachycarpus fortunei*, 5 Feb 2023, Y.R. Xiong, XG432 (MHZU 24-0468, holotype), ex-type ZHKUCC 25-0081, other living culture ZHKUCC 25-0082.

GenBank numbers: ZHKUCC 25-0081: ITS – PV578226, LSU – PV578392, *rpb2* – PV595346; ZHKUCC 25-0082: ITS – PV578227, LSU – PV578393, *rpb2* – PV595347.

Notes: Two collections from this study formed a separate lineage and clustered with *Pirozynskiomyces sinensis* in the phylogenetic tree with 91% ML bootstrap support and 1.00 BYPP (Figure 2.121). The nucleotide differences excluding gaps between *Pir. trachycarpi* (ZHKUCC 25-0081) and *Pir. sinensis* (UAMH 11913) were checked and given as follows, ITS: 2.90% (16/550 base pairs). *Pirozynskiomyces trachycarpi* have setae with coiled in 1–2 coiledloops which differs from *Pir. sinensis* have setae with straight or flexuous (Li et al., 2017). Based on phylogenetic placement and morphological variations, we introduce *Pir. trachycarpi* as a new species.



Note a, b Colonies on substrate surface. c–k Setae. f, g Conidia. h Germinating conidium. i Conidiogenous cell. m The front of culture on PDA at 25℃ and the reverse of culture on PDA at 25℃. Scale bars: c–i = 10 μm.

Figure 2.123 *Pirozynskiomyces trachycarpi* (MHZU 24-0468, holotype)

Pseudoconiocessia L. Lu & Tibpromma, Phytotaxa 641 (2): 130 (2024)

Notes: Lu et al. (2024) established *Pseudoconiocessia* (*Pseudoci.*) with *Pseudoci. xishuangbannaensis* as the type species based on morphological evidence and phylogenetic analysis of combined ITS, LSU, and *rpb*2. *Pseudoconiocessia* was only reported from its sexual morph which is characterized by carbonaceous and clypeus ascomata, unitunicate, furcate pedicel and apical ring of asci with 4–8-spored, ascospores uniseriate, fusiform or ellipsoid and aseptate with germ slit present when mature (Lu et al., 2024). In this study, we use ITS, LSU, and *rpb*2 to update phylogenetic analyses of *Pseudoconiocessia* (Figure 2.121). *Pseudoconiocessia* is a monotypic genus (Index Fungorum, 2025 January) with all species associated with molecular data. Here we

described a new species which is the first time reported from palm species (Xiong et al., 2025).

Pseudoconiocessia arengicola Y.R. Xiong, Manawas. & K.D. Hyde, ***sp. nov.***

Figure 2.124

Etymology: The epithet refers to the host genus name "*Arenga*", from which the species was collected.

Saprobic on dead petiole of *Arenga tremula*. Asexual morph: Not observed. Sexual morph: *Ascomata* pseudothecium, immersed, hemispherical to lenticular, immersed under a black clypeus, black, coriaceous, solitary to gregarious, unilocular or multilocular, forming black round spots. *Clypeus* up to 850 μm, black, considerably exceeding the locular in size. *Locular* 220–300 × 130–190 μm ($\bar{x}$ = 264 × 154 μm, n = 10), globose to subglobose, single. *Peridium* 25–45 μm, multilayers, comprising several layers, outer layer brown, thick-walled *textura angular* cells, inner layer light brown to hyaline. *Hamathecium* 1–2 μm wide paraphyses, numerous, branched, septate, hyaline, embedded in a gelatinous matrix. *Asci* 50–70 × 4–5 μm ($\bar{x}$ = 63 × 4.3 μm, n = 25) 8-spored, unitunicate, long-cylindrical to clavate, short-pedicellate, pedicellate, straight or slightly curved, apically rounded, with a wedge-shaped apical ring. *Ascospores* 6.5–8 × 3–4 μm ($\bar{x}$ = 7.1 × 3.4 μm, n = 40) uniseriate, brown, aseptate, with conspicuous warts, germ slit on ventral side of the ascospore, straight, nearly the spore-length, lacking mucilaginous sheath.

Culture characteristics: Colonies on PDA fast growing, after 2 weeks reaching 2 cm diam., at 25°C, irregular, corvex, dense, mycelium cream towards the lobate margin; reverse brown.

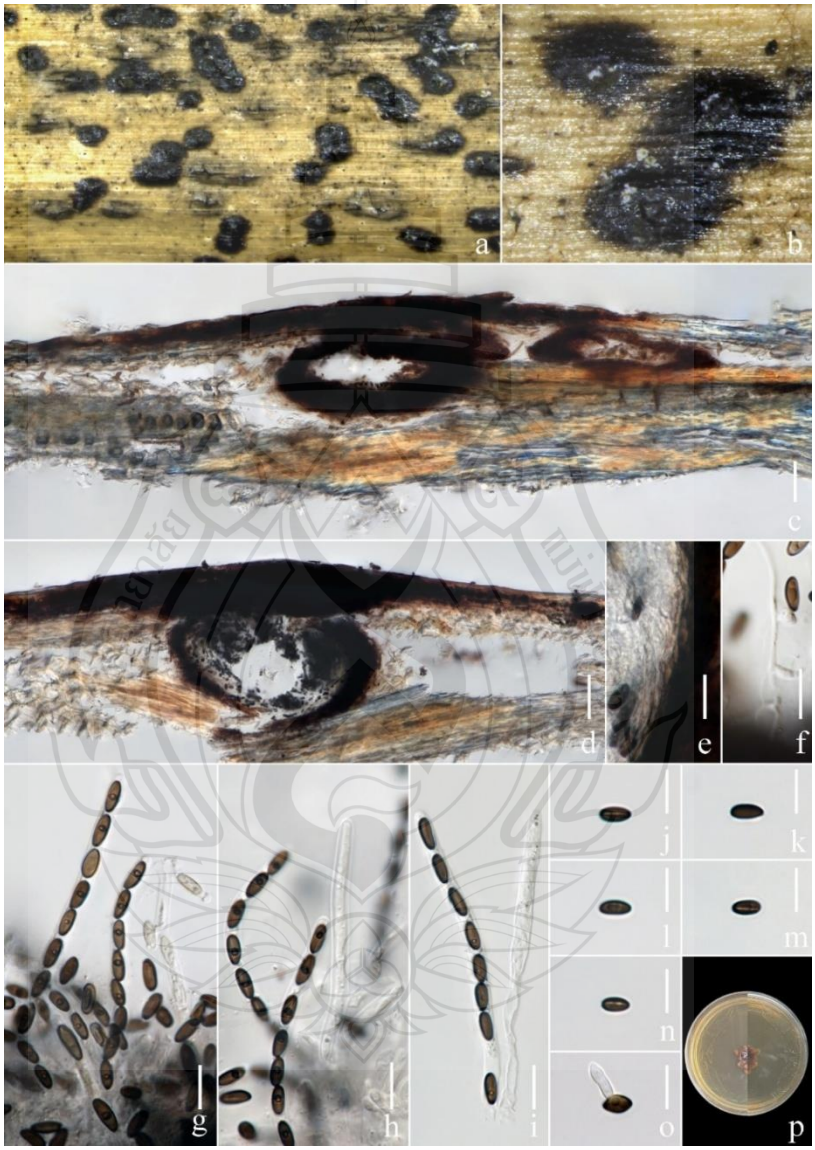
Known distribution: China (this study).

Material examined: China, Yunnan Province, Xishuangbanna City, unknown forest, on dead petiole of *Arenga tremula*, 4 Feb 2023, Y.R. Xiong & L. Lu, XG307 (MHZU 25-1055, holotype), ex-type ZHKUCC 25-0089, other living culture ZHKUCC 25-0090.

GenBank numbers: ZHKUCC 25-0089: ITS – PV578234, LSU – PV578400, *tub*2 – PV607966, *tef* 1-α – PV608882; ZHKUCC 25-0090: ITS – PV578235, LSU – PV578401, *tub*2 – PV607967, *tef* 1-α – PV608883.

Notes: Two collections from this study clustered in *Pseudoconiocessia* clade in Coniocessiaceae and formed a sister lineage to *Pseudoci. xishuangbannaensis* in the phylogenetic tree with 100% ML bootstrap support and 1.00 BYPP (Figure 2.121). The

nucleotide differences excluding gaps between *Pseudoci. arengicola* and *Pseudoci. xishuangbannaensis* were checked and given as follows; ITS: 1.67% (9/538 base pairs), and LSU: 13.35% (112/839 base pairs). *Pseudoconiocessia arengicola* differs from *Pseudoci. xishuangbannaensis* by clypeus considerably exceeding the locular in size (Lu et al., 2024). Based on phylogenetic placement and morphological variations, we introduce *Pseudoci. arengicola* as a new species.



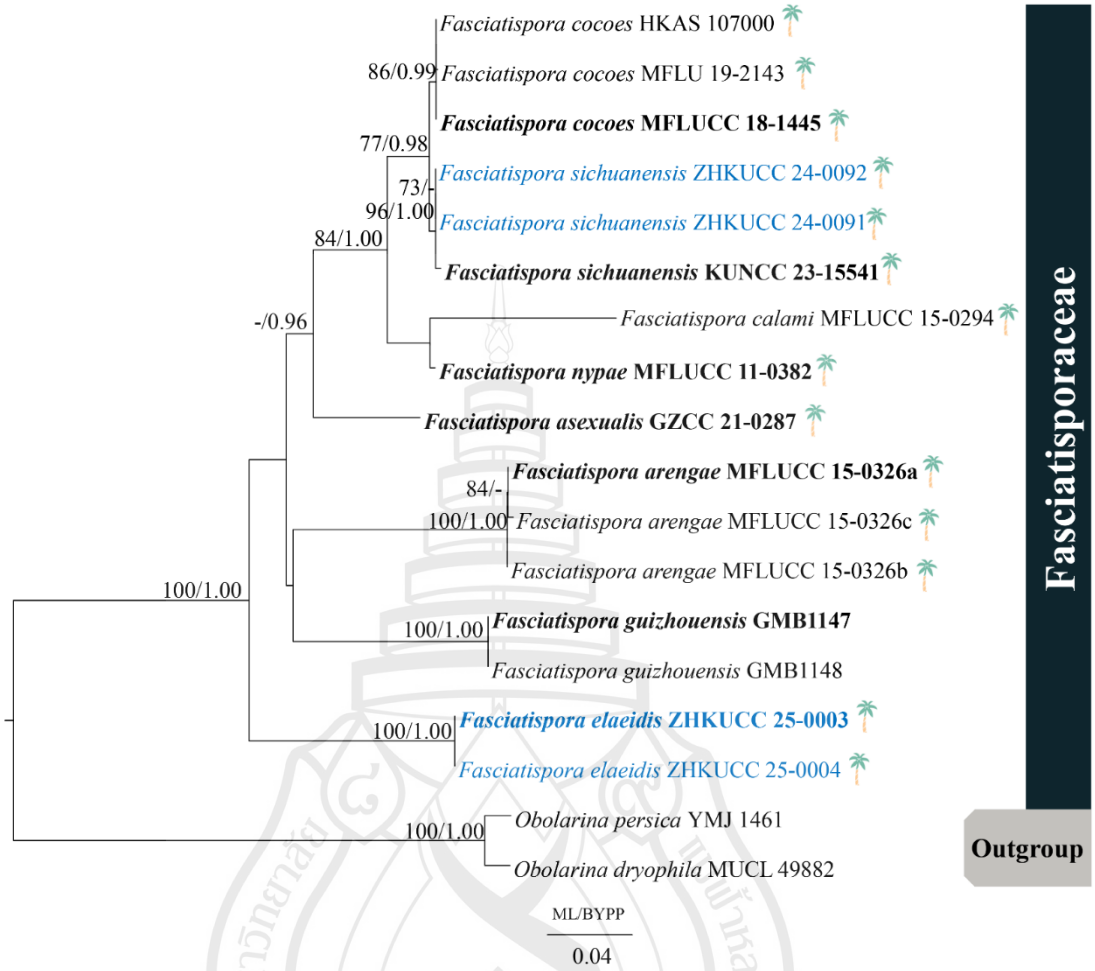
Note a, b Ascomata on substrate. c, d Vertical sections of ascomata. e Peridium. f Hamathecium. g–i Asci. j–n Ascospore. o Germinating ascospore. p The front of culture on PDA at 25℃ and the reverse of culture on PDA at 25℃. Scale bars: c, d = 50 µm, e–o = 10 µm.

Figure 2.124 *Pseudoconiocessia arengicola* (MHZU 25-1055, holotype)

Fasciatisporaceae S.N. Zhang, K.D. Hyde & J.K. Liu, Fungal Diversity 100: 227 (2020)

Fasciatispora K.D. Hyde, Transactions of the Mycological Society of Japan 32: 265 (1991)

Notes: Hyde et al. (1991) established *Fasciatispora* (*Fa*.) with *Fa. nypae* as type species. The sexual morph *Fasciatispora* is characterized by beneath a clypeus of ascomata, wedge-shaped subapical ring of asci, and pale brown to brown, ellipsoidal, ovoid or rhomboid, aseptate ascospores with a central pallid band (Hyde et al., 2020). Asexual morph is characterized by colonies on the substratum superficial, conidiophores arising from the stromata with macronematous and unbranched, conidiogenous cells holoblastic and integrated, conidia brown or reddish-brown and with or without a hyaline inconspicuous longitudinal slit (Zhang et al., 2024). Based on morphological evidence and phylogenetic analysis combined ITS, LSU, *rpb*2, *tub*2, SSU and *tef* 1-α data, Hyde et al. (2020) placed *Fasciatispora* in Fasciatisporaceae. Subsequently, phylogenetic studies mainly use LSU, SSU, *rpb2* and *tef* 1-α or *tub*2 data in species delineation (Dissanayake et al., 2024; Zhang et al., 2024). In this study, we use ITS, LSU, *rpb*2, *tub*2, SSU and *tef* 1-α to update phylogenetic studies for *Fasciatispora* (Figure 2.125). Currently, 13 epithets are listed under *Fasciatispora* (Index Fungorum, 2025 January), and only seven species are associated with molecular data. Totally 12 species have been reported from palm species including one new species and one new host recorded and described in this study (Xiong et al., 2025).



Note Phylogram generated from maximum likelihood analysis of some of Fasciatisporaceae based on combined ITS, LSU, *rpb*2, *tub*2, SSU and *tef* 1-α sequence data. Bootstrap values for maximum likelihood (ML) equal to or greater than 70 are indicated above the branches. The new collections are indicated in blue and ex-type strains are indicated in bold.

Figure 2.125 Phylogenetic tree of Fasciatisporaceae

Fasciatispora elaeidis Y.R. Xiong, Manawas. & K.D. Hyde, ***sp. nov.***

Figure 2.126

Etymology: The epithet refers to the host genus name "*elaeis*", from which the species was collected.

Saprobic on dead petiole of *Elaeis guineensis*. Asexual morph: Not observed. Sexual morph: *Ascomata* 380–460 × 130–150 µm ($\bar{x}$ = 410 × 135 µm, n = 10), immersed,

visible as black, circular convex, sometimes solitary, mostly aggregated into small groups, globose, multilocular, beneath a clypeus. *Locular* 100–180 × 90–150 µm ($\bar{x}$ = 134 × 111 µm, n = 10), globose to sub-globose. *Peridium* 10–20 µm wide, 3–5-layered, comprising brown, thick-walled cells of *textura angularis* and *textura globulosa*. *Hamathecium* 3–5 µm wide, septate, branched, hyaline, numerous, paraphysoids. *Asci* 70–100 × 10–15 µm ($\bar{x}$ = 82 × 12.5 µm, n = 25), 8-spored, unitunicate, cylindrical, short pedicellate, inconspicuous wedge-shaped apical ring, apex rounded. *Ascospores* 14–17 × 7–9 µm ($\bar{x}$ = 15.8 × 7.9 µm, n = 25), uniseriate, or biseriate at middle of asci, ellipsoidal to obovoid, aseptate, hyaline when immature, brown when mature, with wide umbilicated at medium or upper part, verruculose, surround by a mucilaginous sheath.

Culture characteristics: Colonies on PDA fast growing, after 2 weeks reaching 4 cm diam. at 25°C, circular, with fluffy, dense mycelium on the surface, medium yellowish, white margin; in reverse yellow in the middle and white at the margin.

Known distribution: China (this study).

Material examined: China, Yunnan Province, Xishuangbanna City, in an unidentified forest beside National Highway 219, on dead petiole of *Elaeis guineensis*, 5 Feb 2023, Y.R. Xiong and L. Lu, XG178 (MHZU 24-0452, holotype), ex-type ZHKUCC 25-0003, other living culture ZHKUCC 25-0004.

GenBank numbers: ZHKUCC 25-0003: ITS – PV578174, LSU – PV578338, SSU – PV578496, *tef* 1-α – PV608844, *rpb*2 – PV595324, *tub*2 – PV584061; ZHKUCC 25-0004: ITS – PV578175, LSU – PV578339, SSU – PV578497, *tef* 1-α – PV608845, *rpb*2 – PV595325, *tub*2 – PV584062.

Notes: Two collections from this study formed a distinct lineage within *Fasciatispora* in the phylogenetic tree with 100% ML bootstrap support and 1.00 BYPP (Figure 2.125). Based on a MegaBLAST (Query cover ≥ 70%) search using the ITS sequence, the closest matches in NCBIs GenBank nucleotide database were *Xylaria sp.* (GenBank JX156382; Identities 348/373 (93.30%), 4 gap), *Vamsapriya* sp. (GenBank PQ568141; Identities 342/370 (92.43%), 6 gaps) and *Vamsapriya uniseptata* (GenBank PP407904; Identities 334/363 (92.01%), 8 gaps). The highest similarities using the LSU sequence were *Fasciatispora nypae* (GenBank KP744484; Identities 825/844 (97.75%), 4 gap), *Fasciatispora cocoes* (GenBank PP593428; Identities 827/848 (97.52%), 5 gaps) and *Fasciatispora calami* (GenBank NG066198; Identities 826/847 (97.52%), 5 gaps). The

highest similarities using the SSU sequence were *Induratia apiospora* (GenBank NG242948; Identities 1013/1025 (98.83%), 0 gap), *Astrocystis* sp. (GenBank OM836751; Identities 1013/1026 (98.73%), 1 gaps) and *Geniculisynnema termiticola* (GenBank AB274812; Identities 1013/1026 (98.73%), 2 gaps). The highest similarities using the *tef* 1-α sequence were *Vamsapriya* sp. (GenBank MW759506; Identities 812/937 (86.66%), 10 gap), *Metacordyceps liangshanensis* (GenBank EF468756; Identities 817/943 (86.64%), 7 gaps) and Cordycipitaceae sp. (GenBank OR115233; Identities 820/948 (86.50%), 8 gaps). The highest similarities using the *tub*2 sequence were *Fusarium lactis* (GenBank FR870322; Identities 230/268 (85.82%), 9 gap), *Clonostachys solani* (GenBank OQ982853; Identities 241/281 (85.77%), 18 gaps) and *Clonostachys aureofulvella* (GenBank OQ982576; Identities 241/281 (85.77%), 18 gaps). The highest similarities using the *rpb*2 sequence were *Biscogniauxia citriformis* (GenBank JX507780; Identities 794/1004 (79.08%), 20 gap), *Biscogniauxia cylindrispora* (GenBank JX507782; Identities 788/998 (78.96%), 10 gaps) and *Biscogniauxia marginata* (GenBank KU684310; Identities 786/996 (78.92%), 14 gaps). Morphologically, *Fa. elaeidis* differs from other species in *Fasciatispora* by multilocular ascomata and verruculose ascospores. Based on phylogenetic placement and morphological variations, we introduce *Fa. elaeidis* as a new species.



Note a, b Ascomata on substrate. c Vertical sections of ascomata. d Peridium. e Hamathecium. f–k Asci. l–r Ascospore (r ascospore in Indian ink). s Germinating ascospore. t The front of culture on PDA at 25°C and the reverse of culture on PDA at 25°C. Scale bars: c = 50 µm, d–s = 10 µm.

Figure 2.126 *Fasciatispora elaeidis* (MHZU 24-0452, holotype)

Fasciatispora sichuanensis L.S. Dissan., K.D. Hyde & J.C. Kang, Mycosphere 15(1), 1675–1793 (2024)

Figure 2.127

Saprobic on dead leaf sheath of *Arenga obtusifolia*. Asexual morph: Not observed. Sexual morph: *Ascomata* 200–290 × 130–180 μm ($\overline{x}$ = 242 × 160 μm, n = 10), pseudothecium, semi-immersed, visible as black, circular dots, mostly solitary, sometimes aggregated into small groups, globose, beneath a clypeus, with ostioles. *Peridium* 20–30 μm wide, multi-layered, outer layer comprising brown, thick-walled cells of *textura angularis*. *Hamathecium* 2–3 μm wide, septate, branched, hyaline, numerous, filamentous, paraphysoids. *Asci* 70–110 × 8–11 μm ($\overline{x}$ = 89 × 9.5 μm, n = 25), 8-spored, unitunicate, cylindrical, short pedicellate, inconspicuous apical ring, apex rounded. *Ascospores* 13–16 × 6–8 μm ($\overline{x}$ = 14.4 × 6.8 μm, n = 25), uniseriate, ellipsoidal to obovoid, aseptate, hyaline when immature, brown when mature, with wide umbilicated equatorial pallid band, smooth, guttulate (1–2 large guttules at the center), without a mucilaginous sheath and lacking a germ slit.

Culture characteristics: Colonies on PDA fast growing, after 2 weeks reaching 4 cm diam. at 25°C, circular, with fluffy, white mycelium on the surface, sparse at the edge, dense in the middle and outwardly strongly radiating; in reverse cream.

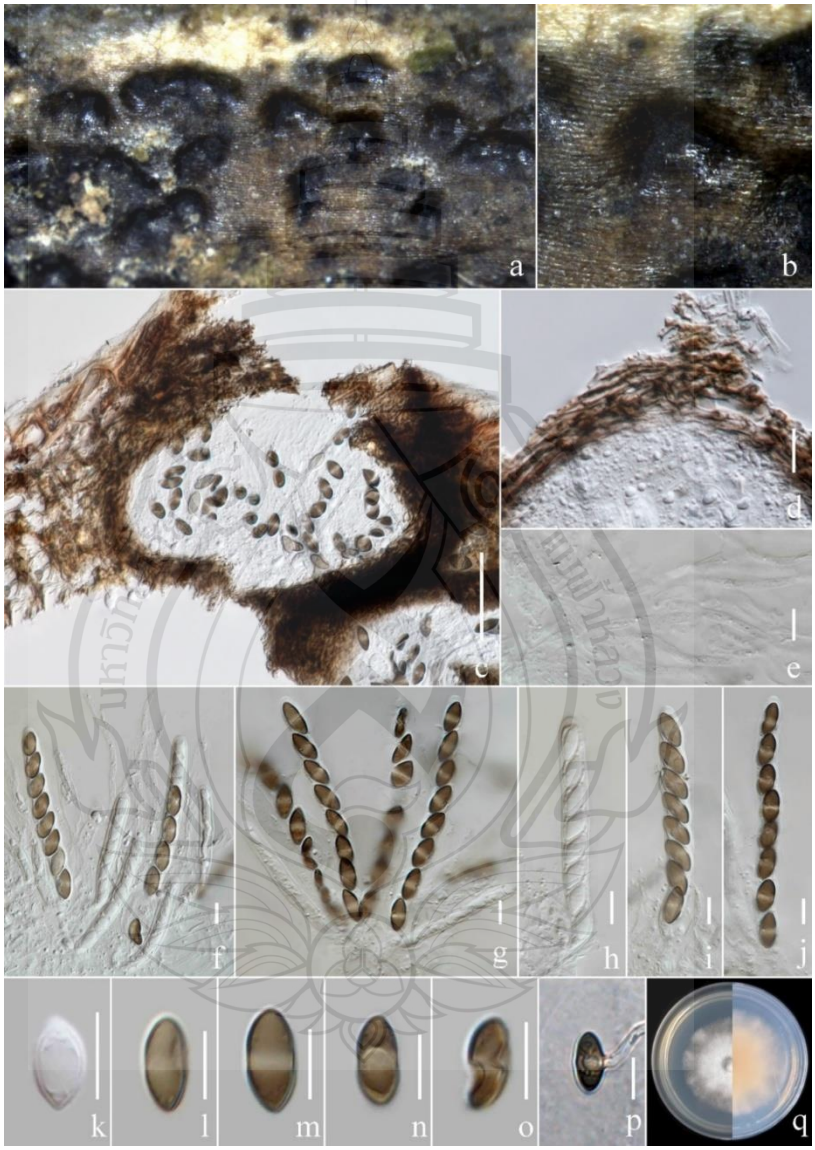
Known distribution: China (Dissanayake et al., 2024, this study).

Material examined: China, Yunnan Province, Xishuangbanna City, in an unidentified forest beside National Highway 219, on dead leaf sheath of *Arenga obtusifolia*, 5 Feb 2023, Y.R. Xiong and L. Lu, XG161 (MHZU 23-0142, new host record) – ex-type ZHKUCC 24-0091, other living culture ZHKUCC 24-0092.

GenBank numbers: ZHKUCC 24-0091: ITS – PV578176, LSU – PV578340, SSU – PV578498, *tef* 1-α – PV608846, *rpb*2 – PV595326, *tub*2 – PV584063; ZHKUCC 24-0092: ITS – PV578177, LSU – PV578341, SSU – PV578499, *tef* 1-α – PV608847, *rpb*2 – PV595327, *tub*2 – PV584064.

Notes: Two collections obtained in this study clustered with *Fasciatispora sichuanensis* by 100% ML bootstrap support and 0.99 BYPP (Figure 2.125). The nucleotide differences excluding gaps between our collections and *Fa. sichuanensis* (KUNCC 23-15541) in ITS is 0.42% (2/478 base pairs). Morphological evidence of unitunicate, cylindrical asci and ascospore with wide equatorial pallid band are well fit with

Fa. sichuanensis (Dissanayake et al., 2024). Therefore, based on morphology and phylogenetic analysis, we identified our collections as *Fa. sichuanensis*. *Fasciatispora sichuanensis* was first introduced as a dead twig of *Poacea*e sp. from China by Dissanayake et al. (2024), Xiong et al. (2025) reported a new record on dead petiole of *Wodyetia bifurcate* from China. To our knowledge, this is the first report of *Fa. sichuanensis* from *Arenga obtusifolia.*



Note a, b Ascomata on substrate. c Vertical sections of ascomata. d Peridium. e Hamathecium. f–j Asci. l–o Ascospore. p Germinating ascospore. q The front of culture on PDA at 25℃ and the reverse of culture on PDA at 25℃. Scale bars: c = 50 µm, d–p = 10 µm.

Figure 2.127 *Fasciatispora sichuanensis* (MHZU 23-0142, new host record)

Cannoniaceae Y.R. Xiong, Manawas. & K.D. Hyde, ***fam. nov.***

Etymology: refers to the name of the type genus.

Type genus: *Cannonia* Joanne E. Taylor & K.D. Hyde

Saprobic on dead palm substrates. Asexual morph: Not observed. Sexual morph: *Ascomata* perithecium, solitary, hair, venter immersed in wood, long neck. *Venter* globose to subglobose, unilocular. *Neck* cylindrical, periphysate, composing *textura porrecta* cells. *Peridium* multilayers, composing *textura angularis* cells with pit connections. *Hamathecium* paraphyses, periphysoids, unbranched, septate, hyaline, embedded in a gelatinous matrix. *Asci* 8-spored, bitunicate, cylindric-clavate, with a short stalked, apical ring indistinct or absent. *Ascospores* overlapping biseriate, aseptate, cymbiform, ovoid to ellipsoidal, hyaline to brown, with an obvious collapsed germ slit with a unilateral depression, smooth-walled.

Notes: Cannoniaceae is introduced to accommodate the genus *Cannonia* (*Can*.) which formed a sister branch with Spirodecosporaceae within Xylariales (Figure 2.128). Cannoniaceae is typical of Xylariales in having ascospores with a germ-slit (Samarakoon et al., 2022). However, Cannoniaceae is characterised by ascomata with long necks, which is different from Spirodecosporaceae have cylindrical, and periphysate ascomata (Sugita et al., 2022). Moreover, Cannoniaceae is distinctive within Xylariales by peridium composed of *textura angularis* cells with pit connections. Based on phylogenetic placement and morphological variation, we proposed Cannoniaceae as a new family in Xylariales.

Cannonia Joanne E. Taylor & K.D. Hyde, Mycol. Res. 103 (11): 1398 (1999)

Notes: Taylor and Hyde (1999) established the genus *Cannonia* based on morphological differences, with *Can. australis* as the type species. *Cannonia* only reported sexual morph which characterized by long ostiola ascomata and aseptate ascospores with germ slit (Taylor & Hyde, 1999, this study). *Cannonia* was originally placed in the Xylariaceae based on the morphological characteristics that the basis of ascomata being immersed beneath a clypeus and surrounded by some stromatic tissues (Taylor & Hyde, 1999). Although Trierveiler-Pereira et al. (2012) reported *Can. australis* again, there is still no corresponding molecular data. Wendt et al. (2017) transferred *Cannonia* to Xylariales genera *incertae sedis*. Subsequently, Daranagama et al. (2018) suggest placing this genus in Coniochaetales pending fresh collections as it is atypical of Xylariales. Our study provides molecular data for *Cannonia* for the first time and described a new species.

According to phylogenetic analysis of combined ITS, LSU, *tef* 1-α, *tub*2 and *rpb*2, we determined the position of *Cannonia* in Xylariales (Figure 2.128). Based on the phylogenetic results and morphological variations, we supported that it is necessary to propose a new family to accommodate *Cannonia*. Two species have been reported from palms including a new species described in this study (Xiong et al., 2025).

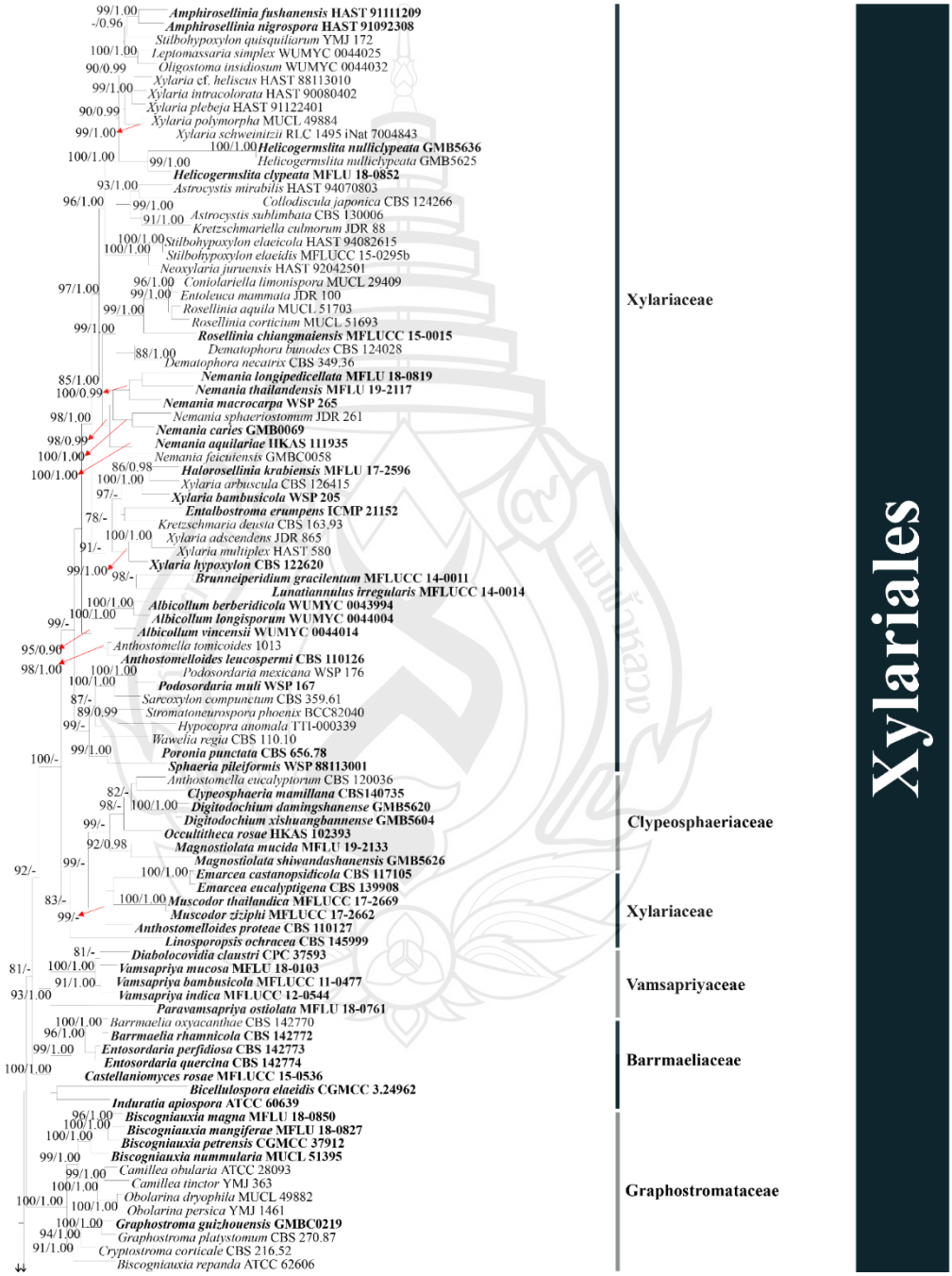


Figure 2.128 Phylogenetic tree of Xylariales

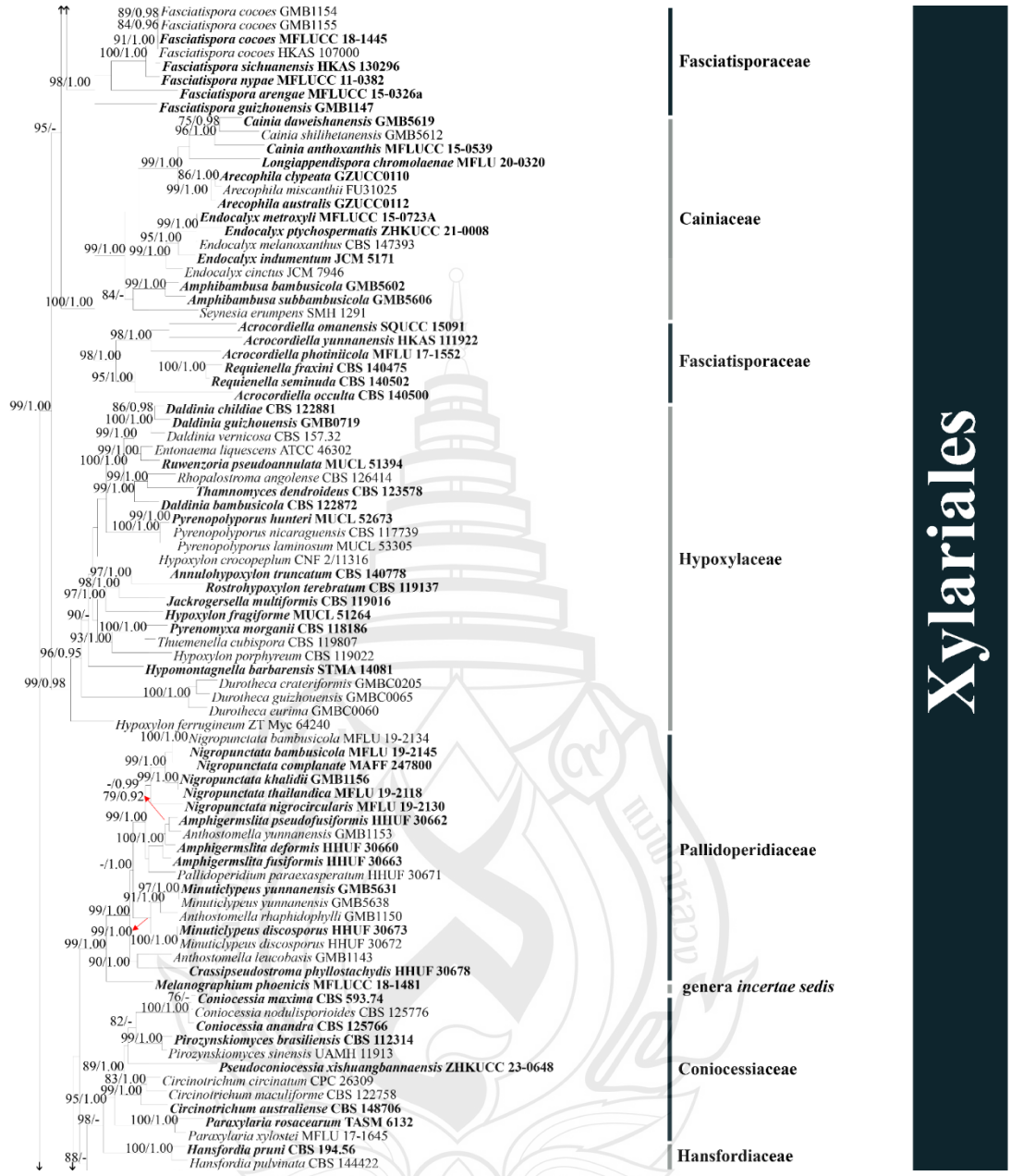
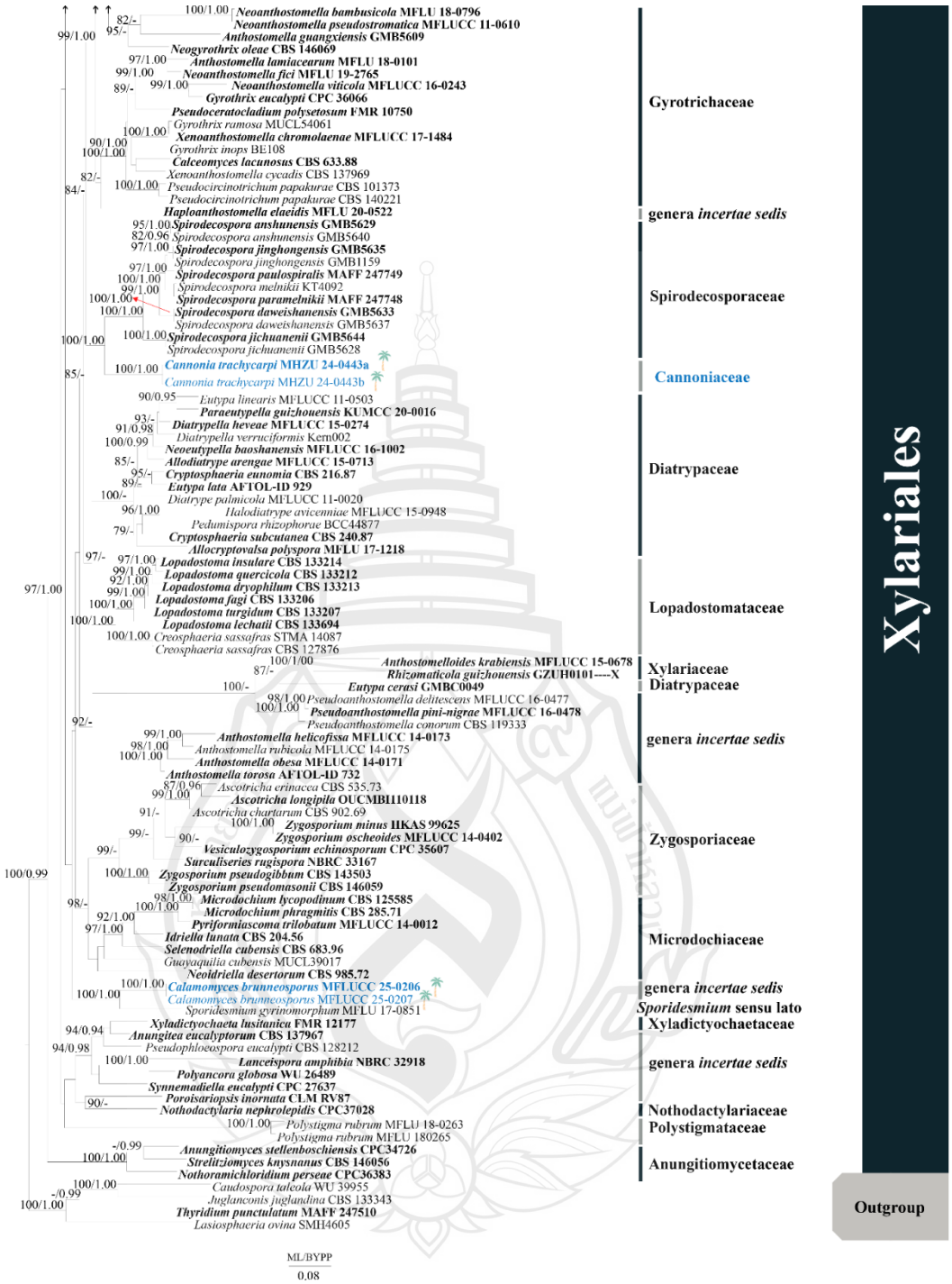


Figure 2.128 (continued)



Note Phylogram generated from maximum likelihood analysis of Xylariales based on combined ITS, LSU, *tef* 1-α, *tub*2 and *rpb*2 sequence data. Bootstrap values for maximum likelihood (ML) equal to or greater than 70 and BYPP values xxx are indicated above the branches. The new collections are indicated in blue and ex-type strains are indicated in bold.

Figure 2.128 (continued)

Cannonia trachycarpi Y.R. Xiong, Manawas. & K.D. Hyde, ***sp. nov.***

Figure 2.129

Etymology: The epithet refers to the host genus name "*Trachycarpus*", from which the species was collected.

Saprobic on dead leaf sheath of *Trachycarpus fortunei*. Asexual morph: Not observed. Sexual morph: *Ascomata* perithecial, solitary, scattered to gregarious, columnar, venter, with a dark, erumpent, central neck. *Venter* 200–260 × 250–350 μm ($\overline{x}$ = 232 × 292 μm, n = 10), globose to subglobose, unilocular, brown to dark brown. *Ostiola* 680–770 × 45–55 μm ($\overline{x}$ = 733 × 52 μm, n = 10), apex widest part 80–100 μm, cylindrical, dark brown, periphysate, composing *textura porrecta* cells, ascospores forming a sticky mass at the tip of the perithecial neck. *Peridium* 40–80 μm, multilayers, brown, composing *textura angularis* cells with pit connections. *Hamathecium* 2–3 μm wide paraphyses, periphysoids, numerous, unbranched, septate, hyaline, embedded in a gelatinous matrix. *Asci* 45–60 × 10–13 μm ($\overline{x}$ = 50 × 12 μm, n = 25) 8-spored, bitunicate, cylindric-clavate, short stalked, curved, apically rounded, apical ring indistinct or absent. *Ascospores* 9–12 × 4–8 μm ($\overline{x}$ = 11 × 5.6 μm, n = 40), overlapping biseriate, aseptate, hyaline with guttules when immature, cymbiform, ovoid to ellipsoidal, becoming brown when mature, with rounded end, with an obvious collapsed germ slit with a unilateral depression, smooth-walled.

Culture characteristics: Colonies on PDA fast growing, after 2 weeks reaching 2 cm diam. at 25°C, circular, margin entire, dense, surface filamentous, cream at the margin, olivaceous in the center; reverse cream at the margin, dark olivaceous in the center.

Known distribution: China (this study).

Material examined: China, Yunnan Province, Kunming City, the way near Kunming Institute of Botany, on dead leaf sheath of *Trachycarpus fortunei*, 7 May 2021, Y.R. Xiong & L. Lu, XG023 (MHZU 24-0443, holotype).

GenBank numbers: MHZU 24-0443a: ITS – PV578194, LSU – PV578360, *rpb*2 – PV595332, *tub*2 – PV607964; MHZU 24-0443b: ITS – PV578195, LSU – PV578361, *rpb*2 – PV595333, *tub*2 – PV607965.

Notes: Two collections formed a separate lineage in the phylogenetic tree with 100% ML bootstrap support and 1.00 BYPP (Figure 2.128). Based on a MegaBLAST (Query cover ≥ 70%) search using the LSU sequence, the closest matches in NCBI GenBank nucleotide database were *Lopadostoma meridionale* (GenBank KC774595;

Identities 864/900 (96.00%), 11 gap), *Spirodecospora* sp. (GenBank PQ885427; Identities 886/925 (95.78%), 9 gaps) and *Barrmaelia rhamnicola* (GenBank MF488990; Identities 883/937 (94.24%), 11 gaps). The highest similarities using the ITS sequence were *Daldinia korfii* (GenBank NR_152500; Identities 495/574 (86.24%), 25 gaps), *D. childiae* (GenBank MN341622; Identities 497/578 (85.99%), 28 gaps) and *D. bambusicola* (GenBank OQ831975; Identities 489/571 (85.64%), 24 gaps). The highest similarities using the *rpb*2 sequence were *Lopadostoma linospermum* (GenBank KC774544; Identities 729/909 (80.20%), 20 gaps) and *Lopadostoma lechatii* (GenBank KC774543; Identities 735/926 (79.37%), 23 gaps), *Eutypa cerasi* (GenBank MW814894; Identities 726/923 (78.66%),

25 gap). The highest similarities using the *tub*2 sequence were *Sporidesmium gyrinomorphum* (GenBank KX090080; Identities 835/923 (90.47%), 16 gaps) and *Stilbochaeta novae-guineensis* (GenBank AY951711; Identities 830/921 (90.12%), 10 gaps), *Codinaea assamica* (GenBank MF489024; Identities 829/921 (90.01%), 11 gap). *Cannonia trachycarpi* is character by ascoma periphysate and pit connections in peridium which are distinct with *Can. australis* character by ascoma aperiphysata (Taylor & Hyde, 1999). In addition, there are first molecular report in *Cannonia*. Based on phylogenetic placement and morphological variation, we introduce *Can. trachycarpi* as a new species.



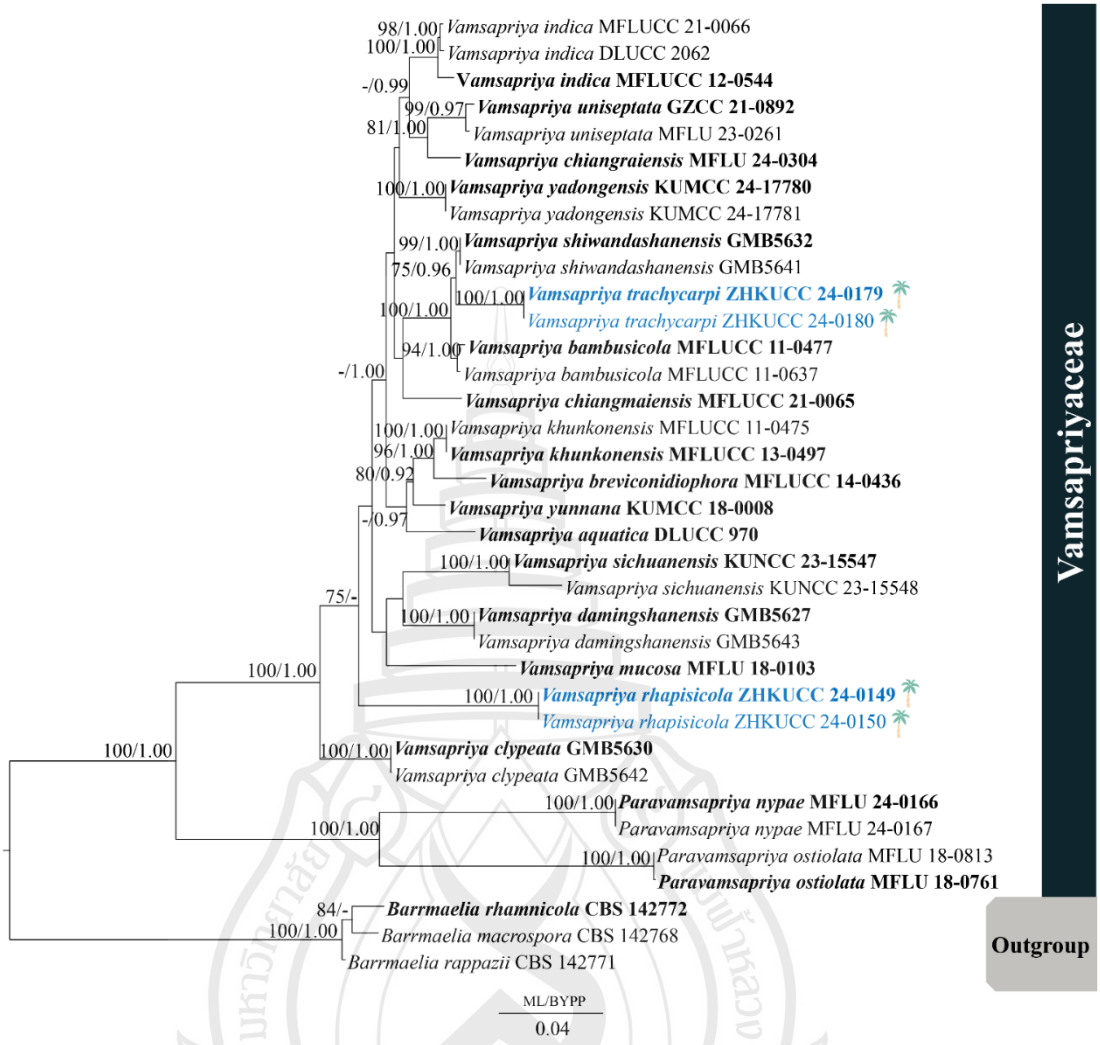
Note a–c Ascomata on substrate. d Vertical sections of ascomata. e, f Vertical sections of neck. g Vertical sections of venter. h Peridium. i, j Hamathecium. k–n Asci. o–s Ascospore. Scale bars: d, g = 100 µm, e, f = 20 µm, h–s = 10 µm.

Figure 2.129 *Cannonia trachycarpi* (MHZU 24-0443, holotype)

Vamsapriyaceae Y.R. Sun, Yong Wang bis & K.D. Hyde, in Sun, et al., Journal of Fungi 7(891), 7 (2021)

Vamsapriya Gawas & Bhat, Mycotaxon 94: 150 (2006)

Notes: Gawas and Bhat (2005) established *Vamsapriya* (*Va*.) with *Va. indicaas* as the type species. *Vamsapriya* is holomorphic genus which asexual morph characterized by brown to dark, simple, straight synnemata, monotretic conidiogenous cells and solitary, obclavate, multi-septate, septate, verruculose, dark brown conidia (Gawas & Bhat, 2005; Sun et al., 2021); and sexual morph characterized by scattered, ostiolate ascomata, unitunicate with a J+ apical ring asci and apiosporous, hyaline, surrounded by a mucilaginous sheath ascospore (Dai et al., 2016; Sun et al., 2021). Sun et al. (2021) introduced the family, Vamsapriyaceae, based on morphological evidence and phylogenetic analysis of combined ITS, LSU, *rpb*2 and *tub*2 to accommodate *Diabolocovidia*, *Didymobotryum*, *Podosporium*, *Tretophragmia*, and *Vamsapriya*. Subsequent phylogenetic studies mainly use ITS, LSU, *rpb*2, *tub*2 and *tef* 1-α or without *tef* 1-α in updated phylogenetic analyses (Samarakoon et al., 2022; Chethana et al., 2023). In this study, we use ITS, LSU, *rpb*2, *tub*2 and *tef* 1-α to update the phylogenetic tree of *Vamsapriya* (Figure 2.130). Currently, 18 species are listed under *Vamsapriya* (Index Fungorum, 2025 January), and only 11 species are associated with molecular data. Here we described two new species of *Vamsapriya* which is the first time reported from palm species (Xiong et al., 2025).



Note Phylogram generated from maximum likelihood analysis of Vamsapriyaceae based on combined ITS, LSU, *rpb2*, *tub2* and *tef* 1-α sequence data. Bootstrap values for maximum likelihood (ML) equal to or greater than 70 are indicated above the branches. The new collections are indicated in blue and ex-type strains are indicated in bold.

Figure 2.130 Phylogenetic tree of Vamsapriyaceae

Vamsapriya rhapidicola Y.R. Xiong, Manawas. & K.D. Hyde, ***sp. nov.***

Figure 2.131

Etymology: The epithet refers to the host genus name "*Rhapis*", from which the species was collected.

Saprobic on dead petiole of *Rhapis excelsa*. Asexual morph: Hyphomycetous. *Colonies* on the substrate superficial, effuse, dark brown, hairy, scattered. *Synnemata* 800–

1100 × 20–30 µm ($\bar{x}$ = 936 × 24.6 µm, n = 10), erect, rigid, dark brown, composed of compact parallel conidiophores. *Conidiophores* macronematous, synnematous, single, erect, cylindrical, straight or slightly flexuous, dark brown, smooth-wall. *Conidiogenous cells* 9–15 × 4.5–6 µm ($\bar{x}$ = 11.1 × 5.4 µm, n = 25), monotretic, integrated, terminal, brown, cylindrical to clavate, apically rounded, verrucose. *Conidia* was not observed in the examined specimens. Sexual morph: Not observed.

Culture characteristics: Colonies on PDA fast growing, after 2 weeks reaching 4 cm diam., at 25°C, circular, with fluffy, dense, white mycelium on the surface with entire margin; in reverse white.

Known distribution: China (this study).

Material examined: China, Yunnan Province, Xishuangbanna City, in an unidentified forest beside National Highway 219, on dead petiole of *Rhapis excelsa*, 5 Feb 2023, Y.R. Xiong and L. Lu, XG222 (MHZU 23-0171, holotype), ex-type ZHKUCC 24-0149, other living culture ZHKUCC 24-0150.

GenBank numbers: ZHKUCC 24-0149: ITS – PV578262, LSU – PV578430, *tef* 1-α – PV608900, *rpb*2 – PV595366, *tub*2 – PV584069; ZHKUCC 24-0150: ITS – PV578263, LSU – PV578431, *tef* 1-α – PV608901, *rpb*2 – PV595367, *tub*2 – PV584070.

Notes: Two collections from this study formed a separate lineage within *Vamsapriya* in the phylogenetic tree with 75% ML bootstrap support (Figure 2.130). Based on a MegaBLAST (Query cover ≥ 70%) search using the ITS sequence, the closest matches in NCBIs GenBank nucleotide database were *Va. uniseptata* (GenBank PP407904; Identities 441/468 (94.23%), 6 gap), *Va. yunnana* (GenBank MG833874; Identities 480/510 (94.12%), 8 gaps) and *Va. bambusicola* (GenBank KM462835; Identities 532/568 (93.66%), 7 gaps). The highest similarities using the LSU sequence were *Va. indica* (GenBank MZ420762; Identities 820/822 (99.76%), 0 gap), *Va. uniseptata* (GenBank PP407717; Identities 804/807 (99.63%), 0 gaps) and *Va. khunkonensis* (GenBank NG_066165; Identities 786/791 (99.37%), 0 gaps). The highest similarities using the *rpb*2 sequence were *Va. indica* (GenBank OK560921; Identities 692/758 (91.29%), 0 gap), *Va. khunkonensis* (GenBank KM462829; Identities 731/807 (90.58%), 0 gaps) and *Va. bambusicola* (GenBank KM462834; Identities 731/808 (90.47%), 0 gaps). The highest similarities using the *tef* 1-α sequence were *Va. bambusicola* (GenBank KU940209; Identities 889/961 (92.51%), 3 gaps), *Va. indica* (GenBank MZ442694; Identities 854/924

(92.42%), 1 gap) and *Va. khunkonensis* (GenBank KU940211; Identities 888/961 (92.40%), 3 gaps). The highest similarities using the *tub*2 sequence were *Daldinia theissenii* (GenBank KU684130; Identities 735/796 (92.34%), 0 gap), *Daldinia clavata* (GenBank AY951693; Identities 734/796 (92.21%), 0 gaps) and *Colletotrichum johnstonii* (GenBank MT456875; Identities 837/925 (90.49%), 6 gaps). Although we do not observe absolute conidia in the examined specimens, we got pure culture from germinating conidiogenous cells to obtain molecular data. Based on verrucose conidiogenous cells and differences of molecular evidence, we introduce *Va. rhapidicola* as a new species.



Note a, b Colonies on substrate surface. c Conidiophores. d–g Conidiogenous cells. j, k Germinating conidiogenous cells. l The front of culture on PDA at 25°C and the reverse of culture on PDA at 25°C. Scale bars: c–e = 50 µm, f–k = 10 µm.

Figure 2.131 *Vamsapriya rhapidicola* (MHZU 23-0171, holotype)

Vamsapriya trachycarpi Y.R. Xiong, Manawas. & K.D. Hyde, ***sp. nov.***

Figure 2.132

Etymology: The epithet refers to the host genus name "*Trachycarpus*", from which the species was collected.

Saprobic on dead leaf sheath of *Trachycarpus fortunei*. Asexual morph: Hyphomycetous. *Colonies* on the substrate superficial, effuse, dark brown, hairy, scattered. *Synnemata* 700–860 × 30–40 μm ($\bar{x}$ = 790 × 32 μm, n = 10), erect, rigid, dark brown, composed of compact parallel conidiophores. *Conidiophores* macronematous, synnematous, single, erect, cylindrical, straight or slightly flexuous, dark brown, smooth-walled. *Conidiogenous cells* 10–17 × 4–5 μm ($\bar{x}$ = 13.6 × 4.7 μm, n = 25), monotretic, integrated, terminal, brown, cylindrical to clavate, apically rounded, verrucose. *Conidia* were not observed in the examined specimens. Sexual morph: Not observed.

Culture characteristics: Colonies on PDA fast growing, after 2 weeks reaching 2 cm diam. at 25°C, circular, with fluffy, dense, white mycelium on the surface with entire margin; in reverse white.

Known distribution: China (this study).

Material examined: China, Yunnan Province, Xishuangbanna City, on dead leaf sheath of *Trachycarpus fortunei*, 5 Feb 2023, Y.R. Xiong and L. Lu, XG267 (MHZU 23-0186, holotype), ex-type ZHKUCC 24-0179, other living culture ZHKUCC 24-0180.

GenBank numbers: ZHKUCC 24-0179: ITS – PV578264, LSU – PV578432, *tef* 1-α – PV608902, *rpb*2 – PV595368; ZHKUCC 24-0180: ITS – PV578265, LSU – PV578433, *tef* 1-α – PV608903, *rpb*2 – PV595369.

Notes: Two collections from this study formed a separate lineage and clustered with *Vamsapriya bambusicola* in the phylogenetic tree with 75% ML bootstrap support and 0.96 BYPP (Figure 2.130). The nucleotide differences excluding gaps between *Va. trachycarpi* (ZHKUCC 24-0179) and *Va. bambusicola* (MFLUCC 11-0477) were checked and given as follows, ITS: 2.03% (12/590 base pairs), LSU: 0.22% (2/897 base pairs), *rpb*2: 0.57% (6/1049 base pairs), *tef* 1-α: 7.27% (73/1004 base pairs). *Vamsapriya trachycarpi* have verrucose conidiogenous cells which differ from *Va. bambusicola* have smooth-wall conidiogenous cells (Dai et al., 2014). Although we did not observe absolute conidia in the examined specimens, we got pure culture from germinating conidiogenous cells to obtain molecular data. Thus, we introduce *Va. trachycarpi* as a new species.



Note a, b Colonies on the substrate surface. c Conidiophores. d–j Conidiogenous cells. k Germinating conidiogenous cells. l The front of culture on PDA at 25°C and the reverse of culture on PDA at 25°C. Scale bars: c–k = 10 µm.

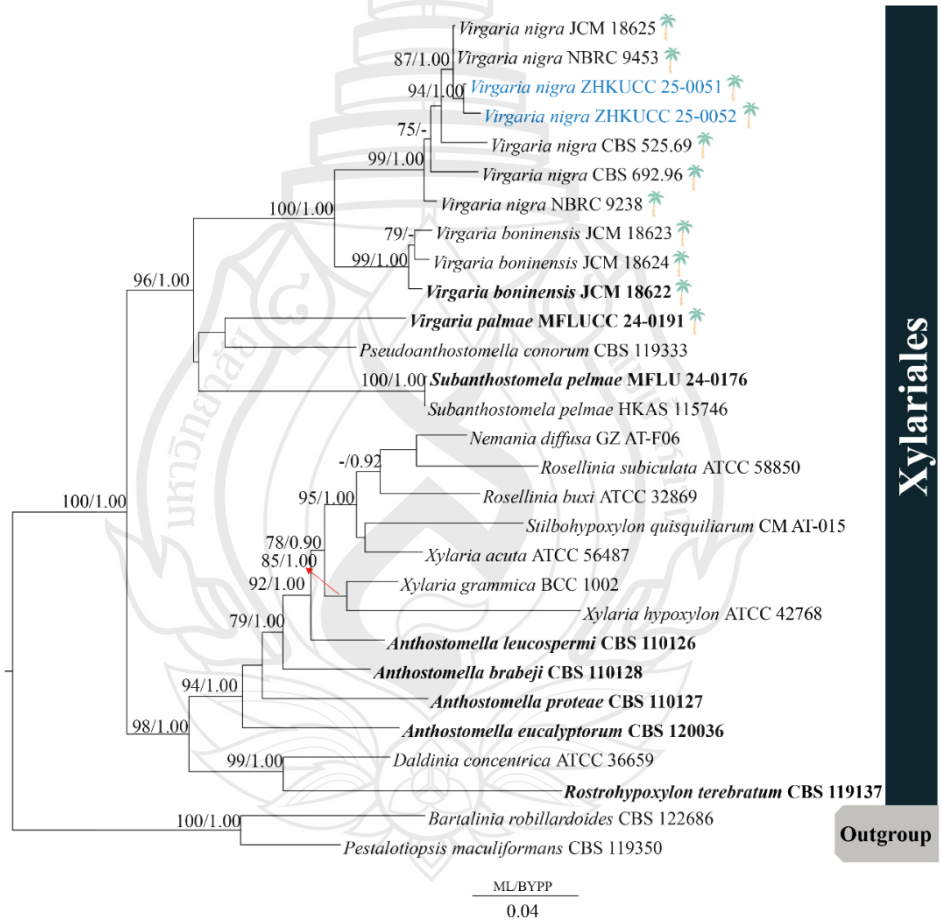
Figure 2.132 *Vamsapriya trachycarpi* (MHZU 23-0186, holotype)

Xylariaceae Tul. & C. Tul., Selecta Fungorum Carpologia, Tomus Secundus. Xylariei - Valsei - Sphaeriei 2: 3 (1863)

Virgaria Nees, System der Pilze und Schwämme: 54 (1817)

Notes: *Virgaria* (*Vi.*) was first proposed by Nees von Esenbeck (1816), and classified within the family Xylariaceae, typified by a hyphomycete species *Vi. nigra* (Seifert et al., 2011). The asexual morph of *Virgaria* is characterized by macronematous,

mononematous, and branched conidiophores, with polyblastic, sympodial conidiogenous cells and reniform to ellipsoidal, aseptate conidia (Liu et al., 2024). *Virgaria* has been synonymous with *Ascovirgaria*, though *Virgaria* is the recommended name (Zhang et al., 2024). In this study, we use ITS and LSU to update phylogenetic studies for *Virgaria* (Figure 2.133). There are 11 species accepted in *Virgaria* (Index Fungorum, 2025 January), and only three species are associated with molecular data (Liu et al., 2024; Zhang et al., 2024). In total, three species have been reported from palm species (Xiong et al., 2025), including a new host and new geography record of *Vi. nigra* was introduced from *Trachycarpus fortunei* from China in this study.



Note Phylogram generated from maximum likelihood analysis of some genera of Xylariales based on combined ITS and LSU sequence data. Bootstrap values for maximum likelihood (ML) equal to or greater than 70 are indicated above the branches. The new collections are indicated in blue and ex-type strains are indicated in bold.

Figure 2.133 Phylogenetic tree of some genera of Xylariales

Virgaria nigra (Link) Nees, System der Pilze und Schwämme: 54 (1817)

Index Fungorum number: IF 213598; *Facesoffungi number*: FoF 03079; Figure 2.134

Saprobic on dead segment of *Trachycarpus fortunei*. Asexual morph: Hyphomycetous. *Colonies* on natural substrate, effuse, brown to black, dense, velvety. *Mycelium* 2–3 µm wide ($\overline{x}$ = 2.3 µm, n = 20), hyphae immersed, composed of hyaline to brown, branched, septate, smooth-walled. *Conidiophores* 1–3 µm wide ($\overline{x}$ = 2 µm, n = 20), macronematous, mononematous, fasciculate to procumbent, straight or flexuous, brown at the base, paler towards the apex, branched, septate, verruculose, thick-walled. *Conidiogenous cells* 1.5–3.5 µm wide ($\overline{x}$ = 2.9 µm, n = 20), polyblastic, integrated, terminal, subcylindrical, tip tapered to a pointed tip, subhyaline to pale brown, denticulate. *Conidia* 4–5 × 2.5–3 µm ($\overline{x}$ = 4.4 × 2.8 µm, n = 30), solitary, subglobose to ellipsoidal, some ovoid, brown, aseptate, smooth-walled, guttulate. Sexual morph: Not observed.

Culture characteristics: Colonies on PDA slowly growing, after 2 weeks reaching 2–3 cm diam., at 25°C, circular, flat, with entire edge, above brown in the middle and cream in the outer, yellowish in reverse.

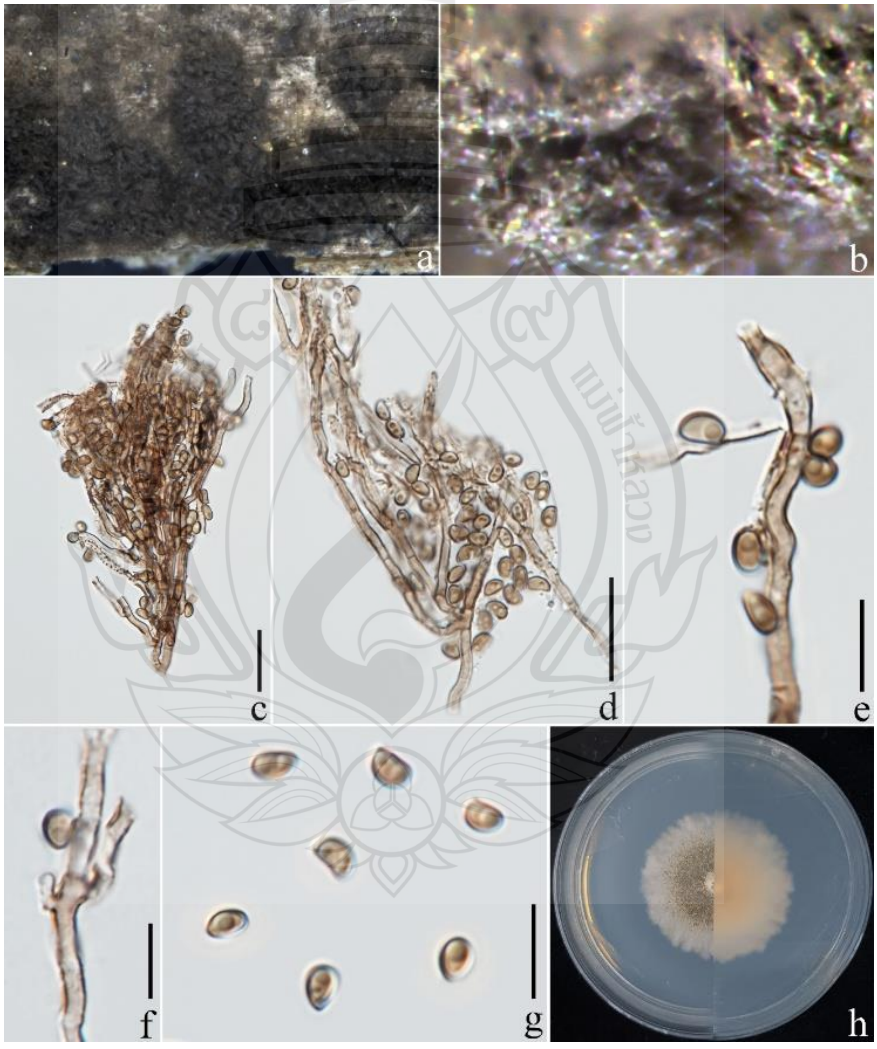
Known distribution: Cuba, Canada, France, Italy, Spain, United States of America (Matsushima, 1975; Hughes, 1978; Seifert et al., 2011; Nonaka et al., 2013). Thailand (Liu et al., 2024; Zhang et al., 2024), China (this study).

Material examined: China, Jiangxi Province, Nanchang City, Meiling National Forest Park, on dead segment of *Trachycarpus fortunei*, 11 April 2024, Y.R. Xiong, XG394 (MHZU 24-0489, new host and new geography record), living culture ZHKUCC 25-0051, other living culture ZHKUCC 25-0052.

GenBank numbers: ZHKUCC 25-0051: ITS – PV578272, LSU – PV578440; ZHKUCC 25-0052: ITS – PV578273, LSU – PV578441.

Notes: Two collections obtained in this study clustered with *Vi. nigra* by 87% ML bootstrap support and 1.00 BYPP (Figure 2.133). Based on a MegaBLAST (Query cover ≥ 70%) search using the ITS and LSU sequence, the closest matches in NCBIs GenBank nucleotide database were *Vi. nigra* (GenBank AB670716; Identities 604/608(99%), 1 gap), *Vi. nigra* (GenBank AB670711; Identities 603/608(99%), 1 gap) and *Vi. nigra* (GenBank: MN844242; Identities 599/606(99%), 2 gaps) for ITS; *Vi. nigra* (GenBank MH866907; Identities 884/887(99%), 1 gap), *Vi. nigra* (GenBank MH870170;

Identities 880/889(99%), 3 gaps) and *Vi. nigra* (GenBank: MH871129, Identities 879/888(99%), 2 gaps) for LSU. Morphological evidence of conidiogenous cells and brown conidia are well fit with *Vi. nigra* (Liu et al., 2024, Figure 126). *Virgaria nigra* is the type species of *Virgaria* and many records have been introduced from different hosts worldwide (Matsushima, 1975; Hughes, 1978; Seifert et al., 2011; Nonaka et al., 2013; Liu et al., 2024). Some research indicates that the species *Vi. nigra* has the potential to produce novel metabolites, with antimicrobial activity (Ishii et al., 2012). Therefore, based on morphology and phylogenetic analysis, we identified our collections as new a record of *Vi. nigra*.



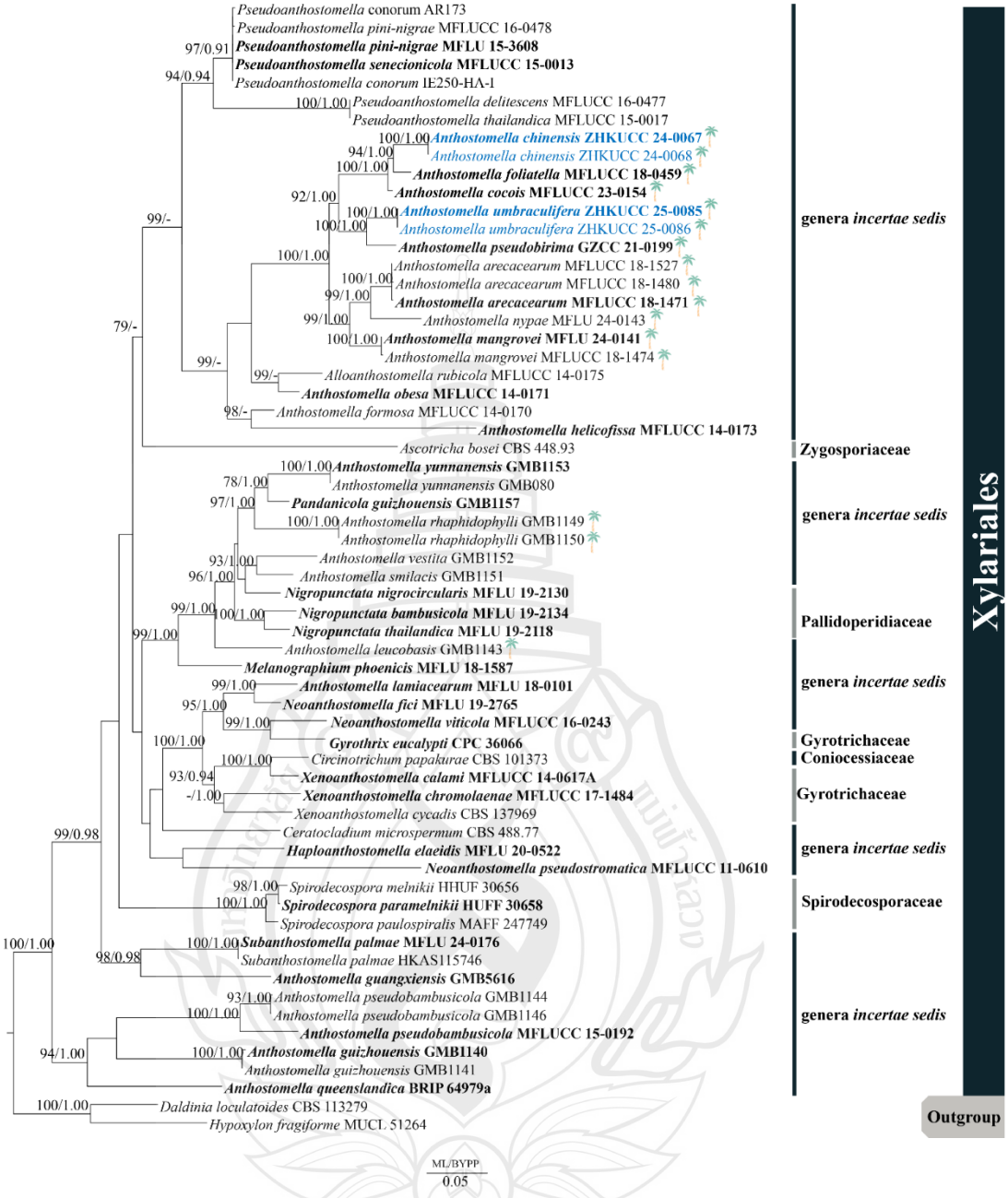
Note a, b Colonies on natural substrate. c, d Conidiophores and conidia. e, f Conidiogenous cells with conidia. g Conidia. h The front of culture on PDA at 25°C and the reverse of culture on PDA at 25°C. Scale bars: c, d = 20 µm; e–g = 10 µm.

Figure 2.134 *Virgaria nigra* (MHZU 24-0489, new host and new geography record)

Xylariales *genera Incertae sedis*

Anthostomella Sacc., Atti Soc. Veneto-Trent. Sci. Nat., Padova, Sér. 4 4: 84 (1875)

Notes: Saccardo (1875) established *Anthostomella (Anth*.) to accommodate *Anth. limitata*, *Anth. tomicoides* and *Anth. perfidiosa*, without designating a type. Eriksson (1966) designated *Anth. limitata* as the type species for *Anthostomella* based on its non-appendiculate ascospores. However, Francis (1975) argued that the lack of a clypeus in *Anth. limitata* was inconsistent with the genus *Anthostomella* and subsequently redesignated *Anth. tomicoides* as the type species. Although Lu and Hyde (2000) reported the presence of a dark clypeus in *Anth. limitata*, they accepted *Anth. tomicoides* as the type species. *Anthostomella* is a polyphyletic genus characterized by immersed ascomata beneath a dark clypeus, periphysate ostiolar canals, unitunicate, cylindrical asci with or without a J+, apical ring and mostly brown, aseptate ascospores with or without a dwarf cell or appendages at the ends and presence or absence of a germ slit (Lu & Hyde, 2000; Daranagama et al., 2015; Samarakoon et al., 2022). Daranagama et al. (2015) revised the genus *Anthostomella* based on morphology and phylogenetic analysis of combined ITS, *rpb*2, *tub*2 and LSU. Subsequently Samarakoon et al. (2022) re-evaluated and revised the genus *Anthostomella* based on morphological characteristics and phylogenetic analyses incorporating combined ITS, LSU, SSU, *rpb*2, *tub*2, and *tef* 1-α sequence data. In this study, we use ITS, LSU, SSU, *rpb*2, *tef* 1-α and *tub*2 to update phylogenetic studies for *Anthostomella* (Figure 2.135). Currently, 179 epithets are listed under *Anthostomella* (Index Fungorum, 2025 January), and only 16 species are associated with molecular data. To date, a total of 82 species have been reported from palm species including two new species described in this study (Xiong et al., 2025).



Note Phylogram generated from maximum likelihood analysis of some families of Xylariales based on combined ITS, LSU, SSU, *rpb*2, *tef* 1-α and *tub*2 sequence data. Bootstrap values for maximum likelihood (ML) equal to or greater than 70 and BYPP values equal to or greater than 0.90 are indicated above the branches. The new collections are indicated in blue and ex-type strains are indicated in bold.

Figure 2.135 Phylogenetic tree of some families of Xylariales

Anthostomella chinensis Y.R. Xiong, Manawas. & K.D. Hyde, ***sp. nov.***

Figure 2.136

Etymology: The epithet refers to the host species name "*Livistona chinensis*", from which the species was collected.

Saprobic on dead leaf sheath of *Livistona chinensis*. Asexual morph: Not observed. Sexual morph: *Ascomata* 150–180 × 180–200 μm ($\overline{x}$ = 160 × 190 μm, n = 10), sub-immersed, scattered or gregarious, solitary, raising host epidermal and producing a black area, with a poorly developed clypeus, papillate, subglobose to globose in vertical section. *Ostioles* centric, ostiolar canal periphysate. *Peridium* 10–20 μm wide, multi-layered, attached to the host with yellowish to hyaline innert substrate, outer layer comprising brown, thick-walled cells of *textura angularis*. *Paraphyses* 2.5–3.5 μm wide, hypha-like, fexuose, numerous, unbranched, without septa, guttulate. *Asci* 60–90 × 8–10 μm ($\overline{x}$= 84 × 9 μm, n = 30), 8-spored, unitunicate, long-cylindrical, short pedicellate, apex rounded, with a discoid apical apparatus. *Ascospores* 10–13 × 5–6.5 μm ($\overline{x}$ = 11.4 × 5.7 μm, n = 25), uniseriate, unicellular, with broadly rounded ends, with straight germ slit, brown, fusiform or ellipsoidal, smooth, surrounded by a thin mucilaginous sheath, lacking appendages.

Culture characteristics: Colonies on PDA fast growing, after 2 weeks reaching 4 cm diam. at 25°C, irregular, floccose, lobate edge, dusty green with grey marge; in reverse dark brown.

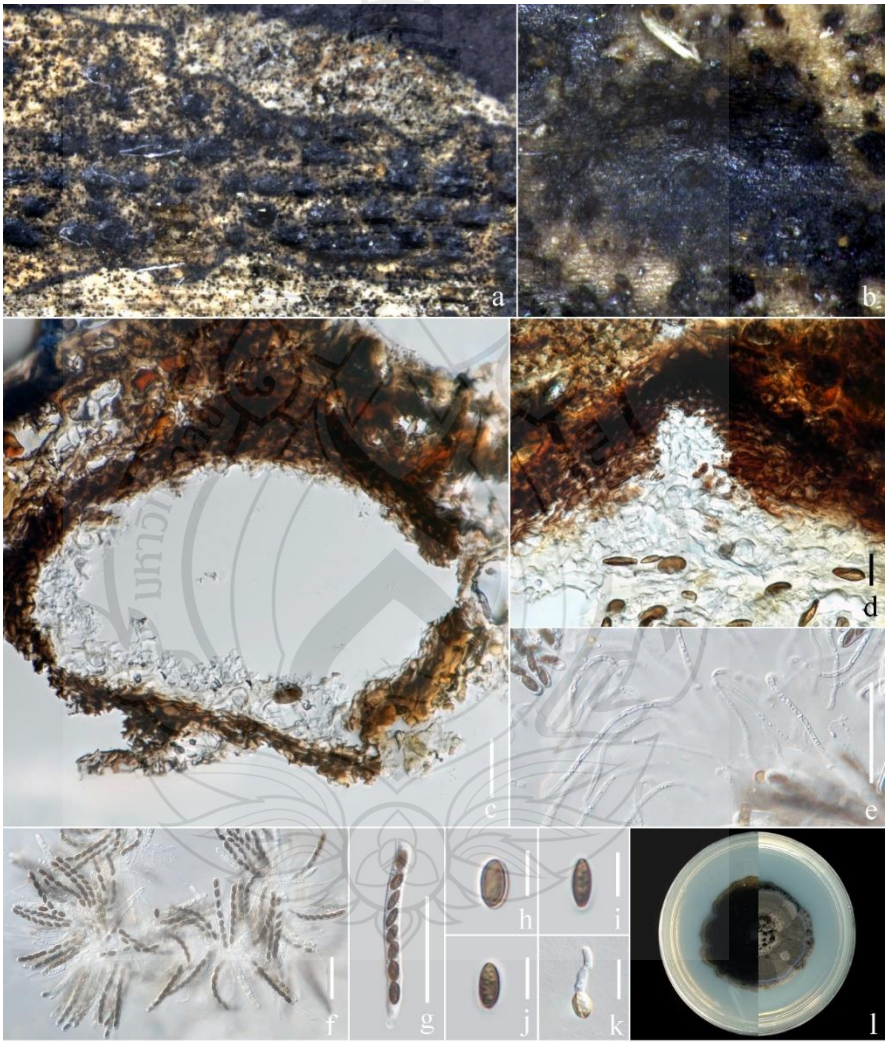
Known distribution: China (this study).

Material examined: China, Yunnan Province, Qujing City, Sanyuan District, on dead leaf sheath of *Livistona chinensis*, 29 Dec 2022, Y.R. Xiong and L. Lu, XG137 (MHZU 23-0130, holotype) – ex-type ZHKUCC 24-0067, other living culture ZHKUCC 24-0068.

GenBank numbers: ZHKUCC 24-0067: ITS – PV578130, LSU – PV578300, SSU – PV578484, *tef* 1-α – PV608814, *rpb*2 – PV595302, *tub*2 – PV584053; ZHKUCC 24-0068: ITS – PV578131, LSU – PV578301, SSU – PV578485, *tef* 1-α – PV608815, *rpb*2 – PV595303, *tub*2 – PV584054.

Notes: Two collections from this study formed a sister lineage with *Anthostomella foliatella* in the phylogenetic tree with 100% ML bootstrap support and 1.00 BYPP. The nucleotide differences excluding gaps between *Anth. chinensis* (ZHKUCC 24-

0067) and *Anth. foliatella* (MFLUCC 18-0459) were checked and given as follows, ITS: 4.75% (27/568 base pairs), LSU: 1.25% (14/1117 base pairs), SSU: 0% (1/1014 base pairs), *rpb2*: 5.26% (53/1007 base pairs), *tub2*: 8.09% (66/816 base pairs), *tef* 1-α: 8.18% (77/941 base pairs). *Anthostomella chinensis* has conidia with fusiform or ellipsoidal and is surrounded by a thin mucilaginous sheath which is different from *Anth. foliatella* have oblong-ellipsoidal to ellipsoid-fusiform and ends acute without sheath (Zhang et al., 2024, Figure 2.136). Based on phylogenetic placement and morphological variations, we introduce *Anth. chinensis* as a new species.



Note a, b Ascomata on substrate. c Vertical sections of ascomata. d Cells of peridium. e Pseudoparaphyses. f, g Asci. h–j Ascospores. k Germinating ascospore. l The front of culture on PDA at 25°C and the reverse of culture on PDA at 25°C. Scale bars: c = 20 µm, d, h–k = 10 µm, e–g = 50 µm.

Figure 2.136 *Anthostomella chinensis* (MHZU 23-0130, holotype

Anthostomella umbraculiferae Y.R. Xiong, Manawas. & K.D. Hyde, ***sp. nov.***

Figure 2.137

Etymology: The epithet refers to the host species name "*Corypha umbraculifera*", from which the species was collected.

Saprobic on dead petiole of *Corypha umbraculifera*. Asexual morph: Coelomycetous. *Conidiomata* 130–270 × 100–250 μm ($\overline{x}$ = 200 × 175 μm, n = 10), pycnidial, semi-immersed, solitary, globose to pyriform, unilocular, ostioles, Papillate structure with a centrally depressed apex. *Clypeus* thick, comprising host cells mixed with dark-brown intracellular fungal hyphae. *Peridium* 15–30 μm, composed of thick-walled, dark-brown cells, *textura angularis*, inner wall with hyaline cells. *Conidiophores* reduced to conidiogenous cells. *Conidiogenous cell* 5–10 × 2–3 μm ($\overline{x}$ = 7 × 2.3 μm, n = 25), enteroblastic, tretic (pore), phialidic to cylindrical, hyaline, smooth-walled. *Conidia* 10–11.5 × 5–6 μm ($\overline{x}$ = 10.9 × 5.6 μm, n = 25), unicellular, dark brown to black brown, ovate or ellipsoidal-inequilaterally ellipsoidal, smooth, with broadly rounded ends, with a slightly oblique germ slit running longitudinally, a separation pore at basal, lacking appendages and sheaths. Sexual morph: Not observed.

Culture characteristics: Colonies on PDA fast growing, after 2 weeks reaching 4 cm diam., at 25°C, circular, with fluffy, velvety, milky white to yellowish white; in reverse cream in the middle and white at the margin.

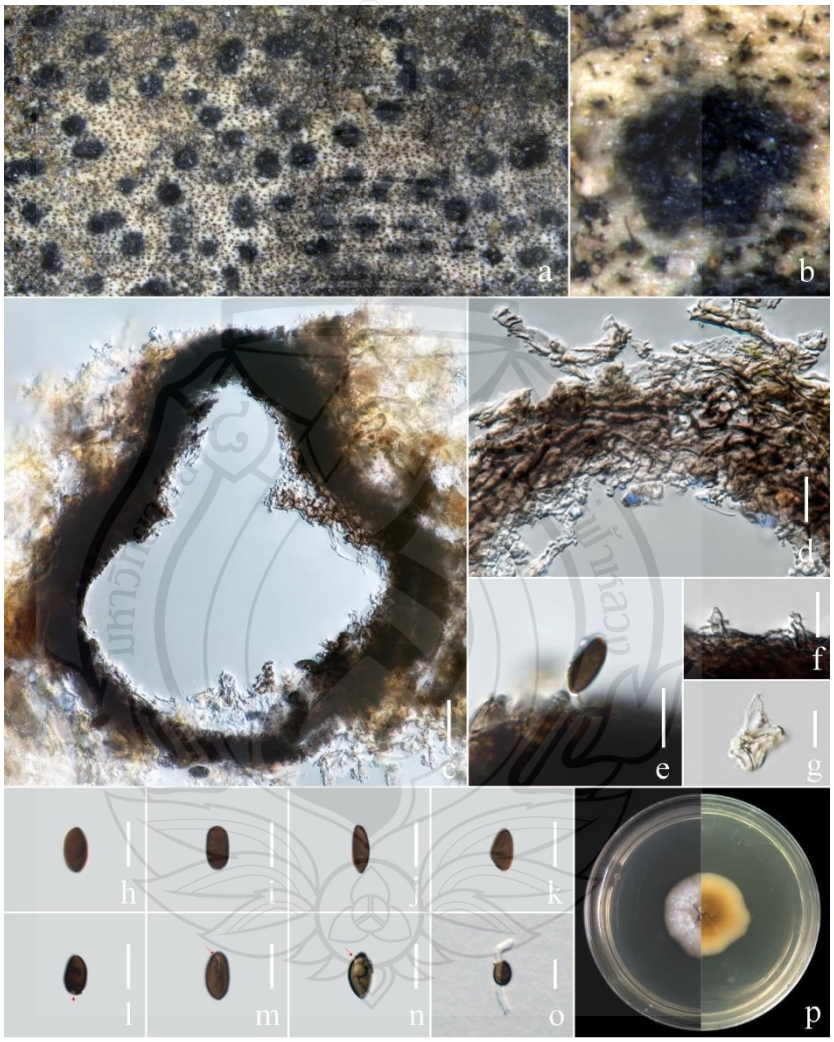
Known distribution: China (this study).

Material examined: China, Yunnan Province, Xishuangbanna City, in an unidentified forest beside National Highway 219, on dead petiole of *Corypha umbraculifera*, 5 Feb 2023, Y.R. Xiong and L. Lu, XG145 (MHZU 25-1053, holotype), ex-type ZHKUCC 25-0085, other living culture ZHKUCC 25-0086.

GenBank numbers: ZHKUCC 25-0085: ITS – PV578132, LSU – PV578302, *rpb*2 – PV595304, *tef* 1-α – PV608816; ZHKUCC 25-0086: ITS – PV578133, LSU – PV578303, *rpb*2 – PV595305, *tef* 1-α – PV608817.

Notes: Two collections from this study formed a sister lineage with *Anthostomella pseudobirima* in the phylogenetic tree with 100% ML bootstrap support and 1.00 BYPP. The nucleotide differences excluding gaps between *Anth. umbraculiferae* (ZHKUCC 25-0085) and *Anth. pseudobirima* (GZCC 21-0199) were checked and given as follows, ITS: 5.35% (30/561 base pairs), LSU: 0.55% (5/912 base pairs), *rpb*2: 9.21% (96/1043 base

pairs), *tef* 1-α: 5.74% (54/940 base pairs). Morphologically, *Anth. umbraculifera* have dark brown to black brown and ovate or ellipsoidal-inequilaterally ellipsoidal which fits with *Anthostomella* (Li et al., 2024). However, *Anth. umbraculiferae* is distinct in *Anthostomella* which have conidia with a slightly oblique germ slit running longitudinally and a separation pore at basal. Moreover, *Anth. pseudobirima* is a sexual morph which not observed asexual morph can't compare with *Anth. umbraculiferae* (Zhang et al., 2024). Based on phylogenetic placement and morphological variations, we introduce *Anth. umbraculiferae* as a new species.



Note a, b Conidiomata on the substrate. c Sections through conidiomata. d Peridium. e–g Conidiogenous cells and developing conidia. h–n Conidia. o Germinating conidium. p The front of culture on PDA at 25°C and the reverse of culture on PDA at 25°C. Scale bars: c = 20 µm, d–o = 10 µm.

Figure 2.137 *Anthostomella umbraculiferae* (MHZU 25-1053, holotype)

Calamomyces Y.R. Xiong, Manawas. & K.D. Hyde, ***gen. nov.***

Etymology: referring to the name of the host "*calamus*" from which type species was collected

Type species: *Calamomyces brunneisporus* Y.R. Xiong, Manawas. & K.D. Hyde

Saprobic on dead palm substrates. Asexual morph: Hyphomycetous. *Colonies* on natural substrate superficial, irregular, effuse, hairy, velvety, black. *Mycelium* mostly immersed in substratum, consisting of branched, septate, brown, smooth hyphae. *Conidiophores* macronematous, mononematous, caespitose, cylindrical, unbranched, erect, slight curved at the medium part, smooth, dark brown, septate. *Conidiogenous cell* monoblastic, holoblastic, terminal, determinate, cylindrical. *Conidia* acrogenous, solitary, fusiform to fusoid, 1-sepate, slightly constricted at septa, sometime flexuous, guttulate, truncate at base with a pore, rounded at apex, brown to dark brown. Sexual morph: Not observed.

Notes: Based on our phylogenetic result (Figure 2.128), our collection (*Calamomyces*; *Cal.*) formed a sister clade with *Sporidesmium gyrinomorphum* in Xylariales. *Calamomyces* is a hyphomycetous genus which is characterised by macronematous, mononematous and unbranched, erect conidiophore. In addition, *Calamomyces* have conidia which are characterised by fusiform to fusoid, truncate at the base with a pore, rounded at the apex with 1-septate are different from *Sporidesmium gyrinomorphum* which are characteristic by conidia are rostrate, 7–8-euseptate and obclavate to obspathulate (Yang et al., 2018). Although *Sporidesmium* belongs to Sporidesmiaceae (Sporidesmiales), Yang et al. (2018) placed *Sporidesmium gyrinomorphum* within *Sporidesmium sensu lato* according to its distinctive conidiophores, cylindrical conidiogenous cells with percurrent proliferation and obclavate, rostrate conidia. Our collections were also distinctive in Xylariales by unbranched conidiophore, determined conidiogenous cells and conidia truncate at the base with a pore, acrogenous with 1-sepate (Figure 2.138). Based on morphological variations and phylogenetic results, we proposed a monotypic genus *Calamomyces* to accommodate the type species *Cal. brunneisporus*. However, we provisionally treated it as *incertae sedis* within the order Xylariales according to is closed with *Sporidesmium gyrinomorphum* in the phylogenetic result. Thus, more fresh collections of *Calamomyces* are needed to stabilize the placement of this genus.

Calamomyces brunneisporus Y.R. Xiong, Manawas. & K.D. Hyde, ***sp. nov.***

Figure 2.138

Etymology: The epithet refers to the conidia character “brown to dark brown”.

Saprobic on dead leaf sheath of *Calamus* sp. Asexual morph: Hyphomycetous. *Colonies* on natural substrate superficial, irregular, effuse, hairy, velvety, black. *Mycelium* mostly immersed in substratum, consisting of branched, septate, brown, smooth hyphae. *Conidiophores* 80–100 × 5.5–8.5 µm ($\bar{x}$ = 93 × 6.7 µm, n = 15), macronematous, mononematous, caespitose, cylindrical, unbranched, erect, slight curved at the medium part, smooth, dark brown, septate. *Conidiogenous cells* 15–20 × 4–5 µm ($\bar{x}$ = 16.8 × 4.6 µm, n = 25), monoblastic, holoblastic, terminal, determinate, cylindrical. *Conidia* 20–30 × 5–6 µm ($\bar{x}$ = 23 × 5.8 µm, n = 25), acrogenous, solitary, fusiform to fusoid, 1-sepate, slightly constricted at septa, sometime flexuous, guttulate, truncate at base with a pore, rounded at apex, brown to dark brown. Sexual morph: Not observed.

Culture characteristics: Colonies on PDA fast growing, after 2 weeks reaching 2 cm diam. at 25°C, circular, margin entire, dense, grey mycelium velvety towards the margin; reverse dark at the center, grey in the margin.

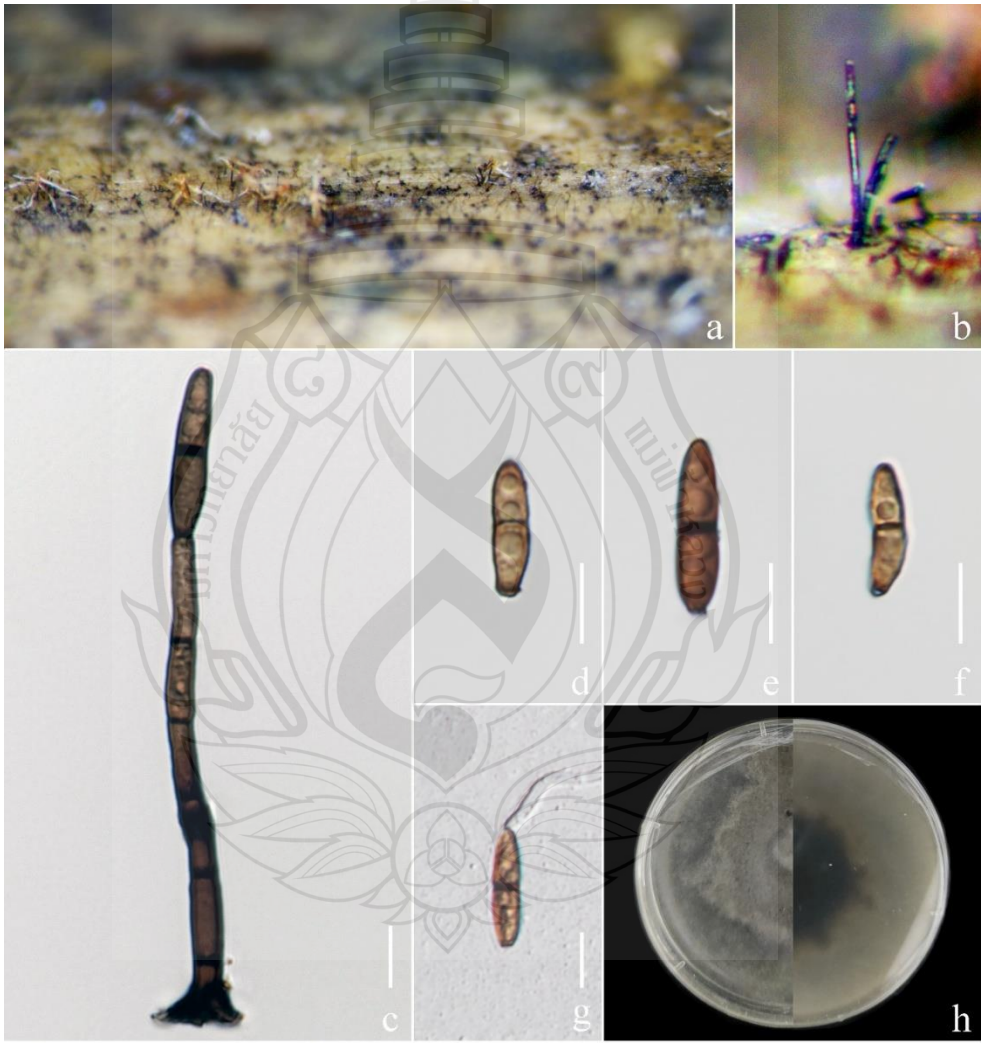
Known distribution: Thailand (this study).

Material examined: Thailand, Narathiwat Province, in an unidentified beach, on dead petiole of *Calamus* sp., 6 Aug 2024, Y.R. Xiong, XG332 (MFLU 25-0148, holotype), ex-type MFLUCC 25-0206, other living culture MFLUCC 25-0207.

GenBank numbers: MFLUCC 25-0206: ITS – PV578142, LSU – PV578312, *tef* 1-α – PV608824; MFLUCC 25-0207: ITS – PV578143, LSU – PV578313, *tef* 1-α – PV608825.

Notes: Two collections from this study formed a sister clade with *Sporidesmium gyrinomorphum* in the phylogenetic tree with 100% ML bootstrap support and 1.00 BYPP (Figure 2.128). Based on a MegaBLAST (Query cover ≥ 70%) search using the LSU sequence, the closest matches in NCBIs GenBank nucleotide database were *Xyladictyochaeta lusitanica* (GenBank MH107972; Identities 816/844 (96.68%), 0 gap), *Ellisembia calyptrata* (GenBank DQ408564; Identities 817/846 (96.57%), 2 gaps) and *Pseudophloeospora eucalypti* (GenBank HQ599593; Identities 835/866 (96.42%), 2 gaps). The highest similarities using the ITS sequence were *Xylaria hypoxylon* (GenBank MH864103; Identities 490/595 (82.35%), 47 gap), *Xylaria adscendens* (GenBank KP133287; Identities 504/613 (82.22%), 42 gaps) and *Xylaria schweinitzii* (GenBank

KP133459; Identities 488/594 (82.15%), 37 gaps). The highest similarities using the *tef* 1-α sequence were *Sporidesmium gyrinomorphum* (GenBank MF135656; Identities 874/933 (93.68%), 0 gaps) and *Stilbochaeta novae-guineensis* (GenBank OL654060; Identities 882/968 (91.12%), 3 gaps), *Codinaea assamica* (GenBank OL653997; Identities 877/964 (90.98%), 2 gap). *Calamomyces brunneisporus* were distinct by monoblastic and terminal conidiogenous cells, conidia 1-sepate, slightly constricted at septa, sometimes flexuous with brown to dark brown. Based on phylogenetic placement and morphological variations, we introduce *Cal. brunneisporus* as a new species.

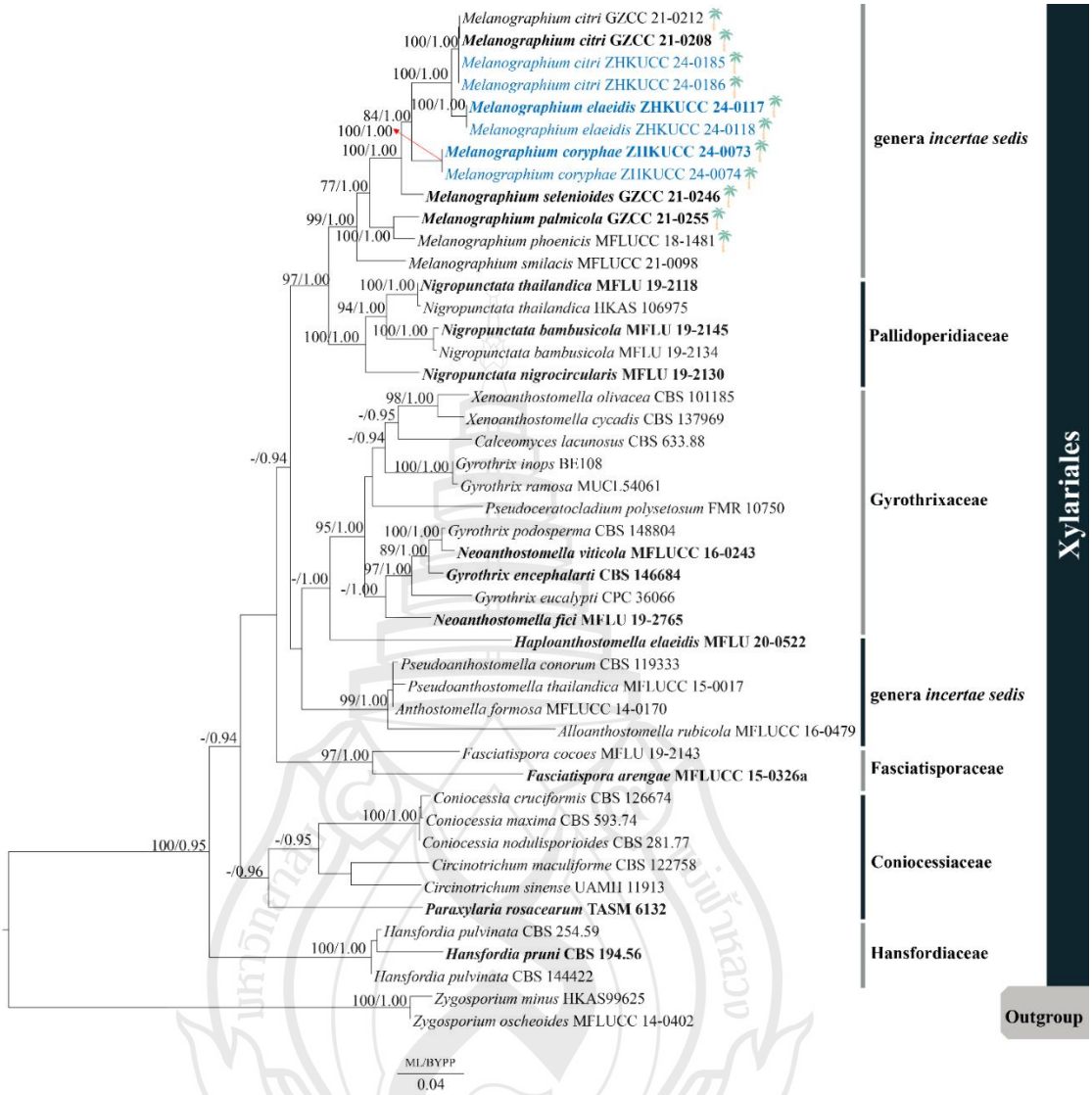


Note a, b Colonies on substrate surface. c Conidiophores, conidiogenous cells with growing conidia. d–f Conidia. g Germinating conidium. h The front of culture on PDA at 25°C and the reverse of culture on PDA at 25°C. Scale bars: c–g = 10 µm.

Figure 2.138 *Calamomyces brunneisporus* (MFLU 25-0148, holotype)

Melanographium Sacc., Annls mycol. 11(6): 557 (1913)

Notes: Saccardo (1913) established *Melanographium* (*M.*) with *M. spleniosporum* as the type species. *Melanographium* is a hyphomycetous genus characterized by superficial colonies or arising in a group from immersed stromata, unbranched conidiophores; polyblastic conidiogenous cells with sympodial proliferation; holoblastic, reniform, aseptate, frequently reniform and often with a hyaline germ slit (Ellis, 1963, 1971). Moreover, the length of conidiophores, a pattern of conidiophore grouping (single, synnemata, loosely or dense fascicles), conidial shape (straight, curved, or strongly curved), and conidial size are morphological traits of identified species in this genus (Goh & Hyde, 1997; Somrithipol & Jones, 2005). Hyde et al. (2020) first provide molecular data (ITS, LSU, SSU and *tef* 1-α) for *Melanographium*, and based on morphological evidence and phylogenetic analysis combined ITS, LSU, SSU, *rpb*2, *tub*2 and *tef* 1-α to place it in Xylariales. Subsequently, phylogenetic studies mainly use SSU, LSU, *tef* 1-α and *rpb*2 or without SSU for analysis (Liu et al., 2024; Zhang et al., 2024). In this study, we use ITS, LSU, SSU and *tef* 1-α to update phylogenetic studies for *Melanographium* (Figure 2.139). Currently, 14 epithets are listed under *Melanographium* (Index Fungorum, 2025 January), and only 5 species are associated with molecular data. Totally 13 species have been reported from palm species including two new species and one new geography record described in this study (Xiong et al., 2025).



Note Phylogram generated from maximum likelihood analysis of some families of Xylariales based on combined ITS, LSU, SSU and *tef* 1-α sequence data. Bootstrap values for maximum likelihood (ML) equal to or greater than 70 and BYPP values equal to or greater than 0.90 are indicated above the branches. The new collections are indicated in blue and ex-type strains are indicated in bold.

Figure 2.139 Phylogenetic tree of some families of Xylariales

Melanographium citri (Gonz. Frag. & Cif.) M.B. Ellis, Mycological Papers 93: 21 (1963)

Figure 2.140

Saprobic on dead leaf sheath of *Trachycarpus fortunei*. Asexual morph: Hyphomycetous. *Colonies* on natural substratum superficial, effuse, velvety or tufted, black. *Mycelium* immersed. *Conidiophores* 170–320 × 4–6 μm ($\overline{x}$ = 294 × 4.7 μm, n = 15), fasciculate, macronematous, mononematous, unbranched, usually straight, flexuous and sometimes slightly swollen near the medium, septate, forming moderately dense, dark brown fascicles, often paler and spreading in the upper part, smooth. *Conidiogenous cells* polyblastic, integrated, terminal, cylindrical, subhyaline to pale brown, smooth-walled. *Conidia* 16–20 × 10–14 μm ($\overline{x}$ = 17.8 × 11.5 μm, n = 25), solitary, curved, smooth or verrucose, reniform, integrated, terminal, often with a longitudinal germ slit, pale to dark brown, aseptate. Sexual morph: Not observed.

Culture characteristics: Colonies on PDA, after 2 weeks reaching 4 cm diam., at 25°C, circular, with fluffy, sparse, white mycelium on the surface with entire margin; in reverse yellow in the middle and white at the margin.

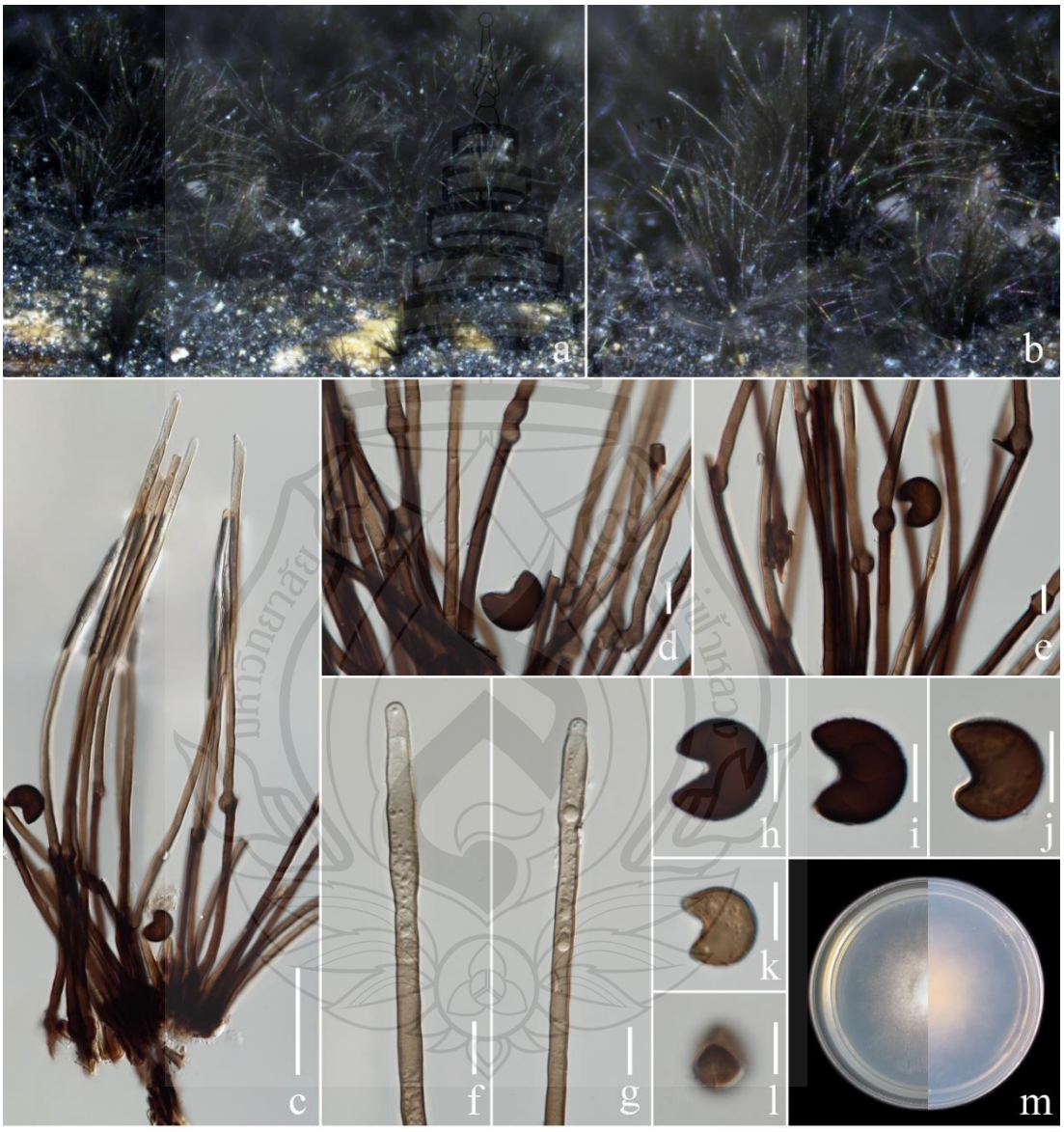
Known distribution: China (this study).

Material examined: China, Yunnan Province, Xishuangbanna City, on dead leaf sheath of *Trachycarpus fortunei*, 5 Feb 2023, Y.R. Xiong and L. Lu, XG277 (MHZU 23-0189, new geography record); living culture ZHKUCC 24-0185, other living culture ZHKUCC 24-0186.

GenBank numbers: ZHKUCC 24-0185: ITS – PV578196, LSU – PV578364, SSU – PV578510, *tef* 1-α – PV608858; ZHKUCC 24-0186: ITS – PV578197, LSU – PV578365, SSU – PV578511, *tef* 1-α – PV608859.

Notes: Two collections from this study clustered with *Melanographium citri* in the phylogenetic tree with 100% ML bootstrap support and 1.00 BYPP (Figure 2.139). The nucleotide differences excluding gaps between the strain obtained in this study (ZHKUCC 24-0185) and *Melanographium citri* (GZCC 21-0208) were checked and given as follows, ITS: 0% (0/564 base pairs), LSU: 0% (1/846 base pairs), SSU: 0% (0/1001 base pairs), *tef* 1-α: 3.43% (1/933 base pairs). Morphologically, the strains well fit with *M. citri* which have conidia with solitary, curved and often with a longitudinal germ slit (Prasher & Verma, 2016; Zhang et al., 2024). Although the conidiophore length of our collections is 170–320 μm

which is shorter than previously reported on *M. citri* which are 800 µm and 1200 µm, the different measurements may be due to local habitat or environmental differences (Ellis, 1963; Zhang et al., 2024). Moreover, this is the first time reported *M. citri* from Xishuangbanna City. Based on phylogenetic placement and morphological variations, we introduce our collections as a new geography record of *M. citri*.



Note a, b Colonies on substrate. c–g Conidiophores. h–l Conidia. m The front of culture on PDA at 25°C and the reverse of culture on PDA at 25°C. Scale bars: c = 50 µm, d–l = 10 µm.

Figure 2.140 *Melanographium citri* (MHZU 23-0189, new geography record)

Melanographium coryphae Y.R. Xiong, Manawas. & K.D. Hyde, ***sp. nov.***

Figure 2.141

Etymology: The epithet refers to the host genus name "*Corypha*", from which the species was collected.

Saprobic on dead petiole of *Corypha umbraculifera*. Asexual morph: Hyphomycetous. *Colonies* on natural substratum superficial, effuse, velvety or tufted, black. *Mycelium* superficial, adhering conidia with clusters, composed of hyaline to pale brown, smooth, hyphae. *Conidiophores* 220–420 × 4–7 μm ($\overline{x}$ = 298 × 5.5 μm, n = 15), 3–5 in loose fared fascicle or rarely single, straight or flexuous, with "Z" shape nodose near apex, brown below, paler near apex, multi-septate, smooth. *Conidiogenous cells* holoblastic, integrated, terminal, pale brown, smooth-walled. *Conidiogenous cells* polyblastic, integrated, terminal, cylindrical, subhyaline to pale brown, smooth-walled. *Conidia* 14–18 × 11–15 μm ($\overline{x}$ = 16 × 12.5 μm, n = 25), holoblastic, slight curved, aseptate, guttulate, verruca lose, smooth, with a subhyaline longitudinal germ-slit. Sexual morph: Not observed.

Culture characteristics: Colonies on PDA, after 2 weeks reaching 4 cm diam., at 25°C, circular, with fluffy, dense, white mycelium on the surface with entire margin; in reverse yellow in the middle and white at the margin.

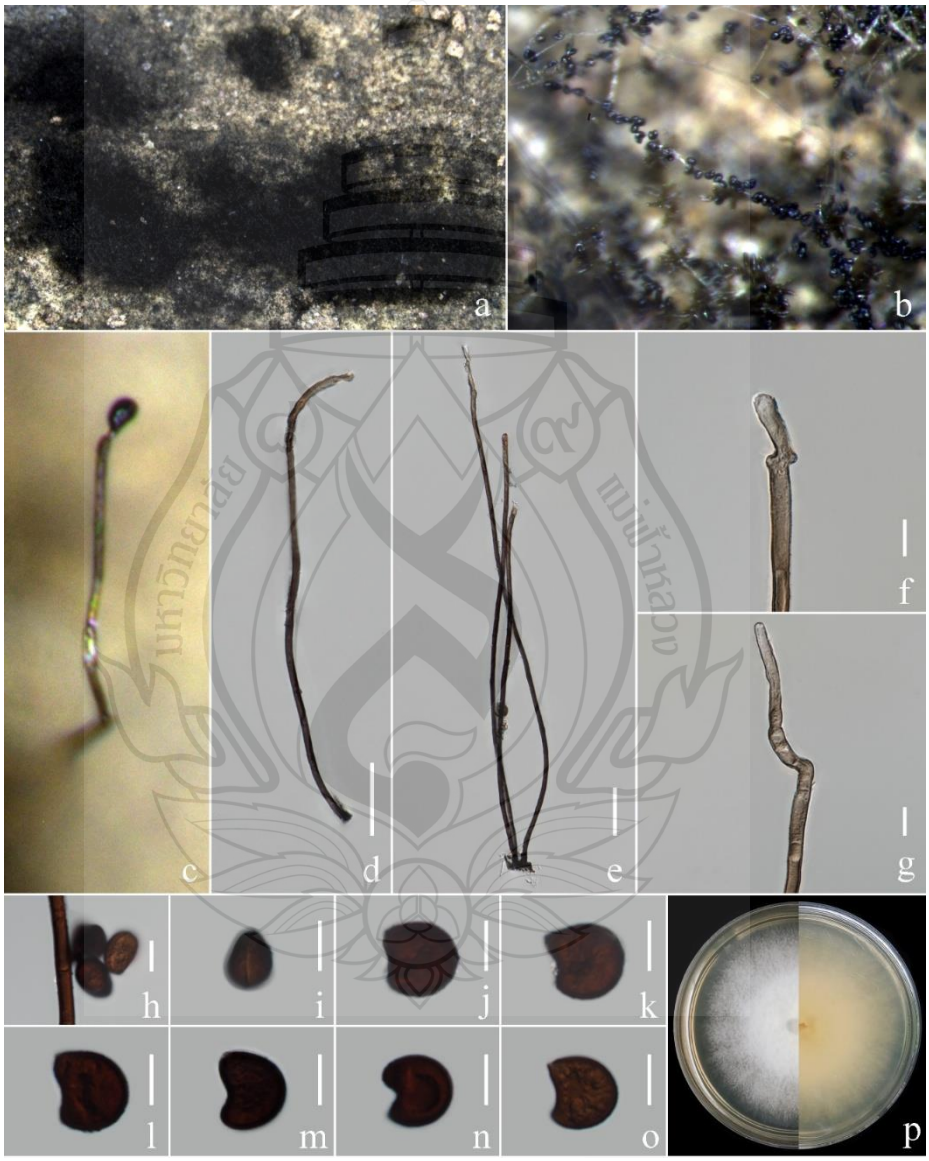
Known distribution: China (this study).

Material examined: China, Yunnan Province, Xishuangbanna City, in an unidentified forest beside National Highway 219, on dead petiole of *Corypha umbraculifera*, 5 Feb 2023, Y.R. Xiong and L. Lu, XG149 (MHZU 23-0133, holotype); ex-type ZHKUCC 24-0073, other living culture ZHKUCC 24-0074.

GenBank numbers: ZHKUCC 24-0073: ITS – PV578198, LSU – PV578366, SSU – PV578512, *tef* 1-α – PV608860; ZHKUCC 24-0074: ITS – PV578199, LSU – PV578367, SSU – PV578513, *tef* 1-α – PV608861.

Notes: Two collections from this study formed an independent lineage within *Melanographium* in the phylogenetic tree with 100% ML bootstrap support and 1.00 BYPP (Figure 2.139). The nucleotide differences excluding gaps between *M. coryphae* (ZHKUCC 24-0073) and its phylogenetically related species were checked and given as follows, *M. citri* (GZCC 21-0208) - ITS: 8.98% (51/568 base pairs), LSU: 1.98% (17/860 base pairs), SSU: 0.39% (4/1001 base pairs), *tef* 1-α: 6.44% (60/932 base pairs); *M. elaeis*

(ZHKUCC 24-0117) - ITS: 8.78% (49/558 base pairs), LSU: 2.29% (20/870 base pairs), SSU: 0.39% (4/1025 base pairs), *tef* 1-α: 7.58% (73/963 base pairs); *M. selenioides* (GZCC 21-0246) - ITS: 5.37% (29/540 base pairs), LSU: 1.63% (14/861 base pairs), SSU: 0.39% (4/1010 base pairs), *tef* 1-α: 5.61% (51/909 base pairs). *Melanographium coryphae* differs from its closely related species by mycelium adhering conidia with clusters and having "Z" shape nodose near the apex of the conidiophore. Based on phylogenetic placement and morphological variations, we introduce *M. coryphae* as a new species.



Note a, b Colonies on substrate. c–g Conidiophores. h–o Conidia. p The front of culture on PDA at 25°C and the reverse of culture on PDA at 25°C. Scale bars: d, e = 50 µm, g–o = 10 µm.

Figure 2.141 *Melanographium coryphae* (MHZU 23-0133, holotype)

Melanographium elaeidis Y.R. Xiong, Manawas. & K.D. Hyde, ***sp. nov.***

Figure 2.140

Etymology: The epithet refers to the host genus name "*Elaeis*", from which the species was collected.

Saprobic on dead segment of *Elaeis guineensis*. Asexual morph: Hyphomycetous. *Colonies* on natural substrate superficial, effuse, velvety, tufted, dark brown. *Mycelium* immersed, composed of smooth, pale brown hyphae. *Conidiophores* 300–400 × 4.5–7 μm ($\overline{x}$ = 346 × 5.7 μm, n = 15), macronematous, densely, fascicle or tufted, unbranched, multiseptated, erect, straight or broadly curved, brown at base, paler towards the apex. *Conidiogenous cells* polyblastic, integrated, terminal and intercalary, cylindrical, subhyaline to pale brown, smooth. *Conidia* 15–20 × 11–13 μm ($\overline{x}$ = 17.5 × 12.5 μm, n = 25), solitary, simple, olivaceous brown to brown, frequently reniform, aseptate, rough-walled, verrucose, with a germ slit running longitudinally. Sexual morph: Not observed.

Culture characteristics: Colonies on PDA fast growing, after 2 weeks reaching 4 cm diam., at 25°C, circular, with fluffy, dense, white mycelium on the surface with entire margin; in reverse white.

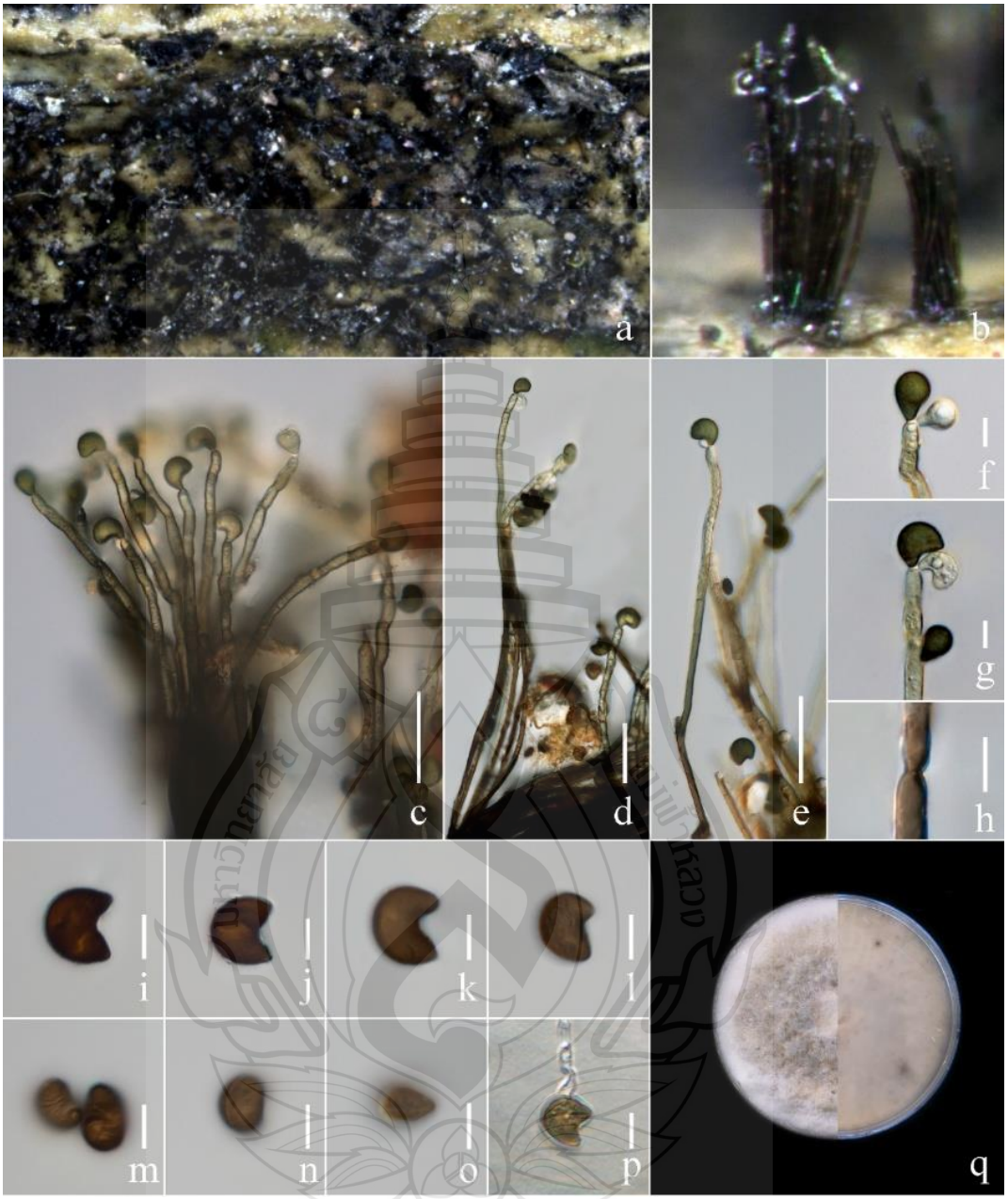
Known distribution: China (this study).

Material examined: China, Yunnan Province, Xishuangbanna City, in an unidentified forest beside National Highway 219, on dead rachis of *Elaeis guineensis*, 5 Feb 2023, Y.R. Xiong and L. Lu, XG195 (MHZU 23-0155, holotype), ex-type ZHKUCC 24-0117, other living culture ZHKUCC 24-0118.

GenBank numbers: ZHKUCC 24-0117: ITS – PV578200, LSU – PV578368, SSU – PV578514, *tef* 1-α – PV608862; ZHKUCC 24-0118: ITS – PV578201, LSU – PV578369, SSU – PV578515, *tef* 1-α – PV608863.

Notes: Two collections from this study formed a separate lineage and clustered with *Melanographium citri* in the phylogenetic tree with 84% ML bootstrap support and 1.00 BYPP (Figure 2.139). The nucleotide differences excluding gaps between *M. elaeidis* (ZHKUCC 24-0117) and *M. citri* (GZCC 21-0208) were checked and given as follows, ITS: 2.48% (14/564 base pairs), LSU: 0.23% (2/884 base pairs), SSU: 0% (0/1001 base pairs), and *tef* 1-α: 2.36% (22/933 base pairs). Morphologically, *M. elaeidis* have terminal and intercalary conidiophore which are different from *M. citri* have only terminal conidiophore (Ellis 1963, Zhang et al., 2024, this study). Based on phylogenetic placement

and morphological variations, we introduce *M. elaeidis* as a new species.

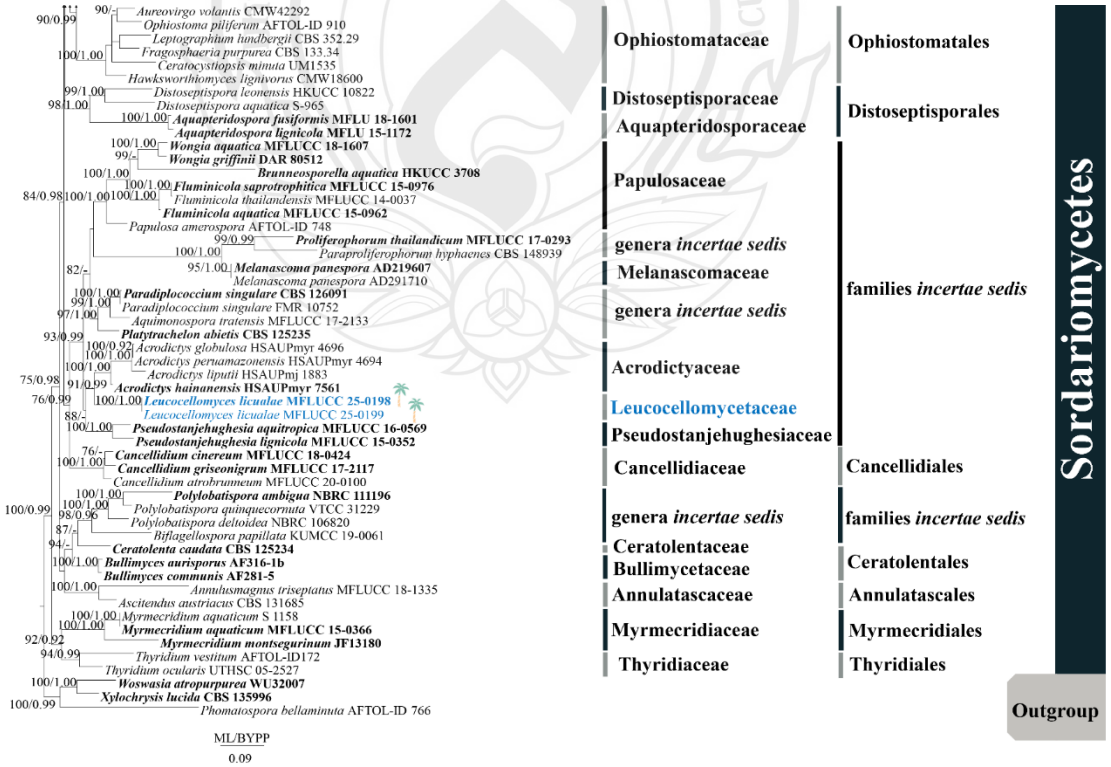


Note a, b Colonies on substrate. c–h Conidiophores. i–o Conidia. p Germinating conidium. q The front of culture on PDA at 25°C and the reverse of culture on PDA at 25°C. Scale bars: c–e = 50 µm, f–p = 10 µm.

Figure 2.142 *Melanographium elaeidis* (MHZU 23-0155, holotype)



Figure 2.143 Phylogenetic tree of some orders in Sordariomycetes



Note Phylogram generated from maximum likelihood analysis of some orders in Sordariomycetes based on combined ITS, LSU, SSU, *tef* 1-α and *rpb*2 sequence data. Bootstrap values for maximum likelihood (ML) equal to or greater than 70 and BYPP values equal to or greater than 0.90 are indicated above the branches. The new collections are indicated in blue and ex-type strains are indicated in bold.

Figure 2.143 (continued)

Leucocellomycetaceae Y.R. Xiong, Manawas. & K.D. Hyde, ***fam. nov.***

Etymology: refers to the name of the type genus.

Type genus: *Leucocellomyces* Y.R. Xiong, Manawas. & K.D. Hyde

Saprobic on dead palm substrates. Asexual morph: Hyphomycetous. *Colonies* on natural substrate effuse, hairy, punctiform. *Mycelium* partly immersed in substratum, consisting of branched hyphae. *Conidiophores* macronematous, mononematous, unbranched, erect to flexuous, dark olive-brown to subhyaline, septate, proliferating, constricted at remnants of proliferation, smooth. *Conidiogenous cells* monoblastic, integrated, terminal, determinate, light coloured, septum at the junction of conidiogenous cell with conidiophore constricted. *Conidia* solitary, fusiform, globose to subglobose, septate, smooth-walled, guttulate. Sexual morph: Not observed.

Notes: Leucocellomycetaceae is introduced and typified by *Leucocellomyces* (*Le*.) which forms a sister clade with Acrodictyaceae within Diaporthomycetidae (Sordariomycetes) (Figure 2.143). Leucocellomycetaceae and Acrodictyaceae both have macronematous, mononematous conidiophores that sometimes proliferate (Xia et al., 2017; Yu et al., 2024). However, in Leucocellomycetaceae the conidiogenous cell is paler than the conidiophore and the septum at the junction of conidiogenous cell with conidiophore is constricted, features not observed in Acrodictyaceae (Figure 2.143; Xia et al., 2017). Acrodictyaceae is a family *incertae sedis* in Diaporthomycetidae (Yu et al., 2024), we propose Leucocellomycetaceae as a new family *incertae sedis* in Diaporthomycetidae (Sordariomycetes).

Leucocellomyces Y.R. Xiong, Manawas. & K.D. Hyde, ***gen. nov.***

Etymology: referring to the light coloured conidiogenous cell characteristic and hyaline apical cell of type species

Type species: *Leucocellomyces licualae* Y.R. Xiong, Manawas. & K.D. Hyde

Saprobic on dead palm substrates. Asexual morph: Hyphomycetous. *Colonies* on natural substrate effuse, hairy, velvety, gregarious. *Mycelium* mostly immersed in substratum, consisting of branched, septate, smooth hyphae. *Conidiophores* macronematous, mononematous, single to caespitose, cylindrical, unbranched, erect to slight curved, dark olive-brown, light olive to hyaline at the apex, septate, percurrently proliferating, not constricted at the septa, constricted at remnants of proliferation, smooth. *Conidiogenous cells* monoblastic, integrated, terminal, cylindrical, septum at the junction of conidiogenous cell with conidiophore constricted, often with localized swelling, light olive to hyaline at the apex, percurrently proliferating. *Conidia* solitary, fusiform, 1-septate, olive to dark brown, truncate conidiogenous loci with pore, basal cell erect and short, upper cell tapering and pointed, slightly bent to geniculate and long, guttulate. Sexual morph: Not observed.

Notes: In our phylogenetic result (Figure 2.143), *Leucocellomyces* clustered with *Acrodictys*. Although they have similar morphology in conidiophores shape, they are different in the shape of conidia and conidiogenous cells (Xia et al., 2017). *Leucocellomyces* has conidia which are 1-septate, basal cell erect and short, upper cell tapering and pointed, slightly bent to geniculate and long, while *Acrodictys* has conidia with both transverse and longitudinal septa, the transverse septa typically spanning the whole conidial width, the longitudinal septa incomplete and short (Xia et al., 2017). According to morphological differences and phylogenetical results, we propose the genus *Leucocellomyces* to accommodate the type species *Le. licualae*. More fresh collections of *Leucocellomyces* are needed to stabilize placement of this genus.

Leucocellomyces licualae Y.R. Xiong, Manawas. & K.D. Hyde, ***sp. nov.***

Figure 2.144

Etymology: The epithet refers to the host genus name "*Licuala*", from which the species was collected.

Saprobic on dead petiole of *Licuala* sp. Asexual morph: Hyphomycetous. *Colonies* on natural substrate effuse, black, hairy, velvety, gregarious. *Mycelium* mostly immersed in substratum, consisting of branched, septate, pale brown to brown, smooth hyphae. *Conidiophores* 70–190 × 4–5.5 µm ($\overline{x}$ = 143 × 4.7 µm, n = 15), macronematous, mononematous, single to caespitose, cylindrical, unbranched, erect to slight curved, dark olive-brown, light olive to hyaline at the apex, septate, percurrently proliferating, not

constricted at septa, constricted at remnants of proliferation, smooth. *Conidiogenous cells* 20–30 × 4–4.5 µm ($\overline{x}$ = 21.6 × 4.3 µm, n = 25), monoblastic, integrated, terminal, cylindrical, septum at the junction of conidiogenous cell with conidiophore constricted, often with localized swelling, light olive to hyaline at the apex, percurrently proliferating. *Conidia* 30–40 × 5.5–6.5 µm ($\overline{x}$ = 33.5 × 5.9 µm, n = 25), fusiform, 1-septate, olive to dark brown, truncate conidiogenous loci with pore, basal cell erect and short, upper cell tapering and pointed, slightly bent to geniculate and long, guttulate. Sexual morph: Not observed.

Culture characteristics: Colonies on PDA fast growing, after 2 weeks reaching 2 cm diam. at 25°C, circular, margin entire, raised, surface dense filamentous; reverse cream at the margin, dark in the center.

Known distribution: Thailand (this study).

Material examined: Thailand, Narathiwat City, Toh Daeng Peat swamp, on dead petiole of *Licuala* sp., 4 Aug 2023, Y.R. Xiong, XG321 (MFLU 25-0144, holotype), ex-type MFLUCC 25-0198, other living culture MFLUCC 25-0199.

GenBank numbers: MFLUCC 25-0198: LSU – PV578358, SSU – PV578508; MFLUCC 25-0199: LSU – PV578359, SSU – PV578509.

Notes: Two collections from this study formed a separate lineage in the phylogenetic tree with 90% ML bootstrap support and 1.00 BYPP (Figure 2.143). Based on a MegaBLAST (Query cover ≥ 70%) search using the LSU sequence, the closest matches in NCBIs GenBank nucleotide database were *Pararamichloridium verrucosum* (GenBank MH873621; Identities 844/897 (94.09%), 7 gap), *Pseudoproboscispora caudae-suis* (GenBank MH868307; Identities 833/887 (93.91%), 6 gaps) and *Cancellidium applanatum* (GenBank NG_064107; Identities 839/894 (93.85%), 4 gaps). The highest similarities using the SSU sequence were *Acrodictys pyriformis* (GenBank PQ066568; Identities 743/813 (98.48%), 1 gap), *Papulosa amerospora* (GenBank AF064050; Identities 830/912 (98.43%), 2 gaps) and *Acrodictys pyriformis* (GenBank NG_242861; Identities 838/924 (98.43%), 2 gaps). The highest similarities using the ITS sequence were *Acrodictys* sp. (GenBank MH267821; Identities 469/563 (83.30%), 34 gaps) and *Lecythophora* sp. (GenBank JX910080; Identities 478/575 (83.13%), 42 gaps), *Acrodictys* sp. (GenBank ON606324; Identities 474/572 (88.56%), 34 gaps). *Leucocellomyces licualae* has distinct conidiophores that are constricted at remnants of proliferation, conidiogenous cell septum at the junction of conidiogenous cell with conidiophore

constricted and often with localized swelling, conidia 1-septate, olive to dark brown and truncate conidiogenous loci with pore. Based on phylogenetic separate placement and morphological variation, we introduce *Le. licualae* as a new species.



Note a, b Colonies on natural substrate. c–f Conidiophores, conidiogenous cells with conidia. g–l Conidia. m The front of culture on PDA at 25°C and the reverse of

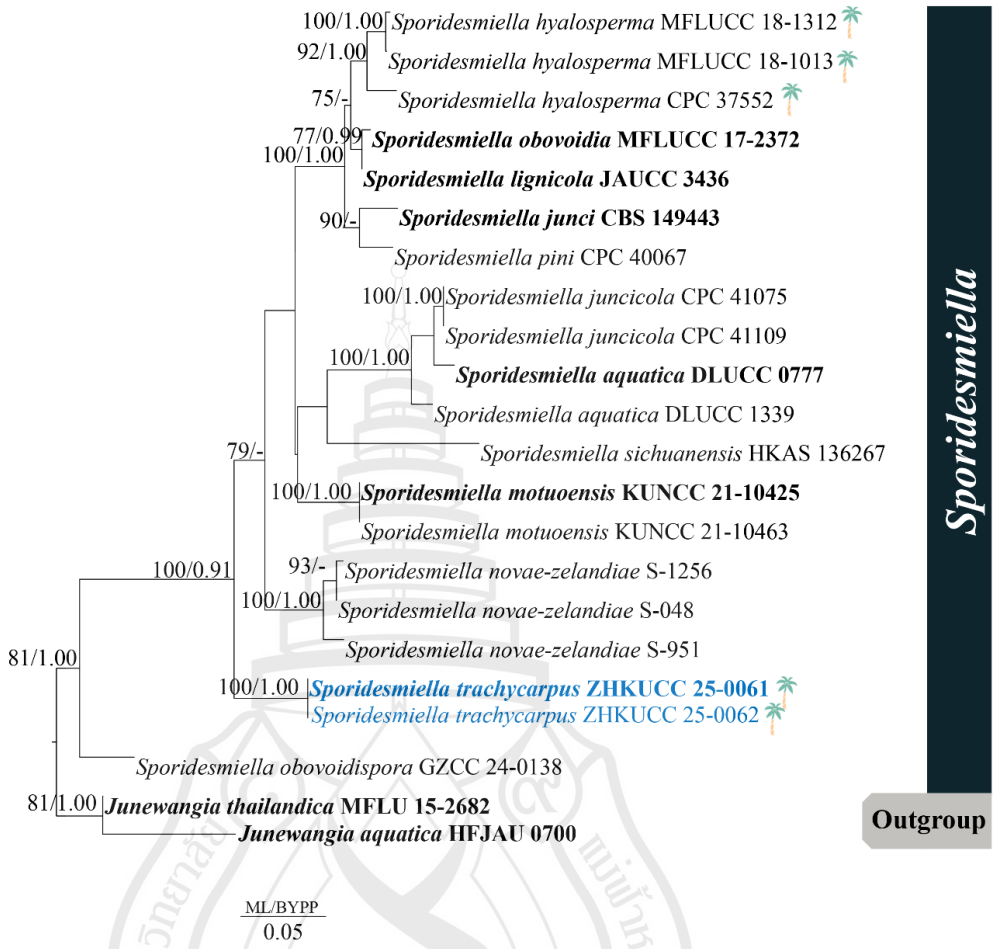
culture on PDA at 25°C. Scale bars: c–f = 50 µm; g–l = 10 µm.

Figure 2.144 *Leucocellomyces licualae* (MFLU 25-0144, holotype)

Junewangiaceae J.W. Xia & X.G. Zhang, Scientific Reports 7: 12 (2017)

Sporidesmiella P.M. Kirk, Transactions of the British Mycological Society 79 (3): 479 (1982)

Notes: Kirk (1982) established *Sporidesmiella* (*Spo*.) with *Spo. claviformis* as the type species. *Sporidesmiella* is a hyphomycetous genus characterized by conidiophore that are macronematous, mononematous and branched or unbranched, conidiogenous cell monoblastic or polyblastic and enteroblastic percurrent elongated, conidia acrogenous or acropleurogenous and mostly distoseptate (Kirk, 1982; Luo et al., 2019). Based on morphological evidence and phylogenetic analysis of combined SSU, LSU, *rpb*2 and *tef* 1-α, Luo et al. (2019) placed *Sporidesmiella* in Junewangiaceae. Subsequently, ITS, LSU, *rpb*2 and *tef* 1-α are mainly used in phylogenetic studies (Yuan et al., 2020; Liu et al., 2024). We used ITS, LSU and *rpb*2 to update phylogenetic studies for *Sporidesmiella* (Figure 2.145). Fifty species are listed under *Sporidesmiella* (Index Fungorum, 2025 February), and only 11 species have molecular data. Four species have been reported from palms including a new species described in this study (Xiong et al., 2025).



Note Phylogram generated from maximum likelihood analysis of *Sporidesmiella* based on combined ITS, LSU and *rpb*2 sequence data. Bootstrap values for maximum likelihood (ML) equal to or greater than 70 are indicated above the branches. The new collections are indicated in blue and ex-type strains are indicated in bold.

Figure 2.145 Phylogenetic tree of *Sporidesmiella*

Sporidesmiella trachycarpi Y.R. Xiong, Manawas. & K.D. Hyde, ***sp. nov.***

Figure 2.146

Etymology: The epithet refers to the host genus name "*Trachycarpus*", from which the species was collected.

Saprobic on dead rachis of *Trachycarpus fortunei*. Asexual morph: Hyphomycetous. *Colonies* on natural substratum effuse, hairy, yellow-brown to brown, velvety, scattered. *Mycelium* immersed, composed of smooth, septate, branched, pale brown hyphae. *Conidiophores* 120–160 × 5–6 µm ($\bar{x}$ = 143 × 5.8 µm, n = 10),

macronematous, mononematous, erect, straight or slightly flexuous, cylindrical, septate, unbranched, smooth, yellow-brown, paler towards the apex. *Conidiogenous cells* 15–18 × 4–5 µm ($\overline{x}$ = 16.7 × 4.8 µm, n = 25), integrated, terminal, monoblastic or rarely polyblastic, holoblastic, subhyaline to pale brown, cylindrical, taper towards the apex. *Conidia* 18–25 × 8–12 µm ($\overline{x}$ = 21.7 × 10 µm, n = 25), acrogenous, solitary, 3–4-distoseptate, clavate–obclavate, widened and rounded at the apex, uneven width, truncate at the base, sometimes flexuous, subhyaline to pale brown, thick-walled, smooth. Sexual morph: Not observed.

Culture characteristics: Colonies on PDA fast growing, after 2 weeks reaching 1 cm diam., at 25°C, circular, with fluffy, dense, white mycelium on the surface with entire margin, PDA surface ochreous; in reverse brown in the middle and cream at the margin.

Known distribution: China (this study).

Material examined: China, Jiangxi Province, Pingxiang City, Wugong Mountain National Scenic Area, on dead rachis of *Trachycarpus fortunei*, 12 Apr 2024, Y.R. Xiong, XG413 (MHZU 24-0494, holotype), ex-type ZHKUCC 25-0061, other living culture ZHKUCC 25-0062.

GenBank numbers: ZHKUCC 25-0061: ITS – PV578254, LSU – PV578422, *rpb2* – PV595362; ZHKUCC 25-0062: ITS – PV578255, LSU – PV578423, *rpb2* – PV595363.

Notes: Two collections from this study formed an independent lineage within *Sporidesmiella* in the phylogenetic tree with 100% ML bootstrap support and 1.00 BYPP. Based on a MegaBLAST (Query cover ≥ 70%) search using the ITS sequence, the closest matches in NCBIs GenBank nucleotide database were *Sporidesmiella* sp. (GenBank OL435555; Identities 550/560 (98.21%), 4 gaps), *Sporidesmiella* sp. (GenBank OP626349; Identities 518/546 (94.87%), 15 gaps) and *Sporidesmiella* sp. (GenBank PQ168238; Identities 510/538 (94.80%), 15 gaps). The highest similarities using the LSU sequence were *Sporidesmiella* sp. (GenBank OL376601; Identities 844/844 (100%), 0 gap), *Sporidesmiella* sp. (GenBank ON124905; Identities 831/831 (100%), 0 gaps) and *Sporidesmiella* sp. (GenBank PQ455346; Identities 780/783 (99.63%), 2 gaps). The highest similarities using the *rpb2* sequence were *Sporidesmiella novae-zelandiae* (GenBank MN124525; Identities 789/875 (90.17%), 0 gaps), *Spo. juncicola* (GenBank OK651165; Identities 602/674 (89.32%), 0 gaps) and *Spo. aquatica* (GenBank MN124524; Identities 678/767 (88.40%), 2 gaps). *Sporidesmiella trachycarpi* fits well with

morphological characterize *Sporidesmiella* by conidia widened and rounded at the apex, uneven width, truncate at the base (Kirk, 1982; Luo et al., 2019, Figure 2.146). However, according to significant disparity molecular variations, we introduce *Spo. trachycarpi* as a new species.



Note a, b Colonies on substrate surface. c–e Conidiophore, conidiogenous cells with conidia. f–i Conidia. j The front of culture on PDA at 25°C and the reverse of culture on PDA at 25°C. Scale bars: c–i = 10 µm.

Figure 2.146 *Sporidesmiella trachycarpi* (MHZU 24-0494, holotype)

Pseudoconlariaceae Y.R. Xiong, Manawas. & K.D. Hyde, ***fam. nov.***

Etymology: refers to the name of the type genus.

Type genus: *Pseudoconlarium* N.G. Liu, K.D. Hyde & J.K. Liu

Saprobic on dead palm substrates. Asexual morph: Hyphomycetous. *Colonies* on natural substrate effuse, scattered, punctiform. *Mycelium* partly immersed, partly superficial. *Conidiophores* micronematous or semi-macronematous, mononematous, septate, branched, flexuous, subhyaline to pale brown. *Conidiogenous cell* monoblastic, integrated, terminal, subhyaline to pale brown, determinate, coliform. *Conidia* solitary, brown to median brown, irregularly globose to sub globose, or trapeziform, muri form, obpyriform, constricted at the septa, smooth-walled, thick wall. Sexual morph: Not observed.

Notes: Pseudoconlariaceae is introduced here to accommodate the genus *Pseudoconlarium* (*Pseudoc*.) which was treated as Diaporthomycetidae (Sordariomycetes) genus *incertae sedis* (Hyde et al., 2020a). Pseudoconlariaceae which formed a sister branch with Xenospadicoidaceae which is supported by 89% ML Bootstrap values within Sordariomycetes (Figure 2.143). The phylogenetic result was similar to previous phylogenetic analysis (Réblová et al., 2018; Luo et al., 2019; Hyde et al., 2021; Liu et al., 2024). Pseudoconlariaceae is distinct by conidiophores micronematous or semi-macronematous and irregular shape of conidia, Xenospadicoidaceae is characterised by conidiophores macronematous, mononematous and conidia solitary or in chains (Hernández-Restrepo et al., 2017). Although Pseudoconlariaceae was similar to Conlariaceae in conidia character which is irregularly globose or subglobose, septate, and constricted at the septa (Hyde et al., 2021), they did not share the same ancestral clade. Thus, based on the phylogenetic results and special morphological characters, it is necessary to propose Pseudoconlariaceae to accommodate *Pseudoconlarium* at a higher taxonomic level.

Pseudoconlarium N.G. Liu, K.D. Hyde & J.K. Liu, Fungal Diversity 100: 191 (2020)

Type species: *Pseudoconlarium punctiforme* N.G. Liu, K.D. Hyde & J.K. Liu.

Notes: Hyde et al. (2020a) established *Pseudoconlarium* with *Pseudoc. punctiforme* as type species based on morphological evidence and phylogenetic analysis combined SSU, LSU, and *tef* 1-α. Due to its unstable phylogenetic placement, the genus

was assigned to Diaporthomycetidae (Sordariomycetes) as *incertae sedis* (Hyde et al., 2020a). *Pseudoconlarium* is hyphomycetous genus characterized by punctiform colonies, micronematous or semi-macronematous conidiophores, and subglobose and muriform conidia with multi-septum (Hyde et al., 2020a). In this study, our new collection was analyzed using ITS, LSU, SSU, and *tef1-α* and updated the phylogenetic analysis of Sordariomycetes in which we, provide a stable placement for *Pseudoconlarium* in Sordariomycetes. *Pseudoconlarium* is a monotypic genus (Index Fungorum, 2025 January), the accepted species associated with molecular data. Here we described a new species of *Pseudoconlarium* which is the first time reported from palm species (Xiong et al., 2025).

Pseudoconlarium trachycarpi Y.R. Xiong, Manawas. & K.D. Hyde, ***sp. nov.***

Figure 2.147

Etymology: The epithet refers to the host genus name "*Trachycarpus*", from which the species was collected.

Saprobic on dead primary rachis of *Trachycarpus fortunei*. Asexual morph: Hyphomycetous. *Colonies* on natural substrate effuse, scattered, punctiform, raised, dark brown to black. *Mycelium* partly immersed, partly superficial, composed of light brown, septate, branched hyphae. *Conidiophores* micronematous, mononematous, septate, branched, flexuous, subhyaline to pale brown. *Conidiogenous cell* 6–9 × 2–4 μm ($\overline{x}$ = 8 × 3.2 μm, n = 15), monoblastic, integrated, terminal, subhyaline to pale brown, determinate, doli form. *Conidia* 25–35 × 15–20 μm ($\overline{x}$ = 28 × 16.9 μm, n = 25), solitary, median brown, irregularly globose or sub globose, muri form, obpyriform, slight constricted at the transverse septum, smooth-walled, thick wall. Sexual morph: Not observed.

Culture characteristics: Colonies on PDA fast growing, after 2 weeks reaching 2 cm diam. at 25°C, circular, margin entire, dense, cream, mycelium velvety and black towards the margin, cream; reverse black at the margin.

Known distribution: China (this study).

Material examined: China, Jiangxi Province, Pingxiang City, Wugong Mountain National Scenic Area, on dead primary rachis of *Trachycarpus fortunei*, 12 Apr 2024, Y.R. Xiong, XG405 (MHZU 24-0464, holotype), ex-type ZHKUCC 25-0057, other living culture ZHKUCC 25-0058.

GenBank numbers: ZHKUCC 25-0057: LSU – PV578404, SSU – PV578538;

ZHKUCC 25-0058: LSU – PV578405, SSU – PV578539.

Notes: Two collections from this study formed a separate lineage and clustered with *Pseudoc. punctiforme* in the phylogenetic tree with 94% ML bootstrap support and 1.00 BYPP (Figure 2.143). The nucleotide differences excluding gaps between *Pseudoc. trachycarpi* (ZHKUCC 25-0057) and *Pseudoc. punctiforme* (GZCC 20-0009) were checked and given as follows, ITS: 15.80% (82/519 base pairs), LSU: 5.15% (42/815 base pairs), SSU: 1.86% (19/1021 base pairs), *tef* 1-α: 9.47% (88/929 base pairs). *Pseudoconlarium trachycarpi* fits well with *Pseudoc. punctiforme* on conidia shape. However, in *Pseudoconlarium trachycarpi* trapeziform conidia were not observe and only slightly constricted at the transverse septum which is different from *Pseudoc. punctiforme* have trapeziform conidia and are constricted at the septa (Hyde et al., 2020a). Thus, based on significant molecular differences and morphological variations, we introduce *Pseudoc. trachycarpi* as a new species.



Note a, b Colonies on natural substrate. c–h Conidiogenous cells with conidia. i The front of culture on PDA at 25°C and the reverse of culture on PDA at 25°C. Scale bars: c = 20 µm; d–h = 10 µm.

Figure 2.147 *Pseudoconlarium trachycarpi* (MHZU 24-0464, holotype)

Sporodochyalomycetaceae Y.R. Xiong, Manawas. & K.D. Hyde, ***fam. nov.***

Etymology: refers to the name of the type genus.

Type genus: *Sporodochyalomyces* Y.R. Xiong, Manawas. & K.D. Hyde

Saprobic on dead palm substrates. Asexual morph: Hyphomycetous. *Colonies* on natural substrate effuse, scattered, coalescing, punctiform. *Mycelium* partly immersed, partly superficial. *Conidiophores* micronematous, reduced to conidiogenous cell. *Conidiogenous cell* holoblastic, at the base of the spore, hyaline. *Conidia* non-complanate, cheiroid, clavate, ellipsoidal, subcylindrical, slight bent to geniculate, brown to dark brown, acrogenous, smooth-walled, tightly fasciculate structure, composed of multiple rows of cells, multi-euseptate in each row, rows of cells tapering and converging at the conidial base, each row of cells bears a hyaline, elongated apex cell at the top. Conidial secession: schizolytic. Sexual morph: Not observed.

Notes: Sporodochyalomycetaceae is introduced to accommodate the new genus *Sporodochyalomyces* (*Spo.*) which formed an independent branch with Trichosphaeriaceae within Diaporthomycetidae in Sordariomycetes (Figure 2.143). The phylogenetic result was similar to previous phylogenetic analyses (Réblová et al., 2018; Luo et al., 2019; Hyde et al., 2021; Liu et al., 2024). *Sporodochyalomyces* is distinct in Diaporthomycetidae by having tightly fasciculate structures, composed of multiple rows of cells, each row of cells bears an elongated apex cell. Although those characteristics are different from hyphomycetous (*Brachysporium*) morph of Trichosphaeriaceae which are usually pendulous, clavate, ellipsoidal, fusiform, limoniform, obovoid or pyriform, septate, brown, often with polar cells paler than middle cells (Hyde et al., 2020b). *Sporodochyalomyces* formed a stable lineage with *Brachysporium*, which is a genus of *Trichosphaeriaceae* placed as *incertae sedis* due to its unclear taxonomic position (Crous et al., 2023). Thus, we propose *Sporodochyalomycetaceae* as a Diaporthomycetidae family *incertae sedis*, pending further evidence for re-evaluating its taxonomic placement.

Sporodochyalomyces Y.R. Xiong, Manawas. & K.D. Hyde, ***gen. nov.***

Etymology: referring to the conidia characteristic “fasciculate structure” and “hyaline cell at apex” of type species

Type species: *Sporodochyalomyces trachycarpi* Y.R. Xiong, Manawas. & K.D. Hyde

Saprobic on dead palm substrates. Asexual morph: Hyphomycetous. *Colonies*

on natural substrate effuse, scattered, coalescing, punctiform, dark brown to black. *Mycelium* is partly immersed, partly superficial, and composed of septate, branched hyphae. *Conidiophores* micronematous, reduced to conidiogenous cell. *Conidiogenous cell* holoblastic, at the base of the spore, hyaline. *Conidia* non-complanate, cheiroid, clavate, ellipsoidal, subcylindrical, slightly bent to geniculate, brown to dark brown, acrogenous, smooth-walled, and without appendages or mucilaginous sheaths, form a tightly fasciculate structure, composed of multiple rows of cells, multi-euseptate in each row, slightly constricted at septa, rows of cells tapering and converging at the conidial base, each row of cells bears a hyaline, elongated apex cell at the top, tapering towards the apex, rounded to truncate at apex. Conidial secession: schizolytic. Sexual morph: Not observed.

Notes: Based on our phylogenetic result (Figure 2.143), *Sporodochyalomyces* formed a distinct clade in Pleosporales and clustered with *Brachysporium*. *Sporodochyalomyces* has micronematous conidiophore or they are reduced to conidiogenous cells and tightly sporodochium structure conidia while *Brachysporium* has macronematous, mononematous conidiophores and conidia that are ellipsoid, obovoid or broadly fusiform (Markovskaja & Treigienė, 2007). It also differs from *Biflagellospora* which has have macronematous, mononematous, erect, conidiophores and conidia which are composed of 8–9 cells consisting of the two upper and larger ones having 4–8 distal tapering arms attached filiform, hyaline appendages (Sivichai & Hywel-Jones, 1999). The only species of *Biflagellospora* with molecular data is *Biflagellospora papillata* (=*Aquidictyomyces appendiculatus*) (Dong et al., 2021; Koukol & Delgado, 2021). According to morphological differences evidence and phylogenetical results, we propose a monotypic genus *Sporodochyalomyces* to accommodate the type species *Spo. trachycarpi*. More fresh collections of *Sporodochyalomyces* are needed to stabilize and evaluate placement of this genus and family Sporodochyalomycetaceae.

Sporodochyalomyces trachycarpi Y.R. Xiong, Manawas. & K.D. Hyde, ***sp. nov.***

Figure 2.148

Etymology: The epithet refers to the host genus name "*Trachycarpus*", from which the species was collected.

Saprobic on dead primary rachis of *Trachycarpus fortunei*, Asexual morph: Hyphomycetous. *Colonies* on natural substrate effuse, scattered, coalescing, punctiform, raised, dark brown to black. *Mycelium* partly immersed, partly superficial, composed of

light brown, septate, branched hyphae. *Conidiophores* micronematous, reduced to conidiogenous cell. *Conidiogenous cell* holoblastic, at the base of the spore, hyaline. *Conidia* 50–110 × 25–40 µm ($\bar{x}$ = 76 × 30 µm, n = 25), non-complanate, cheiroid, clavate, ellipsoidal, subcylindrical, slight bent to geniculate, brown to dark brown, acrogenous, smooth-walled, and without appendages or mucilaginous sheaths, form a tightly fasciculate structure, composed of multiple rows of cells, 11–18 euseptate in each row, slightly constricted at septa, rows of cells tapering and converging at the conidial base, each row of cells bears a hyaline, elongated apex cell at the top, 10–17 × 2.5–4.5 µm ($\bar{x}$ = 13.5 × 3.3 µm, n = 25), tapering towards the apex, rounded to truncate at apex. Conidial secession: schizolytic. Sexual morph: Not observed.

Culture characteristics: Colonies on PDA fast-growing, after 2 weeks reaching 1 cm diam., at 25°C, circular, lobate entire, umbonate, dense, mycelium velvety towards the margin, brown; reverse dark brown at the margin, black in the center.

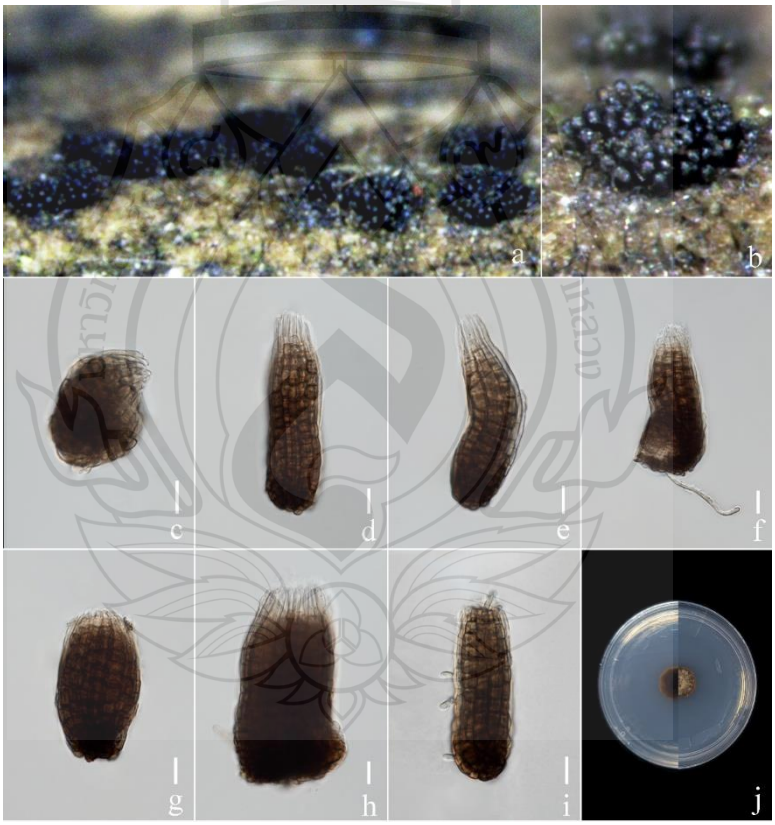
Known distribution: China (this study).

Material examined: China, Jiangxi Province, Pingxiang City, Wugong Mountain National Scenic Area, on dead primary rachis of *Trachycarpus fortunei*, 12 Apr 2024, Y.R. Xiong, XG406 (MHZU 24-0465, holotype), ex-type ZHKUCC 25-0059, other living culture ZHKUCC 25-0060.

GenBank numbers: ZHKUCC 25-0059: ITS – PV578178, LSU – PV578342, *tef* 1-α – PV608848; ZHKUCC 25-0060: ITS – PV578179, LSU – PV578343, *tef* 1-α – PV608849.

Notes: Two collections from this study formed a separate lineage in the phylogenetic tree with 99% ML bootstrap support and 1.00 BYPP (Figure 2.143). Based on a MegaBLAST (Query cover ≥ 70%) search using the LSU sequence, the closest matches in the NCBI GenBank nucleotide database were *Cryptadelphia groenendalensis* (GenBank AY281104; Identities 859/884 (97.17%), 2 gap), *Brachysporium* sp. (GenBank PQ345849; Identities 799/823 (97.08%), 3 gaps) and *Cryptadelphia groenendalensis* (GenBank EU528007; Identities 863/889 (97.08%), 3 gaps). The highest similarities using the SSU sequence were *Xylolentia* sp. (GenBank OP378025; Identities 1014/1035 (97.97%), 0 gap), *Conlarium aquaticum* (GenBank MN994331; Identities 1009/1030 (97.96%), 1 gap) and *Conlarium aquaticum* (GenBank MN994323; Identities 1008/1029 (97.96%), 1 gap). The highest similarities using the ITS sequence were *Pseudoproboscispora caudae-suis*

(GenBank KU975070; Identities 470/587 (80.07%), 43 gaps) and *Longicollum biappendiculatum* (GenBank KU975062; Identities 468/589 (79.46%), 44 gaps), *Annulusmagnus triseptatus* (GenBank OK298393; Identities 463/583 (79.42%), 40 gaps). The highest similarities using the *tef* 1-α sequence were *Distoseptispora rostrata* (GenBank MG988425; Identities 791/869 (91.02%), 0 gaps) and *Cancellidium cinereum* (GenBank MT370488; Identities 860/952 (90.34%), 2 gaps), *Rhodoveronaea nieuwwulvenica* (GenBank OQ627955; Identities 791/877 (90.19%), 0 gap). *Sporodochyalomyces trachycarpi* is distinct by conidia that are ellipsoidal to subcylindrical, slightly bent to geniculate, forming a tightly fasciculate structure, composed of multiple rows of cells, slightly constricted at septa, rows of cells tapering and converging at the conidial base, each row of cells bears a hyaline, elongated apical cell. Based on phylogenetic placement and morphological variation, we introduce *Spo. trachycarpi* as a new species.



Note a, b Colonies on natural substrate. c–h Conidia. i Germinating conidia. j The front of culture on PDA at 25°C and the reverse of culture on PDA at 25°C. Scale bars: c–i = 10 µm.

Figure 2.148 *Sporodochyalomyces trachycarpi* (MHZU 24-0465, holotype)

2.4 Discussion

Rich fungal diversity is essential for maintaining the function and stability of ecosystems (Dighton & White, 2017; Grossart et al., 2019; Liu et al., 2022). The unique structure and rich diversity of palm trees support a huge diversity of palm fungi (Zhang et al., 2024). As previously discussed, studies on plam fungi has been flourished over the years yet diversity, composition and the boundaries of species need to be further updated to adapt modern fungal taxonomy to this end, our results provide a large number of new taxa and records of palm fungi to supplement the diversity of palm fungi with the new clues for the host preference of palm fungi. Furthermore, our study also provides new interpretations for predicting the total number of palm fungal diversity from the perspectives of time, space and climate.

2.4.1 Host Preference of Palm Fungi

The host specificity of palm fungi has always been a focus of researchers. Zhou and Hyde (2001) proposed a more accurate description of "host preference", which refers to repeated occurrence on the same host and absence or seldom occurrence on adjacent hosts of the same family. Pereira and Phillips (2023) believed that palm fungi have fungal specificity at the family, genus and species levels, and proposed that palm fungi have tissue specificity on palm hosts. In addition, Zhang et al. (2024) has considered *Anthostomella*, *Linocarpon* and *Oxydothis* to be major palm-specific fungal genera. However, "host preference" had limitations in describing high-level plant groups. To this end, based on the definition of "host preference", we took palm fungi as the analysis object and provided a new perspective to explain "host preference". Based on the data of this study, we propose three terms 'typical palm preferring fungal genus'', "atypical palm host-preferring fungal genus" and "conjectured palm host-preferring fungal genus". We would like to elaborate on these definitions and relationships as follows.

A "typical palm preferring fungal genus" is defined based on two characteristics: (1) the species in a particular genus that use palm species (Arecaceae) as their host or over 50% of species in the genus host palm species (Arecaceae) and (2) more than half of the palm fungal species in the genus clustered together and shared the same ancestor in the phylogenetic tree of the genus. *Fissuroma* in this study is a "typical palm host-preferential fungal genus". *Fissuroma* was first proposed to include *Fissuroma aggregatum* from bamboo and *Fissuroma maculans* from palm (Liu et al., 2011). Subsequent studies mostly reported on *Fissuroma* species from the palm family (Phookamsak et al., 2015; Niranjan

& Sarma, 2018; Konta et al., 2020). To date, 10 of the 15 species of *Fissuroma* have palm host records (Index Fungurum, 2025; Checklist). Our phylogenetic results also showed that all *Fissuroma* species with palm host records clustered in the branch represented by *Fissuroma maculans* (Figure 2.16) with significant bootstrap support (100% ML). Another fungal genus with such a striking palm host preference is *Melanographium*. To date, 13 of the 16 species of *Melanographium* have been reported to occur on palm hosts (Index Fungorum, 2025; Checklist). In the phylogenetic analysis results of this study, *Melanographium* showed clustering of palm host groups similar to *Fissuroma* (Figure 2.139, 100% ML). In addition, *Fasciatispora* is also an underestimated fungal genus with a strong palm host preference. *Fasciatispora* was originally established based on *Fasciatispora nypae* from *Nypa fruticans* (Hyde, 1991). This special palm preference characteristic has become increasingly prominent in subsequent studies. To date, 13 of the 15 species of *Fasciatispora* have been introduced based on palm hosts and have only been reported on palm hosts (Index Fungorum, 2025; Checklist). The phylogenetic results of *Fasciatispora* also showed the clustering of palm host groups (Figure 2.125). The palm host preference of these three genera makes them considered representative genera of palm host preference that should be focused on after *Anthostomella*, *Linocarpon* and *Oxydothis*. It is noteworthy that many genera meet the definition of palm host preference in this study, including *Phellinocrescentia*, *Pseudomassarina*, *Inflatispora*, *Fusichloridium*, *Verticimonosporium*, *Pseudoconiocessia* and newly introduced genera. However, most of these genera have only two species and are not representative of the study. Therefore, further collections are necessary to understand the relationship of these poorly represented genera.

If a particular genus only fulfils the definition based on the fungal genus perspective (1) the species that use palm trees as a host or one of their hosts account for 25% to 50% of the total number of species in the genus, we call it as "atypical palm host-preferring fungal genus". For instance, *Neomassaria*, although four out of 12 species (33%) have been reported from palms, in the phylogenetic analyses, these palm fungi are scattered at different positions (Figure 2.39). In addition, when constructing a phylogenetic analysis of *Neomassaria*, we observed that the developmental positions between palm host species of this genus were almost all interspersed with species from coffee hosts. This may be caused by the host-jumping phenomenon of the fungus from palm to coffee, as there is a clear host-

jumping phenomenon in coffee (Lu et al., 2025). In addition, two of the eight (25%) species of *Xylolentia* are from palm trees, and these two species are scattered at different positions in the phylogenetic tree (Figure 2.111). We speculate that the fungal genera of this group may represent a stage of transition to typical palm-preferring fungal genera or non-palm-preferring fungal genera. Future data from studies on this type of fungi may support our conjecture.

If a particular genus only fulfils the definition based on the phylogenetic perspective (2) more than half of the palm host fungal species in the genus appear clustered in the phylogenetic results of the genus, we call it a "conjectured palm host-preferring fungal genus". For example, *Byssosphaeria* and *Distoseptispora* in this study, more than half of their palm host members clustered in one clade in the phylogenetic results (Figure 2.33, Figure 2.91). The unique structure of fungi helps them to reproduce and spread in nature (Gwynne-Vaughan, 2021; Bahram & Netherway, 2022), which may explain this phenomenon. *Byssosphaeria* has a unique spherical perithecia structure, and *Distoseptispora* has a multi-distoseptate structure, which also gives them a unique advantage among hyphomycetes (Luo et al., 2018; Xiong et al., 2023). Therefore, it is possible that they were once palm-preferring fungi. However, their advantageous structures made their habitats no longer restricted, and they have since turned into non-palm-preferring fungi. However, this view still needs more data to support it.

2.4.2 Palm Fungi Collection, Culture, and Challenges in Identification

Isolating fungi from their host or substrate and obtaining pure cultures has always been challenging (Goh, 1999). Most mycologists consider single spore collection the best method for obtaining pure cultures and outline standard procedures (Kirsop & Doyle, 1991; Goh, 1999; Senanayake et al., 2020). However, conidia from contaminants present on the specimen may be transferred along with the target conidia or spores (Bernadovičová & Ivanová, 2011). If the fungus grows slowly, bacterial or fungal contaminants may overgrow it, potentially leading to incorrect identification (Smith, 1969; Goh, 1999). Furthermore, not all spores can germinate on artificial culture media, necessitating the development of alternative techniques (Choi et al., 1999). Numerous palm-associated fungal species were described before the molecular era, but some could not be obtained in pure culture (Taylor & Hyde, 2003). These challenges were also encountered in the present study.

Our study collected a total of 645 samples from tropical and subtropical regions of

China and Thailand. Various methods were used to isolate fungi and extract DNA from these samples following Senanayake et al. (2020). Pure cultures were obtained, and DNA was successfully extracted from 437 samples. Despite attempting multiple methods, the remaining 214 samples failed to yield the corresponding pure culture. Subsequent attempts to extract DNA directly from the fruiting bodies, according to Zeng et al. (2018), were also unsuccessful. Finally, we fully characterized 105 samples and identified them phylogenetically and morphologically.

To explore the possible reasons why palm fungi samples did not germinate, a germination rate distribution diagram of the corresponding morphology was provided according to the different fruiting body morphologies of fungi (Figure 2.149). We found that the germination rate of asexual fungi (Coelomycete 69.39% and Hyphomycete 71.36%) was significantly higher than that of fungi with sexual reproductive structures (Ascomata 59.25%). This may be because ascospores usually have a dormancy mechanism, and in nature, they often require specific stimuli (such as temperature changes, chemical signals, light cycles, etc.) to break dormancy and germinate (Rämä & Quandt, 2021). The laboratory conditions we used may not meet the triggering factors required for germination, failing some Ascomata samples to germinate.

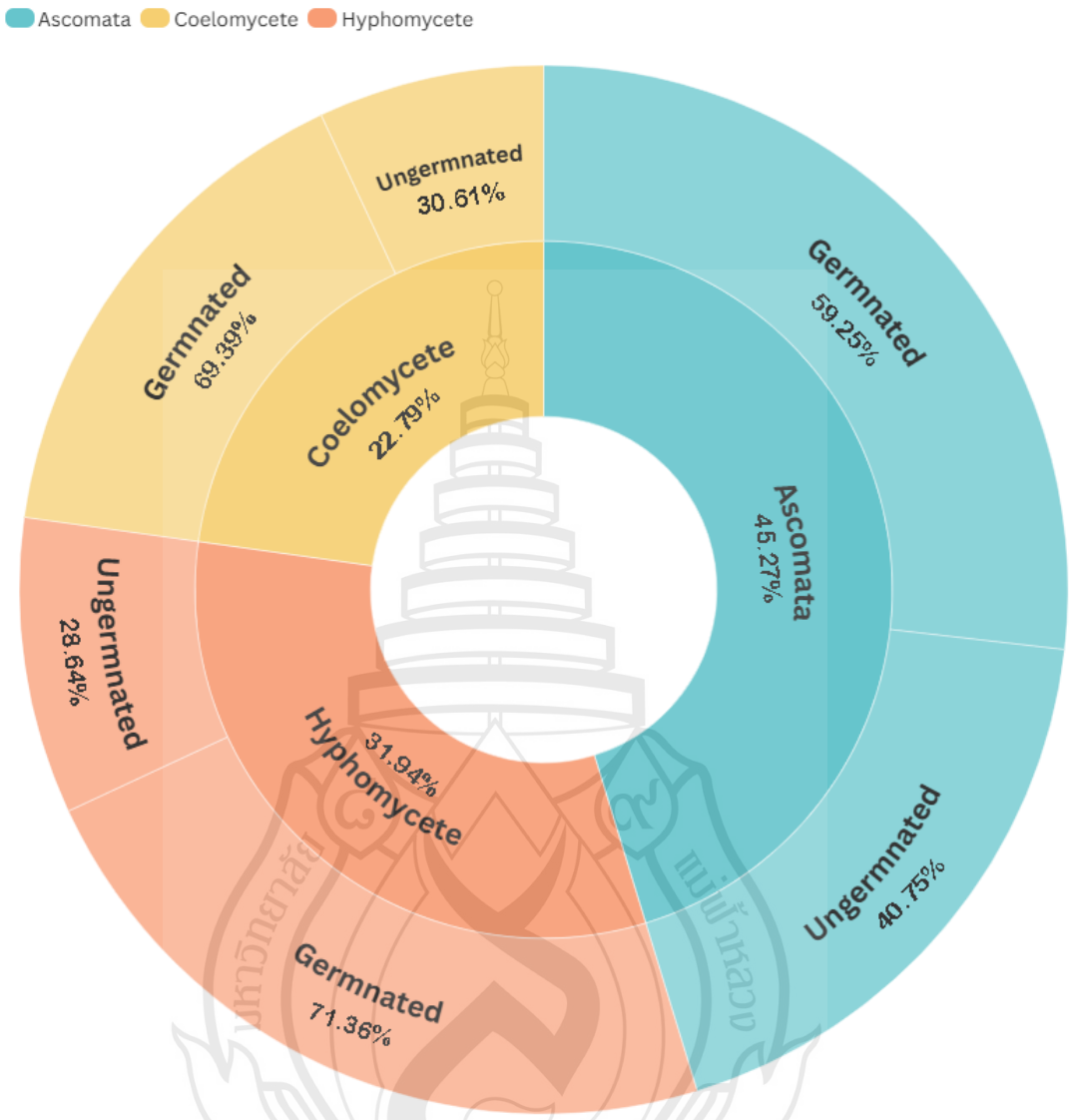


Figure 2.149 Germination rate based on different fruiting body morphologies

In addition, the germination rates also varied markedly by collection location (Figure 2.150). Southern China and Thailand exhibited a wide range: the highest germination was observed in Jiangxi (76.0% germinated) and Yunnan (70.2%), whereas Guangdong had the lowest (46.5%). Guangxi (56.3%) and southern Thailand (Narathiwat, 56.6%) were intermediate. Thus, more than 70% of collections from Jiangxi and Yunnan provinces grew, whereas less than half did from Guangdong province. These regional differences may be caused by a variety of factors. Climate and environmental conditions can affect the life cycle and spore viability of fungi (Tapia et al., 2025). These provinces

are home to different palm species, each of which may have different fungal communities. The Yunnan and Jiangxi provinces flora may favor fungi (or fungal morphotypes) that germinate easily, whereas the Guangdong palms may favor taxa that germinate poorly. Geographic origin significantly affects fungal germination success, but the underlying causes are likely complex and multifactorial, involving interactions between the local environment, the condition of the host palm, the composition of the specific fungal community, and post-collection handling.

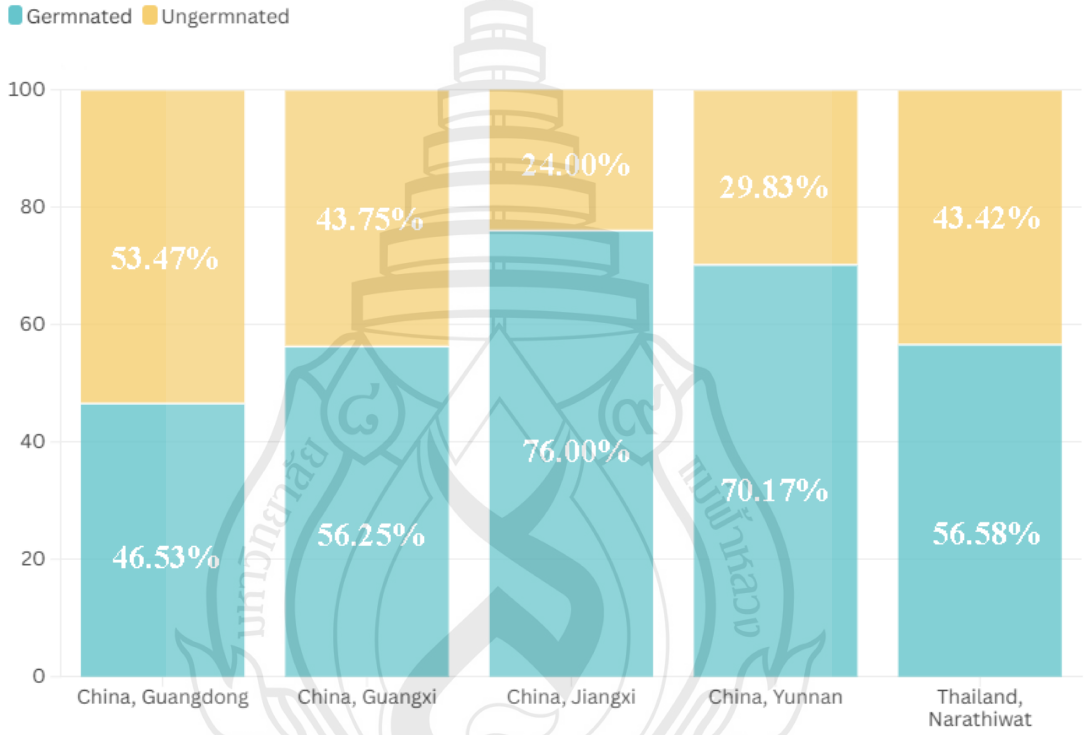


Figure 2.150 Germination rate based on collection locations

During the collection of palm fungi, it is essential to prioritize distinct preservation methods for specimens from different habitats. Samples obtained from humid environments should be promptly dried after collection to prevent mite infestation and mold development. Newly acquired specimens brought back to the laboratory must also undergo immediate observation and isolation to avoid extended storage periods that may lead to the complete release of internal contents from the sporocarp, leaving only an empty cavity (Figure 2.151). For samples that fail to germinate or yield viable sporocarp DNA, taxonomic identification—at the family or genus level, or designated as incertae sedis—is conducted based on morphological comparisons (Figure 2.151). All unidentified specimens

are temporarily archived in the specimen repository, awaiting future technological advances for accurate identification.

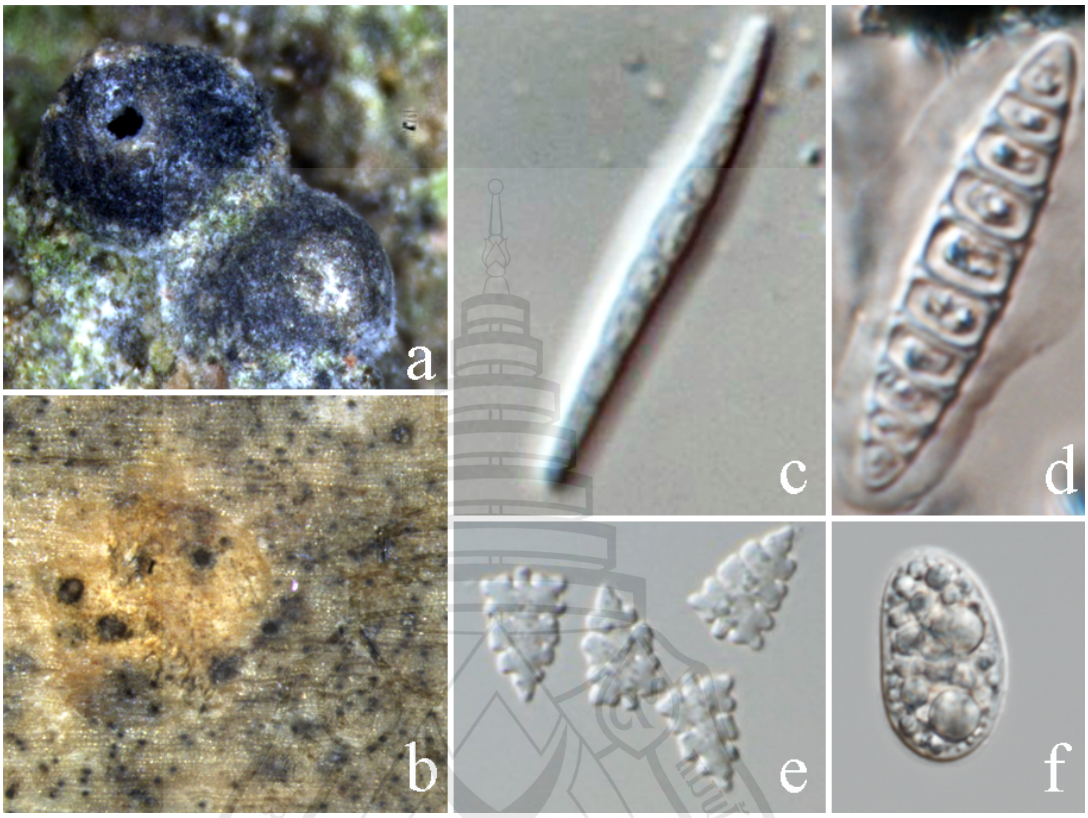


Figure 2.151 Unidentified fruiting bodies and spores

CHAPTER 3

PALM FUNGI DATA PLATFORM

3.1 Introduction

To document the diversity and distribution of different organismal taxa, it is important to set out recording and standardised monitoring programmes, often with the help of citizen scientists (Mueller et al., 2004; Halme et al., 2012; Haelewaters et al., 2024). Fungi are an ancient and thriving group of organisms that play a vital role in natural ecosystems (Stubblefield et al., 1985; Taylor et al., 2014; Xie et al., 2023). As early as the beginning of the 20th century, evidence of fungi living in the Tertiary period was found in fossils and, since then, a large number have been documented (Kidston & Lang, 1921; Edwards, 1922). In the 21st century, the description of new species and the recording of fungi have been occurring at a higher frequency (Hawksworth & Lücking, 2017; Fisher et al., 2020). Over the centuries, mycologists have been working to study the diversity of fungi. The “Sylloge Fungorum”, published by Pier Andrea Saccardo in 1882, stimulated extensive research and discussion on fungal diversity amongst modern mycologists (Bolman, 2023). This discussion continues to this day, with Hawksworth (2001) suggesting that the number of fungi might be 1.5 million species, O’Brien et al., (2005) estimating there might be 3.5 to 5.1 million species, while Schmit and Mueller (2007) suggest that there may be as few as 712,000 species. According to a more recent study by Niskanen et al. (2023), the current estimates for global fungal richness range between 2 and 3 million species, with a “best guess” at 2.5 million, of which only about 150,000 fungi have been described (Species Fungorum, 2024, http://www.speciesfungorum.org). There are three major ecological strategies of fungi: saprotrophic, parasitic and mutualistic (Willis, 2018). To adapt to different ecological settings, fungi have a variety of life modes, including endophytes, pathogens or saprobes and, depending on environmental conditions, they may be able to shift from one lifestyle to another, such as endophytes becoming pathogens (Hyde et al., 2014; Bhunjun et al., 2023). These diverse lifestyles allow fungi to have a wide range of hosts, from animals to plants. Amongst these, the relationship between fungi

and plants has been well-studied (Senanayake et al., 2020; Jayawardena et al., 2021; Maharachchikumbura et al., 2021; Manawasinghe et al., 2021).

Arecaceae, which is commonly known as palms, ranks fifth in species richness amongst monocot families (Chen et al., 2022). According to APG IV (Angiosperm Phylogeny Group et al., 2016), Arecaceae contains five subfamilies, namely Arecoideae, Calamoideae, Ceroxyloideae, Coryphoideae and Nypoideae. To better record palm species data, Kissling et al., (2019) established the PalmTraits 1.0 database and a species information retrieval website, palmweb (https://palmweb.org). An increasing number of palm fungi are also being continuously recorded and reported. As represented by monographs of Fröhlich and Hyde (2000), Hyde et al. (2000) and Taylor and Hyde (2003), a large number of palm fungi have been recorded, laying a solid foundation for subsequent research on fungal diversity on palm plants and exploring the diversity of the entire fungal population.

According to the database of Farr and Rosaman (2021), there are about 9500 records of palm fungi, distributed within 99 palm genera. The diversity of palm fungi is extremely broad, covering almost all major fungal taxa (Taylor et al., 1999; Fröhlich & Hyde, 2000). Fungi on palms may be saprobes (Taylor et al., 1999; Fröhlich & Hyde, 2000), pathogens (Douanla-Meli & Scharnhorst, 2021; Xiong et al., 2022b), endophytes (Taylor et al., 1999) or epiphytes (Marasinghe et al., 2022, 2023). Earlier focal studies by Pinruan et al., (2007) reported fungi on the *Licuala longicalycata*, while Pinnoi et al. (2006) reported those on the *Eleiodoxa conferta*, both from a peat swamp in southern Thailand. Recent introductions of new saprobic taxa on palms are by Konta et al., (Konta et al., 2020; Konta et al., 2021; Konta et al., 2023b) and Xiong et al. (2022a), who have expanded our understanding of palm-associated fungal diversity. Zheng et al. (2017), Pandian et al. (2021) and Xiong et al. (2022b) reported pathogenic fungi on palms, and Guo et al. (1998) and Mahmoud et al. (2016, 2017) reported endophytic fungi on palms. However, the research on palm fungi is scattered, lacking a comprehensive and up to date source of knowledge to precisely document them. Many asexual palm fungi have also not been linked to their sexual morphs (Hyde et al., 2011; Wijayawardene et al., 2017). To overcome these gaps, we proposed a website dedicated to palm fungi which will be an interactive platform for mycologists, as well the those who are interested in palms in general.

In recent years, web pages dedicated to fungal groups have become important resources to retrieve information. Other than the traditional fungal databases dedicated to fungal classification, several new databases were introduced as websites. Taxa depository databases include MycoBank (Crous et al., 2004) and Index Fungorum (Index Fungorum, 2024, https://www.indexfungorum.org). Other generally important databases are Facesoffungi (Jayasiri et al., 2015, https://www.facesoffungi.org), Outlineoffungi (Wijayawardene et al., 2020, 2022b, https://www.outlineoffungi.org) and Fungalpedia (Hyde et al., 2023). In addition, there are several recently introduced fungal web pages which are dedicated to specific hosts, ecosystems and localities, allowing researchers to easily access and cite relevant data. A few examples are dothideomycetes.org (Pem et al., 2019, Dothideomycetes, botryosphaeriales.org) dedicated to (Wu et al., 2021) dedicated to Botryosphaeriales, coelomycetes.org (Huanraluek et al., 2021) dedicated to Coelomycetes, Italian microfungi.org (Wijesinghe et al., 2021) dedicated to fungi associated with Italian flora, Soilfun.org on soil-inhabiting Ascomycota (Yasanthika et al., 2023) and Beeltehangers.org (de Groot et al., 2024) dedicated to exploring spatiotemporal trends of *Hesperomyces harmoniae*.

As a timely and significant addition to the palm fungal studies, herein we introduce palmfungi.org, an online platform dedicated to fungi associated with various palm species worldwide. This study uses palmfungi.org and related data to briefly discuss the current status of research on the distribution of palm fungi populations, showing how palmfungi.org serves as a bridge between the available data on fungi and their palm hosts, providing researchers with a sustainable platform for fungal information. In addition, this website will be the global consortium for studies on various aspects of palm fungi.

3.2 Why Do We Need Palmfungi.Org?

Palm fungi research and records have a long history. Based on the language and frequency of reports, Pereira and Phillips (2023) divide the history of palm fungus research into three phases: 1880s – 1920s, 1920s – 1990s and 1990s – the present. However, we redefine the time ranges of these three phases after adding the standard based on the method of fungal identification. We named the first phase as “Historical

palm fungi era", which has been reported sporadically using short Latin paragraphs and relatively subjective identification methods, from the 1820s to the 1990s. The second phase we named as "Classical palm fungi era", which was led by K.D. Hyde and co-authors used standard morphological methods to identify fungi on palms from the 1990s to around 2005. The third phase is named "Molecular palm fungi era", which combined molecular analysis with morphology for standardised fungal identification, started around 2005 to continues today. Taylor and Hyde (2003) reported the classification of a large number of palm fungi, prompting researchers to pay more attention to how to collect and integrate palm fungi. However, the decentralised reporting of palm fungi means that data cannot be collected and integrated simultaneously, which might cause misjudgment of the diversity of palm fungi. Most of the fungal species introduced in the early 20th century lacked molecular data or living cultures. Furthermore, these data are mostly published in printed books and are not frequently referred to or cited. Palmfungi.org, as an integrated sustainable data platform, will facilitate solving this issue. This website will provide researchers with concise, relatively complete information on palm fungal species and serve as a directory of palm fungal diversity and host-specificity (Zhou & Hyde, 2001).

In addition to connecting the history of palm fungi with modern data, this website also correlates palm fungi and palm plant taxa by citing the identification and classification of palms by Kissling et al. (2019) and Yao et al. (2023). In recent years, the research on palms has not been limited to the classification and identification of species. Most people have focused on the application and uses of palms (Khan et al., 2023). By establishing itself as a data bridge between available data on fungi and palms, Palmweb (https:// palmweb.org) has the potential to become an important tool in applied research.

3.3 What Is Palmfungi.Org?

The role of palmfungi.org is to establish a retrieval database based on fungi species that use palms as hosts. The operation process of the website is shown in Figure 4.1. In terms of host data, we listed the names of all known species of Arecaceae.

According to Kissling et al. (2019) and Palmweb (2023), the taxonomic status of Arecaceae species will be kept updated. In terms of fungal classification, we followed the "Outline of Fungi" (Wijayawardene et al., 2022b, https://www.outlineoffungi.org). Meanwhile, we have added the vast majority of fungal species names from palms and dedicated entries for some of the species for which information is available. In addition, we implemented interactive searches for palm plant species and fungal species through hyperlinks and dual-function tags.

We will further refine the summary, including the order, family, genus of fungi and other important data. Readers can click on relevant links from the palm fungi website which will redirect to the other databases including "Faces of Fungi" (Jayasiri et al., 2015, http://www.facesoffungi.org); onestopshopfungi.org "Onestopshop Fungi" (Jayawardena et al., 2019); "Marine fungi" (Jones et al., 2019, http://marinefungi.org); "Freshwater fungi" (Calabon et al., 2020, http://freshwaterfungi.org); "Sordariomycetes" (Bundhun et al., 2020, https://sordariomycetes.org); "Fungal Genera" (Monkai et al., 2020, https://www.fungalgenera.org); "Outline of Fungi" (Wijayawardene et al., 2020, https://www.outlineoffungi.org).

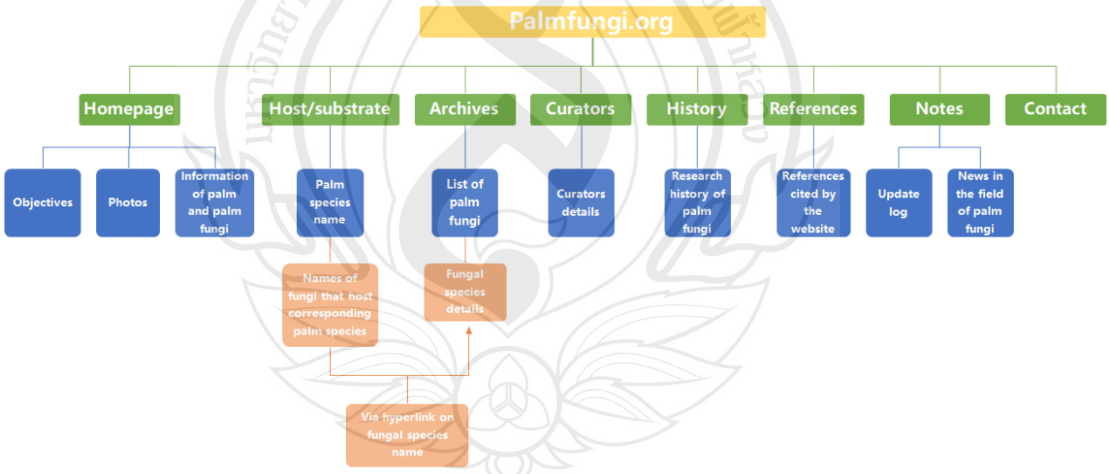


Figure 3.1 Palmfungi.org operation process

3.4 Association with Plant Classification

According to APG IV (Angiosperm Phylogeny Group et al., 2016), Arecaceae (Palm) is the largest family within the order Arecales. Kissling et al. (2019) reported that there are 181 genera and nearly 2,600 species of palms. Despite this, taxonomic studies on palm plants are still common in recent years (Bellot et al., 2020; Helmstetter et al., 2020; Hodel et al., 2021; Jiménez et al., 2021; Eiserhardt et al., 2022). For fungi, especially saprophytic fungi, confirming the host species is a key step in taxonomic identification (Senanayake et al., 2020). Palmfungi.org cites identification and classification information of palm trees by Kissling et al. (2019) and Yao et al. (2023) and keeps it updated. Thus, Palmfungi.org will be a useful platform to solve this challenge and, together with Palmweb (https:// palmweb.org), it will build a data bridge between the fungi and plants.

3.5 Construction

Following the Outline of Ascomycetes (Wijayawardene et al., 2022b), all fungi using palm plants as hosts are included in the database. The database of palmfungi.org will be updated periodically as new information becomes available. Outlines, detailed descriptions and relevant information on each entry on the website will be carefully verified by the expert curators (Table 3.1).

Table 3.1 List of expert curators with their contact information

Position	Name	Address	Contact information
Head Curators	Kevin D. Hyde	Center of Excellence in Fungal Research, School of Science, Mae Fah Luang University, Chiang Rai, Thailand 57100	kdhyde3@gmail.com
	Ishara S. Manawasinghe	Innovative Institute for Plant Health, Zhongkai University of Agriculture and Engineering, Guangzhou 510225, P.R. China	ishara9017@gmail.com
Managing curator	Yinru Xiong	Center of Excellence in Fungal Research, School of Science, Mae Fah Luang University, Chiang Rai, 57100, Thailand	richard_xyr@163.com
Curators	Joanne Taylor	Royal Botanic Garden Edinburgh, 20A Inverleith Row, Edinburgh EH3 5LR, United Kingdom	drjotaylor@yahoo.co.uk
	Alan J.L. Phillips	Biosystems and Integrative Sciences Institute, Faculdade de Ciências, 1749-016 Lisboa, Portugal	alan.jl.phillips@gmail.com
	Diana Santos Pereira	Biosystems and Integrative Sciences Institute, Faculdade de Ciências, 1749-016 Lisboa, Portugal	santospereira.dsp@gmail.com
	Shengnan Zhang	School of Life Science and Technology, Center for Informational Biology, University of Electronic Science and Technology of China, Chengdu, 611731, P.R. China	zshengnanbio@gmail.com
	Shiping Zou	Center of Excellence in Fungal Research, Faculty of Agriculture, Chiang Mai University, Chiang Mai, Thailand	wss20020108@163.com

Database Interface and Visualisation

Palmfungi.org is an online fungi-palm interactive retrieval platform that compiles published information based on the taxonomy of fungi that host palm plants. The functions of the website are diverse, and the interface is simple and user-friendly. The website consists of eight tabs: home, hosts substrate, archives, curators, history, references, notes and contact details, each tab with different functions. In addition, there is a right toolbar for searching and displaying recent updates. Finally, the lower border is for displaying copyright and entry content to display fungal species details.

In total, there are 11 different features and functional details of the website. This includes the “species entry” which is the building block of this website. For all these sections, detailed descriptions are as follows:

3.5.1 A Species Entry

A single entry comprises species name, taxonomic classification database numbers such as Faces of Fungi number, Index Fungorum and MycoBank number, description, host, distribution, coloured photo plate and illustrations, culture characteristics and references (Figure 3.2).

Xylariales » Cainiaceae » Endocalyx

Endocalyx ptychospermatis

Endocalyx ptychospermatis

Y.R. Xiong, Manawas. & K.D. Hyde *Fungal Diversity* 114 (1) (2022)

Classification:Ascomycota-Pezizomycotina-Sordariomycetes-Xylariomycetidae-Xylariales-*Cainiaceae-Endocalyx*

Host species: *Ptychosperma macarthurii*

Holotype: ZHKU 21-0001

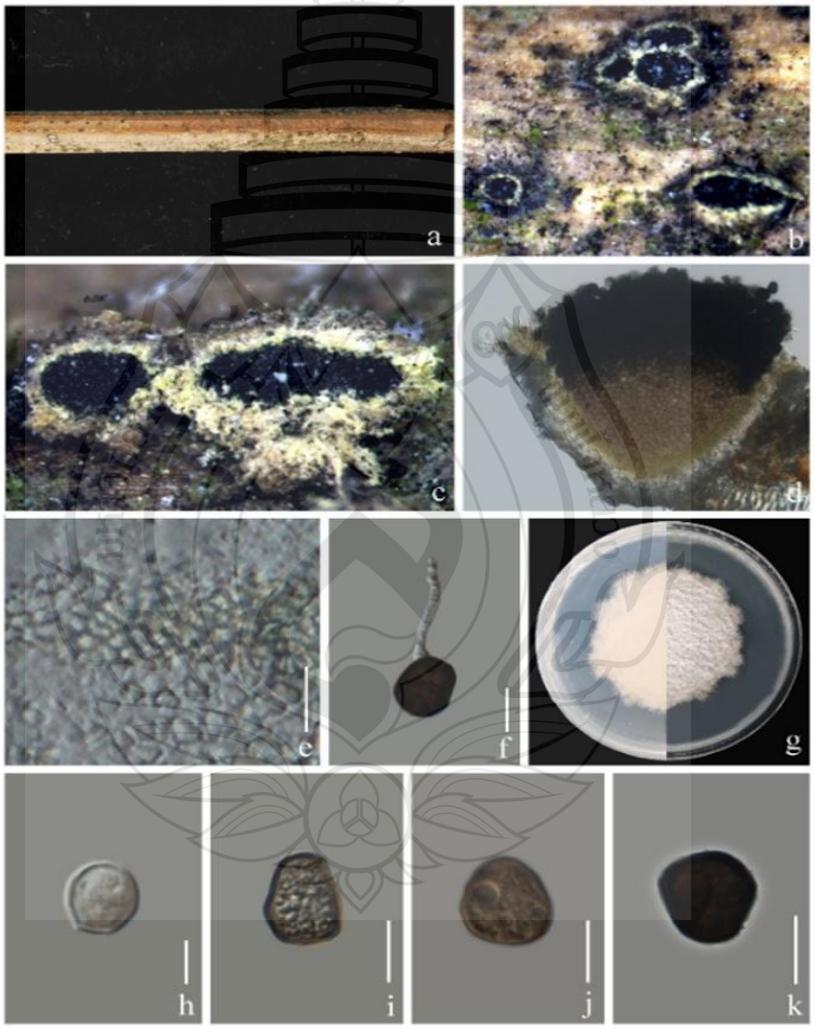
Known distribution: Guangdong, China

IF Number: IF558846 **Mycobank Number**: 558846 **FOF Number**: FoF10540

Description

Saprobic on dead petiole of *Ptychosperma macarthurii*. Sexual morph: Undetermined. Asexual morph: Conidiomata 470–520 µm diam., up to 100 µm high, light yellow to light green, raised, cup-shaped or cylindrical, surrounded by yellow hyphal rings and hyaline conidiophores. Conidiogenous cells 4–6 µm long ($\bar{x}$ = 5 um, n = 20), integrated, unicellular, hyaline, knob-like. Conidia 10–20 × 7–15 µm ($\bar{x}$ =13 × 11 um, n = 40), unicellular, dark brown, elliptical to closed polygonal with verrucous inclusions.

Culture conditions: Colonies on PDA reaching 6 cm diam., after seven days at 25 °C, white at first, irregular, raised, undulate, rough, after maturity, smooth at the margin, white from above, pale-brown from below.



Endocalyx ptychospermatis (ZHKU 21-0001 Holotype): a–c. Conidiomata on host surface. d. Section of conidioma. e. Conidioma wall. f. Conidia. g. Culture on PDA. h–k. Conidia. Scale bars: e = 10 µm, f = 10 µm, h = 5 µm, i–k = 10 µm.

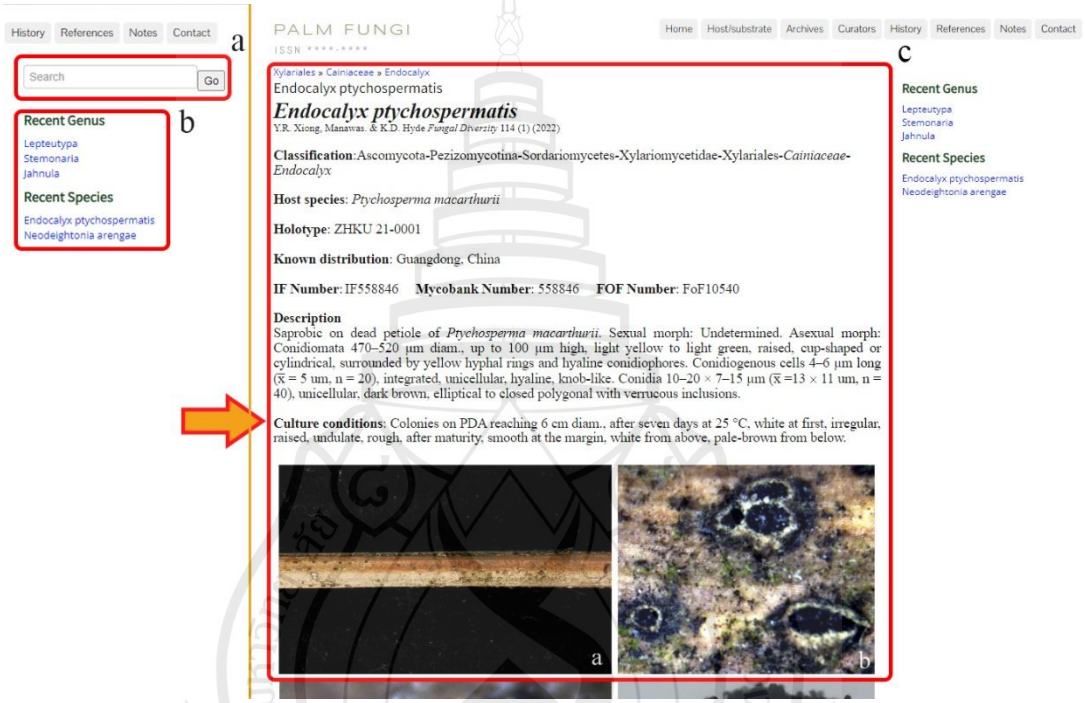
Reference

Phukhamsakda, C. et al. (2022) The numbers of fungi: Contributions from traditional taxonomic studies and challenges of metabarcoding. *Fungal Diversity* 114(1): 327–386.

Figure 3.2 A single species entry of the palm web

3.5.2 Right Toolbar

The right toolbar consists of three sections, the search toolbar (a), recent genus and recent species (b), which are fixed on the right side of the entire website (Figure 4.3). The fungal genus or taxon of interest can be entered in the search toolbar. Then a pop-up window will prompt the target fungus, including its taxonomic level. Clicking on the corresponding entry name will lead you to the species entry interface.

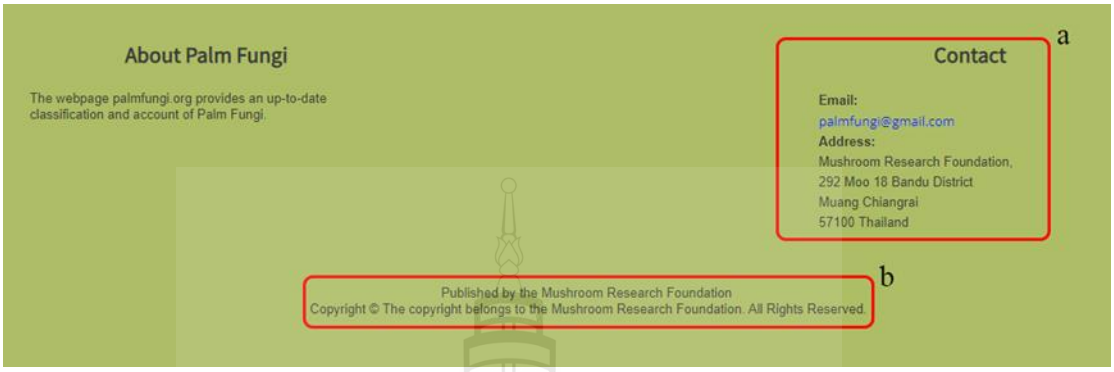


Note a Search toolbar. b Recently updated news, recent genera and species. c The entry details the interface of fungi species.

Figure 3.3 Right toolbar and search result

3.5.3 Lower Border

This information shows contact details and copyright ownership (Figure 4.4).

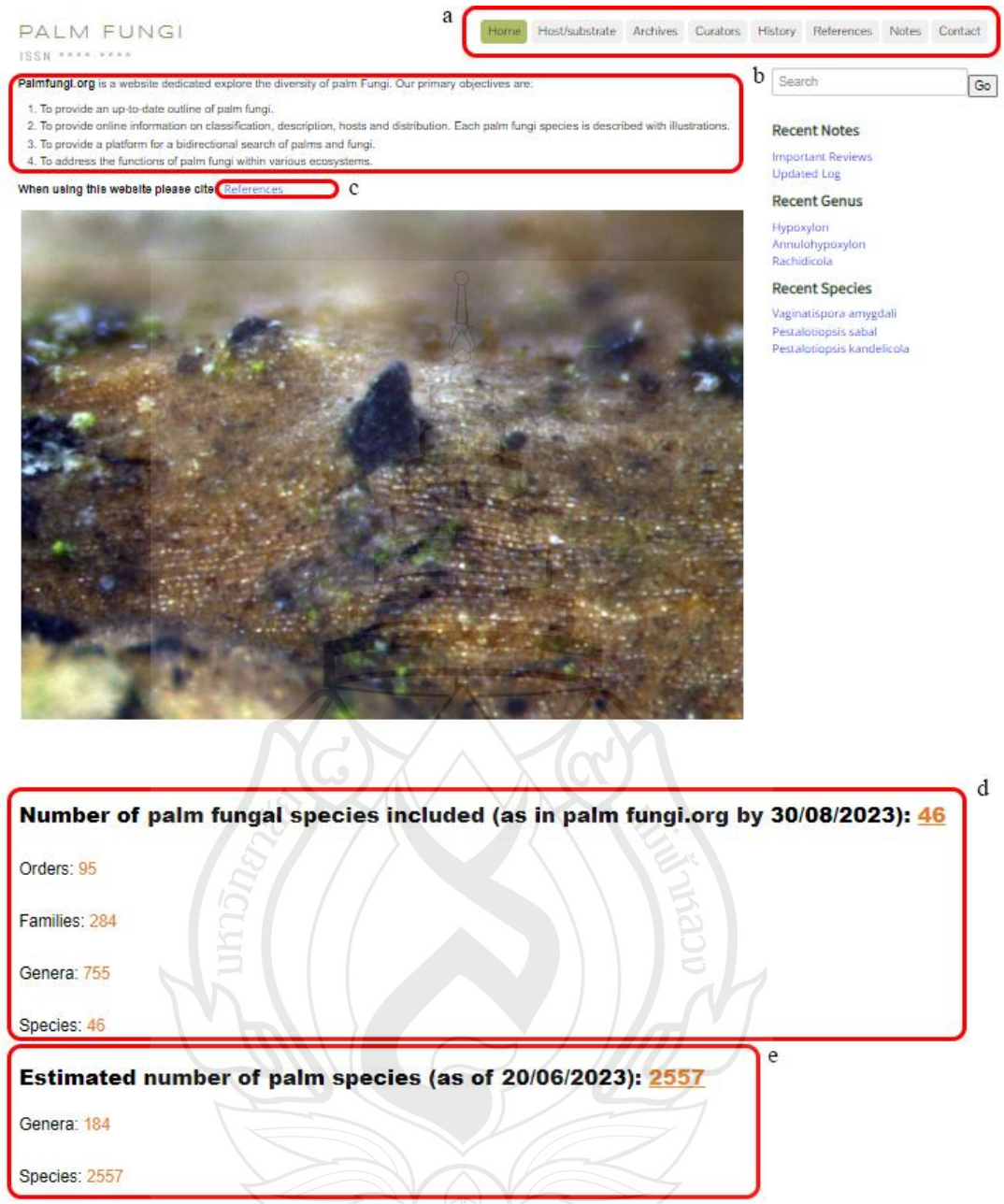


Note a Contact details. b Publisher and copyright information.

Figure 3.4 Bottom border

3.5.4 Homepage

The homepage (Figure 3.5) shows the objectives of the website and the general information of the web (the function menu includes the search toolbar, home page, host/substrate, archive, curator, history, references, notes, and contact). In addition, Figure 4.5.5c shows users the reference materials when citing this website. In addition, the number of palm fungi (including each classification level) and the number of palm species (including each classification level) currently included on the website are also shown.



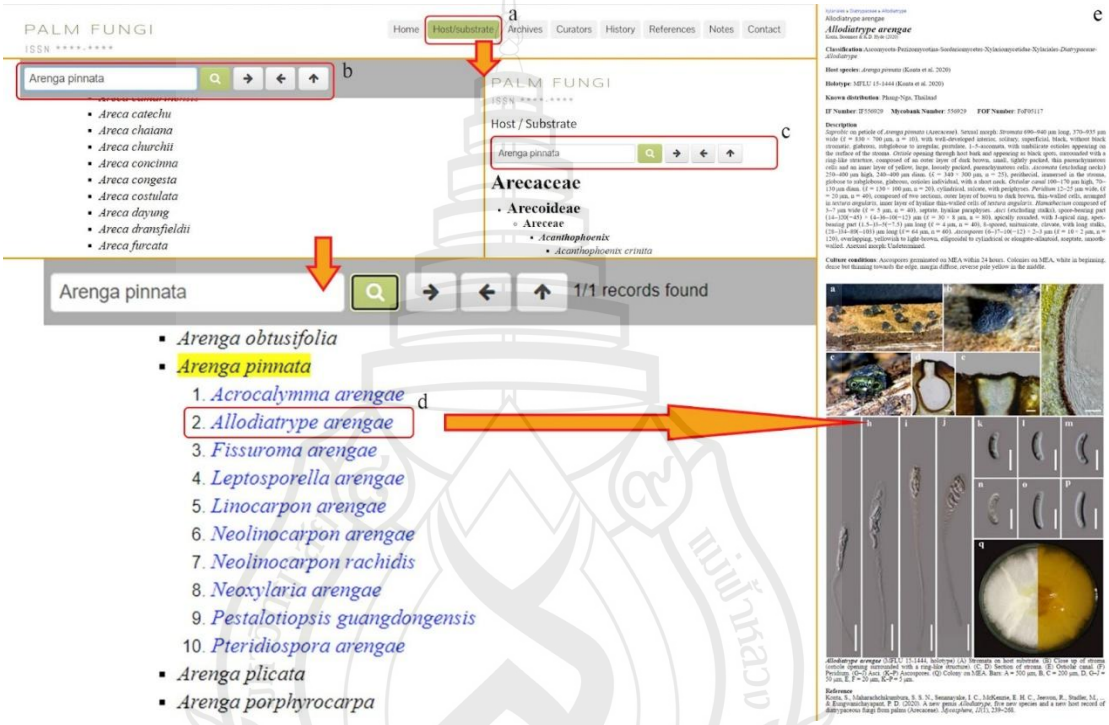
Note a Headers. b Objectives of the webpage. c Citation of the webpage. d Number of palm fungi (including each classification level). e Number of palm species (including each classification level).

Figure 3.5 Homepage

3.5.5 Host/Substrate

By entering this tab, users can obtain information regarding all currently known palm species based on their classification (https://palmweb.org) (Figure 4.6). Users can

intuitively find the fungal species and quantities reported on each palm species. At the same time, each palm species provides entry to the fungal species that host this palm species. In addition, there is also a search bar frozen at the top of the page, where you can enter the palm genus or taxon of interest and the fungus genus or taxon and the page will automatically lock to the target entry. Clicking on the corresponding entry name will guide users to the entry's detailed information interface.

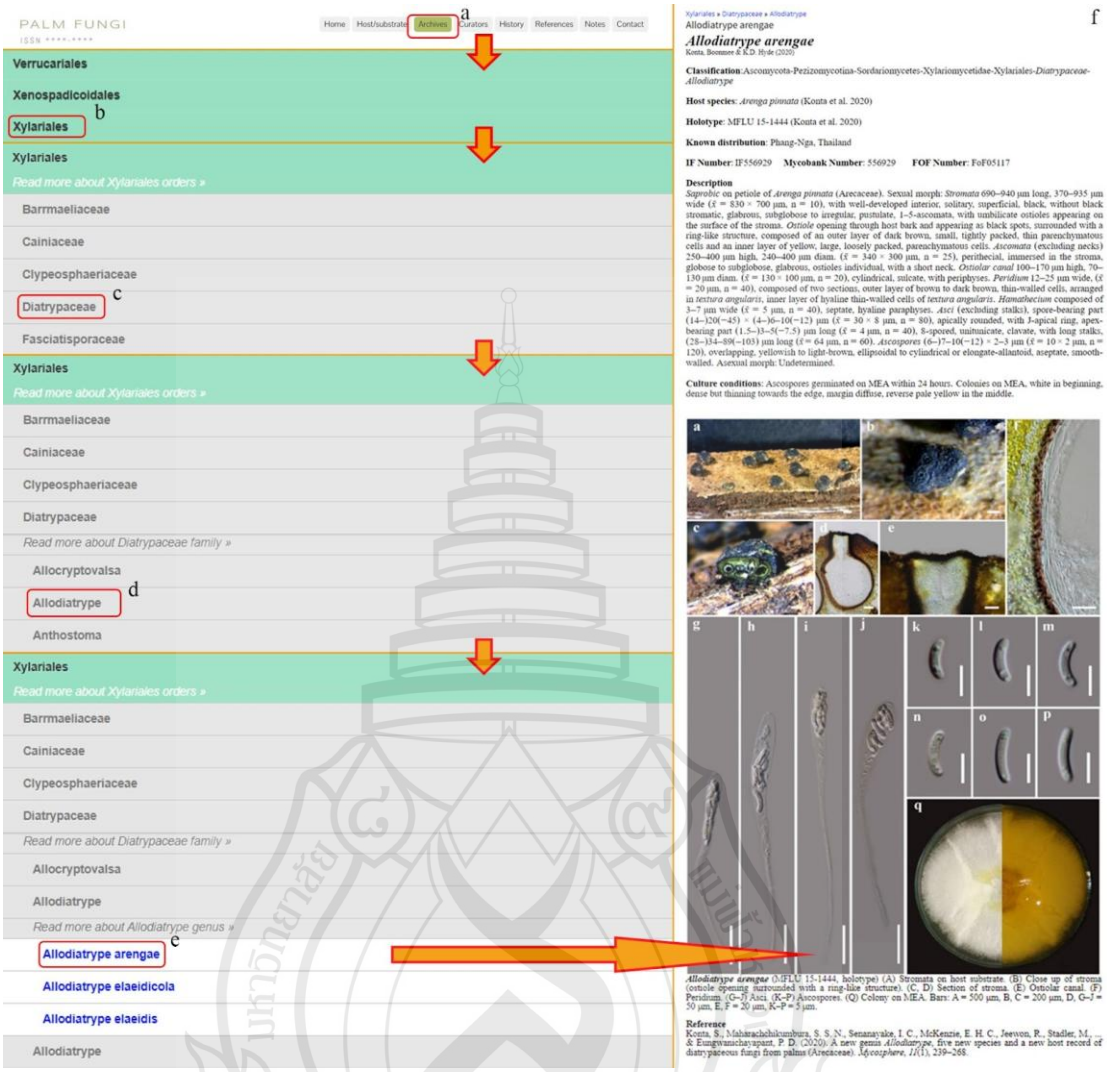


Note a Host/Substrate tag. b Frozen search bar. c Search bar. d Palm fungus species names with hyperlinks. e The entry details the fungal species that host this palm species.

Figure 3.6 Host/Substrate

3.5.6 Archives

Provides users with a relevant list of palm fungi at various classification levels (highest classification level is order, lowest classification level is species) (Figure 4.7). By clicking on the relevant term, the user is presented with options for "Read more about this entry" and a list of sub-categories.



Note a Archive tag. b Order list. c Family list. d Genus list. e Species list. f The entry details the fungal species.

Figure 3.7 Archive

3.5.7 Curators

Provides the contact information and affiliation of the website curators (Figure 3.8).

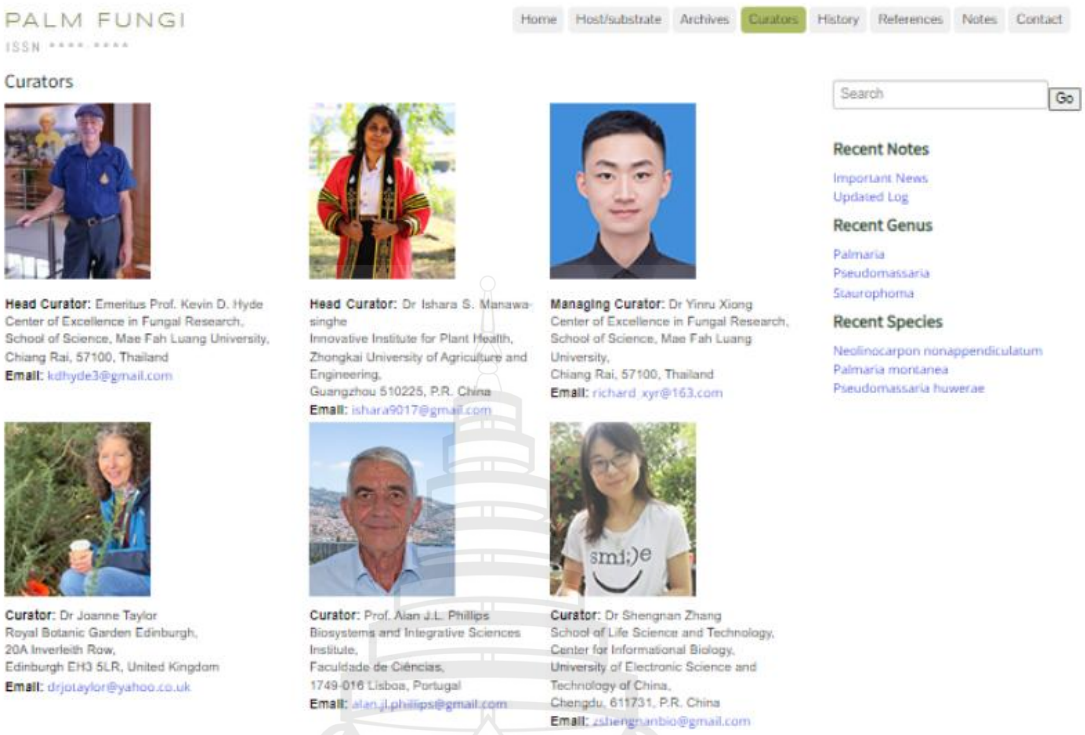
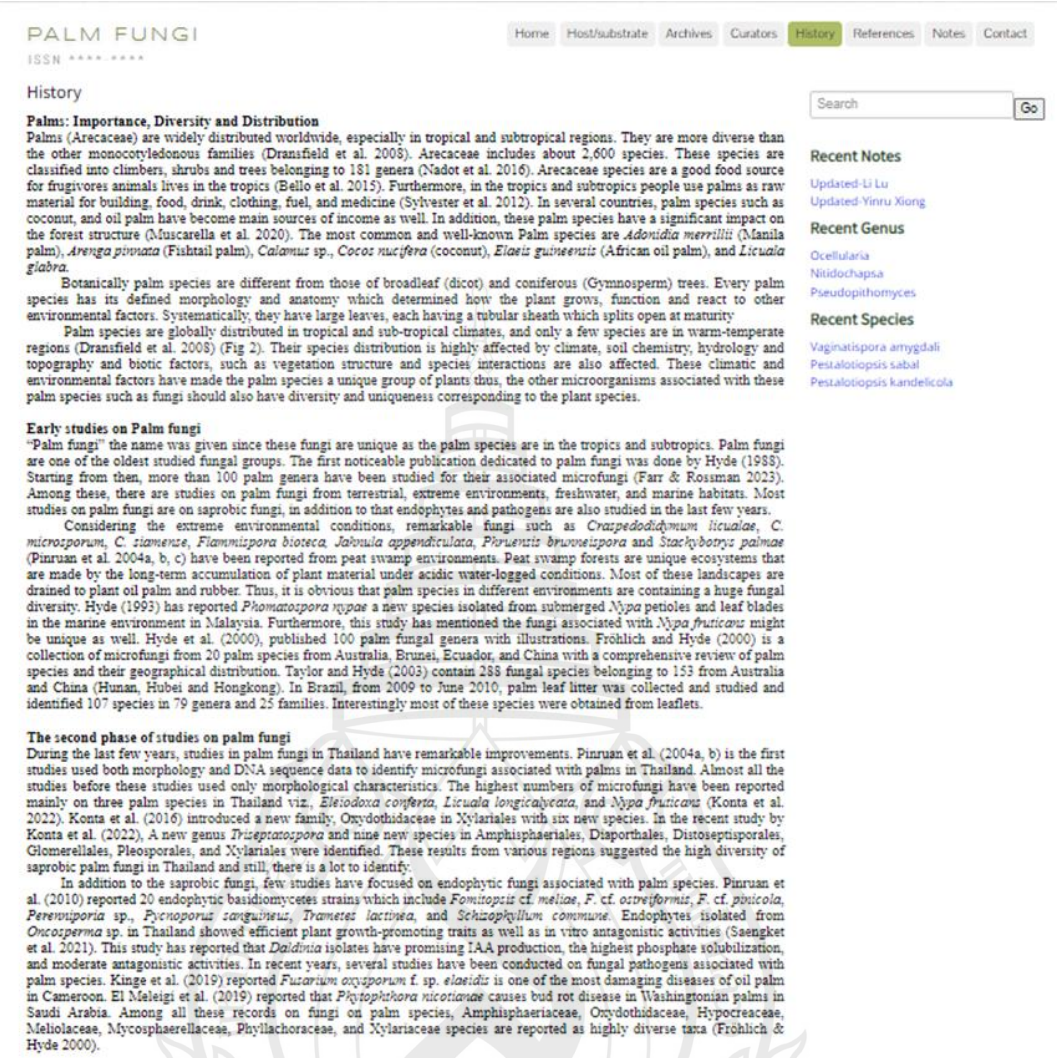


Figure 3.8 Curators: Website curator information

3.5.8 History

Shows the palm fungi collected, examined and recorded with a brief historical background (Figure 3.9).


PALM FUNGI

ISSN ****-****

Home | Host/substrate | Archives | Curators | History | References | Notes | Contact

History

Search Go

Palms: Importance, Diversity and Distribution

Palms (Arecaceae) are widely distributed worldwide, especially in tropical and subtropical regions. They are more diverse than the other monocotyledonous families (Dransfield et al. 2008). Arecaceae includes about 2,600 species. These species are classified into climbers, shrubs and trees belonging to 181 genera (Nadot et al. 2016). Arecaceae species are a good food source for frugivores animals lives in the tropics (Bello et al. 2015). Furthermore, in the tropics and subtropics people use palms as raw material for building, food, drink, clothing, fuel, and medicine (Sylvester et al. 2012). In several countries, palm species such as coconut, and oil palm have become main sources of income as well. In addition, these palm species have a significant impact on the forest structure (Muscarella et al. 2020). The most common and well-known Palm species are *Adonidia merrillii* (Manila palm), *Arenga pinnata* (Fishtail palm), *Calamus* sp., *Cocos nucifera* (coconut), *Elaeis guineensis* (African oil palm), and *Licuala glabra*.

Botanically palm species are different from those of broadleaf (dicot) and coniferous (Gymnosperm) trees. Every palm species has its defined morphology and anatomy which determined how the plant grows, function and react to other environmental factors. Systematically, they have large leaves, each having a tubular sheath which splits open at maturity

Palm species are globally distributed in tropical and sub-tropical climates, and only a few species are in warm-temperate regions (Dransfield et al. 2008) (Fig 2). Their species distribution is highly affected by climate, soil chemistry, hydrology and topography and biotic factors, such as vegetation structure and species interactions are also affected. These climatic and environmental factors have made the palm species a unique group of plants thus, the other microorganisms associated with these palm species such as fungi should also have diversity and uniqueness corresponding to the plant species.

Early studies on Palm fungi

"Palm fungi" the name was given since these fungi are unique as the palm species are in the tropics and subtropics. Palm fungi are one of the oldest studied fungal groups. The first noticeable publication dedicated to palm fungi was done by Hyde (1988). Starting from then, more than 100 palm genera have been studied for their associated microfungi (Farr & Rossman 2023). Among these, there are studies on palm fungi from terrestrial, extreme environments, freshwater, and marine habitats. Most studies on palm fungi are on saprobic fungi, in addition to that endophytes and pathogens are also studied in the last few years.

Considering the extreme environmental conditions, remarkable fungi such as *Craspedodidymum licualae*, *C. microsporum*, *C. siamense*, *Flammispora bioteca*, *Jahnula appendiculata*, *Phruensis brunneispora* and *Stachybotrys palmae* (Pinruan et al. 2004a, b, c) have been reported from peat swamp environments. Peat swamp forests are unique ecosystems that are made by the long-term accumulation of plant material under acidic water-logged conditions. Most of these landscapes are drained to plant oil palm and rubber. Thus, it is obvious that palm species in different environments are containing a huge fungal diversity. Hyde (1993) has reported *Phomatospora nypae* a new species isolated from submerged *Nypa* petioles and leaf blades in the marine environment in Malaysia. Furthermore, this study has mentioned the fungi associated with *Nypa fruticans* might be unique as well. Hyde et al. (2000), published 100 palm fungal genera with illustrations. Fröhlich and Hyde (2000) is a collection of microfungi from 20 palm species from Australia, Brunei, Ecuador, and China with a comprehensive review of palm species and their geographical distribution. Taylor and Hyde (2003) contain 288 fungal species belonging to 153 from Australia and China (Hunan, Hubei and Hongkong). In Brazil, from 2009 to June 2010, palm leaf litter was collected and studied and identified 107 species in 79 genera and 25 families. Interestingly most of these species were obtained from leaflets.

The second phase of studies on palm fungi

During the last few years, studies in palm fungi in Thailand have remarkable improvements. Pinruan et al. (2004a, b) is the first studies used both morphology and DNA sequence data to identify microfungi associated with palms in Thailand. Almost all the studies before these studies used only morphological characteristics. The highest numbers of microfungi have been reported mainly on three palm species in Thailand viz., *Eleiodoxa conferta*, *Licuala longicalycata*, and *Nypa fruticans* (Konta et al. 2022). Konta et al. (2016) introduced a new family, Oxydothidaceae in Xylariales with six new species. In the recent study by Konta et al. (2022), A new genus *Trieptaxospora* and nine new species in Amphisphaeriales, Diaporthales, Distoseptisporales, Glomerellales, Pleosporales, and Xylariales were identified. These results from various regions suggested the high diversity of saprobic palm fungi in Thailand and still, there is a lot to identify.

In addition to the saprobic fungi, few studies have focused on endophytic fungi associated with palm species. Pinruan et al. (2010) reported 20 endophytic basidiomycetes strains which include *Fomitopsis* cf. *meliae*, *F.* cf. *ostreiformis*, *F.* cf. *pinicola*, *Perenniporia* sp., *Pycnoporus sanguineus*, *Trametes lactinea*, and *Schizophyllum commune*. Endophytes isolated from *Oncosperma* sp. in Thailand showed efficient plant growth-promoting traits as well as in vitro antagonistic activities (Saengket et al. 2021). This study has reported that *Daldinia* isolates have promising IAA production, the highest phosphate solubilization, and moderate antagonistic activities. In recent years, several studies have been conducted on fungal pathogens associated with palm species. Kinge et al. (2019) reported *Fusarium oxysporum* f. sp. *elaeidis* is one of the most damaging diseases of oil palm in Cameroon. El Meleigi et al. (2019) reported that *Phytophthora nicotianae* causes bud rot disease in Washingtonian palms in Saudi Arabia. Among all these records on fungi on palm species, Amphisphaeriaceae, Oxydothidaceae, Hypocreaceae, Meliolaceae, Mycosphaerellaceae, Phyllachoraceae, and Xylariaceae species are reported as highly diverse taxa (Fröhlich & Hyde 2000).

Recent Notes

Updated-Li Lu

Updated-Yinru Xiong

Recent Genus

Ocellularia

Nitidochapsa

Pseudopithomyces

Recent Species

Vaginatispora amygdali

Pestalotiopsis sabal

Pestalotiopsis kandelicola

Figure 3.9 History: Website history information.

3.5.9 References

Assembly of the main literature (such as books, reviews, monographs and articles) and websites (Figure 3.10).

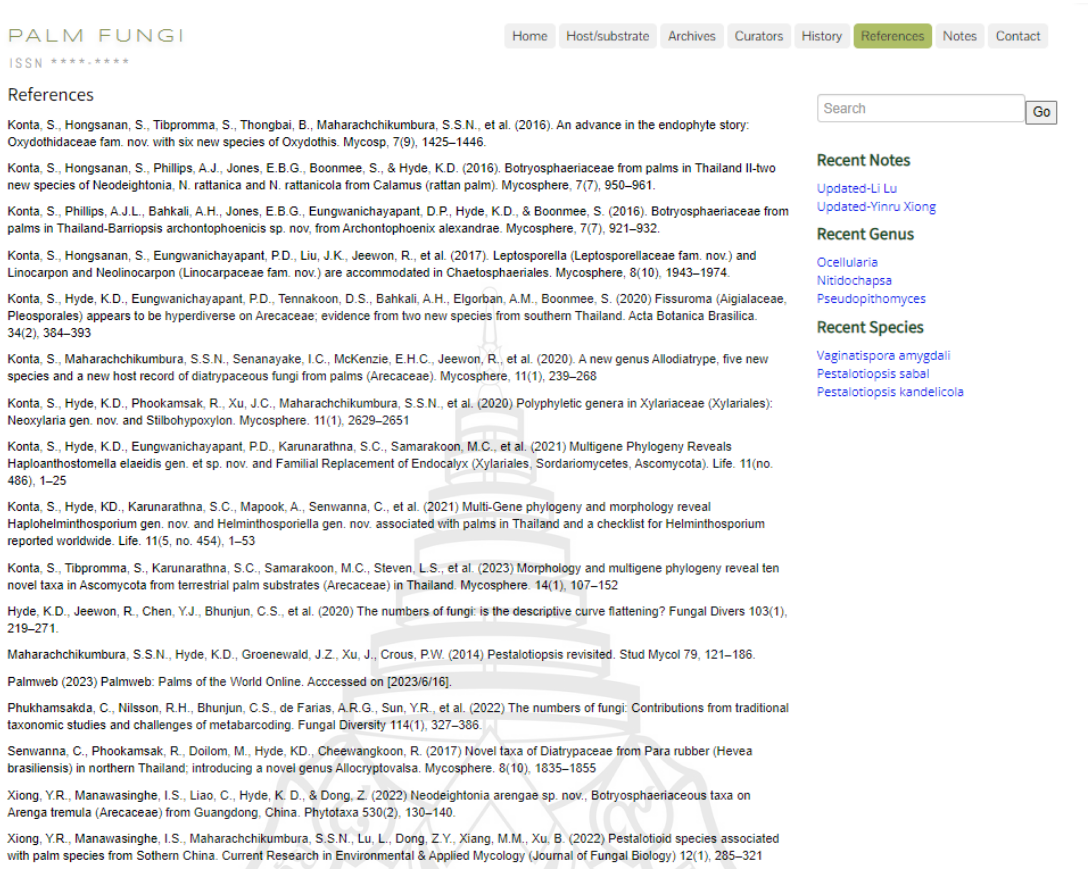


Figure 3.10 References: Website reference information

3.5.10 Notes

The note section is dedicated to additional details relevant to the palm fungi, with two sections (Figure 3.11). One link is for Important News (a) and will link to the recent reviews, publications, events, or other updated news relevant to the palm fungi. The second is the Updated Log (b), which shows the updated time and person who updated the website and includes the hyperlink of the update log.

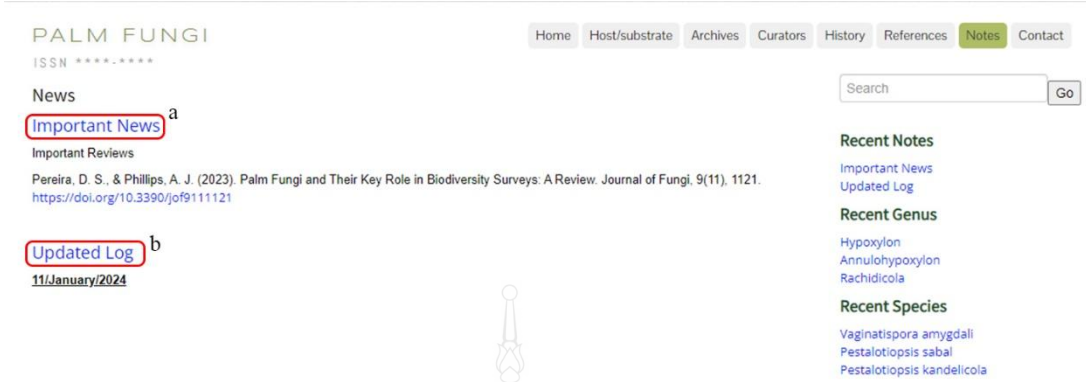


Figure 3.11 Notes: a important news. b updated log

3.5.11 Contact

Provides the contact information of the website and allows users to provide any comments or suggestions (Figure 3.12).

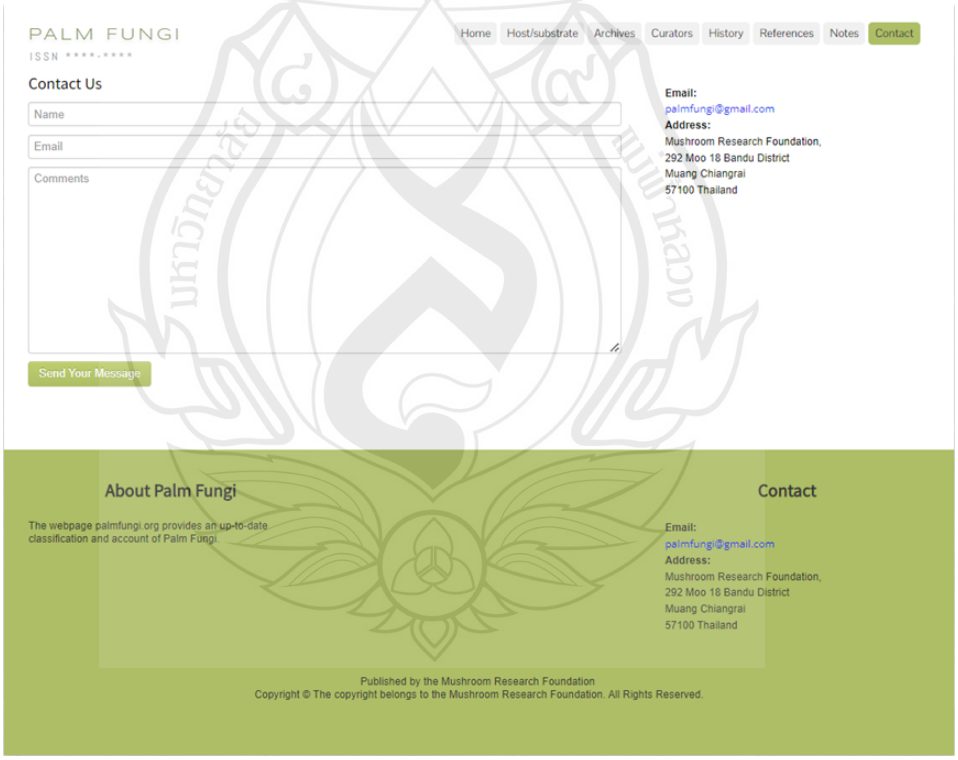


Figure 3.12 Contact: Website contact information

3.6 Use Palmfungi.Org to Briefly Discuss the Current Status of Research on the Population Distribution of Palm Fungi

Palm species have many uses (Dransfield et al., 2008), and Cámara-Leret et al. (2017) reported that 208 species of palm plants can be used as cash crops. Data from FAOSTAT (Food and Agriculture Organization of the United Nations 2024, https://www.fao.org/ faostat/en/#data) also show that palms, especially oil palms and coconuts, have huge economic benefits. Based on data from Index Fungorum (2024) and Farr and Rosaman (2021), palmfungi.org reviewed and included 1,521 fungal species associated with palm.

Based on the above data, this study briefly analysed the reported distribution of fungi in the cash crops and non-cash crops of the palm. The results show in (Figure 3.13a): 784 fungal species were reported from cash crop palm hosts, accounting for 51.55%; 421 fungal species were reported on non-cash crop palm hosts, accounting for 27.68%; 316 fungal species were reported from unidentified palm species, accounting for 20.78%. Simultaneously, utilising the information from Host/Substrate in palmfungi.org, this study conducted a basic analysis to determine the number of palm species that have fungus records. The results showed as follows (Figure 3.13b): there were 316 species of palm with fungi recorded, accounting for 12.36%, and 2241 species of Palm without fungi recorded, accounting for 87.64%.

Leveraging palmfungi.org as a platform, this study successfully conducted a basic analysis of the population distribution of palm fungi. The findings suggest that, while there is widespread documentation of palm fungi, the study focuses on a limited number of economically valuable palm species and overlooks the vast majority of naturally occurring palm species.

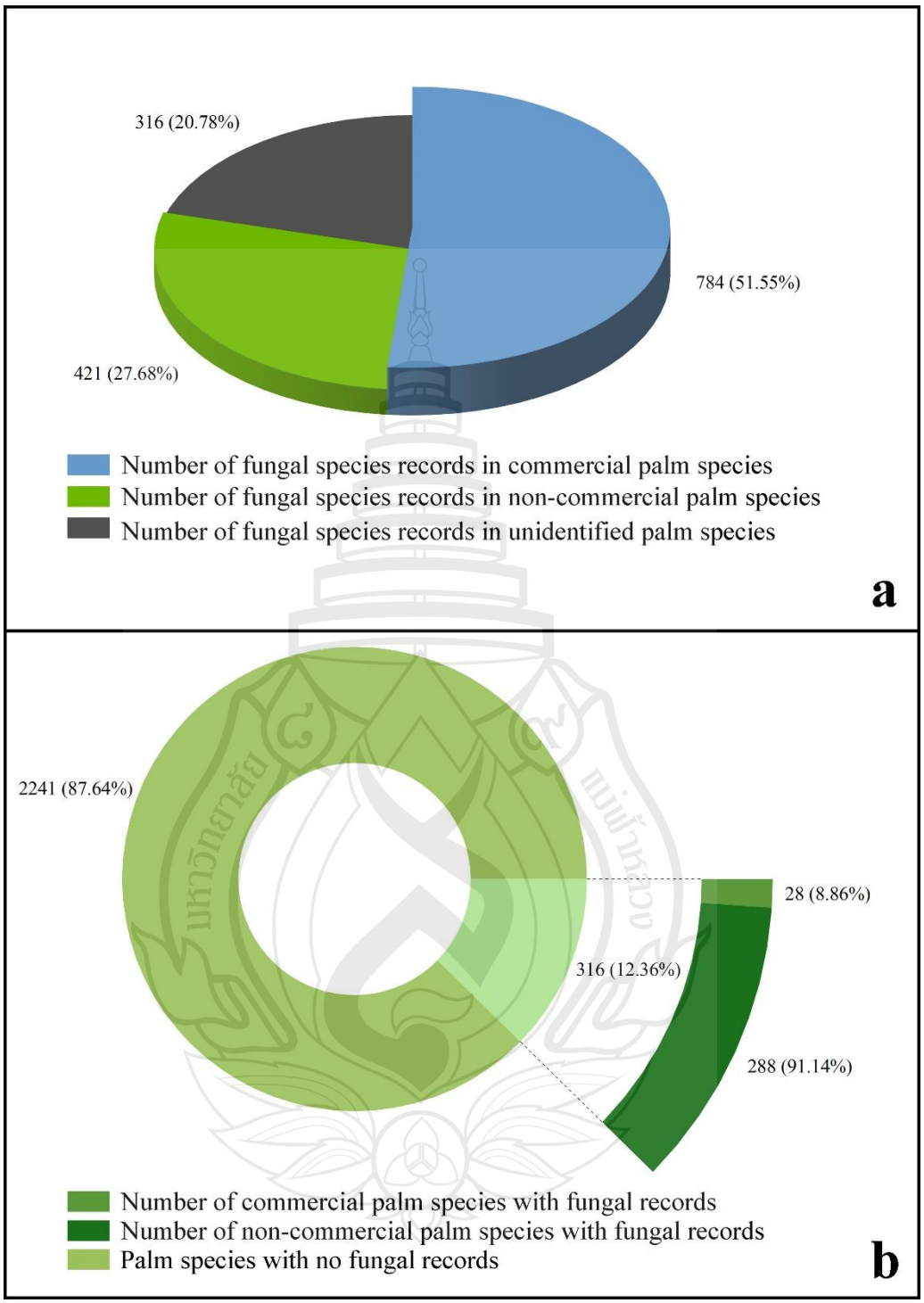


Figure 3.13 A diagram of the numbers of palm fungi vs. the number of palm species or Arecaceae

3.7 Discussion

The advancement of modern online platforms has greatly affected the ease of gathering information, which connects various databases about different biological information (Chaiwan et al., 2021). Basic information on related fungi can be found in several global fungal nomenclature and classification databases outlined in this paper. Those resources provide users with fungal host records and, as fungal species are continually being discovered, new host records and regional records are constantly being reported (Hyde et al., 2024). In recent years, studies have recorded the fungal host-specificity (Zhou & Hyde, 2001). Bubner (2013) reported the host-specificity of ectomycorrhizal fungi in pure and mixed stands of Scots pine (*Pinus sylvestris* L.) and beech (*Fagus sylvatica* L.). Miao et al. (2021) found that plant genetics are a deciding factor affecting *Nitraria tangutorum* endophytic fungal composition. Wang et al. (2019) pointed out that soil plant pathogenic fungi are specialised in low-level host taxa and Li et al. (2020) describe and discuss host specific genes in most fungi at the molecular level. In addition, Hyde et al. (2007) pointed out that there are also differences in fungi from different locations on the same host. Even though fungi are so closely associated with plants, the only fungal-plant database available is for fungi on rice (https://mycolab.pp.nchu.edu.tw/rice_fungi/contact.php). However, this website cannot be used to explore fungal host specificity and is not interlinked with other large databases. The brief discussion of the distribution of palm fungi populations in this study fully demonstrates the effective application of palmfungi.org after interconnection with other large databases. Therefore, the operation of palmfungi.org provides a platform for the exploration of the host-fungus relationship.

We have presently uploaded 50 species entries to palmfungi.org and the website content will be continuously updated with the assistance of all curators. In the future, the palm fungi website will establish links between large and small fungal classification websites to form an integrated and interactive data collection platform. More attention will be paid to links with palm-related taxonomic websites such as PalmWeb (https://palmweb.org), where associations with palm species will further improve the understanding of the relationship between fungi and palm hosts. Palmfungi.org will

also be the first retrieval platform to record and retrieve taxonomic data on fungi and their specifically corresponding palm hosts. This platform will enable a new direction for exploring the host specificity of palm fungi and even the whole fungal kingdom.

CHAPTER 4

CHECKLIST OF PALM FUNGI

4.1 Weighted Data Processing Methods

Palm fungus record data from 1990 to 2025 were first obtained through the US National Fungus Collections Fungus–Host Database (Farr et al., 2021) and Index Fungorum (http://www.indexfungorum.org/Names/Names.asp), and then collected based on a year-by-year examination of palm fungi papers from 1990 to 2025 by Google Scholar. All collected data were compared and screened, and only records with unique NAME OF FUNGUS, CURRENT NAME, HOST, LOCATION, and YEAR OF PUBLICATION were retained. If these entries were repeated, they were reviewed in the corresponding articles to determine whether they were from the same collection site or the same record, and only the first published record was retained. All the data were summarized and sorted to obtain a checklist (Xiong et al., 2025). Climate classification is based on the Köppen-Geiger climate classification diagram provided by Beck et al. (2018), following the merging method of the U.S. Department of Energy (2014). The detailed classification is shown in Table 4.1. The land area and climate zone proportions were generated and exported through Google Earth Engine (Gorelick et al., 2017). Based on the PyCharm environment (Van Horn & Nguyen, 2023), Python programming language (Van Rossum and Drake) was used to perform the corresponding local outlier factor (LOF) test (Breunig et al., 2000), Kolmogorov-Smirnov (KS) test (Massey, 1951), negative binomial generalized linear model (GLM) (Hilbe, 2011; Lord et al., 2012), mixed effect test (Zuur et al., 2009), and Monte Carlo simulation (Mooney, 1997). RAWGraphs 2.0 (Mauri et al., 2017) was used to draw the analysis graphs.

Table 4.1 Macro-classification of climate zones based on the U.S. Department of Energy (2014) merging perspective and the Köppen-Geiger climate classification (Beck et al., 2018)

Macro-climate zone	Included subtypes (full name and code)	Grouping logic
Tropical	Tropical rainforest climate (Af), Tropical monsoon climate (Am), Tropical savanna climate (Aw)	All Group A subtypes: year-round high temperatures; variation in precipitation between monsoon/wet seasons.
Arid	Hot desert climate (BWh), Cold desert climate (BWk), Hot semi-arid climate (BSh), Cold semi-arid climate (BSk)	All Group B subtypes: potential evapotranspiration exceeds precipitation; differentiated into hot vs. cold deserts and steppes.
Subtropical	Hot-summer Mediterranean climate (Csa), Warm-summer Mediterranean climate (Csb), Cold-summer Mediterranean climate (Csc), Monsoon-influenced humid subtropical climate (Cwa), Subtropical highland climate with dry winters (Cwb), Cold subtropical highland climate (Cwc)	Selected Group C subtypes in mid-latitudes: Mediterranean (summer-dry) and monsoon/dry-winter highland variants.
Temperate	Humid subtropical climate (Cfa), Temperate oceanic climate (Cfb), Subpolar oceanic climate (Cfc), Hot-summer continental Mediterranean climate (Dsa), Warm-summer continental Mediterranean climate (Dsb), Subarctic climate with dry, cold summers (Dsc), Subarctic climate with severe dry winters (Dsd), Monsoon-influenced hot-summer humid continental climate (Dwa), Monsoon-influenced warm-summer humid continental climate (Dwb), Monsoon-influenced subarctic climate (Dwc)	Remaining Group C subtypes plus Group D “summer-dry”/“summer-wet” variants in the warmer D-range.
Subarctic	Monsoon-influenced extremely cold subarctic climate (Dwd), Hot-summer humid continental climate (Dfa), Warm-summer humid continental climate (Dfb), Subarctic climate (Dfc)	Colder D-group subtypes: coldest month well below 0 C, with mild to short summers.
Polar	Extremely cold subarctic climate (Dfd), Tundra climate (ET), Ice cap climate (EF)	Dfd plus all Group E subtypes: all months average below 10 C (tundra) or 0 C (ice cap), unsuitable for trees.

4.1.1 Weight System Construction

Time compensation weights proposed based on palm fungal records and palm host species growth trends over time (Figure 4.1):

$$w_{\text{time}} = \alpha(1 + \gamma \Delta t)$$

Δt: Indicates the time since the first record for each climate zone.

Based on the results of Figure 4.2, palm fungus records are extremely unevenly distributed in different countries and regions. In order to quantify the original data, this study uses climate distribution instead of national distribution and uses space-climate to weight and quantify the original data. The final spatial-climate weight formula is unevenly distributed in terms of number and country area:

$$w_{(l)} = \frac{\left(\frac{A_{(c)}}{A_{(to\text{-}c)}}\right)\left(\frac{A_{(all\text{-}c)}}{A_{(a)}}\right) N_{samples}}{\sum_{o} w_{(o)}}$$

$A_{(c)}$: Total area of each climate zone in the sample country.

$A_{(to\text{-}c)}$: Total area of the sample country.

$A_{(all\text{-}c)}$: Total area of each climatic zone in all sample countries.

$A_{(all\text{-}a)}$: Total area of all sample countries.

$N_{samples}$: The number of observations available in the partition.

$w_{(o)}$: Total "climate weight" for all climate zones.

In order to adjust the discreteness of weighted data and make the data usable for subsequent analysis, we proposed the data discrete adjustment formula:

$$w_{\text{CV}} = \beta F(\text{CV}_n)$$

$F(\text{CV}_n)$ Discrete adjustment function the penalty model is $(\text{CV}_n + 10^{-10})^{-1}$ and the reward model is CV_n

Parameter optimization via grid search yielded: α = 0.6, β = 0.3, γ = 0.1.

4.1.2 Triple Integration Weights

Taking into account the weights of spatial and temporal conditions and the discreteness of weighted data, we constructed a triple-integrated weight system $w_{(k)}$ to correct the bias. Local outlier factor (LOF) detection with a neighborhood parameter k = 20 (determined by the elbow method) identified 137 outliers (2.25% of the total), which were excluded from subsequent analyses. Based on the Kolmogorov-Smirnov (KS) test, we found that the data distribution morphology was a typical non-normal distribution (P = 0).

$$w_{(k)} = w_{(l)}[a(1 + \gamma\Delta t) + \beta F(\mathrm{CV}_n)]$$

In order to fully account for spatial dispersion, a temporal compensation model was proposed to fit the spatially discrete reward/penalty contrast. A negative binomial generalized linear model (GLM) with a logarithmic link function was used to validate the model, and the model fit was tested using mixed effects. The results showed satisfactory dispersion parameters (penalty model: 10.35; reward model: 11.58), confirming the appropriate treatment of overdispersion.

4.1.3 Weighted Mean Response Variable Prediction

Therefore, the generalized linear model (GLM) framework was adopted to construct the response variable prediction equation based on the above two models with a logarithmic link function to predict the fungal diversity density under the corresponding model conditions:

$$\hat{Y}_k = \exp(Intercept + \beta_{YEAR} \times YEAR + \beta_{Climate})$$

The subarctic was used as the reference zone, and the optimal $\beta_{Climate}$ value, β_{YEAR} value and $Intercept$ value of each climate were calculated by iterative weighted least squares (IRLS) based on the negative binomial distribution model (Table 3). Through Monte Carlo simulations (n=10,000 iterations), the prediction intervals (PI) generated by the two models (reward/penalty) cover 96.2% (reward) and 92.3% (penalty) of the holdout samples, respectively, demonstrating the robust generalization ability of the data and models.

Table 4.2 The optimal $\beta_{Climate}$ value, β_{YEAR} value and $Intercept$ value of each climate in this study

Model Type	Intercept	β_{YEAR}	$\beta_{Climate}$					
			Tropical	Arid	Subtropical	Temperate	Subarctic	Polar
Dispersion Penalty	-1.1002	0.0196	1.7914	1.7609	-0.6162	0.8749	0	-1.6842
Dispersion Reward	-0.6410	0.0121	1.8012	1.7600	-0.5728	0.8527	0	-1.6952

4.2 Results with Discussion

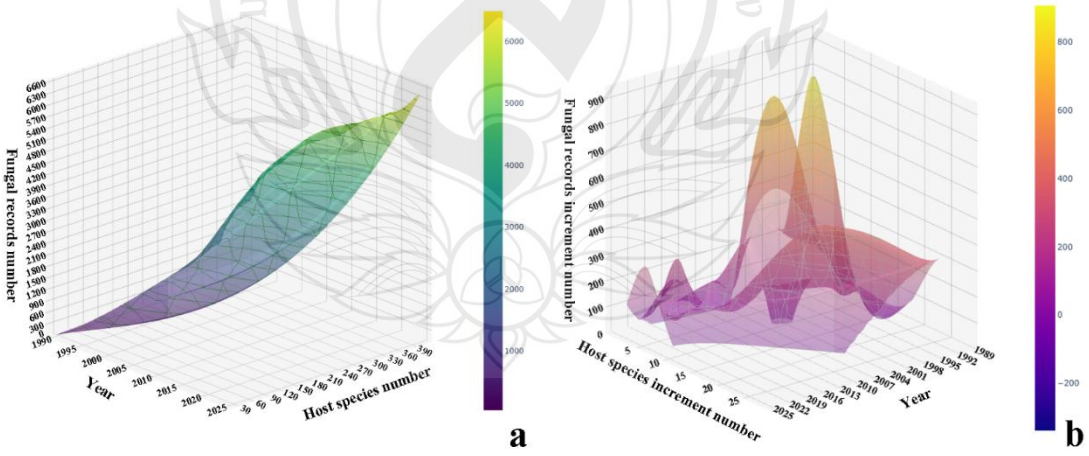
4.2.1 Palm Fungal Diversity Prediction

The diversity of palm fungi is a microcosm of the overall diversity of fungi, and previous studies have been exploring the overall diversity of palm fungi (Hyde, 1996; Fröhlich & Hyde, 1999; Taylor et al., 2000; Taylor & Hyde, 2003; Pereira & Phillips, 2023). Although the plant-fungus ratio is considered a reliable predictor, previous predictions of palm fungal diversity are basically based on the plant-fungus ratio under specific research conditions. However, biodiversity detection schemes and data processing methods need to be flexible to adapt to samples to cope with changes in different biodiversity conditions (Kühl et al., 2020). In response to the complex situation of palm fungal diversity, we collected 6,099 palm-associated fungal records from 1990 to 2025, and drew a three-dimensional trend chart of the total number of fungi and the annual growth of fungi-host-year (Figure 4.1a, b) and a multidimensional data bubble chart based on the country's major climate zones-total land area-national palm fungal records (Figure 4.2). According to the trend in the three-dimensional graph, we observed that the number of fungal records and the number of recorded palm species have increased significantly over time (Figure 4.1). Based on the results of the multidimensional data bubble chart, we found that palm fungal records are unevenly distributed among 109 countries with different land areas (Figure 4.2). This complex situation makes us realize that integrating palm fungal records worldwide and finding the characteristics that balance the imbalance of these records is a necessary means to make more accurate predictions of palm fungal diversity. Based on previous estimates of the total expected diversity of palm fungi (Hyde, 1996; Taylor & Hyde, 2003),

we believe that it is necessary to flexibly handle fungal records from different countries and climate zones to accurately reflect the true contribution of each record to the total diversity of palm fungi. Combined with the method of Chiarucci et al. (2011), we propose that the fungal records of different countries can be represented by climate zones and classified and processed to accurately reflect the true contribution of each record to the total diversity of palm fungi.

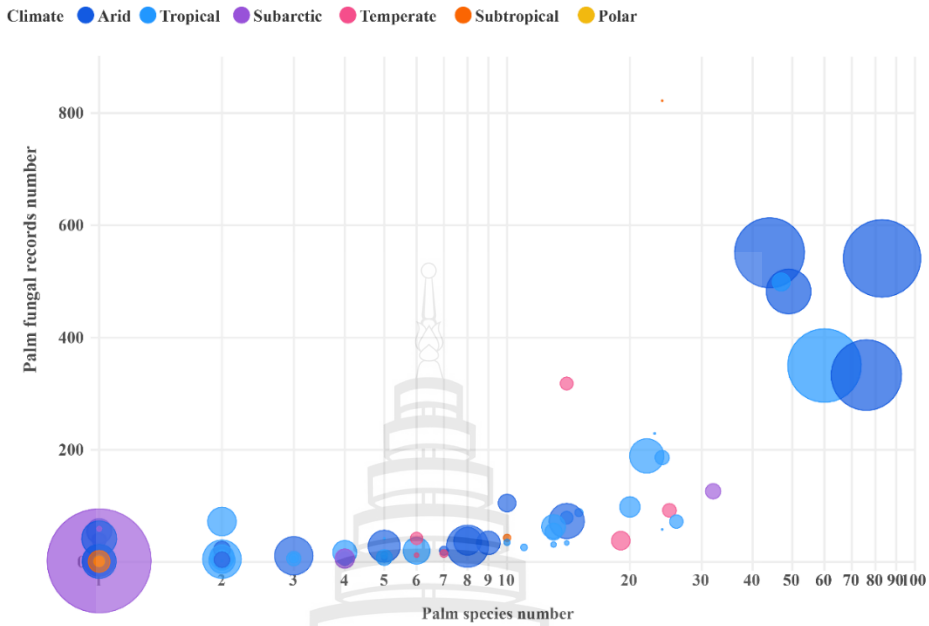
Therefore, we proposed a plant-fungus ratio based on the three-phase weighted processing of time-space-data discreteness. In addition, based on the results of the triple integral weight calculation, we used the data of climate zone area-climate zone fungal record weight-year to draw a triple integral weight distribution waterfall chart. The result shows the imbalance of fungal records in the six climate zones after data weighting, which is biased towards tropical and arid zones, and less distributed in subarctic and polar regions, which is consistent with the facts (Figure 4.3). We then constructed an improved prediction method for the total amount of palm fungi diversity based on the final weighted formula $w_{(P)}$.

Based on our weighted data and two discrete opposition models, the final fungus-plant ratio was obtained according to the final weighted formula. Based on the palm tree species baseline data (2558 accepted species) of Xiong et al. (2024), our model prediction results are shown in Table 4.3.



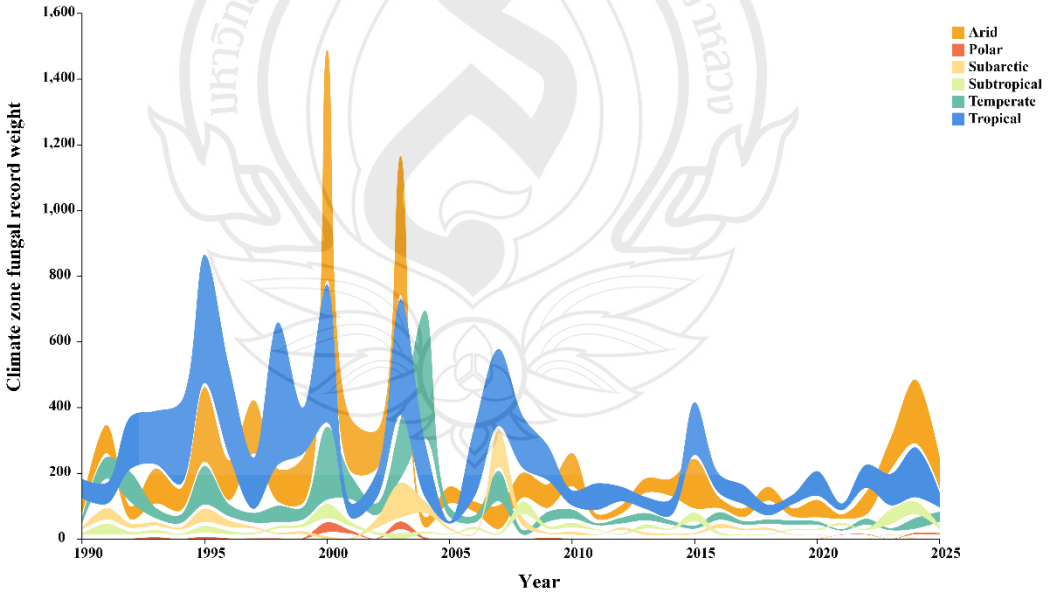
Note a Overall growth trend of palm fungi and palm host species (reported fungal records).
b Annual growth trend of palm fungi and palm host species (reported fungi records)

Figure 4.1 Palm fungi population trend chart from 1990 to 2025



Note The size of the bubble represents the area of the corresponding country or region.

Figure 4.2 Data on palm fungus records and palm species by climate within countries (reported fungus records)



Note The width of the waterfall belt represents the value.

Figure 4.3 Based on triple integration weights data, the data of palm fungi in each climate zone are presented each year

Table 4.3 Model prediction results

Model Type	Plant: Fungi Ratio	Estimated Diversity (number)
Dispersion Penalty	1:17.4	44,509
Dispersion Reward	1:28.2	72,136

CHAPTER 5

CONCLUSIONS

5.1 Overall Conclusion

The current study mainly focuses on four main areas; (1) exploring the diversity, taxonomy, and phylogeny of palm saprobic fungi in tropical and subtropical regions of China and tropical regions of Thailand, (2) data digitalisation, (3) comprehensive checklist of plam fungi with the prediction of the number of palm fungi and (4) provide new insights into the palm fungal host association. Overall, we collected and studied 105 palm saprobic specimens, and five diseased palm species as part of exploring the diversity, taxonomy, phylogeny, and pathogenicity of palm fungi.

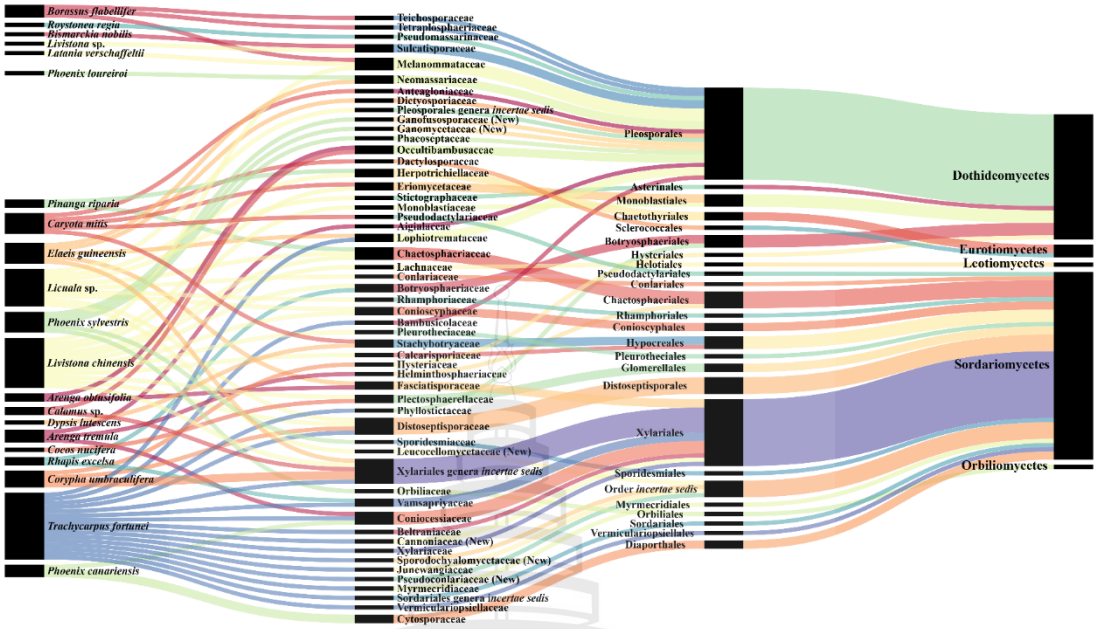
Beyond taxonomic contributions, this study established a sustainable digital platform for palm-associated fungi and compiled a comprehensive checklist (1995–2025) of all recorded taxa, including their taxonomy, host associations, and distributions. This enabled us to redefine total palm fungal diversity and introduce the concept of palm host-preferential genera, offering a framework for future ecological and evolutionary studies. Furthermore, these findings not only fill gaps in the understanding of palm-fungal interactions but also provide a foundation for applied research in plant pathology and conservation. Future work should expand sampling to underrepresented regions, integrate omics tools to explore functional roles and utilize the new data platform to monitor emerging palm pathogens. This study underscores the importance of documenting fungal diversity in the face of ecological change and highlights the need for ongoing collaboration to refine taxonomic and ecological knowledge of palm-associated fungi. For each section of this study, expanded conclusions are given in the next section.

5.1.1 Diversity of Palm-associated Saprobic Fungi

This study, research followed an in-depth investigation of fungal diversity in southern China and the peat swamp regions of southern Thailand and described 105 species based on morphology and phylogenetic analyses. These species are widely

distributed across five classes, 27 orders (including four *incertae sedis* orders within Dothideomycetes), 51 families, and 70 genera (including one *incertae sedis* genus in Pleosporales, one in Sordariales, and six in Xylariales) of Ascomycota. These results show that Dothideomycetes and Sordariomycetes are the two largest classes, while data on Eurotiomycetes, Leotiomycetes and Orbiliomycetes are very scarce. This may be because Dothideomycetes and Sordariomycetes are the dominant classes among palm fungi. Similar results have been observed in previous studies. However, future studies should focus more on fungi from other classes to ensure adequate sampling and collection frequencies, thereby accurately reflecting the diversity of palm fungi. At the same time, our study also reflects the distribution trend of fungi on palm species. *Trachycarpus fortunei* is the most recorded species of fungi in this study, followed by *Livistona chinensis* (Figure 5.1). This may be because *Trachycarpus fortunei* and *Livistona chinensis* are widely distributed as landscape plants in southern China.

One of the major challenges faced in assessing diversity via collection was obtaining pure culture and sequence data. This study found that in the process of standardized species separation (Senanayake et al., 2020), a considerable number of collections could not get living cultures or have good fruiting bodies, yet sequence results are unsuitable for phylogenetic analyses. Samples were collected mainly from subtropical and tropical regions in China, where the annual average rainfall is 1398.2 mm, and the temperature is 19.5°C. After following standard protocols by Fröhlich and Hyde (2000), Senanayake et al. (2020), and Zhang et al. (2024), over 200 samples were unable to either sporulate or obtain quality sequences for the phylogenetic analyses. Thus, we conclude the plam fungi might require specific approaches to (1) isolate and obtain pure cultures and (2) obtain sequences using direct DNA extraction of fruiting bodies. Therefore, future studies should be carried on to develop novel techniques to overcome these hurdles. Also, this study proposed to develop methods to preserve these non-culturable taxa and index them in the fungal databases. By doing so, we believe that these improvements in methods will surely make the diversity of palm fungi complete and accurate. Due to the lack of germination data and molecular data, here in this study presents the diversity of palm fungi known from culture.



Note From left to right are the host species of the sample, the family, order and class to which the fungal species belongs. The streamline represents the number of species.

Figure 5.1 Host-fungus Sankey diagram based on the number of species

5.1.2 Palmfungi.org Digitalization of Records and Dissemination of Fungal Knowledge

palmfungi.org is a comprehensive, interactive database designed to integrate and modernize global knowledge on fungi associated with palm hosts (Arecaceae). This platform bridges historical, classical, and molecular data, which standardizes fungal-host records, offers curated taxonomic entries, and visualises host specificity and fungal diversity through searchable, interconnected modules. The study highlights critical gaps in palm fungal research, particularly the underdocumentation of non-cash crop palms and uneven global research coverage, while emphasizing the need for centralized, accessible data systems. Palmfungi.org not only facilitates taxonomic and ecological studies but also lays a foundation for future collaborations across mycology, botany, and applied sciences, setting a new standard for biodiversity informatics in fungal research.

5.1.3 Palm Fungi Records from 1990 to 2025 Provide New Insights into Expected Palm Fungal Diversity

This study highlights the necessity for flexible and adaptive biodiversity detection and data processing methods to accurately reflect the true diversity of palm fungi. By integrating spatiotemporal weighting and discrete data adjustments, this study provides a refined approach to estimate palm fungal diversity. By reconciling two opposing discrete models, this study has derived plant-to-fungus ratios of 1:17.4 and 1:28.2. Overall, significant progress has been made over the past three decades, yet challenges remain.

Despite a steady rise in total palm fungal records, the annual species introduction rate has stagnated since its peak (2000–2005). However, this could be biased due to limited specialist engagement and geography. Notably, research has concentrated disproportionately in only eight countries, leaving regions like Mexico severely understudied. Meanwhile, temperate palm fungi, which are an emerging component of diversity, likely driven by anthropogenic host migration remain overlooked. Equally concerning is the declining focus on palm species with no prior fungal records, signaling a need for renewed exploratory efforts.

To address these challenges, I propose three priorities:

1. Global Collaboration: Strengthen networks among palm fungal taxonomists to systematically document unexplored diversity.
2. Geographic Expansion: Diversify sampling efforts to mitigate biases and refine diversity estimates.
3. Temperate/Subtropical Focus: Intensify studies on landscape palms in these zones and on underreported host species.

These steps are essential to unlock the full scope of palm-fungal interactions, ensuring robust foundational knowledge for ecological, conservation, and applied research in an era of rapid environmental change.

5.1.4 Host Preference of Palm Fungi: Conclusion and Definitions

In the present study, the concept of host preference in palm-associated fungi was re-evaluated. However, this study noticed limitations in applying terms such as tissue specificity, host specificity, and host preference to higher taxonomic levels. To address this, this study introduces a refined classification system for palm host-preferring fungi,

defining three distinct categories:

1. Typical palm-preferring fungal genera – These exhibit strong phylogenetic clustering of palm-associated species (>50% of genus members) and a shared evolutionary origin. Examples include *Fissuroma*, *Melanographium*, and *Fasciatispora*, where most species are palm-associated and form well-supported clades.

2. Atypical palm-preferring fungal genera – These meet the species that use palm trees as a host or one of their hosts account for 25% to 50% of the total number of species in the genus, but lack phylogenetic clustering, suggesting possible host jumps (e.g., *Neomassaria* and *Xylolentia*, where palm-associated species are phylogenetically scattered, possibly due to shifts to non-palm hosts like coffee, rubber).

3. Conjectured palm-preferring fungal genera – These show phylogenetic clustering of palm-associated species but do not meet the >50% host association threshold, implying a past preference that has since broadened (e.g., *Byssosphaeria* and *Distoseptispora*, where unique morphological adaptations may have enabled habitat expansion).

Findings from this study highlight the complexity of host-fungus interactions, demonstrating that palm fungi exhibit varying degrees of specialization, from strict preference to evolutionary flexibility. This refined framework provides a more nuanced understanding of fungal ecology and evolution, while also identifying key genera (e.g., *Fissuroma*, *Melanographium*) that require further study due to their strong palm associations. However, limitations remain such as particularly for genera with few described species. Also, it is necessary to expand sampling and genomic analyses to validate evolutionary hypotheses.

5.2 Research Advantages

5.2.1 This study substantially advances our understanding of palm-associated fungal diversity in tropical and subtropical regions. Although palm fungi have been investigated for many years, their true diversity remains far from fully explored. By uncovering seven new families, nine new genera, 61 new species, and 44 new records, we have significantly expanded the known spectrum of palm fungi from cultures and

highlighted the vast richness still awaiting discovery.

5.2.2 The Development of www.palmfungi.org is a resource for mycological and botanical Research. With the growing demand for systematic and sustainable data platforms in mycology, we have developed www.palmfungi.org, which is the first searchable, integrated database dedicated to palm-fungal interactions. This platform serves as a centralized knowledge hub, bridging the gap between fungal taxonomy and their specific palm hosts, with several key advantages. Unlike traditional databases that focus solely on fungal taxonomy or host records, our platform directly links fungi to their palm hosts, enabling researchers to explore species-specific relationships with ease. This website also interfaces with existing databases (e.g., Index Fungorum, MycoBank), ensuring seamless data verification and updates. Even though this website is primarily designed for mycologists, the platform could extend its utility to plant biologists, ecologists, and horticulturists who study palms but lack specialized fungal expertise. This will emphasise the interdisciplinary research on palm diseases, biodiversity, and ecosystem health. In the future, this platform is designed to evolve into an educational resource for conservationists, agriculturists, and even palm enthusiasts.

5.2.3 This study provided a new estimation of the number of palm fungi. The comprehensive checklist of palm fungi from 1990 to 2025 consolidates nearly allrecords from the past 35 years. Based on this dataset and a three-phase weighted analysis, we estimate global palm-associated fungal diversity to be between 44,509 and 72,136 species. This resource will support worldwide biodiversity assessments and inform effective conservation strategies in the face of climate change.

5.2.4 Host preference remains a complex and debated topic. Drawing on our experimental results, the palm fungus platform data, and phylogenetic analyses, we propose three categories of host preference among palm-associated fungi: “typical,” “atypical,” and “conjectured” palm-preferring genera. By refining the classification of palm-associated fungi, this study advances fungal ecology and offers a foundation for future research on host specificity, coevolution, and biodiversity conservation in palm-dominated ecosystems. As one of the simplest advantages over the number of possible applications of these categories, this could be guided by targeted research and sampling. For instance, for typical genera, future studies could prioritize aspects like coevolution,

for atypical genera, understanding of host-switching mechanisms and conjectured genera further sampling could be the priority.

5.3 Future Work

5.3.1 Biodiversity Exploration

Future research on the biodiversity of palm fungi should proceed along two main fronts. First, it is necessary to deepen our understanding of fungal assemblages in economically important palms. Comparing taxonomic and functional profiles of fungi across different commercially important palm species should be prioritised under varying climatic conditions. This will help address key scientific questions: (1) Which fungal taxa contribute to growth promotion and fruiting, and what are their precise roles? (2) How is fungal biodiversity distributed among cash-crop palms, and which environmental or ecological drivers shape these patterns? (3) Do healthy versus diseased individuals of the same cash-crop species harbour distinct fungal communities, and how do these taxa influence host health and disease recovery?

Second, we should investigate fungal diversity in non-cash-crop palms, especially those with no existing mycological records, aiming to address the following key scientific questions: (1) What is the true global richness of palm-associated fungi, and can we develop more rigorous methods to estimate total fungal diversity? (2) How do fungal community structures in non-cash-crop palms compare to those in cash-crop species, and what factors underlie any differences?

5.3.2 Maintenance and Expansion of the Palm Fungus Platform

Although this study has successfully built an integrated interactive data platform, more key information still needs to be added to provide for the majority of palm fungus researchers. First, it is necessary to improve and continuously supplement the palm fungus species information as comprehensively as possible. Then, it was required providing annotations of life forms (saprophytic, endophytic, or pathogenic) for each palm fungus species. In addition, it could link with AntiSMASH-DB, SciFinder, ChEBI, and ChemSpider to provide secondary metabolite information or synthetic gene cluster information for the corresponding fungal species. These additions can make the palm

fungus website out of classification move beyond classification and provide stronger support for solving ecological problems, such as biological control.

5.3.3 Genetic Representation of Host Preference

Future research on host preference could utilize greater palm fungus diversity data, next-generation sequencing technology, and genomic methods to explore the relationship between fungi and palm plants at the genetic level. By investigating the key genetic loci of underlying palm fungus host preference and their corresponding protein synthesis pathways, we can explore can elucidate the biological formation mechanism underlying biological mechanisms and ecological influencing factors governing host preference. This will provide new insights for solving to advance environmental protection as well as the conservation and breeding of endangered plant species.

5.3.4 Discovery and Characterization of Metabolites from Palm Endophytes and Pathogens

Future studies should employ advanced metabolomics techniques, such as liquid chromatography-mass spectrometry (LC-MS) and gas chromatography-mass spectrometry (GC-MS) combined with bioassay-guided fractionation to isolate and identify antimicrobial or plant defence-inducing compounds. These metabolites could serve as lead molecules for developing next-generation biofungicides. Furthermore, given the well-established role of endophytic fungi in drug discovery, promising compounds produced by palm-associated fungi may also hold potential for pharmaceutical development.

5.4 Publications

List of publications

5.4.1 First Author

Xiong, Y. R., Manawasinghe, I. S., Maharachchikumbura, S. S. N., Lu, L., Dong, Z. Y., Xiang, M. M., . . . Xu, B. (2022). Pestalotioid species associated with palm species from Southern China. *Current Research in Environmental & Applied Mycology (Journal of Fungal Biology), 12*(1), 285–321. https://doi.org/10.5943/cream/12/1/18

Xiong, Y., Hyde, K. D., Lu, L., Harishchandra, D. L., Mapook, A., Xu, B., . . . Manawasinghe, I. S. (2024). Novel *Helicoma* and *Neohelicosporium* (Tubeufiaceae, Tubeufiales) species and two new host records of *Helicoma* on tropical palms (Arecaceae) from China. *MycoKeys, 108*, 287–315. https://doi.org/10.3897/mycokeys.108.128889

Xiong, Y., Manawasinghe, I. S., Hyde, K. D., Taylor, J. E., Phillips, A., Pereira, D., . . . Xu, B. (2024). Introducing palmfungi.org, an integrated fungal-host data platform. *Biodiversity Data Journal, 12*, e126553. https://doi.org/10.3897/BDJ.12.e126553

Xiong, Y., Manawasinghe, I. S., Liao, C., Hyde, K. D., & Dong, Z. (2022). *Neodeightonia arengae* sp. nov., Botryosphaeriaceous taxa on *Arenga tremula* (Arecaceae) from Guangdong, China. *Phytotaxa, 530*(2), 130–140.

Xiong, Y., Manawasinghe, I. S., Lu, L., Mapook, A., Alotibi, F., & Hyde, K. D. (2025). *Neodeightonia guineensis* sp. nov., a palmicolus species from Guangdong, China. *Phytotaxa, 681*(1), 81–92.

Xiong, Y., Manawasinghe, I. S., Wanasinghe, D. N., Hongsanan, S., Hyde, K. D., Biao, X., . . . Dong, Z. (2024). Two new species and a new host record of Pleosporales (Dothideomycetes) from palm (Arecaceae) in Guangdong Province, China. *New Zealand Journal of Botany, 62*(2–3), 165–191.

Xiong, Y. R., Lu, L., Mapook, A., Maharachchikumbura, S. S. N., McKenzie, E. H. C., Hyde, K. D., . . . Manawasinghe, I. S. (in press). Fungal safari on palm trees: New discoveries from East Asia and 1990-2025 years of global records. *Fungal Diversity*.

Xiong, Y. R., Manawasinghe, I. S., & Mapook, A. (in press). Addition to tropical palm fungi: Ten new Records from China and Thailand. *Asian Journal of Mycology*.

Xiong, Y. R., Mapook, A., Chen, C., Han, M. Y., Hyde, K. D., & Manawasinghe, I. S. (in press). *Pleopunctum livistonae*, a new species on *Livistona chinensis* in Jiangxi Province, China. *Chiang Mai Journal of Science*.

5.4.2 Co-author

Cao, B., Phurbu, D., Ralaiveloarisoa, A., Liimatainen, K., Niskanen, T., Ramírez-Cruz, V., . . . Zhao, R. L. (2025). Fungal diversity notes 1919–2016: Taxonomic and phylogenetic contributions to fungal taxa. *Fungal Diversity, 132*, 425-651. https://doi.org/10.1007/s13225-025-00556-z

Hongsanan, S., Khuna, S., Manawasinghe, I. S., Tibpromma, S., Chethana, K. W. T., Xie, N., . . . Karunarathna, S. C. (2025). Mycosphere notes 521–571: A special edition of fungal biodiversity to celebrate Kevin D. Hyde's 70th birthday and his exceptional contributions to mycology. *Mycosphere, 16*(2), 1–178. https://doi.org/10.5943/mycosphere/16/2/1

Hyde, K. D., Abdel-Wahab, M. A., Abdollahzadeh, J., Abeywickrama, P. D., Absalan, S., Afshari, N., . . . Ertz, D. (2023). Global consortium for the classification of fungi and fungus-like taxa. *Mycosphere*, *14*(1), 1960–2012. https://doi.org/10.5943/mycosphere/14/1/23

Hyde, K. D., Amuhenage, T. B., Apurillo, C. C. S., Asghari, R., Aumentado, H. D., Bahkali, A. H., . . . Dai, D. Q. (2023). Fungalpedia, an illustrated compendium of the fungi and fungus-like taxa. *Mycosphere, 14*(1),1835–1959. https://doi.org/10.5943/mycosphere/14/1/22

Hyde, K. D., Noorabadi, M. T., Thiyagaraja, V., Mq, H., Johnston, P. R., Wijesinghe, S. N., . . . Dianese, J. (2024). The 2024 outline of fungi and fungus-like taxa. *Mycosphere*, *15*(1), 5146–6239. https://doi.org/10.5943/mycosphere/15/1/25

Hyde, K. D., Wijesinghe, S. N., Amuhenage, T. B., Bera, I., Bhunjun, C. S., Chethana, K. W. T., . . . Zhao, H. J. (2024). Current research in applied and environmental mycology fungal profiles 1-30. *Current Research in Environmental & Applied Mycology (Journal of Fungal Biology), 14*(1), 167–266. https://doi.org/10.5943/cream/14/1/11

Lu, L., Karunarathna, S. C., Dai, D. Q., Xiong, Y. R., Suwannarach, N., Stephenson, S. L., . . . Tibpromma, S. (2022). Description of four novel species in pleosporales associated with coffee in Yunnan, China. *Journal of Fungi*, *8*(10), 1113. https://doi.org/10.3897/mycokeys.87.79433

Lu, L., Karunarathna, S. C., Rajeshkumar, K. C., Elgorban, A. M., Jayawardena, R. S., Hongsanan, S., . . . Tibpromma, S. (2025). Unveiling fungal diversity associated with coffee trees in China using a polyphasic approach and a global review of coffee saprobic fungi. *IMA Fungus*, *16*, e144874. https://doi.org/10.3897/imafungus.16.144874

Manawasinghe, I. S., Hyde, K. D., Wanasinghe, D. N., Karunarathna, S. C., Maharachchikumbura, S. S., Samarakoon, M. C., . . . Zhang, W. (2025). Fungal diversity notes 1818–1918: Taxonomic and phylogenetic contributions on genera and species of fungi. *Fungal Diversity*, *130*(1), 1-261.

Manawasinghe, I. S., Zhang, Y. X., Liao, C. F., Xiong, Y. R., Kularathnage, N. D., Luo, M., . . . Gafforov, Y. S. (2022). Mycosphere notes 345–386. *Mycosphere*, *13*(1), 454-557.

Phukhamsakda, C., Nilsson, R. H., Bhunjun, C. S., de Farias, A. R. G., Sun, Y. R., Wijesinghe, S. N., . . . Hyde, K. D. (2022). The numbers of fungi: Contributions from traditional tax onomic studies and challenges of metabarcoding. *Fungal Divers, 114*, 327–386. https://doi.org/10.1007/s13225-022-00502-3.

Tan, Q., Zhang, Y., Zhou, T., Xiong, Y., Huang, Q., Liu, G., . . . Manawasinghe, I. (2025). Endophytic Trichoderma (Sordariomycetes, Hypocreaceae) species associated with citrus in Guangdong province, China. *New Zealand Journal of Botany*, *63*(2-3), 251-277.

REFERENCES

Adamčík, S., Cai, L., Chakraborty, D., Chen, X. H., Cotter, V. T. H., Dai, D. Q., . . . Buyck, B. (2015). Fungal biodiversity profiles 1–10. *Cryptogamie, Mycologie, 36*(2), 121–166. https://doi.org/10.7872/crym/v36.iss2.2015.121

Adams, G. C., Wingfield, W. J., & Common, R. (2005). Phylogenetic relationships and morphology of *Cytospora* species and related teleomorphs (Ascomycota, Diaporthales, Valsaceae) from *Eucalyptus*. *Studies in Mycology, 52*, 1–144.

Akinsanmi, O. A., Nisa, S., Jeff-Ego, O. S., Shivas, R. G., & Drenth, A. (2017). Dry flower disease of macadamia in Australia caused by *Neopestalotiopsis macadamiae* sp. nov. and *Pestalotiopsis macadamiae* sp. nov. *Plant Disease, 101*(1), 45–53.

Alfenas, A., Zauza, E., Mafia, R., & Assis, T. (2009). *Clonagem e doenças do eucalipto*. UFV.

Amrutha, P., & Vijayaraghavan, R. (2018). Evaluation of fungicides and biocontrol agents against *Neopestalotiopsis clavispora* causing leaf blight of strawberry (*Fragaria* × *ananassa* Duch.). *International Journal of Current Microbiology and Applied Sciences, 7*(8), 622–628. https://doi.org/10.20546/ijcmas.2018.708.067

An, J., Fan, C., Fu, Z., Zhang, H., & Yang, P. (2022). Analyses of the complete mitochondrial genome of *Paraconiothyrium* sp. and gene rearrangement diversity in the Pleosporales. *Diversity*, *14*(8), 601. https://doi.org/10.3390/d14080601

Andersson, M. A., Salo, J., Mikkola, R., Marik, T., Kredics, L., Kurnitski, J., . . . Salonen, H. (2021). Melinacidin-producing *Acrostalagmus luteoalbus*, a major constituent of mixed mycobiota contaminating insulation material in an outdoor wall. *Pathogens, 10*(7), 843. https://doi.org/10.3390/pathogens10070843

Andreasen, M., Skrede, I., Jaklitsch, M. W., Voglmayr, H., & Nordén, B. (2021). Multi-locus phylogenetic analysis of lophiostomatoid fungi motivates a broad concept of *Lophiostoma* and reveals nine new species. *Persoonia, 46*, 240–271. https://doi.org/10.3767/persoonia.2021.46.09

Ariyawansa, H. A., & Hyde, K. D. (2018). Additions to *Pestalotiopsis* in Taiwan. *Mycosphere, 9*(5), 999–1013. https://doi.org/10.5943/mycosphere/9/5/4

Ariyawansa, H. A., Hyde, K. D., Jayasiri, S. C., Buyck, B., Thilini Chethana, K. W., Dai, D. Q., . . . Hernawati. (2015). Fungal diversity notes 111–252: Taxonomic and phylogenetic contributions to fungal taxa. *Fungal Diversity, 75*(1), 27–274. https://doi.org/10.1007/s13225-015-0346-5

Ariyawansa, H. A., Jaklitsch, W. M., & Voglmayr, H. (2018). Additions to Taiwan fungal flora 1: *Neomassariaceae* fam. nov. *Cryptogamie, Mycologie, 39*(3), 359–372. https://doi.org/10.7872/crym/v39.iss3.2018.359

Ariyawansa, H. A., Tanaka, K., Thambugala, K. M., Phookamsak, R., Tian, Q., Camporesi, E., . . . Hyde, K. D. (2014). A molecular phylogenetic reappraisal of the Didymosphaeriaceae (= Montagnulaceae). *Fungal Diversity, 68*, 69–104. https://doi.org/10.1007/s13225-014-0305-6

Ariyawansa, H. A., Tsai, I., Hozzein, W. N., & Thambugala, K. M. (2020). *Leucaenicola osmanthi* sp. nov. (Bambusicolaceae, Pleosporales), causing leaf spot of *Osmanthus fragrans* in Taiwan. *Phytotaxa, 437*(1), 23–31. https://doi.org/10.11646/phytotaxa.437.1.3

Artigues, M., & Davet, P. (1984). β-(1→3)-glucanase and chitinase activities in some fungi in relation to their capacity to destroy sclerotia of *Corticium rolfsii* in sterile soil. *Soil Biology and Biochemistry, 16*(5), 527–528. https://doi.org/10.1016/0038-0717(84)90064-6

Arx, J. A. V., & Müller, E. (1975). A re-evaluation of the bitunicate Ascomycetes with keys to families and genera. *Studies in Mycology, 9*, 1–159.

Arzanlou, M., Groenewald, J. Z., Gams, W., Braun, U., Shin, H. D., & Crous, P. W. (2007). Phylogenetic and morphotaxonomic revision of *Ramichloridium* and allied genera. *Studies in Mycology, 58*, 57–93. https://doi.org/10.3114/sim.2007.58.03

Ayasiri, S. C., Hyde, K. D., Jones, E. B. G., McKenzie, E. H. C., Jeewon, R., Phillips, A. J. L., . . . Karunarathna, S. C. (2019). Diversity, morphology and molecular phylogeny of Dothideomycetes on decaying wild seed pods and fruits. *Mycosphere, 10*, 1–186. https://doi.org/10.5943/mycosphere/10/1/1

Ayoubi, N., & Soleimani, M. J. (2016). Strawberry fruit rot caused by *Neopestalotiopsis iranensis* sp. nov. and *N.* mesopotamica. *Current Microbiology, 72*(3), 329–336.

Azuddin, N. F., Mohd, M. H., Rosely, N. F. N., Mansor, A., & Zakaria, L. (2021). Molecular phylogeny of endophytic fungi from rattan (*Calamus castaneus* Griff.) spines and their antagonistic activities against plant pathogenic fungi. *Journal of Fungi, 7*(4), 301. https://doi.org/10.3390/jof7040301

Bachmann, F. M. (1909). Discomycetes in the vicinity of Oxford, Ohio. *Contributions from the Botanical Laboratory of Miami University I. Proceedings of the Ohio State Academy of Science, 5*, 18–70.

Bacon, C. D., & Bailey, C. D. (2006). Taxonomy and conservation: A case study from *Chamaedorea alternans*. *Annals of Botany, 98*(4), 755–763. https://doi.org/10.1093/aob/mcl158

Badali, H., Gueidan, C., Najafzadeh, M. J., Bonifaz, A., Gerrits van den Ende, A. H. G., & De Hoog, G. S. (2008). Biodiversity of the genus *Cladophialophora*. *Studies in Mycology, 61*, 175–191. https://doi.org/10.3114/sim.2008.61.18

Bahram, M., & Netherway, T. (2022). Fungi as mediators linking organisms and ecosystems. *FEMS Microbiology Reviews, 46*(2), fuab058. https://doi.org/10.1093/femsre/fuab058

Baker, W. A., Partridge, E. C., & Morgan-Jones, G. (2001). Notes on Hyphomycetes. LXXXIV. *Pseudotrichoconis* and *Rhexodenticula*, two new monotypic genera with rhexolytically disarticulating conidial separating cells. *Mycotaxon, 79*, 361–373.

Baker, W. J., & Dransfield, J. (2016). Beyond genera palmarum: Progress and prospects in palm systematics. *Botanical Journal of the Linnean Society, 182*(2), 207–233. https://doi.org/10.1111/boj.12401

Bao, D. F., Hyde, K. D., McKenzie, E. H. C., Jeewon, R., Liu, N. G., Phukhamsakda, C., . . . Boonmee, S. (2021). Biodiversity of lignicolous freshwater hyphomycetes from China and Thailand and description of sixteen species. *Journal of Fungi, 7*(8), 669. https://doi.org/10.3390/jof7080669

Baral, H. O., Weber, E., & Marson, G. (2020). *Monograph of Orbiliomycetes (Ascomycota) based on vital taxonomy. Part 1 and 2*. Muséum National d'Histoire Naturelle.

Barr, M. E. (1979). A classification of Loculoascomycetes. *Mycologia, 71*(5), 935–957. https://doi.org/10.1080/00275514.1979.12021099

Barr, M. E. (1980). On the family Tubeufiaceae (Pleosporales). *Mycotaxon, 12*, 137–167.

Barr, M. E. (1984). *Herpotrichia* and its segregates. *Mycotaxon, 20*(1), 1–38.

Barr, M. E. (1987). *Prodromus to class Loculoascomycetes*. University of Massachusetts, Amherst.

Barr, M. E. (2002). Teichosporaceae, another family in the Pleosporales. *Mycotaxon, 82*, 373–389.

Basavand, E., Pakdin-Parizi, A., Mirhosseini, H. A., & Dehghan-Niri, M. (2020). Occurrence of leaf spot disease on date palm caused by *Neopestalotiopsis clavispora* in Iran. *Journal of Phytopathology, 102*(3), 959–959. https://doi.org/10.1007/s42161-020-00530-5

Basu, S., Sengupta, R., & Zandi, P. (2014). *Arecaceae: The majestic family of palms*. https://www.researchgate.net/profile/Peiman-Zandi/publication/266081210_Arecaceae_The_Majestic_Family_of_Palms/links/5424f5070cf238c6ea73bd81/Arecaceae-The-Majestic-Family-of-Palms.pdf

Beck, H. E., Zimmermann, N. E., McVicar, T. R., Vergopolan, N., Berg, A., & Wood, E. F. (2018). Present and future Köppen-Geiger climate classification maps at 1-km resolution. *Scientific Data, 5*(1), 214. https://doi.org/10.1038/sdata.2018.214

Belisário, R., Aucique-Pérez, C. E., Abreu, L. M., Salcedo, S. S., Cotta, S. R., Souza, R. C., . . . Glienke, C. (2020). Infection by *Neopestalotiopsis* spp. occurs on unwounded eucalyptus leaves and is favoured by long periods of leaf wetness. *Plant Pathology, 69*(2), 194–204. https://doi.org/10.1111/ppa.13132

Bellemère, A., & Hafellner, J. (1982). Ultrastructure des asques de genre *Dactylospora* (Discomycetes) et son intérêt taxonomique. *Cryptogamie, Mycologie, 3*, 71–93. https://doi.org/10.5962/p.354108

Bensch, K., Braun, U., Groenewald, J. Z., & Crous, P. W. (2012). The genus *Cladosporium*. *Studies in Mycology, 72*, 1–401. https://doi.org/10.3114/sim0003

Berkeley, M. J., & Broome, C. E. (1850). Notices of British fungi (438–501). *Annals and Magazine of Natural History, 5*, 455–466. https://doi.org/10.1080/03745486009494947

Bernadovičová, S., & Ivanová, H. (2011). Hyphomycetes and Coelomycetes fungi isolated from affected leaves and twigs of cherry laurel trees. *Folia Oecologica, 38*, 137–145.

Bezerra, J. D. P., Machado, A. R., Firmino, A. L., Rosado, A. W. C., & Pereira, O. L. (2018). Mycological diversity description I. *Acta Botanica Brasilica, 32*(4), 656–666. https://doi.org/10.1590/0102-33062018abb0154

Bhat, D. J. (2008). The forests of Western Ghats, an abode of novel and interesting microfungi. *Kavaka, 36*, 1–11.

Bhunjun, C. S., Niskanen, T., Suwannarach, N., Wannathes, N., Chen, Y. J., Lin, C. G., . . . Hyde, K. D. (2022). The numbers of fungi: Are the most speciose genera truly diverse?. *Fungal Diversity, 114*, 387-462. https://doi.org/10.1007/s13225-022-00501-4

Bien, S., & Damm, U. (2020). *Arboricolonus simplex* gen. et sp. nov. and novelties in *Cadophora*, *Minutiella* and *Proliferodiscus* from *Prunus* wood in Germany. *MycoKeys, 63*, 119. https://doi.org/10.3897/mycokeys.63.46836

Boehm, E. W., Schoch, C. L., & Spatafora, J. W. (2009). On the evolution of the Hysteriaceae and Mytilinidiaceae (Pleosporomycetidae, Dothideomycetes, Ascomycota) using four nuclear genes. *Mycological Research, 113*, 461–479. https://doi.org/10.1016/j.mycres.2008.12.001

Bondarenko, S. A., Georgieva, M. L., & Bilanenko, E. N. (2016). Alkalitolerant micromycetes in acidic and neutral soils of the temperate zone. *Microbiology, 85*, 737–744. https://doi.org/10.1134/S0026261716060035

Bondarenko, S. A., Ianutsevich, E. A., Sinitsyna, N. A., Georgieva, M. L., Bilanenko, E. N., & Tereshina, B. M. (2018). Dynamics of the cytosol soluble carbohydrates and membrane lipids in response to ambient pH in alkaliphilic and alkalitolerant fungi. *Microbiology, 87*, 21–32. https://doi.org/10.1134/S0026261718010034

Bonifaz, A., Davoudi, M. M., De Hoog, G. S., Padilla-Desgarennes, C., Vázquez-González, D., Navarrete, G., . . . Badali, H. (2013). Severe disseminated phaeohyphomycosis in an immunocompetent patient caused by *Veronaea botryosa*. *Mycopathologia, 175,* 497–503. https://doi.org/10.1007/s11046-013-9632-5

Boonmee, S., D'souza, M. J., Luo, Z. L., Pinruan, U., Tanaka, K., Su, H. Y., . . . Hyde, K. D. (2016). Dictyosporiaceae fam. nov. *Fungal Diversity, 80,* 457–482. https://doi.org/10.1007/s13225-016-0363-z

Boonmee, S., Rossman, A. Y., Liu, J. K., Li, W. J., Dai, D. Q., Bhat, J. D., . . . Hyde, K. D. (2014). Tubeufiales, ord. nov., integrating sexual and asexual generic names. *Fungal Diversity, 68*(1), 239–298. https://doi.org/10.1007/s13225-014-0304-7

Boonmee, S., Wanasinghe, D. N., Calabon, M. S., Huanraluek, N., Chandrasiri, S. K. U., Jones, E. B. G., . . . Hyde, K. D. (2021). Fungal diversity notes 1387–1511: Taxonomic and phylogenetic contributions on genera and species of fungal taxa. *Fungal Diversity, 111,* 1–335. https://doi.org/10.1007/s13225-021-00489-3

Boonmee, S., Zhang, Y., Chomnunti, P., Chukeatirote, E., Tsui, C. K. M., Bahkali, A. H., . . . Hyde, K. D. (2011). Revision of lignicolous Tubeufiaceae based on morphological reexamination and phylogenetic analysis. *Fungal Diversity, 51*(1), 63–102. https://doi.org/10.1007/s13225-011-0147-4

Borelli, D. (1980). Causal agents of chromoblastomycosis (Chromomycetes). In *Proceedings of the 5th International Conference on Mycoses* (pp. 335–340). Organización Mundial de la Salud.

Brahamanage, R. S., Lu, Y. Z., Bhat, D. J., Wanasinghe, D. N., Yan, J. Y., Hyde, K. D., . . . Boonmee, S. (2017). Phylogenetic investigations on freshwater fungi in Tubeufiaceae (Tubeufiales) reveals the new genus *Dictyospora* and new species *Chlamydotubeufa aquatica* and *Helicosporium flavum*. *Mycosphere, 8*(7), 917–933. https://doi.org/10.5943/mycosphere/8/7/8

Brahmanage, R. S., Dayarathne, M. C., Wanasinghe, D. N., Thambugala, K. M., Jeewon, R., Chethana, K. W. T., . . . Hyde, K. D. (2020). Taxonomic novelties of saprobic Pleosporales from selected dicotyledons and grasses. *Mycosphere, 11*(1), 2481–2541. https://doi.org/10.5943/mycosphere/11/1/15

Breunig, M. M., Kriegel, H. P., Ng, R. T., & Sander, J. (2000). LOF: Identifying density-based local outliers. In *Proceedings of the 2000 ACM SIGMOD International Conference on Management of Data* (pp. 93–104). ACM. https://doi.org/10.1145/342009.335388

Cai, W. Q., Wang, Z., & Deng, J. Y. (2007). Occurrence status and control strategies of dangerous palm plant diseases and insect pests in Guangdong Province. *Hunan Forestry Science and Technology, 3,* 48–50. https://kns.cnki.net/kcms/detail/detail.aspx?FileName=HLKJ200703016&DbName=CJFQ2007

Calabon, M. S., Bagacay, J. F. E., Nim, J. A., Aposaga, D. M., Collado, G. J., & Sadaba, R. B. (2024). The asexual morph of *Seriascoma acutisporum* (Occultibambusaceae, Pleosporales). *Biol Bull Russ Acad Sci, 51*, 1614–1621. https://doi.org/10.1134/S1062359024608334

Calabon, M. S., Jones, E. B. G., Boonmee, S., Doilom, M., Lumyong, S., & Hyde, K. D. (2021). Five novel freshwater ascomycetes indicate high undiscovered diversity in lotic habitats in Thailand. *Journal of Fungi, 7*(2), 117. https://doi.org/10.3390/jof7020117

Cámara-Leret, R., Faurby, S., Macía, M. J., Balslev, H., Göldel, B., Svenning, J. C., . . . Saslis-Lagoudakis, C. H. (2017). Fundamental species traits explain provisioning services of tropical American palms. *Nature Plants, 3*, 16220. https://doi.org/10.1038/nplants.2016.220

Cao, X., Xu, X., Che, H., West, J., & Luo, D. (2019). Eight *Colletotrichum* species, including a novel species, are associated with areca palm anthracnose in Hainan, China. *Plant Disease, 104*(5), 1369–1377. https://doi.org/10.1094/PDIS-10-19-2077-RE

Capdet, M., & Romero, A. I. (2010). Fungi from palms in Argentina. 1. *Mycotaxon, 112*(1), 339–355. https://doi.org/10.5248/112.339

Capella-Gutiérrez, S., Silla-Martínez, J. M., & Gabaldón, T. (2009). trimAl: A tool for automated alignment trimming in large-scale phylogenetic analyses. *Bioinformatics, 25*(15), 1972–1973. https://doi.org/10.1093/bioinformatics/btp348

Carbone, I., & Kohn, L. M. (1999). A method for designing primer sets for speciation studies in filamentous ascomycetes. *Mycologia, 91*(3), 553–556. https://doi.org/10.1080/00275514.1999.12061051

Chaiwan, N., Lu, Y. Z., Tibpromma, S., Bhat, D. J., Hyde, K. D., & Boonmee, S. (2017). *Neotubeufa* gen. nov. and *Tubeufa guangxiensis* sp. nov. (Tubeufiaceae) from freshwater habitats. *Mycosphere, 8*(9), 1443–1456. https://doi.org/10.5943/mycosphere/8/9/9

Chaiwan, N., Wanasinghe, D. N., Mapook, A., Jayawardena, R. S., Norphanphoun, C., & Hyde, K. D. (2020). Novel species of *Pestalotiopsis* fungi on *Dracaena* from Thailand. *Mycology, 11*(4), 306–315. https://doi.org/10.1080/21501203.2020.1801873

Chandrasiri, S. K. U., Liu, Y. L., Huang, J. E., Samarakoon, M. C., Boonmee, S., Calabon, M. S., . . . Hu, D. M. (2021). *Veronaea aquatica* sp. nov. (Herpotrichiellaceae, Chaetothyriales, Eurotiomycetes) from submerged bamboo in China. *Biodiversity Data Journal, 9,* e64505. https://doi.org/10.3897/BDJ.9.e64505

Chang, R., Wang, Y., Liu, Y., Wang, Y., Li, S., Zhao, G., . . . Si, H. (2023). Nine new species of black lichenicolous fungi from the genus *Cladophialophora* (Chaetothyriales) from two different climatic zones of China. *Frontiers in Microbiology, 14,* 1191818. https://doi.org/10.3389/fmicb.2023.1191818

Chen, J., Hao, Z., Xu, H., Yang, L., Liu, G., Sheng, Y., . . . Shi, J. (2015). The complete chloroplast genome sequence of the relict woody plant *Metasequoia glyptostroboides* Hu et Cheng. *Frontiers in Plant Science, 6,* 447. https://doi.org/10.3389/fpls.2015.00447

Chen, Y. J., Zeng, L., Shu, N., Jiang, M. Y., Qang, H., Huang, Y., & Tong, H. (2018). *Pestalotiopsis*-like species causing gray blight disease on *Camellia sinensis* in China. *Plant Disease, 102*(1), 98–106. https://doi.org/10.1094/PDIS-05-17-0642-RE

Chen, Y. Y., Maharachchikumbura, S. S. N., Liu, J. K., Hyde, K. D., Nanayakkara, R. R., Zhu, G. S., . . . Liu, Z. Y. (2017). Fungi from Asian karst formations I. *Pestalotiopsis photinicola* sp. nov., causing leaf spots of *Photinia serrulata. Mycosphere, 8,* 103–110. https://doi.org/10.5943/mycosphere/8/1/9

Chethana, K. W. T., Manawasinghe, I. S., Hurdeal, V. G., Bhunjun, C. S., Appadoo, M. A., Gentekaki, E., . . . Hyde, K. D. (2021). What are fungal species and how to delineate them? *Fungal Diversity, 109*(1), 1–25. https://doi.org/10.1007/s13225-021-00483-9

Chethana, K. W. T., Rathnayaka, A. R., Samarakoon, B. C., Wu, N., Wijesinghe, S. N., Yasanthika, W. A. E., . . . Hyde, K. D. (2023). AJOM new records and collections of fungi: 151–200. *Asian Journal of Mycology, 6*(2), 89–243. https://doi.org/10.5943/ajom/6/2/7

Chiarucci, A., Bacaro, G., & Scheiner, S. M. (2011). Old and new challenges in using species diversity for assessing biodiversity. *Philosophical Transactions of the Royal Society B: Biological Sciences, 366*(1576), 2426–2437. https://doi.org/10.1098/rstb.2011.0065

Choi, Y. W., Hyde, K. D., & Ho, W. W. H. (1999). Single spore collection of fungi. *Fungal Diversity, 3,* 29–38.

Christenhusz, M. J. M., & Byng, J. W. (2016). The number of known plant species in the world and its annual increase. *Phytotaxa, 261*(3), 201-217. https://doi.org/10.11646/phytotaxa.261.3.1

Ciferi, R., & Montemartini, A. (1957). Sui generi Muchmoria Sacc. e Veronaea n. gen. (Dematiaceae, Didymosporae). *Atti Ist Bot Univ Lab Crittogam Pavia Ser, 5*(15), 67–72. https://doi.org/10.1484/J.EUPHR.5.127844

Cole, G. T. (1983). Graphiola phoenicis: A taxonomic enigma. *Mycologia, 75,* 93–116.

Cooke, M. C., & Plowright, C. B. (1879). British Sphaeriacei. *Grevillea, 7,* 77–89.

Corda, A. C. J. (1837). *Icones fungorum hucusque cognitorum* (vol. 1). JG Calve.

Corda, A. C. J. (1838). Abbildungen der Pilze und Schwämme. *Icones Fungorum Hucusque Cognitorum, 2,* 1–43.

Crous, P. W., & Palm, M. E. (1999). Reassessment of the anamorph genera Botryodiplodia, Dothiorella and Fusicoccum. *Sydowia, 51,* 167–175.

Crous, P. W., Akulov, A., Balashov, S., Boers, J., Braun, U., Castillo, J., . . . Groenewald, J. Z. (2023). New and interesting fungi. 6. *Fungal Systematics and Evolution, 11*, 109–156. https://doi.org/10.3114/fuse.2023.11.09

Crous, P. W., Luangsa-Ard, J. J., Wingfield, M. J., Carnegie, A. J., Hernández-Restrepo, M., Lombard L, . . . Groenewald, J. Z. (2018a). Fungal planet description sheets: 785–867. *Persoonia, 41*, 238–417. https://doi.org/10.3767/persoonia.2018.41.12

Crous, P. W., Schubert, K., Braun, U., De Hoog, G. S., Hocking, A. D., Shin, H. D., . . . Groenewald, J. Z. (2007). Opportunistic, human-pathogenic species in the Herpotrichiellaceae are phenotypically similar to saprobic or phytopathogenic species in the Venturiaceae. *Stud Mycol, 58*, 185–217. https://doi.org/10.3114/sim.2007.58.07

Crous, P. W., Schumacher, R. K., Wingfield, M. J., Akulov, A., Denman, S., Roux, J., . . . Groenewald, J. Z. (2018b). New and interesting fungi. 1. *Fungal Syst Evol, 1*, 169–215. https://doi.org/10.3114/fuse.2018.01.08

Crous, P. W., Schumacher, R. K., Wingfield, M. J., Lombard, L., Giraldo, A., Christensen, M, . . . Groenewald, J. Z. (2015). Fungal systematics and evolution: FUSE 1. *Sydowia, 67*, 81–118.

Crous, P. W., Shivas, R. G., Quaedvlieg, W. V., Van der Bank, M., Zhang, Y., Summerell, B. A., . . . Groenewald, J. Z. (2014). Fungal planet description sheets: 214–280. *Persoonia, 32*, 184–306. https://doi.org/10.3767/003158514X682395

Crous, P. W., Slippers, B., Wingfield, M. J., Rheeder, J., Marasas, W. F. O., Phillips, A. J. L., . . . Groenewald, J. Z. (2006). Phylogenetic lineages in the Botryosphaeriaceae. *Stud Mycol, 55*, 235–253. https://doi.org/10.3114/sim.55.1.235

Crous, P. W., Summerell, B. A., Swart, L., Denman, S., Taylor, J. E., Bezuidenhout, C. M., . . . Groenewald, J. Z. (2011). Fungal pathogens of Proteaceae. *Persoonia, 27*, 20–45. https://doi.org/10.3767/003158511X606239

Crous, P. W., Wingfield, M. J., Burgess, T. I., Carnegie, A. J., Hardy, G. E. S. J., Smith, D., . . . Groenewald, J. Z. (2017). Fungal planet description sheets: 625–715. *Persoonia, 39*, 270–467. https://doi.org/10.3767/persoonia.2017.39.11

Crous, P. W., Wingfield, M. J., Burgess, T. I., Hardy, G. E. S. J., Crane, C., Barrett, S., . . . Groenewald, J. Z. (2016). Fungal planet description sheets: 469–557. *Persoonia, 37*, 218–403. https://doi.org/10.3767/003158516X694499

Crous, P. W., Wingfield, M. J., Cheewangkoon, R., Carnegie, A. J., Burgess, T. I., Summerell, B. A., . . . Groenewald, J. Z. (2019). Foliar pathogens of eucalypts. *Stud Mycol, 94*, 125–298. https://doi.org/10.1016/j.simyco.2019.08.001

Crous, P. W., Wingfield, M. J., Chooi, Y. H., Gilchrist, C. L. M., Lacey, E., Pitt, J. I., . . . Groenewald, J. Z. (2020). Fungal planet description sheets: 1042–1111. *Persoonia, 44*, 301–459. https://doi.org/10.3767/persoonia.2020.44.11

Crous, P. W., Wingfield, M. J., Le Roux, J. J., Richardson, D. M., Strasberg, D., Shivas, R. G, . . . Groenewald, J. Z. (2015). Fungal planet description sheets: 371–399. *Persoonia, 35*, 264–327. https://doi.org/10.3767/003158515X690269

Crous, P. W., Wingfield, M. J., Schumacher, R. K., Akulov, A., Bulgakov, T. S., Carnegie, A. J., . . . Groenewald, J. Z. (2020). New and interesting fungi. 3. *Fungal Syst Evol, 6*, 157–231. https://doi.org/10.3114/fuse.2020.06.09

Dai, D.Q., Bahkali, A. H., Li, Q. R., Bhat, D. J., Wijayawardene, N. N., Li, W. J., . . . Hyde, K. D. (2014). Vamsapriya (Xylariaceae) re-described, with two new species and molecular sequence data. *Cryptogam Mycol, 35*, 339–357. https://doi.org/10.7872/crym.v35.iss4.2014.339

Dai, D.Q., Phookamsak, R., Wijayawardene, N. N., Li, W. J., Bhat, D. J., Xu, J. C., . . . Chukeatirote, E. (2017). Bambusicolous fungi. *Fungal Divers, 82*, 1–105. https://doi.org/10.1007/s13225-016-0367-8

Daranagama, D. A., Camporesi, E., Tian, Q., Liu, X., Chamyuang, S., Stadler, M., . . . Hyde, K. D. (2015). Anthostomella is polyphyletic comprising several genera in Xylariaceae. *Fungal Divers, 73*, 203–238. https://doi.org/10.1007/s13225-015-0329-6

Darapanit, A., Boonyuen, N., Leesutthiphonchai, W., Nuankaew, S., & Piasai, O. (2021). Identification, pathogenicity and effects of plant extracts on Neopestalotiopsis and Pseudopestalotiopsis causing fruit diseases. *Sci Rep, 11*, 22606. https://doi.org/10.1038/s41598-021-02113-5

Das, K., Lee, S. Y., & Jung, H. Y. (2020). *Pestalotiopsis kaki* sp. nov., a novel species isolated from persimmon tree (Diospyros kaki) bark in Korea. *Mycobiology, 49*(1), 54–60. https://doi.org/10.1080/12298093.2020.1852703

David, H. L. (1931). Brief notes on the Helicosporeae with descriptions of four new species. *Ann Missouri Bot Gard, 18*(1), 9–16. https://doi.org/10.2307/2394042

De Hoog, G. S., & Papendorf, M. C. (1976). The genus Phaeoisaria. *Persoonia, 8,* 407–414.

De Hoog, G. S., Guarro, J., Gené, J., & Figueras, M. J. (2000). *Atlas of clinical fungi* (2nd ed.). Centraalbureau voor Schimmelcultures.

De Hoog, G. S., Nishikaku, A. S., Fernandez-Zeppenfeldt, G., Padín-González, C., Burger, E., Badali, H., . . . Gerrits van den Ende, A. H. G. (2007). Molecular analysis and pathogenicity of the Cladophialophora carrionii complex, with the description of a novel species. *Stud Mycol, 58,* 219–234. https://doi.org/10.3114/sim.2007.58.08

De Notaris, G. (1847). Prime linee di una nuova disposizione dei Pirenomiceti Isterini. *Giorn Bot Ital, 2*(7–8), 5–52.

de Silva, N. I., Hyde, K. D., Lumyong, S., Phillips, A. J. L., Bhat, D. J., Maharachchikumbura, S. S. N., . . . Karunarathna, S. C. (2022). Morphology, phylogeny, host association and geography of fungi associated with plants of Annonaceae, Apocynaceae and Magnoliaceae. *Mycosphere, 13*(1), 955–1076. https://doi.org/10.5943/mycosphere/13/1/12

de Silva, N. I., Maharachchikumbura, S. S. N., Thambugala, K. M., Bhat, D. J., Jeewon, R., Chukeatirote, E., . . . Hyde, K. D. (2021). Morphomolecular taxonomic studies reveal a high number of endophytic fungi from Magnolia candolii and M. garrettii in China and Thailand. *Mycosphere, 12*(1), 163–237. https://doi.org/10.5943/mycosphere/12/1/3

de Silva, N. I., Thambugala, K. M., Jeewon, R., Phookamsak, R., Goonasekara, I. D., Lumyong, S., . . . Hyde, K. D. (2018). Morphology and phylogeny of Atrocalyx acervatus sp. nov. (Lophiotremataceae) from Acer species. *Phytotaxa, 333,* 199–208. https://doi.org/10.11646/phytotaxa.333.2.3

de Silva, N. I., Thambugala, K. M., Tennakoon, D. S., Karunarathna, S. C., Kumla, J., Suwannarach, N., . . . Lumyong, S. (2022). Taxonomy and phylogenetic appraisal of Dothideomycetous fungi associated with Magnolia, Lilium longiflorum and Hedychium coronarium. *J Fungi, 8*, 1094. https://doi.org/10.3390/jof8101094

Deighton, F. C. (1985). Three leaf-spotting hyphomycetes on palms. *Trans Br Mycol Soc, 85*, 739–742. https://doi.org/10.1016/S0007-1536(85)80275-8

Delgado, G. (2013). South Florida microfungi: A new species of Ellisembia (hyphomycetes) with new records from the USA. *Mycotaxon, 123*, 445–450

Delgado, G., Koukol, O., Cáceres, O., & Piepenbring, M. (2017). The phylogenetic placement of Ernakulamia cochinensis within Pleosporales (Dothideomycetes, Ascomycota). *Cryptog Mycol, 38*, 435–451. https://doi.org/10.7872/crym/v38.iss4.2017.435

Dhillon, B., Graham, F., Laughinghouse, H. D., & Chakrabarti, S. (2024). Assessment of endophytic fungal community in palm leaves and their biocontrol potential. *Phyto Frontiers, 4*(3), 296–304. https://doi.org/10.1094/PHYTOFR-04-23-0053-R

Diederich, P., Ertz, D., Lawrey, J. D., Sikaroodi, M., & Untereiner, W. A. (2013). Molecular data place the hyphomycetous lichenicolous genus Sclerococcum close to Dactylospora (Eurotiomycetes) and S. parmeliae in Cladophialophora (Chaetothyriales). *Fungal Divers, 58*, 61–72. https://doi.org/10.1007/s13225-012-0179-4

Diederich, P., Lawrey, J. D., & Ertz, D. (2018). The 2018 classification and checklist of lichenicolous fungi, with 2000 non-lichenized, obligately lichenicolous taxa. *Bryologist, 121,* 340–425. https://doi.org/10.1639/0007-2745-121.3.340

Dighton, J., & White, J. F. (2017). *The fungal community: Its organization and role in the ecosystem*. CRC Press. https://doi.org/10.1201/9781315119496

Dissanayake, A. J., Bhunjun, C. S., Maharachchikumbura, S. S. N., & Liu, J. K. (2020). Applied aspects of methods to infer phylogenetic relationships amongst fungi. *Mycosphere, 11*, 2652–2676. https://doi.org/10.5943/mycosphere/11/1/18

Dissanayake, A. J., Phillips, A. J. L., Hyde, K. D., & Li, X. H. (2016). Botryosphaeriaceae: Current status of genera and species. *Mycosphere, 7*, 1001–1073. https://doi.org/10.5943/mycosphere/si/1b/13

Dissanayake, L. S., Samarakoon, M. C., Maharachchikumbura, S. S. N., Hyde, K. D., Tang, X., Li, Q. R., . . . Wanasinghe, D. N. (2024). Exploring the taxonomy and phylogeny of Sordariomycetes taxa emphasizing Xylariomycetidae in Southwestern China. *Mycosphere, 15*, 1675–1793. https://doi.org/10.5943/mycosphere/15/1/15

Döbbeler, P., & Buck, W. R. (2017). Dactylospora inopina (Lecanorales), a new biotrophic parasite on Radula (Hepaticae) from the Cape Horn Archipelago, Chile. *Nova Hedwigia, 105*, 87–93. https://doi.org/10.1127/nova_hedwigia/2017/0403

Doilom, M., Dissanayake, A. J., Wanasinghe, D. N., Boonmee, S., Liu, J. K., Bhat, D. J., . . . Hyde, K. D. (2017). Microfungi on Tectona grandis (teak) in Northern Thailand. *Fungal Divers, 82*, 107–182. https://doi.org/10.1007/s13225-016-0368-7

Doilom, M., Hyde, K. D., Phookamsak, R., Dai, D. Q., Tang, L. Z., Hongsanan, S., . . . Promputtha, I. (2018). Mycosphere notes 225–274: Types and other specimens of some genera of Ascomycota. *Mycosphere, 9*(4), 647–754. https://doi.org/10.5943/mycosphere/9/4/3

Dong, W., Hyde, K. D., Bhat, D. J., & Zhang, H. (2018). Introducing *Aculeata aquatica* gen. et sp. nov., *Minimelanolocus thailandensis* sp. nov. and *Thysanorea aquatica* sp. nov. (Herpotrichiellaceae, Chaetothyriales) from freshwater in northern Thailand. *Mycol Prog, 17*, 617–629. https://doi.org/10.1007/s11557-018-1389-2

Dong, W., Hyde, K. D., Jeewon, R., Doilom, M., Yu, X. D., Wang, G. N., . . . Zhang, H. (2021). Towards a natural classification of annulatascaceae-like taxa II: introducing five new genera and eighteen new species from freshwater. *Mycosphere, 12*, 1–88. https://doi.org/10.5943/mycosphere/12/1/1

Dong, W., Wang, B., Hyde, K. D., McKenzie, E. H. C., Raja, H., Tanaka, K., . . . Zhang, H. (2020). Freshwater Dothideomycetes. *Fungal Divers, 105*, 319–575. https://doi.org/10.1007/s13225-020-00463-5

Dong, W., Zhang, H., Doilom, M., Yu, X. D., Wang, G. N., & Nalumpang, S. (2021). Rhexodenticula aquatica (Sordariomycetidae genera incertae sedis), a novel hyphomycete from freshwater in Thailand. *Phytotaxa, 483*, 129–138. https://doi.org/10.11646/phytotaxa.483.2.5

Dransfield, J., Uhl, N. W., Asmussen, C. B., Baker, W. J., Harley, M. M., & Lewis, C. E. (2008). *Genera Palmarum – The evolution and classification of the palms*. Royal Botanic Gardens.

Du, H. Z., Liu, N. G., Wu, N., Cheewangkoon, R., & Liu, J. K. (2025). Morpho-phylogenetic evidence reveals novel hyphomycetous fungi on medicinal plants in Southwestern China. *Mycology,* 1–60. https://doi.org/10.1080/21501203.2024.2444436

Ehrenberg, C. G. (1818). *Sylvae mycologicae berolinenses*. Formis Theophili Bruschcke.

Ekanayaka, A. H., Hyde, K. D., Gentekaki, E., McKenzie, E. H. C., Zhao, Q., Bulgakov, T. S., . . . Camporesi, E. (2019). Preliminary classification of Leotiomycetes. *Mycosphere, 10*(1), 310–489. https://doi.org/10.5943/mycosphere/10/1/7

Ekanayaka, A. H., Jones, E. B. G., Hyde, K. D., & Zhao, Q. (2019). A stable phylogeny for Dactylosporaceae. *Cryptogamie, Mycologie, 40*(1), 23–44. https://doi.org/10.5252/cryptogamie-mycologie2019v40a3

Elliott, M. L. (2011). First report of Fusarium wilt caused by *Fusarium oxysporum* f. sp. palmarum on Canary Island date palm in Florida. *Plant Disease, 95*(3), 356. https://doi.org/10.1094/PDIS-11-10-0851

Elliott, M. L., & Des Jardin, E. A. (2014). Serenomyces associated with palms in southeastern USA: Collection, culture storage and genetic variation. *Mycologia, 106*(4), 698–707. https://doi.org/10.3852/13-353

Ellis, M. B. (1957). Haplobasidion, Lacellinopsis and Lacellina. *Mycological Papers, 67*, 1–15.

Ellis, M. B. (1963). Dematiaceous hyphomycetes. V. *Mycological Papers, 93*, 1–33.

Ellis, M. B. (1967). Dematiaceous hyphomycetes. VIII. Periconiella, Trichodochium, etc. *Mycological Papers, 111*, 1–46.

Ellis, M. B. (1971). *Dematiaceous hyphomycetes*. Commonwealth Mycological Institute. https://doi.org/10.1079/9780851986180.0000

Eriksson, O. E. (1966). On Anthostomella Sacc., Entosordaria (Sacc.) Hohn. and some related genera (pyrenomycetes). *Svensk Botanisk Tidskrift, 60,* 315–324.

Eriksson, O., & Hawksworth, D. L. (1986). An alphabetical list of the generic names of ascomycetes. *Systema Ascomycetum, 5*, 3–111.

Fan, X. L., Hyde, K. D., Liu, M., Liang, Y. M., & Tian, C. M. (2015a). Cytospora species associated with walnut canker disease in China, with description of a new species C. gigalocus. *Fungal Biology*, *119*(5), 310–319. https://doi.org/10.1016/j.funbio.2014.12.011

Fan, X. L., Hyde, K. D., Yang, Q., Liang, Y. M., Ma, R., & Tian, C. M. (2015b). Cytospora species associated with canker disease of three anti-desertification plants in northwestern China. *Phytotaxa, 197*(4), 227–244. https://doi.org/10.11646/phytotaxa.197.4.1

Farman, M. L., Ascari, J. P., Rahnama, M., Ponte, E. M. D., Pedley, K. F., Martinez, S., . . . Valent, B. (2024). A reevaluation of phylogenomic data reveals that current understanding in wheat blast population biology and epidemiology is obfuscated by oversights in population sampling. *Phytopathology, 114*(1), 220–225. https://doi.org/10.1094/PHYTO-01-23-0025-R

Farr, D. F., Rossman, A. Y., & Castlebury, L. A. (2021). *United States National Fungus Collections Fungus-Host Dataset.* Ag Data Commons. https://doi.org/10.15482/USDA.ADC/1524414

Fehr, V., Buitenwerf, R., & Svenning, J. C. (2020). Non-native palms (Arecaceae) as generators of novel ecosystems: A global assessment. *Diversity and Distributions, 26*(11), 1523–1538. https://doi.org/10.1111/ddi.13150

Feng, P. Y., De Hoog, G. S., Najafzadeh, M. J., Gerrits van den Ende, A. H. G., Stielow, J. B., Badali, H., . . . Vicente, V. A. (2014). Cladophialophora abundans, a novel species of Chaetothyriales isolated from the natural environment. *Mycological Progress, 13*(2), 381–391. https://doi.org/10.1007/s11557-013-0924-4

Feng, Y., Zhang, S. N., Chen, Y. Y., & Liu, Z. Y. (2022). *Fissuroma bambucicola* sp. nov. (Aigialaceae, Pleosporales) from bamboo in Guizhou, China. *Phytotaxa, 543*(1), 64–72. https://doi.org/10.11646/phytotaxa.543.1.6

Francis, S. M. (1975). Anthostomella Sacc. (Part 1). *Mycological Papers, 139*, 1–97.

Freitas, E. F. S., Da Silva, M., Barros, M. V. P., & Kasuya, M. C. M. (2019). *Neopestalotiopsis hadrolaeliae* sp. nov., a new endophytic species from the roots of the endangered orchid Hadrolaelia jongheana in Brazil. *Phytotaxa, 416*(3), 211–220. https://doi.org/10.11646/phytotaxa.416.3.2

Fries, E. M. (1819). *Novitiae florae suecicae* (Part V). Typographia Academia.

Fries, E. M. (1825). *Systema orbis vegetabilis*. Typographia Academia.

Fries, E. M. (1836). *Corpus Florarum provincialium suecicae I. Floram Scanicam*. Upsaliae, Typis Palmblad, Sebell & Co. https://doi.org/10.5962/bhl.title.47083

Fröhlich, J., & Hyde, K. D. (1999). Biodiversity of palm fungi in the tropics: Are global fungal diversity estimates realistic?. *Biodiversity and Conservation, 8*(7), 977–1004. https://doi.org/10.1023/A:1008895913857

Fröhlich, J., & Hyde, K. D. (2000). Palm microfungi. *Fungal Diversity Research Series, 3*, 1–393.

Fröhlich, J., Hyde, K. D., & Petrini, O. (2000). Endophytic fungi associated with palms. *Mycological Research, 104*(10), 1202–1212. https://doi.org/10.1017/S095375620000263X

Gams, W., O'Donnell, K., Schroers, H. J., & Christensen, M. (1998). Generic classification of some more hyphomycetes with solitary conidia borne on phialides. *Canadian Journal of Botany, 76*(10), 1570–1583. https://doi.org/10.1139/b98-104

Gao, W., Tu, R. X., Li, H., Fang, Y. L., & Que, Q. M. (2020). In the subtropical monsoon climate high-density city, what features of the neighborhood environment matter most for public health?. *International Journal of Environmental Research and Public Health, 17*(24), 9566. https://doi.org/10.3390/ijerph17249566

Garcia, J. F., Lawrence, D. P., Morales-Cruz, A., Travadon, R., Minio, A., Hernandez-Martinez, R., . . . Cantu, D. (2021). Phylogenomics of plant-associated Botryosphaeriaceae species. *Frontiers in Microbiology, 12*, 652802. https://doi.org/10.3389/fmicb.2021.652802

Gawas, P., & Bhat, D. J. (2005). *Vamsapriya indica* gen. et sp. nov., a bambusicolous, synnematous fungus from India. *Mycotaxon, 94*, 149–154.

Geng, K., Zhang, B., Song, Y., Hyde, K. D., Kang, J. C., & Wang, Y. (2013). A new species of *Pestalotiopsis* from leaf spots of *Licuala grandis* from Hainan, China. *Phytotaxa, 88*(3), 49–54. https://doi.org/10.11646/phytotaxa.88.3.2

Gerardo-Lugo, S. S., Tovar-Pedraza, J. M., Maharachchikumbura, S. S. N., Apodaca-Sánchez, M. A., Correia, K. C., Sauceda-Acosta, C. P., . . . Beltrán-Peña, H. (2020). Characterization of *Neopestalotiopsis* species associated with mango grey leaf spot disease in Sinaloa, Mexico. *Pathogens, 9*(10), 788. https://doi.org/10.3390/pathogens9100788

Glass, N. L., & Donaldson, G. C. (1995). Development of primer sets designed for use with the PCR to amplify conserved genes from filamentous ascomycetes. *Applied and Environmental Microbiology, 61*(4), 1323–1330. https://doi.org/10.1128/aem.61.4.1323-1330.1995

Goh, T. K. (1999). Single–spore collection using a hand–made glass needle. *Fungal Diversity, 2*, 47–63.

Goh, T. K., & Hyde, K. D. (1997). *Melanographium palmicolum* sp. nov. from Hong Kong, and a key to the genus. *Mycological Research, 101*(9), 1097–1100. https://doi.org/10.1017/S0953756297003675

Goh, T. K., & Hyde, K. D. (1998). A new hyphomycete genus, *Conioscyphopsis*, from wood submerged in a freshwater stream and a review of *Conioscypha*. *Mycological Research, 102*(3), 308–312. https://doi.org/10.1017/S0953756297004942

Gonçalves, M. F., Esteves, A. C., & Alves, A. (2020). Revealing the hidden diversity of marine fungi in Portugal with the description of two novel species, *Neoascochyta fuci* sp. nov. and *Paraconiothyrium salinum* sp. nov. *International Journal of Systematic and Evolutionary Microbiology, 70*(8), 5337–5354.

Gongfu, Z., Yuanlue, H., & Guozhao, L. (1990). Characteristics and regional diversity of tropical China. *Acta Geographica Sinica, 45*(2), 245–252.

González Fragoso, R. (1917). Hongos de la provincia de Málaga (recolectados por D. Cándido Bolívar y D. Enrique Rioja). *Boletín de la Real Sociedad Española de Historia Natural, 17*, 299–311.

Goos, R. D. (1986). A review of the anamorph genus *Helicoma*. *Mycologia, 78*(5), 744–761. https://doi.org/10.1080/00275514.1986.12025318

Gorelick, N., Hancher, M., Dixon, M., Ilyushchenko, S., Thau, D., & Moore, R. (2017). Google Earth Engine: Planetary-scale geospatial analysis for everyone. *Remote Sensing of Environment, 202*, 18–27. https://doi.org/10.1016/j.rse.2017.06.031

Griffiths, D. A., & Swart, H. J. (1974a). Conidial structure in two species of *Pestalotiopsis. Transactions of the British Mycological Society, 62*(2), 295–IN220.

Griffiths, D. A., & Swart, H. J. (1974b). Conidial structure in *Pestalotia pezizoides. Transactions of the British Mycological Society, 63*(1), 1–X. https://doi.org/10.1016/S0007-1536(74)80149-X

Grossart, H. P., Van den Wyngaert, S., Kagami, M., Wurzbacher, C., Cunliffe, M., & Rojas-Jimenez, K. (2019). Fungi in aquatic ecosystems. *Nature Reviews Microbiology, 17*(6), 339–354. https://doi.org/10.1038/s41579-019-0175-8

Grum-Grzhimaylo, A. A., Georgieva, M. L., Bondarenko, S. A., Debets, A. J., & Bilanenko, E. N. (2016). On the diversity of fungi from soda soils. *Fungal Diversity*, *76*, 27–74. https://doi.org/10.1007/s13225-015-0320-2

Gruyter, J., Woudenberg, J. H. C., Aveskamp, M. M., Verkley, G. J. M., Groenewald, J. Z., & Crous, P. (2013). Redisposition of *Phoma*-like anamorphs in Pleosporales. *Studies in Mycology*, *75*(1), 1–36. https://doi.org/10.3114/sim0004

Gualberto, G. F., Catarino, A. D. E. M., Sousa, T. F., Cruz, J. C., Hanada, R. E., Caniato, F. F., . . .Silva, G. F. (2021). *Pseudopestalotiopsis gilvanii* sp. nov. and *Neopestalotiopsis formicarum* leaf spot pathogens from guarana plant: A new threat to global tropical hosts. *Phytotaxa, 489*(2), 121–139. https://doi.org/10.11646/phytotaxa.489.2.2

Guarro, J., Vieira, L. A., De Freitas, D., Gené, J., Zaror, L., Hofling-Lima, A. L., . . . Figueras, M. J. (2000). *Phaeoisaria clematidis* as a cause of keratomycosis. *Journal of Clinical Microbiology, 38*(6), 2434–2437. https://doi.org/10.1128/JCM.38.6.2434-2437.2000

Guba, E. F. (1960). Monograph of *Monochaetia* and *Pestalotia. Mycologia, 52*(6), 966. https://doi.org/10.2307/3755860

Guindon, S., Dufayard, J. F., Lefort, V., Anisimova, M., Hordijk, W., & Gascuel, O. (2010). New algorithms and methods to estimate maximum-likelihood phylogenies: Assessing the performance of PhyML 3.0. *Systematic Biology, 59*(3), 307–321. https://doi.org/10.1093/sysbio/syq010

Guo, J. W., Yang, L. F., Liu, Y. H., Yang, J., Wang, H. F., Li, L., . . . Li, W. J. (2016). First report of pseudostem black spot caused by *Pestalotiopsis microspora* on Tsao-ko in Yunnan, China. *Plant Disease, 100*(5), 1021. https://doi.org/10.1094/PDIS-12-15-1460-PDN

Gutiérrez del Pozo, D., Martín-Gómez, J., Tocino, Á., & Cervantes, E. (2020). Seed geometry in the Arecaceae. *Horticulturae, 6*(4), 64. https://doi.org/10.3390/horticulturae6040064

Gwynne-Vaughan, H. C. I. (2021). *The structure and development of the fungi*. CUP Archive.

Haase, G., Sonntag, L., Melzer-Krick, B., & De Hoog, G. S. (1999). Phylogenetic inference by SSU-gene analysis of members of the Herpotrichiellaceae with special reference to human pathogenic species. *Studies in Mycology, 43*, 80–97.

Hafellner, J. (1979). Karschia: Revision einer Sammelgattung an der Grenze von lichenisierten und nichtlichenisierten Ascomyceten. *Beihefte zur Nova Hedwigia, 62*, 1–248.

Haines, J. H., & Dumont, K. P. (1983). Studies in the Hyaloscyphaceae II: Proliferodiscus, a new genus of Arachnopezizoideae. *Mycologia, 75*(3), 535–543. https://doi.org/10.1080/00275514.1983.12023717

Hall, T. A. (1999). BioEdit: A user-friendly biological sequence alignment editor and analysis program for Windows 95/98/NT. *Nucleic Acids Symposium Series, 41*, 95–98.

Haq, I. U., & Ijaz, S. (2020). *Etiology and integrated management of economically important fungal diseases of ornamental palms*. Springer.

Harishchandra, D. L., Aluthmuhandiram, J. V. S., Yan, J., & Hyde, K. D. (2020). Molecular and morpho-cultural characterisation of *Neopestalotiopsis* and *Pestalotiopsis* species associated with ornamental and forest plants in China.

Harkness, H. W. (1884). New species of Californian fungi. *Bulletin of the California Academy of Sciences, 1*, 29–47.

Harrison, S., Spasojevic, M. J., & Li, D. (2020). Climate and plant community diversity in space and time. *Proceedings of the National Academy of Sciences of the United States of America, 117*(9), 4464–4470. https://doi.org/10.1073/pnas.1921724117

Hashimoto, A., Matsumura, M., Hirayama, K., & Tanaka, K. (2017). Revision of Lophiotremataceae (Pleosporales, Dothideomycetes): Aquasubmersaceae, Cryptocoryneaceae, and *Hermatomycetaceae fam*. nov. *Persoonia, 39*, 51–73. https://doi.org/10.3767/persoonia.2017.39.03

Hassan, N. S. M., Hossain, M. S., Balakrishnan, V., Zuknik, M. H., Mustaner, M., Easa, A. M., . . . Yahaya, A. N. A. (2021). Influence of fresh palm fruit sterilization in the production of carotenoid-rich virgin palm oil. *Foods, 10*(11), 2838. https://doi.org/10.3390/foods10112838

Hawksworth, D. L. (2012). Global species numbers of fungi: Are tropical studies and molecular approaches contributing to a more robust estimate?. *Biodiversity and Conservation*, *21*(9), 2425–2433. https://doi.org/10.1007/s10531-012-0299-5

Hawksworth, D. L., & Lücking, R. (2017). Fungal diversity revisited: 2.2 to 3.8 million species. *Microbiology Spectrum*, *5*(2), 17. https://doi.org/10.1128/microbiolspec.FUNK-0052-2016

Hennings, P. (1902). Fungi blumenaviensis II, a cl. Alfr Möller lecti. *Hedwigia, 41*, 1–33.

Heredia, G., & Mercado, A. (1998). Tropical hyphomycetes of Mexico. III. Some species from the Calakmul Biosphere Reserve, Campeche. *Mycotaxon, 68*, 137–143.

Heredia-Abarca, G., Mena Portales, J., Mercado Sierra, A., & Reyes Estebanez, M. (1997). Tropical hyphomycetes of Mexico. II. Some species from the tropical biology station “Los Tuxtlas”, Veracruz, Mexico. *Mycotaxon, 64*, 203–223.

Hernández-Hernández, J., Espino, A., Rodríguez-Rodríguez, J. M., Pérez Sierra, A., León, M., Abad-Campos, P., . . . Armengol, J. (2010). Survey of diseases caused by *Fusarium* spp. on palm trees in the Canary Islands. *Phytopathologia Mediterranea, 49*, 84–88.

Hernández-Restrepo, M., Decock, C. A., Costa, M. M., & Crous, P. W. (2022). Phylogeny and taxonomy of *Circinotrichum, Gyrothrix, Vermiculariopsiella* and other setose hyphomycetes. *Persoonia, 49*, 99–135. https://doi.org/10.3767/persoonia.2022.49.04

Hernández-Restrepo, M., Gené, J., Castañeda-Ruiz, R. F., Mena-Portales, J., Crous, P. W., & Guarro, J. (2017). Phylogeny of saprobic microfungi from Southern Europe. *Studies in Mycology, 86*, 53–97. https://doi.org/10.1016/j.simyco.2017.05.001

Hernández-Restrepo, M., Giraldo, A., Van Doorn, R., Wingfield, M. J., Groenewald, J. Z., Barreto, R. W., . . . Crous, P. W. (2020). The genera of fungi–G6: *Arthrographis, Kramasamuha, Melnikomyces, Thysanorea*, and *Verruconis. Fungal Systematics and Evolution, 6*, 1–24. https://doi.org/10.3114/fuse.2020.06.01

Hidayat, I., Meeboon, J., & To-anun, C. (2007). *Anthostomella* and *Fasciatispora* species (Xylariaceae) from palms including *Fasciatispora ujungkulonensis* sp. nov. *Mycotaxon, 102*, 347–354.

Hilbe, J. M. (2011). *Negative binomial regression*. Cambridge University Press. https://doi.org/10.1017/CBO9780511973420

Hirayama, K., & Tanaka, K. (2011). Taxonomic revision of *Lophiostoma* and *Lophiotrema* based on reevaluation of morphological characters and molecular analyses. *Mycoscience*, *52*(6), 401–412. https://doi.org/10.1007/s10267-011-0114-8

Ho, M. H. M., Castañeda, R. F., Dugan, F. M., & Jong, S. C. (1999). *Cladosporium* and *Cladophialophora* in culture: Descriptions and an expanded key. *Mycotaxon, 72*, 115–157.

Ho, W. H., Yanna, Hyde, K. D., & Goh, T. K. (2005). *Endosporoideus* gen. nov., a mitosporic fungus on *Phoenix hanceana. Mycologia*, *97*(1), 238–245. https://doi.org/10.1080/15572536.2006.11832867

Hoang, D. T., Chernomor, O., Von Haeseler, A., Minh, B. Q., & Vinh, L. S. (2018). UFBoot2: Improving the ultrafast bootstrap approximation. *Molecular Biology and Evolution, 35*(2), 518–522.

Höhnel, F. von. (1909). Fragmente zur Mykologie. (VI. Mitteilung, Nr. 182 bis 288). *Sitzungsberichte der Kaiserlichen Akademie der Wissenschaften, Mathematisch-Naturwissenschaftliche Klasse, Abteilung I, 118*(4), 275–452.

Holubová-Jechová, V. (1987). Studies on hyphomycetes from Cuba V. Six new species of dematiaceous hyphomycetes from Havana Province. *Česká Mykologie, 41*(1), 29–36.

Hongsanan, S., Hyde, K. D., Phookamsak, R., Wanasinghe, D. N., McKenzie, E. H. C., Sarma, V. V., . . . Xie, N. (2020a). Refined families of Dothideomycetes: Dothideomycetidae and Pleosporomycetidae. *Mycosphere, 11*, 1553–2107. https://doi.org/10.5943/mycosphere/11/1/13

Hu, H. H., & Cheng, W. C. (1948). On the new family Metasequoiaceae and on *Metasequoia glyptostroboides*, a living species of the genus *Metasequoia* found in Szechuan and Hupeh. *Bulletin of the Fan Memorial Institute of Biology, New Series, 1*, 153–163.

Hu, H., Jeewon, R., Zhou, D., Zhou, T., & Hyde, K. D. (2007). Phylogenetic diversity of endophytic *Pestalotiopsis* species in *Pinus armandii* and *Ribes* spp.: Evidence from rDNA and β-tubulin gene phylogenies. *Fungal Diversity, 24*, 1–22.

Hu, S. Y. (1980). The Metasquoia flora and its phytogeographic significance. *Journal of the Arnold Arboretum, 61*, 41–94.

Hu, Y. F., Liu, J. W., Luo, X. X., Xu, Z. H., Xia, J. W., Zhang, X. G., . . . Ma, J. (2023). Multi-locus phylogenetic analyses reveal eight novel species of *Distoseptispora* from southern China. *Microbiology Spectrum, 11*, e02468–e02423. https://doi.org/10.1128/spectrum.02468-23

Huanaluek, N., Jayawardena, R. S., Maharachchikumbura, S. S. N., & Harishchandra, D. (2021). Additions to pestalotioid fungi in Thailand: *Neopestalotiopsis hydeana* sp. nov. and *Pestalotiopsis hydei* sp. nov. *Phytotaxa, 479*, 23–43.

Huelsenbeck, J. P., & Ronquist, F. (2001). MrBayes: Bayesian inference of phylogeny. *Bioinformatics, 17*, 754–755.

Hughes, S. J. (1951). Studies on micro-fungi. III. *Mastigosporium, Camposporium,* and *Ceratophorum. Mycological Papers, 36*, 1–43.

Hughes, S. J. (1953). Fungi from the Gold Coast. II. *Mycological Papers, 50*, 1–104.

Hughes, S. J. (1978). New Zealand fungi. 25. Miscellaneous species. *New Zealand Journal of Botany, 16*, 311–370.

Huson, D. H., & Bryant, D. (2006). Application of phylogenetic networks in evolutionary studies. *Molecular Biology and Evolution, 23*, 254–267. https://doi.org/10.1093/molbev/msj030

Hyde, K. D. (1991). A new amphisphaeriaceous fungus from intertidal fronds of Nypa fruticans. *Transactions of the Mycological Society of Japan, 32*, 265–271.

Hyde, K. D. (1992). Fungi from palms. I. The genus Linocarpon, a revision. *Sydowia, 44*, 32–54.

Hyde, K. D. (1995). Fungi from palms XVII. The genus Fasciatispora, with notes on Amphisphaerella. *Nova Hedwigia, 61*, 249–268.

Hyde, K. D. (1995). Measuring biodiversity of microfungi in the wet tropics of North Queensland. In T. J. B. Boyle & B. Boontawee (Eds.), *Measuring and monitoring biodiversity of tropical and temperate forests: Proceedings of a workshop, Chiang Mai, Thailand* (pp. 271–286). CIFOR.

Hyde, K. D. (1996a). Fungi from palms XXVI. The genus Anthostomella, with ten new species. *Nova Hedwigia, 62*, 273–340.

Hyde, K. D. (1996b). Biodiversity of microfungi in North Queensland. *Australian Systematic Botany, 9*, 261–271.

Hyde, K. D. (1997). Diversity of ascomycetes on palms in the tropics. In K. D. Hyde (Ed.), *Biodiversity of tropical microfungi* (pp. 141–156). Hong Kong University Press.

Hyde, K. D. (1999a). *Byssosphaeria, Chaetosphaeria, Niesslia* and *Ornatispora* gen. nov. from palms. *Mycological Research, 103*, 1423–1439.

Hyde, K. D. (2001). Non-lichenised Australian ascomycetes. *Australian Systematic Botany, 14*, 357–375.

Hyde, K. D., & Cannon, P. F. (1999). Fungi causing tar spots on palms. *Mycological Papers, 175*, 1–114.

Hyde, K. D., Bao, D. F., Hongsanan, S., Chethana, K. W. T., Yang, J., & Suwannarach, N. (2021). Evolution of freshwater Diaporthomycetidae (Sordariomycetes) provides evidence for five new orders and six new families. *Fungal Diversity, 107*, 71–105. https://doi.org/10.1007/s13225-021-00469-7

Hyde, K. D., Chaiwan, N., Norphanphoun, C., Boonmee, S., Camporesi, E., Chethana, K. W. T., . . . Zhao, Q. (2018). Mycosphere notes 169–224. *Mycosphere, 9*, 271–430.

Hyde, K. D., de Silva, N. I., Jeewon, R., Bhat, D. J., Phookamsak, R., Doilom, M., . . . Bulgakov, T. S. (2020b). AJOM new records and collections of fungi: 1–100. Asian Journal of Mycology, 3(1), 22–294. https://doi.org/10.5943/ajom/3/1/3

Hyde, K. D., Dong, Y., Phookamsak, R., Jeewon, R., Bhat, D. J., Gareth Jones, E. B., . . . Sheng, J. (2020). Fungal diversity notes 1151–1276: Taxonomic and phylogenetic contributions on genera and species of fungal taxa. *Fungal Diversity*, *100*, 5–277. https://doi.org/10.1007/s13225-020-00439-5

Hyde, K. D., Fröhlich, J. (2003). *Nigramammilla calami* gen. et sp. nov. and *Arecomyces calami, A. licualae and Pseudohalonectria palmae* spp. nov. from palms. *Cryptogamie Mycologie, 24*, 13–20.

Hyde, K. D., Fröhlich, J., & Taylor, J. E. (1997). Diversity of ascomycetes on palms in the tropics. In K. D. Hyde (Ed.), *Biodiversity of tropical microfungi* (pp. 141–156). Hong Kong University Press.

Hyde, K. D., Goh, T. K., Taylor, J. E., & Fröhlich, J. (1999). *Byssosphaeria, Chaetosphaeria, Niesslia* and *Ornatispora* gen. nov. from palms. *Mycological Research*, *103*(11), 1423–1439. https://doi.org/10.1017/S0953756299008679

Hyde, K. D., Hongsanan, S., Jeewon, R., Bhat, D. J., McKenzie, E. H. C., Jones, E. B. G., … Zhu, L. (2016). Fungal diversity notes 367–490: Taxonomic and phylogenetic contributions to fungal taxa. *Fungal Diversity, 80*, 1–270. https://doi.org/10.1007/s13225-016-0373-x

Hyde, K. D., Jeewon, R., Chen, Y. J., Bhunjun, C. S., Calabon, M. S., Jiang, H. B., . . . Lumyong, S. (2020). The numbers of fungi: Is the descriptive curve flattening?. *Fungal Diversity, 103*, 219–271. https://doi.org/10.1007/s13225-020-00458-2

Hyde, K. D., Jones, E. G., Liu, J. K., Ariyawansa, H., Boehm, E., Boonmee, S., . . . Zhang, M. (2013). Families of Dothideomycetes. *Fungal Diversity, 63*, 1–313. https://doi.org/10.1007/s13225-013-0263-4

Hyde, K. D., Noorabadi, M. T., Thiyagaraja, V., He, M. Q., Johnston, P. R., Wijesinghe, S. N., . . . Zvyagina, E. (2024). The 2024 outline of fungi and fungus-like taxa. *Mycosphere, 15*(1), 5146–6239. https://doi.org/10.5943/mycosphere/15/1/25

Hyde, K. D., Norphanphoun, C., Abreu, V. P., Bazzicalupo, A., Chethana, K. W. T., Clericuzio, M., . . . Mortimer, P. E. (2017). Fungal diversity notes 603–708: Taxonomic and phylogenetic notes on genera and species. *Fungal Diversity, 87*(1), 1–235. https://doi.org/10.1007/s13225-017-0391-3

Hyde, K. D., Norphanphoun, C., Maharachchikumbura, S. S. N., Bhat, D. J., Jones, E. B. G., Bundhun, D., . . . Xiang, M. M. (2020d). Refined families of Sordariomycetes. *Mycosphere, 11*(1), 305–1059. https://doi.org/10.5943/mycosphere/11/1/7

Hyde, K. D., Norphanphoun, C., Maharachchikumbura, S. S. N., Bhat, D. J., Jones, E. B. G., Bundhun, D., … Xiang, M. M. (2020a). Refined families of sordariomycetes. *Mycosphere, 11*(1), 305–1059. https://doi.org/10.5943/mycosphere/11/1/7

Hyde, K. D., Saleh, A., Aumentado, H. D. R., Boekhout, T., Bera, I., Khyaju, S., . . . Wanasinghe, D. N. (2024a). Fungal numbers: Global needs for a realistic assessment. *Fungal Diversity, 128*, 191–225. https://doi.org/10.1007/s13225-024-00545-8

Hyde, K. D., Suwannarach, N., Jayawardena, R. S., Manawasinghe, I. S., Liao, C. F., Doilom, M., . . . Bao, D. F. (2021). Mycosphere notes 325–344 – Novel species and records of fungal taxa from around the world. *Mycosphere, 12*(1), 1101–1156. https://doi.org/10.5943/mycosphere/12/1/14

Hyde, K. D., Taylor, J. E., & Fröhlich, J. (2000). Genera of ascomycetes from palms. *Fungal Diversity Research Series, 2*, 1–247.

Hyde, K. D., Tennakoon, D. S., Jeewon, R., Bhat, D. J., Maharachchikumbura, S. S. N., Rossi, W., . . . Xu, J. C. (2019). Fungal diversity notes 1036–1150: Taxonomic and phylogenetic contributions on genera and species of fungal taxa. *Fungal Diversity, 96*, 1–242. https://doi.org/10.1007/s13225-019-00429-2

Hyde, K. D., Wijesinghe, S. N., Afshari, N., Aumentado, H. D., Bhunjun, C. S., Boonmee, S., . . . Zhang, J. Y. (2024). Mycosphere notes 469–520. *Mycosphere, 15*(1), 1294–1454. https://doi.org/10.5943/mycosphere/15/1/11

Hyde, K. D., Wijesinghe, S. N., Amuhenage, T. B., Bera, I., Bhunjun, C. S., Chethana, K. W. T., . . . Zhao, H. J. (2024). Current research in applied and environmental mycology fungal profiles 1–30. *Current Research in Environmental & Applied Mycology (Journal of Fungal Biology), 14*(1), 167–266. https://doi.org/10.5943/cream/14/1/11

Ichinoe, M. (1971). Camposporium species from Japan. *Transactions of the Mycological Society of Japan, 12*, 79–88.

Index Fungorum. (2024). *Index Fungorum*. http://www.indexfungorum.org/Names/Names.asp

Ishii, T., Nonaka, K., Iwatsuki, M., Masuma, R., Ōmura, S., & Shiomi, K. (2012). Virgaricin produced by Virgaria sp. FKI-4860. *The Journal of Antibiotics, 65*(3), 139–141. https://doi.org/10.1038/ja.2011.123

Ismail, S. I., Zulperi, D., Norddin, S., & Ahmad-Hamdani, S. (2017). First report of *Neopestalotiopsis saprophytica* causing leaf spot of oil palm (*Elaeis guineensis*) in Malaysia. *Plant Disease, 101*(10), 1821–1822. https://doi.org/10.1094/pdis-02-17-0271-pdn

Jackson, G. V. H., & McKenzie, E. H. C. (1988). *Marasmiellus cocophilus* on coconuts in Solomon Islands. *FAO Plant Protection Bulletin, 36*, 91–97.

Jaklitsch, W. M., Fournier, J., & Voglmayr, H. (2018). Two unusual new species of Pleosporales: *Anteaglonium rubescens* and *Atrocalyx asturiensis. Sydowia, 70*, 129–140.

Jaklitsch, W. M., Gardiennet, A., & Voglmayr, H. (2016). Resolution of morphology-based taxonomic delusions: *Acrocordiella, Basiseptospora, Blogiascospora, Clypeosphaeria, Hymenopleella, Lepteutypa, Pseudapiospora, Requienella, Seiridium*, and *Strickeria. Persoonia, 37*(1), 82–105.

Jaklitsch, W. M., Olariaga, I., & Voglmayr, H. (2016). *Teichospora* and the Teichosporaceae. *Mycological Progress, 15*, 1–20. https://doi.org/10.1007/s11557-016-1171-2

Jami, F., Marincowitz, S., Slippers, B., & Wingfield, M. (2018). New Botryosphaeriales on native red milkwood (*Mimusops caffra*). *Australasian Plant Pathology, 47*, 475–484. https://doi.org/10.1007/s13313-018-0586-4

Jamilah, I. Y. (2018). Collection and identification of exopolysaccharide producing endophytic fungi from leaf midribs of oil palm. *Journal of Physics: Conference Series, 1116*, 052080. https://doi.org/10.1088/1742-6596/1116/5/052080

Jamilah, I., Hartanto, A., & Lutfia, A. (2021). Screening of endophytic fungi from oil palm (*Elaeis guineensis*) in producing exopolysaccharides. *Biodiversitas, 22*, 1467–1473. https://doi.org/10.13057/biodiv/d220350

Jayasiri, S. C., Hyde, K. D., Ariyawansa, H. A., Bhat, J., Buyck, B., Cai, L., . . . Promputtha, I. (2015). The faces of fungi database: Fungal names linked with morphology, phylogeny and human impacts. *Fungal Diversity, 74*(1), 3–18. https://doi.org/10.1007/s13225-015-0351-8

Jayasiri, S. C., Hyde, K. D., Ariyawansa, H. A., Bhat, J., Buyck, B., Cai, L., . . . Promputtha, I. (2015). The faces of fungi database: Fungal names linked with morphology, phylogeny and human impacts. *Fungal Divers, 74*, 3–18.

Jayasiri, S. C., Hyde, K. D., Jones, E. B. G., & Lu, Y. Z. (2017). *Neohelicosporium fusisporum* sp. nov. (Tubeufiaceae) and a first record of a sexual morph within *Neohelicosporium. Studies in Fungi, 2*(1), 210–217. https://doi.org/10.5943/sif/2/1/24

Jayasiri, S. C., Hyde, K. D., Jones, E. B. G., Peršoh, D., Camporesi, E., & Kang, J. C. (2018). Taxonomic novelties of hysteriform Dothideomycetes. *Mycosphere, 9*(4), 803–837. https://doi.org/10.5943/mycosphere/9/4/8

Jayasiri, S. C., Jones, E. B. G., Kang, J. C., Promputtha, I., Bahkali, A. H., & Hyde, K. D. (2016). A new species of genus *Anteaglonium* (Anteagloniaceae, Pleosporales) with its asexual morph. *Phytotaxa, 263*, 233–244. https://doi.org/10.11646/phytotaxa.263.3.4

Jayawardena, R. S., Hyde, K. D., Chethana, K. W. T., Dissanayake, A. J., Goonasekara, I. D., Manawasinghe, I. S., . . . Yan, J. Y. (2018). Mycosphere notes 102–168: Saprotrophic fungi on Vitis in China, Italy, Russia and Thailand. *Mycosphere, 9*(1), 1–114. https://doi.org/10.5943/mycosphere/9/1/1

Jayawardena, R. S., Hyde, K. D., de Farias, A. R. G., Bhunjun, C. S., Ferdinandez, H. S., Manamgoda, D. S., . . . Thines, M. (2021). What is a species in fungal plant pathogens?. *Fungal Diversity, 109*(1), 239–266. https://doi.org/10.1007/s13225-021-00484-8

Jayawardena, R. S., Hyde, K. D., Wang, S., Sun, Y. R., Suwannarach, N., Sysouphanthong, P., . . . Wang, Y. (2023). Fungal diversity notes 1512–1610: Taxonomic and phylogenetic contributions on genera and species of fungal taxa. *Fungal Diversity*, *117*, 1–272. https://doi.org/10.1007/s13225-022-00513-0

Jayawardena, R. S., Liu, M., Maharachchikumbura, S. S. N., Zhang, W., Xing, Q. K., Hyde, K. D., . . . Yan, J. Y. (2016). *Neopestalotiopsis vitis* sp. nov. causing grapevine leaf spot in China. *Phytotaxa*, *258*(1), 63–74.

Jiang, N., Bonthond, G., Fan, X. L., & Tian, C. M. (2018). *Neopestalotiopsis rosicola* sp. nov. causing stem canker of Rosa *chinensis* in China. *Mycotaxon, 133*(2), 271–283.

Jiang, N., Fan, X., & Tian, C. (2021). Identification and characterization of leaf-inhabiting fungi from *Castanea* plantations in China. *Journal of Fungi*, *7*(1), 64. https://doi.org/10.3390/jof7010064

Johnston, P. R. (2022). New *Rhizodiscina* and saprobic *Sclerococcum* species from Aotearoa New Zealand. *Index Fungorum, 519*, 1–6.

Kalyaanamoorthy, S., Minh, B. Q., Wong, T. K. F., von Haeseler, A., & Jermiin, L. S. (2017). ModelFinder: Fast model selection for accurate phylogenetic estimates. *Nature Methods*, *14*(6), 587–589.

Karimi, O., Chethana, K. W. T., de Farias, A. R., Asghari, R., Kaewchai, S., Hyde, K. D., & Li, Q. (2024). Morphology and multigene phylogeny reveal three new species of *Distoseptispora* (Distoseptisporales, Distoseptisporaceae) on palms (Arecaceae) from peatswamp areas in southern Thailand. *MycoKeys, 102*, 55.

Katoh, K., & Standley, D. M. (2013). MAFFT multiple sequence alignment software version 7: improvements in performance and usability. *Molecular Biology and Evolution, 30*(4), 772–780.

Kiffer, E., & Morelet, M. (2000). *The deuteromycetes, mitosporic fungi, classification and generic keys*. Science Publishers.

Kirk, P. M. (1982). New or interesting microfungi VI. *Sporidesmiella* gen. nov. (hyphomycetes). *Transactions of the British Mycological Society, 79*, 479–489.

Kirk, P. M. (1983). New or interesting microfungi X. Hyphomycetes on *Laurus nobilis* leaf litter. *Mycotaxon, 18*, 259–298.

Kirk, P. M., Cannon, P. F., David, J. C., & Stalpers, J. A. (2001). *Ainsworth and Bisby's dictionary of the fungi* (9th ed.). CABI.

Kirk, P. M., Cannon, P. F., Minter, D. W., & Stalpers, J. A. (2008). *Dictionary of the fungi* (10th ed.). CABI.

Kirschner, R., & Hsieh, S. Y. (2023). *Xylolentia simplex*, a hyphomycete from dead petioles of the fern *Angiopteris lygodiifolia* in Taiwan. *Fungal Science, 38*(1), 13–21.

Kirsop, B. E., & Doyle, A. (1991). *Maintenance of microorganisms and cultured cells, a manual of laboratory methods* (2nd ed.). Academic Press.

Klaubauf, S., Tharreau, D., Fournier, E., Groenewald, J. Z., Crous, P. W., de Vries, R. P., . . . Lebrun, M. H. (2014). Resolving the polyphyletic nature of *Pyricularia* (Pyriculariaceae). *Studies in Mycology, 79*, 85–120.

Klotz, L. J., & Fawcett, H. S. (1932). Black scorch of the date palm caused by *Thielaviopsis paradoxa*. *Journal of Agricultural Research, 44*, 155–166.

Kodsueb, R., Jeewon, R., Vijaykrishna, D., McKenzie, E. H. C., Lumyong, P., Lumyong, S., . . . Hyde, K. D. (2006). Systematic revision of Tubeufiaceae based on morphological and molecular data. *Fungal Diversity, 21*, 105–130.

Kohlmeyer, J., Volkmann-Kohlmeyer, B., & Eriksson, O. E. (1996). Fungi on *Juncus roemerianus*. 8. New bitunicate ascomycetes. *Canadian Journal of Botany, 74*, 1830–1840.

Konta, S., Hongsanan, S., Phillips, A. J. L., Jones, E. B. G., Boonmee, S., & Hyde, K. D. (2016). Botryosphaeriaceae from palms in Thailand II: two new species of *Neodeightonia*, *N. rattanica* and *N. rattanicola* from *Calamus* (rattan palm). *Mycosphere, 7*(7), 950–961.

Konta, S., Hongsanan, S., Tibpromma, S., Thongbai, B., Maharachchikumbura, S. S. N., Bahkali, A. H., . . . Boonmee, S. (2016). An advance in the endophyte story: Oxydothidaceae fam. nov. with six new species of *Oxydothis*. *Mycosphere, 7*, 1425–1446.

Konta, S., Hyde, K. D., Eungwanichayapant, P. D., Tennakoon, D. S., Bahkali, A. H., Elgorban, A. M., . . . Boonmee, S. (2020). *Fissuroma* (Aigialaceae, Pleosporales) appears to be hyperdiverse on Arecaceae; evidence from two new species from southern Thailand. *Acta Botanica Brasilica, 34*(2), 384–393.

Konta, S., Tibpromma, S., Karunarathna, S. C., Samarakoon, M. C., Steven, L. S., Mapook, A., . . . Hyde, K. D. (2023). Morphology and multigene phylogeny reveal ten novel taxa in Ascomycota from terrestrial palm substrates (Arecaceae) in Thailand. *Mycosphere, 14*(1), 107–152.

Koukol, O. (2010). Revision of *Septonema ochraceum* revealed three new species of Venturiaceae and Herpotrichiellaceae. *Mycological Progress, 9*(3), 369–378.

Koukol, O., & Delgado, G. (2021). Why morphology matters: the negative consequences of hasty descriptions of putative novelties in asexual ascomycetes. *IMA Fungus, 12*, 26.

Koukol, O., Delgado, G., Hofmann, T. A., & Piepenbring, M. (2018). Panama, a hot spot for Hermatomyces (Hermatomycetaceae, Pleosporales) with five new species, and a critical synopsis of the genus. *IMA Fungus, 9*, 107–141.

Kühl, H. S., Bowler, D. E., Bösch, L., Bruelheide, H., Dauber, J., & Eichenberg, D. (2020). Effective biodiversity monitoring needs a culture of integration. *One Earth, 3*(4), 462–474.

Kularathnage, N. D., Senanayake, I. C., de Hoog, S., Quan, Y., Jayawardena, R. S., Hyde, K. D., . . . Qi, Z. (2025). Systematics and physiology of *Cladophialophora matsushimae* (Chaetothyriales) associated with ant carton and five new combinations in *Cladophialophora* and *Epibryon. New Zealand Journal of Botany, 63*(5), 2138-2159. https://doi.org/10.1080/0028825X.2025.2479092

Kularathnage, N. D., Wanasinghe, D. N., Senanayake, I. C., Yang, Y., Manawasinghe, I. S., Phillips, A. J. L., . . . Song, J. (2022). Microfungi associated with ornamental palms: *Byssosphaeria phoenicis* sp. nov. (Melanommataceae) and *Pseudocoleophoma rhapidis* sp. nov. (Dictyosporiaceae) from south China. *Phytotaxa, 568*(2), 149–169.

Kumar, V., Cheewangkoon, R., Gentekaki, E., Maharachchikumbura, S. S. N., Brahmanage, R. S., & Hyde, K. D. (2019). *Neopestalotiopsis alpapicalis* sp. nov., a new endophyte from tropical mangrove trees in Krabi Province Thailand. *Phytotaxa, 393*(3), 251–262.

Kunze, G., & Schmidt, J. C. (1817). *Mycologische Hefte, 1*, i–xvi, 1–109.

Lan, C. Z., Dai, Y. L., Gan, L., Yao, J. A., & Yang, X. J. (2020). First report of *Fusarium oxysporum* f. sp. *canariensis* causing Fusarium wilt on Canary Island date palm (*Phoenix canariensis* Hort. ex Chabaud) in China. *Journal of Plant Pathology, 102*(2), 569–570.

Larsson, A. (2014). AliView: A fast and lightweight alignment viewer and editor for large datasets. *Bioinformatics, 30*(22), 3276–3278. https://doi.org/10.1093/bioinformatics/btu531

Lee, S., & Crous, P. W. (2003). New species of Anthostomella on fynbos, with a key to the genus in South Africa. *Mycological Research, 107*(3), 360–370. https://doi.org/10.1017/S0953756203007184

Leuchtmann, A. (1985). Kulturversuche mit einigen Arten der Gattung *Lophiostoma Ces.* & De Not. *Sydowia, 38*, 158–170.

Levis, C., Costa, F. R. C., Bongers, F., Peña-Claros, M., Clement, C. R., Junqueira, A. B., . . . Steege, H. T. (2017). Persistent effects of pre-Columbian plant domestication on Amazonian forest composition. *Science, 355*(6328), 925–931. https://doi.org/10.1126/science.aal0157

Li, C. J. Y., Chethana, K. W. T., Lu, Z. Y., & Zhao, Q. (2022). Two novel species of Lachnaceae (Helotiales, Leotiomycetes) from southwestern China. *Creative Microbiology Research, 12*(1), 20. https://doi.org/10.5943/cream/12/1/20

Li, D. W., Schultes, N. P., Chen, J. Y., & Wang, Y. X. (2017). Circinotrichum sinense, a new asexual fungus from Hubei, China. *Botany, 95*(12), 1099–1108. https://doi.org/10.1139/cjb-2017-0132

Li, G., Wu, W., Lu, L., Chen, B., & Chen, S. (2023). Characterization of *Pseudofusicoccum* species from diseased plantation-grown *Acacia mangium, Eucalyptus* spp., and *Pinus massoniana* in southern China. *Pathogens, 12*(4), 574. https://doi.org/10.3390/pathogens12040574

Li, L. L., Shen, H. W., Bao, D. F., Wanasinghe, D. N., Lu, Y. Z., Feng, Y., . . . Luo, Z. L. (2022). The plethora of Tubeufiaceae in lakes of the northwestern Yunnan plateau, China. *Frontiers in Microbiology, 13*, 1056669. https://doi.org/10.3389/fmicb.2022.1056669

Li, L., Pan, H., Chen, M. Y., & Zhong, C. H. (2016). First report of Pestalotiopsis microspora causing postharvest rot of kiwifruit in Hubei Province, China. *Plant Disease, 100*(10), 2161.

Li, L., Yang, Q., & Li, H. (2021). Morphology, phylogeny, and pathogenicity of pestalotioid species on Camellia oleifera in China. *Journal of Fungi, 7*(12), 1080. https://doi.org/10.3390/jof7121080

Li, Q. R., Habib, K., Long, S. H., Wu, Y. P., Zhang, X., Hu, H. M., . . . Kang, J. C. (2024). Unveiling fungal diversity in China: New species and records within the Xylariaceae family. *Mycosphere, 15*(1), 275–364. https://doi.org/10.5943/mycosphere/15/1/2

Li, W. J., McKenzie, E. H., Liu, J. K., Bhat, D. J., Dai, D. Q., Camporesi, E., . . . Zhang, J. F. (2020). Taxonomy and phylogeny of hyaline-spored coelomycetes. *Fungal Diversity, 100*, 279–801. https://doi.org/10.1007/s13225-020-00440-y

Li, W. L., Liang, R. R., Dissanayake, A. J., & Liu, J. K. (2023). Botryosphaerialean fungi associated with woody oil plants cultivated in Sichuan Province, China. *MycoKeys, 97*, 71–116. https://doi.org/10.3897/mycokeys.97.103118

Li, W. L., Liang, R. R., Dissanayake, A. J., & Liu, J. K. (2023). Mycosphere notes 413–448: Dothideomycetes associated with woody oil plants in China. *Mycosphere, 14*(1), 1436–1529. https://doi.org/10.5943/mycosphere/14/1/16

Liang, J., Li, G., Zhou, S., Zhao, M., & Cai, L. (2019). Myrothecium-like new species from turfgrasses and associated rhizosphere. *MycoKeys, 51*, 29. https://doi.org/10.3897/mycokeys.51.31957

Liao, C. F., Yang, Y. H., Dong, W., Tangtrakulwanich, K., Zhang, Y. X., Khan, S., . . . Doilom, M. (2024). *Tetraploa wurfbainiae* sp. nov. (Tetraplosphaeriaceae, Pleosporales) isolated from *Wurfbainia villosa* in Guangdong, China. *New Zealand Journal of Botany, 62*(2-3), 303-316. https://doi.org/10.1080/0028825X.2024.2311964

Ligoxigakis, E. K., Markakis, E. A., Papaioannou, I. A., & Typas, M. A. (2013). First report of palm rot of *Phoenix* spp. caused by *Neodeightonia phoenicum* in Greece. *Plant Disease, 97*(2), 286. https://www.researchgate.net/publication/263040162

Lin, C. G., McKenzie, E. H. C., Bhat, D. J., Liu, J. K., Hyde, K. D., & Lumyong, S. (2018). *Pseudodactylaria brevis* sp. nov. from Thailand confirms the status of Pseudodactylariaceae. *Phytotaxa, 369*(4), 241–250. https://doi.org/10.11646/phytotaxa.369.4.1

Lin, L., Bai, Y. K., Pan, M., Tian, C. M., & Fan, X. L. (2023). Morphology and molecular analyses reveal three new species of Botryosphaeriales isolated from diseased plant branches in China. *MycoKeys, 97*, 1–19. https://doi.org/10.3897/mycokeys.97.102653

Lin, L., Fan, X. L., Groenewald, J. Z., Jami, F., Wingfield, M. J., Voglmayr, H., . . . Crous, P. W. (2024). Cytospora: An important genus of canker pathogens. *Studies in Mycology, 109*, 323–401. https://doi.org/10.3114/sim.2024.109.05

Linder, D. H. (1929). A monograph of the helicosporous fungi imperfecti. *Annals of the Missouri Botanical Garden, 16*(3), 22–388. https://doi.org/10.2307/2394038

Link, H. F. (1809). Observationes in ordines plantarum naturales. Dissertatio prima complectens Anandrarum ordines Epiphytas, Mucedines, Gastromycos et Fungos. *Magazin der Gesellschaft Naturforschender Freunde zu Berlin, 3*(1), 3–42.

Liu, F., Bonthond, G., Groenewald, J. Z., Cai, L., & Crous, P. W. (2019). Sporocadaceae, a family of coelomycetous fungi with appendage-bearing conidia. *Studies in Mycology, 92*, 287–415. https://doi.org/10.1016/j.simyco.2018.11.001

Liu, F., Hou, L., Raza, M., & Cai, L. (2017). Pestalotiopsis and allied genera from Camellia, with description of 11 new species from China. *Scientific Reports, 7*(1), 866. https://doi.org/10.1038/s41598-017-00972-5

Liu, F., Hu, D. M., & Cai, L. (2012). *Conlarium duplumascospora* gen. et sp. nov. and *Jobellisia guangdongensis* sp. nov. from freshwater habitats in China. *Mycologia, 104*(5), 1178–1186. https://doi.org/10.3852/11-379

Liu, F., Wang, J., Li, H., Wang, W., & Cai, L. (2019). *Setophoma* spp. on *Camellia sinensis*. *Fungal Systematics and Evolution, 15*(4), 43–57. https://doi.org/10.3114/fuse.2019.04.05

Liu, J. K., Chomnunti, P., Cai, L., Phookamsak, R., Chukeatirote, E., Jones, E. B. G., . . . Hyde, K. D. (2010). Phylogeny and morphology of *Neodeightonia palmicola* sp. nov. from palms. *Sydowia, 62*, 261–276.

Liu, J. K., Hyde, K. D., Jeewon, R., Phillips, A. J., Maharachchikumbura, S. S., Ryberg, M., . . . Zhao, Q. (2017). Ranking higher taxa using divergence times: A case study in Dothideomycetes. *Fungal Diversity, 84*, 75–99. https://doi.org/10.1007/s13225-017-0385-1

Liu, J. K., Hyde, K. D., Jones, E. B. G., Ariyawansa, H. A., Bhat, D. J., Boonmee, S., . . . Camporesi, E. (2015). Fungal diversity notes 1–110: Taxonomic and phylogenetic contributions to fungal species. *Fungal Diversity, 72*, 1–197.

Liu, J. K., Lu, Y. Z., Cheewangkoon, R., & To-Anun, C. (2018). Phylogeny and morphology of *Helicotubeufa* gen. nov., with three new species in Tubeufiaceae from aquatic habitats. *Mycosphere, 9*(3), 495–509.

Liu, J. K., Phookamsak, R., Doilom, M., Wikee, S., Li, Y. M., Ariyawansha, H., . . . Hyde, K. D. (2012). Towards a natural classification of Botryosphaeriales. *Fungal Diversity, 57*, 149–210.

Liu, J. K., Phookamsak, R., Doilom, M., Wikee, S., Li, Y. M., Ariyawansha, H. A., . . . Hyde, K. D. (2012). Towards a natural classification of Botryosphaeriales. *Fungal Diversity, 57*, 149–210.

Liu, J. K., Phookamsak, R., Jones, E. B. G., Zhang, Y., Ko-Ko, T. W., Hu, H. L., . . . Hyde, K. D. (2011). Astrosphaeriella is polyphyletic, with species in *Fissuroma* gen. nov. and *Neoastrosphaeriella* gen. nov. *Fungal Diversity, 51*, 135–154.

Liu, L. L., Yang, J., Liu, N. G., Chen, Y. Y., Gui, X. X., & Liu, Z. Y. (2019). *Sporidesmium guizhouense* sp. nov. (Sordariomycetes incertae sedis), a new species from a freshwater habitat in Guizhou Province, China. *Phytotaxa, 422*(2), 144–156.

Liu, N. G., Hyde, K. D., Bhat, D. J., Jumpathong, J., & Liu, J. K. (2019). Morphological and phylogenetic studies of *Pleopunctum* gen. nov. (Phaeoseptaceae, Pleosporales) from China. *Mycosphere, 10*(1), 757–775.

Liu, N. G., Hyde, K. D., Sun, Y. R., Bhat, D. J., Jones, E. B. G., Jumpathong, J. J., . . . Liu, J. K. (2024). Notes, outline, taxonomy and phylogeny of brown-spored hyphomycetes. *Fungal Diversity, 129*, 1–281.

Liu, N. G., Lu, Y. Z., Bhat, D. J., McKenzie, E. H. C., Lumyong, S., Jumpathong, J., . . . Liu, J. K. (2019). *Kevinhydea brevistipitata* gen. et sp. nov. and *Helicoma hydei* sp. nov. (Tubeufiaceae) from decaying wood habitats. *Mycological Progress, 18*, 671–682.

Liu, S. L., Wang, X. W., Li, G. J., Deng, C. Y., Rossi, W., Leonardi, M., . . . Zhou, L. W. (2024). Fungal diversity notes 1717–1817: Taxonomic and phylogenetic contributions on genera and species of fungal taxa. *Fungal Diversity, 124*, 1–216.

Liu, S. L., Zhao, P., Cai, L., Shen, S., Wei, H. W., Na, Q., . . . Zhou, L. W. (2024). Catalogue of fungi in China 1. New taxa of plant-inhabiting fungi. *Mycology, 16*, 1–58. https://doi.org/10.1080/21501203.2024.2316066

Liu, S., García-Palacios, P., Tedersoo, L., Guirado, E., van der Heijden, M. G., Wagg, C., . . . Delgado-Baquerizo, M. (2022). Phylotype diversity within soil fungal functional groups drives ecosystem stability. *Nature Ecology & Evolution, 6*, 900–909.

Liu, X., Tibpromma, S., Zhang, F., Xu, J., Kandawatte, T. C., Karunarathna, S. C., . . . Mortimer, P. E. (2021). *Neopestalotiopsis cavernicola* sp. nov. from Gem Cave in Yunnan Province, China. *Phytotaxa, 512*(1), 1–27. https://doi.org/10.11646/phytotaxa.512.1.1

Liu, Y. J., Whelen, S., & Hall, B. D. (1999). Phylogenetic relationships among ascomycetes: Evidence from an RNA polymerase II subunit. *Molecular Biology and Evolution, 16*(12), 1799–1808.

Lombard, L., Houbraken, J., Decock, C., Samson, R. A., Meijer, M., Réblová, M., . . . Crous, P. W. (2016). Generic hyper-diversity in Stachybotriaceae. *Persoonia, 36*, 156–246.

Lord, D., Park, B. J., & Model, P. G. (2012). *Negative binomial regression models and estimation methods: Probability density and likelihood functions*. Texas A&M University, Korea Transport Institute.

Lu, B. S., & Hyde, K. D. (2000). A world monograph of Anthostomella. *Fungal Diversity Research Series, 4*, 1–376.

Lu, B. S., Hyde, K. D., & Liew, E. C. Y. (2000). Eight new species of Anthostomella from South Africa. *Mycological Research, 104*(6), 742–754.

Lu, L. M., Chen, G. Q., Hu, X. R., Du, D. C., Pu, Z. X., Peng, A. T., . . . Cheng, B. P. (2015). Identification of Pestalotiopsis clavispora causing brown leaf spot on Chinese bayberry in China. *Canadian Journal of Plant Pathology, 37*(4), 397–402.

Lu, L., Karunarathna, S. C., Dai, D. Q., Jayawardena, R. S., Suwannarach, N., & Tibpromma, S. (2022) Three new species of *Nigrograna* (Dothideomycetes, Pleosporales) associated with Arabica coffee from Yunnan Province, China. *MycoKeys, 94*, 51–71.

Lu, L., Karunarathna, S. C., Dai, D. Q., Xiong, Y. R., Suwannarach, N., Stephenson, S. L., . . . Tibpromma, S. (2022). Description of four novel species in Pleosporales associated with coffee in Yunnan, China. *Journal of Fungi, 8*(11), 1113.

Lu, L., Karunarathna, S. C., Liu, Y., Elgorban, A. M., Tibpromma, S., & Jayawardena, R. S. (2024). *Pseudoconiocessia xishuangbannaensis* gen. et sp. nov. in Coniocessiaceae, Xylariales from *Coffea liberica* in China. *Phytotaxa, 641*(2), 125–137.

Lu, L., Karunarathna, S. C., Xiong, Y. R., Han, L. S., Chen, X. M., Xu, R. F., . . . Tibpromma, S. (in press). Taxonomy and systematics of micro-fungi associated with Coffea in southern China and northern Thailand. *Fungal Diversity*.

Lu, Y. H., Zhang, S. N., Du, H. Z., Cheewangkoon, R., & Liu, J. K. (2024). Additions to Crassiparies and *Neobrevicollum* (Neohendersoniaceae, Pleosporales) associated with woody hosts in Southwest China. *Phytotaxa, 636*(2), 126–138.

Lu, Y. Z., Boonmee, S., Bhat, D. J., Hyde, K. D., & Kang, J. C. (2017). Helicosporium luteosporum sp. nov. and Acanthohelicospora aurea (Tubeufiaceae, Tubeufiales) from terrestrial habitats. Phytotaxa, 319(3), 241–253.

Lu, Y. Z., Boonmee, S., Dai, D. Q., Liu, J. K., Hyde, K. D., Bhat, D. J., . . . Kang, J. C. (2017). Four new species of Tubeufia (Tubeufiaceae, Tubeufiales) from Thailand. *Mycological Progress, 16*, 403–417.

Lu, Y. Z., Boonmee, S., Liu, J. K., Hyde, K. D., Bhat, D. J., Eungwanichayapant, P. D., . . . Kang, J. C. (2017). Novel Neoacanthostigma species from aquatic habitats. Cryptogamie, Mycologie, 38, 169–190.

Lu, Y. Z., Boonmee, S., Liu, J. K., Hyde, K. D., McKenzie, E. H. C., Eungwanichayapant, P. D., . . . Kang, J. C. (2018). Multi-gene phylogenetic analyses reveals *Neohelicosporium* gen. nov. and five new species of helicosporous hyphomycetes from aquatic habitats. *Mycological Progress, 17*, 631–646.

Lu, Y. Z., Liu, J. K., Hyde, K. D., Jeewon, R., Kang, J. C., Fan, C., . . . Eungwanichayapant, P. D. (2018). A taxonomic reassessment of Tubeufiales based on multi-locus phylogeny and morphology. *Fungal Diversity, 92*, 131–344.

Lu, Y. Z., Ma, J., Xiao, X. J., Zhang, L. J., Ma, X. Y., Xiao, Y. P., . . . Kang, J. C. (2023). Two novel species and one new record of Helicoma from tropical China. *Mycosystema, 42*(1), 263–277.

Lumbsch, H. T., & Huhndorf, S. M. (2010). Outline of Ascomycota 2009. *Myconet, 14*, 1–64.

Luo, L., Chethana, K. T., Zhao, Q., Thiyagaraja, V., Al-Otibi, F., & Hyde, K. D. (2025). Unveiling fungal diversity: A novel species of Proliferodiscus (Lachnaceae, Helotiales) discovered in China. *Phytotaxa, 682*(3), 227–239. https://doi.org/10.11646/phytotaxa.682.3.3

Luo, Z. L., Bhat, D. J., Jeewon, R., Boonmee, S., Bao, D. F., Zhao, Y. C., . . . Hyde, K. D. (2017). Molecular phylogeny and morphological characterization of asexual fungi (Tubeufiaceae) from freshwater habitats in Yunnan, China. Cryptogamie, *Mycologie, 38*(1), 27–53. https://doi.org/10.7872/crym/v38.iss1.2017.27

Luo, Z. L., Hyde, K. D., Bhat, D. J., Jeewon, R., Maharachchikumbura, S. S. N., Bao, D. F., . . . Su, H. Y. (2018). Morphological and molecular taxonomy of novel species Pleurotheciaceae from freshwater habitats in Yunnan, China. *Mycological Progress, 17*, 511–530. https://doi.org/10.1007/s11557-018-1377-6

Luo, Z. L., Hyde, K. D., Liu, J. K., Bhat, D. J., Bao, D. F., Li, W. L., . . . Su, H. Y. (2018). Lignicolous freshwater fungi from China II: Novel Distoseptispora (Distoseptisporaceae) species from northwestern Yunnan Province and a suggested unified method for studying lignicolous freshwater fungi. *Mycosphere, 9*(3), 444–461. https://doi.org/10.5943/mycosphere/9/3/2

Luo, Z. L., Hyde, K. D., Liu, J. K., Maharachchikumbura, S. S. N., Jeewon, R., Bao, D. F., . . . Su, H. Y. (2019). Freshwater Sordariomycetes. *Fungal Diversity, 99*, 451–660. https://doi.org/10.1007/s13225-019-00438-1

Ma, J., Hyde, K. D., Tibpromma, S., Gomdola, D., Liu, N. G., Norphanphoun, C., . . . Lu, Y. Z. (2024). Taxonomy and systematics of lignicolous helicosporous hyphomycetes. *Fungal Diversity, 129*, 365-653. https://doi.org/10.1007/s13225-024-00544-9

Ma, J., Xiao, X. J., Liu, N. G., Boonmee, S., Xiao, Y. P., & Lu, Y. Z. (2023). Morphological and multi-gene phylogenetic analyses reveal *Pseudotubeufia* gen. nov. and two new species in Tubeufiaceae from China. *Journal of Fungi, 9*(7), 742. https://doi.org/10.3390/jof9070742

Ma, X. Y., Maharachchikumbura, S. S. N., Chen, B. W., Hyde, K. D., Mckenzie, E. H. C., Chomnunti, P., . . . Kang, J. C. (2019). Endophytic pestalotiod taxa in Dendrobium orchids. *Phytotaxa, 419*(3), 268–286. https://doi.org/10.11646/phytotaxa.419.3.2

Mack, J. N., Sproule, A., Shields, S. W., Seifert, K. A., Smith, M., & Overy, D. P. (2024). Two novel Pleosporales species isolated from the bark of Acer saccharum. *Fungal Systematics and Evolution, 13*, 1–14. https://doi.org/10.3114/fuse.2024.13.01

Maharachchikumbura, S. S. N., Chen, Y., Ariyawansa, H. A., Hyde, K. D., Haelewaters, D., Perera, R. H., . . . Stadler, M. (2021). Integrative approaches for species delimitation in Ascomycota. *Fungal Diversity, 109*(1), 155–179. https://doi.org/10.1007/s13225-021-00486-6

Maharachchikumbura, S. S. N., Chukeatirote, E., Guo, L. D., Crous, P. W., McKenzie, E. H. C., & Hyde, K. D. (2013). Pestalotiopsis species associated with Camellia sinensis (tea). *Mycotaxon, 123*(1), 47–61. https://doi.org/10.5248/123.47

Maharachchikumbura, S. S. N., Guo, L. D., Cai, L., Chukeatirote, E., Wu, W. P., Sun, X., . . . Hyde, K. D. (2012). A multi-locus backbone tree for Pestalotiopsis, with a polyphasic characterization of 14 new species. *Fungal Diversity, 56*(1), 95–129. https://doi.org/10.1007/s13225-012-0198-1

Maharachchikumbura, S. S. N., Guo, L. D., Chukeatirote, E., & Hyde, K. D. (2013). Improving the backbone tree for the genus *Pestalotiopsis*; addition of *P. steyaertii* and *P. magna* sp. nov. *Mycological Progress, 13*(3), 617–624. https://doi.org/10.1007/s11557-013-0944-0

Maharachchikumbura, S. S. N., Guo, L. D., Chukeatirote, E., McKenzie, E. H. C., & Hyde, K. D. (2013). A destructive new disease of Syzygium samarangense in Thailand caused by the new species Pestalotiopsis samarangensis. *Tropical Plant Pathology, 38*(3), 227–235. https://doi.org/10.1590/S1982-56762013005000002

Maharachchikumbura, S. S. N., Hyde, K. D., Groenewald, J. Z., Xu, J., & Crous, P. W. (2014). Pestalotiopsis revisited. *Studies in Mycology, 79*, 121–186. https://doi.org/10.1016/j.simyco.2014.09.005

Maharachchikumbura, S. S. N., Larignon, P., Hyde, K. D., Al-Sadi, A. M., & Liu, Z. Y. (2016). Characterization of *Neopestalotiopsis*, *Pestalotiopsis*, and *Truncatella* species associated with grapevine trunk diseases in France. *Phytopathologia Mediterranea, 55*(3), 380–390.

Maharachchikumbura, S. S. N., Zhang, Y. M., Wang, Y., & Hyde, K. D. (2013). *Pestalotiopsis anacardiacearum* sp. nov. (Amphisphaeriaceae) has an intricate relationship with Penicillaria jocosatrix, the mango tip borer. *Phytotaxa, 99*(2), 49–57. https://doi.org/10.11646/phytotaxa.99.2.1

Mahmoud, F. M., Krimi, Z., Maciá-Vicente, J. G., Errahmani, M. B., & López-Llorca, L. V. (2017). Endophytic fungi associated with roots of date palm (Phoenix dactylifera) in coastal dunes. *Revista Iberoamericana de Micología, 34*, 116–120. https://doi.org/10.1016/j.riam.2016.06.007

Manawasinghe, I. S., Calabon, M. S., Jones, E. B. G., Zhang, Y. X., Liao, C. F., Xiong, Y. R., . . . Hyde, K. D. (2022). Mycosphere notes 345–386. *Mycosphere, 13*(1), 454–557. https://doi.org/10.5943/mycosphere/13/1/3

Manawasinghe, I. S., Hyde, K. D., Wanasinghe, D. N., Karunarathna, S. C., Maharachchikumbura, S. S. N., Samarakoon, M. C., . . . Xu, B. (2024). Fungal diversity notes 1818–1918: Taxonomic and phylogenetic contributions on genera and species of fungi. *Fungal Diversity, 130*, 1–261. https://doi.org/10.1007/s13225-024-00541-y

Manawasinghe, I. S., Jayawardena, R. S., Li, H. L., Zhou, Y. Y., Zhang, W., Phillips, A. J. L., . . . Yan, J. Y. (2021). Microfungi associated with Camellia sinensis: A case study of leaf and shoot necrosis on tea in Fujian, China. *Mycosphere, 12*(1), 430–518.

Manawasinghe, I. S., Phillips, A. J. L., Xu, J., Balasuriya, A., Hyde, K. D., Stępień, Ł., . . . Cheewangkoon, R. (2021). Defining a species in fungal plant pathology: Beyond the species level. *Fungal Diversity, 109*, 267–282. https://doi.org/10.1007/s13225-021-00481-x

Mao, Y. X., Lu, Y. T., Hu, Z. J., & Zhao, Y. (2020). Genetic diversity of Trachycarpus fortunei (Hook.) H. Wendl germplasm resources in Guizhou by SRAP molecular markers analysis. *Journal of Southern Agriculture, 51*, 27–35.

Marasinghe, D. S., Hongsanan, S., Wanasinghe, D. N., Boonmee, S., Lumyong, S., Hyde, K. D., . . . Ning, X. (2022). Morpho-molecular characterization of Brunneofissuraceae fam. nov., Cirsosia mangiferae sp. nov., and Asterina neomangiferae nom. nov. *Mycological Progress, 21*, 279–295. https://doi.org/10.1007/s11557-021-01767-9

Marín-Félix, Y., Hernández-Restrepo, M., Wingfield, M. J., Akulov, A., Carnegie, A. J., Cheewangkoon, R., . . . Crous, P. W. (2019). Genera of phytopathogenic fungi: GOPHY 2. *Studies in Mycology, 92*, 47–133. https://doi.org/10.1016/j.simyco.2018.04.002

Markovskaja, S., & Treigienė, A. (2007). A new and a rare species of Cryptadelphia and their Brachysporium anamorphs. *Nova Hedwigia, 84*(3–4), 495–501. https://doi.org/10.1127/0029-5035/2007/0084-0495

Mason, E. W., & Hughes, S. J. (1951). *Phragmocephala* gen. nov., hyphomycetarum. *The Naturalist, 76*(838), 97-105.

Massey, F. J., Jr. (1951). The Kolmogorov-Smirnov test for goodness of fit. *Journal of the American Statistical Association, 46*(253), 68–75. https://doi.org/10.1080/01621459.1951.10500769

Matsunaga, K. K. S., & Smith, S. Y. (2021). Fossil palm reading: Using fruits to reveal the deep roots of palm diversity. *American Journal of Botany, 108*, 472–494. https://doi.org/10.1002/ajb2.1616

Matsushima, T. (1971). *Microfungi of the Solomon Islands and Papua-New Guinea*. Matsushima.

Matsushima, T. (1975). *Icones microfungorum: A Matsushima lectorum.* Matsushima.

Mauri, M., Elli, T., Caviglia, G., Uboldi, G., & Azzi, M. (2017). RAWGraphs: A visualisation platform to create open outputs. In *Proceedings of the 12th Biannual Conference on Italian SIGCHI Chapter* (pp. 28:1–28:5). ACM. https://doi.org/10.1145/3125571.3125585

McKenzie, E. H. C., Buchanan, P. K., & Johnston, P. R. (2004). Checklist of fungi on nikau palm (*Rhopalostylis sapida* and *R. baueri var. cheesemanii*) in New Zealand. *New Zealand Journal of Botany, 42*, 335–355. https://doi.org/10.1080/0028825X.2004.9512908

Mehl, J. W. M., Slippers, B., Roux, J., & Wingfield, M. J. (2011). Botryosphaeriaceae associated with Pterocarpus angolensis (kiaat) in South Africa. *Mycologia, 103*(3), 534–553. https://doi.org/10.3852/10-003

Mel'nik, V. A. (2012). *Phaeoisaria vietnamensis* sp. nov. and *P. clematidis* (hyphomycetes) from Vietnam. *Mycosphere, 3*(6), 957–960. https://doi.org/10.5943/mycosphere/3/6/10

Mendes, J., Portilho, A., Aguiar-Dias, A., Sampaio, K., & Farias, L. (2019). Arecaceae: Uma estratégia diferenciada para o ensino de botânica em uma escola de ensino médio na ilha de Cotijuba, Pará, Brasil. *Enciclopédia Biosfera, 16*(29), 2226–2240. https://doi.org/10.18677/EnciBio_2019A170

Miadlikowska, J., Kauff, F., Högnabba, F., Oliver, J. C., Molnár, K., Fraker, E., . . . Stenroos, S. (2014). A multigene phylogenetic synthesis for the class Lecanoromycetes (Ascomycota): 1307 fungi representing 1139 infrageneric taxa, 317 genera and 66 families. *Molecular Phylogenetics and Evolution, 79*, 132–168. https://doi.org/10.1016/j.ympev.2014.04.003

Miller, M. A., Pfeiffer, W., & Schwartz, T. (2010). Creating the CIPRES science gateway for inference of large phylogenetic trees. *In Proceedings of the 2010 Gateway Computing Environments Workshop (GCE)* (pp. 1–8). IEEE. https://doi.org/10.1109/GCE.2010.5676129

Minnis, A. M., Kennedy, A. H., Grenier, D. B., Palm, M. E., & Rossman, A. Y. (2012). Phylogeny and taxonomic revision of the Planistromellaceae including its coelomycetous anamorphs: Contributions towards a monograph of the genus Kellermania. *Persoonia, 29*, 11–28. https://doi.org/10.3767/003158512X658766

Mohammadi, A. C., & Amini, Y. (2015). Molecular characterization and identification of Acrostalagmus luteoalbus from saffron in Iran. *Agricultural Science Developments*, *4*, 16–18.

Mooney, C. Z. (1997). *Monte Carlo simulation* (No. 116). Sage. https://doi.org/10.4135/9781412985116

Moore, R. T. (1955). Index to the Helicosporae. *Mycologia*, *47*(1), 90–103. https://doi.org/10.1080/00275514.1955.12024431

Mortimer, P. E., Jeewon, R., Xu, J. C., Lumyong, S., & Wanasinghe, D. N. (2021). Morpho-phylo taxonomy of novel dothideomycetous fungi associated with dead woody twigs in Yunnan Province, China. *Frontiers in Microbiology, 12*, 654683. https://doi.org/10.3389/fmicb.2021.654683

Mugambi, G. K., & Huhndorf, S. M. (2009). Parallel evolution of hysterothecial ascomata in ascolocularous fungi (Ascomycota, Fungi). *Systematics and Biodiversity, 7*(4), 453–464. https://doi.org/10.1017/S147720000999020X

Munk, A. (1953). The system of the Pyrenomycetes. *Dansk Botanisk Arkiv, 15*, 1–163.

Muscarella, R., Emilio, T., Phillips, O. L., Lewis, S. L., Slik, F., Baker, W. J., . . . Balslev, H. (2020). The global abundance of tree palms. *Global Ecology and Biogeography, 29*(9), 1495–1514. https://doi.org/10.1111/geb.13123

MycoBank. (2022). *MycoBank*. https://www.mycobank.org/

Nadot, S., Alapetite, E., Baker, W. J., Tregear, J. W., & Barfod, A. S. (2016). The palm family (Arecaceae): A microcosm of sexual system evolution. *Botanical Journal of the Linnean Society, 182*(2), 376–388. https://doi.org/10.1111/boj.12440

Nag Raj, T. R. (1985). Redisposals and redescriptions in the Monochaetia-Seiridium, Pestalotia-Pestalotiopsis complexes. II. *Pestalotiopsis besseyii* (Guba) comb. nov. and *Pestalosphaeria varia* sp. nov. *Mycotaxon, 22*, 52–63.

Nascimento, M. M. F., Vicente, V. A., Bittencourt, J. V. M., Gelinski, J. M. L., Prenafeta-Boldú, F. X., Romero-Güiza, M., . . . de Hoog, G. S. (2017). Diversity of opportunistic black fungi on babassu coconut shells, a rich source of esters and hydrocarbons. *Fungal Biology, 121*(5), 488–500. https://doi.org/10.1016/j.funbio.2017.01.006

Nees von Esenbeck, C. D. G. (1816). *System der Pilze und Schwämme*. Legare Street Press.

Nees von Esenbeck, C. G. (1817). *Das system der Pilze und Schwämme* (vol. 371, p. 18). Stahelsche Buchhandlung. https://doi.org/10.5962/bhl.title.110007

Nguyen, L. T., Schmidt, H. A., von Haeseler, A., & Minh, B. Q. (2015). IQ-TREE: A fast and effective stochastic algorithm for estimating maximum-likelihood phylogenies. *Molecular Biology and Evolution, 32*(1), 268–274.

Nguyen, T. T., Hee Lee, S., Jeong Jeon, S., & Burm Lee, H. (2019). First records of rare ascomycete fungi, Acrostalagmus luteoalbus, Bartalinia robillardoides, and Collariella carteri from freshwater samples in Korea. *Mycobiology, 47*(1), 1–11. https://doi.org/10.1080/12298093.2018.1550894

Niranjan, M., & Sarma, V. V. (2018). New ascomycetous fungi in the family Aigialaceae from Andaman Islands, India. *Current Research in Environmental & Applied Mycology, 8*(3), 351–359. https://doi.org/10.5943/cream/8/3/6

Niranjan, M., & Sarma, V. V. (2019). New species and new records of Melanommataceae (Pleosporales) from Andaman Islands. *Kavaka, 52*, 103–108. https://doi.org/10.36460/Kavaka/54/2020/38-42

Nisa, H., Kamili, A. N., Nawchoo, I. A., Shafi, S., Shameem, N., & Bandh, S. A. (2015). Fungal endophytes as prolific source of phytochemicals and other bioactive natural products: A review. *Microbial Pathogenesis, 82*, 50–59. https://doi.org/10.1016/j.micpath.2015.04.001

Nonaka, K., Ishii, T., Shiomi, K., Ōmura, S., & Masuma, R. (2013). Virgaria boninensis, a new hyphomycete (Xylariaceae) from soils in the Bonin Islands, Japan. *Mycoscience, 54*(5), 394–399. https://doi.org/10.1016/j.myc.2013.01.004

Norphanphoun, C., Jayawardena, R. S., Chen, Y., Wen, T. C., Meepol, W., & Hyde, K. D. (2019). Morphological and phylogenetic characterization of novel pestalotioid species associated with mangroves in Thailand. *Mycosphere, 10*(1), 531–578. https://doi.org/10.5943/mycosphere/10/1/9

NSII. (2017). *The NSII specimen search, version 2020*. http://www.nsii.org.cn/2017/query.php?name=广东

Nuin, P. (2007). *MrMTgui v1.0: MrModelTest/ModelTest graphical interface for Windows/Linux*. Google Scholar.

Nylander, J. (2008). *MrModeltest2 v. 2.3 (Program for selecting DNA substitution models using PAUP)*. Evolutionary Biology Centre.

Nylander, J. A. A. (2004). *MrModeltest v2. Program distributed by the author*. Evolutionary Biology Centre, Uppsala University.

O'Donnell, K., & Cigelnik, E. (1997). Two divergent intragenomic rDNA ITS2 types within a monophyletic lineage of the fungus Fusarium are nonorthologous. *Molecular Phylogenetics and Evolution, 7*, 103–116. https://doi.org/10.1006/mpev.1996.0376

O'Donnell, K., Sarver, B. A., Brandt, M., Chang, D. C., Noble-Wang, J., Park, B. J., . . . Ward, T. J. (2007). Phylogenetic diversity and microsphere array-based genotyping of human pathogenic Fusaria, including collections from the multistate contact lens-associated US keratitis outbreaks of 2005 and 2006. *Journal of Clinical Microbiology, 45*(7), 2235–2248. https://doi.org/10.1128/JCM.00533-07

Outamamat, E., Bourhia, M., Dounas, H., Salamatullah, A. M., Alzahrani, A., Alyahya, H. K., . . . Ouahmane, L. (2021). Application of native or exotic arbuscular mycorrhizal fungi complexes and monospecific collections from saline semi-arid Mediterranean ecosystems improved *Phoenix dactylifera*'s growth and mitigated salt stress negative effects. *Plants, 10*(11), 2501. https://doi.org/10.3390/plants10112501

Pandian, R. T. P., Thube, S. H., Bhavishya, Merinbabu, Chaithra, Santhoshkumar, P., . . . Hegde, V. (2021). First report of Phytophthora *palmivora* (E.J. Butler) E.J. Butler, 1919 causing fruit rot in *Areca triandra* Roxb. ex Buch.-Ham. from India. *Australasian Plant Pathology, 50*(4), 495–499. https://doi.org/10.1007/s13313-021-00802-3

Papendorf, M. C. (1976). Notes on *Veronaea* including V. compacta sp. nov. *Bothalia, 12*, 119–121. https://doi.org/10.4102/abc.v12i1.1384

Pem, D., Jeewon, R., Bhat, D. J., Doilom, M., Boonmee, S., Hongsanan, S., . . . Hyde, K. D. (2019). Mycosphere notes 275–324: A morphotaxonomic revision and typification of obscure Dothideomycetes genera (incertae sedis). *Mycosphere, 10*, 1115–1246. https://doi.org/10.5943/mycosphere/10/1/22

Pem, D., Jeewon, R., Chethana, K. W. T., Hongsanan, S., Doilom, M., Suwannarach, N., . . . Hyde, K. D. (2021). Species concepts of Dothideomycetes: Classification, phylogenetic inconsistencies and taxonomic standardization. *Fungal Diversity, 109*(1), 283–319. https://doi.org/10.1007/s13225-021-00485-7

Peng, H., Xia, H., Chen, H., Zhi, P., & Xu, Z. (2021). Spatial variation characteristics of vegetation phenology and its influencing factors in the subtropical monsoon climate region of southern China. *PLoS ONE, 16*(4), e0250825. https://doi.org/10.1371/journal.pone.0250825

Penzig, A. J. O., & Saccardo, P. A. (1897). Diagnoses fungorum novorum in insula Java collectorum. *Tipografia di Angelo Ciminago, Genova, Italy, series secunda, 11*, 491–530. https://doi.org/10.5962/bhl.title.4921

Pereira, D. S., & Phillips, A. J. L. (2020). A new leaf spot disease of Chamaerops humilis caused by *Palmeiromyces chamaeropicola* gen. et sp. nov. *Phytopathologia Mediterranea, 59*, 353–363. https://doi.org/10.14601/Phyto-11213

Pereira, D. S., & Phillips, A. J. L. (2023). Palm fungi and their key role in biodiversity surveys: A review. *Journal of Fungi, 9*(11), 1121. https://doi.org/10.3390/jof9111121

Pereira, D. S., & Phillips, A. J. L. (2023b). Botryosphaeriaceae on palms—a new species of Neodeightonia, N. chamaeropicola, and new records from diseased foliage of ornamental palms in Portugal. *Phytotaxa, 627*, 1921–1935. https://doi.org/10.11646/phytotaxa.627.1.1

Phillips, A. J. L., Alves, A., Correia, A., & Luque, J. (2005). Two new species of Botryosphaeria with brown, 1-septate ascospores and Dothiorella anamorphs. *Mycologia, 97*(3), 513–529. https://doi.org/10.1080/15572536.2006.11832826

Phillips, A. J. L., Alves, A., Pennycook, S. R., Johnston, P. R., Ramaley, A., Akulov, A., . . . Crous, P. W. (2008). Resolving the phylogenetic and taxonomic status of dark-spored teleomorph genera in the Botryosphaeriaceae. *Persoonia, 21*, 29–55. https://doi.org/10.3767/003158508X340742

Phillips, A. J. L., Hyde, K. D., Alves, A., & Liu, J. K. (2019). Families in Botryosphaeriales: A phylogenetic, morphological and evolutionary perspective. *Fungal Diversity, 94*, 1–22. https://doi.org/10.1007/s13225-018-0416-6

Phillips, A., Alves, A., Abdollahzadeh, J., Slippers, B., Wingfield, M., Groenewald, J., . . . Crous, P. (2013). The Botryosphaeriaceae: Genera and species known from culture. *Studies in Mycology, 76*, 51–167. https://doi.org/10.3114/sim0021

Phookamsak, R., Hyde, K. D., Jeewon, R., Bhat, D. J., Jones, E. B. G., Maharachchikumbura, S. S. N., . . . Xu, J. (2019). Fungal diversity notes 929–1035: Taxonomic and phylogenetic contributions on genera and species of fungi. *Fungal Diversity, 95*, 1–273. https://doi.org/10.1007/s13225-019-00421-w

Phookamsak, R., Norphanphoun, C., Tanaka, K., Dai, D. Q., Luo, Z. L., Liu, J. K., . . . Hyde, K. D. (2015). Towards a natural classification of *Astrosphaeriella*-like species; introducing Astrosphaeriellaceae and *Pseudoastrosphaeriellaceae* fam. nov. and *Astrosphaeriellopsis* gen. nov. *Fungal Diversity, 74*, 143–197. https://doi.org/10.1007/s13225-015-0352-7

Phukhamsakda, C., McKenzie, E. H. C., Phillips, A. J. L., Jones, E. B. G., Bhat, D. J., Stadler, M., . . . Hyde, K. D. (2020). Microfungi associated with Clematis (Ranunculaceae) with an integrated approach to delimiting species boundaries. *Fungal Diversity, 102*, 1–203. https://doi.org/10.1007/s13225-020-00448-4

Phukhamsakda, C., Nilsson, R. H., Bhunjun, C. S., de Farias, A. R. G., Sun, Y. R., Wijesinghe, S. N., . . . Hyde, K. D. (2022). The numbers of fungi: Contributions from traditional taxonomic studies and challenges of metabarcoding. *Fungal Diversity, 114*, 327–386. https://doi.org/10.1007/s13225-022-00502-3

Pilantanapak, A., Jones, E. G., & Eaton, R. A. (2005). Marine fungi on Nypa fruticans in Thailand. *Botanica Marina, 48,* 365–373. https://doi.org/10.1515/BOT.2005.049

Pinnoi, A., Lumyong, S., Hyde, K. D., & Jones, E. G. (2006). Biodiversity of fungi on the palm Eleiodoxa conferta in Sirindhorn peat swamp forest, Narathiwat, Thailand. *Fungal Diversity, 22,* 205-218.

Pinnoi, A., Phongpaichit, P., Jeewon, R., Tang, A. M. C., Hyde, K. D., & Jones, E. B. G. (2010). Phylogenetic relationships of *Astrocystis eleiodoxae* sp. nov. (Xylariaceae). *Mycosphere, 1,* 1–9.

Pinruan, U., Hyde, K. D., Lumyong, S., McKenzie, E. H. C., & Jones, E. B. G. (2007). Occurrence of fungi on tissues of the peat swamp palm Licuala longicalycata. *Fungal Diversity, 25,* 157–173.

Pinruan, U., Rungjindamai, N., Choeyklin, R., Lumyong, S., Hyde, K. D., & Jones, E. B. G. (2010). Occurrence and diversity of basidiomycetous endophytes from the oil palm, Elaeis guineensis in Thailand. *Fungal Diversity, 41,* 71–88. https://doi.org/10.1007/s13225-010-0029-1

Pinruan, U., Rungjindamai, N., Sakayaroj, J., Lumyong, S., Hyde, K. D., & Jones, E. B. G. (2010). *Baipadisphaeria* gen. nov., a freshwater ascomycete (Hypocreales, Sordariomycetes) from decaying palm leaves in Thailand. *Mycosphere, 1*, 53–63.

Pinruan, U., Sakayaroj, J., Jones, E. B. G., & Hyde, K. D. (2004). *Flammispora* gen. nov., a new freshwater ascomycete from decaying palm leaves. *Studies in Mycology, 50*, 381–386.

Pirozynski, K. A. (1972). Microfungi of Tanzania. I. Miscellaneous fungi on oil palm. II. New hyphomycetes. *Mycological Papers, 129*, 1–64.

Pirozynski, K. A. (1972). *Microfungi of Tanzania. I. Miscellaneous fungi on oil palm*. Commonwealth Mycological Institute.

Poiteau, P. A. (1824). Description du Graphiola, nouveau genre des plantes parasite de la famille des champignons. *Annales des Sciences Naturelles, 3,* 473–476.

Pornsuriya, C., Chairin, T., Thaochan, N., & Sunpapao, A. (2020). Identification and characterization of Neopestalotiopsis fungi associated with a novel leaf fall disease of rubber trees (Hevea brasiliensis) in Thailand. *Journal of Phytopathology, 168*(7–8), 416–427.

Prabhugaonkar, A., & Bhat, D. J. (2009). Rattania setulifera, an undescribed endophytic hyphomycete on rattans from western Ghats, India. *Mycotaxon, 108*, 217–222. https://doi.org/10.5248/108.217

Prasannath, K., Shivas, R. G., Galea, V. J., & Akinsanmi, O. A. (2021). Neopestalotiopsis species associated with flower diseases of Macadamia integrifolia in Australia. *Journal of Fungi, 7*(9), 771. https://doi.org/10.3390/jof7090771

Prasher, I. B., & Sushma. (2014). *Hermatomyces indicus* sp. nov. (Hyphomycetes) from India. *Nova Hedwigia, 99*, 551–556.

Prasher, I. B., & Verma, R. K. (2015). Two new species of Dictyosporium from India. *Phytotaxa, 204*, 193–202. https://doi.org/10.11646/phytotaxa.204.3.2

Prasher, I. B., & Verma, R. K. (2016). Hyphomycetes diversity of Himachal Pradesh-I. *Journal of New Biological Reports, 5*(1), 52–58.

Punithalingam, E. (1969). *Studies on Sphaeropsidales in culture*. Commonwealth Mycological Institute.

Qiang, L. (2014). Current plant landscaping in southern gardens and suggestions for the optimized configuration. *Journal of Landscape Research, 6*(9/10), 26.

Quaedvlieg, W., Binder, M., Groenewald, J. Z., Summerell, B. A., Carnegie, A. J., Burgess, T. I., . . . Crous, P. W. (2014). Introducing the consolidated species concept to resolve species in the Teratosphaeriaceae. *Persoonia, 33*(1), 1–40.

Rajesh, M. K., Ramesh, S. V., Perera, L., & Kole, C. (2021). *The coconut genome*. Springer.

Rämä, T., & Quandt, C. A. (2021). Improving fungal cultivability for natural products discovery. *Frontiers in Microbiology, 12*, 706044. https://doi.org/10.3389/fmicb.2021.706044

Rambaut, A. (2014). *FigTree v1.4.2, a graphical viewer of phylogenetic trees*. http://tree.bio.ed.ac.uk/software/figtree/

Rambelli, A. (2011). Some dematiaceous hyphomycetes from Mediterranean maquis litters. *Flora Mediterranea, 21*, 5–204.

Ran, S. F., Maharachchikumbura, S. S. N., Ren, Y. L., Liu, H., Chen, K. R., Wang, Y. X., . . . Wang, Y. (2017). Two new records in Pestalotiopsidaceae associated with Orchidaceae disease in Guangxi Province, China. *Mycosphere, 8*(1), 121–130. https://doi.org/10.5943/mycosphere/8/1/11

Rannala, B., & Yang, Z. H. (1996). Probability distribution of molecular evolutionary trees: A new method of phylogenetic inference. *Journal of Molecular Evolution, 43*, 304–311. https://doi.org/10.1007/BF02338839

Rao, P. R., & Rao, D. (1964). Some species of Camposporium Harkn. from India. *Antonie van Leeuwenhoek, 30*, 60–64. https://doi.org/10.1007/BF02046701

Rathna, V., Prasanna, S. L., Anandakumar, J., Swathi, B., Patil, S. S., & Kujur, R. S. (2025). Forest alchemists: Microbe-mediated nutrient recycling. In R. K. Kalia & R. Pathak (Eds.), *Tree Biology and Biotechnology* (pp. 67–86). Springer Nature Singapore. https://doi.org/10.1007/978-981-96-0002-1_5

Rathnayaka, A. R., Dayarathne, M. C., Maharachchikumbura, S. S. N., Liu, J. K., Tennakoon, D. S., & Hyde, K. D. (2019). Introducing *Seriascoma yunnanense* sp. nov. (Occultibambusaceae, Pleosporales) based on evidence from morphology and phylogeny. *Asian Journal of Mycology, 2*(1), 245–253. https://doi.org/10.5943/ajom/2/1/15

Rathnayaka, A. R., Tennakoon, D. S., Jones, E. B. G., Wanasinghe, D. N., Bhat, D. J., Priyashantha, A. K. H., . . . Karunarathna, S. C. (2024). Significance of precise documentation of hosts and geospatial data of fungal collections, with an emphasis on plant-associated fungi. *New Zealand Journal of Botany, 63*, 462-489. https://doi.org/10.1080/0028825X.2024.2381734

Rayner, R. W. (1970). *A mycological colour chart*. Commonwealth Mycological Institute & British Mycological Society.

Réblová, M., & Štěpánek, V. (2018). Introducing the *Rhamphoriaceae*, fam. nov. (Sordariomycetes), two new genera, and new life histories for taxa with Phaeoisaria- and Idriella-like anamorphs. *Mycologia, 110*, 750–770. https://doi.org/10.1080/00275514.2018.1475164

Réblová, M., Hernández-Restrepo, M., Sklenář, F., Nekvindová, J., Réblová, K., & Kolařík, M. (2022). Consolidation of Chloridium: New classification into eight sections with 37 species and reinstatement of the genera Gongromeriza and Psilobotrys. *Studies in Mycology, 103*(1), 87–212. https://doi.org/10.3114/sim.2022.103.04

Réblová, M., Kolařík, M., Nekvindová, J., Réblová, K., Sklenář, F., Miller, A. N., . . . Hernández-Restrepo, M. (2021). Phylogenetic reassessment, taxonomy, and biogeography of *Codinaea* and similar fungi. *Journal of Fungi, 7*(12), 1097. https://doi.org/10.3390/jof7121097

Réblová, M., Miller, A. N., Réblová, K., & Štěpánek, V. (2018). Phylogenetic classification and generic delineation of *Calyptosphaeria* gen. nov., *Lentomitella, Spadicoides* and *Torrentispora* (Sordariomycetes). *Studies in Mycology, 89*, 1–62. https://doi.org/10.1016/j.simyco.2017.11.004

Réblová, M., Seifert, K. A., Fournier, J., & Štěpánek, V. (2016). Newly recognised lineages of perithecial ascomycetes: The new orders Conioscyphales and Pleurotheciales. *Persoonia, 37*(1), 57–81. https://doi.org/10.3767/003158516X689819

Reddy, M. S., Murali, T. S., Suryanarayanan, T. S., & Govinda Rajulu, M. B. (2016). Pestalotiopsis species occur as generalist endophytes in trees of Western Ghats forests of southern India. *Fungal Ecology, 24*, 70–75. https://doi.org/10.1016/j.funeco.2016.09.002

Rehm, H. (1914). Ascomycetes Philippinensis, VI. *Leaflets of Philippine Botany, 6*, 2257–2281.

Rehner, S. A., & Buckley, E. (2005). A Beauveria phylogeny inferred from nuclear ITS and EF1-α sequences: Evidence for cryptic diversification and links to Cordyceps teleomorphs. *Mycologia, 97*(1), 84–98. https://doi.org/10.3852/mycologia.97.1.84

Reichgelt, T., West, C. K., & Greenwood, D. R. (2018). The relation between global palm distribution and climate. *Scientific Reports, 8*, 4721. https://doi.org/10.1038/s41598-018-23147

Ren, G. C., Tibpromma, S., Dong, K. X., Gao, C. X., Zhang, C. S., Karunarathna, S. C., . . . Gui, H. (2024). Unveiling fungi associated with Castanopsis woody litter in Yunnan Province, China: Insights into Pleosporales (Dothideomycetes) species. *MycoKeys, 108*, 15. https://doi.org/10.3897/mycokeys.108.127560

Rodrigues, K. F. (1994). The foliar fungal endophytes of the Amazonian palm Euterpe oleracea. *Mycologia, 86*, 376–385. https://doi.org/10.1080/00275514.1994.12026423

Rodrigues, K. F., & Samuels, G. J. (1990). Preliminary study of endophytic fungi in a tropical palm. *Mycological Research, 94*, 827–830. https://doi.org/10.1016/S0953-7562(09)81386-5

Rojas, N. L., Voget, C. E., Hours, R. A. C., & Cavalitto, S. F. (2011). Purification and characterization of a novel alkaline α-L-rhamnosidase produced by Acrostalagmus luteoalbus. J*ournal of Industrial Microbiology & Biotechnology, 38*, 1515–1522. https://doi.org/10.1007/s10295-010-0938-8

Rolland, L. (1896). Aliquot fungi novi vel critici Galliae praecipue meridionalis. *Bulletin de la Société Mycologique de France, 12*, 1–10.

Ronquist, F., Teslenko, M., van der Mark, P., Ayres, D. L., Darling, A., Höhna, S., . . . Huelsenbeck, J. P. (2012). MrBayes 3.2: Efficient Bayesian phylogenetic inference and model choice across a large model space. *Systematic Biology, 61*, 539–542. https://doi.org/10.1093/sysbio/sys029

Rossman, A. Y. (1987). The Tubeufiaceae and similar Loculoascomycetes. *Mycological Papers, 157*, 1–71.

Rossman, A. Y., Adams, G. C., Cannon, P. F., Castlebury, L. A., Crous, P. W., Gryzenhout, M., . . . Walker, D. M. (2015). Recommendations of generic names in Diaporthales competing for protection or use. *IMA Fungus, 6*, 145–154. https://doi.org/10.5598/imafungus.2015.06.01.09

Rungjindamai, N., Pinruan, U., Choeyklin, R., Hattori, T., & Jones, E. B. G. (2008). Molecular characterization of basidiomycetous endophytes isolated from leaves, rachis and petioles of the oil palm, Elaeis guineensis, in Thailand. *Fungal Diversity, 33*, 139–161.

Saccardo, P. A. (1875). Conspectus generum Pyrenomycetum italicorum. *Atti dell'Accademia di Scienze Veneto-Trentino-Istriana, 4*, 101–141.

Saccardo, P. A. (1880). Conspectus generum fungorum Italiae inferiorum nempe ad Sphaeropsideas, Melanconieas et Hyphomyceteas pertinentium, systemate sporologico dispositu. *Michelia, 2*, 1–38.

Saccardo, P. A. (1913). Notae mycologicae. Series XVII. *Annales Mycologici, 11*, 546–568.

Saccardo, P. A., & Paoletti, G. (1888). Mycetes Malacenses. *Funghi della penisola di Malacca raccolti nel 1885 dell'Ab Benedetto Scortechini, 6*, 387–428.

Samarakoon, M. C., Hyde, K. D., Maharachchikumbura, S. S. N., Stadler, M., Jones, E. B. G., Promputtha, I., . . . Liu, J. K. (2021). Taxonomy, phylogeny, molecular dating and ancestral state reconstruction of Xylariomycetidae (Sordariomycetes). *Fungal Diversity, 112*, 1–88. https://doi.org/10.21203/rs.3.rs-935829/v1

Santos, G. S., Mafia, R. G., Aguiar, A. M., Zarpelon, T. G., Damacena, M. B., Barros, A. F., . . . Ferreira, M. A. (2020). Stem rot of eucalyptus cuttings caused by *Neopestalotiopsis* spp. in Brazil. *Journal of Phytopathology, 168*, 311–321. https://doi.org/10.1111/jph.12894

Sayan, M. S. (2001). Landscaping with palms in the Mediterranean. *Palms, 45*, 171–176.

Schuessler, J. A., von Blanckenburg, F., Bouchez, J., Uhlig, D., & Hewawasam, T. (2018). Nutrient cycling in a tropical montane rainforest under a supply-limited weathering regime traced by elemental mass balances and Mg stable isotopes. *Chemical Geology*, *497*, 74–87. https://doi.org/10.1016/j.chemgeo.2018.08.024

Seifert, K., Morgan-Jones, G., Gams, W., & Kendrick, B. (2011). *The genera of hyphomycetes*. CBS-KNAW Fungal Biodiversity Centre.

Selmaoui, K., Touati, J., Chliyeh, M., Touhami, A. O., & et Allal Douira, R. B. (2014). Study of *Pestalotiopsis palmarum* pathogenicity on *Washingtonia robusta* (Mexican palm). *International Journal of Pure and Applied Biosciences, 2*, 138–145.

Senanayake, I. C., Jeewon, R., Chomnunti, P., Wanasinghe, D. N., Norphanphoun, C., Karunarathna, A., . . . Karunarathna, S. C. (2018). Taxonomic circumscription of Diaporthales based on multigene phylogeny and morphology. *Fungal Diversity, 93*, 241–443. https://doi.org/10.1007/s13225-018-0410-z

Senanayake, I. C., Lian, T. T., Mai, X. M., Jeewon, R., Maharachchikumbura, S. S. N., Hyde, K. D., . . . Xie, N. (2020). New geographical records of Neopestalotiopsis and Pestalotiopsis species in Guangdong Province, China. *Asian Journal of Mycology, 3*, 512–533. https://doi.org/10.5943/ajom/3/1/19

Senanayake, I. C., Rathnayaka, A. R., Marasinghe, D. S., Calabon, M. S., Gentekaki, E., Lee, H. B., . . . Xiang, M. M. (2020). Morphological approaches in studying fungi: collection, examination, sporulation and preservation. *Mycosphere, 11*, 2678–2754. https://doi.org/10.5943/mycosphere/11/1/20

Senanayake, I. C., Rossi, W., Leonardi, M., Weir, A., McHugh, M., Rajeshkumar, K. C., . . . Song, J. (2023). Fungal diversity notes 1611–1716: Taxonomic and phylogenetic contributions on fungal genera and species with emphasis in south China. *Fungal Diversity, 122*, 161–403. https://doi.org/10.1007/s13225-023-00523-6

Senwanna, C., Hongsanan, S., Hyde, K. D., & Cheewangkoon, R. (2020). First report of the sexual morph of Pseudofusicoccum adansoniae Pavlic, T. I. Burgess & M. J. Wingf. on para rubber. *Cryptogamie, Mycologie, 41*, 133–146. https://doi.org/10.5252/cryptogamie-mycologie2020v41a7

Senwanna, C., Mapook, A., Samarakoon, M. C., Karunarathna, A., Wang, Y., Tang, A. M. C., . . . Cheewangkoon, R. (2021). Ascomycetes on para rubber (Hevea brasiliensis). *Mycosphere, 12*(1), 1334–1512. https://doi.org/10.5943/mycosphere/12/1/18

Sepúlveda, G., Arismendi, M., Huanca-Mamani, W., Cárdenas-Ninasivincha, S., Salvatierra, R., & Latorre, B. (2017). The presence of false smut (Graphiola phoenicis (Moug. ex Fr.) Poit.) on Canary date palm (Phoenix canariensis) in Easter Island, Chile. *Ciencia e Investigación Agraria, 44*, 307–311. https://doi.org/10.7764/rcia.v44i3.1787

Shao, Y., Baral, H. O., Ou, X., Wu, H., Huang, F., Zheng, H., . . . Liu, B. (2018). New species and records of orbiliaceous fungi from Georgia, USA. *Mycological Progress, 17*, 1225–1235. https://doi.org/10.1007/s11557-018-1438-x

Shearer, C. A., & Motta, J. J. (1973). Ultrastructure and conidiogenesis in Conioscypha (Hyphomycetes). *Canadian Journal of Botany, 51*, 1747–1751. https://doi.org/10.1139/b73-226

Shen, H. W., Bao, D. F., Wanasinghe, D. N., Boonmee, S., Liu, J., & Luo, Z. (2022). Novel species and records of Dictyosporiaceae from freshwater habitats in China and Thailand. *Journal of Fungi, 8*(11), 1200. https://doi.org/10.3390/jof8111200

Shenoy, B. D., Jeewon, R., Wang, H. K., Amandeep, K., Ho, W. H., Bhat, D. J., . . . Hyde, K. D. (2010). Sequence data reveals phylogenetic affinities of fungal anamorphs Bahusutrabeeja, Diplococcium, Natarajania, Paliphora, Polyschema, Rattania, and Spadicoides. *Fungal Diversity, 44*, 161–169. https://doi.org/10.1007/s13225-010-0059-8

Shenoy, B. D., Jeewon, R., Wu, W. P., Bhat, D. J., & Hyde, K. D. (2006). Ribosomal and RPB2 DNA sequence analyses suggest that Sporidesmium and morphologically similar genera are polyphyletic. *Mycological Research, 110*, 916–928. https://doi.org/10.1016/j.mycres.2006.06.004

Shi, T., Wang, H., Li, Y. J., Wang, Y. F., Pan, Q., Wang, B., . . . Shang, E. L. (2023). Genus Acrostalagmus: A prolific producer of natural products. *Biomolecules*, *13*(8), 1191. https://doi.org/10.3390/biom13081191

Shirouzu, T., Hirose, D., Tokumasu, S., To-Anun, C., & Maekawa, N. (2010). Host affinity and phylogenetic position of a new anamorphic fungus Beltraniella botryospora from living and fallen leaves of evergreen oaks. *Fungal Diversity*, *43*, 85–92. https://doi.org/10.1007/s13225-010-0037-1

Shu, J., Yu, Z., Sun, W., Zhao, J., Li, Q., Tang, L., . . . Luo, S. (2020). Identification and characterization of pestalotioid fungi causing leaf spots on mango in southern China. *Plant Disease, 104*(4), 1207–1213. https://doi.org/10.1094/PDIS-03-19-0438-RE

Shu, Y. X., Doilom, M., Boonmee, S., Xu, B., & Dong, W. (2024). Three novel cheiroid hyphomycetes in Dictyocheirospora and Dictyosporium (Dictyosporiaceae) from freshwater habitats in Guangdong and Guizhou Provinces, China. *Journal of Fungi, 10*, 259. https://doi.org/10.3390/jof10040259

Silva, A. C., Diogo, E., Henriques, J., Ramos, A. P., Sandoval-Denis, M., Crous, P. W., . . . Bragança, H. (2020). *Pestalotiopsis pini* sp. nov., an emerging pathogen on stone pine (*Pinus pinea* L.). *Forests, 11*(8), 805. https://doi.org/10.3390/f11080805

Silvério, M. L., Calvacanti, M. A. d. Q., Silva, G. A. d., Oliveira, R. J. V. d., & Bezerra, J. L. (2016). A new epifoliar species of Neopestalotiopsis from Brazil. *Agrotrópica, 28*, 151–158.

Sivichai, S., & Hywel-Jones, N. (1999). Biflagellospora (aero-aquatic hyphomycetes) from submerged wood in Thailand. *Mycological Research, 103*, 908–914. https://doi.org/10.1017/S0953756298007928

Slippers, B., & Wingfield, M. J. (2007). Botryosphaeriaceae as endophytes and latent pathogens of woody plants: diversity, ecology and impact. *Fungal Biology Reviews, 21*, 90–106.

Slippers, B., Boissin, E., Phillips, A. J., Groenewald, J. Z., Lombard, L., Wingfield, M. J., . . . Crous, P. W. (2013). Phylogenetic lineages in the Botryosphaeriales: A systematic and evolutionary framework. *Studies in Mycology, 76*, 31–49. https://doi.org/10.3114/sim0020

Smith, G. (1962). Some new and interesting species of microfungi. III. *Transactions of the British Mycological Society, 45*, 387–394. https://doi.org/10.1016/S0007-1536(62)80077-1

Smith, G. (1969). *An introduction to industrial mycology* (6th ed.). Arnold Ltd.

Solarte, F., Muñoz, C. G., Maharachchikumbura, S. S. N., & Alvarez, E. (2018). Diversity of Neopestalotiopsis and *Pestalotiopsis* spp., causal agents of guava scab in Colombia. *Plant Disease, 102*, 49–59.

Somrithipol, S., & Jones, E. B. G. (2005). An addition to the hyphomycete genus Melanographium from Thailand. *Fungal Diversity, 19*, 137–144.

Song, Y., Geng, K., Hyde, K. D., Zhao, W. S., Wei, J. G., Kang, J. C., . . . Wang, Y. (2013). Two new species of Pestalotiopsis from southern China. *Phytotaxa, 126*, 22–30.

Song, Y., Maharachchikumbura, S. S. N., Jiang, Y. L., Hyde, K. D., & Wang, Y. (2014a). *Pestalotiopsis keteleeria* sp. nov., isolated from Keteleeria pubescens in China. *Chiang Mai Journal of Science, 41*, 885–893.

Song, Y., Tangthirasunun, N., Maharachchikumbura, S. S. N., Jiang, Y. L., Xu, J. J., Hyde, K. D., . . . Wang, Y. (2014b). Novel Pestalotiopsis species from Thailand point to the rich undiscovered diversity of this chemically creative genus. Cryptogamie, *Mycologie, 35*, 139–149.

Soprunov, F. F., & Galiulina, Z. A. C. (1951). Predatory hyphomycetes from Turkmenistan soils. *Mikrobiologiya, 20*, 489–499.

Species Fungorum. (2022). http://www.speciesfungorum.org/

Spegazzini, C. L. (1911). Mycetes Argentinenses. Series V. *Anales del Museo Nacional de Historia Natural de Buenos Aires, 3*, 446.

Spennemann, D. H. (2021). The role of Canary Island date palms in physical amenity provisioning for urban landscape settings. *Horticulturae, 7*, 201. https://doi.org/10.3390/horticulturae7070201

Stamatakis, A. (2014). RAxML version 8: A tool for phylogenetic analysis and post-analysis of large phylogenies. *Bioinformatics, 30*, 1312–1313. https://doi.org/10.1093/bioinformatics/btu033

Stamatakis, A., Hoover, J., & Rougemont, J. (2008). A rapid bootstrap algorithm for the RAxML web servers. *Systematic Biology, 57*, 758–771. https://doi.org/10.1080/10635150802429642

Starbäck, K. (1904). Ascomyceten der ersten Regnell'schen Expedition. III. *Arkiv för Botanik, 2*, 1–22.

Steinbauer, M. J., Grytnes, J. A., Jurasinski, G., Kulonen, A., Lenoir, J., Pauli, H., . . . Wipf, S. (2018). Accelerated increase in plant species richness on mountain summits is linked to warming. *Nature, 556*, 231–234. https://doi.org/10.1038/s41586-018-0005-6

Steyaert, R. L. (1949). Contribution à l'étude monographique de Pestalotia de Not. et Monochaetia Sacc. *Truncatella* gen. nov. et *Pestalotiopsis* gen. nov. *Bulletin du Jardin Botanique de l'État à Bruxelles, 19*, 285–347. https://doi.org/10.2307/3666710

Steyaert, R. L. (1963). Complementary informations concerning Pestalotiopsis guepini (Desmazieres) Steyaert and designation of its lectotype. *Bulletin du Jardin Botanique de l'État à Bruxelles, 33*, 369–373.

Su, H. Y., Udayanga, D., Luo, Z. L., Manamgoda, D. S., Zhao, Y. C., Yang, J., . . . Hyde, K. D. (2015). Hyphomycetes from aquatic habitats in southern China: Species of Curvularia (Pleosporaceae) and Phragmocephala (Melanommataceae). *Phytotaxa, 226,* 201–216.

Su, H., Hyde, K. D., Maharachchikumbura, S. S. N., Ariyawansa, H. A., Luo, Z., Promputtha, I., . . . Zhou, D. Q. (2016). The families *Distoseptisporaceae* fam. nov., *Kirschsteiniotheliaceae, Sporormiaceae* and *Torulaceae*, with new species from freshwater in Yunnan Province, China. *Fungal Diversity, 80,* 375–409. https://doi.org/10.1007/s13225-016-0362-0

Su, P., Chen, Y., Syed, A., Bahkali, A. H., & Maharachchikumbura, S. S. (2023). Taxonomic novelty in Sichuan Province, China: *Veronaea polyconidia* sp. nov. (Herpotrichiellaceae), a new addition to hyphomycetous fungi. *Phytotaxa, 632,* 118–130. https://doi.org/10.11646/phytotaxa.632.2.2

Subramanian, C. V. (1952). Fungi Imperfecti from Madras—III: *Beltraniella* gen. nov. *Proceedings of the Indian Academy of Sciences, 36*, 223–228. https://doi.org/10.1007/BF03050466

Subramanian, C. V. (1957). Two new species of Petrakia. *Beihefte zur Sydowia, 1*, 14–15.

Subramanian, C. V. (1994). Hyphomycetes from South East Asia—Novelties from Singapore and Malaysia. *Kavaka, 22/23*, 52–76.

Subramanian, C. V., & Vittal, B. P. R. (1973). Three new hyphomycetes from litter. *Canadian Journal of Botany*, *51*, 1127–1132. https://doi.org/10.1139/b73-142

Sugita, R., Hirayama, K., Shirouzu, T., & Tanaka, K. (2022). *Spirodecosporaceae* fam. nov. (Xylariales, Sordariomycetes) and two new species of Spirodecospora. *Fungal Systematics and Evolution, 10,* 217–229.

Sun, Y. R., Hyde, K. D., Liu, N. G., Jayawardena, R. S., Wijayawardene, N. N., Ma, J., . . . Wang, Y. (2025). Micro-fungi in southern China and northern Thailand: Emphasis on medicinal plants. *Fungal Diversity*, *131*, 99–299.

Sun, Y. R., Liu, N. G., Samarakoon, M. C., Jayawardena, R. S., Hyde, K. D., & Wang, Y. (2021). Morphology and phylogeny reveal *Vamsapriyaceae* fam. nov. (Xylariales, Sordariomycetes) with two novel Vamsapriya species. *Journal of Fungi, 7,* 891.

Sutton, B. C. (1980). *The coelomycetes: Fungi imperfecti with pycnidia, aceruli and stromata*. Commonwealth Survey.

Suwannarach, N., Kumla, J., Bussaban, B., & Lumyong, S. (2012). New report of leaf blight disease on eucalyptus (Eucalyptus camaldulensis) caused by Pestalotiopsis virgatula in Thailand. *Canadian Journal of Plant Pathology, 34*(2), 306–309.

Swofford, D. L. (2003). *PAUP: Phylogenetic analysis using parsimony, version 4.0 b10. Laboratory of Molecular Systematics, Smithsonian Institution*. http://www.ncbi.nlm.nih.gov/pmc/articles/PMC3348772

Sydow, H., & Sydow, P. (1917). Beitrag zur Kenntnis der Pilzflora der Philippinen–Inseln. *Annales Mycologici, 15*, 12–268.

Tanaka, K., & Harada, Y. (2003). Pleosporales in Japan (2): The genus Lophiotrema. *Mycoscience, 44*(2), 115–121.

Tanaka, K., & Harada, Y. (2005). Bambusicolous fungi in Japan (4): A new combination, Astrosphaeriella aggregata. *Mycoscience, 46*(2), 114–118.

Tanaka, K., Hirayama, K., Yonezawa, H., Hatakeyama, S., Harada, Y., Sano, T., . . . Hosoya, T. (2009). Molecular taxonomy of bambusicolous fungi: Tetraplosphaeriaceae, a new pleosporalean family with Tetraploa–like anamorphs. *Studies in Mycology, 64*, 175–209.

Tanaka, K., Hirayama, K., Yonezawa, H., Sato, G., Toriyabe, A., Kudo, H., . . . Hosoya, T. (2015). Revision of the Massarineae (Pleosporales, Dothideomycetes). *Studies in Mycology, 82*, 75–136.

Tao, Y., Quan, X., Khokhar, I., Anjum, T., Song, H., & Mukhtar, I. (2021). First report of Pseudopestalotiopsis theae causing leaf spot of date palm (Phoenix dactylifera) in China. *Plant Disease, 105*(2), 508. https://doi.org/10.1094/PDIS-06-20-1356-PDN

Tapia, L., Castillo-Novales, D., Riquelme, N., Valencia, A. L., Larach, A., Cautín, R., . . . Besoain, X. (2025). Rainfall and high humidity influence the seasonal dynamics of spores of *Glomerellaceae* and *Botryosphaeriaceae* genera in avocado orchards and their fruit rot association. *Agronomy, 15*(6), 1453. https://doi.org/10.3390/agronomy15061453

Taylor, J. E., Hyde, K. D., & Jones, E. B. G. (1999). Endophytic fungi associated with the temperate palm, Trachycarpus fortunei, within and outside its natural geographic range. *New Phytologist, 142*(2), 335–346.

Taylor, J. E., Hyde, K. D., & Jones, E. B. G. (2000). The biogeographical distribution of microfungi associated with three palm species from tropical and temperate habitats. *Journal of Biogeography, 27*, 297–310.

Taylor, J. E., Hyde, K. D., & Jones, E. B. G. (2003). Microfungi of tropical and temperate palms. *Fungal Diversity Press, 108*(2), 223–223.

Tennakoon, D. S., de Silva, N. I., Maharachchikumbura, S. S. N., Bhat, D. J., Kumla, J., Suwannarach, N., . . . Lumyong, S. (2023). Exploring more on Dictyosporiaceae: The species geographical distribution and intriguing novel additions from plant litter. *Diversity, 15*, 410.

Tennakoon, D. S., Jeewon, R., Thambugala, K. M., Gentekaki, E., Wanasinghe, D. N., Promputtha, I., . . . Hyde, K. D. (2021). Biphasic taxonomic approaches for generic relatedness and phylogenetic relationships of Teichosporaceae. *Fungal Diversity*, *110*(1), 199–241.

Tennakoon, D. S., Kuo, C. H., Maharachchikumbura, S. S., Thambugala, K. M., Gentekaki, E., Phillips, A. J., . . . Hyde, K. D. (2021). Taxonomic and phylogenetic contributions to Celtis formosana, Ficus ampelas, F. septica, Macaranga tanarius and Morus australis leaf litter inhabiting microfungi. *Fungal Diversity, 108*, 1–215.

Tennakoon, D. S., Phookamsak, R., Kuo, C. H., Goh, T. K., Jeewon, R., & Hyde, K. D. (2018). Morphological and phylogenetic evidence reveal *Fissuroma taiwanense* sp. nov. (Aigialaceae, Pleosporales) from Hedychium coronarium. *Phytotaxa, 338*, 265–275.

Tennakoon, D. S., Thambugala, K. M., de Silva, N. I., Song, H. Y., Suwannarach, N., Chen, F. S., . . . Hu, D. M. (2024). An overview of *Melanommataceae* (Pleosporales, Dothideomycetes): Current insight into the host associations and geographical distribution with some interesting novel additions from plant litter. *MycoKeys, 106*, 43–96.

Ter Steege, H., Pitman, N. C. A., Sabatier, D., Baraloto, C., Salomao, R. P., Guevara, J. E., . . . Silman, M. R. (2013). Hyperdominance in the Amazonian tree flora. *Science, 342*(6156), 1243092-1–1243092-9. https://doi.org/10.1126/science.1243092

Thambugala, K. M., Hyde, K. D., Tanaka, K., Tian, Q., Wanasinghe, D. N., Ariyawansa, H. A., . . . Liu, Z. Y. (2015). Towards a natural classification and backbone tree for Lophiostomataceae, Floricolaceae, and Amorosiaceae fam. nov. *Fungal Diversity, 74*, 199–266. https://doi.org/10.1007/s13225-015-0348-3

Thawatchai, S., & Larsen, K. (2013). *Flora of Thailand* (Vol. 11, Part 3). Forest Herbarium, National Park, Wildlife and Plant Conservation Department.

Thiyagaraja, V., Ertz, D., Hyde, K. D., Karunarathna, S. C., To-Anun, C., & Cheewangkoon, R. (2022). Morphological and phylogenetic reassessment of Sclerococcum simplex from China. *Phytotaxa, 559*(2), 167–175.

Tian, Q., Liu, J. K., Hyde, K. D., Wanasinghe, D. N., Boonmee, S., Jayasiri, S. C., . . . Camporesi, E. (2015). Phylogenetic relationships and morphological reappraisal of Melanommataceae (Pleosporales). *Fungal Diversity, 74*, 267–324.

Tian, W. H., Liu, J. W., Jin, Y., Chen, Y. P., Zhou, Y. F., Wu, K., . . . Maharachchikumbura, S. S. N. (2024). Morphological and phylogenetic studies of Ascomycota from gymnosperms in Sichuan Province, China. *Mycosphere, 15*(1), 1794–1900.

Tian, X. G., Bao, D. F., Karunarathna, S. C., Jayawardena, R. S., Hyde, K. D., Bhat, D. J., . . . Tibpromma, S. (2024). Taxonomy and phylogeny of ascomycetes associated with selected economically important monocotyledons in China and Thailand. *Mycosphere, 15*(1), 1–274.

Tian, X., Karunarathna, S. C., Xu, R., Lu, Y., Suwannarach, N., Mapook, A., . . . Tibpromma, S. (2022). Three new species, two new records and four new collections of Tubeufiaceae from Thailand and China. *Journal of Fungi, 8*(2), 206.

Tibpromma, S., Hyde, K. D., Jeewon, R., Maharachchikumbura, S. S. N., Liu, J. K., Bhat, D. J., . . . Karunarathna, S. C. (2017). Fungal diversity notes 491–602: Taxonomic and phylogenetic contributions to fungal taxa. *Fungal Diversity, 83*, 1–261.

Tibpromma, S., Hyde, K. D., McKenzie, E. H. C., Bhat, D. J., Phillips, A. J. L., Wanasinghe, D. N., . . . Karunarathna, S. C. (2018). Fungal diversity notes 840–928: Micro-fungi associated with Pandanaceae. *Fungal Diversity, 93*, 1–160.

Tibpromma, S., Mortimer, P. E., Karunarathna, S. C., Zhan, F. D., Xu, J., Promputtha, I., . . . Yan, K. (2019). Morphology and multi-gene phylogeny reveal *Pestalotiopsis pinicola* sp. nov. and a new host record of Cladosporium anthropophilum from edible pine (Pinus armandii) seeds in Yunnan Province, China. *Pathogens, 8*(4), 285.

Toapanta-Alban, C. E., Ordoñez, M. E., & Blanchette, R. A. (2022). New findings on the biology and ecology of the Ecuadorian Amazon fungus Polyporus leprieurii var. yasuniensis. *Journal of Fungi, 8*(2), 203.

Torrend, C. (1912). Deuxième contribution pour l'étude des Champignons de l'île de Madère. *Broteria Série Botanique, 10*, 29–49.

Torres-Garcia, D., García, D., Réblová, M., Jurjević, Ž., Hubka, V., & Gené, J. (2023). Diversity and novel lineages of black yeasts in Chaetothyriales from freshwater sediments in Spain. *Persoonia, 51*, 194–228. https://doi.org/10.3767/persoonia.2023.51.05

Trakunyingcharoen, T., Lombard, L., Groenewald, J. Z., Cheewangkoon, R., To-anun, C., & Crous, P. W. (2015). Caulicolous Botryosphaeriales from Thailand. *Persoonia, 34*, 87–99. https://doi.org/10.3767/003158515X685841

Tsui, C. K., Sivichai, S., & Berbee, M. L. (2006). Molecular systematics of *Helicoma*, *Helicomyces* and *Helicosporium* and their teleomorphs inferred from rDNA sequences. *Mycologia, 98*(1), 94–104.

U.S. Department of Energy. (2014). *EnergyPlus™ documentation library* (version 8.2). National Renewable Energy Laboratory. https://bigladdersoftware.com/epx/docs/8-2/getting-started/energyplus-documentation-library.html

Untereiner, W. A. (2000). Capronia and its anamorphs: Exploring the value of morphological and molecular characters in the systematics of the Herpotrichiellaceae. *Studies in Mycology, 45*, 141–148.

Valenzuela-Lopez, N., Magaña-Dueñas, V., Cano-Lira, J. F., Wiederhold, N., Guarro, J., & Stchigel, A. M. (2019). Two new species of Gloniopsis (Hysteriales, Ascomycota) from clinical specimens: Morphological and molecular characterisation. *Mycoses, 62*(12), 1164–1173. https://doi.org/10.1111/myc.13006

Van Horn, B. M., & Nguyen, Q. (2023). *Hands-on application development with PyCharm: Build applications like a pro with the ultimate Python development tool*. Packt Publishing.

Van Rossum, G., & Drake, F. L., Jr. (1995). *Python tutorial* (Vol. 620). Centrum voor Wiskunde en Informatica.

Verkley, G. J. M., da Silva, M., Wicklow, D. T., & Crous, P. W. (2004). *Paraconiothyrium*, a new genus to accommodate the mycoparasite *Coniothyrium minitans*, anamorphs of *Paraphaeosphaeria*, and four new species. *Studies in Mycology, 50*, 323–335. https://edepot.wur.nl/23136

Vilgalys, R., & Hester, M. (1990). Rapid genetic identification and mapping of enzymatically amplified ribosomal DNA from several Cryptococcus species. *Journal of Bacteriology, 172*(8), 4238–4246. https://doi.org/10.1128/jb.172.8.4238-4246.1990

Viret, O., Toti, L., Chapela, I. H., & Petrini, O. (1994). The role of the extracellular sheath in recognition and attachment of conidia of Discula umbrinella (Berk. & Br.) Morelet to the host surface. *New Phytologist, 127*(1), 123–131. https://doi.org/10.1111/j.1469-8137.1994.tb04266.x

von Höhnel, F. (1904). Mycologische Fragmente. *Annales Mycologici, 2*, 38–60.

von Höhnel, F. (1918). Mycologische Fragmente, 272 Über die Hysteriaceen. *Annales Mycologici, 16*, 145–154.

von Höhnel, F. (1923). Studien über Hyphomyzeten. Zentralblatt für Bakteriologie, Parasitenkunde, *Abteilung II, 60*, 1–26.

Wanasinghe, D. N., Jeewon, R., Jones, E. B. G., Boonmee, S., Kaewchai, S., Manawasinghe, I. S., . . . Hyde, K. D. (2018). Novel palmicolous taxa within Pleosporales: Multigene phylogeny and taxonomic circumscription. *Mycological Progress, 17*, 571–590. https://doi.org/10.1007/s11557-018-1379-4

Wanasinghe, D. N., Ren, G. C., Xu, J. C., Cheewangkoon, R., & Mortimer, P. E. (2022). Insight into the taxonomic resolution of the pleosporalean species associated with dead woody litter in natural forests from Yunnan, China. *Journal of Fungi*, *8*(4), 375. https://doi.org/10.3390/jof8040375

Wang, H., Zhao, R., Zhang, H., Cao, X., Li, Z., Zhang, Z., . . . Huang, X. (2020). Prevalence of yellow leaf disease (YLD) and its associated areca palm velarivirus 1 (APV1) in betel palm (Areca catechu) plantations in Hainan, China. *Plant Disease*, *104*(10), 2556–2562. https://doi.org/10.1094/PDIS-01-20-0140-RE

Wang, L., Sarnthein, M., Erlenkeuser, H., Grimalt, J., Grootes, P., Heilig, S., . . . Pflaumann, U. (1999). East Asian monsoon climate during the late Pleistocene: High-resolution sediment records from the South China Sea. *Marine Geology*, *156*(1–4), 245–284. https://doi.org/10.1016/S0025-3227(98)00182-0

Wang, R. X., Luo, Z. L., Hyde, K. D., Bhat, D. J., & Su, X. J. (2016). New species and records of Dictyocheirospora from submerged wood in north-western Yunnan, China. *Mycosphere*, *7*, 1357–1367. https://doi.org/10.5943/mycosphere/7/9/9

Wang, W. P., Bhat, D. J., Yang, L., Shen, H. W., & Luo, Z. L. (2024). New species and records of Pleurotheciaceae from karst landscapes in Yunnan Province, China. *Journal of Fungi*, *10*(8), 516. https://doi.org/10.3390/jof10080516

Wang, Y., Hyde, K. D., McKenzie, E. H. C., Jiang, Y. L., Li, D. W., & Zhao, D. G. (2015). Overview of Stachybotrys (Memnoniella) and current species status. *Fungal Diversity*, *71*(1), 17–83. https://doi.org/10.1007/s13225-014-0319-0

Wang, Z., Fan, P., Xue, T. D., Meng, L. L., Gao, W. B., Zhang, J., . . . Luo, D. Q. (2018). Two new isocoumarin derivatives from an endophytic fungus Pestalotiopsis coffeae isolated from a mangrove fishtail palm. *Natural Product Communications*, *13*, 57–59. https://doi.org/10.1177/1934578X1801300117

Watanabe, K., Motohashi, K., & Ono, Y. (2010). Description of Pestalotiopsis pallidotheae: A new species from Japan. *Mycoscience*, *51*(3), 182–188.

Watanabe, K., Nozawa, S., Hsiang, T., & Callan, B. (2018). The cup fungus *Pestalopezia brunneopruinosa* is *Pestalotiopsis gibbosa* and belongs to Sordariomycetes. *PLoS One*, *13*(6), e0197025. https://doi.org/10.1371/journal.pone.0197025

White, T. J., Bruns, T., Lee, S., & Taylor, J. (1990). Amplification and direct sequencing of fungal ribosomal RNA genes for phylogenetics. *PCR Protocols*, *18*(1), 315–322.

Whitton, S. R., McKenzie, E. H. C., & Hyde, K. D. (2002). Microfungi on the Pandanaceae: Two new species of Camposporium and key to the genus. *Fungal Diversity*, *11*, 177–187.

Wijayawardene, N. N., Hyde, K. D., Al-Ani, L. K. T., Tedersoo, L., Haelewaters, D., Rajeshkumar, K. C., . . . Thines, M. (2020). Outline of fungi and fungus-like taxa. *Mycosphere*, *11*(1), 1060–1456. https://doi.org/10.5943/mycosphere/11/1/8

Wijayawardene, N. N., Hyde, K. D., Dai, D. Q., Sánchez-García, M., Goto, B. T., Saxena, R. K., . . . Thines, M. (2022). Outline of fungi and fungus-like taxa – 2021. *Mycosphere*, *13*(1), 53–453. https://doi.org/10.5943/mycosphere/13/1/2

Wijesinghe, S. N., Samarakoon, M. C., Camporesi, E., Hyde, K. D., Jones, E. B. G., Zucconi Galli Fonseca, L., . . . Wang, Y. (2023). Over the footprints of Italian mycology with emphasis on plant-associated Ascomycota. *Current Research in Environmental & Applied Mycology*, *13*(1), 162–276. https://doi.org/10.5943/cream/13/1/11

Wijesinghe, S. N., Wang, Y., Camporesi, E., Wanasinghe, D. N., Boonmee, S., & Hyde, K. D. (2020). A new genus of Bambusicolaceae (Pleosporales) on Corylus avellana (Fagales) from Italy. *Biodiversity Data Journal*, *8*, e59058. https://doi.org/10.3897/BDJ.8.e59058

Wingfield, M. J., Beer, Z. W. D., Slippers, B., Wingfield, B. D., Groenewald, J. Z., Lombard, L., . . . Crous, P. W. (2012). One fungus, one name promotes progressive plant pathology. *Molecular Plant Pathology*, *13*, 604–613. https://doi.org/10.1111/j.1364-3703.2011.00768.x

Winter, G. (1885). Pilze-Ascomyceten. In G. L. Rabenhorst (Ed.), *Kryptogamen-Flora von Deutschland, Österreich und der Schweiz* (vol. 1, pp. 65–528). Verlag Friedrich von Zezschwitz.

Wu, N., Dissanayake, A. J., Chethana, K. W. T., & Liu, J. K. (2022). *Neodeightonia septata* sp. nov. and N. subglobosa (Botryosphaeriaceae) from northern Thailand. *Phytotaxa, 575*(2), 129–139. https://doi.org/10.11646/phytotaxa.575.2.2

Wu, W. P., & Diao, Y. Z. (2022). Anamorphic chaetosphaeriaceous fungi from China. *Fungal Diversity, 116*, 1–546. https://doi.org/10.21203/rs.3.rs-1253155/v1

Wu, Y., Peng, C., Yuan, R., Zhang, M., Hu, Y., & Tian, C. (2024). New species and records of Botryosphaeriales (Dothideomycetes) associated with tree dieback in Beijing, China. *MycoKeys, 106*, 225–250. https://doi.org/10.3897/mycokeys.106.122890

Xia, J. W., Ma, Y. R., Li, Z., & Zhang, X. G. (2017). Acrodictys-like wood decay fungi from southern China, with two new families Acrodictyaceae and Junewangiaceae. *Scientific Reports, 7*, 7888. https://doi.org/10.1038/s41598-017-08318-x

Xia, J. W., Mu, T. C., Zhang, Z. X., Li, Z., & Zhang, X. G. (2022). *Neoacrodictys elegans* gen. & sp. nov. from Hainan Province, China. *Mycotaxon, 137*, 63–71. https://doi.org/10.5248/137.63

Xiong, Y. R., Lu, L., Mapook, A., & Maharachchikumbura, S. S. N. (in press). Fungal safari on palm trees: New discoveries from East Asia and 1990–2025 years of global records. *Fungal Diversity*.

Xiong, Y. R., Lu, L., Mapook, A., Maharachchikumbura, S. S. N., McKenzie, E. H. C., Kevin, D. H., . . . Manawasinghe, I. S. (in press). Fungal safari on palm trees: New discoveries from East Asia and 1990–2025 years of global records. *Fungal Diversity*.

Xiong, Y. R., Manawasinghe, I. S., Ausana Mapook, Alotibi, F., & Hyde, K. D. (in press). Addition to tropical palm fungi: Ten new records from China and Thailand. *Asian Journal of Mycology*.

Xiong, Y. R., Manawasinghe, I. S., Hyde, K. D., Taylor, J. E., Phillips, A., Pereira, D., . . . Xu, B. (2024). Introducing palmfungi.org, an integrated fungal-host data platform. *Biodiversity Data Journal, 12*, e126553. https://doi.org/10.3897/BDJ.12.e126553

Xiong, Y. R., Manawasinghe, I. S., Liao, C. F., Hyde, K. D., & Dong, Z. Y. (2022). *Neodeightonia arengae* sp. nov., botryosphaeriaceous taxa on Arenga tremula (Arecaceae) from Guangdong, China. *Phytotaxa, 530*, 130–140. https://doi.org/10.11646/phytotaxa.530.2.1

Xiong, Y. R., Manawasinghe, I. S., Lu, L., Mapook, A., Alotibi, F., & Hyde, K. D. (2024). *Neodeightonia guineensis* sp. nov., a palmicolous species from Guangdong, China. *Phytotaxa, 681*, 81-92. https://doi.org/10.11646/phytotaxa.681.1.6

Xiong, Y. R., Manawasinghe, I. S., Maharachchikumbura, S. S. N., Lu, L., Dong, Z. Y., Xiang, M. M., . . . Xu, B. (2022). Pestalotioid species associated with palm species from southern China. *Current Research in Environmental & Applied Mycology (Journal of Fungal Biology), 12*(1), 285–321. https://doi.org/10.5943/cream/12/1/18

Xiong, Y. R., Manawasinghe, I. S., Wanasinghe, D. N., Hongsanan, S., Hyde, K. D., Biao, X., . . . Dong, Z. Y. (2023). Two new species and a new host record of *Pleosporales* (Dothideomycetes) from palm (*Arecaceae*) in Guangdong Province, China. *New Zealand Journal of Botany, 62*(2-3), 1–27. https://doi.org/10.1080/0028825X.2023.2258583

Xu, C. Y., Song, H. Y., Zhou, J. P., Zhai, Z. J., Cui, C. Y., & Hu, D. M. (2025). Four new or newly recorded species from freshwater habitats in Jiangxi Province, China. *Journal of Fungi, 11*, 79. https://doi.org/10.3390/jof11010079

Xu, R. J., Thiyagaraja, V., Li, Y., Zhou, D. Q., Boonmee, S., & Zhao, Q. (2024). Two novel lignicolous freshwater fungi, Conioscypha xizangensis and Cordana linzhiensis, from the Tibetan Plateau, China. *New Zealand Journal of Botany, 62*(2-3), 426-442. https://doi.org/10.1080/0028825X.2024.2336044

Xu, R. J., Zhu, Y. A., Liu, N. G., Boonmee, S., Zhou, D. Q., & Zhao, Q. (2023). Taxonomy and phylogeny of hyphomycetous muriform conidial taxa from the Tibetan Plateau, China. *Journal of Fungi, 9*, 560. https://doi.org/10.3390/jof9050560

Yang, E. F., Dai, D. Q., Bhat, J. D., Dawoud, T. M., Promputtha, I., Adikaram, N., . . . Tibpromma, S. (2023). Taxonomic and phylogenetic studies of saprobic fungi associated with Mangifera indica in Yunnan, China. *Journal of Fungi, 9*(6), 680. https://doi.org/10.3390/jof9060680

Yang, E. F., Tibpromma, S., Karunarathna, S. C., Phookamsak, R., Xu, J. C., Zhao, Z. X., . . . Promputtha, I. (2022). Taxonomy and phylogeny of novel and extant taxa in Pleosporales associated with Mangifera indica from Yunnan, China (series I). *Journal of Fungi, 8*, 152. https://doi.org/10.3390/jof8020152

Yang, H. (1999). From fossils to molecules: The Metasequoia tale continues. *Arnoldia, 58–59*, 60–71.

Yang, J., Liu, J. K., Hyde, K. D., Jones, E. B. G., & Liu, Z. Y. (2018). New species in Dictyosporium, new combinations in Dictyocheirospora and an updated backbone tree for Dictyosporiaceae. *MycoKeys, 36*, 83–105. https://doi.org/10.3897/mycokeys.36.27051

Yang, J., Liu, L. L., Jones, E. B. G., Hyde, K. D., Liu, Z. Y., Bao, D. F., . . . Liu, J. K. (2023). Freshwater fungi from karst landscapes in China and Thailand. *Fungal Diversity*, *119*, 1–212. https://doi.org/10.1007/s13225-023-00514-7

Yang, J., Liu, L. L., Jones, E. B. G., Li, W. L., Hyde, K. D., & Liu, Z. Y. (2021). Morphological variety in Distoseptispora and introduction of six novel species. *Journal of Fungi, 7*, 945. https://doi.org/10.3390/jof7110945

Yang, J., Maharachchikumbura, S. S. N., Liu, J. K., Hyde, K. D., Jones, E. B. G., Al-Sadi, A. M., . . . Liu, Z. Y. (2018). *Pseudostanjehughesia aquitropica* gen. et sp. nov. and Sporidesmium sensu lato species from freshwater habitats. *Mycological Progress, 17*, 591–616. https://doi.org/10.1007/s11557-017-1339-4

Yang, Q., Zeng, X. Y., Yuan, J., Zhang, Q., He, Y. K., & Wang, Y. (2021). Two new species of Neopestalotiopsis from southern China. *Biodiversity Data Journal, 9*, e70446. https://doi.org/10.3897/BDJ.9.e70446

Yang, T., Groenewald, J. Z., Cheewangkoon, R., Jami, F., Abdollahzadeh, J., Lombard, L., . . . Crous, P. W. (2017). Families, genera, and species of Botryosphaeriales. *Fungal Biology, 121*, 322–346. https://doi.org/10.1016/j.funbio.2016.11.001

Yanna, Ho, W. H., & Hyde, K. D. (2001). Fungal communities on decaying palm fronds in Australia, Brunei, and Hong Kong. *Mycological Research, 105*, 1458–1471. https://doi.org/10.1017/S0953756201005214

Yoshida, N., Nobe, R., Ogawa, K., & Murooka, Y. (2000). Origin of Livistona chinensis var. subglobosa (Arecaceae) on the "Islet of the Gods": Aoshima, Japan. *American Journal of Botany, 87*, 1066–1067.

Youssef, F. S., & Simal-Gandara, J. (2021). Comprehensive overview on the chemistry and biological activities of selected alkaloid producing marine-derived fungi as a valuable reservoir of drug entities. *Biomedicines, 9*, 485. https://doi.org/10.3390/biomedicines9050485

Yu, X. D., Zhang, S. N., Cheewangkoon, R., & Liu, J. K. (2021). Additions to *Occultibambusaceae* (Pleosporales, Dothideomycetes): Unrevealing palmicolous fungi in China. *Diversity, 13*, 516. https://doi.org/10.3390/d13110516

Yu, X. D., Zhang, S. N., Liang, X. D., Zhu, J. T., Hyde, K. D., & Liu, J. K. (2024). Bambusicolous fungi from Southwestern China. *Mycosphere, 15*(1), 5038–5145. https://doi.org/10.5943/mycosphere/15/1/24

Zare, R., Gams, W., & Schroers, H. J. (2004). The type species of Verticillium is not congeneric with the plant pathogenic species placed in Verticillium and it is not the anamorph of 'Nectria inventa'. *Mycological Research, 108*, 576–582. https://doi.org/10.1017/S0953756204009839

Zelski, S. E., Raja, H. A., Miller, A. N., & Shearer, C. A. (2015). *Conioscypha peruviana* sp. nov., its phylogenetic placement based on 28S rRNA gene, and a report of Conioscypha gracilis from Peru. *Mycoscience, 56*, 319–325. https://doi.org/10.1016/j.myc.2014.09.002

Zeng, X. Y., Tan, T. J., Tian, F. H., Wang, Y., & Wen, T. C. (2023). OFPT: A one-stop software for fungal phylogeny. *Mycosphere, 14*(1), 1730–1741. https://doi.org/10.5943/mycosphere/14/1/20

Zeng, X., Jeewon, R., Wen, T., Hongsanan, S., Boonmee, S., & Hyde, K. D. (2018). Simplified and efficient DNA extraction protocol for Meliolaceae specimens. *Mycological Progress, 17*, 403–415. https://doi.org/10.1007/s11557-017-1361-6

Zhang, H., Dong, W., Hyde, K. D., Maharachchikumbura, S. S. N., Hongsanan, S., Bhat, D. J., . . . Zhang, D. (2017). Towards a natural classification of *Annulatascaceae*-like taxa: Introducing *Atractosporales ord*. nov. and six new families. *Fungal Diversity, 85*, 75–110. https://doi.org/10.1007/s13225-017-0387-z

Zhang, J. F., Liu, J. K., Hyde, K. D., Chen, Y. Y., Ran, H. Y., & Liu, Z. Y. (2023). Ascomycetes from karst landscapes of Guizhou Province, China. *Fungal Diversity, 122*, 1–160. https://doi.org/10.1007/s13225-023-00524-5

Zhang, J. Y. (in press). Checklist, taxonomy and phylogeny of fungi associated with pteridophytes.

Zhang, J. Y., Ma, J., Xiao, Y. P., Boonmee, S., Kang, J. C., & Lu, Y. Z. (2022). Morphological and phylogenetic analyses reveal five new species in *Chaetosphaeriaceae*. *Journal of Fungi, 8*, 643. https://doi.org/10.3390/jof8060643

Zhang, L., Bao, D. F., Shen, H. W., & Luo, Z. L. (2024). Diversity of lignicolous freshwater fungi from Yuanjiang River in Yunnan (China), with the description of four new species. *Journal of Fungi, 10*, 881. https://doi.org/10.3390/jof10120881

Zhang, L., Ma, J., Ma, X., Feng, X., Bai, X., Huang, Y., . . . Lu, Y. (2023). A new record of Neohelicosporium guangxiense and its secondary metabolites. *Warasan Khana Witthayasat Maha Witthayalai Chiang Mai, 50*(2), 1–12. https://doi.org/10.12982/CMJS.2023.010

Zhang, Q., Yang, Z. F., Cheng, W., Wijayawardene, N. N., Hyde, K. D., Chen, Z., . . . Wang, Y. (2020). Diseases of *Cymbopogon citratus* (Poaceae) in China: *Curvularia nanningensis* sp. nov. *MycoKeys, 63*, 49-67. https://doi.org/10.3897/mycokeys.63.49264

Zhang, S. N., Hyde, K. D., Jones, E. B. G., Cheewangkoon, R., & Liu, J. K. (2020). Additions to Fissuroma and Neoastrosphaeriella (Aigialaceae, Pleosporales) from palms. *Mycosphere, 11*, 269–284. https://doi.org/10.5943/mycosphere/11/1/5

Zhang, S. N., Hyde, K. D., Jones, E. B. G., Yu, Y. D., Cheewangkoon, R., & Liu, J. K. (2024). Current insights into palm fungi with emphasis on taxonomy and phylogeny. *Fungal Diversity, 127*, 55–301. https://doi.org/10.1007/s13225-024-00536-9

Zhang, T. (2019). *Flora Fungorum Sinicorum* (Vol. 51, dematiaceous hyphomycetes from soil). Science Press.

Zhang, W., & Song, X. (2022). Occurrence of leaf spot caused by Neodeightonia phoenicum on pygmy date palm (Phoenix roebelenii) in China. *Plant Disease, 106*(8), 2269. https://doi.org/10.1094/PDIS-10-21-2190-PDN

Zhang, W., Groenewald, J. Z., Lombard, L., Schumacher, R. K., Phillips, A. J. L., & Crous, P. W. (2021). Evaluating species in Botryosphaeriales. *Persoonia, 46*, 63–115. https://doi.org/10.3767/persoonia.2021.46.03

Zhang, W., Groenewald, J. Z., Lombard, L., Schumacher, R. K., Phillips, A. J. L., & Crous, P. W. (2021). Evaluating species in Botryosphaeriales. *Persoonia, 46*, 63–115.

Zhang, Y. M., Maharachchikumbura, S. S. N., McKenzie, E. H., & Hyde, K. D. (2012). A novel species of Pestalotiopsis causing leaf spots of Trachycarpus fortunei. *Cryptogamie Mycologie, 33*, 311–318.

Zhang, Y. M., Maharachchikumbura, S. S. N., Wei, J. G., McKenzie, E. H. C., & Hyde, K. D. (2012). Pestalotiopsis camelliae, a new species associated with grey blight of Camellia japonica in China. *Sydowia, 64*, 335–344.

Zhang, Y. Z., Chen, Q. L., Ma, J., Lu, Y. Z., Chen, H. B., & Liu, N. G. (2023). Morphological and multi-gene phylogenetic analyses reveal five new hyphomycetes from freshwater habitats. *Frontiers in Microbiology, 14*, 1253239. https://doi.org/10.3389/fmicb.2023.1253239

Zhang, Y., Crous, P. W., Schoch, C. L., & Hyde, K. D. (2012). Pleosporales. *Fungal Diversity, 53*, 1–221. https://doi.org/10.1007/s13225-011-0117-x

Zhang, Y., Fournier, J., Bahkali, A. H., & Hyde, K. D. (2011). Inflatispora, a novel lignicolous genus of Pleosporales from France. *Sydowia, 62*, 287–295.

Zhang, Y., Schoch, C. L., Fournier, J., Crous, P. W., de Gruyter, J., Woudenberg, J. H. C., . . . Hyde, K. D. (2009). Multi-locus phylogeny of Pleosporales: A taxonomic, ecological and evolutionary re-evaluation. *Studies in Mycology, 64*, 85–102. https://doi.org/10.3114/sim.2009.64.04

Zhao, G. Z., Liu, X., & Wu, W. (2007). Helicosporous hyphomycetes from China. *Fungal Diversity, 26*, 313–524.

Zhao, H. J., Doilom, M., Mapook, A., Wang, G., Hyde, K. D., & Dong, W. (2024). New insights into Tetraplosphaeriaceae based on taxonomic investigations of bambusicolous fungi and freshwater fungi. *Journal of Fungi, 10*, 319. https://doi.org/10.3390/jof10050319

Zhao, H., Mapook, A., Hyde, K. D., Doilom, M., Al-Otibi, F. O., Saichana, N., . . . Dong, W. (2025). Xylolentia bambusae (Rhamphoriaceae, Rhamphoriales), a novel species associated with dead bamboo in Guangdong Province, China. *Phytotaxa, 681*(2), 211–222. https://doi.org/10.11646/phytotaxa.681.2.6

Zheng, L., Xi, P., Tu, J. J., Chen, X., Li, J., Qin, X., . . . Xie, C. (2017). First report of Phoma herbarum causing leaf spot of oil palm (Elaeis guineensis) in China. *Plant Disease, 101*(4), 629–630. https://doi.org/10.1094/PDIS-05-16-0692-PDN

Zhou, D. Q., & Hyde, K. D. (2001). Host-specificity, host-exclusivity, and host-recurrence in saprobic fungi. *Mycological Research, 105*, 1449–1457. https://doi.org/10.1017/S0953756201004713

Zhu, H. (2016). A biogeographical comparison between Yunnan Southwest China, and Taiwan, Southeast China with implications for the evolutionary history of the East Asian flora. *Annals of the Missouri Botanical Garden, 101*(4), 750–771. https://doi.org/10.3417/2011037

Zhu, H. (2017). Tropical flora of southern China. *Shengwu Duoyangxing, 25*(2), 72–79. https://doi.org/10.17520/biods.2016055

Zogg, H. (1962). Die Hysteriaceae s. str. und Lophiaceae. *Beiträge zur Kryptogamenflora der Schweiz, 11*(3), 1–190.

Zou, B., Long, W., & Yang, Wu, L. H. (2021). The complete plastid genome of Phoenix canariensis Chabaud (Arecaceae) and phylogenetic analysis. *Mitochondrial DNA Part B, 6*(1), 140–142. https://doi.org/10.1080/23802359.2020.1852900

Zuur, A. F., Ieno, E. N., Walker, N. J., Saveliev, A. A., & Smith, G. M. (2009). *Mixed effects models and extensions in ecology with R*. Springer. https://doi.org/10.1007/978-0-387-87458-6

APPENDIX A

MEDIA AND CHEMICAL REAGENTS

1. Malt Extract Agar (MEA) used for fungal cultivation

Agar 15 g

Peptone 0.78 g

Glycerol 2.35 g

Dextrin 2.75 g

Maltose, Technical 12.75 g

Suspend 33.6 g of malt extract agar in distilled water and mix thoroughly. Heat with frequent agitation and boil for 1 minute to completely dissolve the power and bring volume to 1000 ml. Autoclave at 121ºC for 20 minutes.

2. Potato dextrose agar (PDA) used for fungal cultivation

Potato starch (from the infusion) 4 g

Dextrose 20 g

Agar 15 g

Suspend 39 g of Potato dextrose agar in distilled water and mix thoroughly. Heat with frequent agitation and boil for 1 minute to completely dissolve the powder and bring the volume to 1000 ml. Autoclave at 121ºC for 20 minutes.

3. Water Agar (WA) used for Fungal Collection

Agar 15 g

Suspend 15 g of agar in distilled water and mix thoroughly. Heat with frequent agitation and boil for 1 minute to completely dissolve the powder and bring the volume to 1000 ml. Autoclave at 121°C for 20 minutes.

4. Melzer's Reagent used for the identification of ascomycete fungi. Amyloid reaction of asci changed to blue or heavily purple colors.

5. Indian ink used for observing gelatinous appendages of ascospores in some species.

APPENDIX B

ABSTRACT OF PUBLICATIONS



Current Research in Environmental & Applied Mycology (Journal of Fungal Biology)
12(1): 285–321 (2022) ISSN 2229-2225
www.creamjournal.org
Article
Doi 10.5943/cream/12/1/18

Pestalotioid species associated with palm species from Southern China

Xiong YR[1,2,5], Manawasinghe IS[1,*], Maharachchikumbura SSN[3], Lu L[2,5,6], Dong ZY[1,4], Xiang MM[1] and Xu B[1]

[1]*Innovative Institute for Plant Health, Zhongkai University of Agriculture and Engineering, Guangzhou 510225, China*
[2]*Center of Excellence in Fungal Research, Mae Fah Luang University, Chiang Rai 57100, Thailand*
[3]*School of Life Science and Technology, Centre for Informational Biology, University of Electronic Science and Technology of China, Chengdu 611731, China*
[4]*Key Laboratory of Green Prevention and Control on Fruits and Vegetables in South China, Ministry of Agriculture and Rural Affairs, China*
[5]*School of Science, Mae Fah Luang University, Chiang Rai 57100, Thailand*
[6]*Center for Yunnan Plateau Biological Resources Protection and Utilization, College of Biological Resource and Food Engineering, Qujing Normal University, Qujing, Yunnan 655011, China*

Xiong YR, Manawasinghe IS, Maharachchikumbura SSN, Lu L, Dong ZY, Xiang MM, Xu B 2022 – Pestalotioid species associated with palm species from Sothern China. Current Research in Environmental & Applied Mycology (Journal of Fungal Biology) 12(1), 285–321, Doi 10.5943/cream/12/1/18

Abstract

Palm is the largest monocot group widely distributed in tropical and subtropical regions. The importance of palm species ranges from food sources to landscape. Therefore, the identification and characterization of pathogens associated with these hosts have economic and ecological significance. During surveys in 2020 to 2021, leaf spots on diseased *Sabal mexicana* and rotting tissues of *Areca triandra*, *Arenga pinnata*, *Dypsis leptocheilos*, *Washingtonia robusta* were collected from three cities in southwestern China. Fungal isolates were identified using morphological characterization and phylogenetic analysis based on the internal transcribed spacer (ITS) region of ribosomal DNA, beta-tubulin (*tub2*) gene and part of the translation elongation factor 1-alpha (*tef* 1-α). Six *Neopestalotiopsis* isolates and 22 *Pestalotiopsis* isolates were obtained. These isolates were further confirmed as two novel species described here as *P. guangdongnsis* and *P. sabal*; and three new host records *N. formicidarum*, *P. diploclisae*, *P. kandelicola*; and one unclassified *Neopestalotiopsis* sp. Pathogenicity assays were conducted on potted *Sabal mexicana* leaves for all isolated taxa. The results revealed that all species isolated from this study induced weak lesions on *Sabal mexicana* leaves. Pathogens were reisolated, and Koch's postulates were fulfilled. The results from this study will be an addition to micro-fungi associated with palm trees. Moreover, pathogenicity test results revealed the opportunistic nature of pestalotioid species on *Sabal mexicana*. These results will provide a basic platform to understand the pathogenic mechanisms and lifestyle of pestalotioid species in the future.

Key words – 2 new species – 3 new host records – *Neopestalotiopsis* – *Pestalotiopsis* – Pathogenicity – *Sporocadaceae*

Introduction

Palm trees (*Arecaceae*) are important and more prominent in the tropics due to their extensive uses as food sources, construction materials, handicrafts, landscaping, and alternative medicine

Submitted 25 August 2022, Accepted 19 October 2022, Published 16 November 2022
Corresponding Author: I.S. Manawasinghe – e-mail – ishara9017@gmail.com

Phytotaxa 530 (2): 130–140
https://www.mapress.com/pt/
Copyright © 2022 Magnolia Press

Article

ISSN 1179-3155 (print edition)
PHYTOTAXA
ISSN 1179-3163 (online edition)

https://doi.org/10.11646/phytotaxa.530.2.1

Neodeightonia arengae sp. nov., Botryosphaeriaceous taxa on *Arenga tremula* (*Arecaceae*) from Guangdong, China

YINRU XIONG[1,2,3,4], ISHARA S. MANAWASINGHE[1,5], CHUNFANG LIAO[1,2,3,6], KEVIN D. HYDE[1,2,7] & ZHANGYONG DONG[1,8]*

[1] *Innovative Institute for Plant Health, Zhongkai University of Agriculture and Engineering, Guangzhou 510225, P.R. China*
[2] *Center of Excellence in Fungal Research, Mae Fah Luang University, Chiang Rai 57100, Thailand*
[3] *School of Science, Mae Fah Luang University, Chiang Rai 57100, Thailand*
[4] *richard_xyr@163.com; https://orcid.org/0000-0002-4673-606X*
[5] *ishara.ishara@yahoo.com; https://orcid.org/0000-0001-5730-3596*
[6] *6371105002@lamduan.mfu.ac.th; https://orcid.org/0000-0002-6309-1101*
[7] *kdhyde3@gmail.com; https://orcid.org/0000-0002-2191-0762*
[8] *dongzhangyong@hotmail.com; https://orcid.org/0000-0001-7524-0226*
**Corresponding author: Zhang-yong Dong, dongzhangyong@hotmail.com*

Abstract

Microfungi associated with palm are a significant fungal group with a unique ecological niche and a broad distribution in tropical regions. Even though many fungal species have been reported from palm hosts, studies on fungi from *Arenga tremula* are considerably few. In this study, we isolated a saprobic *Botryosphaeriaceae* species on *A. tremula*, collected from Guangzhou, Guangdong Province, China. Morphological characteristics and phylogenetic analysis of the internal transcribed spacer (ITS), small subunit nuclear rRNA gene (SSU),part of the large subunit nuclear rRNA gene (LSU) and translation elongation factor 1−alpha gene (*tef* 1-α). Based on phylogenetic results and morphology we introduced *Neodeightonia arengae sp. nov.*, with species description and illustrations. In addition, we provide a comparison of morphological characters of currently accepted *Neodeightonia* species. This is the first report of a *Neodeightonia* species associated with *Arenga tremula* and so represents an additional contribution to the knowledge of fungi associated with palm trees.

Keywords: 1 new species, *Botryosphaeriaceae*, multi-gene, palm fungi, saprobic

Introduction

Palm fungi are one of the most diverse and largest groups of fungi. There are more than 1500 species previously described from palm trees representing almost all major fungal classes (Fröhlich & Hyde 2000, Taylor & Hyde 2003). Up until 2000, a diverse group of fungal species had been described from palm hosts. In total 794 ascomycetes species belonged to 79 families, 278 genera and 79 families had been introduced. (Hyde 1994, Htde & Cannon 1999, Fröhlich & Hyde 2000, Hyde *et al.* 2000, Taylor & Hyde 2003). Thereafter, several new genera and species have been described (Pinruan *et al.* 2010, Ligoxigakis *et al.* 2013). The consistent new discoveries indicate the potential identification of novel fungal taxa from palm trees due to their yet to be fully appreciated diversity.

Guangdong Province is one of the most populated cities with a subtropical climate (Gao *et al.* 2020). During the last decades, more than 70 varieties of palm plants from other provinces and abroad were introduced into the Guangdong Province. Palm trees are mostly used as a greening tree species, ornamental plants and garden plants or natural gardens in Guangdong Province. (Cai *et al.* 2007). According to the data from the National Specimen Information Infrastructure (NSII), 71 palm species in Guangdong Province have been identified. (http://www.nsii.org.cn/2017/query.php?name=\u5e7f\u4e1c data retrieved on 23/5/2021), including *Caryota mitis, C. ochlandra*, and *Rhapis gracilis*. However, microfungi associated with these species have not yet been well studied or documented.

Botryosphaeriaceae (*Botryosphaeriales*, Dothideomycetes) species are well-known plant pathogens, saprobes, and endophytes on a wide range of hosts worldwide (Phillips *et al.* 2013). Their ecological role varies with the host and geography (Slippers & Wingfield 2007, Phillips *et al.* 2013). Currently, there are 24 genera accepted in this

 Accepted by Sinang Hongsanan: 10 Dec. 2021; published: 10 Jan. 2022
Licensed under Creative Commons Attribution-N.C. 4.0 International https://creativecommons.org/licenses/by-nc/4.0/

NEW ZEALAND JOURNAL OF BOTANY
https://doi.org/10.1080/0028825X.2023.2258583

Taylor & Francis
Taylor & Francis Group

RESEARCH ARTICLE

Check for updates

Two new species and a new host record of Pleosporales (Dothideomycetes) from palm (*Arecaceae*) in Guangdong Province, China

Yinru Xiong [a,b,c], Ishara S. Manawasinghe [a,d], Dhanushka N. Wanasinghe [e], Sinang Hongsanan [f,g,h], Kevin D. Hyde [a,b,c,i], Xu Biao [a] and Zhangyong Dong [a]

[a]Innovative Institute for Plant Health, Key Laboratory of Green Prevention and Control on Fruits and Vegetables in South China, Ministry of Agriculture and Rural Affairs, Zhongkai University of Agriculture and Engineering, Guangzhou, People's Republic of China; [b]Center of Excellence in Fungal Research, Mae Fah Luang University, Chiang Rai, Thailand; [c]School of Science, Mae Fah Luang University, Chiang Rai, Thailand; [d]Beijing Key Laboratory of Environment-Friendly Management on Fruit Diseases and Pests in North China, Institute of Plant Protection, Beijing Academy of Agriculture and Forestry Sciences, Beijing, People's Republic of China; [e]Center for Mountain Futures, Kunming Institute of Botany, Chinese Academy of Sciences, Honghe, People's Republic of China; [f]Faculty of Sciences, Research Center of Microbial Diversity and Sustainable Utilization, Chiang Mai University, Chiang Mai, Thailand; [g]Faculty of Agriculture, Department of Entomology and Plant Pathology, Chiang Mai University, Chiang Mai, Thailand; [h]Shenzhen Key Laboratory of Microbial Genetic Engineering, College of Life Sciences and Oceanography, Shenzhen University, Shenzhen, People's Republic of China; [i]CAS Key Laboratory for Plant Diversity and Biogeography of East Asia, Kunming Institute of Botany, Chinese Academy of Science, Kunming, People's Republic of China

ABSTRACT

Pleosporales is the largest order of Ascomycota which is distributed worldwide. Among the wide range of hosts, Pleosporales species are frequently isolated from palms. During the surveys of palm fungi from 2020 to 2021, rotting tissues of *Licuala peltata* var. *sumawongii*, *Phoenix roebelenii* and *Trachycarpus fortunei* were collected in Guangzhou, Guangdong Province, China. Fungal isolates were identified based on morphological characteristics and multi-gene phylogenetic analyses. In the present study, we introduce two new species viz. *Byssosphaeria guangdongense* and *Paraconiothyrium guangdongensis*. In addition, we introduce a new host record for *Trachycarpus fortunei*. Photo plates, detailed descriptions, and in-depth phylogenetic analysis results are provided for all identified taxa. Our findings expand the understanding of the fungi that are associated with palm hosts. Moreover, our data will contribute to the knowledge of the biodiversity of South China.

ARTICLE HISTORY
Received 31 July 2023
Accepted 4 September 2023
First published online 5 October 2023

HANDLING EDITOR
Indunil Senanayake

KEYWORDS
Byssosphaeria; *Magnibotryascoma*; *Paraconiothyrium*; phylogeny; saprobic fungi; 2 new species

Introduction

Palm species (*Arecaceae*) are widely distributed in tropical and subtropical regions and have a significant impact on forest ecosystems, including carbon sequestration, food and resources for a large number of animals and humans (Bacon and Bailey 2006; Cámara-Leret et al. 2017; Levis et al. 2017; Muscarella et al. 2020). *Arecaceae* includes ~2600 species, classified into climbers, shrubs and trees belonging to 181

CONTACT Ishara S. Manawasinghe ishara9017@gmail.com; Kevin D. Hyde kdhyde3@gmail.com
© 2023 The Royal Society of New Zealand

Biodiversity Data Journal

Home Articles About About Pensoft Books Journals Blog

Research Article

Biodiversity Data Journal 12: e126553
https://doi.org/10.3897/BDJ.12.e126553 (02 Oct 2024)

Introducing palmfungi.org, an integrated fungal-host data platform

Yinru Xiong, Ishara S. Manawasinghe, Kevin D. Hyde, Joanne E. Taylor, Alan Phillips, Diana Santos Pereira, Li Lu, Sheng-Nan Zhang, Ausana Mapook, Biao Xu

Abstract

Palm fungi are a diverse and unique group mostly found on Arecaceae hosts. They have been studied for approximately 200 years resulting in a large number of known fungal species representing over 700 genera. The timeline of palm fungal studies could be roughly divided into three phases, based on the methods and frequency of reports. They are the "Historical palm fungi era", "Classical palm fungi era" and "Molecular palm fungi era". In the first two periods, the identification of palm fungi was based on morphology, which resulted in a considerable number of morphological species scattered across the data in books, monographs and papers. With the advancement of molecular techniques, studies on palm fungi accelerated. A large number of new species were introduced in the molecular era, especially from Asia, including China and Thailand. However, there is a necessity to link these three generations of studies into a single platform combining data related to host factors, geography and utilisation. Herein, we introduce the palm fungi website: https://palmfungi.org, an integrated data platform for interactive retrieval, based on palm and fungal species. This website is not only a portal for the latest, comprehensive species information on palm fungi, but also provides a new platform for fungal researchers to explore the host-specificity of palm fungi. Additionally, this study uses palmfungi.org and related data to briefly discuss the current status of research on the distribution of palm fungi populations, showing how palmfungi.org links fungi with their palm hosts. Furthermore, the website will act as a platform for collaboration amongst taxonomists, plant pathologists, botanists, ecologists and those who are interested in palms and their relationship with ecological sustainability.

Keywords

Arecaceae, Ascomycota, Basidiomycetes, website, fungal host interaction

MycoKeys

MycoKeys 108: 287–315 (2024)
DOI: 10.3897/mycokeys.108.128889

Research Article

Novel *Helicoma* and *Neohelicosporium* (Tubeufiaceae, Tubeufiales) species and two new host records of *Helicoma* on tropical palms (Arecaceae) from China

Yinru Xiong[1,2,3], Kevin D. Hyde[2,3,4,8], Li Lu[2,3,5], Dulanjalee L. Harishchandra[6,7], Ausana Mapook[3], Biao Xu[1], Fatimah Alotibi[8], Ishara S. Manawasinghe[1]

1 *Innovative Institute for Plant Health, Zhongkai University of Agriculture and Engineering, Guangzhou 510225, Guangdong, China*
2 *School of Science, Mae Fah Luang University, Chiang Rai 57100, Thailand*
3 *Center of Excellence in Fungal Research, Mae Fah Luang University, Chiang Rai 57100, Thailand*
4 *CAS Key Laboratory for Plant Diversity and Biogeography of East Asia, Kunming Institute of Botany, Chinese Academy of Science, Kunming, China*
5 *Center for Yunnan Plateau Biological Resources Protection and Utilization, College of Biological Resource and Food Engineering, Qujing Normal University, Qujing, Yunnan 655011, China*
6 *Office of Research Administration, Chiang Mai University, Chiang Mai 50200, Thailand*
7 *Department of Entomology and Plant Pathology, Faculty of Agriculture, Chiang Mai University, Chiang Mai 50200, Thailand*
8 *Department of Botany and Microbiology, College of Science, King Saud University, P.O. Box 22452, 11495 Riyadh, Saudi Arabia*
Corresponding authors: Kevin D. Hyde (kdhyde3@gmail.com); Ishara S. Manawasinghe (ishara9017@gmail.com)

OPEN ACCESS

This article is part of:
Exploring the Hidden Fungal Diversity: Biodiversity, Taxonomy, and Phylogeny of Saprobic Fungi
Edited by Samantha C. Karunarathna, Danushka Sandaruwan Tennakoon, Ajay Kumar Gautam

Academic editor: S. C. Karunarathna
Received: 3 June 2024
Accepted: 30 July 2024
Published: 13 September 2024

Citation: Xiong Y, Hyde KD, Lu L, Harishchandra DL, Mapook A, Xu B, Alotibi F, Manawasinghe IS (2024) Novel *Helicoma* and *Neohelicosporium* (Tubeufiaceae, Tubeufiales) species and two new host records of *Helicoma* on tropical palms (Arecaceae) from China. MycoKeys 108: 287–315. https://doi.org/10.3897/mycokeys.108.128889

Copyright: © Yinru Xiong et al.
This is an open access article distributed under terms of the Creative Commons Attribution License (Attribution 4.0 International – CC BY 4.0).

Abstract

Asexual species of Tubeufiaceae are characterised as helicosporous hyphomycetes and are abundantly discovered in tropical and subtropical regions. The present study collected helicosporous fungal samples from rotting tissues of *Caryota mitis*, *Elaeis guineensis* and *E. oleifera* in Xishuangbanna, Yunan Province, China. Fungal isolates were identified, based on the morphological characteristics and multi-gene phylogeny with DNA sequence data of the internal transcribed spacer (ITS), part of the large subunit nuclear rRNA gene (LSU), translation elongation factor 1-alpha gene (*tef* 1-α) and RNA polymerase II second largest subunit gene (*rpb2*). Herein, we introduce three new species viz. *Helicoma oleifera*, *Neohelicosporium guineensis* and *N. xishuangbannaensis*. In addition, we introduce two new host records of *Helicoma guttulatum* and *H. rufum* on *Caryota mitis*. The illustrations of all identified species, detailed descriptions and in-depth phylogenetic analyses are provided. Our results add new knowledge of fungal species associated with palm hosts in southern China. Moreover, our data will contribute to the biodiversity of fungi in tropical China.

Key words: *Caryota mitis*, *Elaeis guineensis*, *Elaeis oleifera*, helicosporous fungi, phylogeny, saprobic fungi, taxonomy, three new species

Introduction

Regions in southern China exhibit characteristics of a monsoon climate and its weather patterns are additionally influenced by the geographical distribution and differentiation of land and sea (Wang et al. 1999; Peng et al. 2021). Therefore, the boundaries of China's tropics are long and incoherent (Gongfu et al. 1990).

Phytotaxa 681 (1): 081–092
https://www.mapress.com/pt/
Copyright © 2025 Magnolia Press

Article

ISSN 1179-3155 (print edition)
PHYTOTAXA
ISSN 1179-3163 (online edition)

https://doi.org/10.11646/phytotaxa.681.1.6

Neodeightonia guineensis sp. nov., a palmicolus species from Guangdong, China

YINRU XIONG[1,2,3,6], ISHARA S. MANAWASINGHE[3,7], LI LU[1,2,4,8], AUSANA MAPOOK[2,9]*, FATIMAH ALOTIBI[5,10] & KEVIN D. HYDE[1,2,3,5,11]*

[1]*School of Science, Mae Fah Luang University, Chiang Rai 57100, Thailand*
[2]*Center of Excellence in Fungal Research, Mae Fah Luang University, Chiang Rai 57100, Thailand*
[3]*Innovative Institute for Plant Health, College of Agriculture and Biology, Zhongkai University of Agriculture and Engineering, Guangzhou 510225, Guangdong, P.R. China*
[4]*Center for Yunnan Plateau Biological Resources Protection and Utilization, College of Biological Resource and Food Engineering, Qujing Normal University, Qujing, Yunnan 655011, China*
[5]*Department of Botany and Microbiology, College of Science, King Saud University, P.O. Box 22452, 11495 Riyadh, Saudi Arabia*
[6] *richard_xyr@163.com; https://orcid.org/0000-0002-4673-606X*
[7] *ishara9017@gmail.com; https://orcid.org/0000-0001-5730-3596*
[8] *6371105004@lamduan.mfu.ac.th; https://orcid.org/0000-0003-0977-6414*
[9] *phung.ausana@gmail.com; https://orcid.org/0000-0001-7929-2429*
[10] *falotibi@ksu.edu.sa; https://orcid.org/0000-0003-3629-5755*
[11] *kdhyde3@gmail.com; https://orcid.org/0000-0002-2191-0762*
**Corresponding authors: kdhyde3@gmail.com, phung.ausana@gmail.com*

Abstract

Palm fungi encompass nearly all major fungal taxa and possess a broad spectrum of ecological roles. *Neodeightonia* species are mainly associated with a wide range of palm trees. In this study, a saprobic *Neodeightonia* species was isolated from *Elaeis guineensis* in Xishuangbanna, Yunnan Province, China. For species delineation, morphological characteristics and phylogenetic analysis of the internal transcribed spacer (ITS), and translation elongation factor 1−alpha gene (*tef* 1-α) were conducted. Based on the phylogenetic results and morphology, *Neodeightonia guineensis* is introduced as a new species along with a description and illustrations. Additionally, the taxonomic status of some species within *Neodeightonia* is discussed. Based on our phylogenetic and morphological comparisons, ITS and *tef* 1-α gene region play the most important role in species delineation in *Neodeightonia* species. This is the first report of a *Neodeightonia* species associated with *Elaeis guineensis*, thereby enhancing the diversity of fungi associated with palm trees.

Key words: 1 new species, Arecaceae, Botryosphaeriaceae, *Elaeis guineensis*, multi-gene, saprobic

Introduction

Palms (Arecaceae) represent a monocot family that includes climbers, shrubs, and trees, and are an important substratum for exploring fungal diversity (Baker & Dransfield 2016, Nadot *et al.* 2016, Pereira *et al.* 2023). In recent years, a series of Dothideomycetes, including Botryosphaeriaceae species, have been frequently described from various palms based on morpho-molecular data (Phookamsak *et al.* 2015, Hongsanan *et al.* 2020a, b, Pereira *et al.* 2023, Samarakoon *et al.* 2024). Botryosphaeriaceae are predominantly pathogens that impact a wide range of crops and forest plants globally, while also exhibiting close associations with palm trees (Sakalidis *et al.* 2011, Ligoxigakis *et al.* 2013, Konta *et al.* 2016, Santos *et al.* 2017, Ramjegathesh *et al.* 2020, Batista *et al.* 2021).

Botryosphaeriaceae constitutes a fungal family rich in species and featuring diverse ecological roles (Phillips *et al.* 2013, Manawasinghe *et al.* 2022, Rathnayaka *et al.* 2023, Zhou *et al.* 2023, Hyde *et al.* 2024). These fungi can be saprobic, endophytic, or latent pathogens (Slippers & Wingfield 2007, Phillips *et al.* 2013). Botryosphaeriaceae was first introduced as a sub-family in the *Pseudosphaeriaceae* by Theissen & Sydow (1918), with *Botryosphaeria* as the type genus. After nearly a century of alterations, Schoch *et al.* (2006) proposed order Botryosphaeriales to accommodate Botryosphaeriaceae, based on a multigene phylogenetic analysis of sequence data from the small subunit nuclear rRNA gene (SSU), 28S rRNA gene (LSU), translation elongation factor 1-alpha (*tef* 1-α), and RNA polymerase second largest subunit (*rpb2*). Currently, Botryosphaeriaceae contains 22 genera including *Neodeightonia* (Wijayawardene *et al.* 2022, Hyde *et al.* 2024, Pem *et al.* 2024).

Accepted by Eric McKenzie: 27 Nov. 2024; published: 8 Jan. 2025

CURRICULUM VITAE

NAME Yinru Xiong

EDUCATIONAL BACKGROUND

2016-2020 Bachelor of School of Food and Pharmaceutical Engineering, Guizhou Institute of Technology, China

PUBLICATIONS

First Author Publications

Xiong, Y. R., Manawasinghe, I. S., Maharachchikumbura, S. S. N., Lu, L., Dong, Z. Y., Xiang, M. M., . . . Xu, B. (2022). Pestalotioid species associated with palm species from Southern China. *Current Research in Environmental & Applied Mycology (Journal of Fungal Biology), 12*(1), 285–321. https://doi.org/10.5943/cream/12/1/18

Xiong, Y., Hyde, K. D., Lu, L., Harishchandra, D. L., Mapook, A., Xu, B., . . . Manawasinghe, I. S. (2024). Novel *Helicoma* and *Neohelicosporium* (Tubeufiaceae, Tubeufiales) species and two new host records of *Helicoma* on tropical palms (Arecaceae) from China. *MycoKeys, 108*, 287–315. https://doi.org/10.3897/mycokeys.108.128889

Xiong, Y., Manawasinghe, I. S., Hyde, K. D., Taylor, J. E., Phillips, A., Pereira, D., . . . Xu, B. (2024). Introducing palmfungi.org, an integrated fungal-host data platform. *Biodiversity Data Journal, 12*, e126553. https://doi.org/10.3897/BDJ.12.e126553

Xiong, Y., Manawasinghe, I. S., Liao, C., Hyde, K. D., & Dong, Z. (2022). *Neodeightonia arengae* sp. nov., Botryosphaeriaceous taxa on *Arenga tremula* (Arecaceae) from Guangdong, China. *Phytotaxa, 530*(2), 130–140.

Xiong, Y., Manawasinghe, I. S., Lu, L., Mapook, A., Alotibi, F., & Hyde, K. D. (2025). *Neodeightonia guineensis* sp. nov., a palmicolus species from Guangdong, China. *Phytotaxa, 681*(1), 81–92.

Xiong, Y., Manawasinghe, I. S., Wanasinghe, D. N., Hongsanan, S., Hyde, K. D., Biao, X., . . . Dong, Z. (2024). Two new species and a new host record of Pleosporales (Dothideomycetes) from palm (Arecaceae) in Guangdong Province, China. *New Zealand Journal of Botany, 62*(2–3), 165–191.

Xiong, Y. R., Lu, L., Mapook, A., Maharachchikumbura, S. S. N., McKenzie, E. H. C., Hyde, K. D., . . . Manawasinghe, I. S. (in press). Fungal safari on palm trees: New discoveries from East Asia and 1990-2025 years of global records. *Fungal Diversity*.

Xiong, Y. R., Manawasinghe, I. S., & Mapook, A. (in press). Addition to tropical palm fungi: Ten new Records from China and Thailand. *Asian Journal of Mycology*.

Xiong, Y. R., Mapook, A., Chen, C., Han, M. Y., Hyde, K. D., & Manawasinghe, I. S. (in press). *Pleopunctum livistonae*, a new species on *Livistona chinensis* in Jiangxi Province, China. *Chiang Mai Journal of Science*.

Co-author

Cao, B., Phurbu, D., Ralaiveloarisoa, A., Liimatainen, K., Niskanen, T., Ramírez-Cruz, V., . . . Zhao, R. L. (2025). Fungal diversity notes 1919–2016: Taxonomic and phylogenetic contributions to fungal taxa. *Fungal Diversity, 132*, 425-651. https://doi.org/10.1007/s13225-025-00556-z

Hongsanan, S., Khuna, S., Manawasinghe, I. S., Tibpromma, S., Chethana, K. W. T., Xie, N., . . . Karunarathna, S. C. (2025). Mycosphere notes 521–571: A special edition of fungal biodiversity to celebrate Kevin D. Hyde's 70th birthday and his exceptional contributions to mycology. *Mycosphere, 16*(2), 1–178. https://doi.org/10.5943/mycosphere/16/2/1

Hyde, K. D., Abdel-Wahab, M. A., Abdollahzadeh, J., Abeywickrama, P. D., Absalan, S., Afshari, N., . . . Ertz, D. (2023). Global consortium for the classification of fungi and fungus-like taxa. *Mycosphere*, *14*(1), 1960–2012. https://doi.org/10.5943/mycosphere/14/1/23

Hyde, K. D., Amuhenage, T. B., Apurillo, C. C. S., Asghari, R., Aumentado, H. D., Bahkali, A. H., . . . Dai, D. Q. (2023). Fungalpedia, an illustrated compendium of the fungi and fungus-like taxa. *Mycosphere, 14*(1),1835–1959. https://doi.org/10.5943/mycosphere/14/1/22

Hyde, K. D., Noorabadi, M. T., Thiyagaraja, V., Mq, H., Johnston, P. R., Wijesinghe, S. N., . . . Dianese, J. (2024). The 2024 outline of fungi and fungus-like taxa. *Mycosphere*, *15*(1), 5146–6239. https://doi.org/10.5943/mycosphere/15/1/25

Hyde, K. D., Wijesinghe, S. N., Amuhenage, T. B., Bera, I., Bhunjun, C. S., Chethana, K. W. T., . . . Zhao, H. J. (2024). Current research in applied and environmental mycology fungal profiles 1-30. *Current Research in Environmental & Applied Mycology (Journal of Fungal Biology), 14*(1), 167–266. https://doi.org/10.5943/cream/14/1/11

Lu, L., Karunarathna, S. C., Dai, D. Q., Xiong, Y. R., Suwannarach, N., Stephenson, S. L., . . . Tibpromma, S. (2022). Description of four novel species in pleosporales associated with coffee in Yunnan, China. *Journal of Fungi*, *8*(10), 1113. https://doi.org/10.3897/mycokeys.87.79433

Lu, L., Karunarathna, S. C., Rajeshkumar, K. C., Elgorban, A. M., Jayawardena, R. S., Hongsanan, S., . . . Tibpromma, S. (2025). Unveiling fungal diversity associated with coffee trees in China using a polyphasic approach and a global review of coffee saprobic fungi. *IMA Fungus*, *16*, e144874. https://doi.org/10.3897/imafungus.16.144874

Manawasinghe, I. S., Hyde, K. D., Wanasinghe, D. N., Karunarathna, S. C., Maharachchikumbura, S. S., Samarakoon, M. C., . . . Zhang, W. (2025). Fungal diversity notes 1818–1918: Taxonomic and phylogenetic contributions on genera and species of fungi. *Fungal Diversity*, *130*(1), 1-261.

Manawasinghe, I. S., Zhang, Y. X., Liao, C. F., Xiong, Y. R., Kularathnage, N. D., Luo, M., . . . Gafforov, Y. S. (2022). Mycosphere notes 345–386. *Mycosphere*, *13*(1), 454-557.

Phukhamsakda, C., Nilsson, R. H., Bhunjun, C. S., de Farias, A. R. G., Sun, Y. R., Wijesinghe, S. N., . . . Hyde, K. D. (2022). The numbers of fungi: Contributions from traditional tax onomic studies and challenges of metabarcoding. *Fungal Divers, 114*, 327–386. https://doi.org/10.1007/s13225-022-00502-3.

Tan, Q., Zhang, Y., Zhou, T., Xiong, Y., Huang, Q., Liu, G., . . . Manawasinghe, I. (2025). Endophytic Trichoderma (Sordariomycetes, Hypocreaceae) species associated with citrus in Guangdong province, China. *New Zealand Journal of Botany*, *63*(2-3), 251-277.